UNIVERSITY OF NEWCASTLE UPON TYNE

DEPARTMENT OF CIVIL ENGINEERING

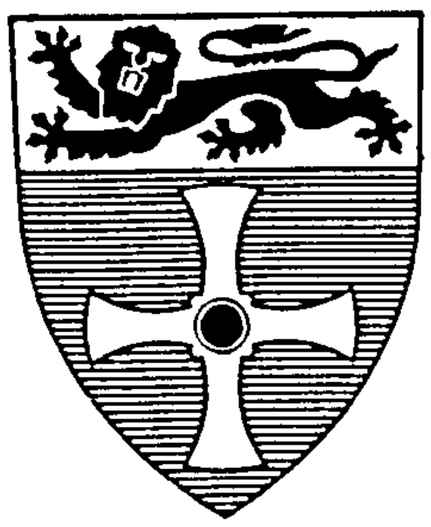

SEDIMENT TRANSPORT IN SEWERS

by

AMINUDDIN AB. GHANI

Thesis submitted in fulfilment of the requirements for the Degree of Doctor of Philosophy in Civil Engineering.

November 1993

ABSTRACT

Sewers have been designed on the concept of self-cleansing where sediments are expected to move continuously without deposition. Due to the intermittent nature of the flow, deposition of solids in sewers could still occur especially at low flows such as during the receding flow or dry weather flow.

The study of sediment movement in sewers will therefore need to cover both rigid (no-deposition) and loose (some deposition) boundary conditions. The present study extended the available data in rigid boundary conditions (clean pipes) to include the effects of surface roughness and pipe size. A complimentary study on the effect of sediment deposits (pipes with deposited beds) was also carried out.

Extensive experiments on bed load transport of non-cohesive sediments without deposition were carried out in pipe channels of 154mm, 305mm and 450mm dia. covering wide ranges of flow depths ($0.15 < y_o/D < 0.80$), sediments ($0.46 < d_{50}$ (mm) < 8.3) and three different bed roughness values ($0.0 < k_o$ (mm) < 1.34). Supplementary data on transport over loose beds were collected in a 450mm dia. channel with various bed thicknesses up to 23% of pipe diameter.

New transport equations based on all variables involved in the process were derived. Extensive uses of data from other relevant studies were made. The combination of the present and other data for both rigid and loose boundary conditions in pipes produced equations which could be applicable over wide range of conditions in sewers. A complimentary study on the rigid bed rectangular channels was also carried out.

Using the newly derived equations, appraisals of the traditional concept of constant velocity criterion were made. The results show the inadequacy of the present design practice for pipe diameters larger than 300mm.

The comparisons made between the newly derived equations for rigid and loose boundaries in pipes suggest that sewers can be designed with clean inverts for diameters up to 1.0m while sewers with larger diameters should be designed allowing for an "optimum" depth of sediment deposits. Design charts based on the newly derived equations were devised.

ACKNOWLEDGEMENTS

I am very grateful to my supervisor Dr. C. Nalluri for his guidance, encouragement, and generous provision of his time throughout the duration of the study period.

I also like to thank Professor P. Novak for his constructive criticism. Also, valuable contributions to this study were made through discussions with Professor K.G. Ranga Raju of Roorkee University, India and Dr. G. Perrusquia of Chalmers University of Technology, Sweden during their visits to Newcastle.

Many thanks are also due to Mr. J. A. Jefferson and Mr. P. Dawber for their assistance in the laboratory at Newcastle.

I am also indebted to Hydraulics Research Ltd. (HRL), Wallingford for the opportunity of undertaking part of this study using its facility. I wish to extend my grateful thanks to Mr. R.W.P May, Mrs. P.M Brown and Mrs. M. Escarameia for their advice and supervision during my stay at HRL. I also wish to express many thanks to Mr. R. Payne and Mr. I. R. Willoughby who were always willing to help me at the laboratory.

Special acknowledgements are due to University Sains Malaysia for providing the fellowship that made possible for me to come to Newcastle to conduct this research.

I am deeply in gratitude to my parents, brothers and sisters for providing encouragement and moral support. Finally, I sincerely acknowledge my wife, Salbiah, for her patience and understanding during the course of this study.

TABLE OF CONTENTS

LIST OF FIGURES

LIST OF TABLES

LIST OF PLATES

LIST OF MAIN SYMBOLS

A	Cross-sectional area of the flow
A_s	Cross-sectional area of the sediment bed
b	cemented sediment bed width, rectangular channel width
B	Water surface width
C	Concentration, constant in Ackers' equation
C_D	Drag coefficient
C_L	Lift force coefficient
C_v	Volumetric sediment concentration
d	Particle size
d_{50}	median diameter of particles in a mixture
D	Internal diameter of pipe channel
D_h	Hydraulic depth (= A/B)
D_{gr}	Dimensionless particle number (= $d_{50}\ (g(S_s-1)/\nu^2)^{1/3}$)
F_{gr}	Mobility parameter in Ackers' equation
F_r	Flow Froude number (= $(BV^2/gA)^{0.5}$)
F_{rm}	Modified Froude number (= $V/(gd_{50}\ (S_s-1))^{1/2}$)
F_s	May's mobility parameter for pipes with deposited beds
g	Gravitational constant
G_{gr}	General transport parameter in Ackers' equation
G_s	Bed load transport (N/s); May's mobility parameter at limit of deposition
H	Dunes' height
J	Ackers' parameter representing sediment transport
k	Linear roughness height
k_0	Clear-water equivalent sand roughness of rigid bed
k_s	Overall equivalent sand roughness with sediment
k_{sb}	Bed equivalent sand roughness with sediment

K Ackers' parameter representing incipient motion

L Dunes' length

m Empirical parameter in Ackers' equation

n Manning roughness coefficient, empirical parameter in Ackers' equation

n_0 Clear-water Manning roughness coefficient of rigid bed

n_s Overall Manning roughness coefficient with sediment

P Wetted parameter of the flow

q Unit flow discharge (= Q/B)

Q Flow discharge

Q_s Absolute sediment discharge

Q_s^* Transport rate ($N.m^{1.5} / s^{2.5}$)

R Overall hydraulic radius (= A/P)

R_0 Bed hydraulic radius

Re Flow Reynolds number (= $4VR/\nu$)

s Standard deviation

S_0 Bed slope

S_c Slope parameter (= $S_0/(S_s - 1)$)

S_s Specific gravity of sediment (= ρ_s/ρ)

T Temperature

u Particle velocity

u_* Shear velocity

V Mean velocity of flow

V_c Mean velocity of flow for incipient motion

W_b Sediment bed width in pipes

W_e Effective width

W_s Width of sediment spread in clean pipes

y_0 Depth of uniform flow

y_s Thickness of sediment bed

Y Overall flow depth ($= y_0 + y_s$)

α Friction angle between the channel and sediment

β Velocity distribution coefficient

γ_s Specific weight of sediment

λ_c Clear water friction factor

λ_s Overall friction factor with sediment

λ_{sb} Bed friction factor with sediment

λ_g Grain roughness

η May's transport parameter (Pipes with deposited beds)

θ May's related transition factor

θ_b Bed mobility number = $(1/\psi_b)$

ν Kinematic viscosity of fluid

ρ Density of water

ρ_s Density of sediment

τ_0 Mean shear stress ($= \rho gRS$)

τ_b Bed shear stress ($= \rho gR_bS$)

Φ Transport parameter ($= C_vVR/(gd^3(S_s-1))^{1/2}$)

ψ Shear intensity or flow parameter ($= (S_s-1)d/SR)$)

Ω May's transport parameter (Clean pipes)

ω Settling velocity of particle

CHAPTER 1

INTRODUCTION

1.1 Background

The movement of sediments in sewers has been the subject of studies in recent years due to the fear of pollution to watercourses. Several studies (Ashley et al 1991, Verbanck 1990, Larson et al 1990) have attempted to relate the presence of sediments in sewers to pollutant concentrations.

Besides pollution, the presence of sediment in sewers might produce several other problems for example, blockage, surcharging, and flooding to name a few. A review of design guide and practice (CIRIA, 1987) shows that most of sewers have been designed mainly on a single critical criterion, either velocity or shear stress with the aim of keeping the sewers free of any sediment deposition. However, recent works (Mayerle et al 1991, May 1982, Ackers 1978) point out that while the single limiting criterion gives conservative results for small sewers (diameters smaller than 500mm), it is not enough to prevent sediment deposition in larger sewers. These studies highlight several important factors influencing sediment deposition such as the supply sediment concentration, the size and density of sediment, and the sewer size. Another important finding from these studies is that the resulting equations obtained give

widely-differing predictions when extrapolated to sewer sizes significantly larger than those originally tested. This result might have been due to small pipes (mostly 150mm dia.) used in the experiments.

Henderson (1984) drew attention to the importance of sewer roughness in relation to the sewer performance. His studies show that the sewer hydraulic roughness is influenced not only by the sewer materials but also the jointing of the sections, sliming, ageing and the presence of sediment deposits. The increase in sewer roughness due to these factors might lead to a loss in their transporting capacities. However, earlier studies (for example, Mayerle 1988) were mostly conducted in smooth pipes.

Ackers et al (1964) reported the presence of permanently-deposited sediments in sewers while conducting the studies on the hydraulic roughness in used sewers. Recent works (Ashley et al 1992, Verbanck 1992, Laplace et al 1992) also found that it is possible for the stationary sediment deposits to occur in sewers. The importance of this finding was conceptually raised by Ackers (1978) where he suggested that a "limited depth of deposits" would lead to milder slopes required for large sewers instead of steeper slopes as produced by the sediment - free criterion. However, limited data available hinders the quantitative studies of the transporting capacity of sewers with stationary sediment deposits.

1.2 Scope of Present Study

The present studies were intended for sewers carrying stormwater, and hence the results are applicable mainly for separate storm sewers. Only non-cohesive sediments were used even though it is acknowledged that cohesion itself would be another factor influencing the sewer transporting capacity (Alvarez 1990). All experiments were conducted under part-full uniform flow conditions with sediments transported as bed load in smooth and rough rigid and loose boundaries. The aims of the research were to gain an improved understanding on the sediment transport process in sewers and to provide improved sediment transport relationships. This is achieved by supplementing the lack of data in the sewer studies on the factors influencing the transporting capacity of sewers namely,

a) sewer texture or wall roughness,
b) sewer size, and
c) sediment deposits

The experiments were carried out at the Hydraulic Laboratories of the University of Newcastle upon Tyne and Hydraulic Research Ltd., Wallingford.

1.3 Outline of The Thesis

This thesis consists of seven chapters and three appendices. Following the introductory chapter, Chapter 2 on the "Nature of Sediments in Sewers" gives a review on the behaviour of sediments

in sewers incorporating the recent results of field works in real sewers and current design criteria used in practice.

Chapter 3 entitled the "Review of Relevant Literature" presents a summary of experimental works on sediment transport in sewers and relevant studies for both rigid and loose boundaries.

Chapter 4 covers the "Experimental Apparatus and Procedures" and describes the experimental apparatus and procedures adopted in the present investigation, with the details of the test pipes, measurement techniques, and sediment characteristics. It also gives the method for the establishment of uniform flow and procedures for the sediment transport experiments.

Chapter 5 on the "Preliminary Analyses" presents the data on pipe roughness. It also presents the bed load results with the aim of highlighting the factors influencing the self-cleansing velocity.

Chapter 6 consists of the "Analyses of Sediment Transport Data" where analyses of the data obtained in the sediment transport experiments for both rigid and loose boundaries are described. For each boundary, the analysis starts with the comparisons among the established transport relationships using the present data. Several functional relationships are then considered and new transport models established with the help of multiple regression analyses. Design examples are later presented to compare the performance of the newly derived transport equations with the

established equations and also to assess the current design practice.

Finally Chapter 7 entitled "Conclusions and Recommendations for Further Research" summarises the conclusions obtained from the present study and suggests several recommendations for further works in light of the present study.

CHAPTER 2

NATURE OF SEDIMENTS IN SEWERS

2.1 Background

Due to variation in flows sediments have always been present to some extent in sewerage systems. The movement of sediments in sewers hence involves a cycle of processes namely erosion, transport and deposition though not strictly in the order mentioned.

CIRIA (1987) conducted extensive studies on problems related to the presence of sediments in sewers in the UK. The most commonly found problems were blockage, surcharging, flooding, premature overflow operation, and water quality. The important sources of sediments were given as winter gritting operations, road surfacing materials and roadworks, ingress of surrounding ground and construction work. The sediment yields were discovered to be affected mainly by geographical location, sewer type, land use, time of year and preceding dry period.

Ashley-Crabtree(1992) reported further works in the UK. New studies (Ashley et al 1992) indicate that there are considerable spatial variations in the sources and origins of sediments where sediment inputs to sewers may differ not only between catchment types but also between adjacent sewer inlets. Other recent studies also give similar results to those of Ashley et al (1992). Xanthopoulos-Augustin (1992) carried out samplings of

sediment types and concentrations at different catchment areas with combined and separate sewerage systems. The results show that the sediment sizes were site-specific and that the main source of solids was the street runoff. Bachoc (1992) found that there are several vulnerable sections for deposition inside the sewers, for instance downstream from flow partition. In general, recent studies produce similar results to the ones obtained from CIRIA's (1987) studies.

Recent studies (Ashley et al 1992, Verbanck 1992, Laplace et al 1992) have also attempted to quantify the sediment concentrations in sewers with stationary sediment deposits. Details of these studies are given in the following section (See Section 2.2.2).

2.2 Characteristics and Quantity of Sediments

2.2.1 Earlier Studies

CIRIA (1987) gave a comprehensive review on the source and quantity of sediments present in the sewerage systems which were found to be dependent on the locations where the samplings were made. A summary of the findings in CIRIA (1987) relating to those samplings made in the invert of sewers is reported herein.

The samplings at eleven cities in the UK (CIRIA 1987) showed that the sediments are generally well-graded with the range ($=d_{50}$) between 0.1 and 9.0mm. May (1982) studied the sediments deposited in storm sewers and reported the average d_{50} size of about 2.5mm. The sediment concentration was found to be 20ppm

by volume with the average depth of deposit of about 40mm in the 1.83m dia. sewer. Ackers et al (1964) measured the depths of sediment deposits in combined sewers and gave the average depths of deposit in the range of 25mm to 300mm made up of sand and gravel with median size between 0.54mm to 12mm.

Urcikan (1984) obtained samples of sediments from combined sewers in Bratislava, Slovakia and found the mean size of sediments between 0.34mm and 2.94mm. Macke (1983) and Shultz (1983) conducted samplings in several cities in Germany and obtained sediments in the range of 0.06 to 2.0mm. Broecker (1984) studied deposition in combined sewers and reported the average specific gravity of the particles of about 2.45 implying coarse sediments.

Mittelstadt et al (1979) compiled volumetric sediment concentrations found by previous researchers where the values varied from 7 to 110 ppm with a mean of about 50 ppm.

These studies suggest (see Table 2.1) that the sediments present in the sewer inverts are mainly coarse with low volumetric concentration.

2.2.2 Recent Studies

Following CIRIA (1987) studies, several new investigations on the occurence of sediment deposits have been going on to quantify the polluting and operational aspect resulting from these sediment deposits. Herein only the results relating to operational

aspects, linked to the costly cleaning operation of the sewers to maintain the designed hydraulic capacity, will be discussed.

TABLE 2.1 SEDIMENT CHARACTERISTICS IN SEWERS
(See CIRIA 1987)

AUTHOR	PARTICLE SIZE (mm)	SPECIFIC GRAVITY	VOLUMETRIC CONCENTRATION (ppm)
CIRIA (1987)	0.10 - 9.00		
MAY (1982)	2.50		20
MACKE (1983)	0.06 - 2.00		
URCIKAN (1984)	0.34 - 2.94		
BROECKER (1984)		2.45	
MITTELSDADT (1979)			7 - 110

Verbanck (1992) obtained sediment accumulation profiles since June 1986 in a Brussels (Belgium) main combined trunk sewer of 4.0m dia. and 5.4km long with an average slope of 0.0004. The longitudinal accumulation profile on the total length of the sewer has been found to be very reproducible in time (Verbanck 1990). Fig. 2.1 shows the evolution with time of the volume of the deposits, calculated for the total length of the main trunk. A closer study of events shown in Fig. 2.1 indicates a development of stationary sediment deposits. The gradual development of stationary deposits during the period without cleaning operations (Fig. 2.2) was observed to be a bed load process. The effects of the cleaning operations on the mean deposit level as shown in Fig. 2.3 were generally very limited. Fig. 2.3 also further illustrates a stable level of deposits over time. Analysis of samples taken along the invert of the sewer

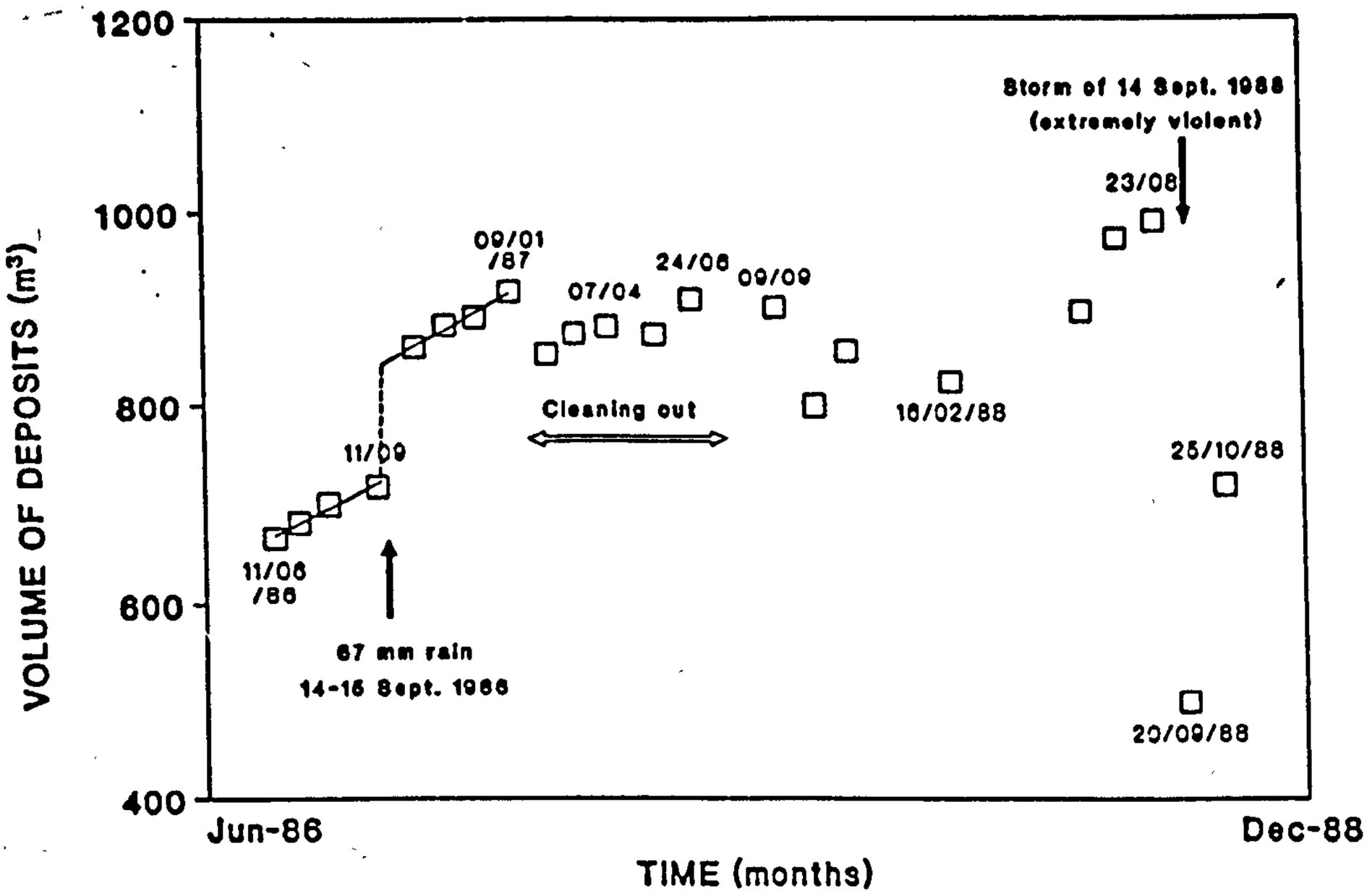

FIG. 2.1 Build-up of sediment on the invert of Brussels main trunk sewer (After Verbanck 1992)

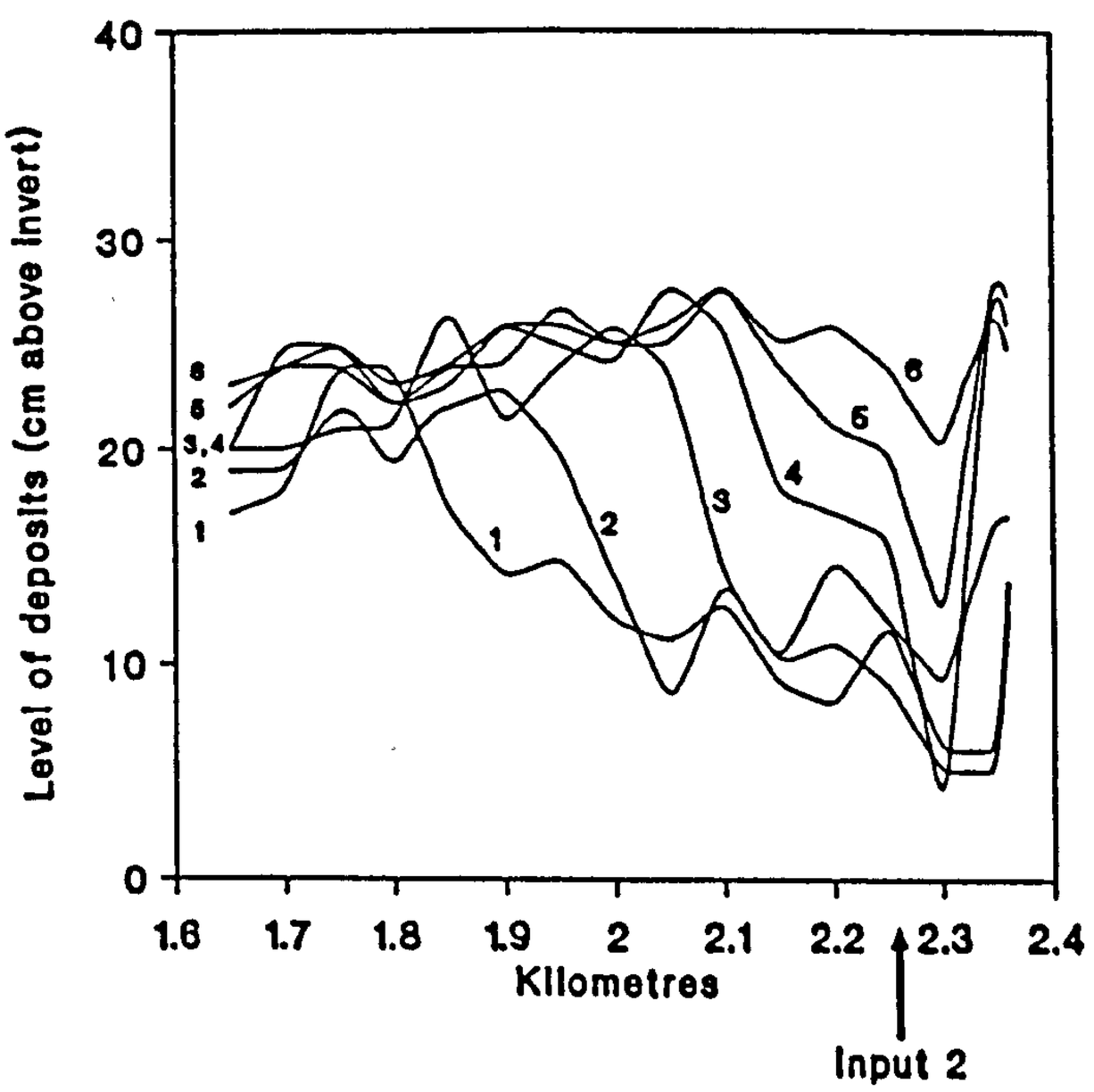

FIG. 2.2 Detailed view of gradual sediment build-up (After Verbanck 1992)

showed that the sediments were made up of well-graded sands ranging from (=d_{50}) 0.2 to 0.5 mm.

Since July 1988 Laplace et al (1992) followed the formation of deposits in a man-entry combined trunk sewer in Marseille (France) for a period of two years. The observations were made along a 460m section of the egg-shape sewer (2.75m high and 1.80m wide) with an average slope of 0.001. Fig. 2.4 shows the level of deposits over the period studied. The asymptotic trend indicates the possibility of the deposits reaching an equilibrium level with time. Fig. 2.5 represents a succession of some profiles which gives an indication of the manner of the formation of the deposits. Based on the sampling of the sediments in the invert of the sewer, which gave an average particle size of between 0.3mm and 3.0mm, Laplace et al concluded that the bed load process was responsible for the formation of stationary beds. Corresponding concentration of sediments transported as bed load was found to be 25ppm.

Ashley et al (1992) studied sediment deposition in an interceptor combined sewer at Dundee (UK) since 1986. The sewer is approximately circular (1500 mm dia.), and 175m long with an average slope of 0.00069. The measurements of the level of sediment deposits do not yet show a tendency to reach an equilibrium level. Samplings of the sediments on the sewer invert gave a size range of 0.1 to 0.5 mm. The volumetric bed load concentrations were found to vary up to 20ppm. Fig. 2.6 (Ashley-Crabtree 1992) shows sediments found in sewers from

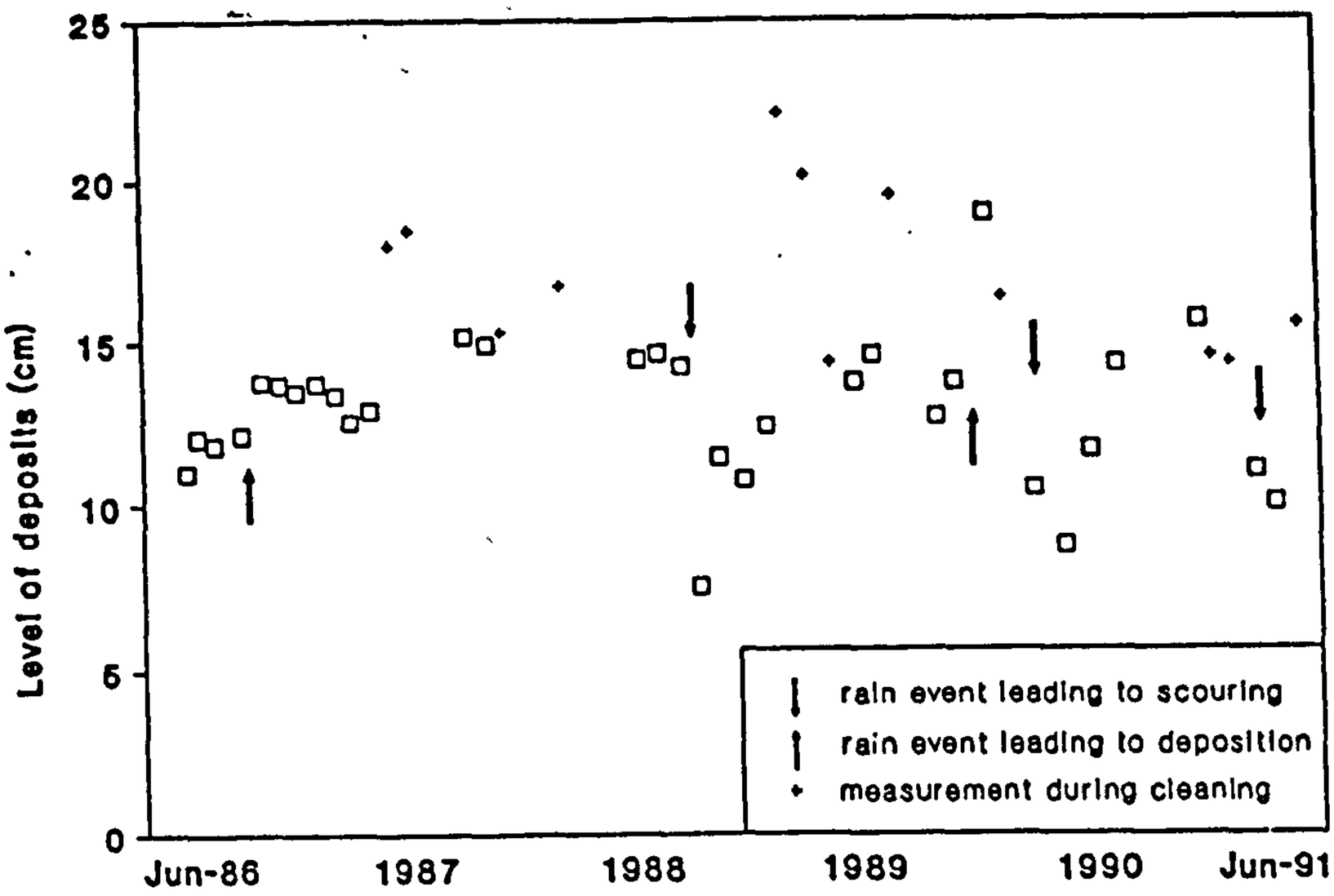

FIG. 2.3 Effect of cleaning operation on sediment deposition (After Verbanck 1992)

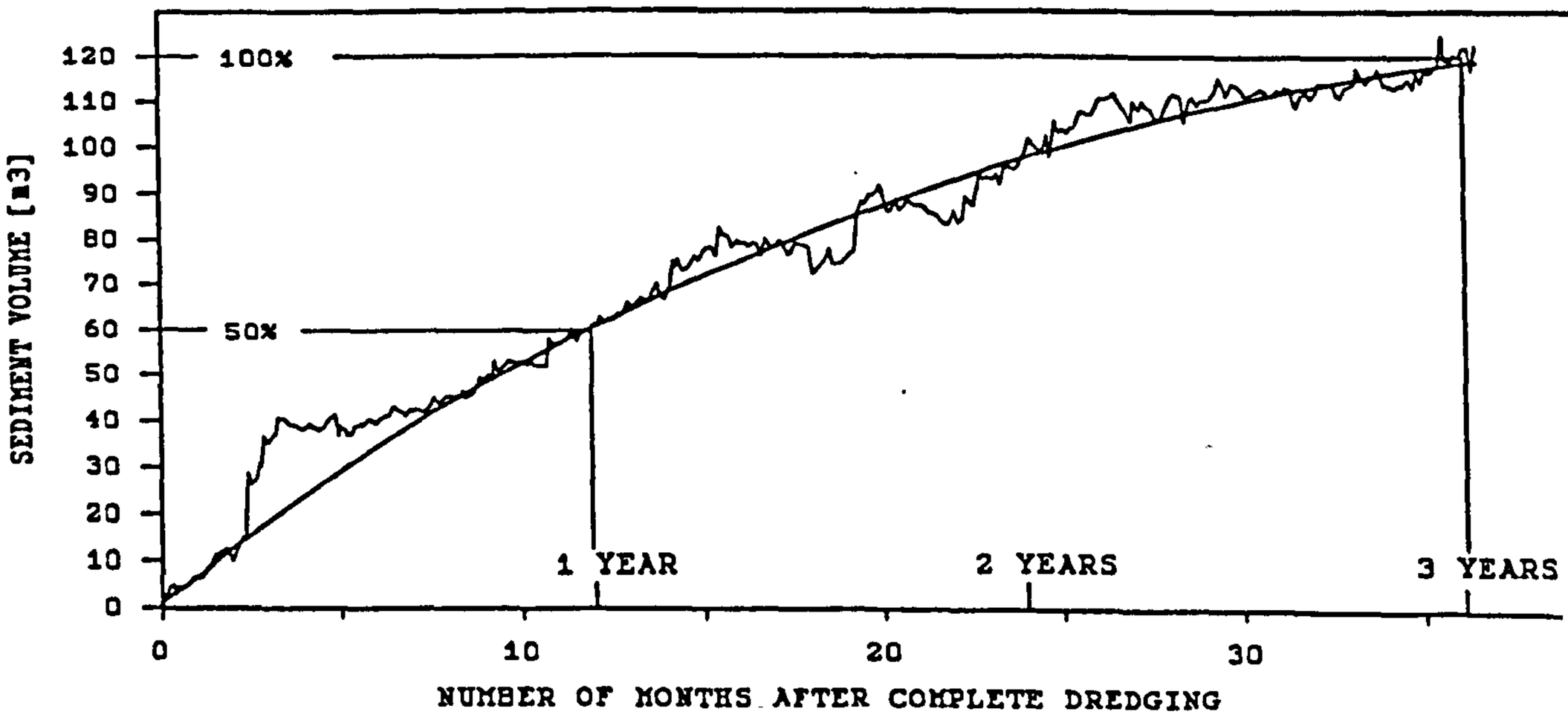

FIG. 2.4 Long-term trend of volume deposited (After Laplace et al 1992)

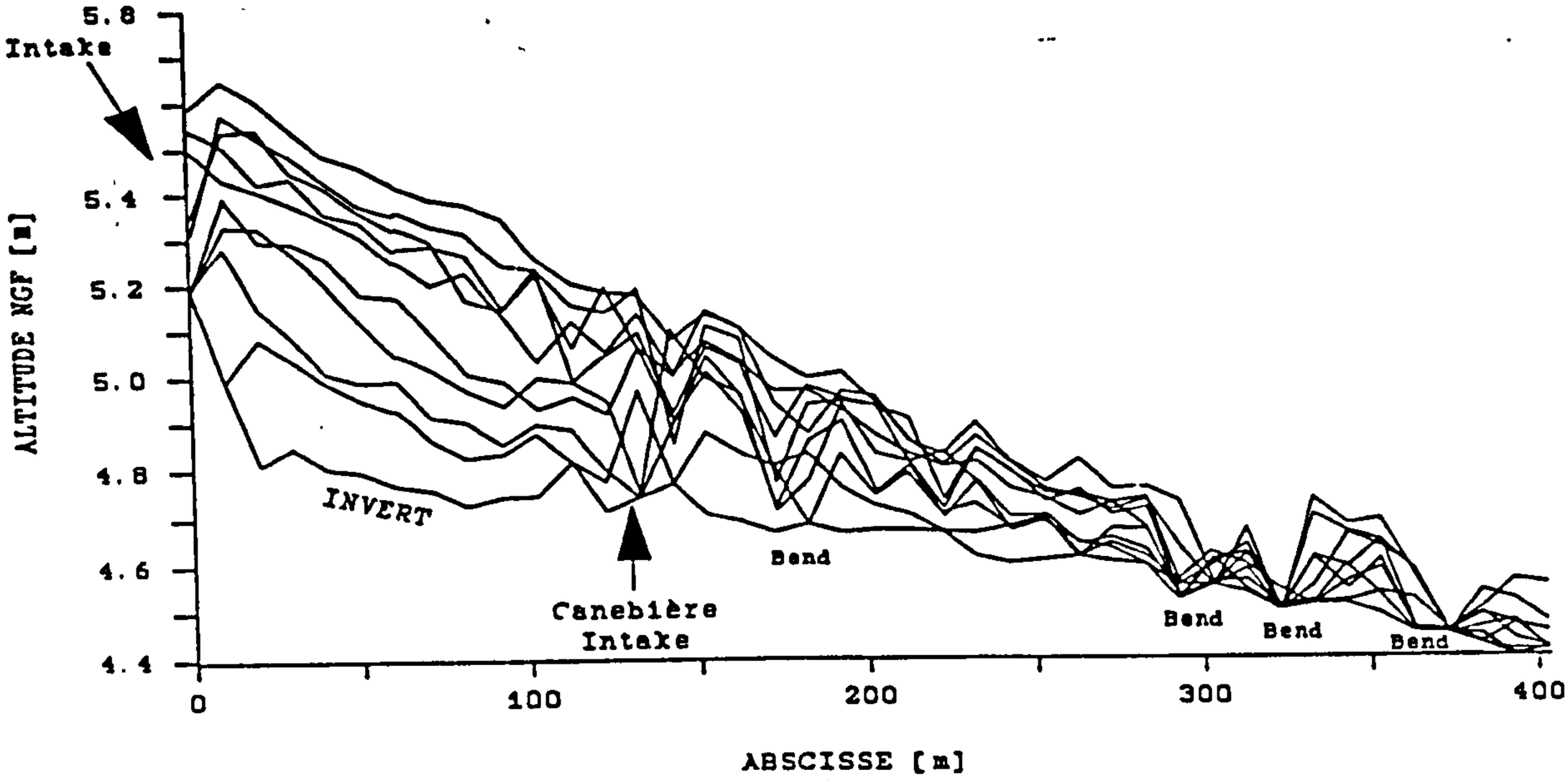

FIG. 2.5 Longitudinal profile of sediment depth (After Laplace et al 1992)

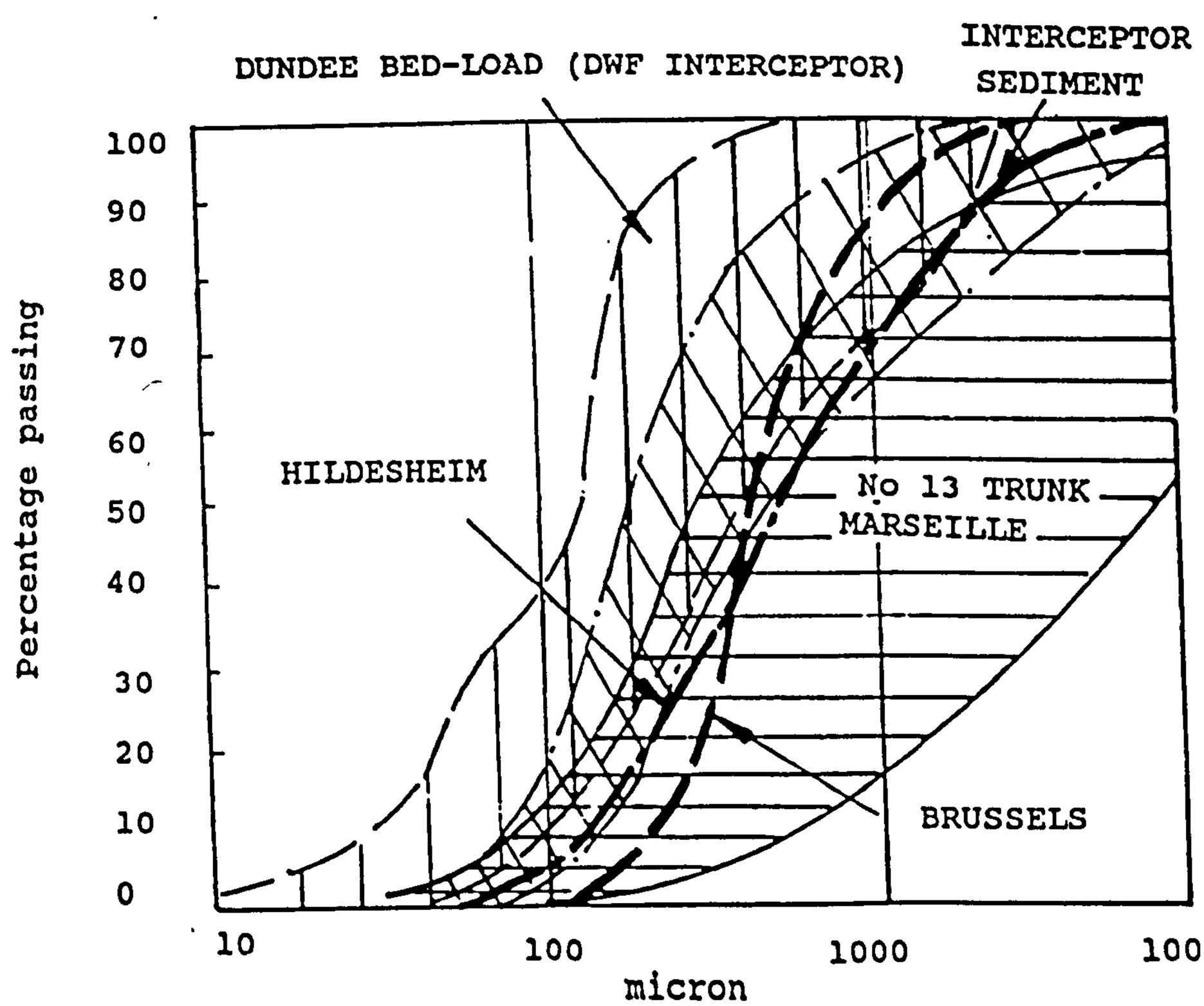

FIG. 2.6 Typical partical sizes found in sewer inverts (After Ashley et al 1992)

recent studies (Ashley et al 1992, Verbanck 1992, Laplace et al, Ristenpart et al 1992).

The results from recent studies show a general agreement on the range of sediment sizes found in the invert of the sewers. It can also be concluded that over time it is possible to reach an equilibrium level of sediment deposits.

2.3 Classification of Sediments and Sewers

Based on studies by CIRIA (1987), Crabtree (1988) revisited sites which showed the presence of sediment deposits to gain a greater insight into the nature of combined sewer sediment deposits. He suggested a five-fold category based on visual appearance, location within a sewerage system, and physical and chemical analysis:

Classes :- A - coarse granular material
B - Class A deposits concreted by greases and mineral cements
C - mobile fine grained - usually overlying A
D - organic wall slimes
E - deposits found in tanks

Among these, Class A represents typical sediments found in the invert of sewers. This is in general agreement with the results mentioned in Section 2.2 suggesting the universal applicability of the classification.

Following their work at Dundee (UK), Ashley et al (1992) attempted to classify sewers based on diameter, slope and cumulative contributing catchment area:

Classes :-	Collectors	- small, local at head of networks
	Trunks	- steeper, convey flows from collectors to disposals or interceptors
	Interceptors	- large, flat gradient

In general these categories are of increasing relative size and distinguishable principally by the relative sediment size. The results at Dundee show that the collector sewer deposits are mainly migrating organic material (Class C). In the trunk sewers, the deposits are coarser (Class A) while the interceptor sewers are deposited with finer organic particles (Class C).

2.4 Modes of Sediment Transport

In general the movement of sediments in sewers could be classified into two categories : 1) transport with clean invert and 2) transport over loose sediment deposits, separated dunes or continuous dunes. The sediments will either move in suspension (suspended-load mode) or roll and/ or saltate (bed-load mode) depending on the physical and chemical characteristics of sediments and also the level of turbulence. Total-load mode is possible if the sediments move both as suspended load and bed load at the same time.

Based on the classifications by Newitt et al (1955) and Spells (1955) May et al (1989) suggest that sediments coarser than 0.4mm are likely to be moving as bed load.

Xanthopoulos-Augustine (1992) proposed a classification of storm water runoff particles where they suggested that fraction larger than 0.6mm will move as bed load.

Verbanck (1992) found that sediments finer than 0.125 mm will move in suspension while sediments larger than 0.4mm will move as bed load.

Based on sediment sizes it can be concluded that for sediments larger than 0.4 mm, the mode of transport for non-cohesive particles will be bed load.

2.5 Hydraulic Sewer Roughness

Henderson (1984) carried out studies on hydraulic roughness in used sewers in the UK to obtain a realistic appraisal of existing sewer capacity. He combined his own data with previous work (mainly of Ackers et al 1964) to come up with suggested equivalent sand roughness, k-values, calculated from the Colebrook-White equation.

Table 2.2 gives pipefull k-values for pipe sewers for the given condition of sewers. These k-values should be modified to account for any misalignment of the sections and the suggested

TABLE 2.2 PIPE-FULL k-VALUES FOR PIPE SEWERS (AFTER HENDERSON, 1984)

TYPICAL CONDITION	SUGGESTED k_s VALUE (mm)	
Virtually as new condition. Light coating of slime (<2mm maximum) to half depth. Free of silt/debris. Peak dwf velocity typically exceeds 1.5m/s.	0.3	Renovation lining design range
Normal condition. Sliming of invert to 3mm maximum. No silt or debris. Peak dwf velocity typically exceeds 1.0m/s.	0.6	
Normal condition. Normal sliming of invert (3 to 5mm). No silt or debris. Peak dwf velocity between 0.7 and 1.0m/s.	1.5	
Normal condition. As above but with light and localised accumulation of silt or heavy sliming exceeding 5mm depth.	3.0	
Normal condition. Mortar loss causing gaps at joints or loss of cross section, not more than 5% caused by root penetration, silt or slight encrustation at joints.	6.0	
Poor condition. Longitudinal cracking/fracturing of pipe with marginal ovality of cross section. Normally slimed. No silt or debris.	6.0	
Poor condition. Multiple fracturing with up to 10% loss of cross section, severe displacement at joints. Standing waves well developed at part full flow.	15.0	
Poor condition. Structurally sound but with heavy encrustation at joints or debris/silt causing 15% loss of cross section.	15.0	
Very poor condition. Multiple fracturing. Pronounced deformation/ovality, causing up to 20% loss of cross section.	30.0	
Partial or total collapse of pipe.	30.0 to 150.0+	

TABLE 2.3 ADDITIONAL ROUGHNESS DUE TO JOINT ECCENTRICITY (AFTER HENDERSON, 1984)

ESTIMATED MEAN JOINT STEP (mm)	k_s DUE TO JOINT ECCENTRICITY (mm)
5- 9	0.15
10-13	0.30
14-18	0.60
19-27	1.5
28-40	3.0
41-55	6.0
>55	15.0

values (Henderson 1984) are given in Table 2.3. Besides pipe material, slime and misalignment of joints, different k-values would be obtained for sewers with sediment deposits.

From Table 2.2 it can be concluded that for sewers with good alignment, minimum sliming of invert and no sediment deposits, the pipefull k-values are in the range between 0.3 to 3.0 mm.

The Water Authorities Association (WAA) suggested in its publication, Sewers for Adoption (WAA, 1989) the k-values to use: 0.6mm for storm water sewers and 1.5mm for combined sewers.

2.6 Current Design Criteria

Sewers are generally designed to be self-cleansing. All sediments entering sewers are expected to move continuously without deposition. Due to the intermittent nature of the flows, deposition is to be expected during receding flows or dry weather conditions. Under these conditions, it is expected that the deposits would be picked-up by high flush hence hindering any long-term deposition.

CIRIA (1987) thoroughly reviewed the available codes of practice and design criteria in the UK and elsewhere. In general, the self-cleansing criterion is based either on minimum mean velocity or shear stress. Tables 2.4 and 2.5 reproduce some of the criteria given in CIRIA (1987).

TABLE 2.4 CONSTANT VELOCITY CRITERIA
(See CIRIA 1987)

REFERENCE SOURCE	COUNTRY	SEWER TYPE	MINIMUM VELOCITY	PIPE CONDITIONS
AMERICAN SOCIETY OF CIVIL ENGINEERS (1970)	USA	FOUL	0.6	FULL/HALF-FULL
		STORM	0.9	FULL/HALF-FULL
BRITISH STANDARD (1987)	UK	STORM	0.75	FULL
		COMBINED	1.0	FULL
ESCRITT (1979)	UK		0.76	FULL
BIELECKI (1982)	GERMANY		1.5	FULL

TABLE 2.5 CONSTANT SHEAR STRESS CRITERIA
(See CIRIA 1987)

REFERENCE SOURCE	COUNTRY	SEWER TYPE	MINIMUM SHEAR STRESS (N/m^2)	PIPE CONDITIONS
MAGUIRE RULE	UK		6.2	FULL/HALF-FULL
YAO (1974)	USA	STORM	3.0 - 4.0	
		FOUL	1.0 - 2.0	
LYSNE (1969)	NORWAY		2.0 - 3.0	
ASVISNINGAR (1976)	SWEDEN		1.5	

Using the transport relationships (Novak-Nalluri 1975, May 1982, Arora et al 1984) based on recent experimental works, the minimum velocity criterion was appraised as shown in Fig. 2.7 (Nalluri, 1985) and Fig. 2.8 (Ackers, 1984). In general, the present design practice overdesigns the slope for small pipe diameters (D < 500mm) and underdesigns the slope for larger pipe diameters.

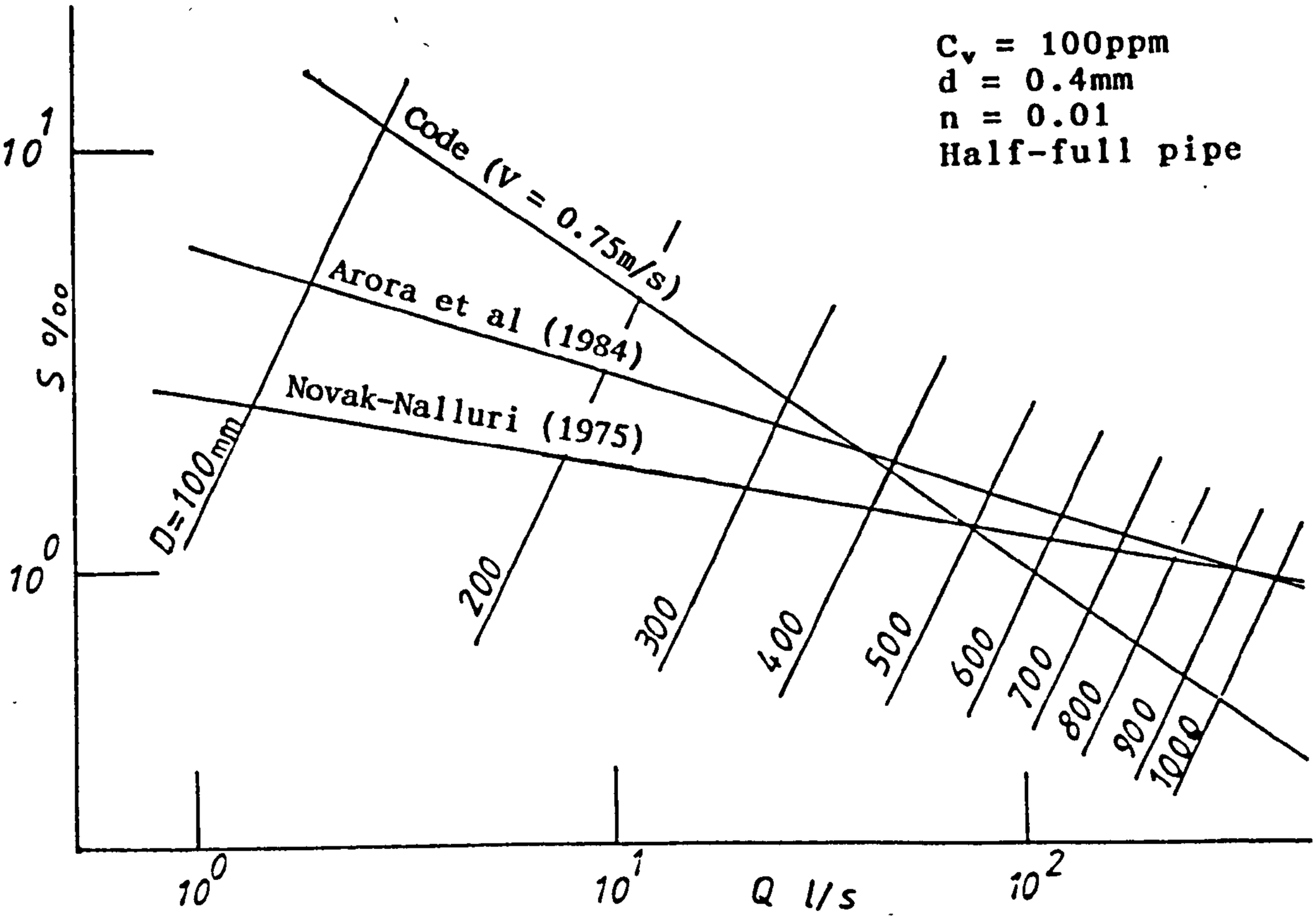

FIG. 2.7 Appraisal of present design practice due to Nalluri (1985)

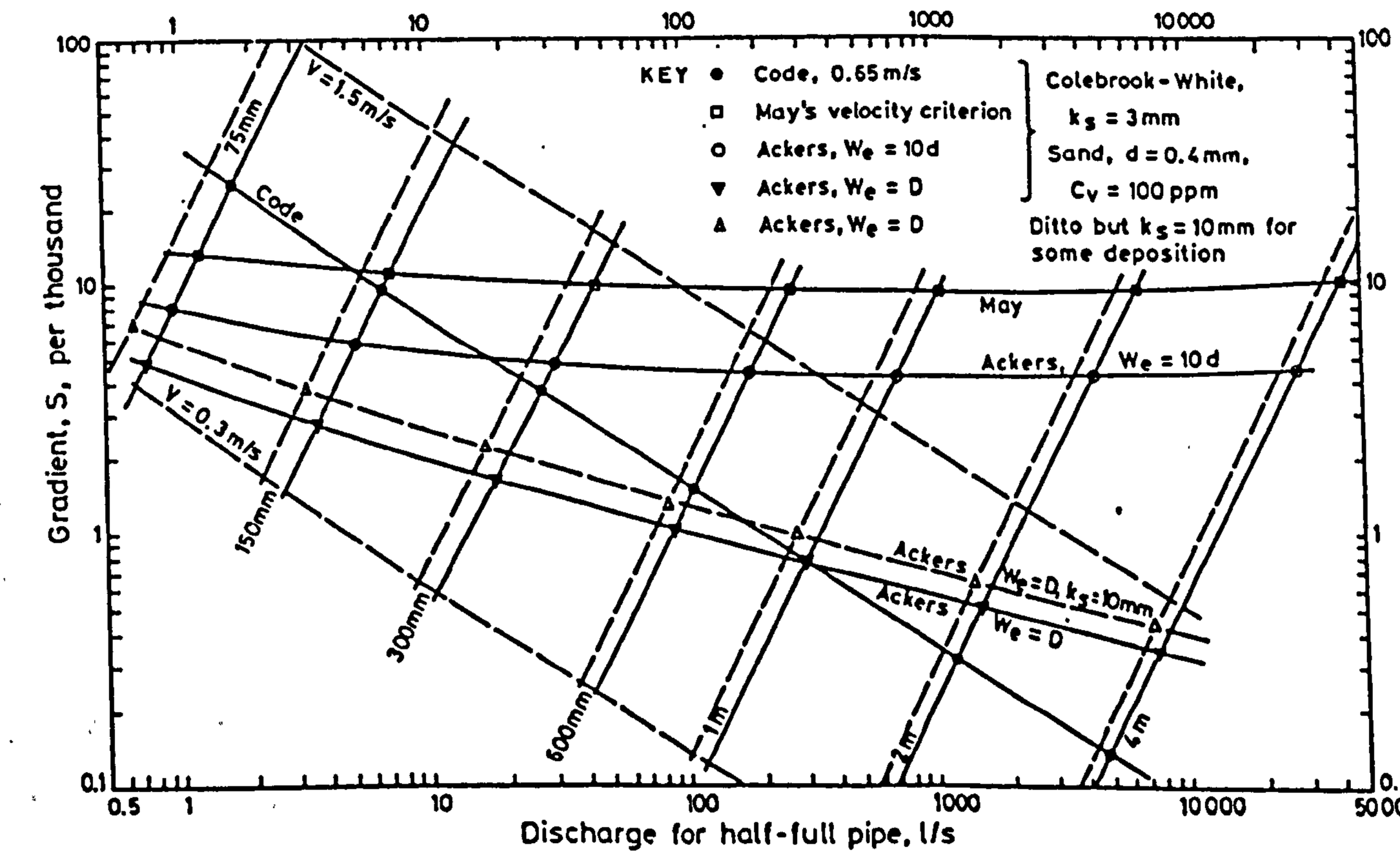

FIG. 2.8 Appraisal of present design practice due to Ackers (1984)

CHAPTER 3

REVIEW OF RELEVANT LITERATURE

3.1 Background

Majority of the works on incipient motion and sediment transport deal with alluvial channels. A good deal of information could be found in standard textbooks such as Vanoni (1975), Graf (1984), Garde-Ranga Raju (1985), Van Rijn (1989) and Raudkivi (1990).

There are however several limitations to the direct application of loose boundary models to the conditions in sewers. Two important differences in the mechanism of sediment transport in alluvial channels and sewers are worthwhile mentioning. Firstly, the supply rate of sediments in an alluvial channel is derived from the channel itself and is effectively unlimited while in sewers the supply rate of sediments is determined from the catchment of the sewerage system as discussed in Section 2.1. Secondly, the effective roughness of sewers varies depending on whether the invert of sewers is clean or made up of loose sediment deposits.

Studies on transportation of slurries in pipelines (Vanoni 1975) also have drawbacks in the direct application to problems in sewers. The sediment concentrations and velocities in slurry transportations are much higher than those attainable in sewers.

The earliest reported studies on sediment transport in sewers were presented by the researchers at Iowa University, USA. Under the guidance of Laursen (1956), Craven (1953), Ambrose (1953) and Valentine (1955) conducted experiments covering sediment transport both with rigid boundary (at the limit of deposition) and over loose beds. However, no further work was reported on this subject until 1970.

Transport studies on rigid boundary in sewers resumed mainly in the UK by Novak-Nalluri (1972) and May (1975). Field data (CIRIA 1987) from used sewers revealed the presence of permanent sediment deposits on their inverts, leading to the studies of transport over deposited beds (May et al 1989, Perrusquia 1991, Kleijwegt 1992). Even with these new works, there still remain areas need to be studied to gain a better understanding of the problems. The following sections summarize existing works and identify those areas which are not yet fully covered by previous studies.

3.2 Incipient Motion

Studies of incipient motion or beginning movement of sediments in alluvial channels (e.g. Graf 1984, Lavelle-Mofjeld 1987, Raudkivi 1990) show that there are two possible definitions of threshold. The first category is based on a minimum transport rate such as the works by Shields and Kramer (see Lavelle-Mofjeld 1987). The second definition constitutes of the visual observations of particle motion on the bed.

Work by Shields (see Graf 1984, Raudkivi, 1990) has been a standard for studies in incipient motion and sediment transport. Shields defined the threshold as a zero transport rate from interpolation of transport data. The results were depicted in a plot (Fig. 3.1) of dimensionless entrainment parameter, $Fr^2_{d,cr}$ (= $\tau_c/[\rho g(S_s-1)d]$) versus shear Reynolds number, $Re_{*,cr}$ (= $u_{*,cr}d/\nu$) where τ_c is the critical shear stress, ρ is the density of water and S_s is the specific gravity of sediment, d is the diameter of sediment, g is the acceleration due to gravity, $u_{*,cr}$ is the critical shear velocity (= $\sqrt{\tau_{cr}/\rho}$), and ν is the kinematic viscosity of water. Van Rijn (1984) expressed Shields' $Fr^2_{d,cr}$ in terms of dimensionless grain diameter, D_{gr} (= $d[g(S_s-1)/\nu^2]^{1/3}$) as given in Table 3.1.

TABLE 3.1 SHIELDS' CURVE ((After VAN RIJN 1984)

RANGE OF D_{gr}	ENTRAINMENT PARAMETER ($Fr^2_{d,cr}$)
$D_{gr} \leq 4$	$0.24\ D_{gr}^{-1.0}$
$4 < D_{gr} \leq 10$	$0.14\ D_{gr}^{-0.64}$
$10 < D_{gr} \leq 20$	$0.04\ D_{gr}^{-0.10}$
$20 < D_{gr} \leq 150$	$0.013\ D_{gr}^{0.29}$
$D_{gr} > 150$	0.055

Only relatively few studies have been carried out on incipient motion in rigid boundary channels (Novak-Nalluri 1975-84, Ojo 1978, El-Zaemey 1991, Kleijwegt 1992). Of importance to present

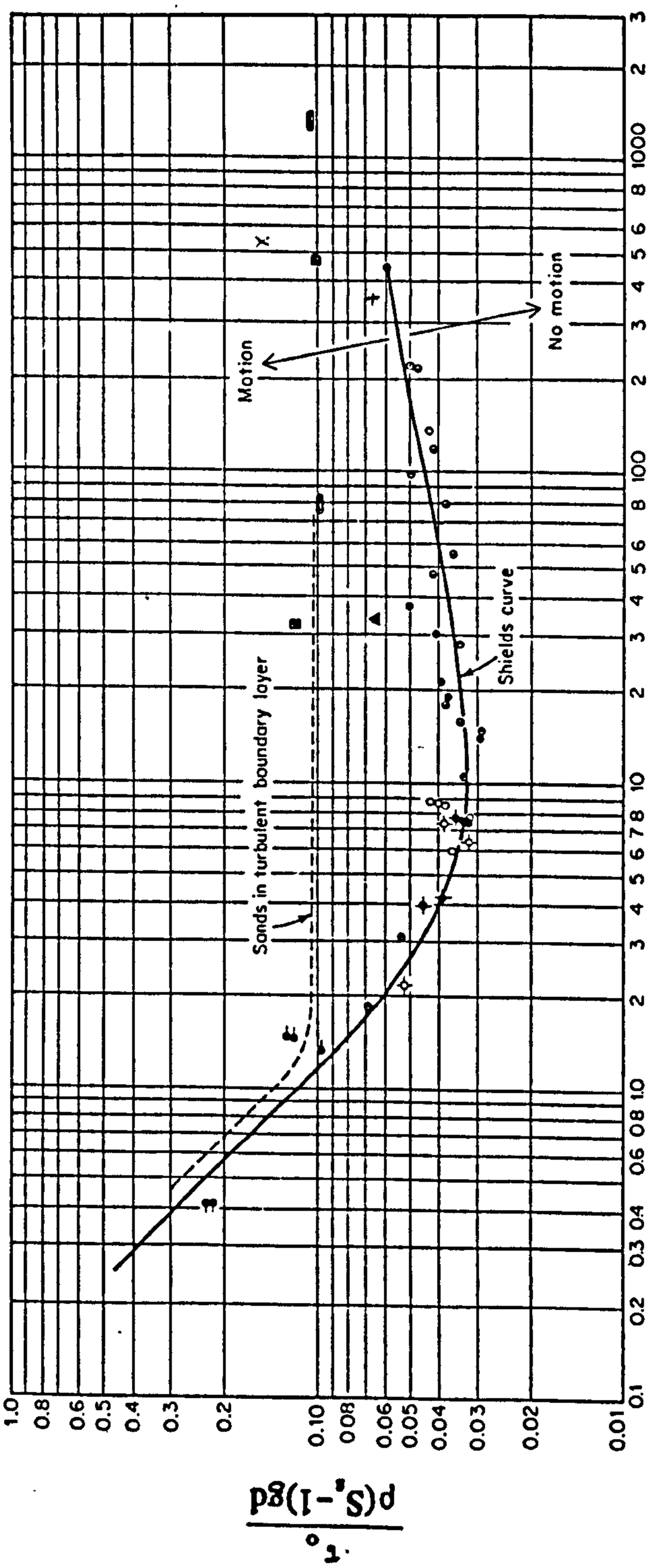

FIG. 3.1 Shields diagram (After Graf 1984)

studies was the work by Novak-Nalluri (1975, 1984). They conducted experimental work (Novak-Nalluri 1975) in smooth circular channels of 152mm and 305mm dia. and a smooth rectangular channel of 305mm wide. Non-cohesive sediments (sand and gravel) were used with sizes ranging from 0.6mm to 50.0mm. All experiments were carried out in part-full uniform flows and the incipient motion of single particles resting on the invert of the channel was identified by a slight sliding or tossing of the particles which were placed along the centre line of the channel.

Novak-Nalluri (1975) performed theoretical analysis by equating the forces acting on a grain resting on a smooth bed and obtained the following form:

$$V_c = C \sqrt{g(S_s-1)d} \qquad (3.1)$$

where V_c is the critical threshold velocity, C is a function of the particle shape, the height of application of the drag force above the bed, the downstream displacement of the point of contact between the bed and particle from the position of the particle centre of gravity, and the surface contact friction coefficient. The experimental results can be approximated (V_c in m/s and d in mm) by:

$$V_c = 0.17\ (S_s-1)^{1/2} d^{0.24} \qquad (3.2)$$

for rectangular channels, and

$$V_c = 0.16\ (S_s-1)^{1/2}\ d^{0.16} \qquad (3.3)$$

for circular channels. Further analyses show that data for both channels could be represented by a single equation by introducing a relative roughness (d/R) in Eqn. 3.1 where R is the hydraulic radius resulting in the following equation (see Fig. 3.2):

$$\frac{V_c}{\sqrt{gd}} = 0.61\ (S_s-1)^{1/2} \left(\frac{d}{R}\right)^{-0.27} \qquad (3.4)$$

for the range $0.01 < (d/R) < 1$.

Ojo (1978) extended the work by Novak-Nalluri (1975) in the 305mm wide rectangular channel to include effects of particle groupings, spacings and channel roughnesses. The range of sand size used for artificial roughnesses studied was 0.3mm to 4.2mm. The grouped particles were placed in three different ways: 1) particles spaced across the width of the flume, 2) particles spaced longitudinally along the centre-line of the flume, and 3) particles touching one another in rows across the width of the flume. Novak-Nalluri (1984) reanalysed their data from earlier work (Novak-Nalluri 1975) in combination with those of Ojo (1978) and presented the following best-fit relationship:

$$\frac{V_c}{\sqrt{gd}} = 0.50\ (S_s-1)^{1/2} \left(\frac{d}{R}\right)^{-0.40} \qquad (3.5)$$

for the range $0.01 < (d/R) < 0.3$ and $3.5 < (d/k) < \infty$ where k is the equivalent sand roughness.

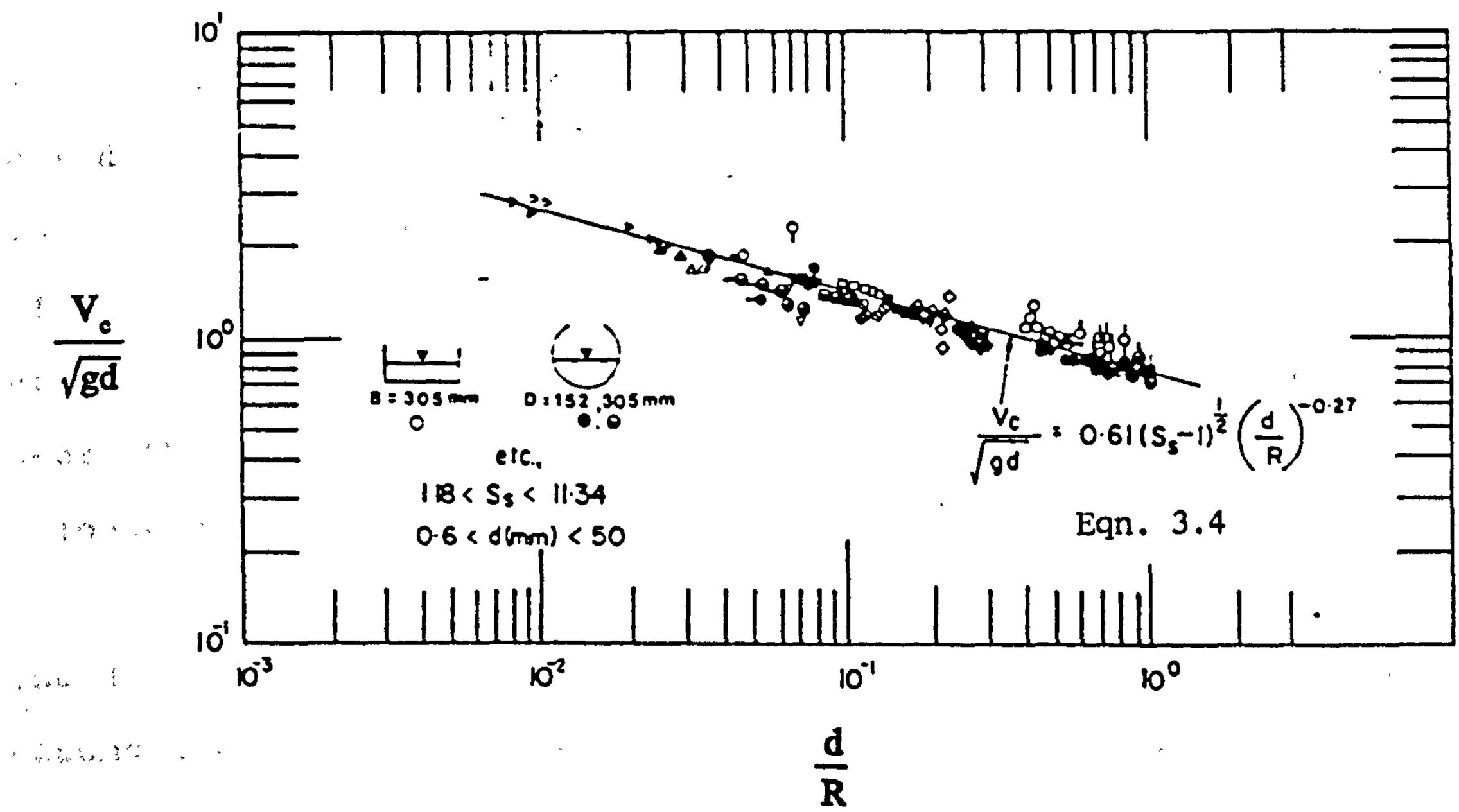

FIG. 3.2 Incipient motion criterion for rigid boundary channels - Eqn. 3.4 (After Novak-Nalluri 1975)

3.3 Sediment Transport

A review of experimental studies on sediment transport in pipes pertaining to the conditions in sewers over the last forty years is presented herein. All studies have been carried out in uniform flows using well graded sediments, a simplification of a complex process involving non-uniform flows and mixture of sediments in real sewers.

Investigations of sediment transport in pipe sewers can be divided into two categories. The aim of the first category is to obtain the maximum rate of sediment transport for the movement of sediments along clean inverts (i.e. rigid boundary) without deposition (limit of deposition studies). The second category seeks the equilibrium transport rates with sediments moving over a loose deposited bed.

The following sections assess each category of investigation accompanied by a review on relevant works in non-circular channels.

3.3.1 Transport at the "Limit of Deposition" Studies in Pipes

Durand (1953) carried out experiments in smooth pipes over a range of diameters (40mm to 700mm) flowing full. A number of uniformly graded sands ranging from 0.02mm to 100mm were used. Both modes of transport were observed with sand sizes between 0.2mm to 2.0mm in the transition region between suspended load

and bed load. The results at the limit of deposition were expressed in terms of a parameter resembling Froude number, hereafter defined as the modified Froude number, Fr_m:

$$Fr_m = \frac{V}{\sqrt{2\ g\ (S_s-1)\ D}} \qquad (3.6)$$

where V is the total transporting flow velocity and D is the pipe diameter. Subsequent works (Robinson-Graf 1972, May 1982, CIRIA 1987) confirmed the importance of Fr_m in transport studies in pipes. Durand (1953) plotted Fr_m against volumetric concentration, C_v, for different sediment diameters, d (Fig. 3.3). The plot shows that Fr_m varies with C_v and d for C_v up to approximately 10-15% and remains constant thereafter at a value of 0.9 for d larger than 0.5mm.

Craven studied deposition in a smooth pipe of 152mm dia. flowing full and used sand sizes of 0.25mm, 0.58mm, and 1.62mm which were transported as bed load. A transport function (see Fig. 3.4) was obtained which would give the sediment volumetric concentration for a given flow discharge, Q, and the proportional depth of sediment deposit, y_s/D. The sediment-free pipe condition is obtained by interpolation of the function for no sediment deposit ($y_s/D = 0.0$) given as:

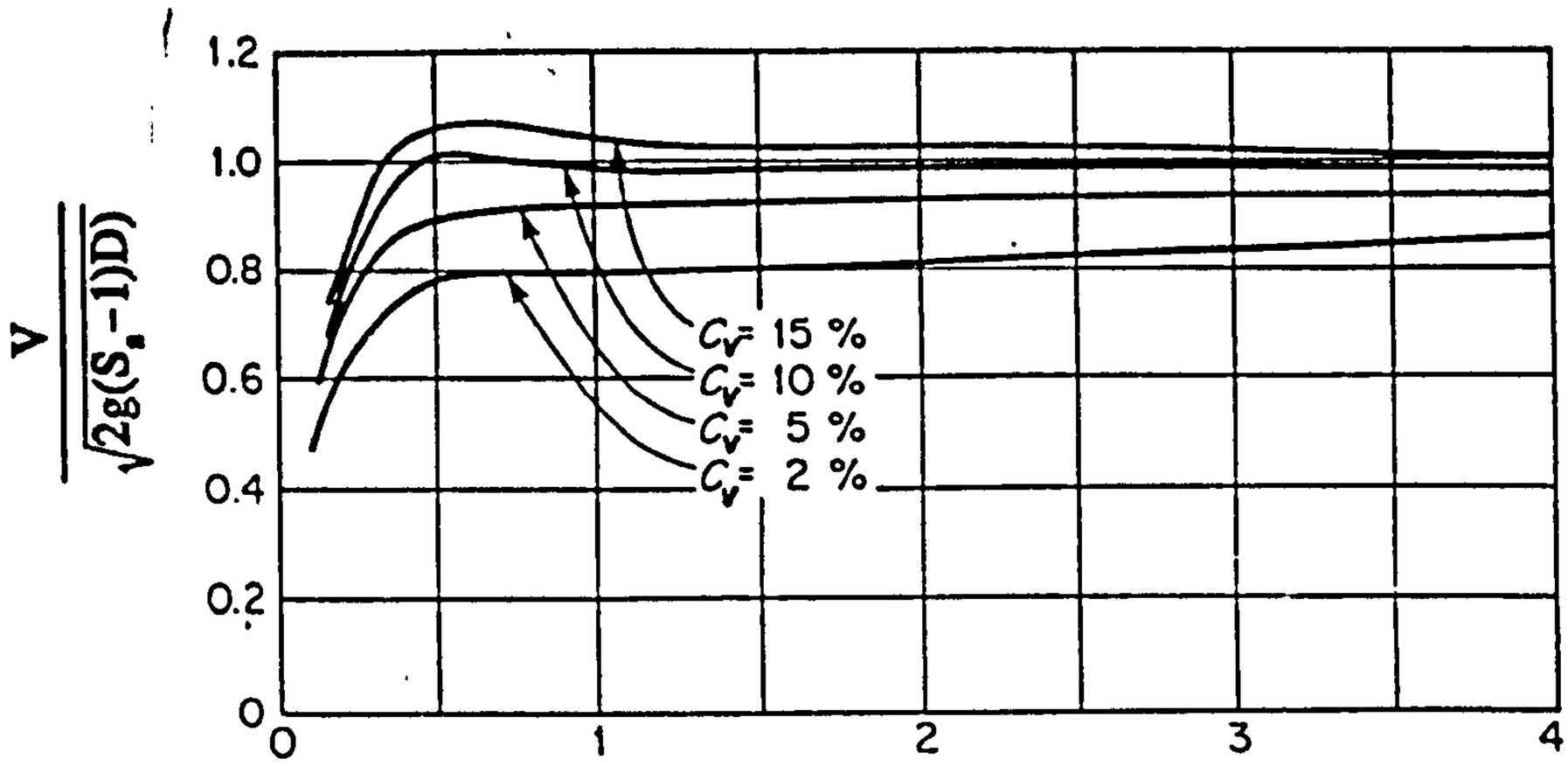

FIG. 3.3 Durand's (1953) criterion at limit of deposition for pipe-full flow (After Graf 1984)

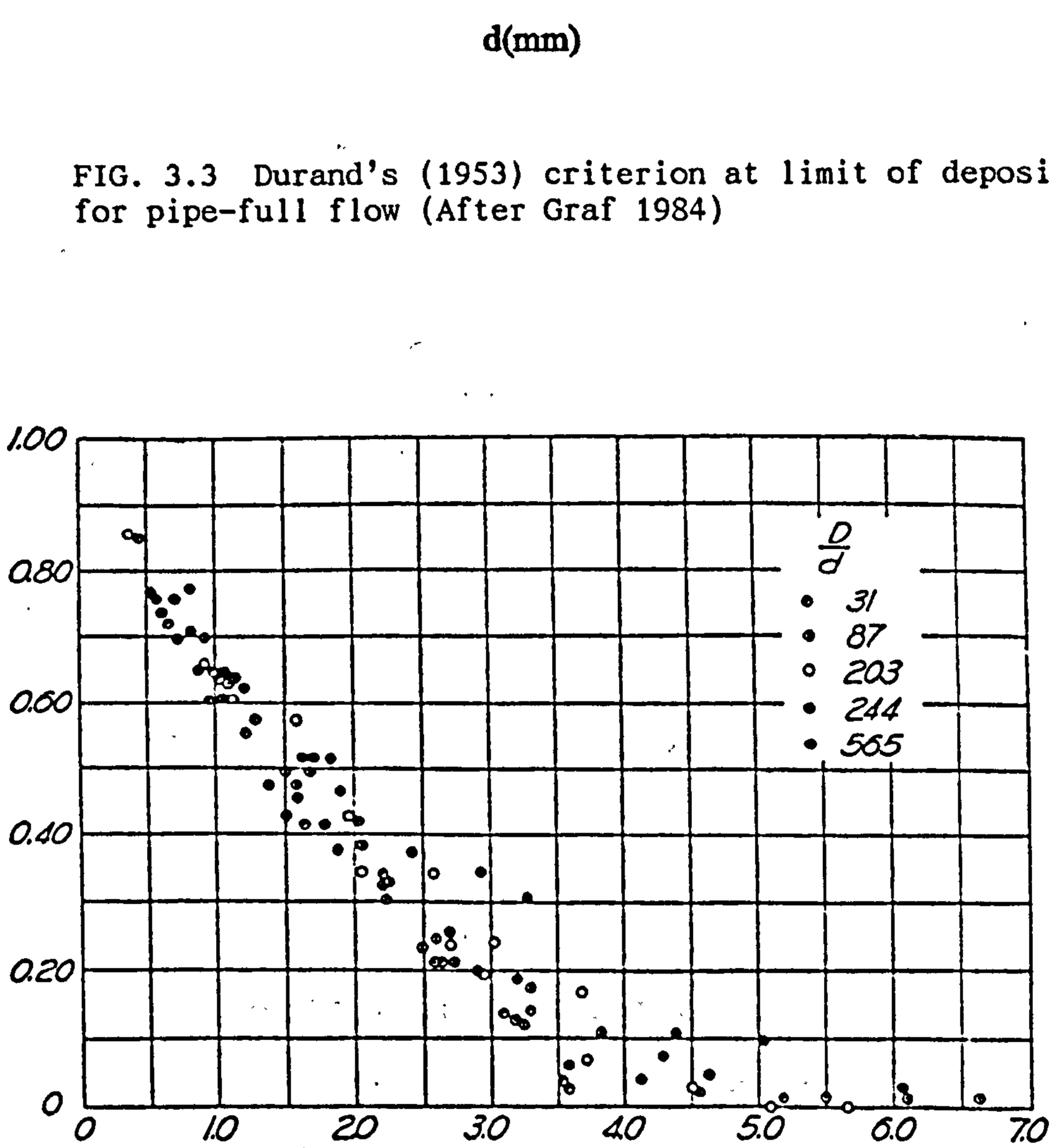

FIG. 3.4 Bed-load transport function for pipes with deposited beds: pipe-full flow (After Craven 1953)

$$\frac{Q}{D^{2.5}\sqrt{g(S_s-1)}}\,C_v^{-1/3} > 5.0 \qquad (3.7)$$

The function can be re-written as:

$$\frac{V}{\sqrt{g(S_s-1)\,D}}\,\frac{A}{D^2}\,C_v^{-1/3} > 5.0 \qquad (3.8)$$

where A is the net cross-sectional flow area above the sediment bed.

Ambrose (1953) extended Craven's (1953) studies and measured sediment concentrations at the limit of deposition for part-full flow conditions. His non-dimensional transport parameter, derived from dimensional analysis on the variables expected to affect bed load transport, correlated well with experimental data as a function of proportional flow depth, y_o/D (Fig. 3.5):

$$\frac{Q}{g^{2/5}\,D^2\,Q_s^{1/5}\,(S_s-1)^{2/5}} = f\left(\frac{y_o}{D}\right) \qquad (3.9)$$

for $10^2 < C_v$ (ppm) $< 6.0\times10^4$ where Q_s is the volumetric sediment discharge. Fig. 3.5 suggests that sediment deposition could be avoided for all part-full flow conditions when the transport parameter equals approximately 2.9. Replacing the right-hand side of Eqn. 3.9 with a constant of 2.9 and re-arranging the equation yields:

$$\frac{V}{\sqrt{g(S_s-1)D}} = 3.78\,C_v^{1/4}\,\frac{A}{D^2} \qquad (3.10)$$

where the dimensionless parameter, A/D^2, represents the shape effects due to variation in flow depths for part-full flow conditions. Here A is the full area of the flow over the clean invert since there is no sediment deposit.

Laursen (1956) re-analysed Ambrose's (1953) data using Craven's (1953) transport parameter (the left-hand side of Eqn. 3.7) and expressed it in terms of proportional flow depth, y_o/D as shown in Fig. 3.6. May (1982) obtained the following relationship for the curve shown in this figure (Fig. 3.6) as:

$$\frac{V}{\sqrt{2\,g\,(S_s-1)\,y_o}} = 7.0\,C_v^{1/3} \qquad (3.11)$$

where y_o is the flow depth.

Robinson-Graf (1972) performed experiments in two smooth pipes (102mm and 152mm dia.) flowing full at the limit of deposition. They used two sands (d_{50} = 0.45mm, 0.88mm) transported as suspended load for the range of velocity of 1.2m/s to 2.5m/s. Dimensional analysis was used to derive transport functions which were fitted to experimental data using multiple regression analyses for the best-fit line as:

$$\frac{V}{\sqrt{2\,g\,(S_s-1)\,D}} = 0.901\,C_v^{0.106}\,(1-S_o)^{-1.0} \qquad (3.12)$$

where S_o is the pipe slope. The range of volumetric sediment concentrations was 10^3ppm to 7.0×10^4ppm.

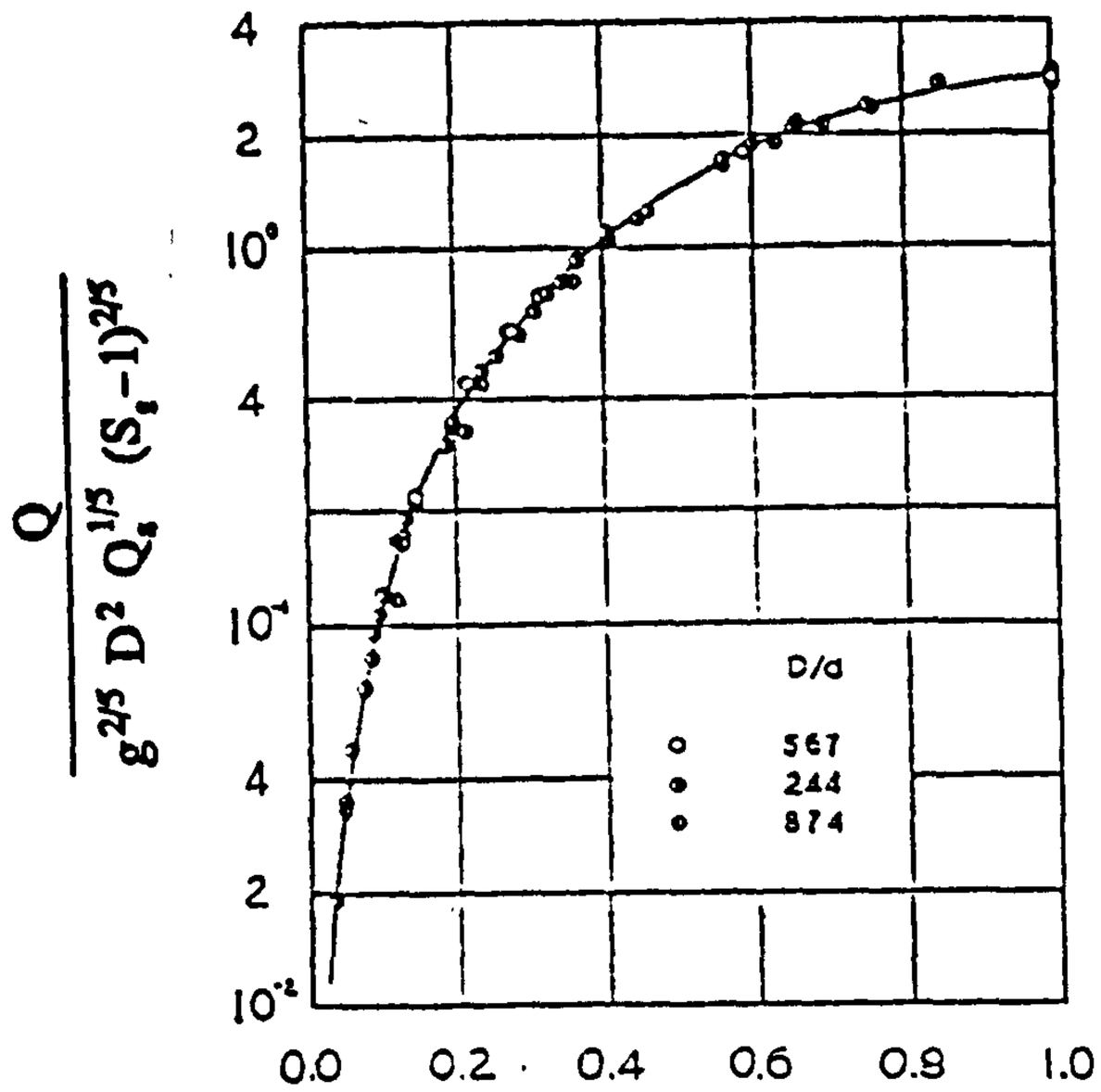

FIG. 3.5 Bed-load transport function for part-full flow in clean pipes (After Ambrose 1953)

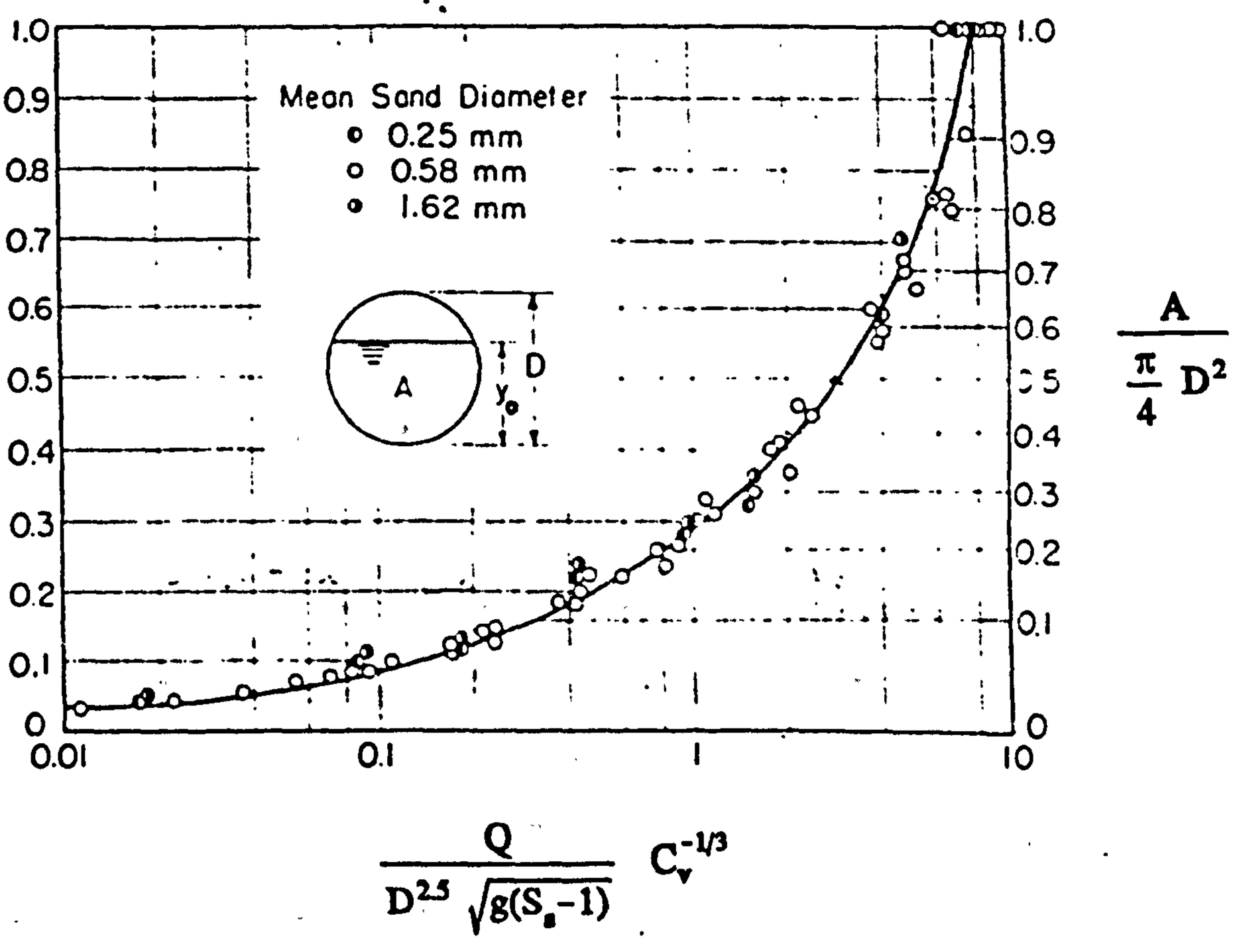

FIG. 3.6 Bed-load transport function for clean pipes at part-full flow (After Laursen 1956)

Novak-Nalluri (1975) carried out experiments at the limit of deposition in smooth pipes of 152mm and 305mm dia. flowing part-full and in a smooth 305mm wide rectangular channel. Uniformly graded sand of sizes between 0.15mm and 2.0mm were used and observed moving as bed load. Applying dimensional analysis and fitting the relevant non-dimensional parameters by eye, they obtained the following relationship applicable for circular channels only (see Fig. 3.7):

$$\frac{\tau_o^{5/4}\, g^{1/4}}{\gamma_s^{5/4}\, d^{1/2}\, \nu^{1/2}} = 0.017 + 0.69\times10^{-5}\left(\frac{G_s\, g^{1/3}}{\gamma_s \nu^{5/3}}\right) \qquad (3.13)$$

where τ_o is the mean shear stress, G_s is the bed load in N/s, γ_s is the specific weight of sediment, and ν is the kinematic viscosity of water. Novak-Nalluri (1975) also derived a relationship applicable for both circular and rectangular channels by utilising a transport parameter, Φ (= $C_v VR/(g(S_s - 1)d^3)^{1/2}$) and a flow parameter, ψ (= $(S_s - 1)d/(RS)$):

$$\phi = 11.6\, \psi^{-2.04} \qquad (3.14)$$

The range of volumetric sediment concentrations was between 20 ppm and 2400 ppm. The range of flow Reynolds numbers , Re (= $4VR/\nu$), was $5.7\text{-}14.0\times10^4$. Eqn. 3.14 can be re-arranged in terms of the modified Froude number by using Darcy-Weisbach's resistance equation ($S_o = \lambda_s V^2/8gR$) yielding:

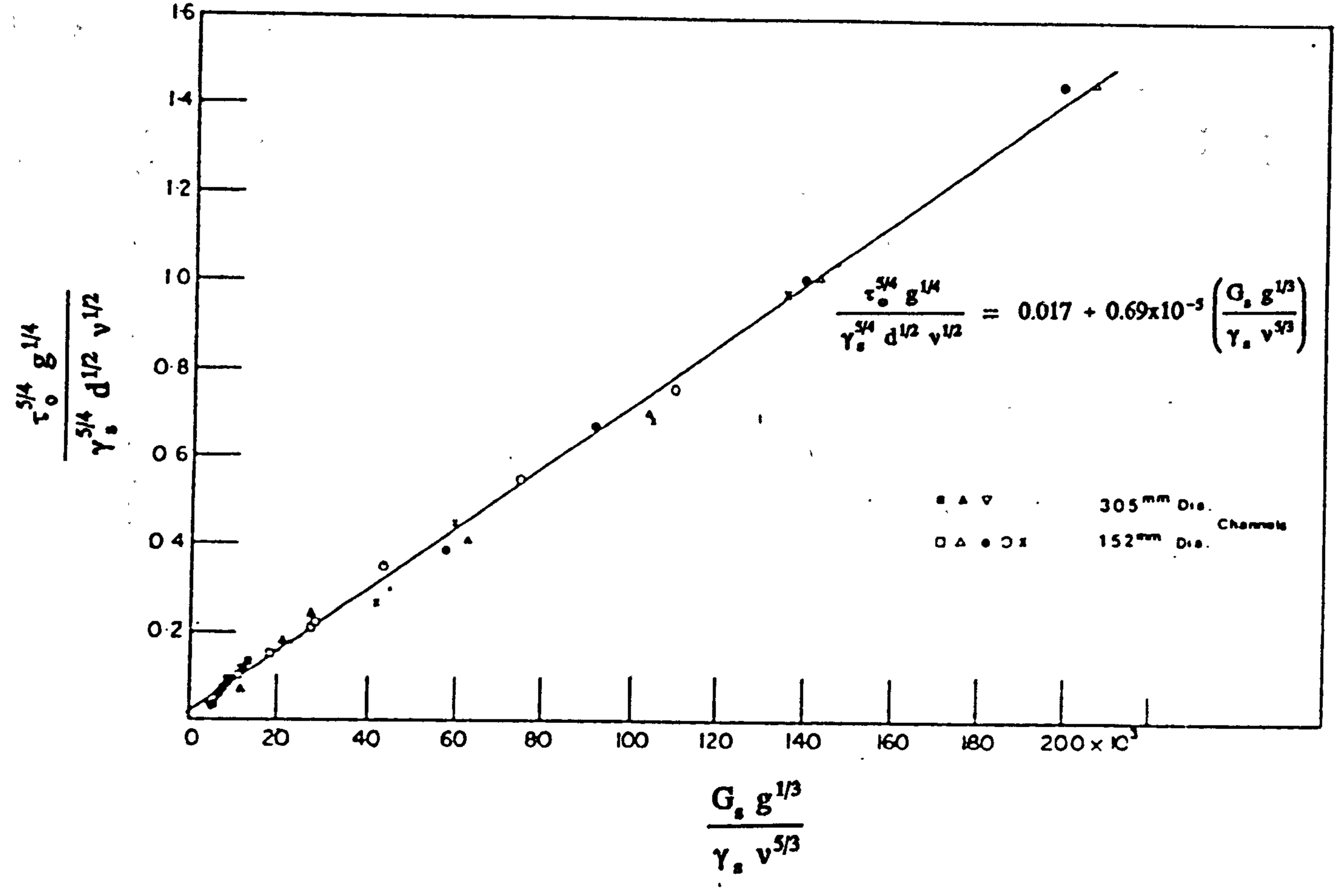

FIG. 3.7 Shear stress criterion for bed load transport in circular channels flowing part-full (After Novak-Nalluri 1975)

$$\frac{V}{\sqrt{g\,(S_s-1)\,d}} = 1.77\,C_v^{1/3}\left(\frac{d}{R}\right)^{-1/3}\lambda_s^{-2/3} \qquad (3.15)$$

Macke (1982) conducted experiments at the limit of deposition using three smooth pipes (192mm, 290mm, and 445mm dia.) flowing part full and used sands with sizes of (= d_{50}) 0.16mm and 0.37mm moving both as suspended and bed loads. He derived a theoretical model and fitted it to experimental data by linear regression analysis for the case of suspended load resulting in the following dimensional equation (see Region I in Fig. 3.8):

$$Q_s^* = Q_s(\rho_s - \rho)g\omega^{1.5} = 1.64 \times 10^{-4}\,\tau_o^3 \qquad (3.16)$$

where Q_s^* is the sediment transport rate in $N.m^{1.5}/s^{2.5}$, ω is the sediment fall velocity in m/s, and, ρ and ρ_s are the water and sediment densities in kg/m^3 respectively. The range of sediment transport rates, Q_s^*, studied was 10^{-6} to $4x10^{-3}$ $Nm^{1.5}/s^{2.5}$. However, Macke (1982) did not attempt to obtain a specific relationship for the case of bed load transport (see Region II in Fig. 3.8) due to the presence of individual curves as functions of sediment size in this region. By using experimental data from previous research (eg. Ambrose 1953, Robinson-Graf 1972) as shown in Fig. 3.8, Macke (1982) established the validity of Eqn. 3.16 for suspended load transport (Region I) and individual curves for bed load transport (Region II). May (1982) re-wrote Eqn. 3.16 as:

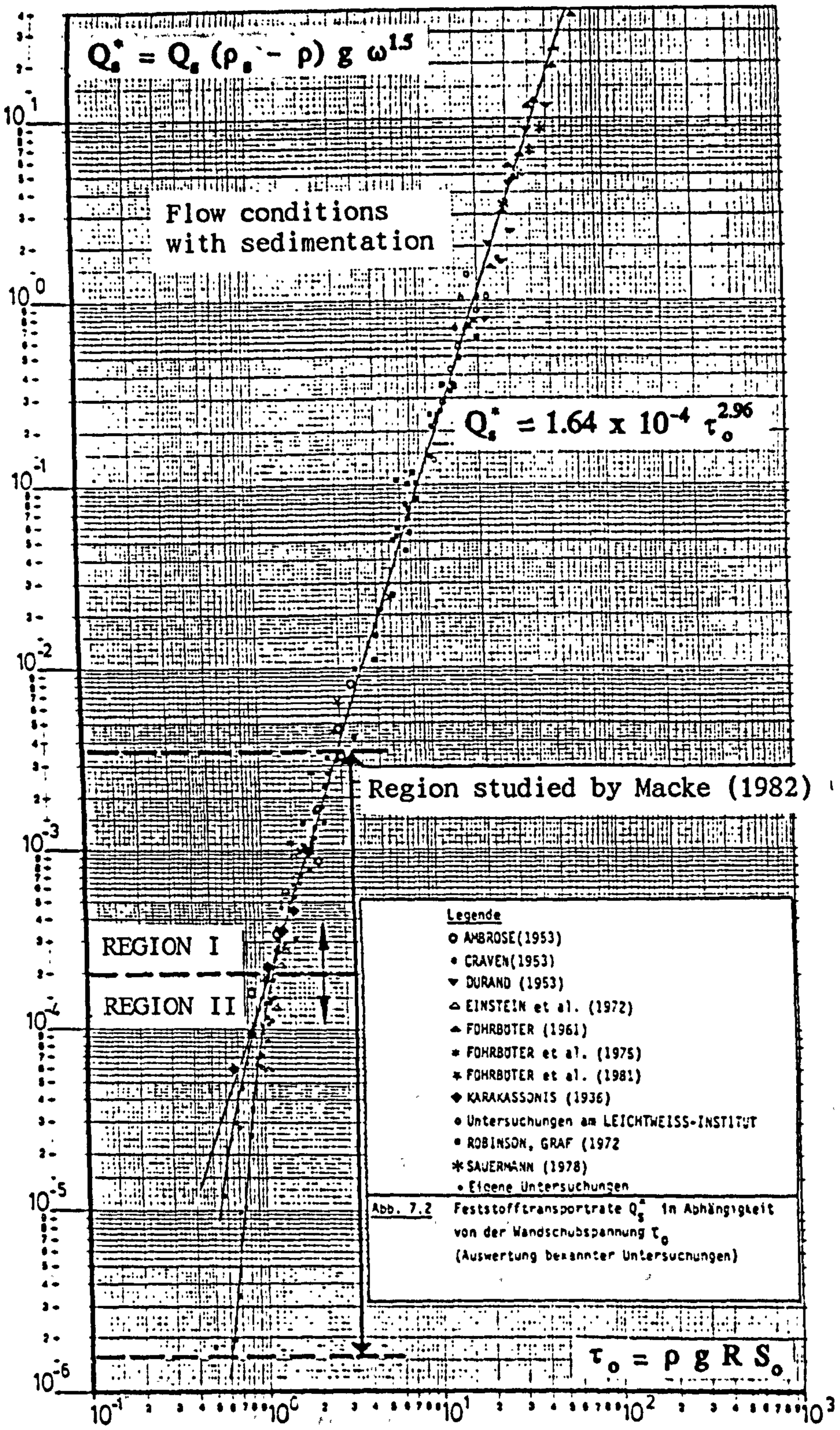

Abb. 7.2 Feststofftransportrate Q_s^* in Abhängigkeit von der Wandschubspannung τ_o (Auswertung bekannter Untersuchungen)

FIG. 3.8 Suspended load model at limit of deposition for part-full flow in pipes (After Macke 1982)

$$V = 1.98\ \lambda_s^{-0.6}\ \omega^{0.3}\ (\ (S_s-1)\ A\ C_v\ )^{0.2} \qquad (3.17)$$

Again, it should be noted that Eqn. 3.17 is dimensional and hence SI units should be used. May (1982) also suggests that the sediment fall velocity, ω in m/s, should be calculated from the following equation:

$$\omega = \frac{\left[9\nu^2 + 10^{-9}\ d^2\ g\ (S_s-1)\ (0.03869 + 0.0248d)\right]^{1/2} - 3\nu}{[0.11607 + 0.074405\ d]\ x\ 10^{-3}} \qquad (3.17a)$$

where ν is in m^2/s, g in m/s^2 and d in mm.

May (1982) studied the limit of deposition using 77mm and 158mm dia. smooth pipes flowing full and part-full. Sediment sizes ranged from 0.64mm to 7.9mm and transported as bed load. May (1982) developed a theoretical bed-load transport model which is based on forces acting on individual sediment particles transported at the limit of deposition. He simplified the theoretical model by utilising dimensional analysis and fitted it to experimental data resulting in the following equation:

$$C_v = 0.0205 \left(\frac{D^2}{A}\right) \left(\frac{d}{R}\right)^{0.6} \left(\frac{V^2}{g\ (S_s-1)\ D}\right)^{3/2} \left(1-\frac{V_c}{V}\right)^4 \qquad (3.18)$$

where V_c is the critical incipient motion velocity given by Novak-Nalluri's (1975) Eqn. 3.4. The experimental data covered the range of $4.7 < C_v$ (ppm) < 2100 for $0.45 < V(m/s) < 1.2$ and $S_s = 2.65$.

May et al (1989) extended the limit of deposition study to a larger pipe using a 300mm concrete pipe with 0.72mm sand transported as bed load. Experimental data in smaller pipes (May 1982) were re-analysed to include the effect of proportional flow depth (y_o/D) and to reduce the scatter in the data for part-full flows, yielding:

$$C_v = 0.0211 \left(\frac{y_o}{D}\right)^{0.36} \left(\frac{D^2}{A}\right) \left(\frac{d}{R}\right)^{0.6} \left(\frac{V^2}{g(s_s-1)D}\right)^{3/2} \left(1-\frac{V_c}{V}\right)^4 \quad (3.19)$$

Analyses on new data (300mm dia.) showed that Eqn. 3.19 produced a reasonable estimate of conditions at the limit of deposition provided the threshold velocity, V_c, could be determined correctly. The 300mm dia. results fall quite close to the best-fit line given by Eqn. 3.19 for V_c = 0.3m/s. The experiments in the 300mm pipe covered the range of $0.3 < C_v$ (ppm) < 443 for $0.5 < V$ (m/s)< 1.5, $S_s = 2.62$, and $3/8 < y_o/D < 1.0$.

May (1993) developed a new semi-empirical transport model at the limit of deposition based on the shear stress acting on the surface layer of sediments . He derived a transport parameter, Ω, and a mobility parameter, G_s as:

$$\Omega = C_v \left(\frac{A}{D^2}\right)\left(\frac{y_o}{D}\right)^{-0.6}\left(\frac{\lambda_g V^2}{8gf\,(S_s-1)\,D}\right)^{-3/2} \qquad (3.20)$$

$$G_s = \left(\frac{y_o}{D}\right)^{0.2}\left(\frac{\lambda_g V^2}{8gf\,(S_s-1)\,d_{50}}\right)^{1/2} \qquad (3.21)$$

where f is a constant representing the surface texture or roughness of the pipe wall (= 1.0 for smooth pipes; = 1.2 for rough pipes) and λ_g is the friction factor due to grain resistance computed from the Colebrook-White equation by assuming the grain roughness, k_g, equals 2.3 d_{50}. Utilising the bed load transport data from earlier work (May et al, 1989), May (1993) determined the values of Ω as a function of G_s (see Table 3.2). May (1993) also suggests that the relationship between Ω and G_s may be extrapolated beyond the limit of $G_s = 0.9$ to be applicable for suspended load transport.

TABLE 3.2 VALUES OF MAY'S TRANSPORT PARAMETER, Ω (EQN. 3.20) FOR SEDIMENT TRANSPORT IN CLEAN PIPES

RANGE OF G_s	Ω
$G_s \leq 0.15$	0.0
$0.15 < G_s \leq 0.55$	$8.25\ G_s - 1.24$
$0.55 < G_s \leq 0.9$	$1.78\ G_s + 2.32$

Arora et al (1984) carried out experiments to determine the limit of deposition in a smooth semi-circular channel of diameter 400mm, a smooth trapezoidal channel of bottom width of 200mm and side slopes 1:1, and a 400mm wide rectangular channel. The rectangular channel was tested with both smooth and artificially roughened beds. The sediments were made up of three uniform sands (0.082mm, 0.106mm, 0.147mm) with specific gravity of 2.65 and coal (0.164mm) with specific gravity of 2.04. All sediments were observed to move as suspended load. Utilising dimensional analysis and eye-fitting, the resulting functional relationship was given as (Fig. 3.9):

$$C_v = f\left(\frac{q\, S_c^{2.5}}{\nu\, \lambda_s^2}\right)\left(\frac{\omega d}{\nu}\right)^{-0.6}\left(\frac{D_h}{y_o}\right)^2 \qquad (3.22)$$

where f is a function, q is the flow unit discharge (= $Q/\mathcal{B}$, Q and $\mathcal{B}$ being flow discharge and water surface width respectively), S_c is the slope parameter (= $S_o/(S_s - 1)$), and D_h is the hydraulic depth (= $A/\mathcal{B}$). Eqn. 3.22 was intended to be applicable for channels of different shapes and boundary roughnesses. The range of volumetric sediment concentrations was 35ppm to 6562ppm for $7x10^4 < Re < 3x10^5$ and $0.55 < Fr < 1.30$ where Fr is the Froude number (= $(V^2\mathcal{B}/gA)^{0.5}$). Nalluri (1985) re-analysed Arora's data (Arora et al, 1984) in terms of transport parameter (Φ) and flow intensity parameter (ψ) yielding:

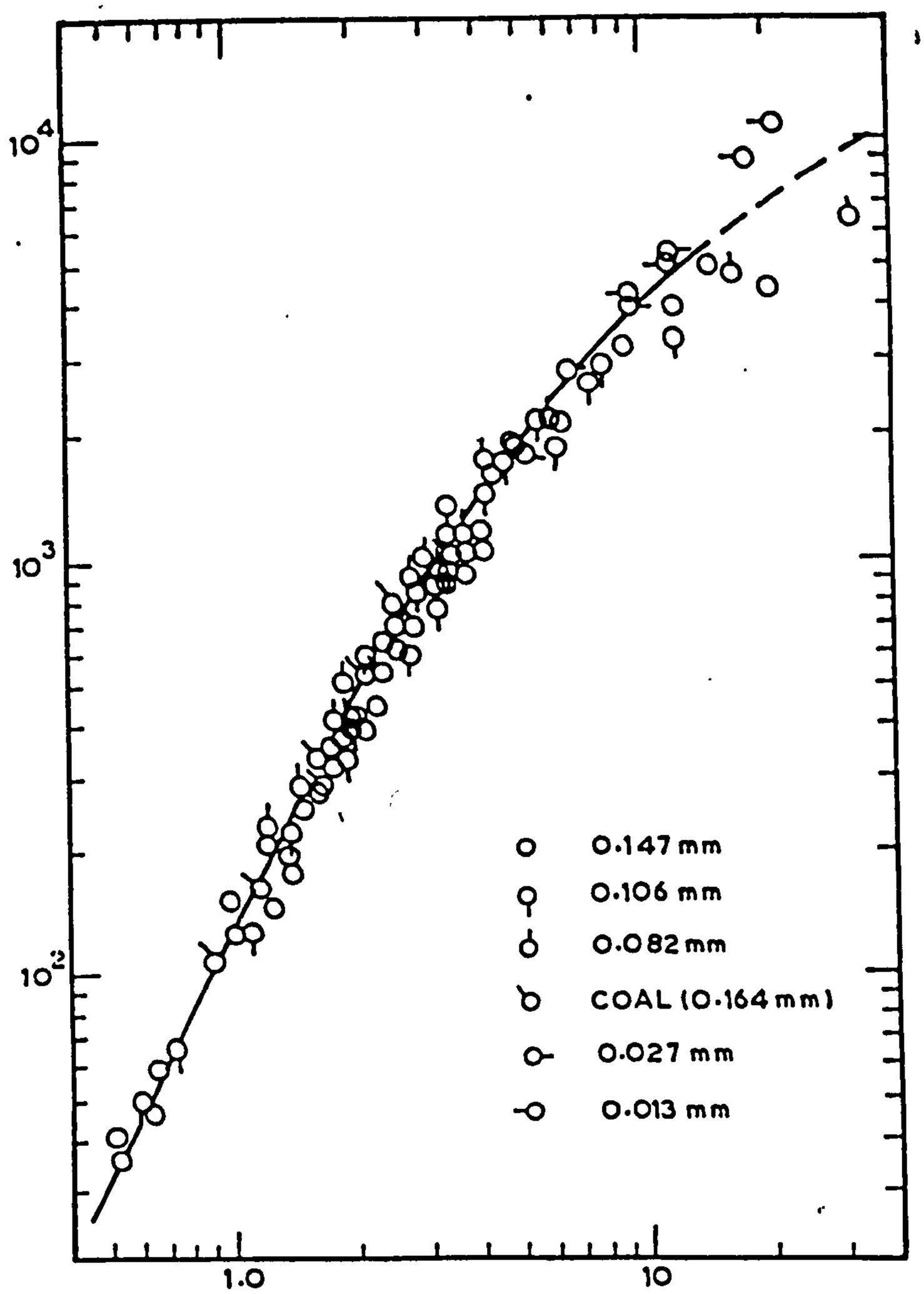

FIG. 3.9 Functional relationship for suspended load transport in rigid boundary channels (After Arora et al 1984)

$$\phi = 100\,\psi^{-4.5} \qquad (3.23)$$

Equation 3.23 can be re-arranged as:

$$\frac{V}{\sqrt{g(S_s-1)d}} = 1.811\,C_v^{0.125}\left(\frac{d}{R}\right)^{-0.125}\lambda_s^{-0.5625} \qquad (3.24)$$

Ackers (1984) modified Ackers-White's (1973) total-load transport model for wide alluvial channels to suit sewer conditions. The original model (Ackers-White 1973) was based on an excess mobility approach (see Fig. 3.10) derived from both physical considerations and dimensional analysis. Two major changes from the original formulation were 1) the use of a fully rough turbulent flow equation for non-rectangular channels, 2) the introduction of an effective width, W_e, to represent the limited availability of sediment for transport at the inverts. The resulting transport equation applicable for all channel shapes was given as:

$$G_{gr} = C\left(\frac{F_{gr}}{A_{gr}} - 1\right)^m \qquad (3.25)$$

with the transport parameter, G_{gr} and the mobility parameter, F_{gr} defined as:

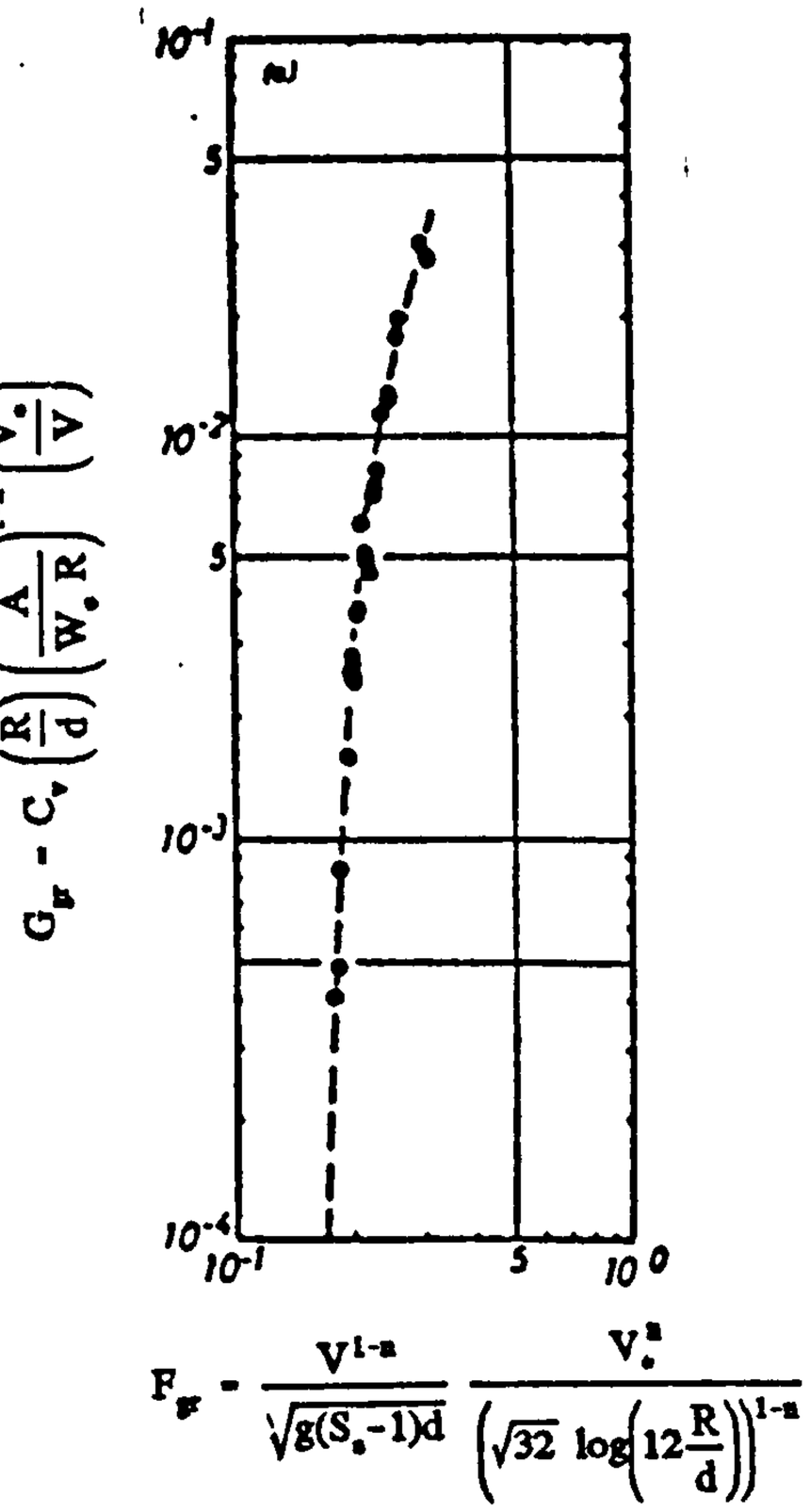

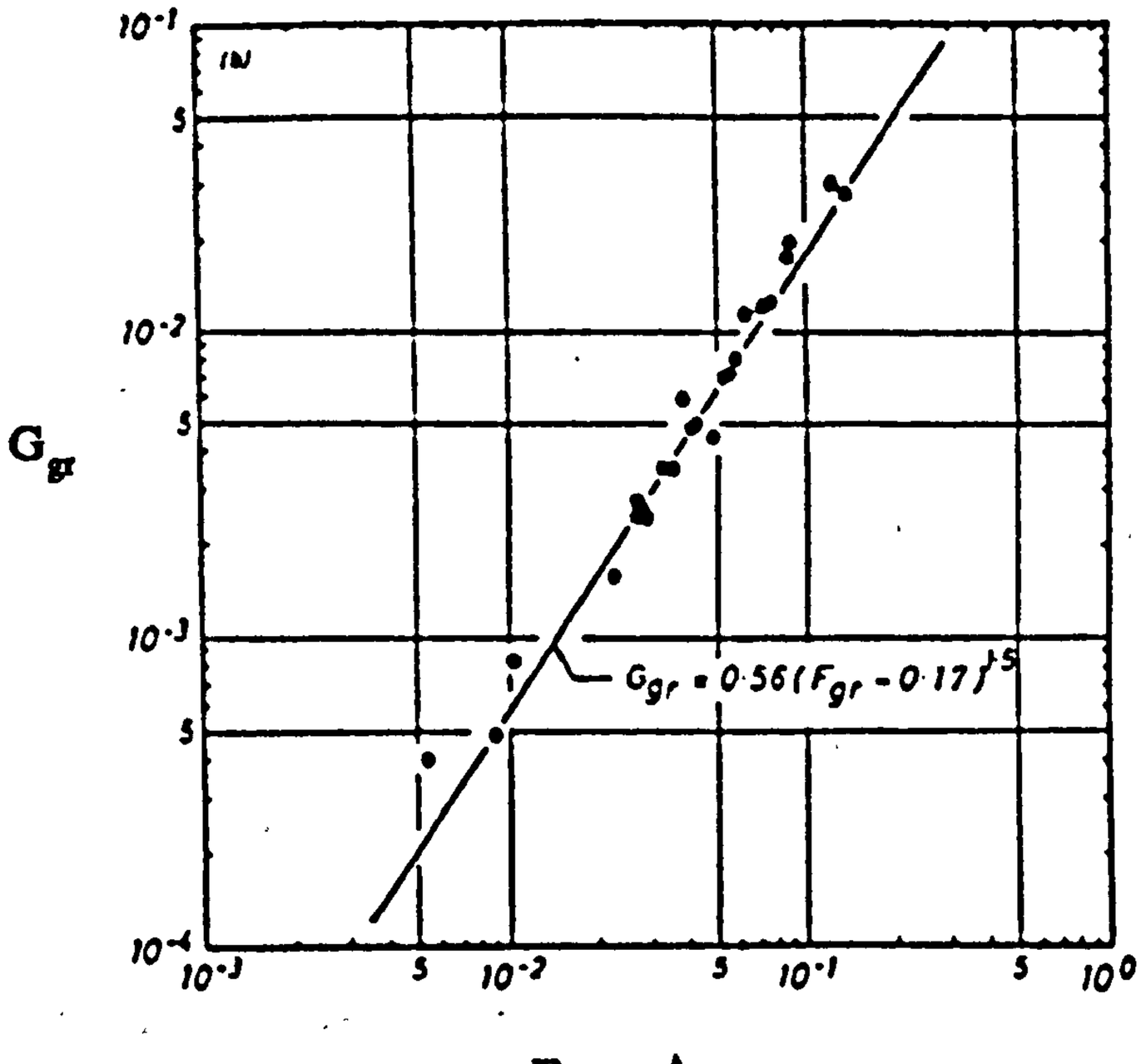

FIG. 3.10 Excess mobility model for total load transport in wide alluvial channels (After Ackers-White 1973)

$$G_{gr} = C_v \left(\frac{R}{d}\right) \left(\frac{A}{W_o R}\right)^{1-n} \left(\frac{V_*}{V}\right)^n \qquad (3.26)$$

$$F_{gr} = \frac{V^{1-n}}{\sqrt{g(S_s-1)d}} \frac{V_*^n}{\left(\sqrt{32}\ \log(12\frac{R}{d})\right)^{1-n}} \qquad (3.27)$$

where A_{gr} (= value of F_{gr} at initial motion condition), C, m and n are constants depending on values of non-dimensional grain diameter, D_{gr}. Values of these constants in relation to D_{gr} were obtained from statistical analyses of experimental data in rectangular channels (Ackers-White 1973) covering the range of 0.04mm < d < 4.94mm, 1.07 < S_s < 2.70, and Fr < 0.8. Ackers (1991) re-computed values of Agr, C, m and n (see Table 3.3) using data from more recent work to include a wider range of sediment sizes than those in their (Ackers-white 1973) original work. The present (Ackers 1991) range of sediment sizes is 0.04mm to 28.65mm. The application of Eqn. 3.25 requires a knowledge of the effective transport width, W_e. Based on the work by May (1982), Ackers (1984, 1991) proposed W_e = 10d for sediment transport in pipes at the limit of deposition.

Ackers (1991) re-arranged Eqns. 3.25, 3.26, and 3.27 in terms of the modified Froude number by replacing the log term in Eqn. 3.27 with an equivalent power law expression:

$$\log\left(12\frac{R}{d}\right) \simeq 2\left(\frac{R}{d}\right)^{0.1} \qquad (3.28)$$

This approximation is valid for the range of relative roughness of $150 < (R/d) < 30000$. Ackers equation is now re-written as:

$$\frac{V}{\sqrt{g(S_s-1)d}} = K\left(1 + J\,C_v^{1/m}\right) \qquad (3.29)$$

with K representing the incipient motion condition which is given by:

$$K = \frac{A_{gr}\left(11.3\,(\frac{R}{d})^{0.1}\right)^{1-n}}{(\lambda_s/8)^{n/2}} \qquad (3.30)$$

and J relating to sediment transport which is defined as:

$$J = \left(\frac{(\frac{R}{d})\,(\frac{A}{W_eR})^{1-n}\,(\frac{\lambda_s}{8})^{n/2}}{C}\right)^{1/m} \qquad (3.31)$$

TABLE 3.3 VALUES OF COEFFICIENTS FOR ACKERS' EQN. 3.29

COARSE SEDIMENT $D_{gr} > 60$ ($d \simeq 2.0$mm)	TRANSITIONAL AND FINE SEDIMENTS $1 < D_{gr} \leq 60$ ($d \simeq 0.02 - 2.00$mm)
$n = 0.0$	$n = 1.00 - 0.56 \log D_{gr}$
$A_{gr} = 0.17$	$A_{gr} = 0.14 + 0.23/\sqrt{D_{gr}}$
$m = 1.78$	$m = 1.67 + 6.83/D_{gr}$
$C = 0.025$	$\log C = -3.46 + 2.79\log D_{gr} - 0.98(\log D_{gr})^2$

Mat Suki (1987) conducted experiments at the limit of deposition in smooth pipes (164mm and 253mm dia.) and rough pipes (155mm, 159mm, 162mm and 249mm dia.) flowing full. The experiments were carried out using a range of sediment size (d_{50} = 1.30mm - 8.00mm) with the specific gravity on the average of 2.65. For rough pipe conditions, the pipes were artificially roughened around the whole perimeter creating uniform roughnesses using sands of diameter 0.83mm (D = 162mm and 249mm), 1.3mm (D = 159mm) and 2.7mm (D = 155mm). The resulting equivalent sand roughnesses, k_o, from the Colebrook-White equation were 1.61mm (D = 249mm), 3.32mm (D = 162mm), 4.73mm (D = 159mm) and 8.84mm (D = 155mm). Mat Suki atttributed these high values of k_o to the effects of joint misalignments. A theoretical bed-load transport model at the limit of deposition, based on forces acting on a single particle, applicable for smooth and rough pipes was derived. Using multiple linear regression analysis to fit the model to experimental data yielded:

$$\frac{V}{\sqrt{g(S_s-1)d}} = 2.86\left(\frac{k_o}{d+k_o}\right)^{0.22}\left(\frac{\log\left(43.13\left(1+\frac{d}{k_o}\right)\right)}{\log\left(4.80\frac{D}{k_o}\right)} - \frac{2.01D(d+k_o)C_v}{dk_o}\right)^{1.0} \quad (3.32)$$

for smooth pipes and,

$$\frac{V}{\sqrt{g(S_s-1)d}} = 3.73\left(\frac{k_o}{d+k_o}\right)^{0.30}\left(\frac{\log\left(43.13(1+\frac{d}{k_o})\right)}{\log\left(4.80\frac{D}{k_o}\right)} - \frac{6.28D(d+k_o)C_v}{dk_o}\right)^{-1.0} \quad (3.33)$$

for rough pipes. Mat Suki suggested that for the application of the smooth pipe equation (Eqn. 3.32), the equivalent sand roughness, k_o, is taken as 0.3mm instead of 0.0mm. Using an equivalent sand roughness of 0.0mm in Eqn. 3.32 will lead to an indeterminate value of velocity. The range of volumetric sediment concentrations was 19.5ppm to 1020ppm for $0.50 < V\ (m/s) < 1.11$.

Mat Suki - Nik Hassan (1990) examined the validity of Ackers' Eqn. 3.25 for sediment transport at the limit of deposition using different values of effective transport width, W_e. Utilising Mat Suki's (1987) experimental data, they compared the predicted sediment concentrations computed using Ackers' Eqn. 3.25 against the measured values. A fairly good agreement was obtained with $W_e = 10d$. They also suggested that W_e might be a function of the sediment characteristics (size and shape) and channel shape.

Mayerle (1988) studied the limit of deposition at part-full flow conditions in a smooth pipe (152mm dia.) and two rectangular channels (311.5mm and 462.3mm wide). The rectangular channels were tested for both smooth and rough bed (k_o =0.64 - 0.73mm) conditions. The sediments used ranged from 0.50mm to 8.74mm with

an average specific gravity of 2.55. Transport functions derived from dimensional analysis were fitted to the experimental data by the use of multiple regression analysis. For the smooth pipe, the best-fit line was given by:

$$\frac{V}{\sqrt{g(S_s-1)d}} = 1.06\, C_v^{0.20} D_{gr}^{-0.41} \left(\frac{d}{R}\right)^{-0.20} \lambda_s^{-1.05} \qquad (3.34)$$

Mayerle (1988) extrapolated the 152mm dia. smooth pipe data with the aid of rough rectangular bed results to give an equation applicable for both smooth and rough pipes. The resulting equation was given as:

$$\frac{V}{\sqrt{g(S_s-1)d}} = 14.43\, C_v^{0.18} D_{gr}^{-0.14} \left(\frac{d}{R}\right)^{-0.56} \lambda_s^{0.18} \qquad (3.35)$$

Mayerle (1988) also proposed an equation to compute the friction factor with sediment, λ_s:

$$\frac{k_s - k_o}{R} = 0.013\, C_v^{0.24} D_{gr}^{0.24} \qquad (3.36)$$

where k_s is the equivalent sand roughness with sediment, computed from the Colebrook-White equation.

Paul-Sakhuja (1990) proposed a bed load function (see Fig. 3.11) at the limit of deposition applicable for any channel shape based on the relationships given by Novak-Nalluri (1975) and Arora et al (1984):

$$C_v = f\left(\left(\frac{q}{v}\right)\left(\frac{S_c^{2.5}}{\lambda_s}\right)\left(\frac{D_h}{y_o}\right)^2\left(\frac{y_o}{d}\right)^{-2.43}\right) \qquad (3.37)$$

The function was tested against data of May (1982), Novak-Nalluri (1975), and Loveless (1986) as shown in Fig. 3.11. Paul-Sakhuja (1990) concluded that the good agreement obtained was due to the use of the dimensionless parameter, D_h/y_o, to represent the shape effects. The best-fit line shown in Fig. 3.11 could be approximated by a power law regression yielding:

$$C_v = 0.50\left(\frac{q}{v}\right)^{0.64} S_c^{1.60}\left(\frac{D_h}{y_o}\right)^{1.28}\left(\frac{y_o}{d}\right)^{-1.56}\lambda_s^{-0.64} \qquad (3.38)$$

Loveless (1991) conducted experiments at the limit of deposition in channels of various shapes (see Fig. 3.12): 1) smooth circular (D=88mm), 2) smooth oval (with a semi-circular invert of 52mm dia.), 3) smooth rectangular (100mm and 59mm wide) and 4) rough U-shaped (with a semi-circular invert of 220mm dia. where k_o = 0.30mm). Two sediment sizes (= d_{50}) 0.45mm and 1.3mm were used in both the smooth and rough channels. A coarser sediment (d_{50} = 6.0mm) was also used for the rough channel. All sediments were observed to move as bed load. Loveless (1986, 1991) presented a theoretical model for bed load transport at the limit of deposition, based on the forces acting on a single particle. He partly followed the treatment of May (1982) and attempted to clarify the importance of the effective transport width, W_e, at

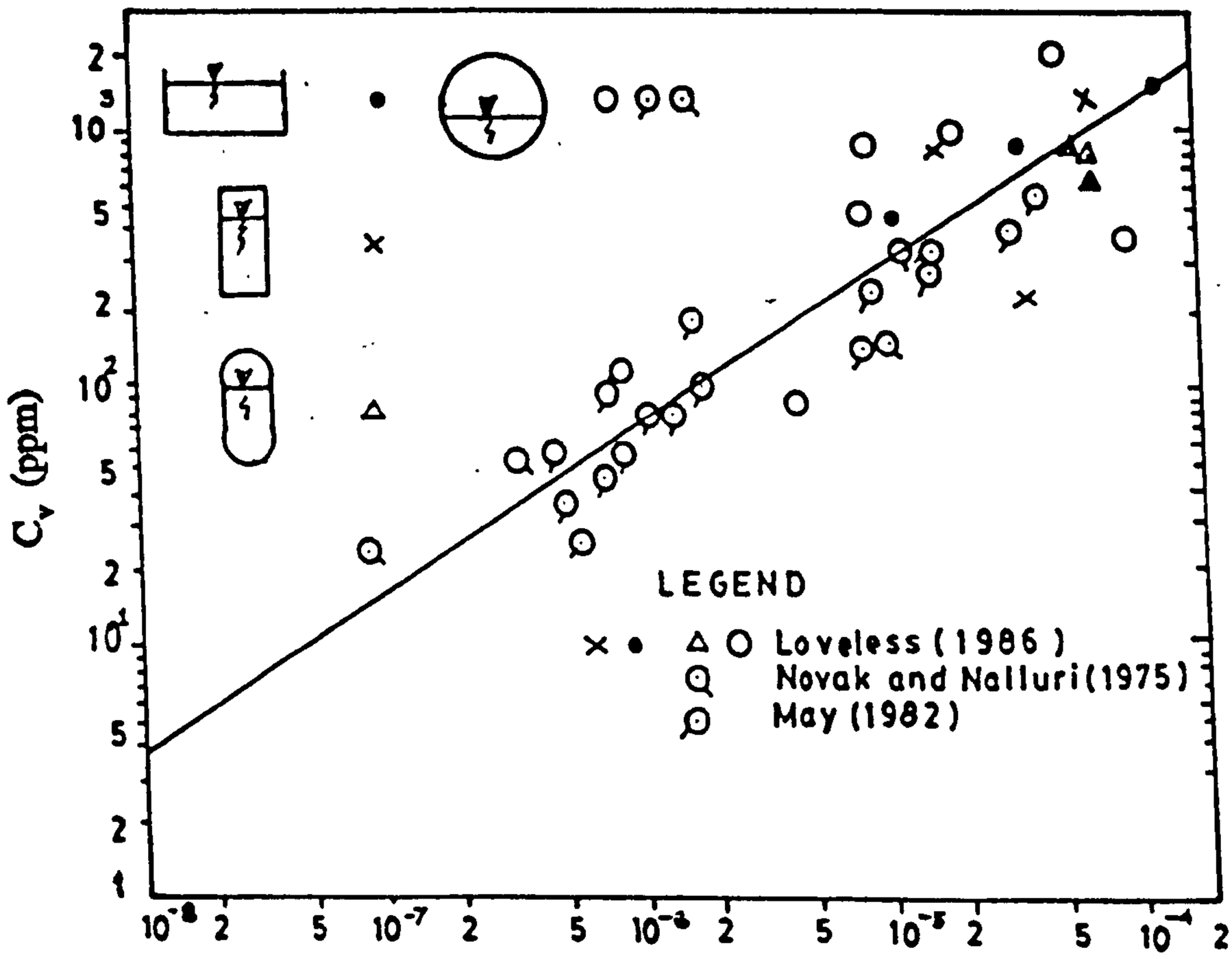

FIG. 3.11 Bed-load functional relationship for rigid boundary channels (After Paul-Sakhuja 1990)

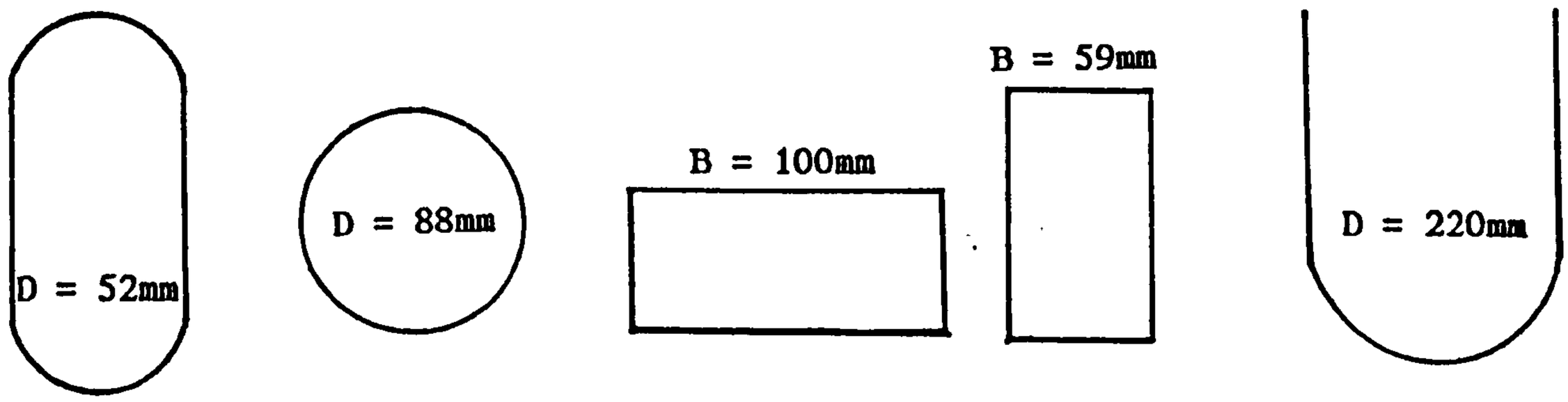

a) Oval b) Circular c) Rectangular d) U-shape

FIG. 3.12 Loveless' (1991) experimental channels

the limit of deposition as raised by Ackers (1984). The general bed load transport equation was given as:

$$\frac{(\beta V-u)^2}{g(S_s-1)} = 2\frac{\alpha_1}{\alpha_2}\frac{\tan\varphi}{(C_D+C_L\tan\varphi)} \qquad (3.39)$$

where u is the particle velocity, α_1 and α_2 are the conduit shape coefficients, φ is the friction angle between the channel and sediment particle, β is the velocity distribution coefficient, and C_D and C_L are the coefficients of drag and lift respectively. Loveless (1991) defined the particle velocity, u as:

$$u = \frac{\left(\frac{\alpha_1}{\alpha_2}\right) C_v V A}{\lambda_p W_e d} \qquad (3.40)$$

where λ_p is the particle spacing parameter. Assuming $\alpha_1/\alpha_2 = 1$ (Loveless 1986), and substituting Eqn. 3.40 into Eqn. 3.39 yields:

$$\frac{V}{\sqrt{g(S_s-1)d}} = \left(\frac{2\tan\varphi}{C_D+C_L\tan\varphi}\right)^{1/2}\left(\beta-\frac{C_v A}{\lambda_p W_e d}\right)^{-1} \qquad (3.41)$$

The evaluation of Eqn. 3.41 will depend on the chosen values of W_e, λ_p, , C_L, and φ (see Table 3.4). Loveless (1991) suggested the following equations to calculate β (see May 1982) and C_D:

$$\beta = 1 + 2.033 \sqrt{\lambda_s} \log(2.18 \frac{y_o}{R}) \qquad (3.42)$$

$$C_D = \left(\frac{100}{R_d} + A_d \right) (1 - \lambda_p^n) \qquad (3.43)$$

where A_d is the roughness coefficient (= 1.0 for smooth channels and 0.8 for rough channels), n is a constant varying between 0.3 and 1.0, and Re_d is the particle Reynolds number (= $\beta V d/\nu$).

TABLE 3.4 SUGGESTED VALUES FOR APPLICATION OF LOVELESS' EQN. 3.41 IN CIRCULAR CHANNELS

PARAMETER	RANGES
W_e (m)	0.11D - 0.20D
λ_p	0.27 - 0.65
C_L	0.20
ϕ	27° - 36°

3.3.2 Transport Over Deposited Bed Studies in Pipes

Craven (1953) expressed his transport parameter for pipe-full flow conditions in terms of proportional sediment depth, y_s/D, as shown in Fig. 3.4:

$$\frac{Q}{D^{2.5}\sqrt{g(S_s-1)}}\,C_v^{-1/3} = \frac{V}{\sqrt{g(S_s-1)D}}\left(\frac{A}{D^2}\right)C_v^{-1/3} - f\left(\frac{y_s}{D}\right) \qquad (3.44)$$

For a given flow rate and sediment concentration in a pipe, Eqn. 3.44 will give an indication of the level of the mean depth of sediment, y_s.

Ambrose (1953) continued his work for part-full flows beyond the limit of deposition (Case III in Fig. 3.13). He also carried out a limited number of tests as Craven (1953) for pipe-full flows (Case II in Fig. 3.13). Ambrose (1953) concluded that a similar transport function (Eqn. 3.9) was possible for both rigid and loose boundaries. He noted that (see Fig. 3.13) as the value of y_s/D approaches zero, the shape of the curves of the constants y_s/D approaches that of the case for the limit of deposition curve. For the same depth of flow, it appears that the values of the transport parameter are higher for loose boundaries than those for rigid boundaries. This implies that for pipes with small depth of deposits, the transport rate is higher than that of clean pipes.

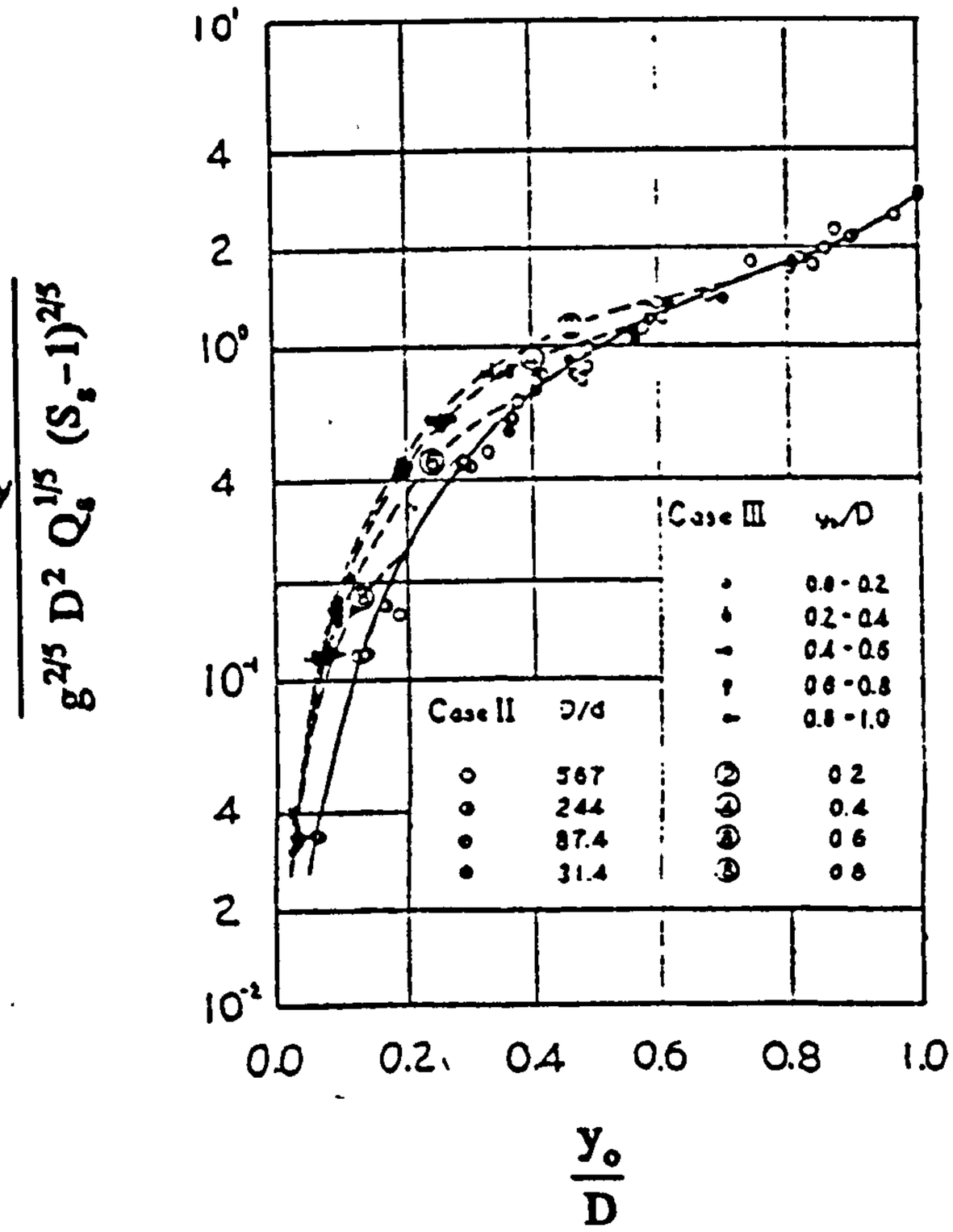

FIG. 3.13 Effect of sediment deposits on flow transporting capacity (After Ambrose 1953)

May et al (1989) conducted experiments with small depths of deposits in a 300mm pipe using 0.72mm sand (S_s= 2.62) transported as bed load. The results show an increase in the transporting capacity with the presence of a limited depth of deposition. With the mean proportional sediment depth, y_s/D, = 1%, they found that the sediment transporting capacity of the flow increased by a factor of two relative to the sediment-free condition without significantly increased head loss. May et al (1989) hence proposed that for y_s/D=1%, a factor of two should be applied to Eqn. 3.19 to give:

$$C_v = 0.04 \left(\frac{y_o}{D}\right)^{0.36} \left(\frac{D^2}{A}\right) \left(\frac{d}{R}\right)^{0.6} \left(\frac{V^2}{\sqrt{g(S_s-1)d}}\right)^{3/2} \left(1 - \frac{V}{V_c}\right)^4 \qquad (3.45)$$

The experimental range was $6 < C_v$ (ppm) < 1165 for $0.5 <$ V(m/s) < 1.5, $0.0008 < y_s/D < 0.1623$, and $0.5 < Y/D < 1.0$ where Y ($= y_o + y_s$) is the overall depth measured from pipe invert.

May (1993) extended his earlier work (May et al, 1989) to include significant depths of deposits in a 450mm concrete pipe. Two uniform sands (d_{50} = 0.47mm and 0.73mm) and two sand mixtures (d_{50} = 0.61mm and 0.58mm) with an average specific gravity of 2.64 were used and observed moving as bed load. May derived a semi-empirical transport relationship based on the shear stress acting on the sediment bed and the active layer concept within which the sediment transport occurs. A transport parameter, η, and a mobility parameter, F_s, were defined as:

$$\eta = C_v \left(\frac{D}{W_b}\right) \left(\frac{A}{D^2}\right) \left(\frac{\theta \lambda_s V^2}{8g(S_s-1)D}\right)^{-1} \qquad (3.46)$$

$$F_s = \left(\frac{\theta \lambda_s V^2}{8g(S_s-1)d_{50}}\right)^{1/2} \qquad (3.47)$$

where W_b is the sediment bed width, θ is the related transition factor given as:

$$\theta = \frac{\exp(R_{*c} / 12.5) - 1}{\exp(R_{*c} / 12.5) + 1} \qquad (3.48)$$

and R_{*c} is the particle Reynolds number given by:

$$R_{*c} = \sqrt{\frac{\lambda_s}{8}} \left(\frac{V d_{50}}{\nu} \right) \qquad (3.49)$$

Values of η were defined as a function of F_s (see Table 3.5) and obtained from the analyses of experimental data in the 450mm dia. pipe (May 1993). The range of volumetric sediment concentrations was 3.9ppm to 1290ppm for 0.5 < V (m/s) < 1.2 and 0.5 < Y/D < 1.0.

TABLE 3.5 VALUES OF TRANSPORT PARAMETER , η (MAY'S EQN. 3.46) FOR SEDIMENT TRANSPORT IN PIPES OVER A LOOSE BED

RANGE OF F_s	η
$F_s \leq 0.10$	0.0
$0.10 < F_s \leq 0.23$	$1.60\ (F_s - 0.10)$
$0.23 < F_s \leq 0.40$	$0.20 + 2.13\ (F_s - 0.23)^{0.60}$
$0.40 < F_s \leq 0.65$	0.95

Alvarez (1990) carried out a limited number of transport experiments with non-cohesive sediments over loose and flat rigid beds in a 154mm dia. pipe flowing part-full. The range of sediment sizes used was ($=d_{50}$) 0.50mm to 4.10mm with an average specific gravity of 2.55. For loose continuous bed tests,

Alvarez expressed his data in terms of transport (Φ) and flow (ψ) parameters yielding:

$$\psi_b = 9.931\ \phi_b^{-0.123} \qquad (3.50)$$

Eqn. 3.50 was derived using values relevant to the bed (hereafter defined by subscript 'b') obtained from Einstein-Vanoni's separation technique (see Alvarez 1990). For flat rigid bed data, Alvarez (1990) obtained the best-fit relationship by the application of multiple linear regression analysis to the transport functions derived from dimensional analysis. Two best-fit equations were proposed based on different parameters (d/R and a combination of d/R and y_o/P) to represent shape effects:

$$\frac{\tau_b}{\rho(S_s-1)gd} = 1.60\ C_v^{0.64} \left(\frac{d}{R_b}\right)^{-1.27} \lambda_{sb}^{0.62} \qquad (3.51)$$

$$\frac{\tau_b}{\rho(S_s-1)gd} = 0.26\ C_v^{0.63} \left(\frac{d}{R_b}\right)^{-1.32} \left(\frac{y_o}{P}\right)^{-0.40} (\lambda_{sb})^{0.35} \qquad (3.52)$$

The experiments on transport over loose beds covered the range of $2 < C_v$ (ppm) < 131 for $0.105 < y_o/D < 0.392$ and $0.30 < Y/D < 0.80$ while the ones for flat rigid beds (at limit of deposition) covered $112 < C_v$ (ppm) < 677 for $y_o/D = 0.265$ and $0.51 < Y/D < 0.76$.

Perrusquia (1991) performed transport experiments over continuous loose beds in pipes (154mm, 225mm and 450mm dia.) flowing part-

full. The sediments used were in the range from 0.72mm to 2.5mm with specific gravity between 2.59 and 2.65. All sediments were observed moving as bed load. Dimensional and multiple linear regression analyses were used to derive the best-fit transport equations. The best-fit relationships (based on smaller pipe data only i.e. 154mm and 225mm dia.) were given as:

$$\phi_b' = 46\ 137\ \theta_b^{2.9}\ D_{gr}^{-1.2} \left(\frac{y_o}{d}\right)^{-0.7} \left(\frac{y_o}{D}\right)^{0.7} \left(\frac{y_s}{D}\right)^{-0.62} \qquad (3.53)$$

and

$$\phi_b' = 7.7\ (\theta_b - \theta_c)^{0.94}\ D_{gr}^{-0.6} \left(\frac{y_o}{d}\right)^{-0.24} \left(\frac{y_o}{D}\right)^{0.46} \left(\frac{y_s}{D}\right)^{-0.82} \qquad (3.54)$$

where Φ_b' is the transport parameter ($= q_s/(g(S_s - 1)d^3)^{1/2}$, q_s being sediment transport rate per unit bed width), θ_b is the mobility number ($= R_bS/(S_s-1)d$), and θ_{bc} is the critical mobility number at threshold computed from Shields' diagram. The experimental ranges were $30 < C_v$ (ppm) < 408 for $0.294 < V$ (m/s) < 0.668, $0.2 < y_s/D < 0.4$ and $0.32 < Y/D < 0.86$. Perrusquia (1992) obtained further data for overall flow depths above half-full (D= 225mm, Y/D > 0.5), and derived the following revised best-fit equation representing his entire data (D = 154 - 225mm):

$$\phi_b' = 3\ 400\ \theta_b^{2.6}\ D_{gr}^{-0.96} \left(\frac{y_o}{d}\right)^{-0.47} \left(\frac{y_o}{D}\right)^{0.66} \left(\frac{y_s}{D}\right)^{-0.70} \qquad (3.55)$$

El-Zaemey (1991) measured transport rates at the limit of deposition in a 305mm dia. pipe with smooth and rough flat rigid

beds flowing part-full. The sediment used ranged in sizes between 0.53mm and 8.4mm with an average specific gravity of 2.59. For rough flat bed conditions, the beds were artificially roughened with two sands of size 0.5mm and 1.0mm (k_o = 0.8mm and 1.40mm respectively). The transport relationships were derived from dimensional and multiple linear regression analyses. The resulting best-fit equations were given as:

$$\frac{\tau_o}{\rho(S_s-1)gd} = 0.55\, C_v^{0.33} \left(\frac{b}{y_o}\right)^{-0.76} \left(\frac{d}{D}\right)^{-1.13} \lambda_s^{1.22} \qquad (3.56)$$

where

$$\lambda_s = 0.88\, C_v^{0.01} \left(\frac{b}{y_o}\right)^{0.03} \lambda_o^{0.94} \qquad (3.57)$$

and

$$\frac{\tau_b}{\rho(S_s-1)gd} = 0.47\, C_v^{0.33} \left(\frac{b}{y_o}\right)^{-0.80} \left(\frac{d}{D}\right)^{-1.14} \lambda_{sb}^{1.2} \qquad (3.58)$$

where

$$\lambda_{sb} = 6.6\, \lambda_s^{1.45} \qquad (3.59)$$

in which b is the flat bed width. The experiments were in the range of $11 < C_v$ (ppm) < 512 for $0.36 < V(m/s) < 0.83$, $1.1 < b/y_o < 7.4$, $0.154 < y_s/D < 0.393$, and $0.34 < Y/D < 0.82$.

Ackers's (1991) equation (Eqn. 3.29) could be used to predict a volumetric sediment concentration in sewers with loose beds provided a suitable value of effective transport width, W_e is applied. Several values of W_e have been suggested: Ackers (1984)

proposed W_e = D for some deposition based on experimental work by May (1982). CIRIA (1987) suggested that the actual width of sediment bed, W_b, should be used for a finite depth of sediment deposits (e.g. y_s/D = 10%). More recently, based on the experimental work by May et al (1989), Ackers (1991) proposed W_e = 0.04D for a modest deposition of 1% of pipe diameter (i.e. y_s/D = 0.01).

Kleijwegt (1992) conducted experiments over loose beds in a 152mm dia. pipe running full and part-full. The sediments were made up of three sand sizes of 0.087mm, 0.2mm and 0.781mm. Both modes of transport, suspended load and bed load were observed. A comparison of various equations for sediment transport was made using the collected experimental data. The results suggested that equations due to Ackers (1984) and van Rijn (1984) could be used to compute transport rates over continuous loose beds with bedforms while equations of Engelund-Hansen (1967) and Graf-Acaroglu (1968) will give reasonable estimates of transport rates over flat loose beds. The range of experimental data was 0.151 < V (m/s) < 0.944, 0.02 < y_s/D < 0.29, and 0.295 < Y/D < 1.0.

3.3.3 Transport in Non-Circular Channels

Mayerle (1988) proposed a transport equation for smooth and rough rigid rectangular channels based on his experimental works in 311.5mm and 462.3mm wide channels. Using multiple regression analysis to fit the non-dimensional transport functions to experimental data yielded:

$$\frac{V}{\sqrt{g(S_s-1)d}} = 11.59\, C_v^{0.15}\, D_{gr}^{-0.14} \left(\frac{d}{R}\right)^{-0.43} \lambda_s^{0.18} \qquad (3.60)$$

The experimental data covered the range of $14 < C_v$ (ppm) < 3030 for $0.5 < V$ (m/s) < 1.2, $3.35 < b/y_o < 12.46$, $0.50 < d$ (mm) < 8.70, and $0.0 < k_o$ (mm) < 0.72.

Kithsiri (1990) extended Mayerle's (1988) experiments in the 311.5mm wide rectangular channel using a wider range of roughnesses (k_o =0.74mm - 5.61mm). The range of sediment sizes used was 1.05mm to 8.40mm with an average density of 2.62. Applying Mayerle equation (Eqn. 3.60) to his data, Kithsiri found that the agreement was rather good (see Fig. 3.14, Nalluri-Kithsiri 1992). Good agreement was also obtained when Eqn. 3.60 was tested against independent data (Pedroli 1963, Loveless 1986) as shown in Fig. 3.15 (Nalluri-Kithsiri 1992). Kithsiri (1990) also proposed an alternative transport equation given as:

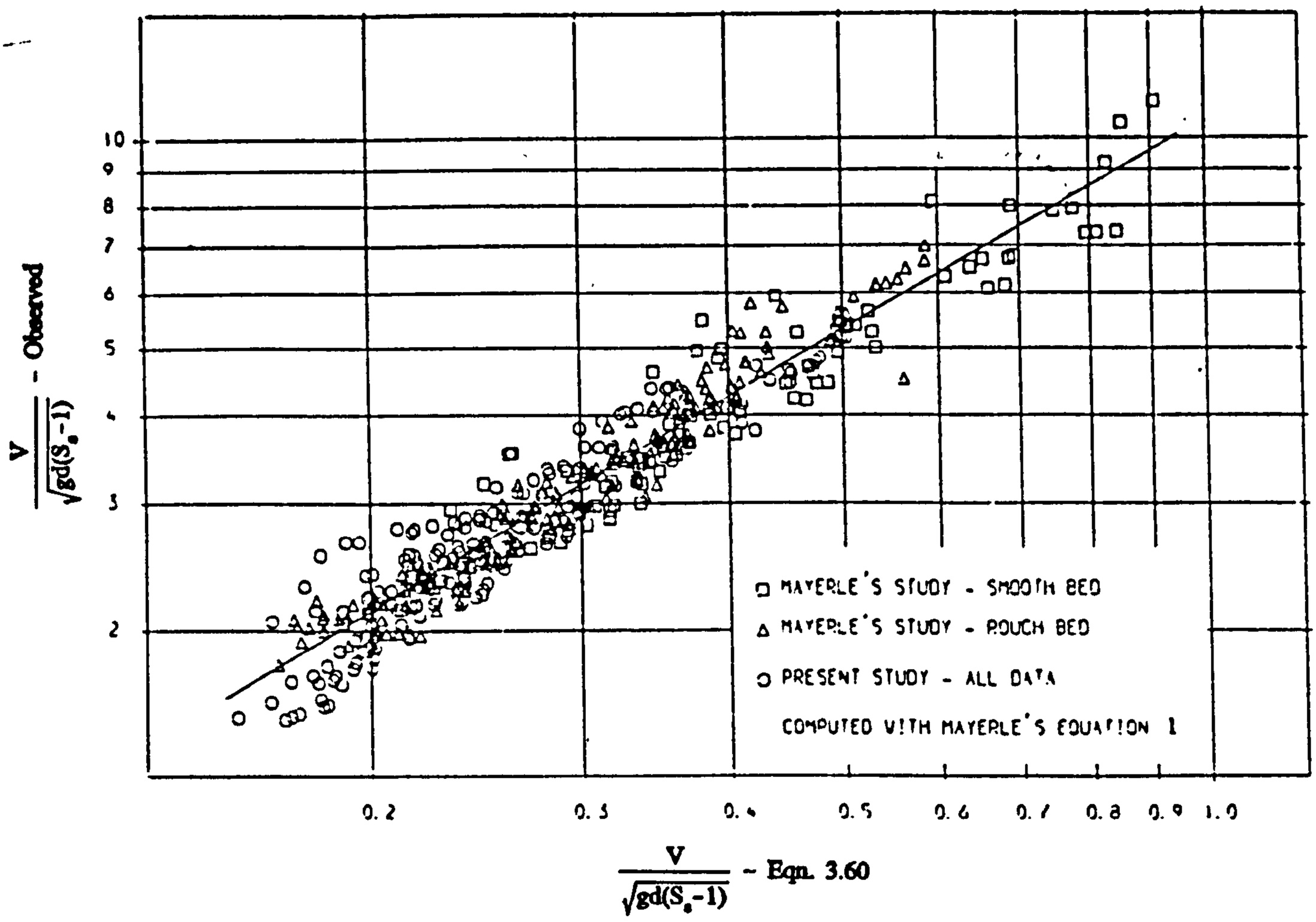

FIG. 3.14 Verification of Eqn. 3.60 with Kithsiri's (1990) data (After Nalluri-Kithsiri 1992)

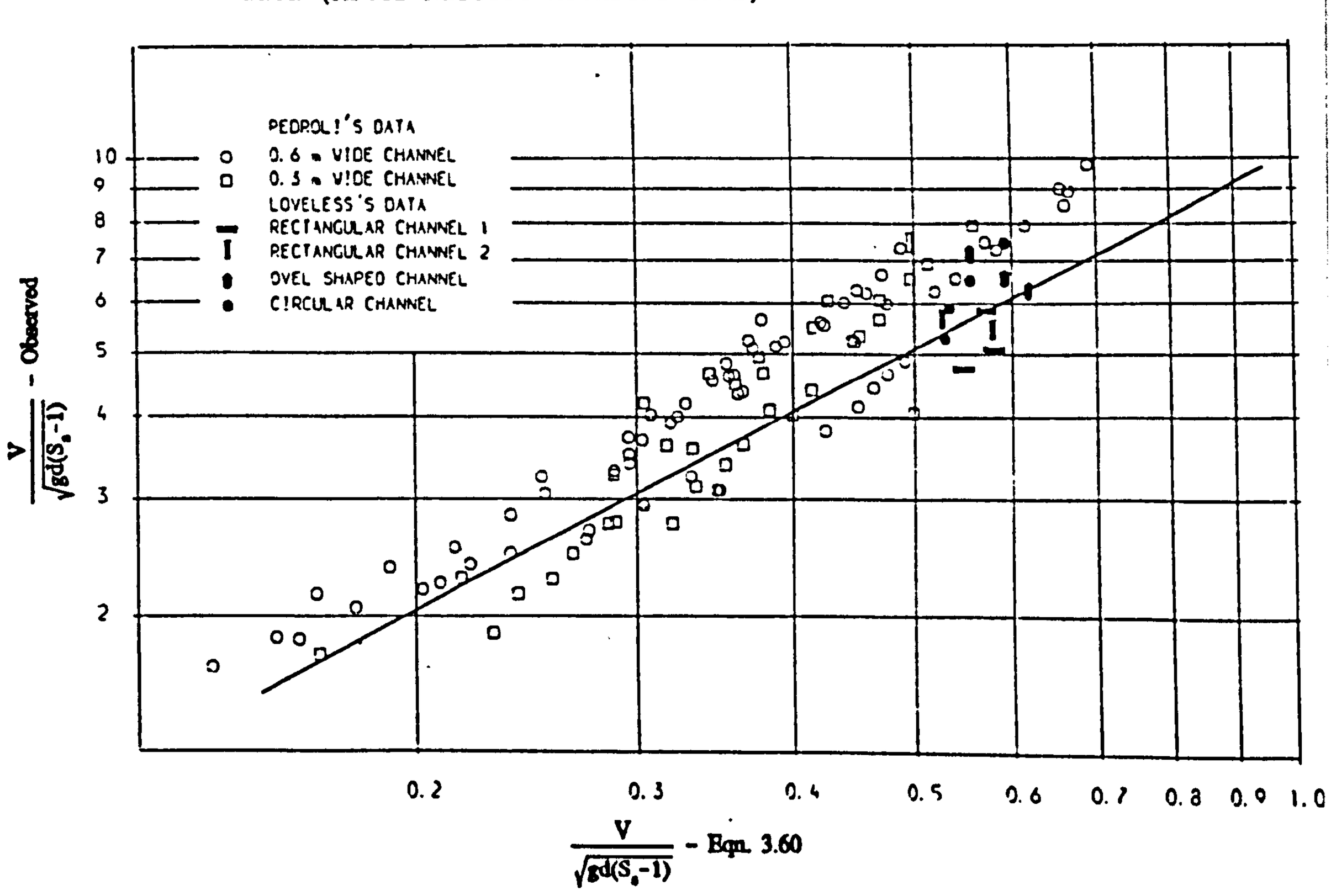

FIG. 3.15 Verification of Eqn. 3.60 with other rectangular channel data (After Nalluri-Kithsiri 1992)

$$\frac{\tau_b}{\rho(S_s-1)gd} = 12.93\, C_v^{0.29} \left(\frac{R_b}{d}\right)^{0.96} \lambda_s^{1.50}\, D_{gr}^{-0.21} \qquad (3.61)$$

where the friction factor with sediment, λ_s, could be evaluated from:

$$\lambda_s = 0.851\, \lambda_o^{0.86} C_v^{0.04} D_{gr}^{0.03} \qquad (3.62)$$

The range of experimental data was $11 < C_v$ (ppm) < 3050 for $0.487 < V$ (m/s) < 0.95 and $2.68 < b/y_o < 6.99$.

Graf-Acaroglu (1968) derived a total load transport model based on physical considerations by establishing the existence of a functional relational between the shear intensity or flow parameter, ψ, and the transport parameter, Φ. They applied linear regression analyses using open channel flow data (transport over loose beds in rectangular channels) from laboratories and field work, and closed conduit data (transport at the limit of deposition in circular and non-circular channels running full). The resulting equation (Fig. 3.16) was expressed as:

$$\phi = 10.39\, \psi^{-2.52} \qquad (3.63)$$

which can be re-arranged as:

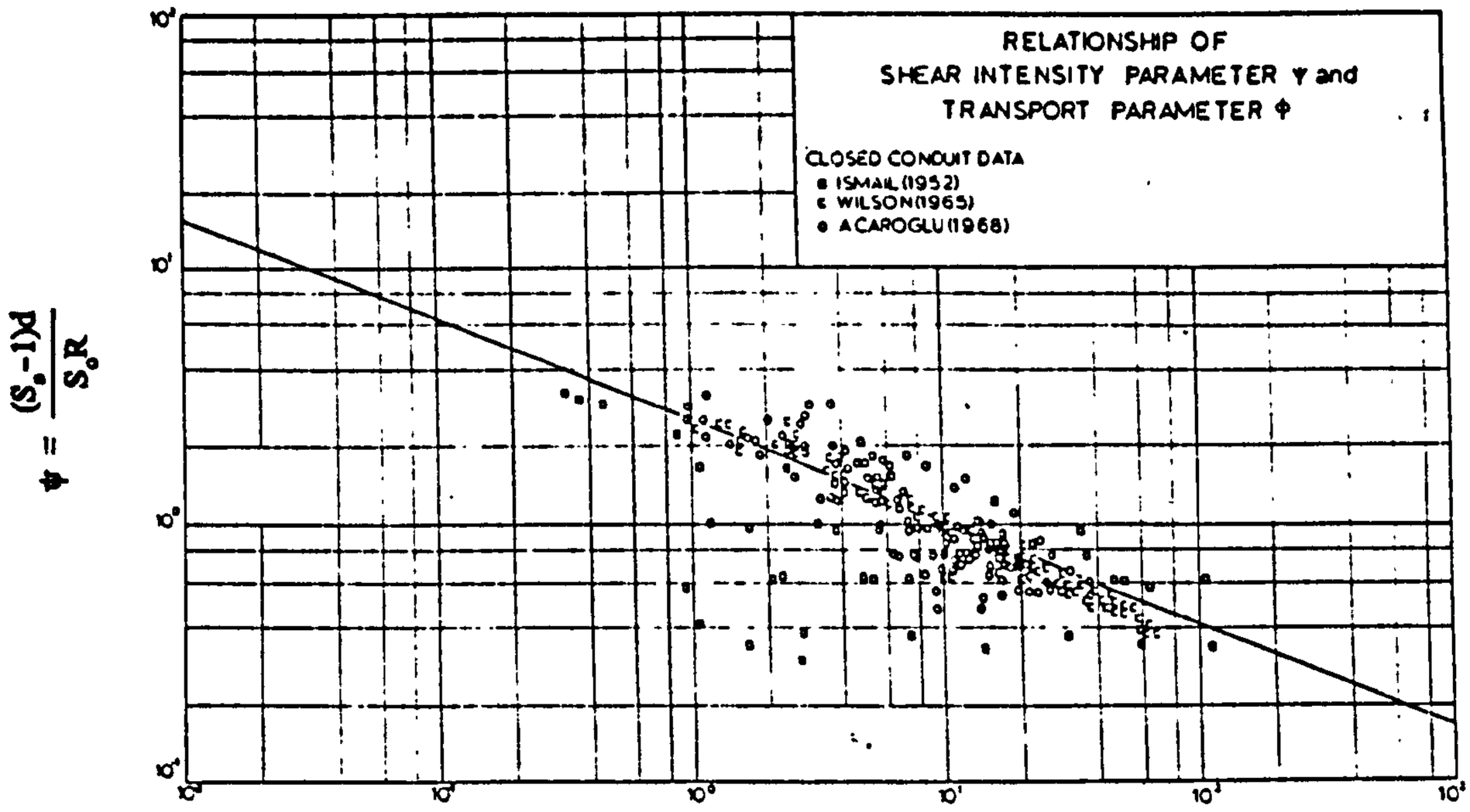

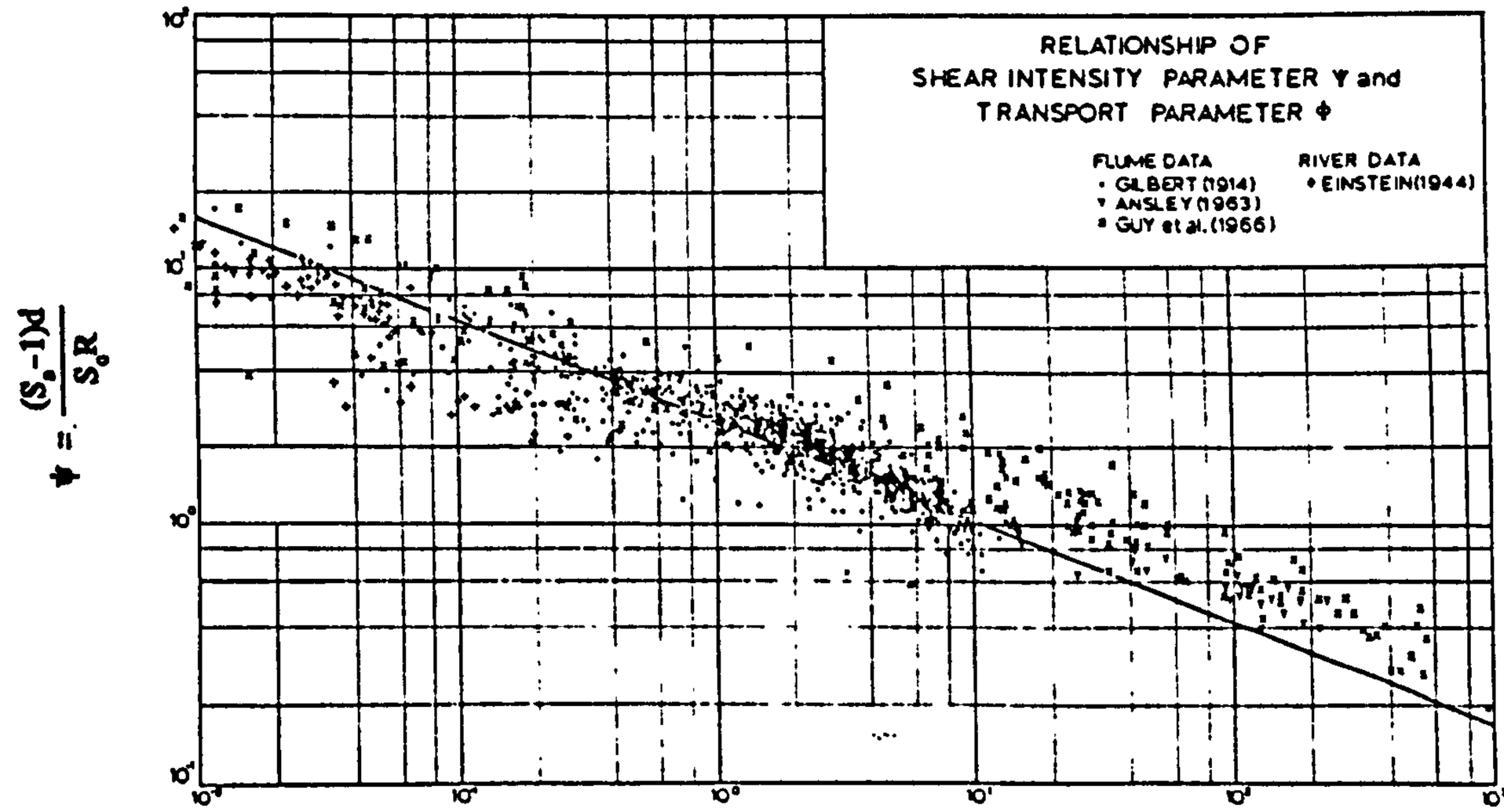

FIG. 3.16 Plots of Φ - Ψ for total load transport in circular and non-circular channels (After Graf-Acaroglu 1968)

$$\frac{V}{\sqrt{g(S_s-1)d}} = 2.07C_v^{0.25}\left(\frac{R}{d}\right)^{0.25}\lambda_s^{-0.624} \qquad (3.64)$$

The ranges of data used to derive Eqn. 3.64 were $0.091 < d\ (mm) < 2.780$, $S_s = 2.65$, and $10^{-2} < \Phi < 10^3$.

3.4. Summary

Based on literature review presented in the previous sections, the following main conclusions can be made regarding the bed-load transport studies in pipes (see Table 3.6):

- Most of experiments were conducted in small smooth rigid pipes (150mm - 250mm dia.) with limited ranges of flow conditions (i.e. depths and velocities) and sediment sizes.

- Only limited data were available for transport over deposited beds in pipes.

The aims of the present experimental work were to supplement these inadequacies in the transport studies in sewers.

TABLE 3.6 EXPERIMENTAL WORKS IN CIRCULAR CHANNELS

a) CLEAN PIPES

AUTHOR	D(mm)	k_o (mm)	d (mm)	C_v (ppm)	V (m/s)	TYPE OF FLOWS
LAURSEN (1956)	152	0.0	0.25 - 1.60	180 - $3x10^5$		FULL/ PART FULL
DURAND (1953)	40 - 700	0.0	0.02 - 100.00	$2x10^4$ - $1.5x10^5$		FULL
NOVAK-NALLURI (1975)	152 - 305	0.0	0.15 - 2.00	20 - 2400	0.45- 0.75	PART FULL
MACKE (1982)	192 - 445	0.0	0.16 - 0.37	1 - 1700	0.5 - 1.2	PART FULL
MAY (1982-1989)	77 - 300	0.0	0.64 - 7.90	2 - 2110	0.5 - 1.2	FULL/ PART FULL
MAT SUKI (1987)	164 - 253	0.0- 2.7	1.30 - 8.00	20 - 1020	0.5 - 1.11	FULL
MAYERLE (1988)	152	0.0	0.5 - 8.74	26 - 1140	0.38 - 1.50	PART FULL
LOVELESS (1991)	88 - 220	0.0- 0.3	0.45 - 6.00	74 - 1914	0.45 - 1.10	PART FULL

b) PIPES WITH DEPOSITED BEDS

AUTHOR	D (mm)	d (mm)	y_s/D	Y/D	V (m/s)	C_v (ppm)
MAY ET AL (1989)	300- 450	0.47- 0.72	0.0008 - 0.22	0.5- 1.0	0.5- 1.5	4 - 1290
ALVAREZ (1990)	152	0.50 - 4.10	0.11 - 0.39	0.30 - 0.80	0.25- 0.65	2 - 131
PERRUSQUIA (1991-1992)	152- 450	0.72 - 2.50	0.20 - 0.40	0.32 - 0.86	0.29- 0.67	30 - 408
KLEIJWEGT (1992)	152	0.09 - 0.78	0.02 - 0.29	0.30 - 1.0	0.151 - 0.944	

CHAPTER 4

EXPERIMENTAL APPARATUS AND PROCEDURE

4.1. Introduction

The experimental work was carried out at the laboratories of University of Newcastle upon Tyne (UNUT) and Hydraulics Research Ltd. (HRL), Wallingford. Two circular channels of 154mm and 305mm dia. were utilised at UNUT while a 450mm dia. concrete pipe was used at HRL. All three pipes were used to collect the smooth rigid boundary data while the rough rigid boundary data were acquired only in the 305mm dia. pipe. The 450mm dia. pipe was also used to obtain the loose boundary data. All the data were collected during the period of November 1990 to April 1993.

4.2 Experimental Work at UNUT

4.2.1 Test Pipes

4.2.1.1 154mm Pipe

This pipe channel, made up of uPVC, was assembled on the top of a steel frame and has a length of 20.5m. Water was supplied to the pipe using two pipe lines which would give a maximum discharge of 40l/s and recirculated over a triangular notch for measurement of flow discharge.

Openings of about 100mm dia. were made on the top of the pipe in several positions to allow for measurements of invert and water levels.

The pipe was laid on circular ring supports and its horizontal position was carefully levelled only allowing for a deviation of about ± 0.5mm from the mean. The alignment of the pipe showed no significant deviation from the straight line.

The slope was varied by a mechanical jack located near the downstream end of the frame. The slope was fixed for each experiment to minimise the sagging of the frame. The frame could be tilted to give a maximum slope of around 0.006.

A vertical tail gate was provided at the end of the channel to allow any adjustment required for flow uniformity.

The arrangement of the 154mm dia. pipe is shown in Fig. 4.1 and Plate 4.1.

4.2.1.2 305mm Pipe

This pipe was constructed of 6.35m long sections of PVC pipe with a total length of 20.5m. The pipe (see Plate 4.2) was placed on the steel frame which was used to support the 154mm pipe hence utilising the same supply lines of water and flow discharge measurement technique.

Each section of the pipe had several 1200mm x 150mm slots cut along the pipe's crown. These large openings were made to allow easy access to pipe wall for artificial roughening process,

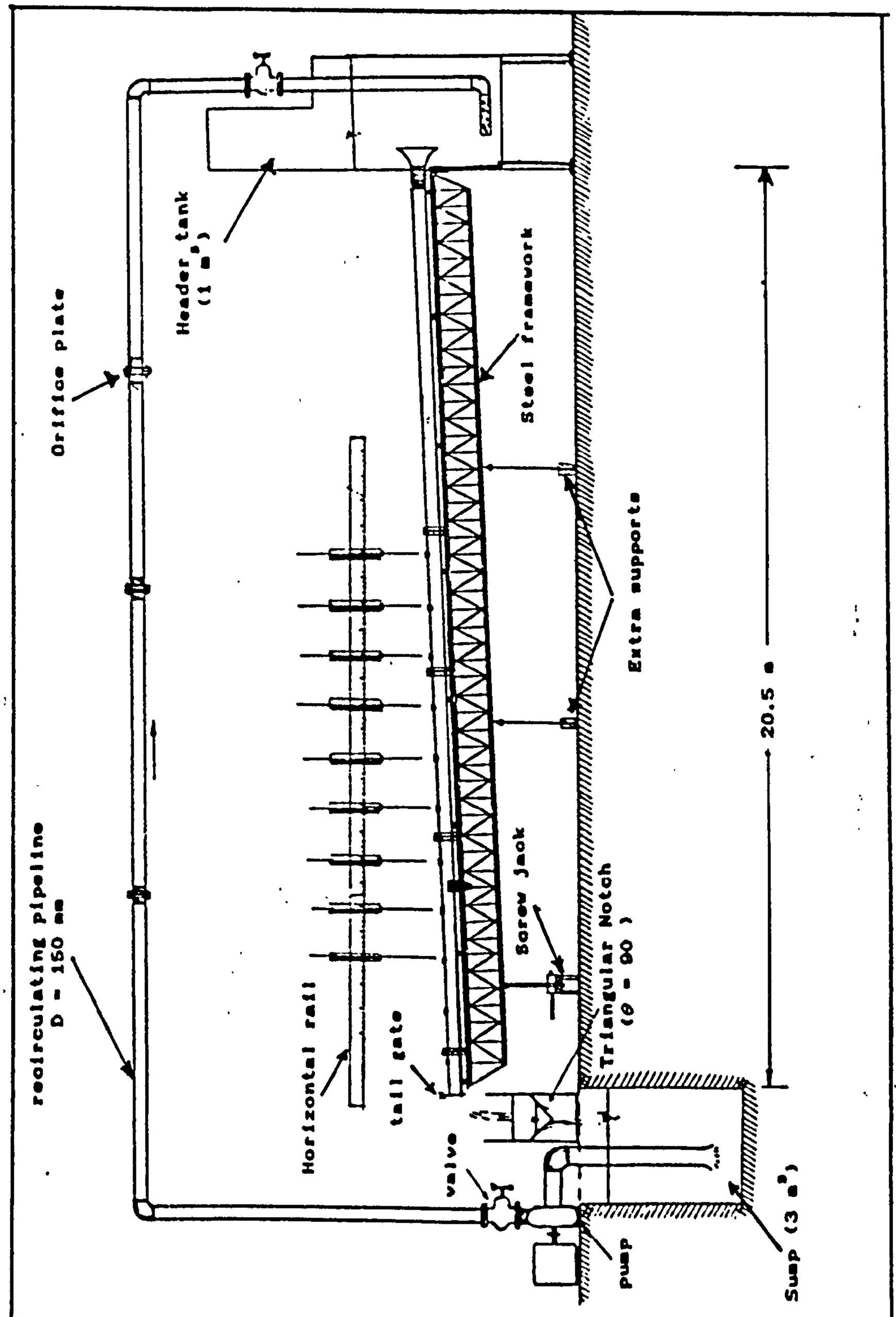

FIG. 4.1 Test arrangement at Newcastle: D = 154mm - 305mm

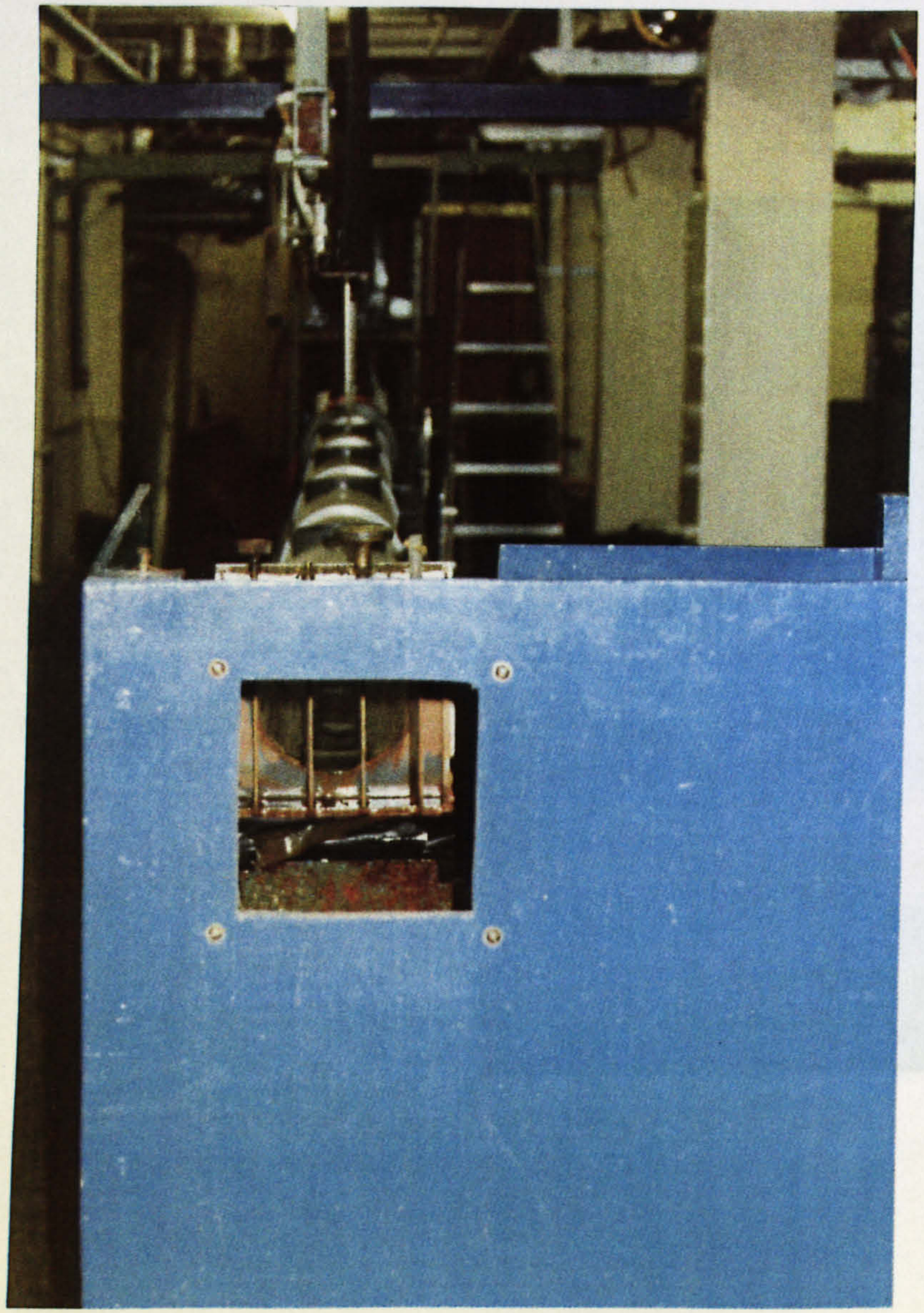

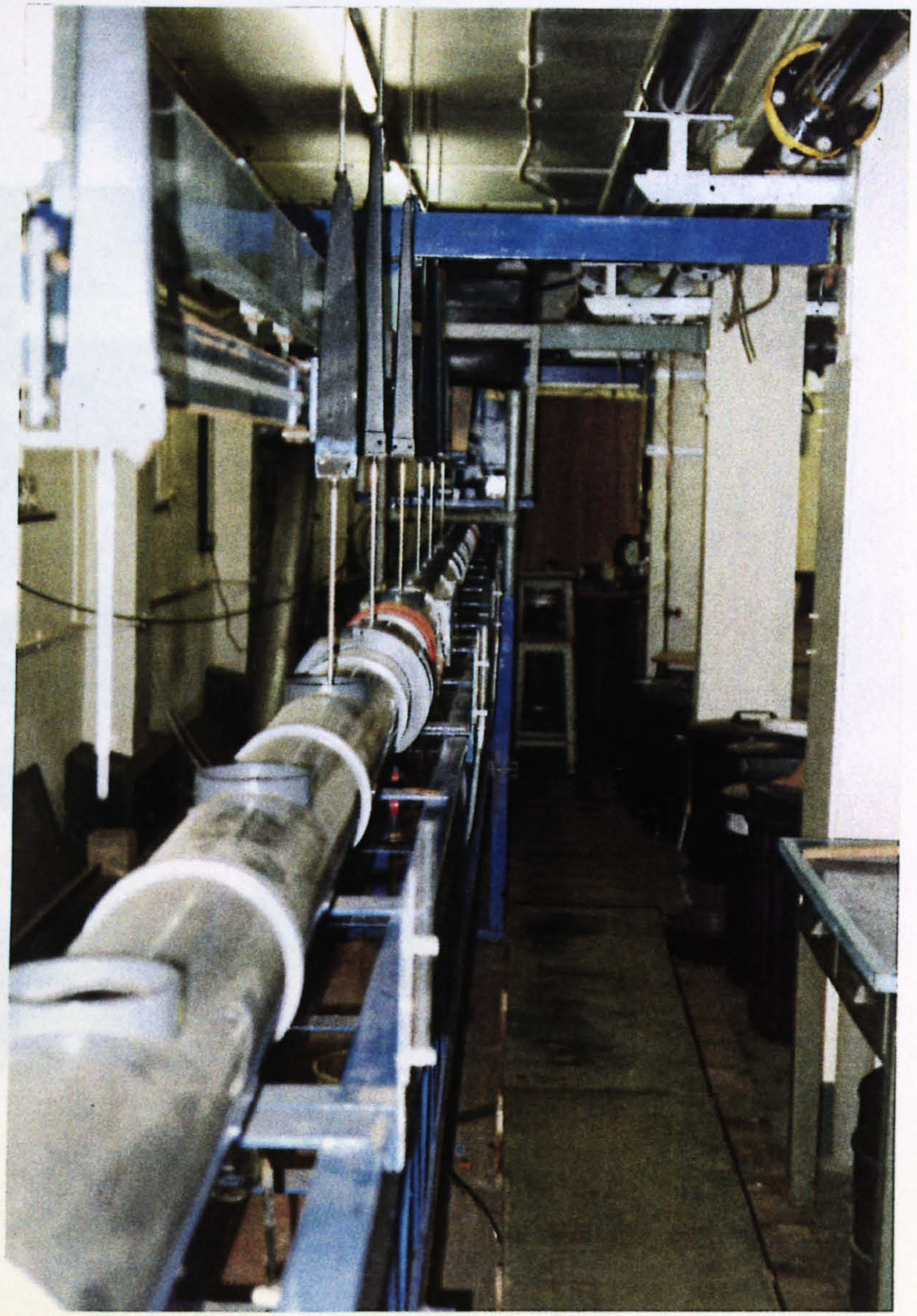

PLATE 4.1 General view of test pipe: D = 154mm

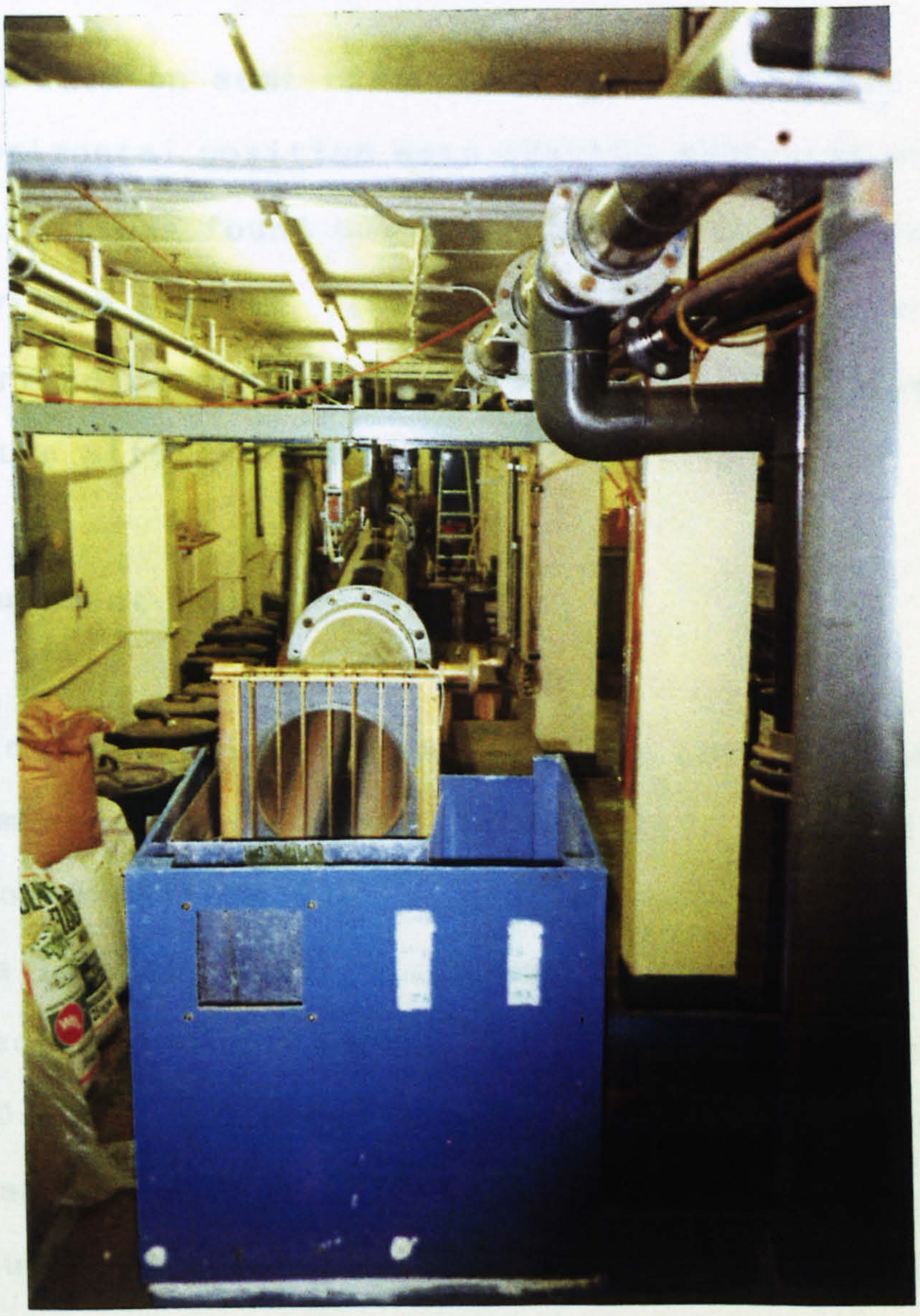

PLATE 4.2 General view of test pipe: D = 305mm

measurement of invert and water levels, and observations of bed conditions along the invert of the pipe.

The pipe was laid on semi-circular ring supports and the invert levels at horizontal position were checked along the whole length of the pipe. It was found out that the deviations from the mean level were within ± 0.5mm. The pipe alignment was also inspected and necessary adjustments were made to bring the pipe within ± 1mm from the straight line.

4.2.2 Measurement Techniques

A test section, approximately 5m long, was located about 10m from the upstream end to give a sufficient entry length to obtain a fully developed uniform flow. Measurements of the invert and water levels in both pipes (D = 154mm and 305mm) were made along this test section using a set of seven point gauges at intervals of average 0.85m. Two extra point gauges each located at about 2.0m upstream and downstream of the test section were used to ensure the uniformity of the flow beyond the test section and also to help in getting the required flow depth quickly. The vertical tail gate, when necessary, was used to adjust the flow to give the required uniform flow. The corresponding slopes of water surface, S_w, and pipe invert, S_p, were then obtained from the best-fit line regression analysis.

Measurements of velocity profile were also made in the newly-installed 305mm pipe for smooth and rough rigid boundaries to ensure the uniformity of the flows. The velocity profiles were obtained along the centre line of the invert in the test section using a 10mm-propeller current meter. The lowest position measured was 7.5mm from the invert. The calibration of the current meter is given in the following form:

$$u = 0.541\,N + 3.822 \quad 50 < N < 250 \tag{4.1}$$

where u is the local velocity in cm/s and N is the current meter frequency reading in Hz. The current meter readings were taken from a digital counter that was set to give an average over 10 seconds. For each position, ten readings were averaged to obtain the local mean velocity. The flow uniformity in the 154mm pipe has been established from previous work (Alvarez 1990).

A 90° triangular notch, located downstream of the flume was used to measure the flow discharge, Q, given by:

$$Q = 1.365\,h^{2.5} \tag{4.2}$$

where Q is in m^3/s and h is the water height above the V-notch vertex in m.

The temperature of water, T in degrees centigrade, was measured using a thermometer placed in the downstream tank. The kinematic viscosity of water, ν in m^2/s, was then calculated from:

$$\nu = \frac{1.79 \times 10^{-6}}{1 + 0.03368T + 0.000221T^2} \qquad (4.3)$$

4.2.3 The Sediments

4.2.3.1 Sediment Characteristics

The sediments were non-cohesive and graded uniformly using the British Standard sieves. The sediments chosen were intended to cover the range of sizes normally found in the invert of sewers (d_{50}= 0.5mm - 10.0mm) as discussed in Section 2.2. Their densities were obtained using water displacement method. The sediment sizes (represented by d_{50}) and densities are given in Table 4.1. The sieve curves for each sediment are shown in Fig. 4.2.

TABLE 4.1 SEDIMENT CHARACTERISTICS

SIZE d_{50} (mm)	DENSITY (kg/m^3)	SPECIFIC GRAVITY
0.46	2593	2.59
0.97	2577	2.58
2.00	2530	2.53
4.20	2569	2.57
5.70	2537	2.54
8.30	2550	2.55

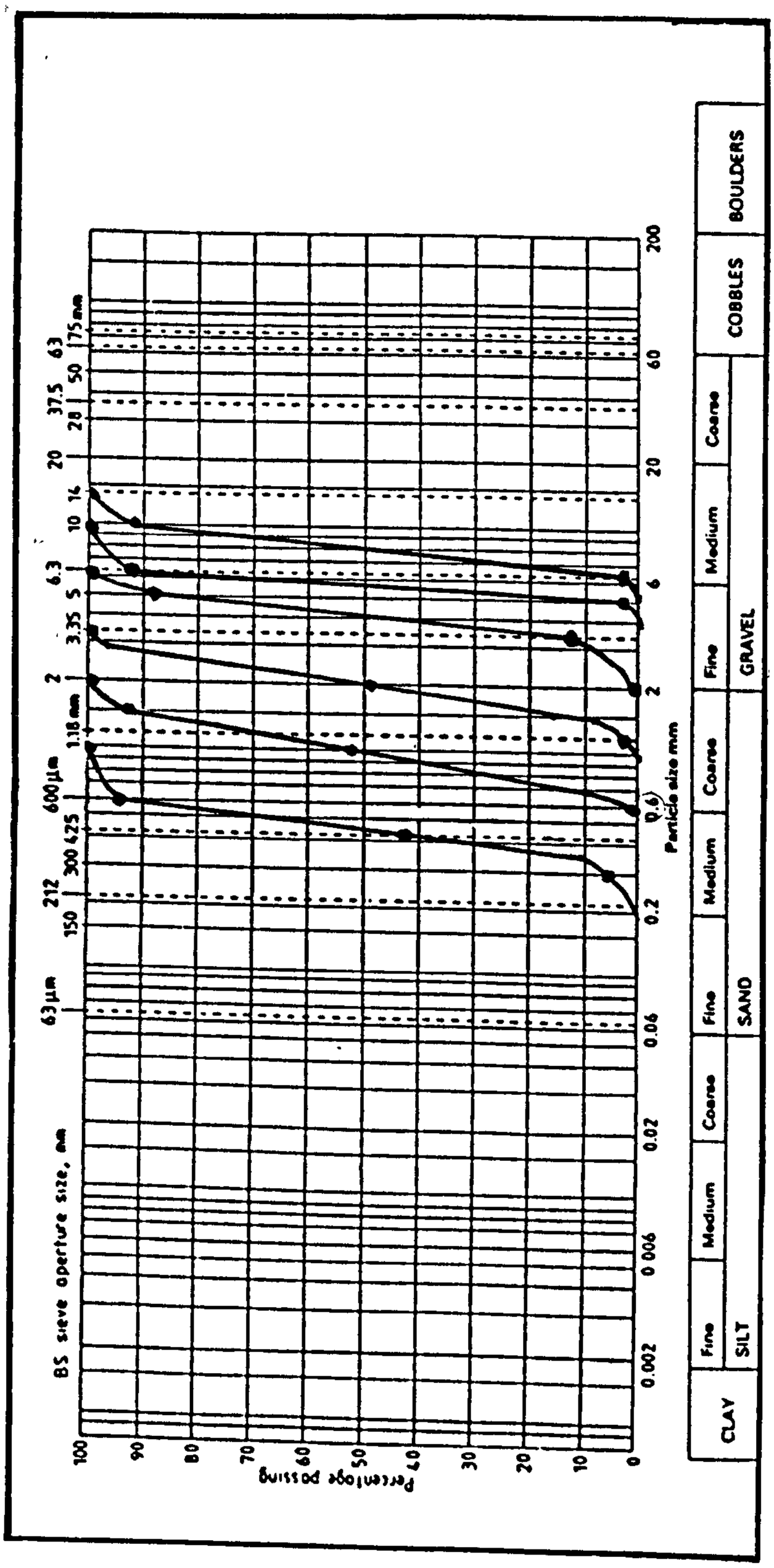

FIG. 4.2 Sediment sizes

4.2.3.2 Sediment Supply System

The sediment supply system, placed 9m from the upstream end, was made up of a container, a sediment tray, and an electromagnetic vibrator (see Plate 4.3). The container, filled with dry sediment, was connected to the tray by a funnel. The rate of sediment supply was adjusted by a vibrator placed under the tray from which the sediments fall into the flow below. A constant rate of sediment supply was maintained by keeping the same amount of sand at the top level of the container, and by adjusting a small gate, if necessary, located near the end of the sediment tray.

The sediment supply rate was measured by weighing the amount of sediments collected over a fixed period of time. After the limit of deposition criterion was reached, the supply rate was recorded for 15 minutes to ensure that the rate was constant. Another measurement of the supply rate was obtained after water level readings were taken. The average value using the rate before and after the test was then adopted. The sediments in the flow were collected at the downstream end using box traps and dried in an oven for re-use.

4.2.4 Artificial Roughening of the 305mm Pipe

For transport experiments in rough rigid boundary, two sizes of sand (d_{50}= 0.5mm and 1.0mm) were used to roughen up to 80% of the

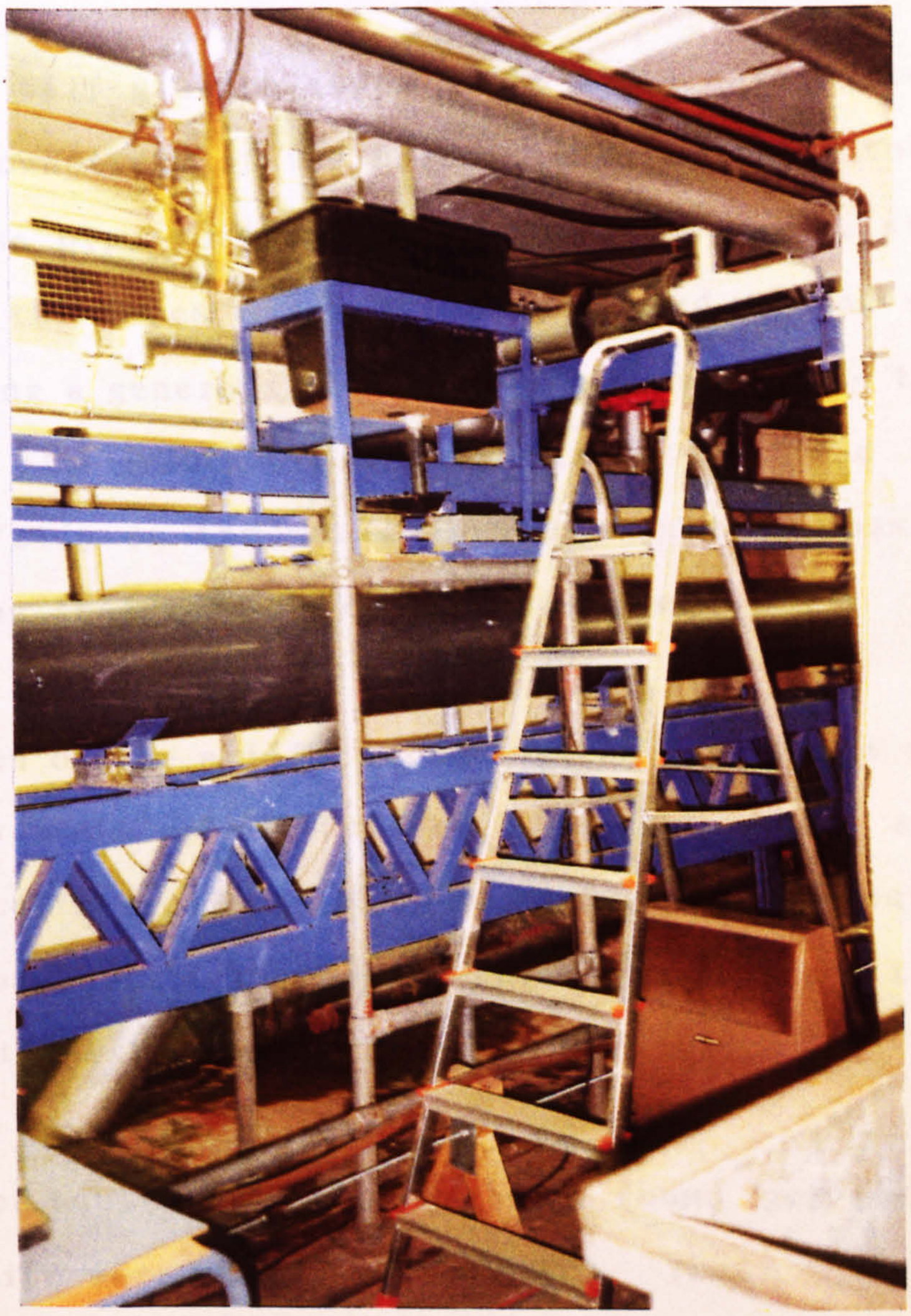

PLATE 4.3 Sediment supply system

pipe diameter which is the upper limit of the proportional flow depth for the present work.

Double-sided self-glueing tapes (50mm wide) were placed between 3m and 19m downstream of the header tank to give a total length of 16m of the pipe roughened. To minimise the bulging of the tape sheet, the tapes were carefully pasted to the pipe wall. After applying a generous coat of gloss paint to the tape sheets to increase the grip on the sand particles, the sands were spread carefully on the wet paint as evenly as possible. The rough bed was then left to dry for two weeks.

An inspection of the artificial roughness (see Plate 4.4) showed that it was made up of a layer of sands having a thickness equivalent to their diameter hence confirming the requirement of a uniform roughness. The sand particles were found to stay firm throughout the experiments.

The values of equivalent sand roughness found from the Colebrook-White equation were given in Table 4.2. These values conformed to those suggested by WAA's Sewers for Adoption (WAA, 1989) (see Section 2.5).

4.2.5 Establishment of Uniform Flow

Prior to each sediment transport test, a clear-water test with uniform flow was obtained. These tests enabled the determination

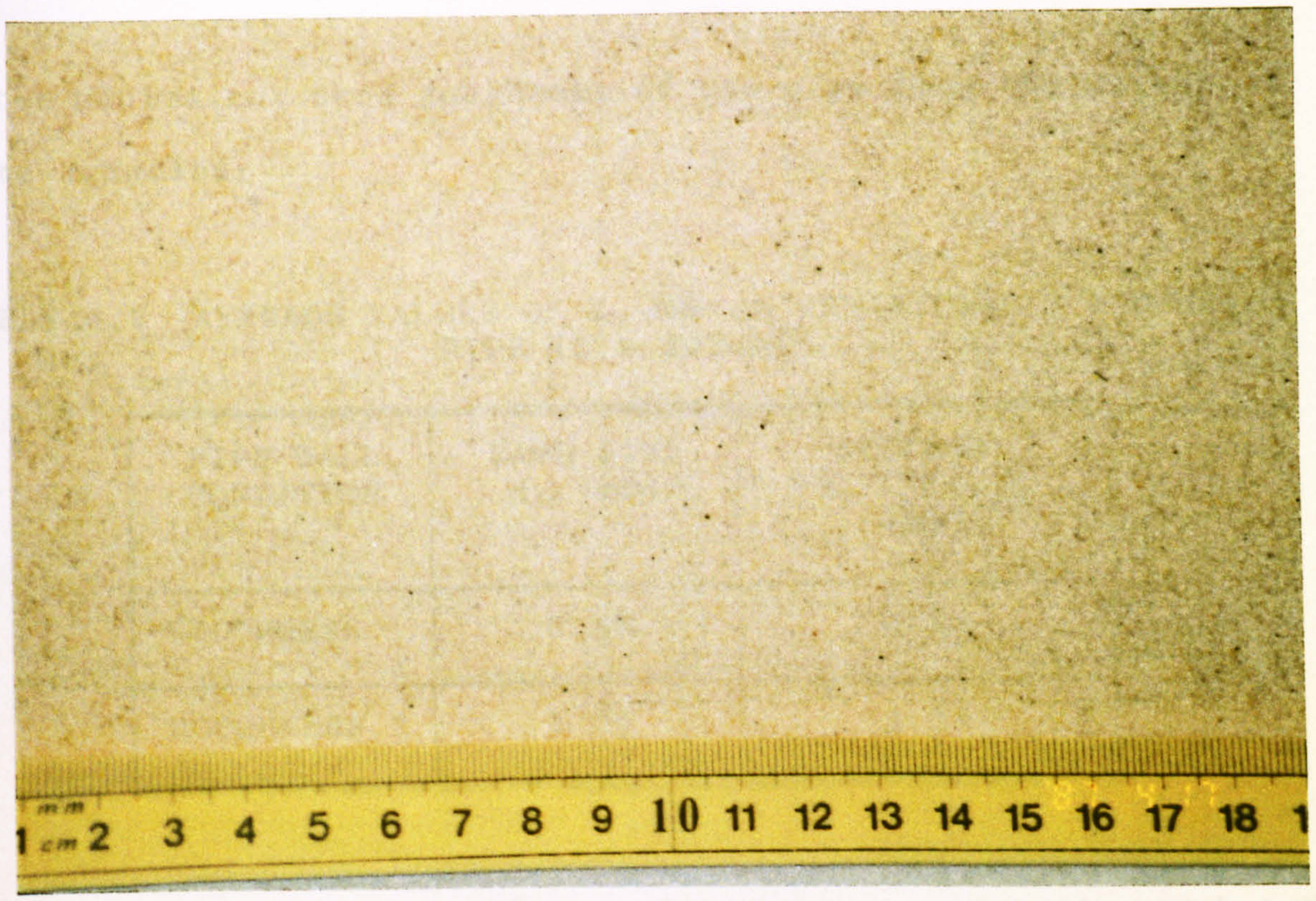

PLATE 4.4a Pipe wall roughness: Roughness 1 (sand size d_{50} = 0.5mm)

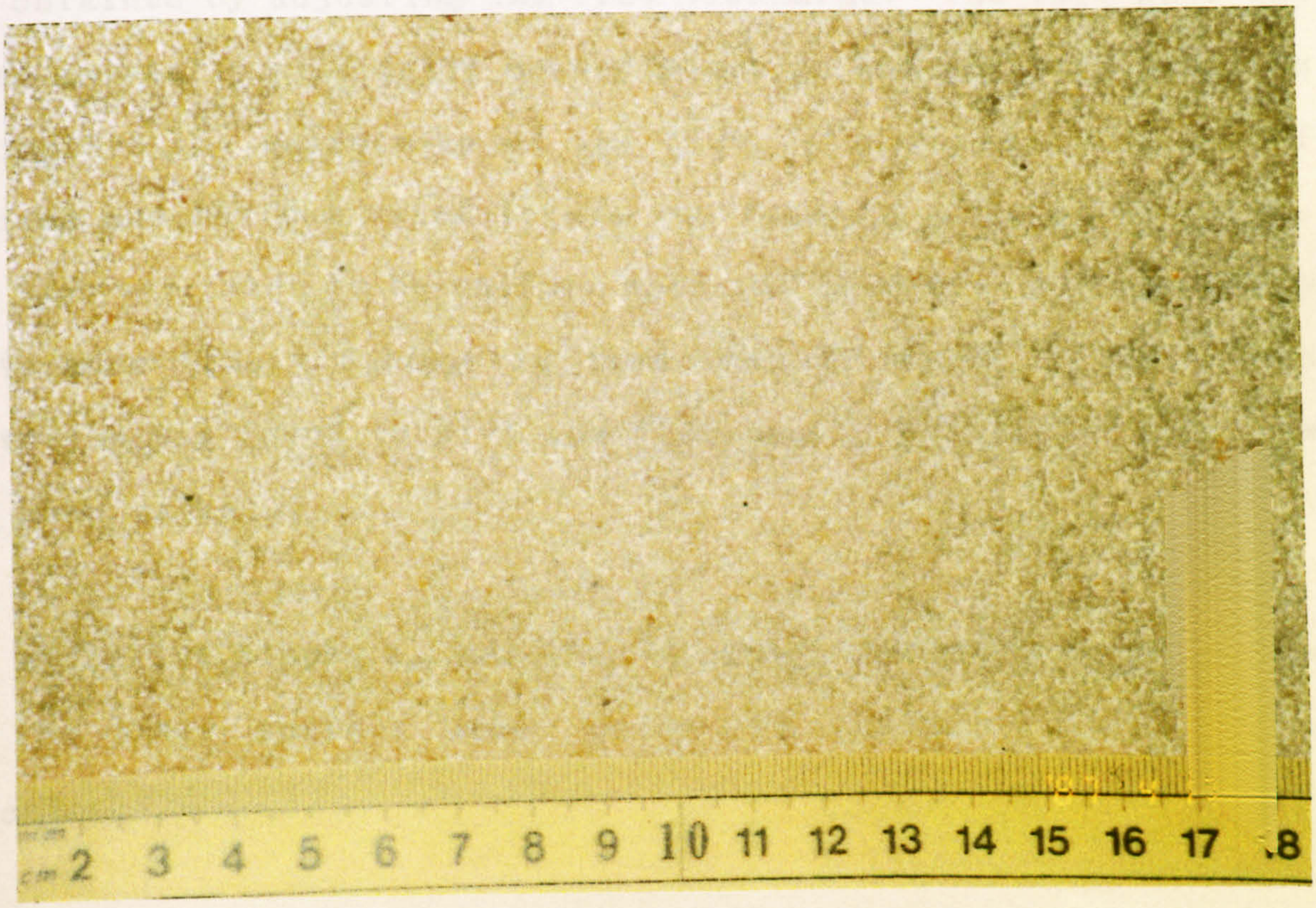

PLATE 4.4b Pipe wall roughness: Roughness 2 (sand size d_{50} = 1.0mm)

of the equivalent sand roughness of the pipe from the Colebrook-White equation.

TABLE 4.2 AVERAGE VALUES OF k_o FOR AN ARTIFICIALLY ROUGHENED PIPE (D = 305mm)

PIPE WALL CONDITION	SAND SIZE d_{50} (mm)	AVERAGE k_o - VALUE (mm)
ROUGHNESS 1	0.50	0.53
ROUGHNESS 2	1.00	1.34

For each test, the slope of the pipe was set using the jack and the invert level readings were recorded. The required flow depth was obtained by adjusting the flow discharge. The tail gate was fixed initially at a fully opened position and adjusted later on to improve the uniformity of the flow, if necessary. A set of minimum and maximum water levels was taken at each point gauge. The flow was taken to be uniform when the absolute relative slope difference ($[S_w - S_p]/S_p$) is less than or equal to 5%. This criterion was found to give the flow depths within +/- 2mm from the mean value.

The effective slope, S_o, was then obtained by making a correction to the water surface slope using the gradually varied flow equation:

$$\frac{dy}{dx} = \frac{(S_p - S_f)}{(1 - F_r^2)} \qquad (4.4)$$

where S_f is the energy gradient and dy/dx is the water surface slope (S_w). For uniform flows, the three slopes should be equal ($S_p=S_w=S_f$). Assuming the flow was nearly uniform, the effective slope can be expressed as:

$$S_o = S_p - (S_p - S_w)(1 - F_r^2) \qquad (4.5)$$

4.2.6 Experimental Procedure for Sediment Transport

After uniform flow was obtained, the sediments were added to the flow at an increasing rate until deposition occurred. The supply rate was then reduced as close as possible to the limit of deposition defined as the point where sediments started to group together and was then dispersed by the flow.

After allowing sediments to move at the limit of deposition for several minutes to ensure no deposition was likely, the flow depths were recorded. Necessary adjustments to the tail gate or flow discharge were made to ensure uniformity of the flow. Sediment transport rates at the limit of deposition were taken before and after the flow depth readings were made.

The width of sediment spread, W_s, at the limit of deposition was measured along the wetted perimeter at several locations and an average value was adopted.

4.3 Experimental Work at HRL

Details of the test arrangement and experimental procedure as summarised here are taken from reports by May et al (1989) and May (1993).

4.3.1 Test Pipe - 450mm Pipe

This pipe (see Fig. 4.3 and Plate 4.5) was made up of 2.52m long sections of spun concrete with a nominal internal diameter of 450mm and a total length of 21m. Flow was supplied to the pipe by up to three pumps and recirculated over a wide rectangular thin plate weir. A small proportion of this flow was extracted by a slurry pump which recirculated sediments through the pipe.

Each pipe section had two 900mm x 90mm slots cut in the top to allow observation of bed conditions along the length of the pipe.

The pipe was laid on wooden blocks and the invert levels at the horizontal position were checked and adjusted as appropriate. The flume could be tilted to give a maximum slope of around 0.01.

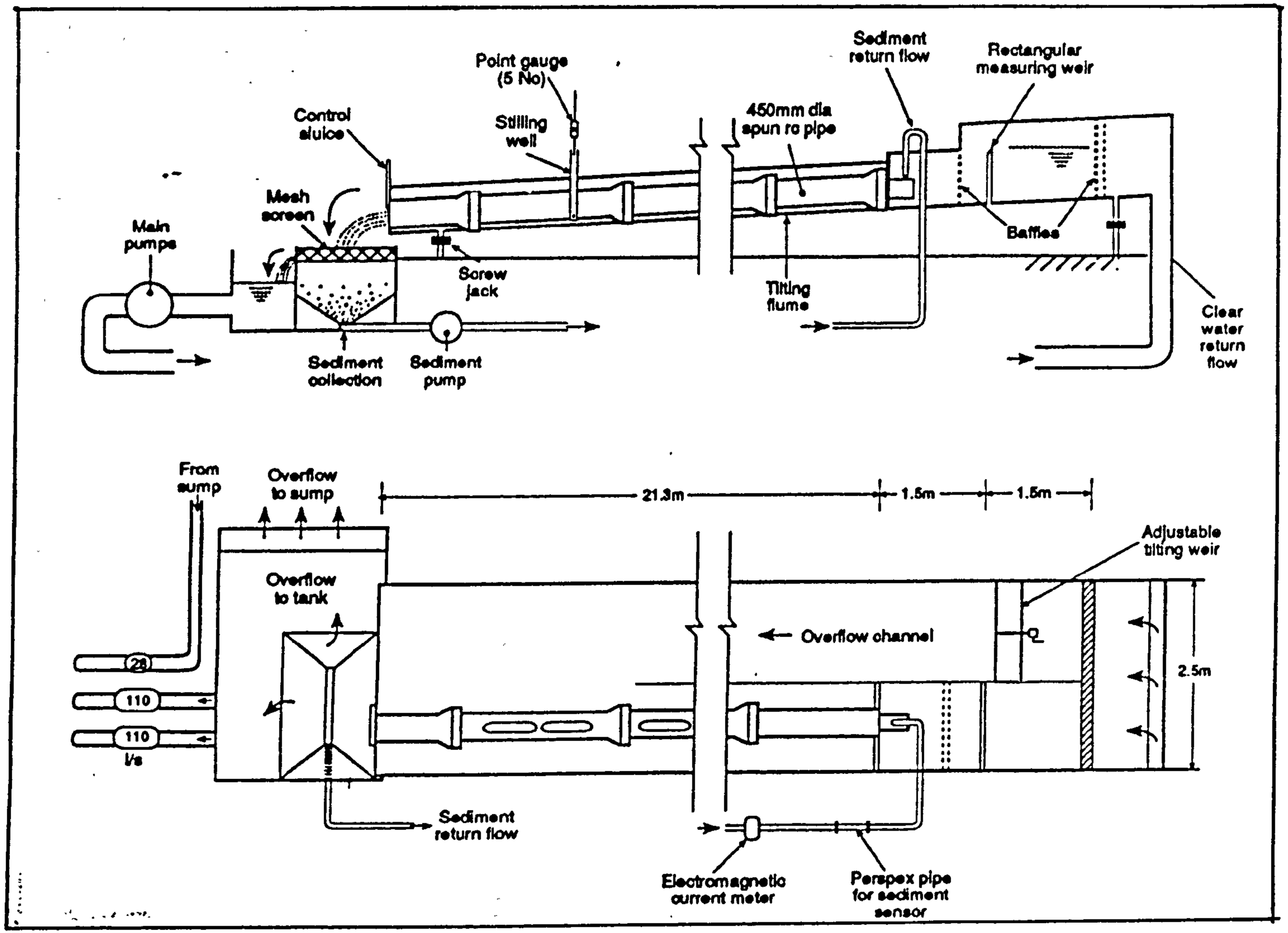

FIG. 4.3 Test arrangement at Hydraulics Research Ltd: D = 450mm
(After May 1993)

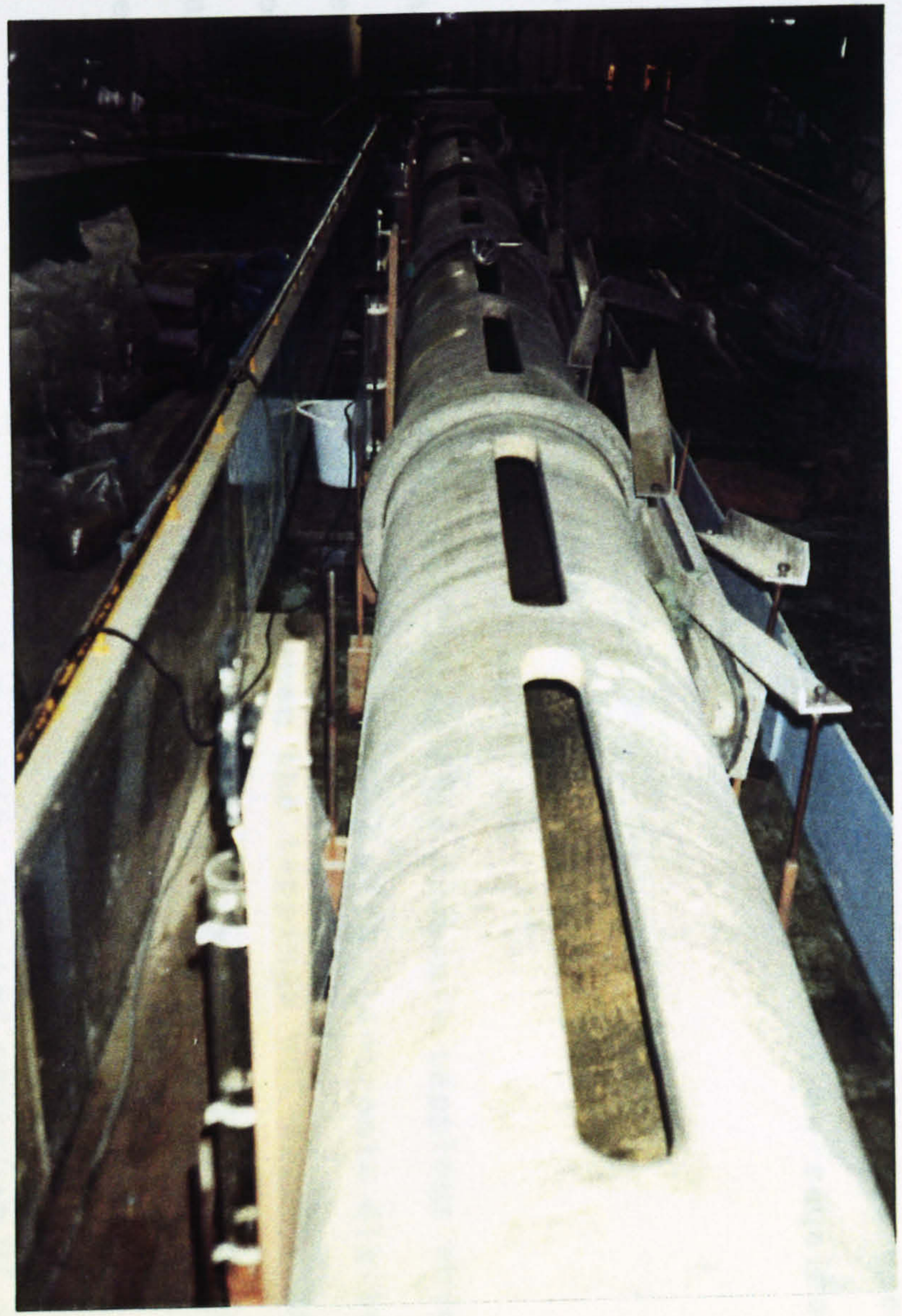

PLATE 4.5 General view of test pipe: D = 450mm

The flow restrictors, made up of two vertical plates, were used to act as tail gates at the downstream end to allow required adjustment for the flow uniformity.

4.3.2 Measurement Techniques

The water levels were measured using five pressure tappings which were connected to stilling wells equipped with electronic digital point gauges. The interval between the tappings was 2.50m. The tapping holes were made 200mm above the invert allowing the flow depths to be measured at half-full and above only.

A 1.22m wide rectangular thin plate weir, located upstream of the test pipe, was used to measure flow discharge from the three pumps using the following relationship:

$$Q_w = \frac{0.38927H_w^2 + 3.5217H_w - 1.5337}{1000} \qquad (4.6)$$

where Q_w is the flow rate over the weir in m^3/s and H_w is the head over the weir in cm. The slurry pump discharge, Q_p in m^3/s, was given by:

$$Q_p = (ECM - 2) \times 0.003065 \qquad (4.7)$$

where ECM is the electro-current meter readings in volts. The total discharge thorough the test pipe, Q (m^3/s), was given by the addition of Q_w and Q_p.

The pipe slope was varied by a mechanical jack connected to a digital counter reading. Calibration of the counter readings was made and the slope was calculated from:

$$S_p = 9.964 \times 10^{-6} \ FSCR - 0.00314 \qquad (4.8)$$

where FSCR is the counter reading.

The temperature was measured using a thermometer placed in the upstream tank. The kinematic viscosity was obtained from Eqn. 4.3.

4.3.3 The Sediments

4.3.3.1 Sediment Characteristics

The sediment used was a narrowly-graded sand with size ($=d_{50}$) 0.72mm and specific gravity of 2.62.

4.3.3.2 Sediment Supply and Discharge

The sediment was introduced in the hopper at the downstream end of the test pipe and recirculated by the slurry pump through the sediment return pipe to the head of the test pipe.

The sediment concentration was measured using an infra-red sensor attached on the outside of a 1m long perspex section of the sediment return pipe (see Fig. 4.4). The sensor mounted opposite the light source detected the signal which were modified by the

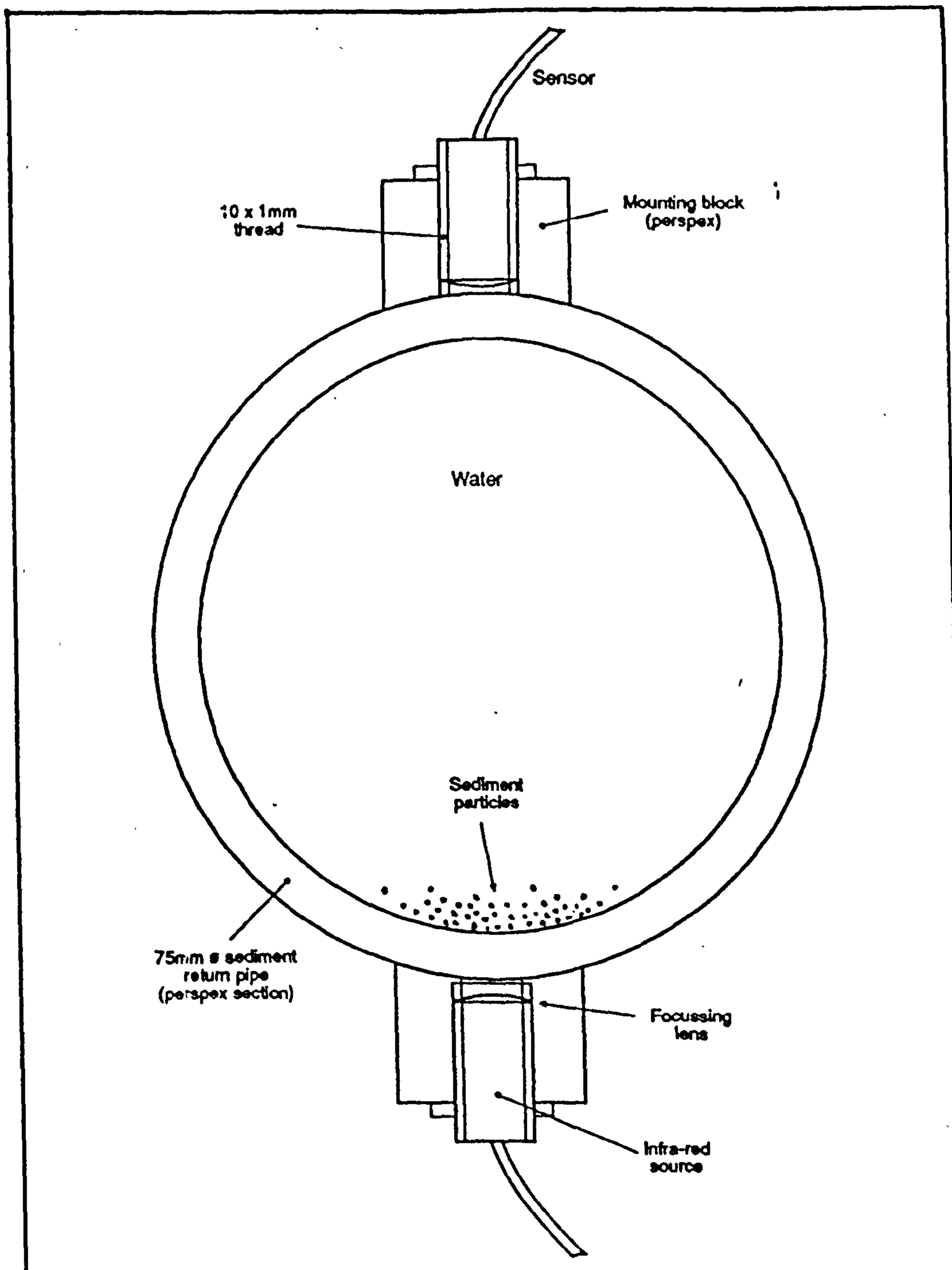

FIG. 4.4 Sediment sensor (After May 1993)

amount of sand passing along the pipe. The signals were fed to an amplifier unit which was connected through a voltage-converter to a counter.

Before the system could be used it was necessary to calibrate the infra-red sensor over a range of sediment concentrations and sediment return pipe velocities. The calibrations were carried out using a 2-litre plastic beaker, with holes of various sizes drilled in the base to allow a range of supply rates. The holes were initially taped over, and the beaker filled with a pre-weighed amount of sands. It was then mounted over the hopper at the downstream end of the test pipe, with a funnel and vertical pipe to catch the sands from the beaker and carry it directly to the slurry pump intake. The sensor readings for clear-water conditions were recorded before introducing the sands into the sediment return pipe. Then with the sediment return pipe set at the required velocity, tape was removed from one or more holes, and a stop watch was started. Ten sensor readings were taken at intervals of 100s. The holes were then resealed and the stopwatch was stopped. The calibration curve for sediment return pipe at velocity of 1.39m/s is shown in Fig. 4.5. Using appropriate calibration curves, the sediment concentration in the test pipe could be determined.

4.3.4 Establishment of Uniform Flow

A series of clear-water tests were carried out to determine the hydraulic roughness of the test pipe, and also to improve the

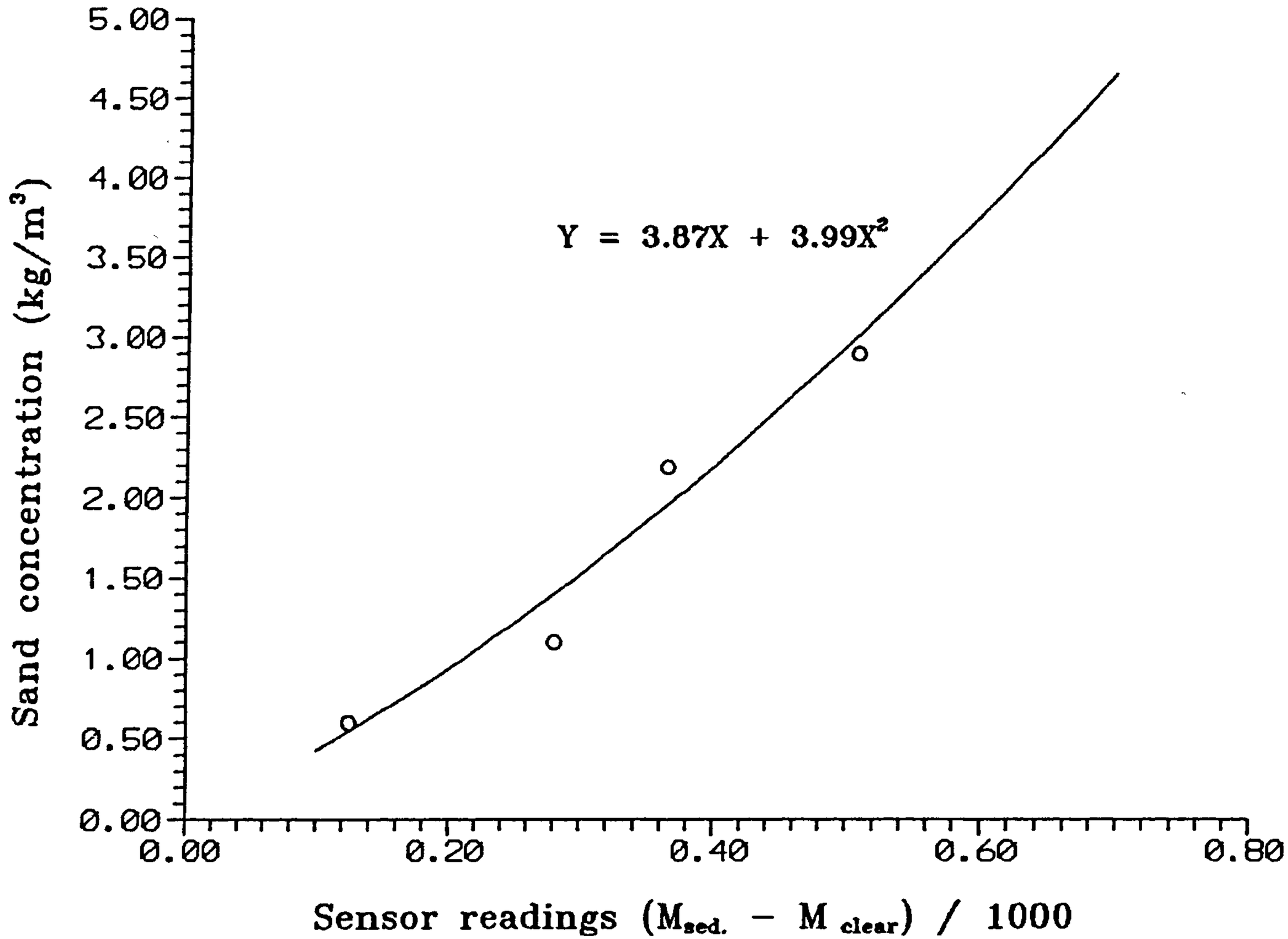

FIG. 4.5 Sediment discharge calibration curve

flow conditions at the upstream end. Initially the sediments were returned to the test pipe via a bend connected to the sediment return pipe. However, the bend restricted the flow at the upstream end of the test pipe. The bend was then replaced with a 600mm long semicircular channel (see Plate 4.6) such that a length of 150mm was inside the test pipe. The channel wall was also raised up to three-quarter of the test pipe diameter with the upstream end closed with a semicircular plate. This was to avoid any sands from escaping the channel and also as to function as the flow entrance to the test pipe. The channel was supported by two PVC plates which were fixed to the floor of the flume.

The clear-water tests were conducted at flow depths of half-full and three-quarter full. For each depth tested, the required discharge was set up and the necessary adjustments of the pipe slope and the flow restrictors were made until uniform flow was obtained. The flows were considered uniform when the point gauge readings were within ± 2mm of the required depth. Any effect of flow non-uniformity was taken by applying Eqn. 4.4 to obtain the effective slope, S_o.

4.3.5 Experimental Procedure for Sediment Transport

4.3.5.1 Transport at the Limit of Deposition

A test section of two 2.52m long sections of the pipe located about 12m from the upstream end was chosen. The observations of the limit of deposition were made along this test section while

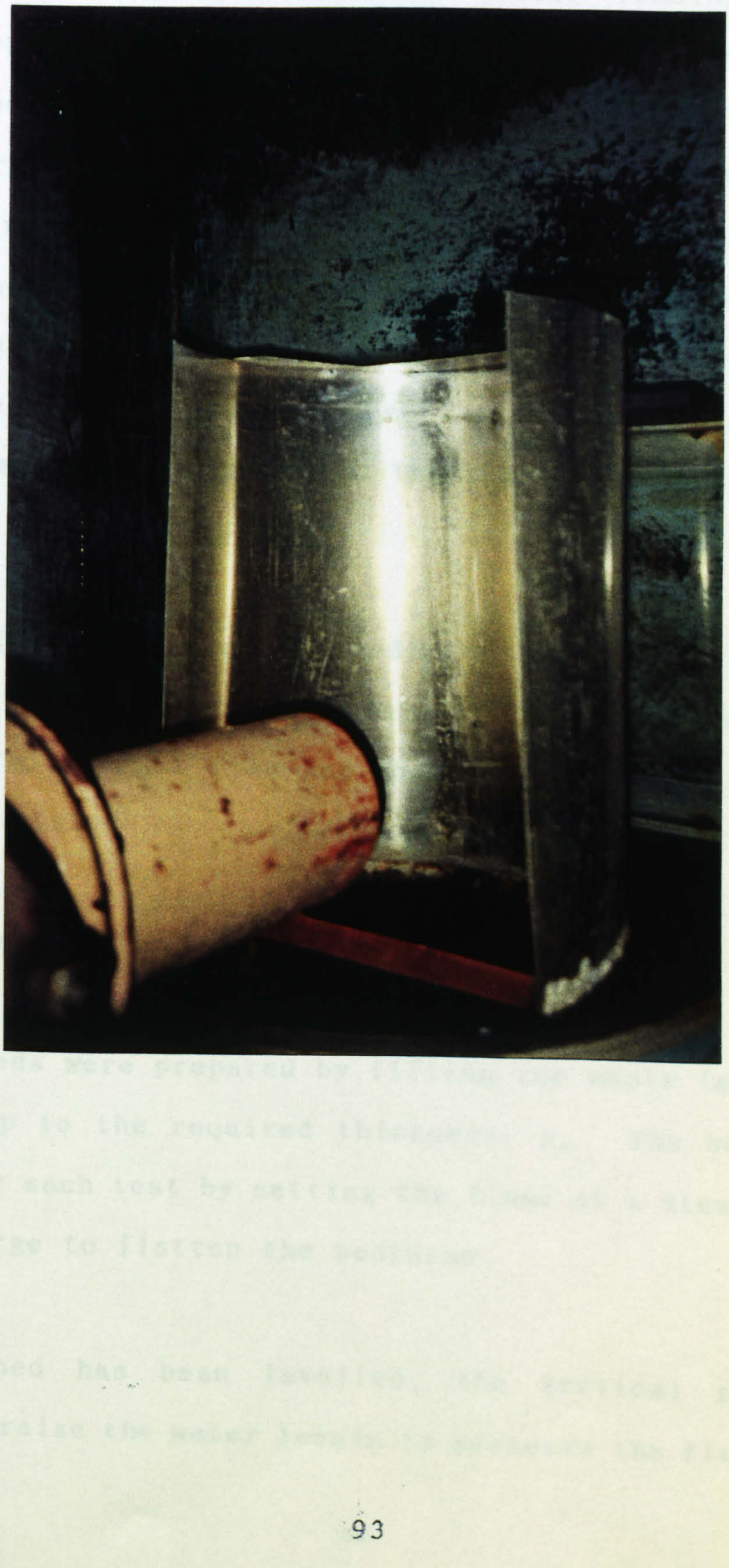

PLATE 4.6 Sediment channel return

the whole length of the pipe was always checked to ensure that local depositions especially at the joints did not occur.

Once the pipe slope and sediment sensor readings had been recorded for clear-water conditions, the sediments were gradually added to the hopper (see Fig. 4.3) until the limit of deposition had been reached. The transport rates up to the limit of deposition were monitored continuously from the sensor readings. At each sediment supply rate, the flow was taken to be at equilibrium when the sensor readings were constant. Once the equilibrium was obtained, observations were made at the test section to see if the flow was at the limit of deposition or not.

A series of 5-10 consecutive sediment sensor readings at 100 seconds interval were taken when the limit of deposition was reached. Two sets of flow depths were also taken between the sensor readings.

4.3.5.2 Transport over Loose Beds

The loose beds were prepared by filling the whole length of the test pipe up to the required thickness, y_s. The bed was then levelled for each test by setting the flume at a steep slope and high discharge to flatten the bedforms.

After the bed has been levelled, the vertical plates were adjusted to raise the water levels to preserve the flat bed. The

flow discharge at the required flow conditions (depth and velocity) was then set. The flume slope and vertical plates were adjusted to obtain uniform flow. Due to the presence of bedforms, the criterion for uniform flow was set at ± 5mm of the required flow depth. It was observed that for low velocity (V= 0.5m/s - 0.7m/s), the criterion could be set at ± 2mm of the required flow depths.

Five sediment sensor readings were taken over 1000s intervals and flow depths were recorded between the sensor readings. Once all the readings had been taken, the downstream end was sealed by closing the vertical plates. The sediment pump and the flow pumps were shut down in that order.

The pipe was left overnight to drain followed by measurements of bedforms. Due to the disturbance of the sediment bed near the upstream and downstream ends of the pipe, the measurement of the bed width and /or thickness were made at each slot (see Plate 4.5) at 10cm intervals over the length of 10m between the first and last point gauges. The bed thickness was measured using a portable point gauge.

CHAPTER 5

PRELIMINARY ANALYSES

5.1 Flow Resistance

This section provides a brief introduction to experimental and theoretical works regarding flow resistance in open channels that is relevant to the present studies. These works can be found in standard textbooks such as Chow (1966), Schlichting (1979), Featherstone-Nalluri (1988), and Chadwick-Morfett (1993).

5.1.1 Clean Pipes

The flow resistance for open channel flows is usually expressed in terms of Darcy-Weisbach equation, developed for pipe-full flows, by replacing pipe diameter, D, with four times the hydraulic radius (4R):

$$S_o = \frac{\lambda V^2}{8gR} \qquad (5.1)$$

where λ is known as Darcy-Weisbach's friction factor. Another frequently used equation is the Manning equation:

$$V = \frac{1}{n} R^{2/3} S_o^{1/2} \qquad (5.2)$$

n being Manning's roughness factor.

An approximate relationship between λ and n could be obtained through Eqn. 5.1 and Eqn. 5.2 yielding:

$$n = \sqrt{\frac{\lambda}{8g}} R^{1/6} \qquad (5.3)$$

Nikuradse carried out extensive experimental work in smooth and rough pipes flowing full. His experimental results show distinctive flow regions: laminar, transition from laminar to turbulence, and turbulence (further divided into three zones - smooth turbulence, transitional turbulence, and rough turbulence). Later, by combining their theories of turbulent boundary layer flows with Nikuradse's experimental results, von Karman and Prandtl developed semi-empirical equations which were expressed as:

$$\frac{1}{\sqrt{\lambda}} = -2 \log \left(\frac{2.51}{Re \sqrt{\lambda}} \right) \qquad (5.4)$$

for smooth pipes, and

$$\frac{1}{\sqrt{\lambda}} = -2 \log \left(\frac{k}{3.7D} \right) \qquad (5.5)$$

for rough pipes where k is the linear roughness height.

Colebrook-White conducted experimental work for commercial pipes and developed a semi-empirical equation, verifying von Karman-Prandtl's equations, for the transitional zone of turbulence given as:

$$\frac{1}{\sqrt{\lambda}} = -2 \log \left(\frac{k}{3.7D} + \frac{2.51}{Re\sqrt{\lambda}} \right) \qquad (5.6)$$

Eqn. 5.6 is also applicable to the whole of the turbulent region for commercial pipes using an effective roughness value, k, determined experimentally for each type of pipe. For application to open channel flows, substitution of D = 4R into Eqn. 5.6 yields:

$$\frac{1}{\sqrt{\lambda}} = -2 \log \left(\frac{k}{14.8R} + \frac{2.51}{Re\sqrt{\lambda}} \right) \qquad (5.7)$$

where Re = 4VR/ν. It must be noted that Colebrook-White's Eqn. 5.6 or 5.7 necessitates iterative solution for λ. One of the direct solutions to the equation (Eqn. 5.6) was proposed by Barr as:

$$\frac{1}{\sqrt{\lambda}} = -2 \log \left(\frac{k}{14.8R} + \frac{5.1286}{Re^{0.89}} \right) \qquad (5.8)$$

after substituting D = 4R for application to open channel flows. Fig. 5.1a shows the cross-sectional geometry of the open channel flow in a clean pipe i.e. without sediment bed.

5.1.2 Pipes with Deposited Beds

The presence of a sediment bed in pipes (Fig. 5.1b) produces the composite resistance made up of the pipe wall and the loose bed

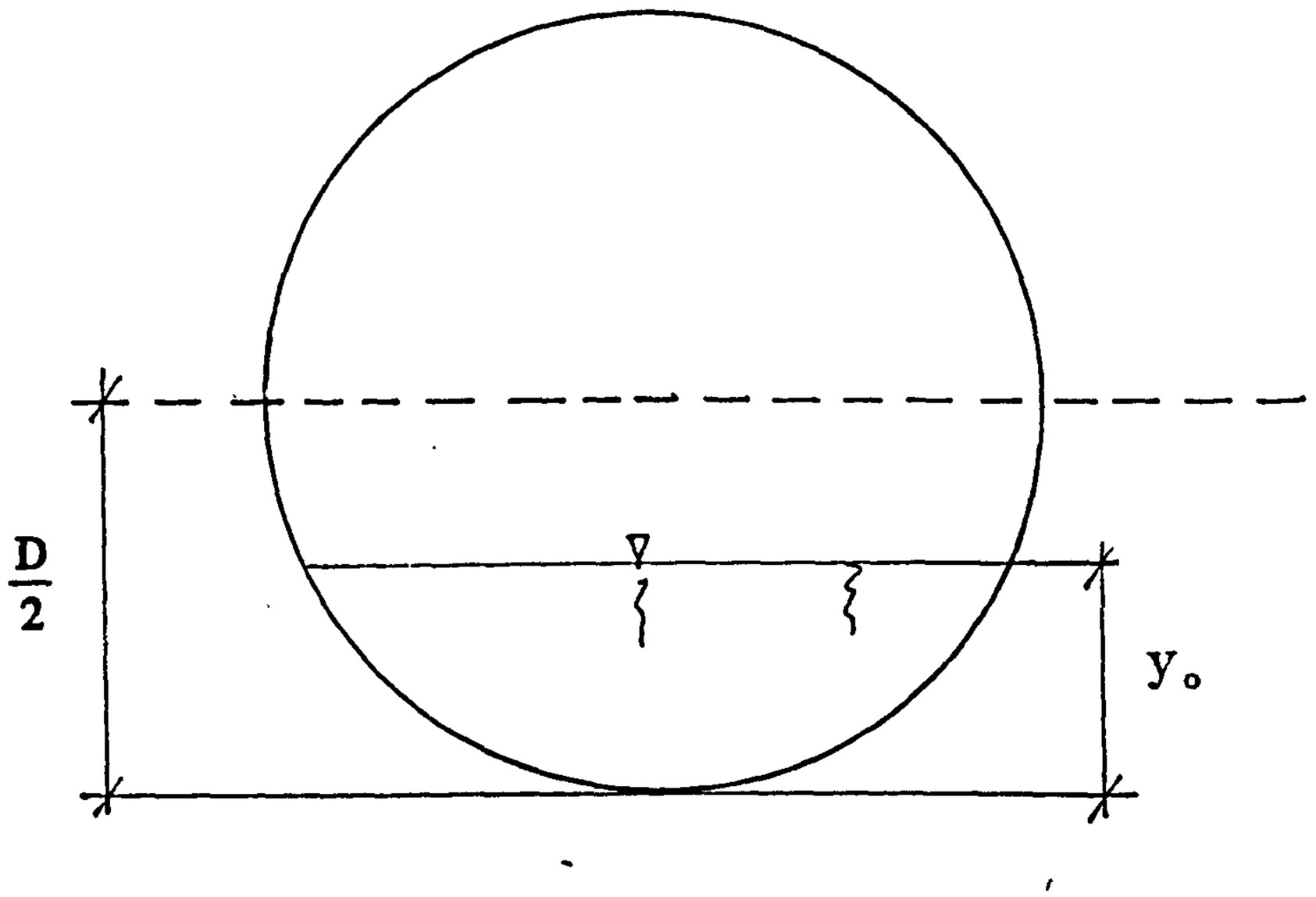

FIG. 5.1a Cross-sectional geometry for clean pipes

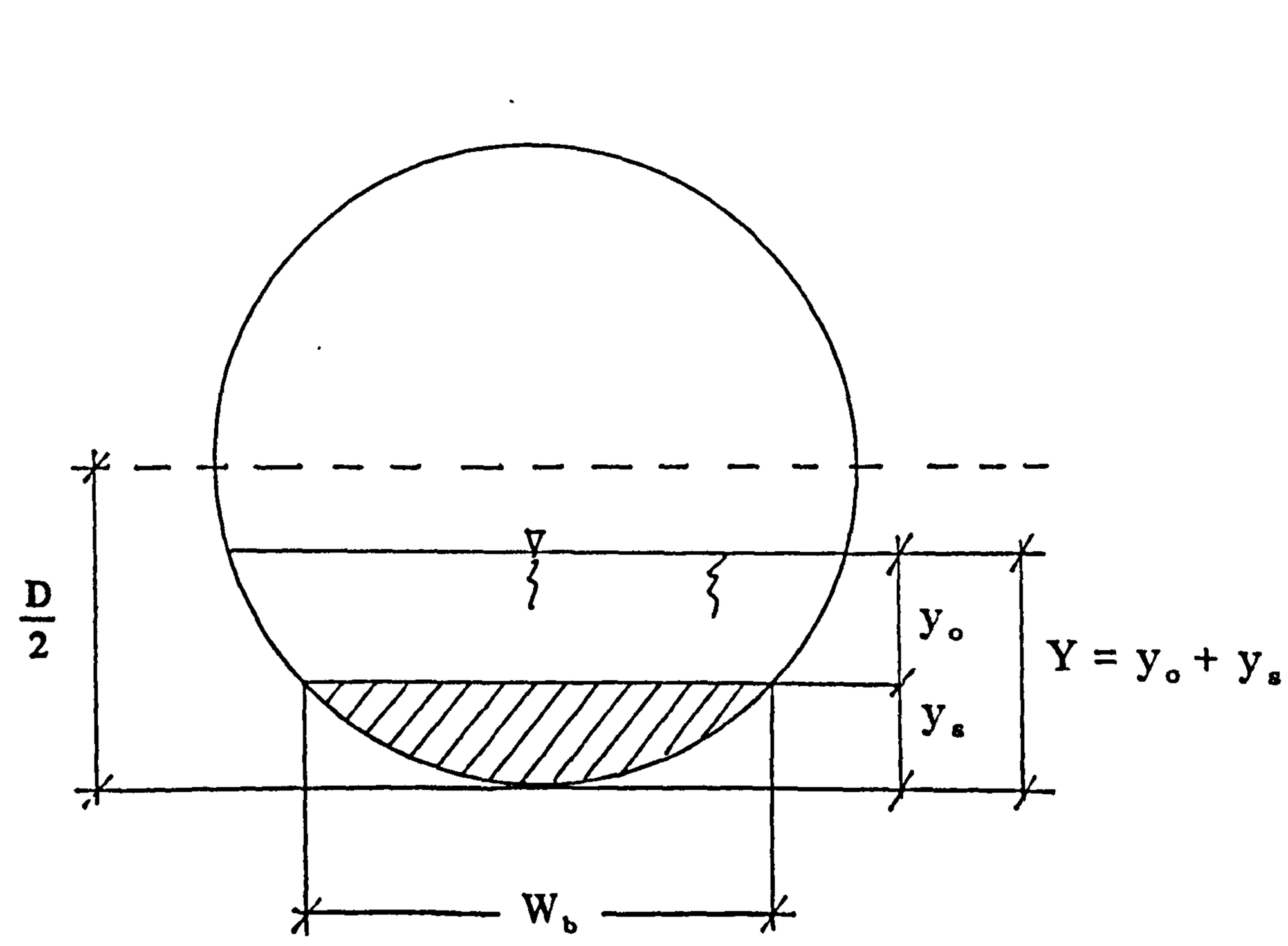

FIG. 5.1b Cross-sectional geometry for pipes with deposited beds

itself. CIRIA (1987) proposed an equation to compute the composite roughness based on the perimeter weighting of the linear roughness value, k:

$$k_s = \frac{P_{sb}k_{sb} + P_w k_w}{P_{sb} + P_w} \qquad (5.9)$$

where P is the wetted perimeter and k_s is the composite effective roughness. The subscripts 'w' and 'sb' refer to the pipe wall and the sediment bed respectively.

Another approach to compute the composite resistance was given by Visvalingam (see May 1993) based on perimeter weighting of shear stress:

$$\tau_s = \frac{P_{sb}\tau_{sb} + P_w\tau_w}{P_{sb} + P_w} \qquad (5.10)$$

where τ_s is the composite shear stress. Equation 5.10 could be transformed in terms of friction factor using Darcy-Weisbach equation:

$$\lambda_s = \frac{P_{sb}\lambda_{sb} + P_w\lambda_w}{P_{sb} + P_w} \qquad (5.11)$$

where λ_s is the composite friction factor.

5.2 Clear-Water Experimental Results - Pipe Wall Roughness

The data for all clear-water tests including those preceding transport tests are given in Appendix A. The details of the calculation of the flow cross-sectional geometry (Fig. 5.1a) are given in Appendix C. The summary of the conditions investigated is listed in Table 5.1.

A total of 345 experiments were conducted where 219 experiments were carried out in smooth clean pipes (D = 154mm, 305mm and 450mm) and the other 126 experiments were performed in rough clean pipes (D = 305mm) with two boundary roughness values of (= k_o) 0.53mm and 1.34mm (see Table 4.2, Section 4.2.4).

The friction factor without sediment, λ_o, was computed from the Darcy-Weisbach's Eqn. 5.1. The corresponding wall roughness, k_o, was obtained from the Colebrook-White's Eqn. 5.7. For comparison, values of Manning's n_o were also computed from Eqn. 5.2.

In general, the values of k_o and n_o were constant over the range of Reynolds numbers studied. The overall average values of k_o and n_o are given in Table 5.1. The present experimental results (see Table 5.1a) suggest that the smooth clean pipes flowing part-full have values of k_o and n_o in the range of 0.0mm - 0.2mm and 0.009 - 0.010 respectively. In the case of the rough clean pipes, the mean values of k_o (= 0.53mm and 1.34mm) are slightly higher than the particle sizes (d_{50} = 0.50mm and 1.0

TABLE 5.1 EXPERIMENTAL RANGES FOR CLEAR WATER DATA

a) SMOOTH CLEAN PIPES

D (mm)	154	305	450
V (m/s)	0.244 - 0.931	0.400 - 1.255	0.395 - 1.194
y_o/D	0.149 - 0.756	0.206 - 0.803	0.500 - 0.750
Re	$0.13x10^5$- $1.49x10^5$	$0.73x10^5$- $2.81x10^5$	$1.59x10^5$- $4.69x10^5$
Fr	0.49 - 1.30	0.32 - 1.51	0.23 - 0.91
S_o	$0.13x10^{-2}$- $0.51x10^{-2}$	$0.06x10^{-2}$- $0.53x10^{-2}$	$0.02x10^{-2}$- $0.30x10^{-2}$
R (m)	0.0142- 0.0465	0.0378- 0.0928	0.111- 0.136
k_o (mm)	0.169	-0.010	0.135
n_o	0.0098	0.0090	0.0103
λ_o	0.0176- 0.0426	0.0111- 0.0224	0.0147- 0.0204
NO. OF DATA	57	111	51

b) ROUGH CLEAN PIPES

D (mm)	305 (ROUGHNESS 1)	305 (ROUGHNESS 2)
V (m/s)	0.390 - 1.109	0.441 - 0.836
y_o/D	0.174 - 0.772	0.200 - 0.756
Re	$0.86x10^5$ - $2.78x10^5$	$0.62x10^5$ - $2.14x10^5$
Fr	0.28 - 1.22	0.38 - 1.02
S_o	$0.06x10^{-2}$ - $0.56x10^{-2}$	$0.10x10^{-2}$ - $0.56x10^{-2}$
R (m)	0.0324 - 0.0925	0.0368 - 0.0922
k_o (mm)	0.53	1.34
n_o	0.0111	0.0127
λ_o	0.0188 - 0.0322	0.0272 - 0.0458
NO. OF DATA	90	36

respectively) used to create the artificial rough boundaries. The corresponding values of Manning's n are 0.011 and 0.012 respectively. It should be noted that the values of k_o as calculated by Colebrook-White's Eqn. 5.7 are sensitive to the measured values of λ_o for the part-full pipe data. This may have resulted in higher average values of k_o. These average values of k_o and n_o are consistent with the suggested values for smooth (k_o = 0.0mm, n_o= 0.010) and rough (k_o = 1.5mm, n_o= 0.012) clean pipes used by Ackers (1984) and Novak-Nalluri (1987) in assessing the present design practice.

The plots of λ_o vs. Reynolds number are shown in Fig. 5.2 for smooth pipes and Fig. 5.3 for rough pipes. By applying the average values of k_o (see Table 5.1) for each set of data, pipe-full curves computed using Colebrook-White's Eqn. 5.6 were also shown on the plots for comparisons.

The results show that the measured values of λ_o tend to be scattered around the computed pipe-full curves. An examination of the ranges of Reynolds numbers for each boundary roughness shows that the experimental data fall within the transitional turbulent zone.

Fig. 5.4 tests the applicability of using Colebrook-white's Eqn. 5.6 for open channel flows in clean pipes by substituting D = 4R or Eqn. 5.7. Good agreements (correlation coefficient, r = 0.95) were obtained confirming the applicability of the Colebrook-White equation (Eqn. 5.7) for the present experimental data.

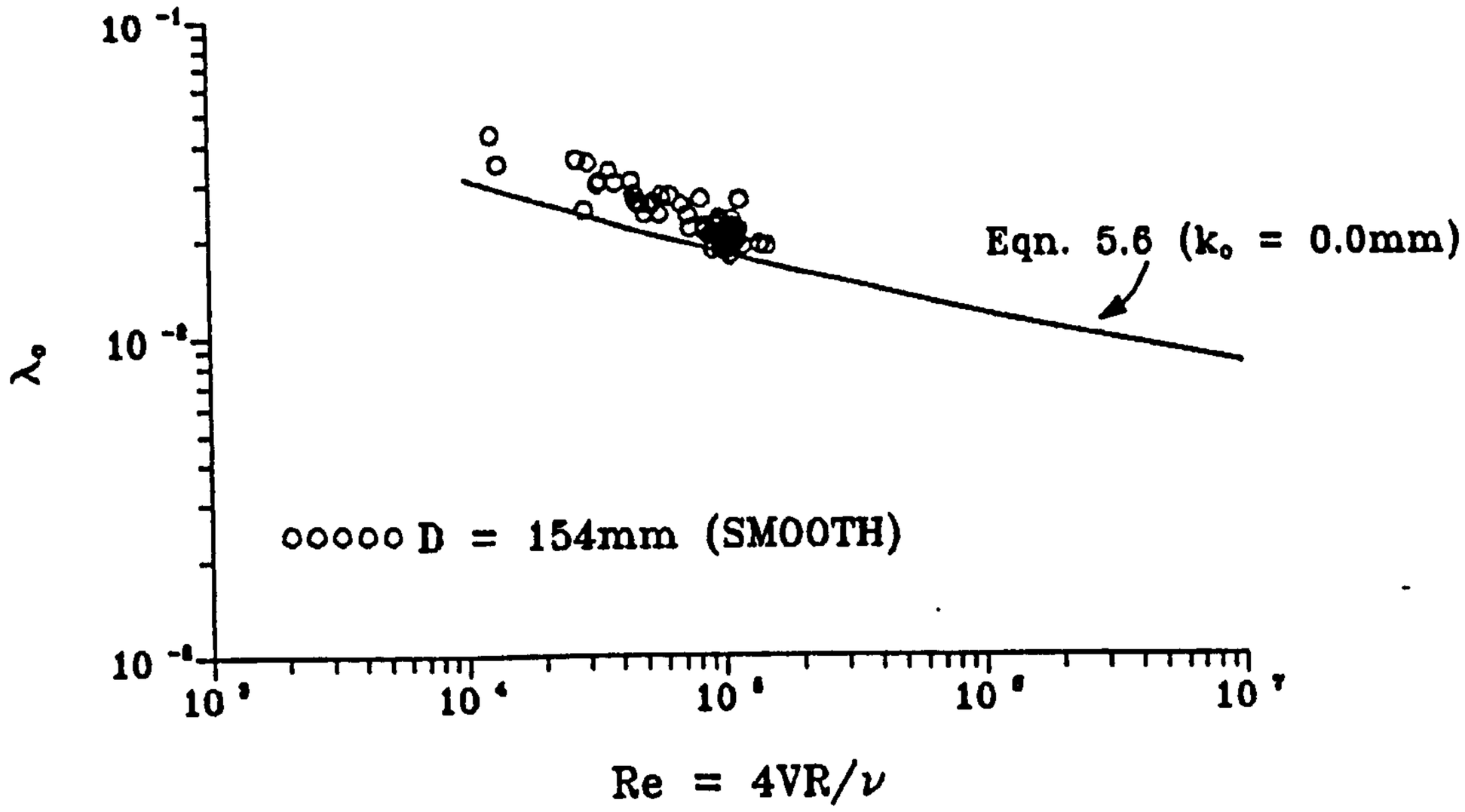

FIG. 5.2a Clear-water friction factor in a smooth 154mm dia. pipe

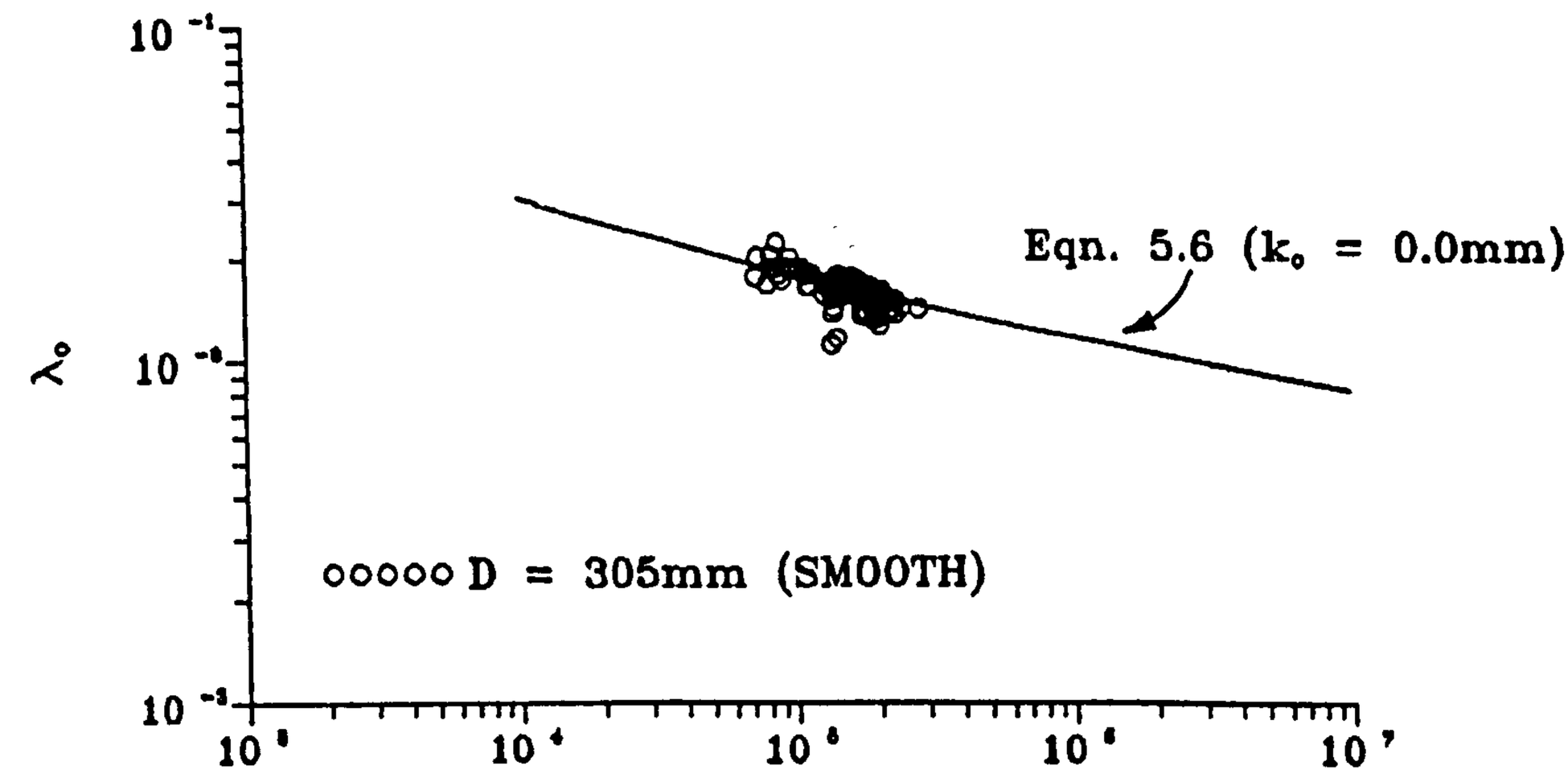

FIG. 5.2b Clear-water friction factor in a smooth 305mm dia. pipe

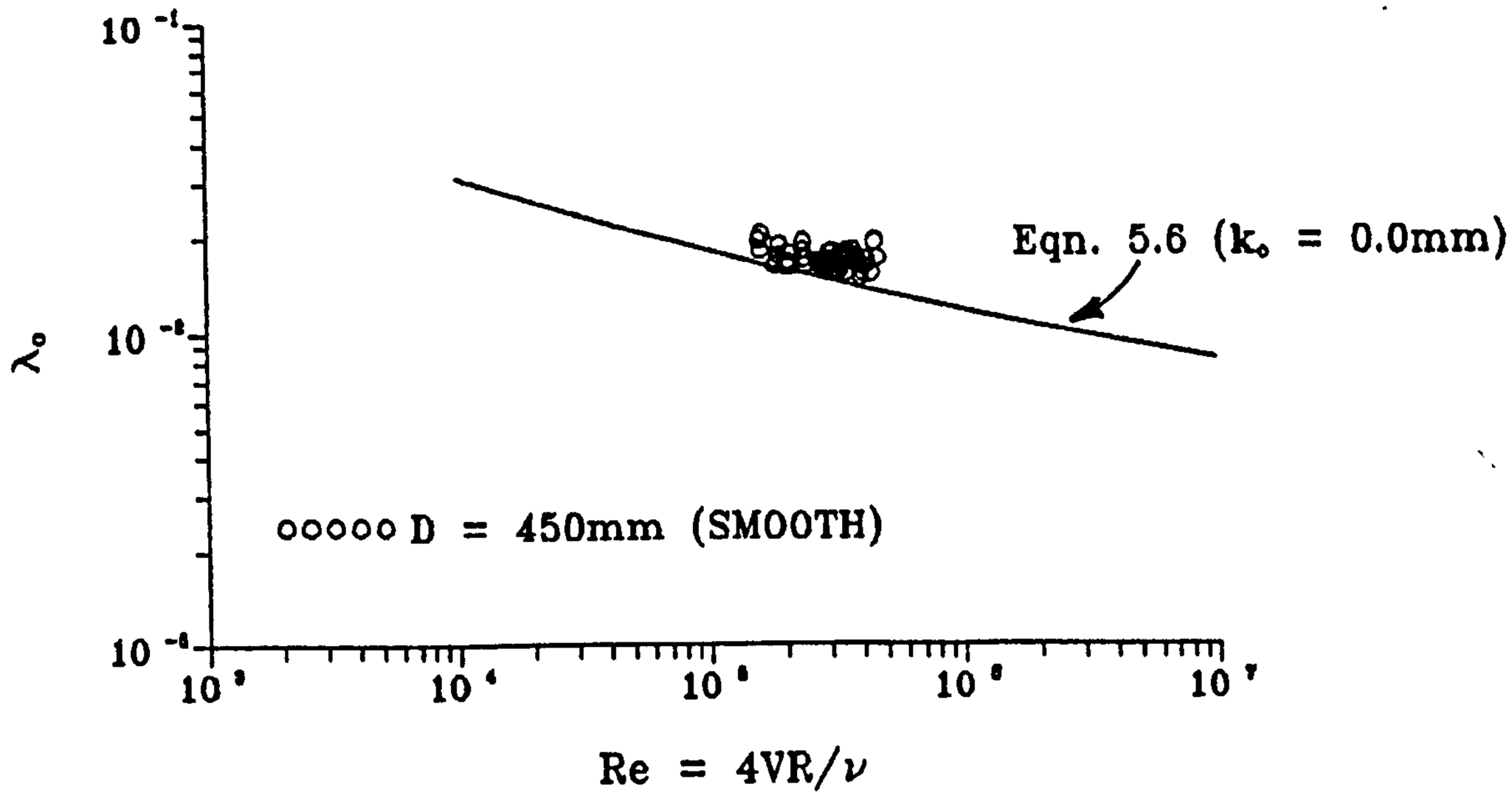

FIG. 5.2c Clear-water friction factor in a smooth 450mm dia. pipe

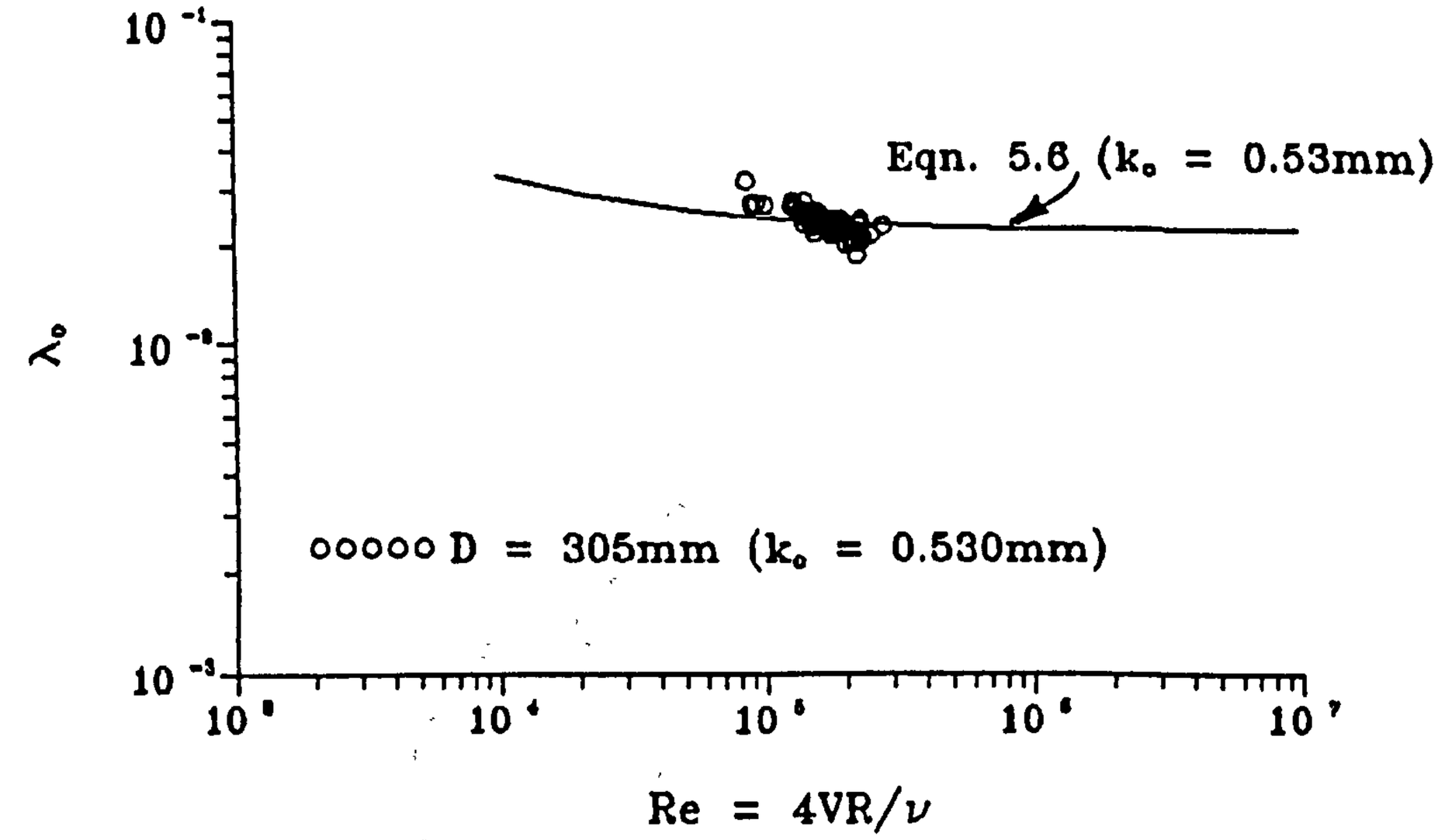

FIG. 5.3a Clear water friction factor in a rough 305mm dia. pipe (Roughness 1)

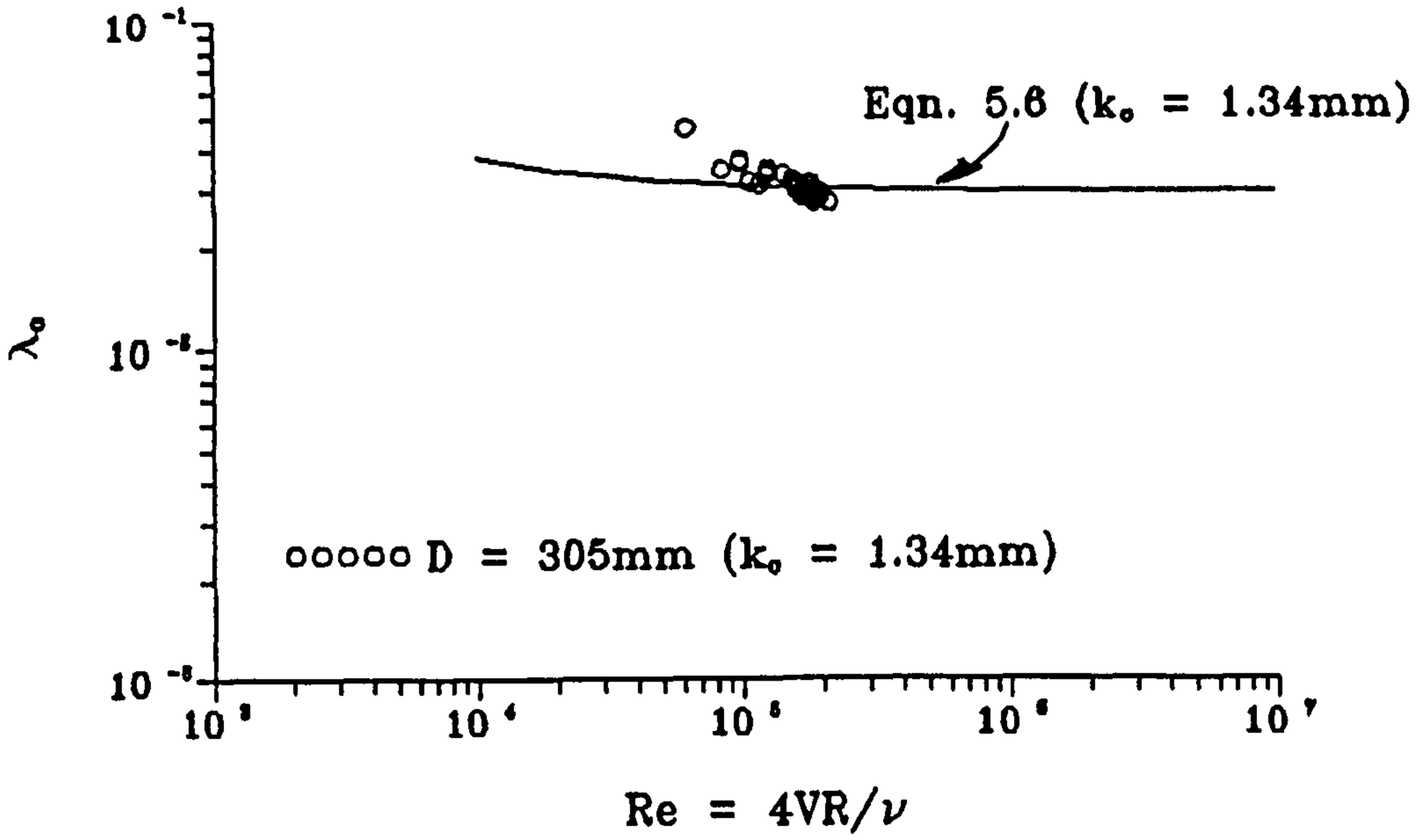

FIG. 5.3b Clear water friction factor in a rough 305mm dia. pipe (Roughness 2)

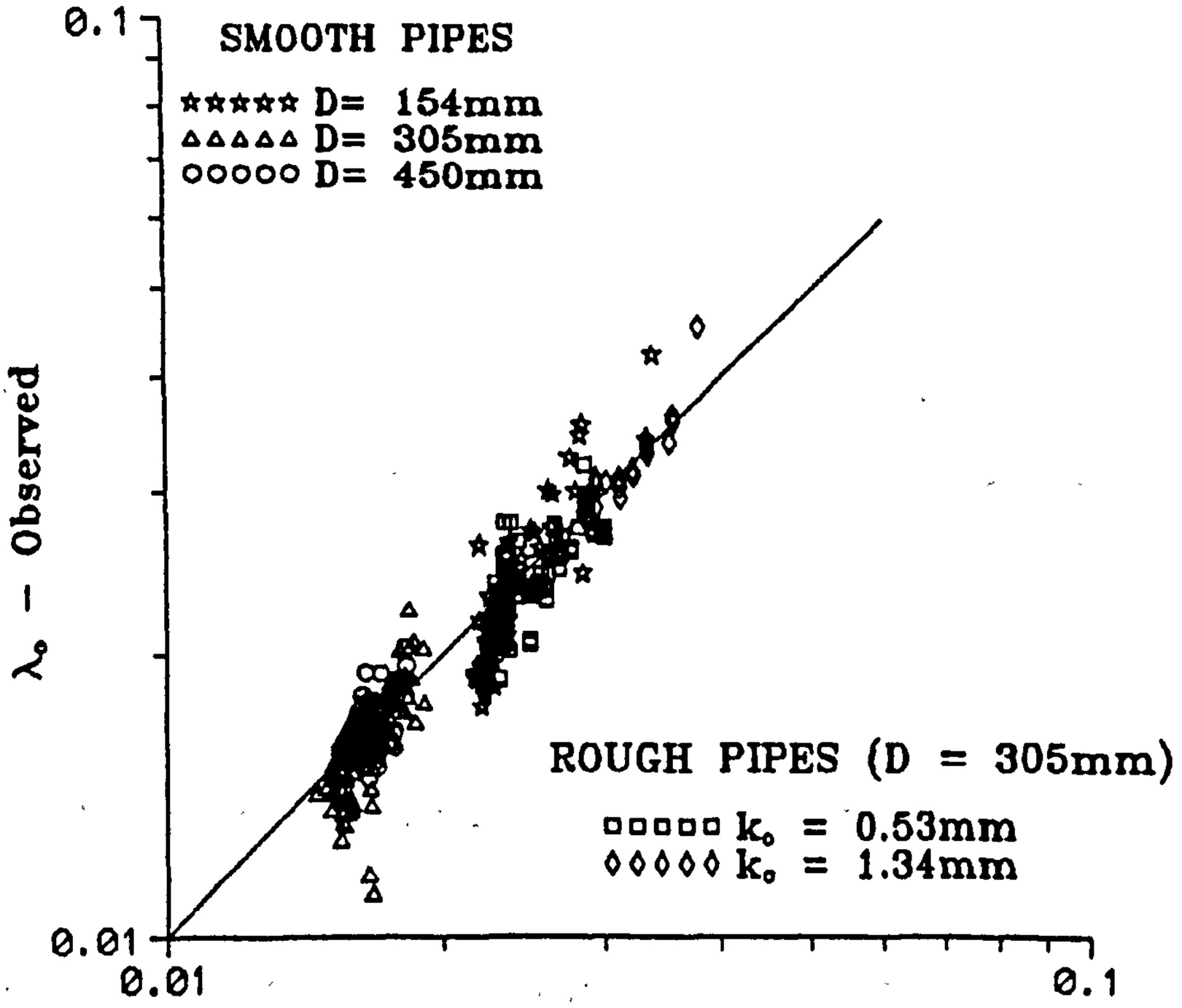

FIG. 5.4 Validity of the Colebrook-White's Eqn. 5.6 for present data (D = 4R)

5.3 Sediment Transport Experimental Results

The data for sediment transport experiments are presented in Appendix B. The summary of conditions investigated for clean pipes and pipes with sediment deposits is given in Table 5.2.

For clean pipes, 155 experiments were conducted in smooth pipes and the other 101 experiments were carried out in rough pipes. For pipes with sediment deposits, 43 experiments, of which 11 of them had been conducted earlier by the author (Ab. Ghani 1990), were performed in a 450mm dia. pipe over different sediment bed thicknesses.

Plots of volumetric sediment concentration (C_v) vs. total velocity (V) are made to identify the effects of sediment concentration, flow depth, sediment size, wall roughness and pipe size on the self-cleansing velocity of the flows at the limit of deposition. The effect of sediment deposits on the transporting capacity of the flow is also highlighted. Also shown are the effects of the presence of sediment in the flow on friction factor.

5.3.1 Effect of Sediment Concentration

In all plots of C_v vs. V (Figs. 5.5 to 5.13), it can be seen that the trend is for the velocity to increase with an increase in sediment concentration. The results highlight the need to take

TABLE 5.2 EXPERIMENTAL RANGES FOR TRANSPORT DATA

a) SMOOTH CLEAN PIPES

D (mm)	154	305	450
V (m/s)	0.240 - 0.862	0.395 - 1.205	0.502 - 1.216
y_o/D	0.153 - 0.757	0.210 - 0.800	0.500 - 0.750
Re	0.13×10^5- 1.43×10^5	0.87×10^5- 2.76×10^5	2.04×10^5- 4.60×10^5
Fr	0.49 - 1.10	0.32 - 1.47	0.28 - 0.93
S_o	0.13×10^{-2}- 0.53×10^{-2}	0.06×10^{-2}- 0.53×10^{-2}	0.04×10^{-2}- 0.31×10^{-2}
R (m)	0.0145- 0.0465	0.0384- 0.0928	0.112- 0.136
d_{50} (mm)	0.93 - 5.70	0.46 - 8.30	0.72
S_s	2.54 - 2.59	2.53 - 2.59	2.62
λ_s	0.0159- 0.0480	0.0129- 0.0206	0.0142- 0.0182
C_v (ppm)	38 - 1452	1 - 1280	2 - 37
NO. OF DATA	39	89	27

b) ROUGH CLEAN PIPES

D (mm)	305 (ROUGHNESS 1)	305 (ROUGHNESS 2)
V (m/s)	0.411 - 1.000	0.566 - 0.827
y_o/D	0.180 - 0.770	0.243 - 0.764
Re	0.89×10^5 - 2.52×10^5	0.98×10^5 - 2.10×10^5
Fr	0.30 - 1.20	0.38 - 1.00
S_o	0.07×10^{-2} - 0.56×10^{-2}	0.13×10^{-2} - 0.56×10^{-2}
R (m)	0.033 - 0.092	0.047 - 0.092
d_{50} (mm)	0.97 - 8.30	2.00 - 8.30
S_s	2.53 - 2.58	2.53 - 2.58
λ_s	0.0210 - 0.0316	0.0261 - 0.0392
C_v (ppm)	1 - 923	7 - 403
NO. OF DATA	71	30

TABLE 5.2 (CONTINUED)

c) PIPES WITH DEPOSITED BEDS - D = 450mm

y_s/D	< 1%	5%	12%	22%
V (m/s)	0.501 - 0.841	0.503 - 1.011	0.492 - 1.206	0.497 - 1.332
Y/D	0.50	0.50 - 0.75	0.50 - 0.75	0.50 - 0.75
Re	1.85×10^5 - 3.16×10^5	1.88×10^5 - 3.72×10^5	1.72×10^5 - 4.10×10^5	1.54×10^5 - 3.77×10^5
Fr	0.38 - 0.64	0.28 - 0.79	0.28 - 0.97	0.31 - 1.25
S_o	0.056×10^{-2} - 0.11×10^{-2}	0.088×10^{-2} - 0.34×10^{-2}	0.087×10^{-2} - 0.46×10^{-2}	0.069×10^{-2} - 0.43×10^{-2}
R (m)	0.1123	0.1089 - 0.1326	0.1011 - 0.1271	0.0834 - 0.1160
d_{50} (mm)	0.72	0.72	0.72	0.72
S_s	2.62	2.62	2.62	2.62
λ_s	0.0176 - 0.0210	0.0269 - 0.0371	0.0260 - 0.0581	0.0031 - 0.0644
C_v (ppm)	4 - 35	11 - 391	21 - 672	55 - 1269
NO. OF DATA	6	11	12	14

the sediment concentration into consideration in designing the required slope for sewers.

5.3.2 Effect of Flow Depth

Fig. 5.5 shows that for a given sediment concentration, a higher velocity is required for flows more than half-full over the range of sediment sizes tested. At high depths, this tendency may be attributed to the "crowning" effect of the pipe through the changes in velocity and shear distributions (Novak-Nalluri 1973, El-Zaemey 1991). The results clearly point out the important influence of shape effects, which are due to variation in flow depths, on the transporting capacity of the flows.

5.3.3 Effect of Sediment Size

Fig. 5.6 indicates that a lower velocity is required as sediment size increases for a given sediment concentration, especially for flows more than half-full. Coarser sediments are subjected to a higher drag due to their larger surface area exposed to the flow. Also, they tend to move less close to each other. This results in less interference between the coarse sediments which leads to higher drag acting on them. As a result a smaller velocity is needed to keep coarser sediments moving without deposition.

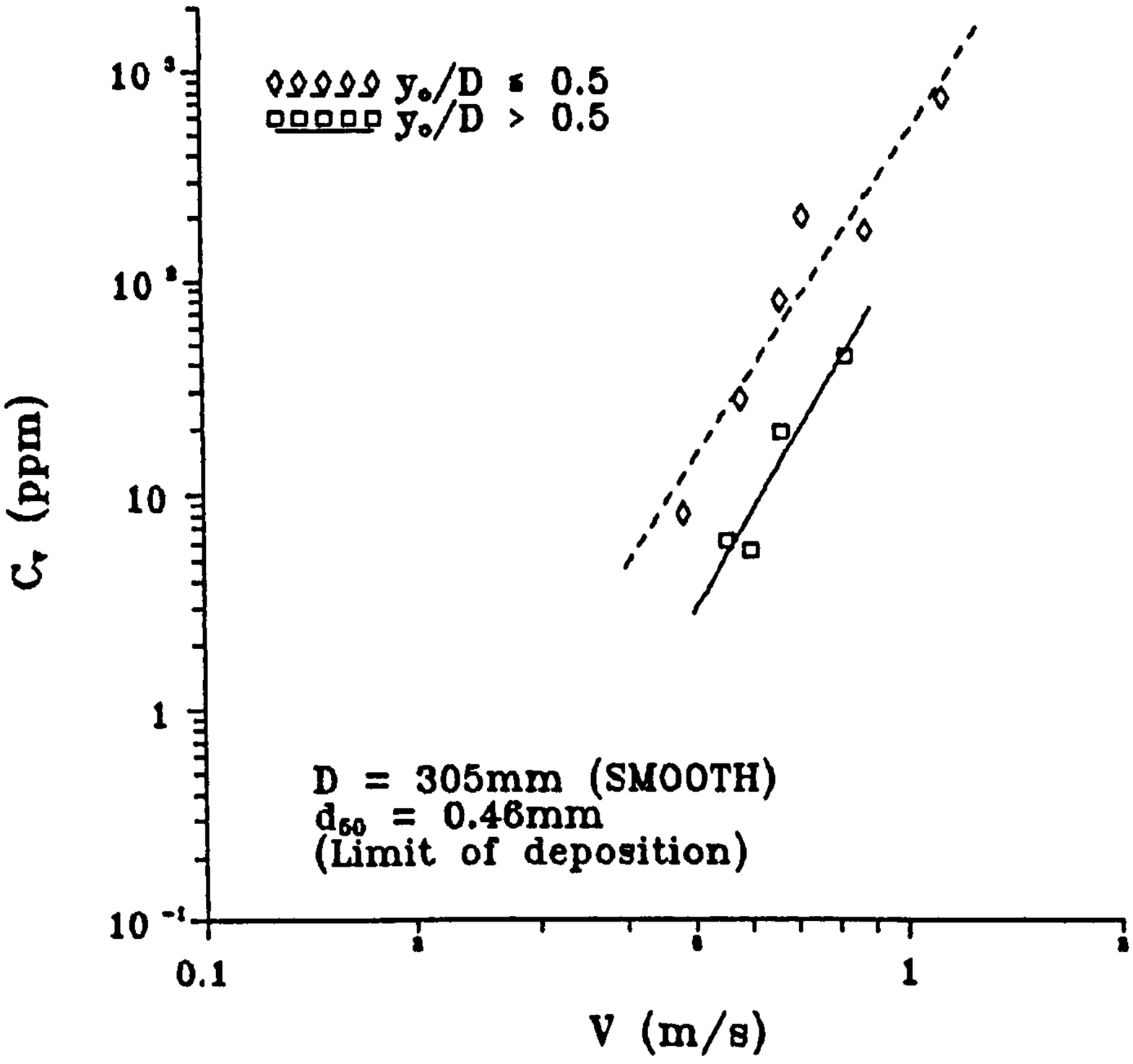

FIG. 5.5a Effect of flow depth – d_{50} = 0.46mm

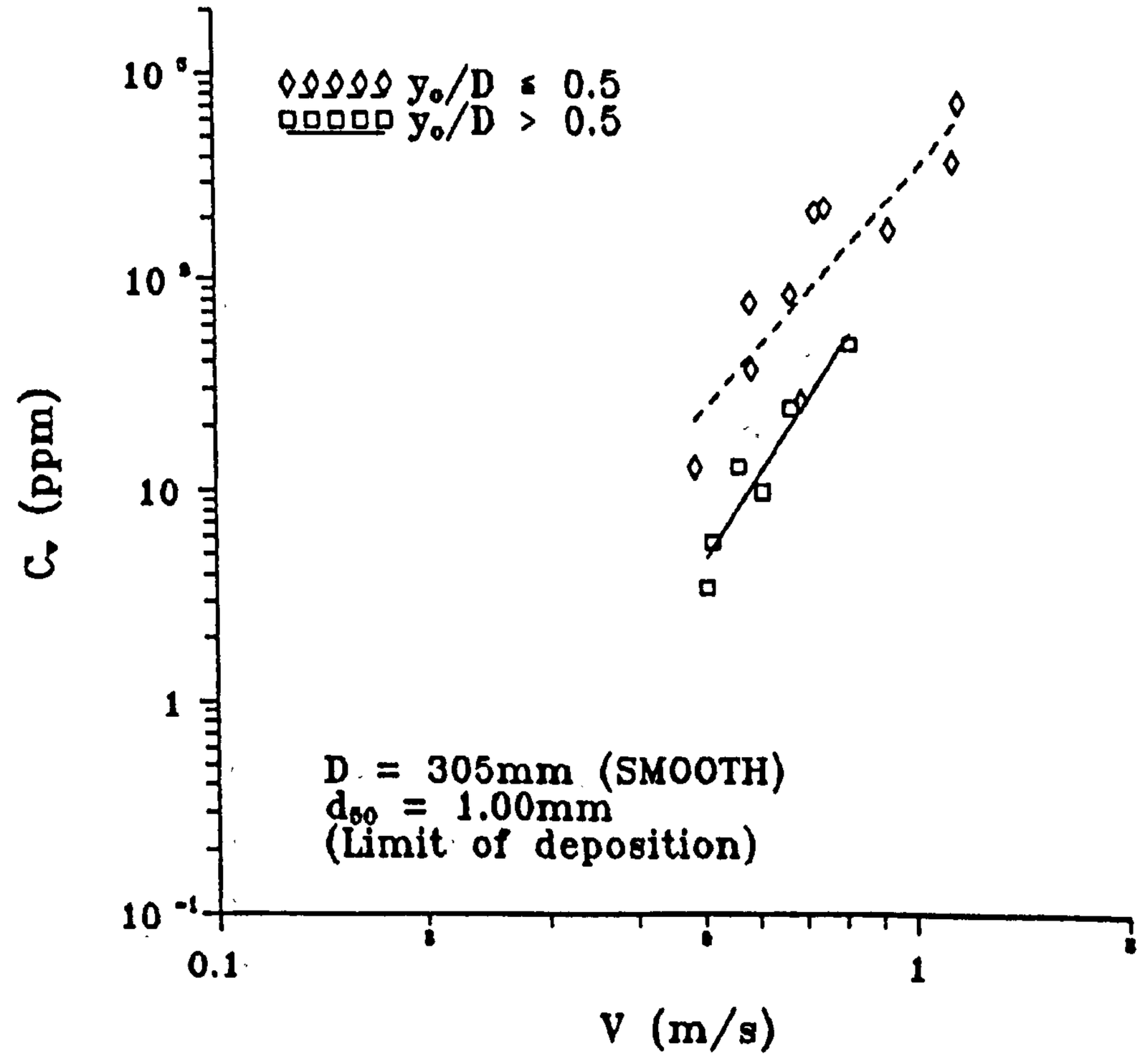

FIG. 5.5b Effect of flow depth – d_{50} = 1.0mm

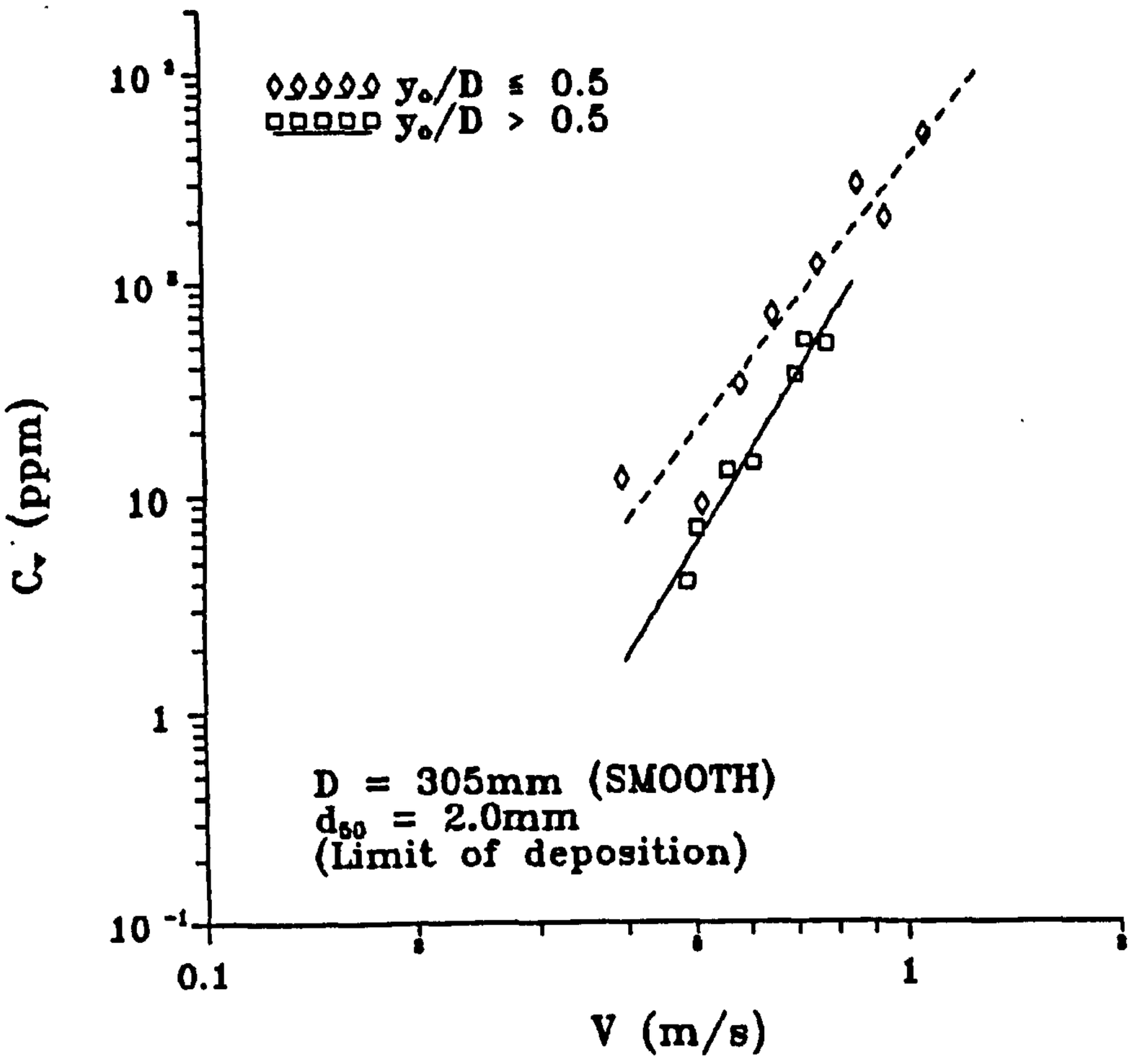

FIG. 5.5c Effect of flow depth – d_{50} = 2.0mm

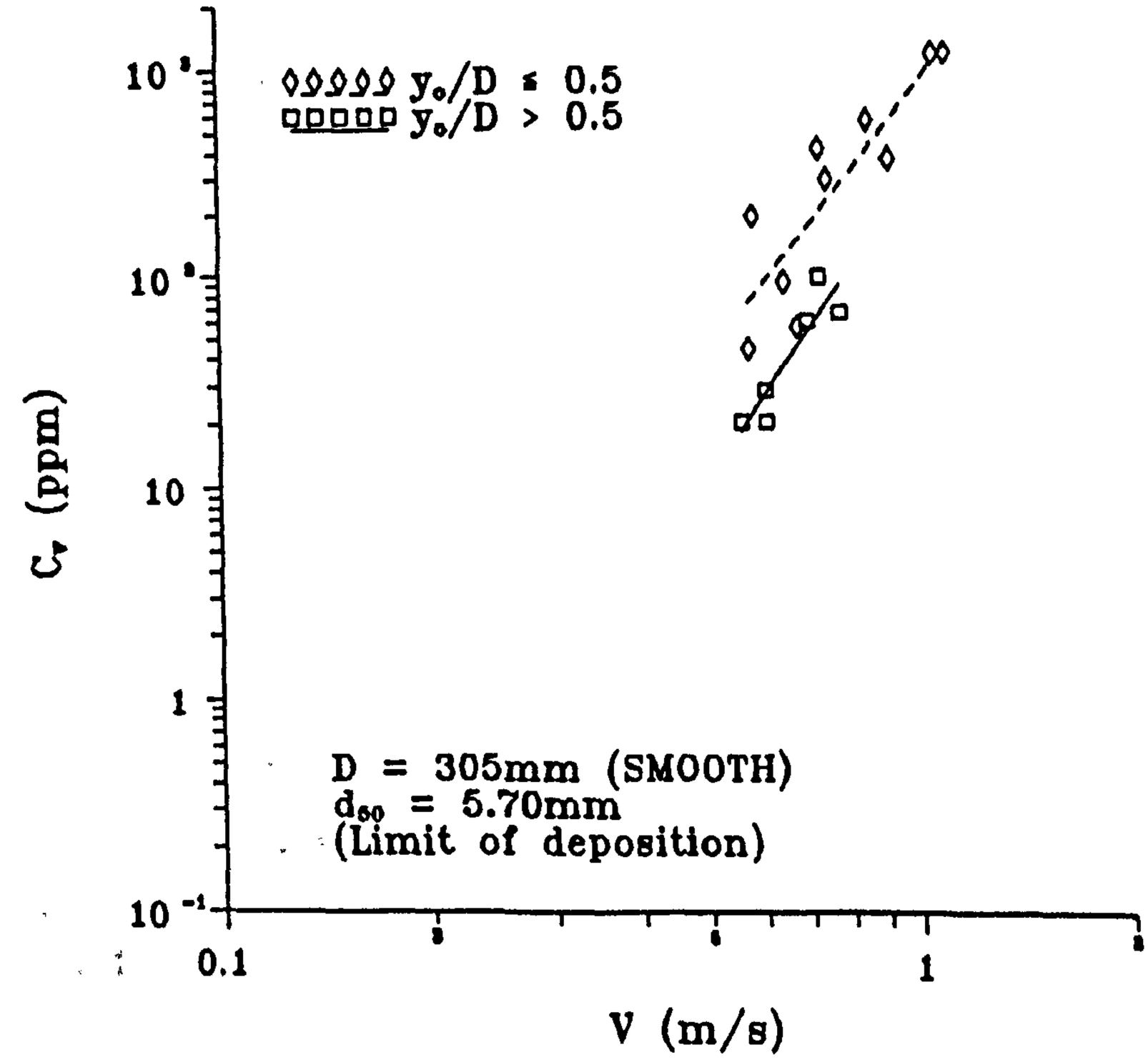

FIG. 5.5d Effect of flow depth – d_{50} = 5.7mm

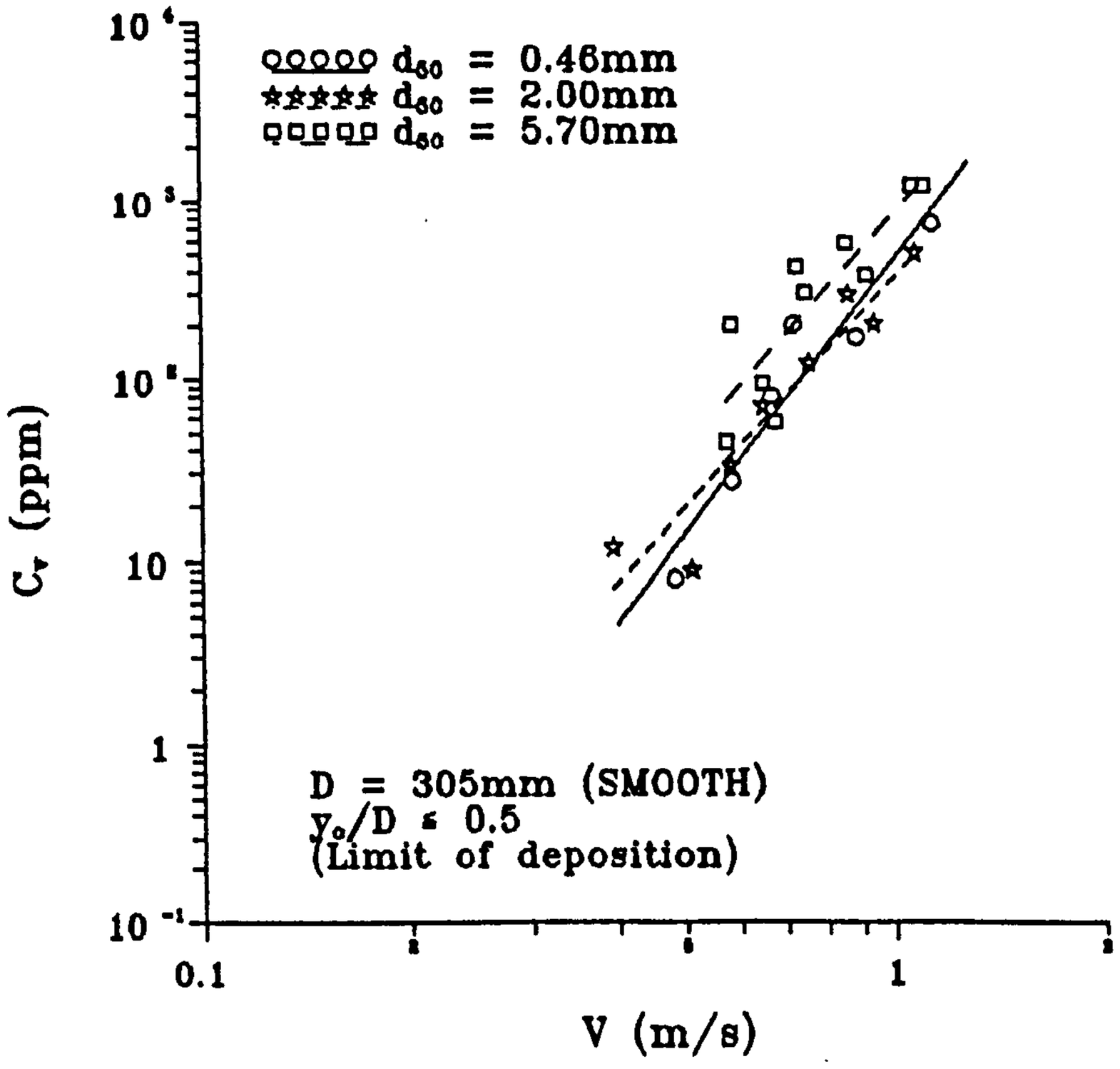

FIG. 5.6a Effect of particle size: flow depths up to half-full

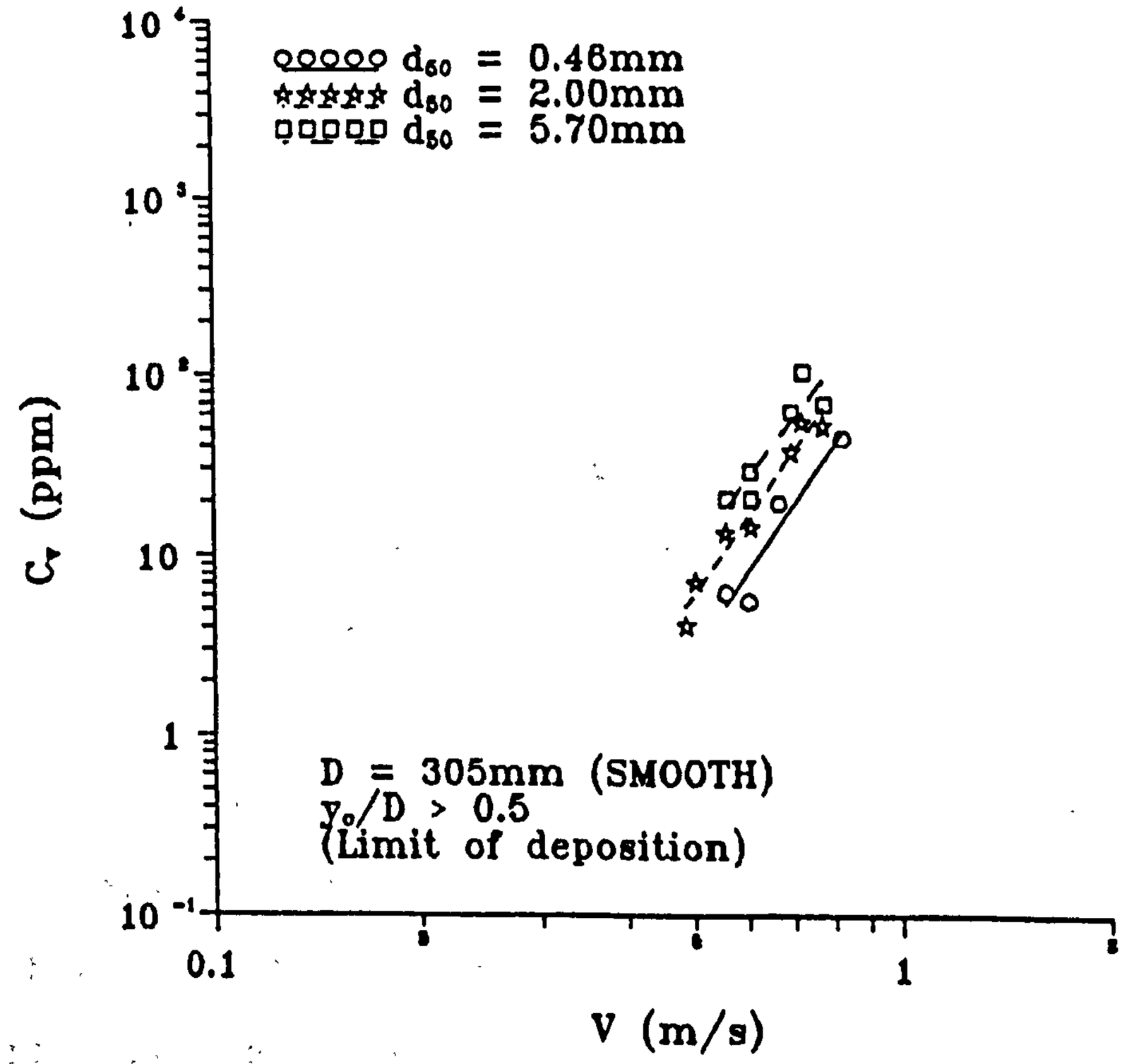

FIG. 5.6b Effect of particle size: flow depths more than half-full

5.3.4 Effect of Wall Roughness

The effect of wall or surface roughness on the self-cleansing velocity is shown in Figs. 5.7 to 5.10. It must be recalled that for experiments in rough clean pipes, the sediment sizes used as the transporting material are always larger than the boundary roughness height itself ($d_{50} > k_o$).

For the first wall roughness made up of 0.5mm sand size, the hydraulic roughness height was 0.53mm as given by the Colebrook-White equation. Therefore the transporting sediments used were in the range of 1.0mm to 8.3mm. Similarly for the second wall roughness, the 1.0mm sand used for the wall roughness resulted in the hydraulic roughness height of 1.34mm. Hence only sediment sizes in the range of 2.0mm to 8.3mm were used as the transporting materials.

The results as shown in Figs. 5.7 to 5.10 indicate that, over the range of sediment sizes tested, the experimental data for rough clean pipes seem to be scattered around those of the smooth clean pipes. There is no clear trend that the velocity will either increase or decrease with the increase in wall roughness.

Semi-empirical models for transport in rigid boundary channels (May 1982, Loveless 1991) point out that an increase in the wall roughness can be expected to be felt in two ways. Firstly, the coefficient of friction between the sediment and the wall increases with increasing surface roughness. Secondly, the flow

resistance is increased which reduces the drag acting on the sediments. Both of these effects will reduce the sediment transporting capacity of the flow for rough clean pipes, hence suggesting that a higher velocity is needed. Although it seems reasonable to assume an increase in velocity with the rigid boundary roughness is required, an increase in secondary currents in rough boundaries (El-Zaemey 1991) creating additional turbulence, may point in the opposite direction.

The results suggest that the effect of flow resistance on the self-cleansing velocity due to wall roughness should not be the sole consideration in designing the required slope. Rather other factors such as the increase in friction factor due to the presence of sediment in the flows (see Section 5.3.7) should also be considered.

5.3.5 Effect of Pipe Size

Fig. 5.11 shows that the limiting velocity required is higher for large pipes confirming the results interpolated from experimental works in small pipes (eg. May 1982, Mayerle 1988). Using a power regression, the best-fit line on the data collected in the 305mm dia. pipe which has the widest range of data is shown in Fig. 5.11. For comparison, parallel lines were also plotted for the data from the 154mm and 450mm dia. pipe. These lines show the existence of distinct regions depending on pipe diameter, hence

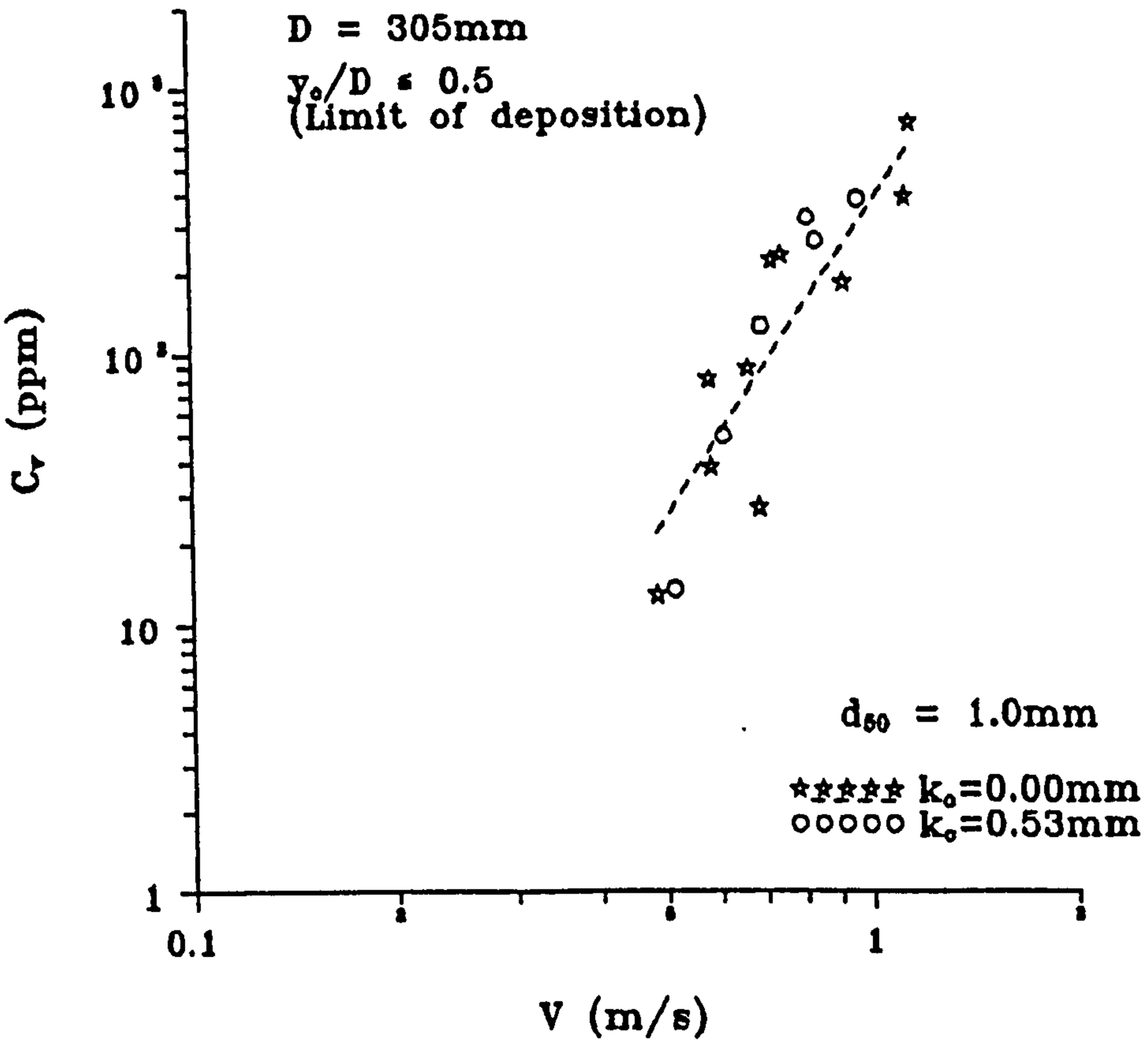

FIG. 5.7a Effect of wall roughness – d_{50} = 1.0mm
(Flow depths up to half-full)

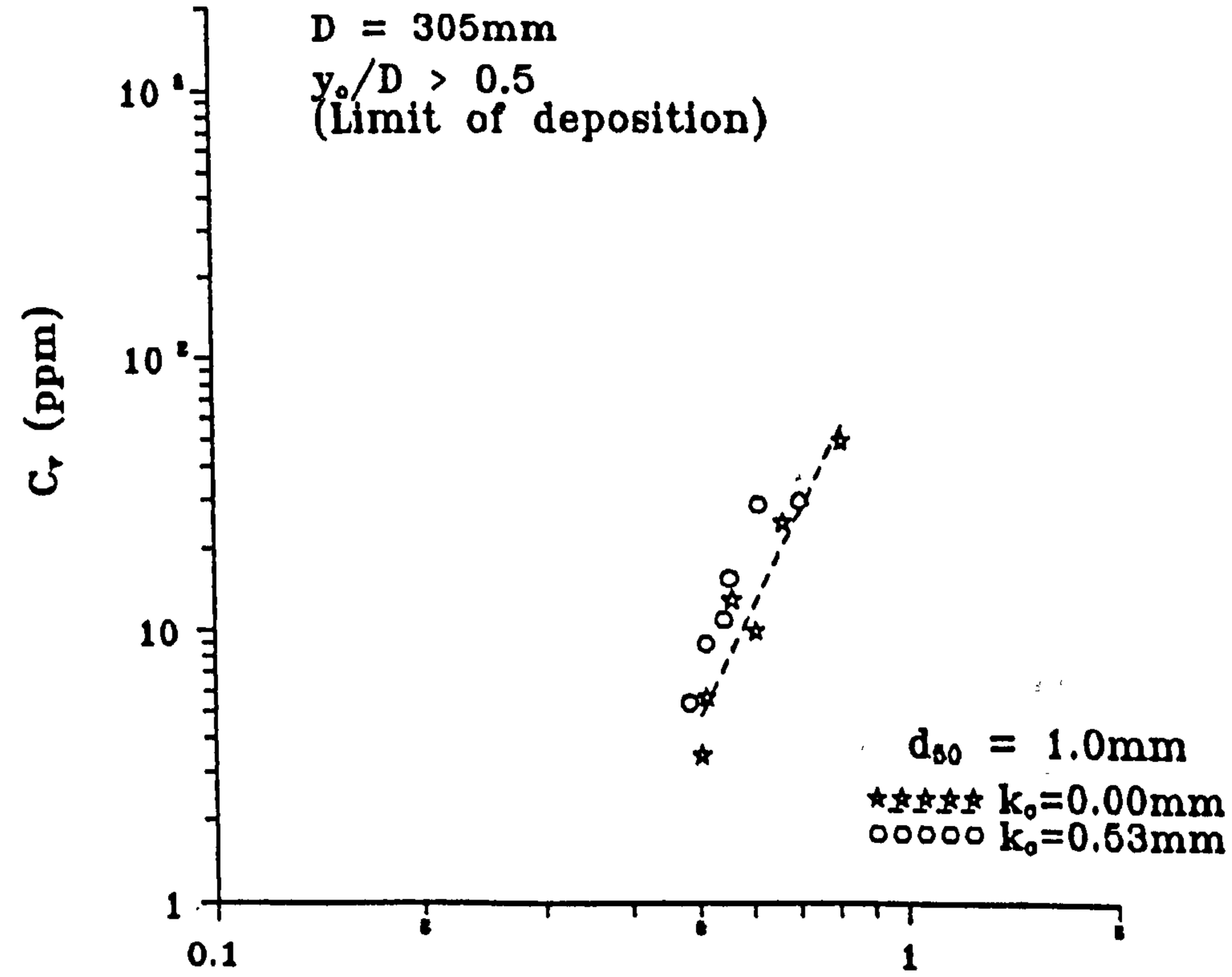

FIG. 5.7b Effect of wall roughness – d_{50} = 1.0mm
(Flow depths more than half-full)

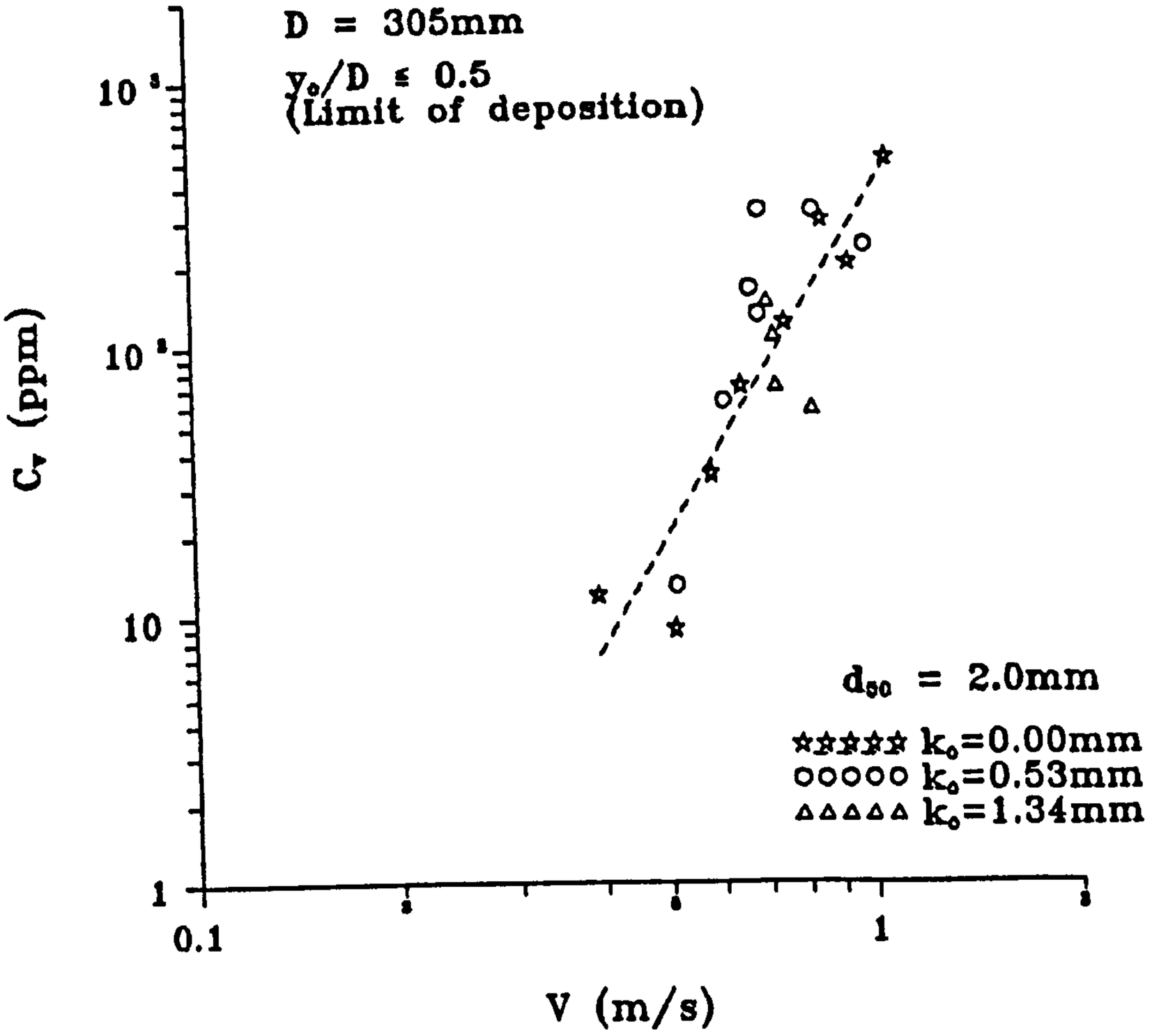

FIG. 5.8a Effect of wall roughness – d_{50} = 2.0mm (Flow depths up to half-full)

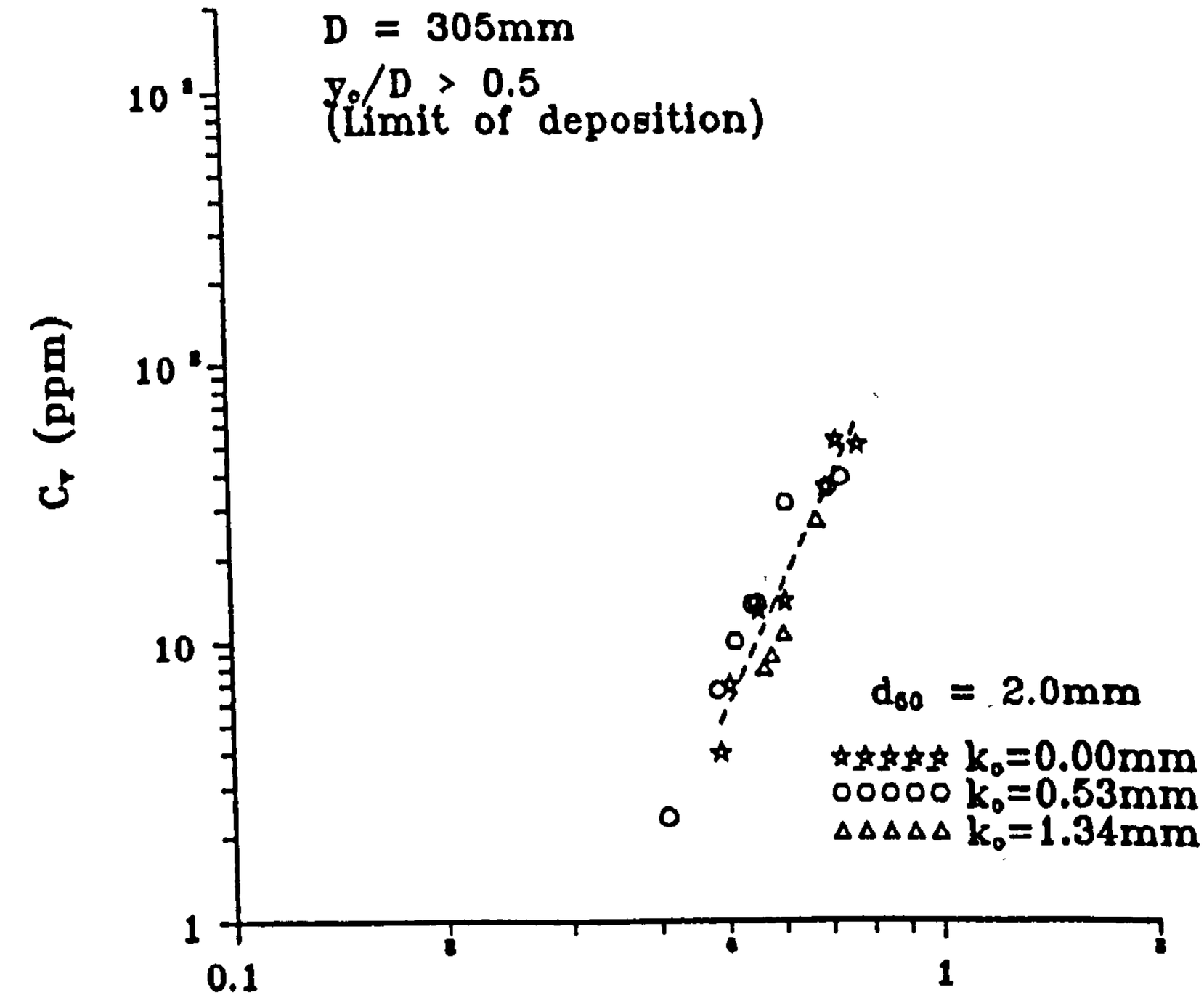

FIG. 5.8b Effect of wall roughness – d_{50} = 2.0mm (Flow depths more than half-full)

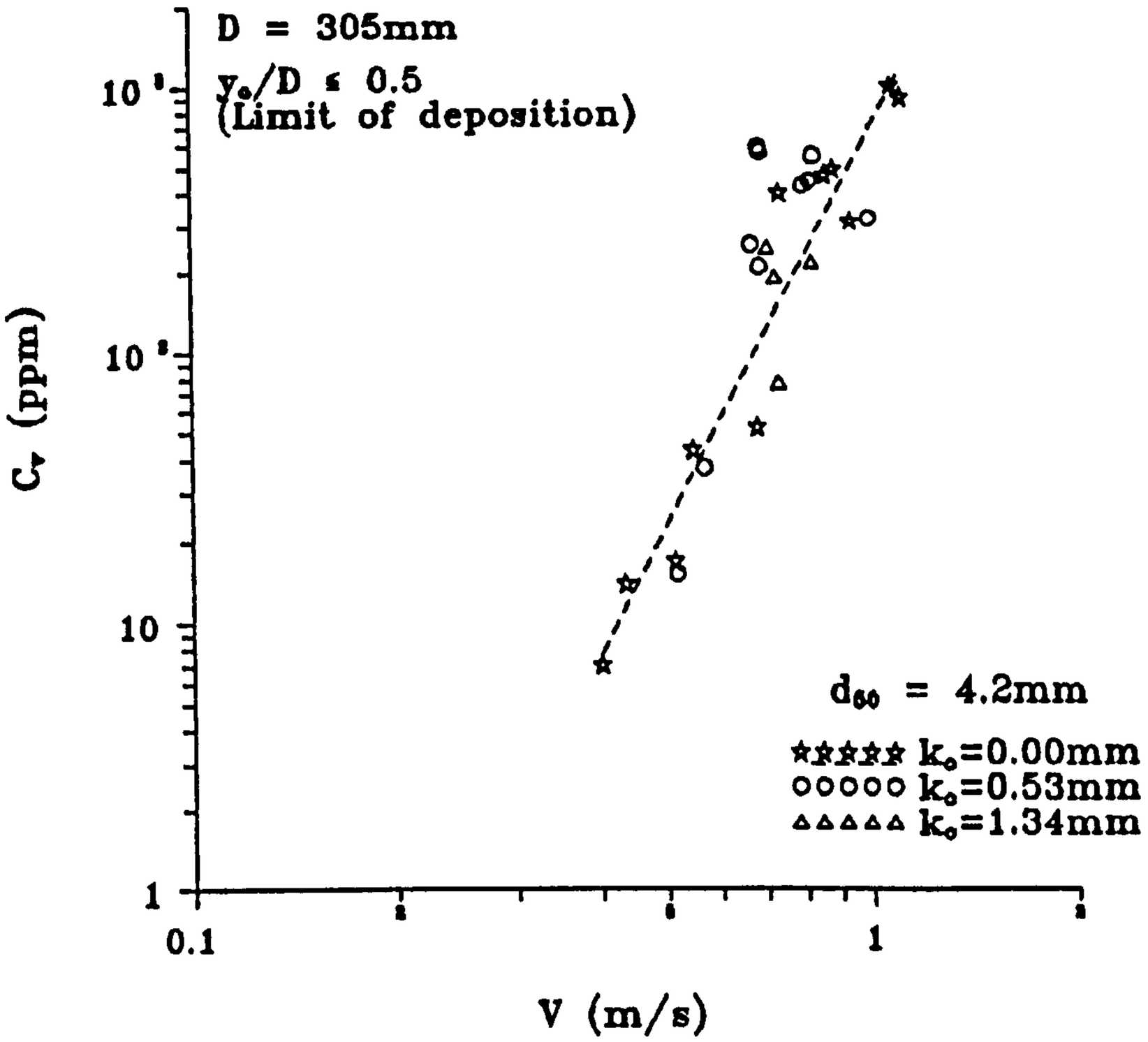

FIG. 5.9a Effect of wall roughness – d_{50} = 4.2mm
(Flow depths up to half-full)

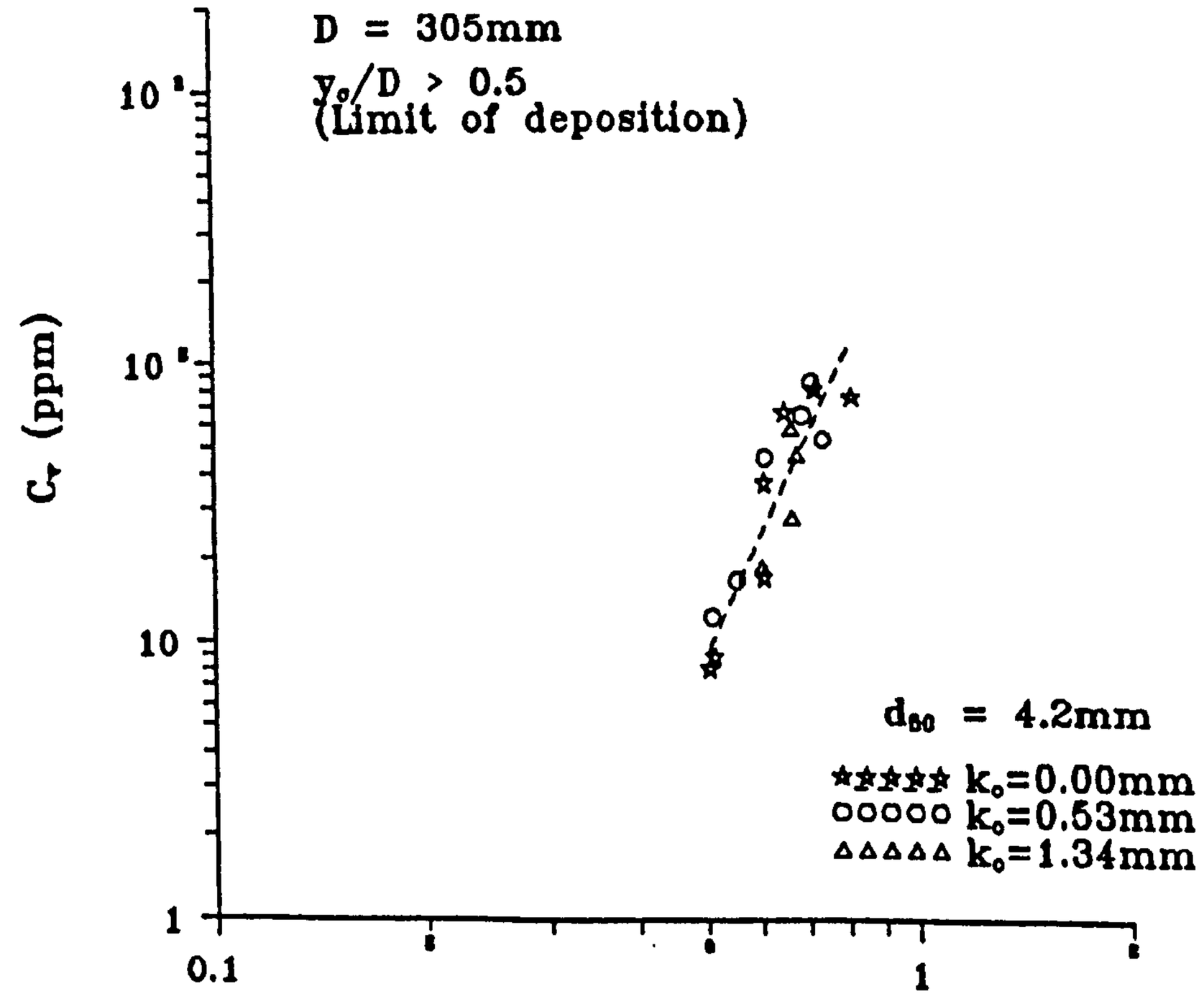

FIG. 5.9b Effect of wall roughness – d_{50} = 4.2mm
(Flow depths more than half-full)

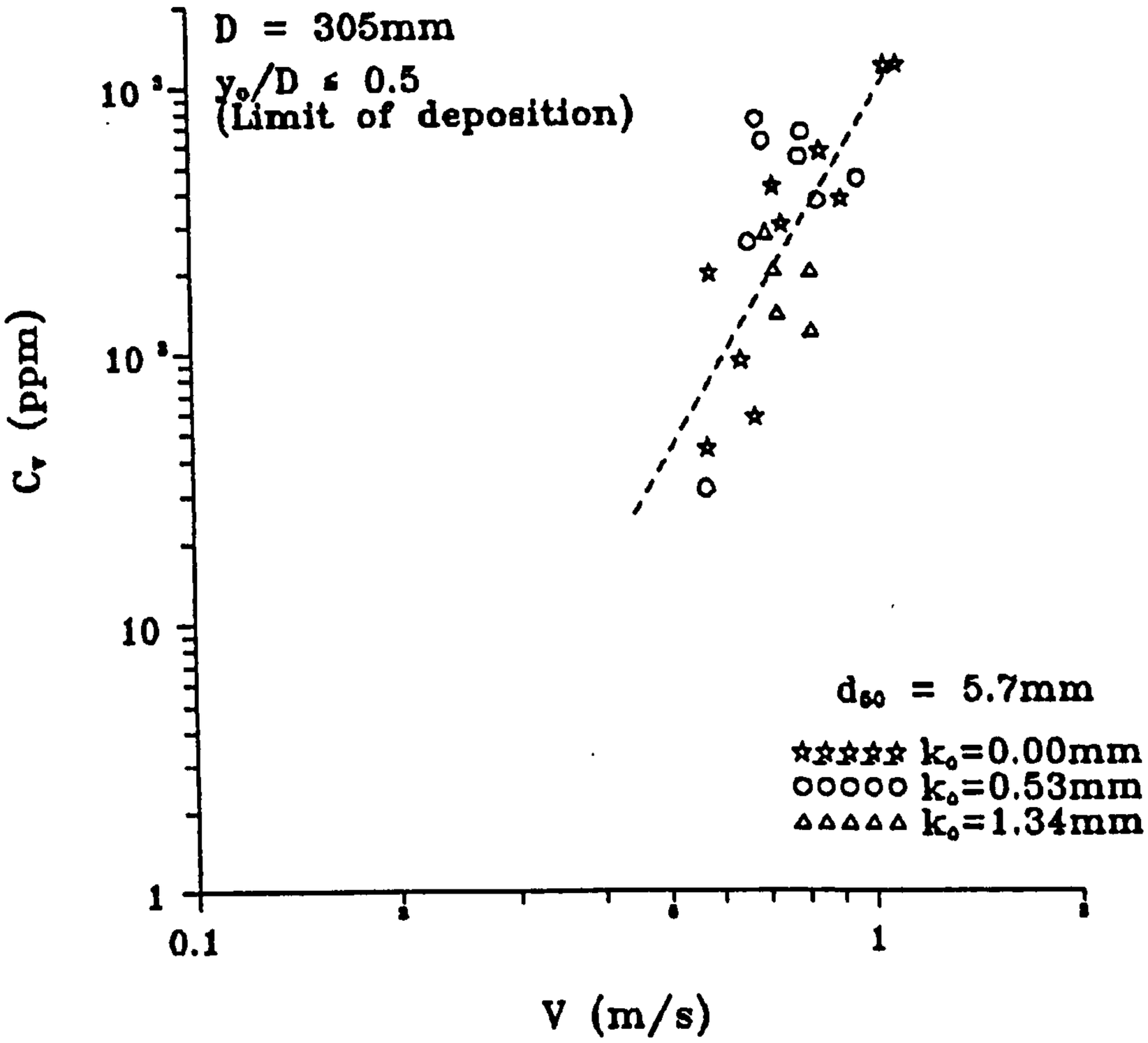

FIG. 5.10a Effect of wall roughness – d_{50} = 5.7mm
(Flow depths up to half-full)

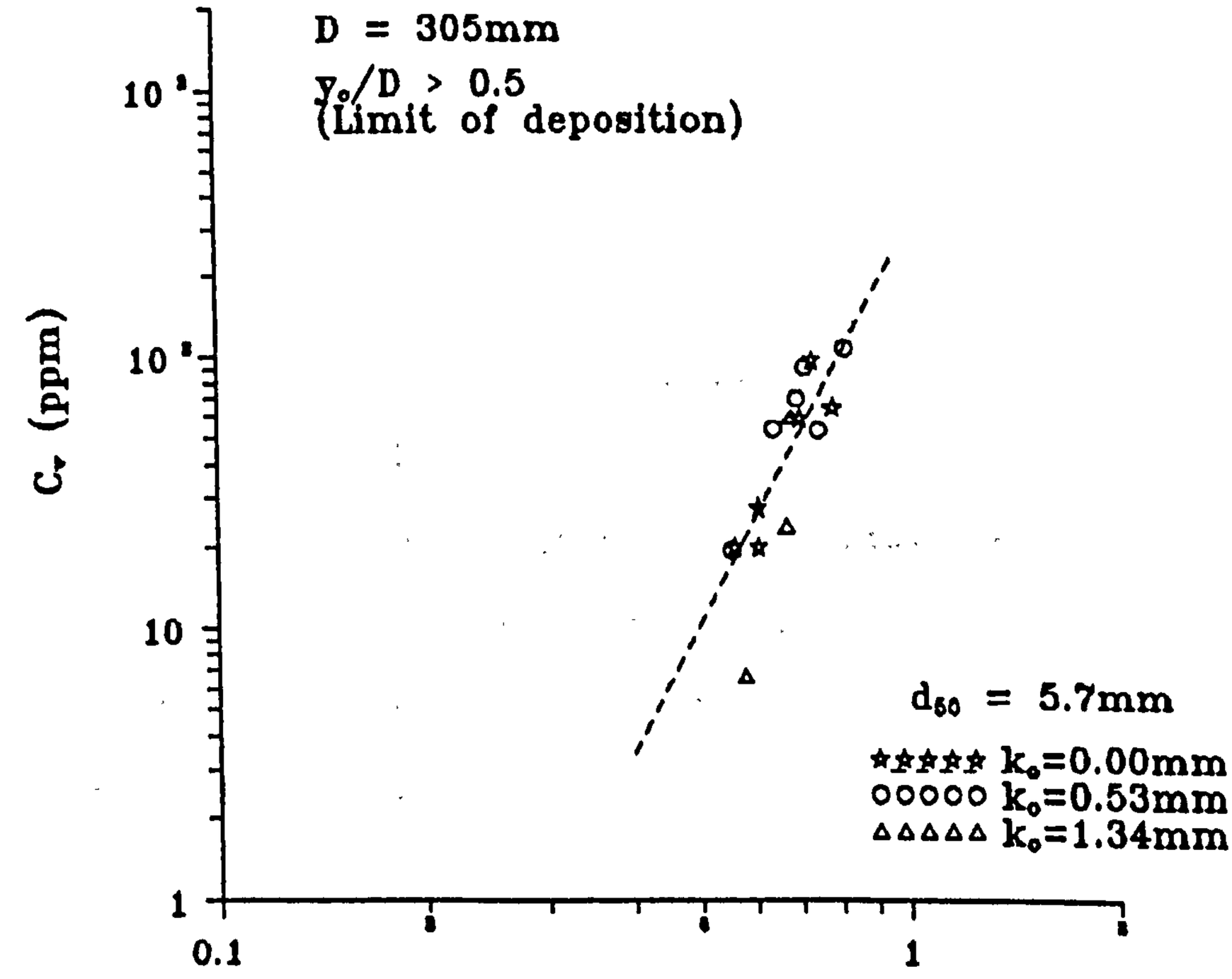

FIG. 5.10b Effect of wall roughness – d_{50} = 5.7mm
(Flow depths more than half-full)

suggesting that different velocities are required for each pipe size.

5.3.6 Effect of Sediment Deposit

Details of the computation of cross-sectional geometry (Fig. 5.1b) for pipes with deposited beds are given in Appendix C. The values of the mean sediment thickness, y_s, were obtained by averaging the volume of sediment bed along the measured section (10m long) of the 450mm dia. pipe (see Fig. 5.12). All flow parameters were then computed based on these mean values of y_s.

Fig. 5.13 illustrates the increase in the transporting capacity with a larger proportional sediment depth, y_s/D. This implies that for a given sediment concentration, a lower velocity is required for pipes with sediment deposits than those with clean inverts. The increase in the transporting capacity of the pipes with sediment beds might be associated with the presence of a finite sediment bed width (May et al 1989, El-Zaemey 1991, Loveless 1991). The author's present experimental data suggest that continuous sediment beds are present when y_s/D is larger than 10%. However, for smaller depths of deposits, the sediments move as trains of separated dunes over the clean inverts (See Fig. 5.12a).

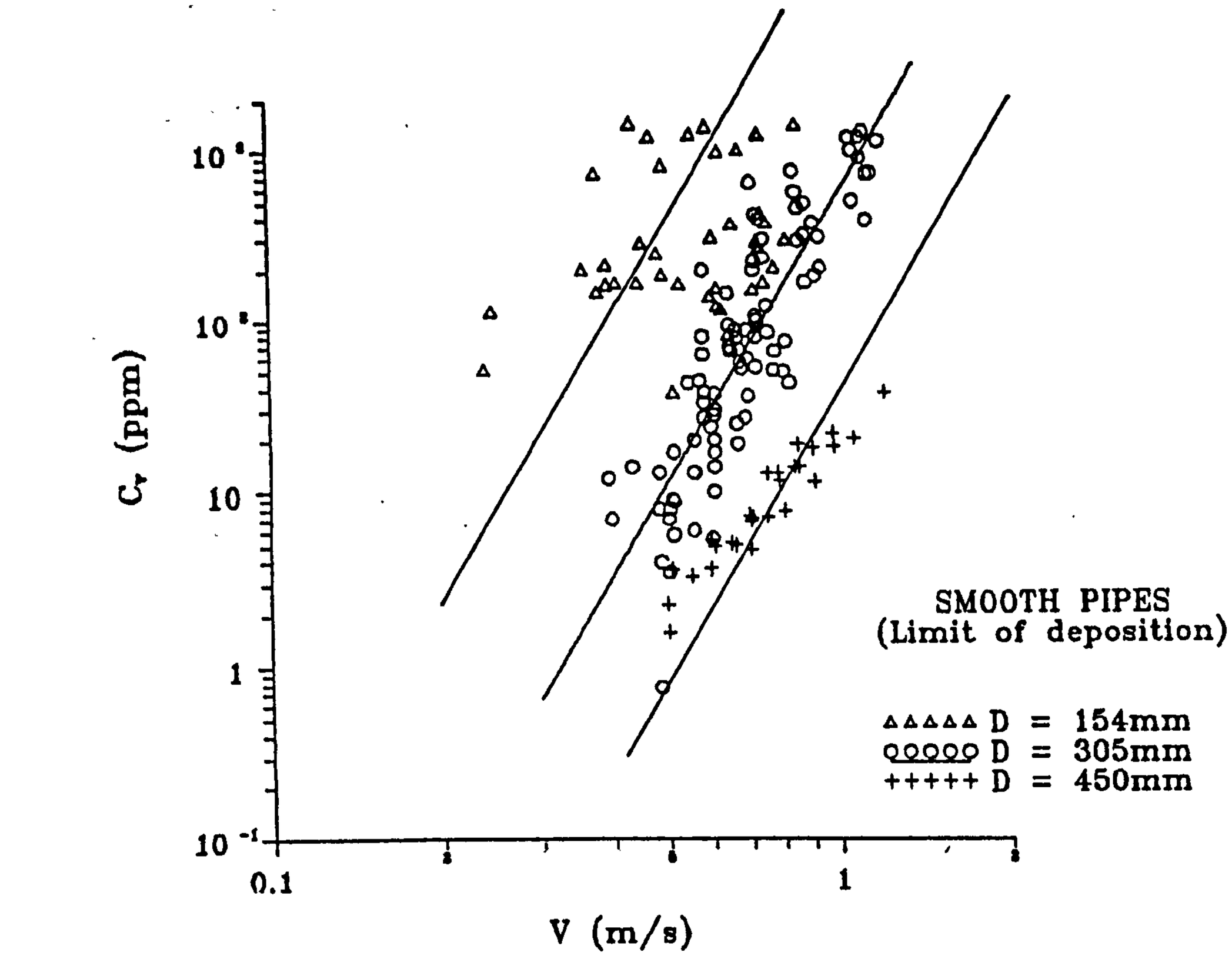

FIG. 5.11 Effect of pipe size

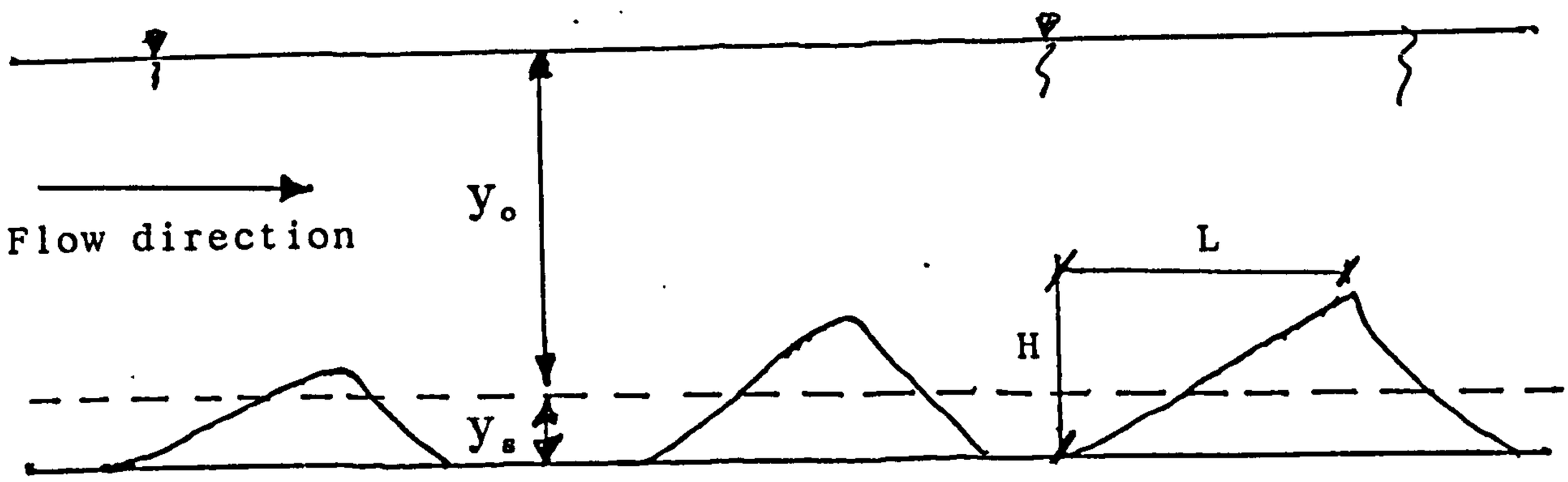

FIG. 5.12a Definitions of mean sediment bed thickness and bedform features (separated dunes)

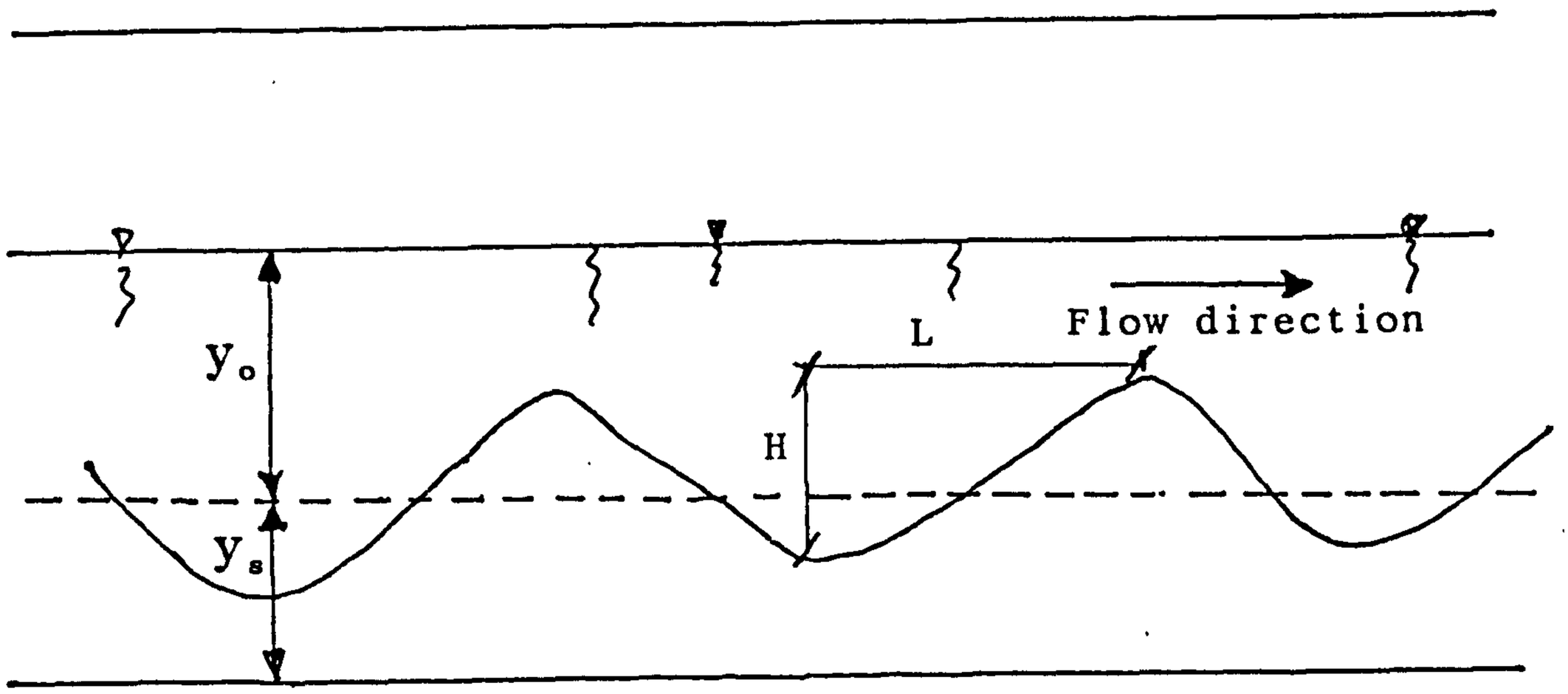

FIG. 5.12b Definitions of mean sediment bed thickness and bedform features (continuous dunes)

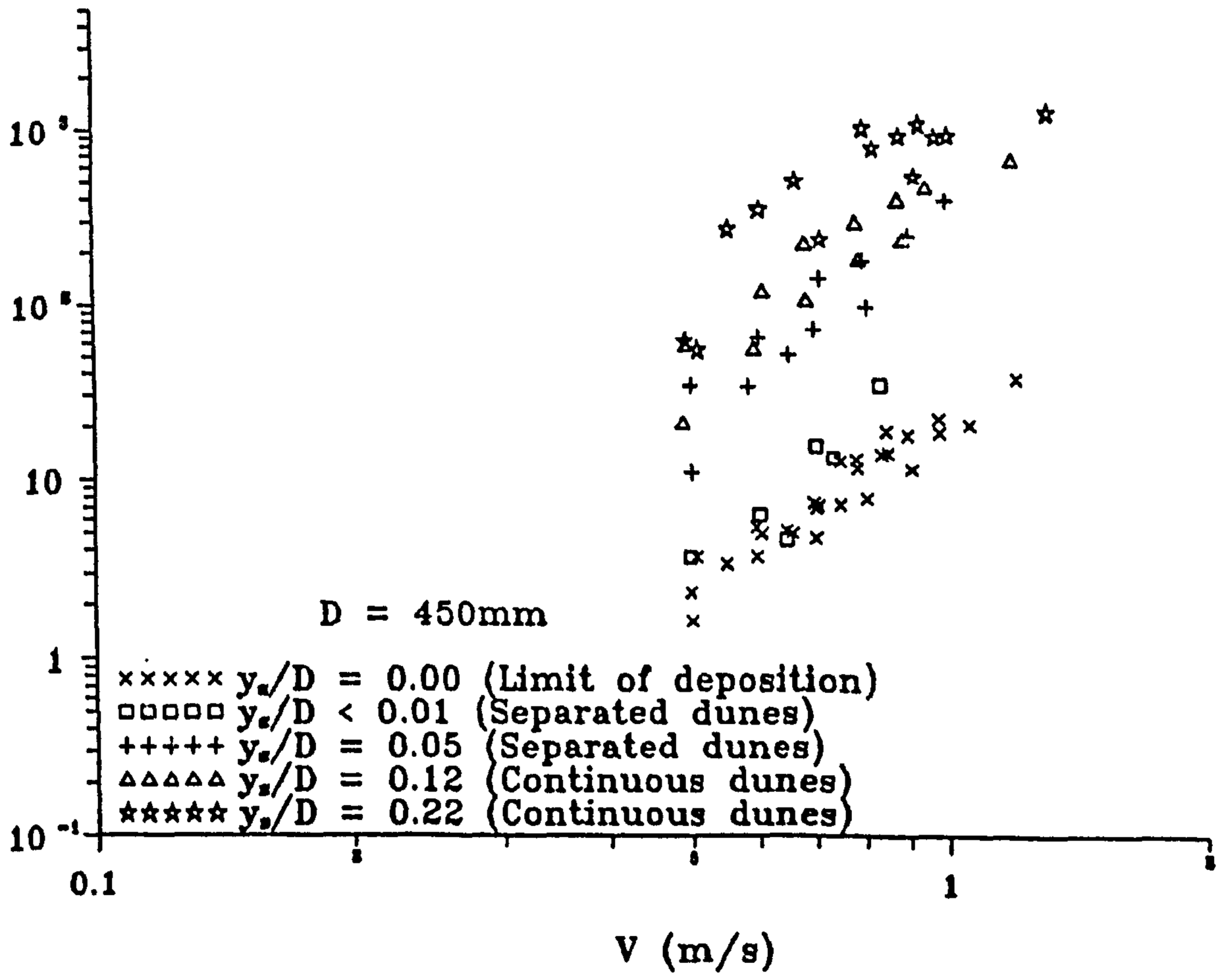

FIG. 5.13 Effect of sediment deposits

5.3.7 Friction Factor with Sediment Transport

The friction factor with sediment, λ_s, and the corresponding roughness height, k_s, were computed from Darcy-Weisbach's Eqn. 5.1 and Colebrook-White's Eqn. 5.7 respectively.

The apparent increase in the friction factor due to the presence of sediments in the case of clean pipes is shown in Figs. 5.14 and 5.15. Both plots consistently indicate the increase in fiction factor ($\lambda_s/\lambda_o > 1$) for both smooth and rough clean pipes over the range of limiting sediment concentrations and the pipe sizes tested. However, the increase in the friction factor for rough pipes appears to be smaller than that of smooth pipes. This could be due to the already larger value of clear water friction factor for rough pipes. The results also suggest that the presence of sediments may create a relatively smoother boundary.

The increase of friction factor in pipes with sediment deposits is shown in Fig. 5.16. It should be mentioned that, during the author's previous work (Ab. Ghani, 1990) where $y_s/D = 0.22$ at half-full flows, the point gauges were mounted over the pipe slots to obtain direct measurements of water levels. However, due to the passage of dunes especially at high velocity ($V > 0.7$m/s), the fluctuations in water level caused difficulties in determining the slope of the water surface accurately. As a result, the values of λ_s for several of the experiments were quite low, and hence these were omitted from the plot shown in

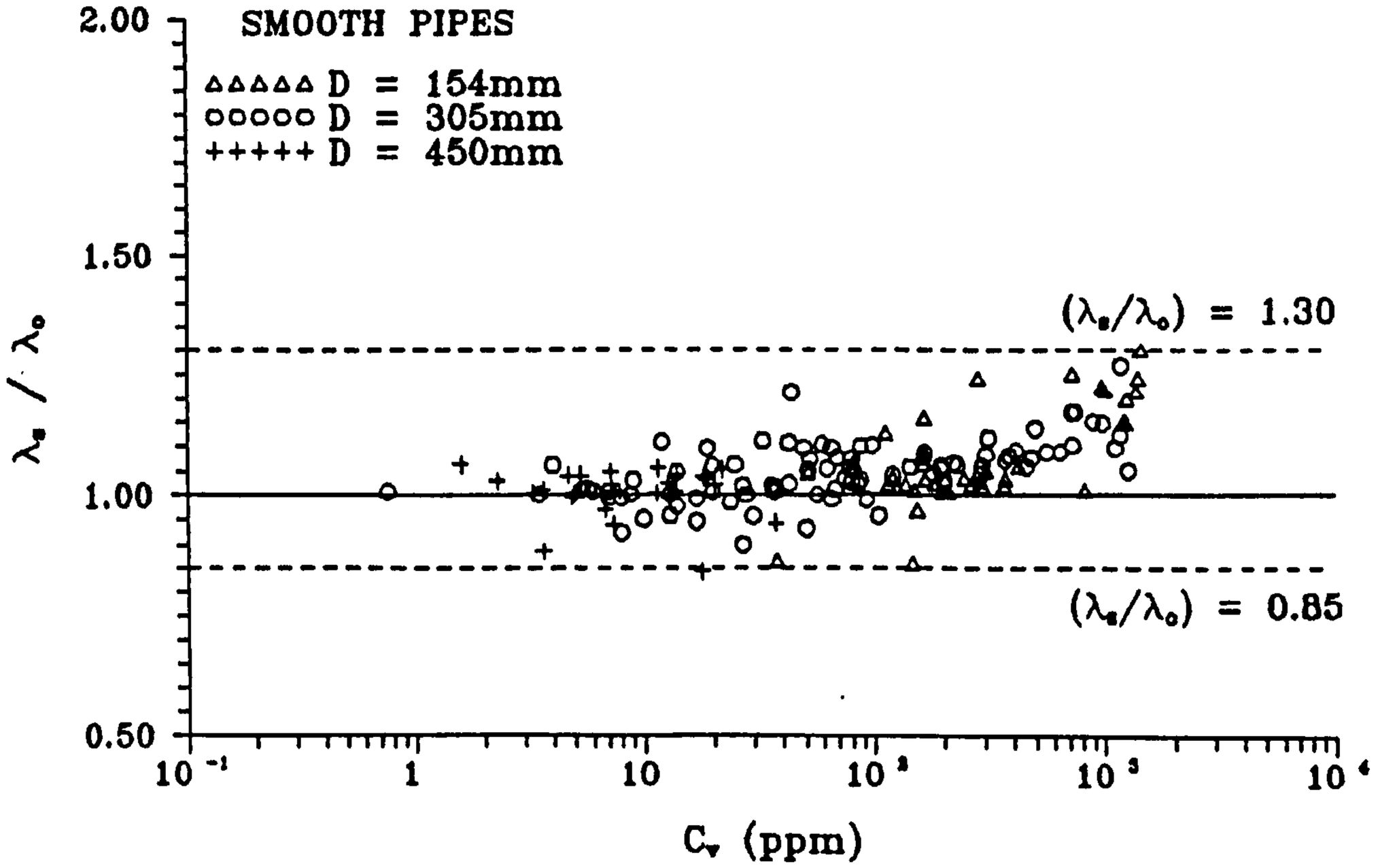

FIG. 5.14 Increase in friction factor at limit of deposition (Smooth pipes)

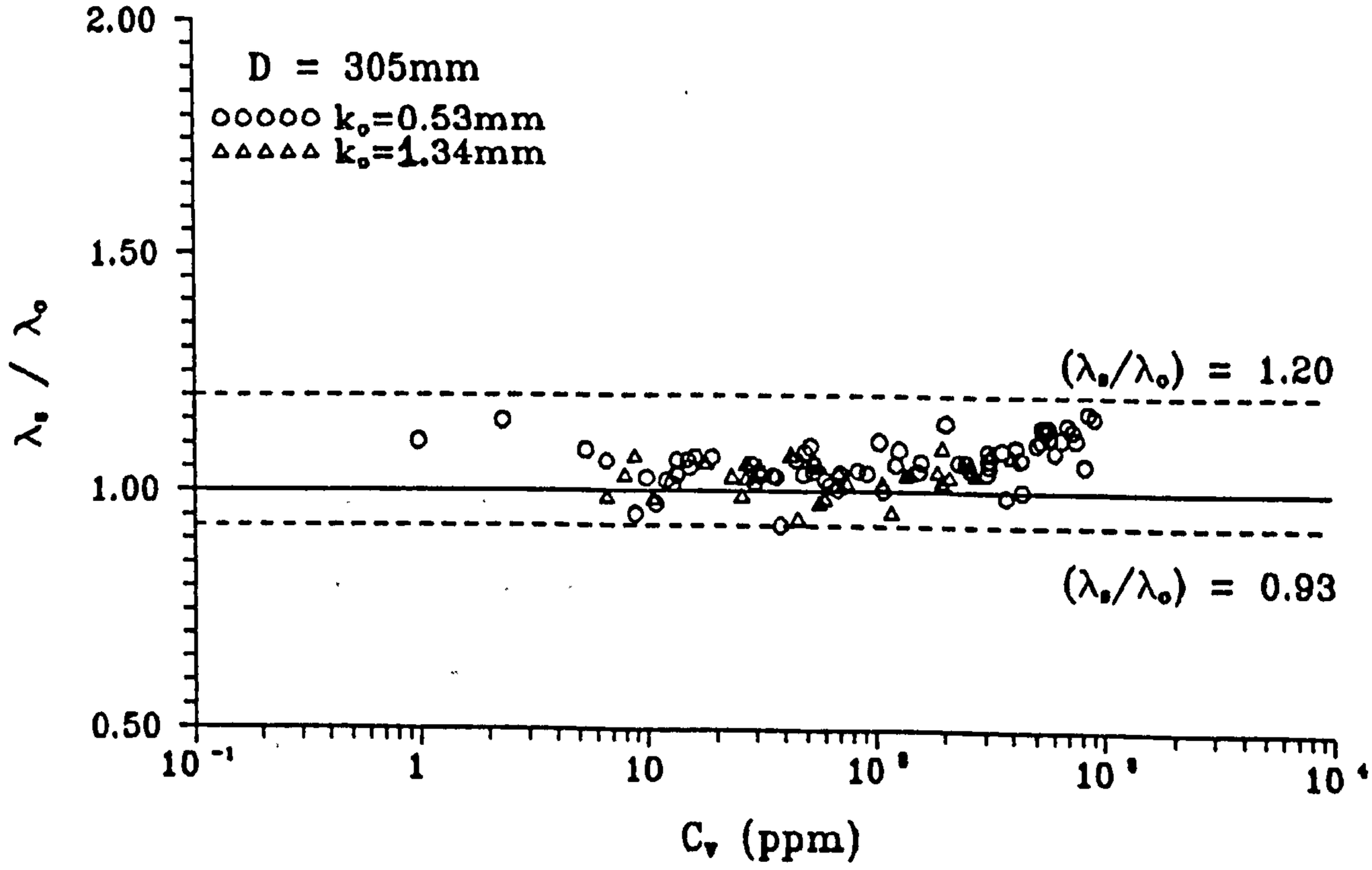

FIG. 5.15 Increase in friction factor at limit of deposition (Rough pipes)

Fig. 5.16. Appropriate adjustments to the measurement of the water level have since been made (May 1993). The water level measurement method for the present studies is as explained in Section 4.3.2.

Overall, Fig. 5.16 shows that for a small depth of deposits (y_s/D < 1%) the value of the composite friction factor, λ_s, is slightly larger than that of clean pipes. However, a larger increase is to be expected for a large depth of sediment deposits (y_s/D > 5%). Also, for y_s/D > 5%, the values of λ_s gets smaller with an increase in the sediment concentration and hence the corresponding velocity.

Fig. 5.17 shows that the composite roughness, k_s, depends on the Froude number. This indicates a similar trend of behaviour of sediment transport in pipes with sediment beds and that of alluvial channels. For a given depth of sediment deposit, the larger the Froude number, the smaller the composite roughness gets and approaches that of the clean pipe roughness. For very small depths of sediment deposits (y_s/D <1%), the values of the composite roughness is scattered around those of the clean pipe roughness. This result agrees with an earlier work of May et al (1989) that suggests y_s/D = 1% would be attractive for a new design criterion especially for large pipes.

Bedform measurements were also made for the present studies. The definitions of the height and length of the individual dunes are as shown in Fig. 5.12. The corresponding mean values of the

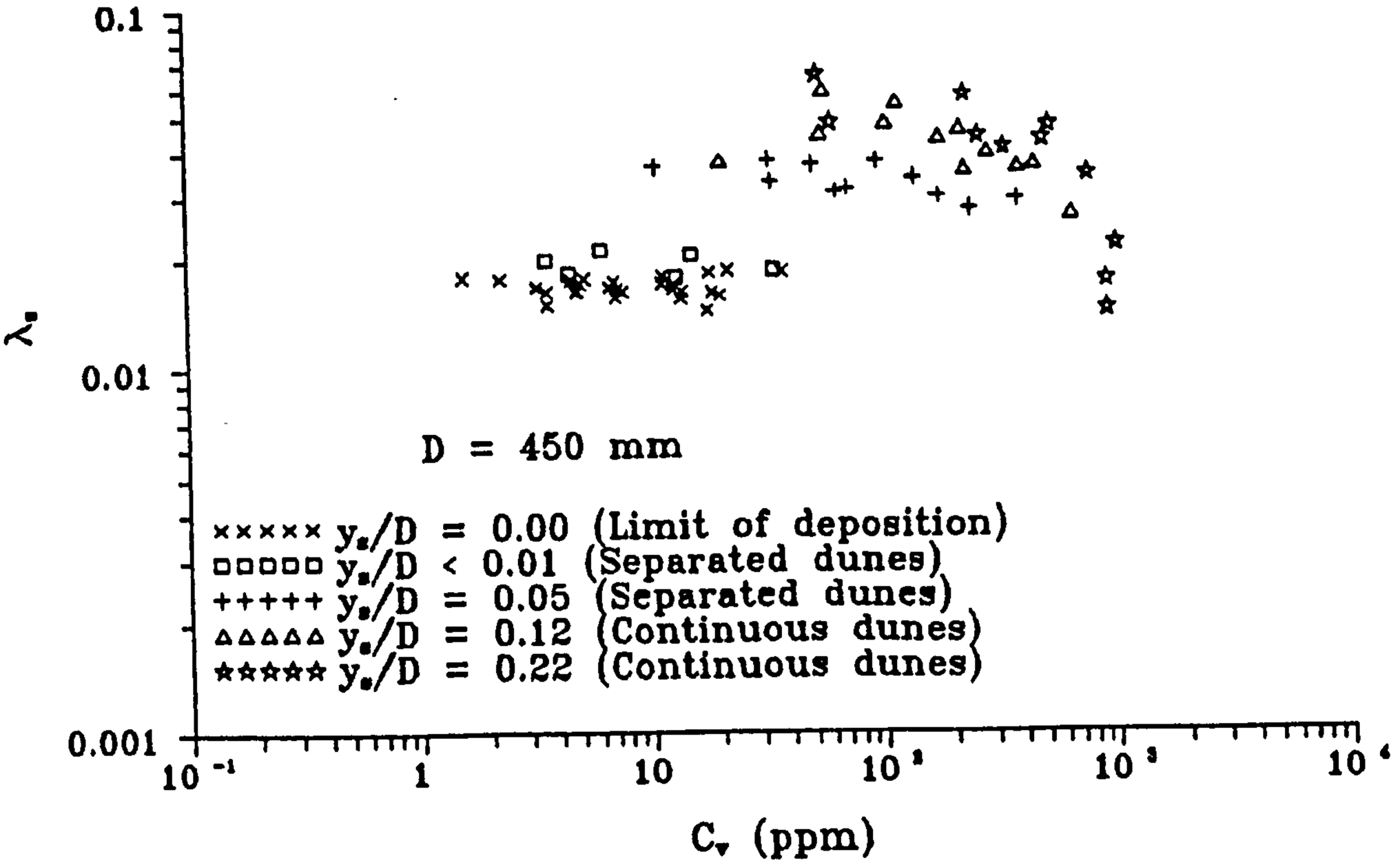

FIG. 5.16 Friction factor at and beyond the limit of deposition

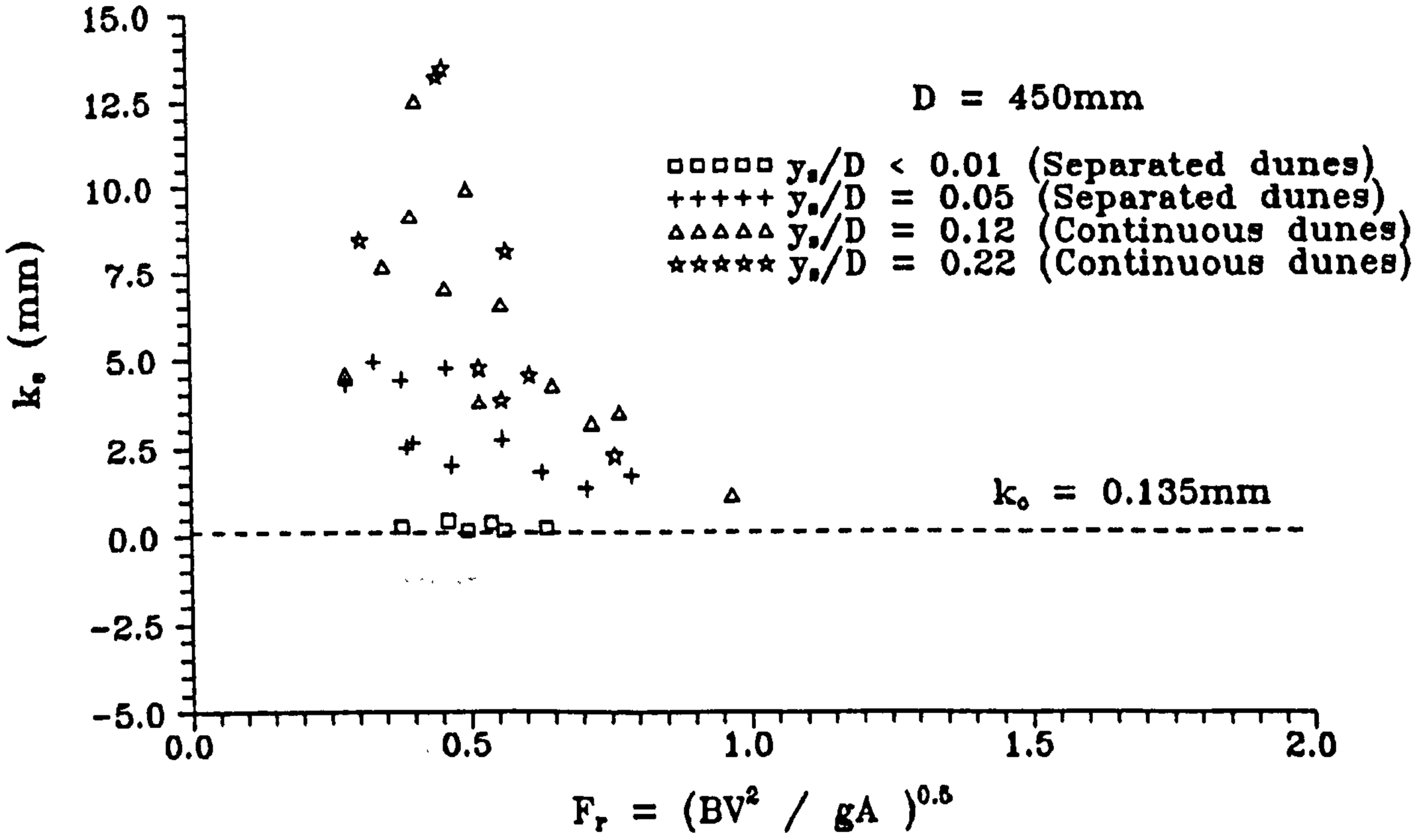

FIG. 5.17 Effect of Froude number on overall flow resistance in pipe with deposited beds

height and length of the dunes for each test was obtained by averaging all values of the individual dunes. The range of the mean values of the height and length of the dunes for each depth of sediment deposit is given in Table 5.3. Due to its simplicity, the Visvalingam method (Eqn. 5.11) was used to compute the values of bed friction factor, λ_{sb}, while the corresponding values of the bed roughness height, k_{sb}, were computed from Colebrook-White's Eqn. 5.7. Figs. 5.18 and 5.19 show the variation of λ_{sb} and k_{sb} with the Froude number, Fr.

TABLE 5.3 FLOW RESISTANCE CHARACTERISTICS:- PIPES WITH DEPOSITED BEDS

D = 450mm d_{50} = 0.72mm

y_s/D	< 1%	5%	12%	22%
λ_{sb}	0.0253 - 0.0349	0.049 - 0.116	0.038 - 0.111	0.011 - 0.108
k_{sb}	0.62 - 37.20	16.60 - 208.50	6.40 - 130.00	7.20 - 98.70
H (mm)	14 - 22	38 - 69	25 - 83	51 - 74
L (mm)	192 - 367	400 - 633	505 - 940	1090 - 1272

NOTE:

For bed thickness of 0.22D, the bedform measurements were made for overall proportional flow depth (Y/D) of 0.75 only.

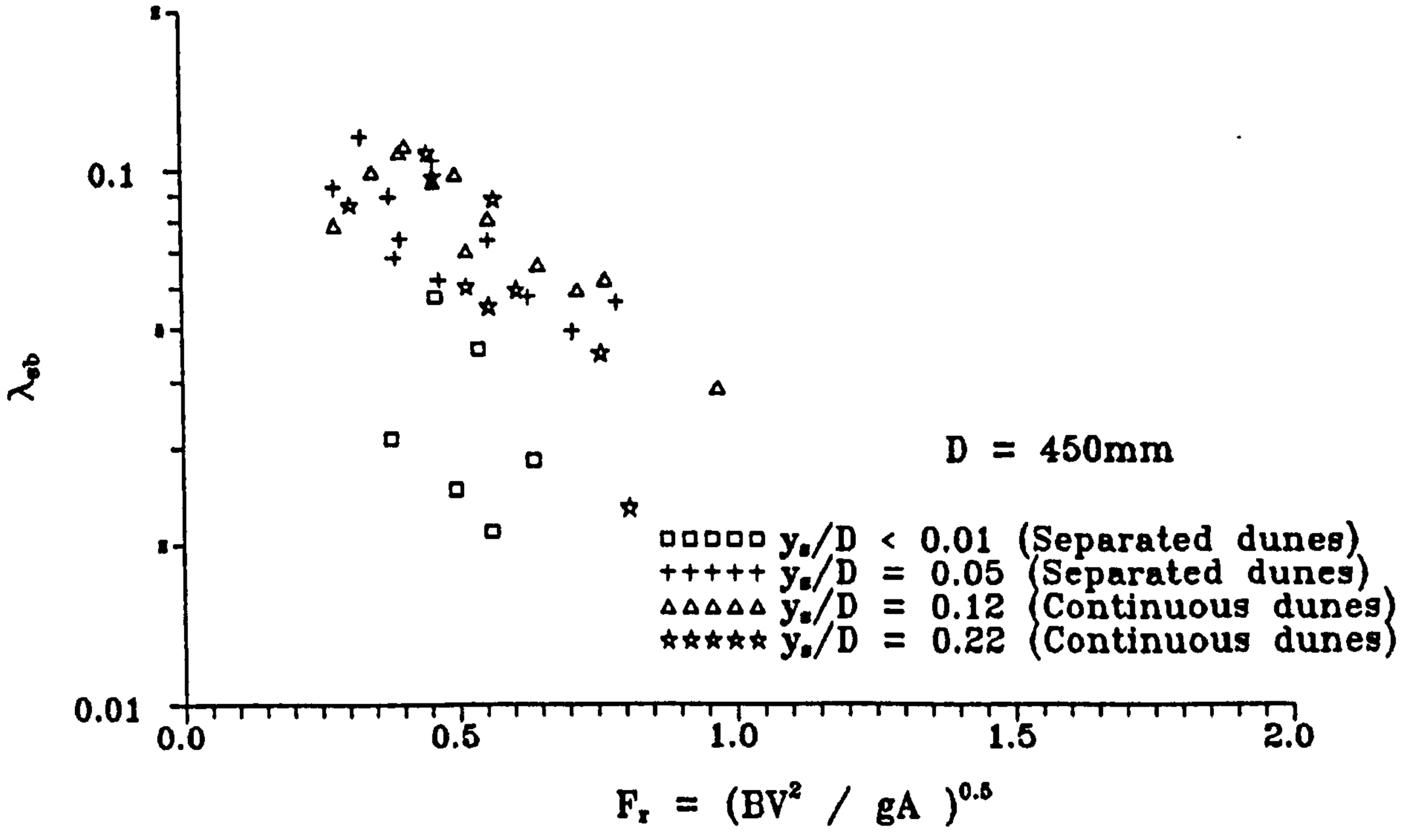

FIG. 5.18 Effect of Froude number on the bed friction factor

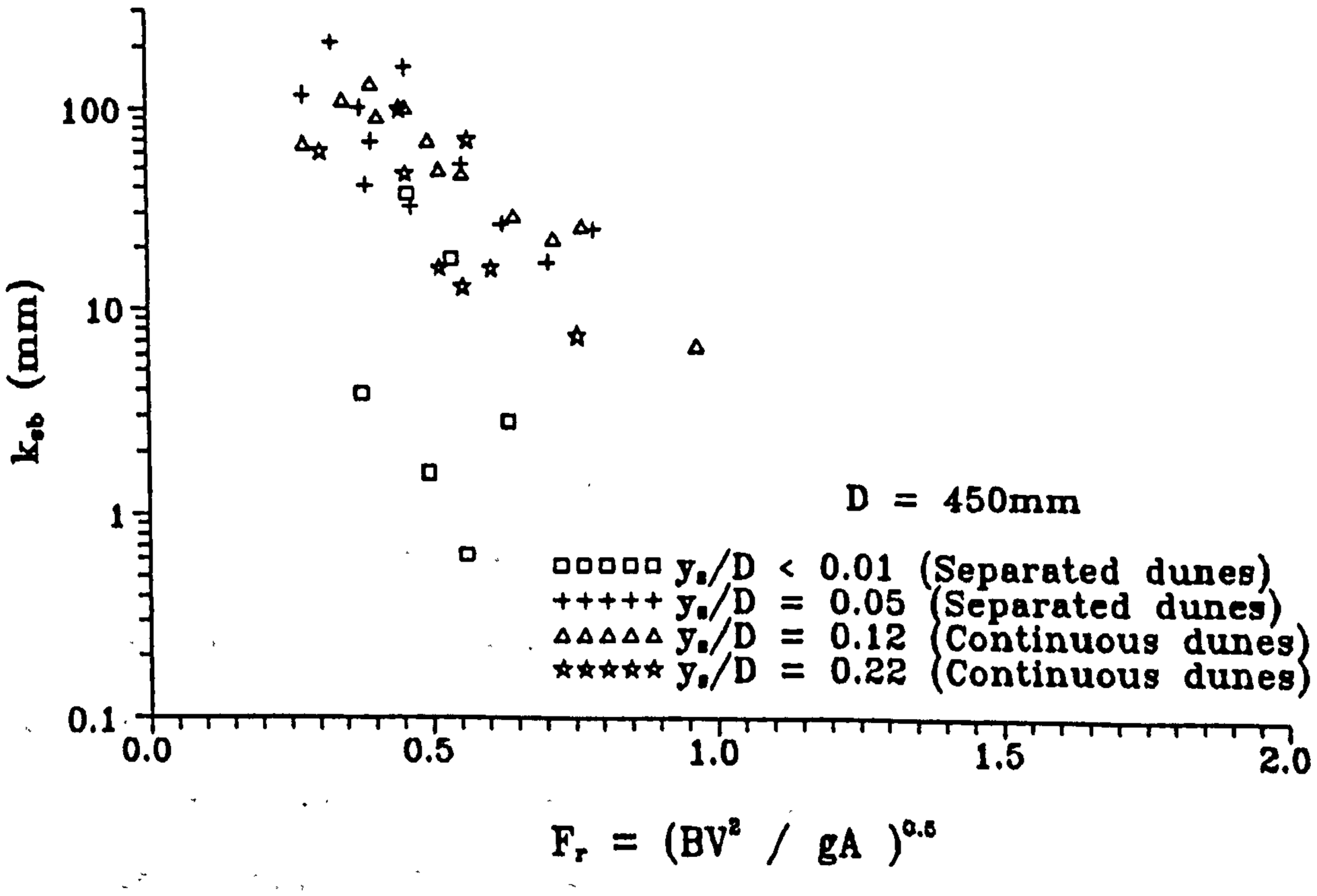

FIG. 5.19 Effect of Froude number on flow resistance due to sediment bed

CHAPTER 6

ANALYSES OF SEDIMENT TRANSPORT DATA

6.1 Clean Pipes

6.1.1 Background

The basic variables that govern the sediment transport process in steady and uniform free surface flow in clean pipe channels include the flow depth (y_o) or hydraulic radius (R), mean flow velocity (V) or mean shear stress (τ_o), kinematic viscosity (ν) and density (ρ) of water, size (d), density (ρ_s) and concentration of sediment, size (D) and roughness (k_o) of pipe, friction factor with sediment (λ_s), bed slope (S_o) and acceleration due to gravity (g).

These variables were usually applied in two ways to obtain a relationship enabling the prediction of the flow transporting capacity. Firstly, dimensional analysis was used extensively to obtain a number of dimensionless group parameters. Previous works (Ambrose 1953, Novak-Nalluri 1975, Mayerle 1988, Paul-Sakhuja 1990) have identified several of these parameters known to have great influence on the sediment transport process in pipes. Several examples of these parameters as highlighted in Chapter 3 are given in Table 6.1.

The second approach was to solve the forces acting on a particle at the equilibrium (May 1982, Mat Suki 1987, Loveless 1991) yielding semi-empirical equations. These equations are usually dimensionally homogeneous with their dimensionless parameters being similar to those obtained by the dimensional analysis approach.

TABLE 6.1 CHARACTERISTIC PARAMETERS FOR SEDIMENT TRANSPORT IN CLEAN PIPE CHANNELS

TYPE OF PARAMETERS	DIMENSIONLESS GROUPS
MOBILITY	$Fr_m = \frac{V}{\sqrt{gd_{50}(S_s-1)}}, \quad \frac{1}{\psi} = \frac{\tau_o}{\rho g(S_s-1)d_{50}}$
TRANSPORT	$C_v, \quad \Phi = \frac{C_v V R}{\sqrt{g(S_s-1)d_{50}^3}}$
SEDIMENT	$D_{gr}, \quad d_{50}/D, \quad S_s$
CONVEYANCE SHAPE	$R/d_{50}, \quad D^2/A, \quad y_o/d_{50}, \quad D_h/y_o, \quad y_o/D$
FLOW RESISTANCE	$\lambda_s, \quad (k_s - k_o)/D$

The analyses of the present experimental data were preceded by a comparison of the existing transport relationships and the final equation was obtained by using multiple regression analyses extensively. The final selection of the best-fit model was based on the values of adjusted determination coefficient (adj. r^2), standard deviation (s) and the simplicity of the model.

6.1.2 Appraisal of Existing Equations

The present experimental data in clean pipe channels (see Table 5.2) were used to evaluate the applicability of several existing equations for sediment transport at the limit of deposition (see Section 3.3.1). This involved the computation of the volumetric sediment concentration (C_v) using other measured quantities such as velocity (V), hydraulic radius (R), and friction factor with sediment (λ_s).

The overall performance of each equation is presented graphically in a plot of observed concentrations against their computed values. A discrepancy ratio, defined as the ratio between computed and measured values, is used as an indication of the accuracy of the equation. Here, the discrepancy ratio in terms of C_v is plotted as a function of the dimensionless sediment size, D_{gr}, an approach introduced by White et al (1975) to assess alluvial transport relationships. It should be noted that other investigators (May 1982 - 1993, Loveless 1991) have also used their experimental data in the appraisal of several of the equations presented in Section 3.3.1.

The equations chosen for the comparisons represent the two broad categories of sediment transport relationships at the limit of deposition. The first category of equations is based on dimensional analysis. In this category, the selected equations were: Laursen's (1956) Eqn. 3.11, Novak-Nalluri's (1975) Eqn. 3.15, and Mayerle's (1988) Eqns. 3.34 and 3.35. The second category of equations is derived from theoretical analysis. In this category, the chosen equations were: Macke's (1982) Eqn. 3.17, and May et al's (1989) Eqn. 3.19 in conjunction with Novak-Nalluri's Eqn. 3.5 to compute the threshold velocity, V_c. It should be emphasized that all of these equations were selected to denote the development of the sediment transport equations at the limit of deposition.

In the comparison of the equations, the present data for clean pipes were grouped into smooth and rough beds to highlight the effect of wall or surface roughness. The results of the comparisons are given in Table 6.2 and plotted on Figures 6.1 - 6.6. In Table 6.2, the overall performance of each equation is presented statistically in terms of the average discrepancy ratio and the percentage of data which can be found in different ranges of variation of the discrepancy ratios.

Laursen's Eqn. 3.11 in Fig. 6.1(a) provides a reasonable fit to the experimental data with a mean discrepancy ratio of 2.37. The agreement is rather good for the limiting concentration between 50ppm and 500ppm. Overall, about 55% of the predicted concentrations using Eqn. 3.11 are within 0.5 and 2 times the

observed values (see Table 6.2). This band of error is usually used as an indication of the reliability of alluvial channel transport relationships (White et al 1975, Yang 1979, Brownlie 1981). Fig. 6.1(a) also shows that Laursen's Eqn. 3.11 produced similar results for both rough and smooth bed data.

TABLE 6.2 DISCREPANCY RATIO (C_v) FOR DIFFERENT EQUATIONS - ALL PRESENT DATA (CLEAN PIPES)

Equations	C_v (predicted) / C_v (observed)							No. of data
	Mean	min	max	0.9-1.1 (%)	0.75-1.25 (%)	0.5-1.5 (%)	0.5-2.0 (%)	
Laursen (Eqn. 3.11)	2.37	0.17	33.82	10	23	42	55	256
Novak-Nalluri (Eqn. 3.15)	3.84	0.14	61.20	7	17	31	38	256
Mayerle (Eqn. 3.34)	3.55	0.01	41.10	5	12	30	35	256
Mayerle (Eqn.3.35)	0.38	0.02	10.41	3	7	21	22	256
May (Eqn. 3.19)	0.18	0.00	1.03	1	2	6	6	256
Macke (Eqn. 3.17)	0.24	0.00	3.04	1	5	14	16	256

Fig. 6.1(b) indicates that Eqn. 3.11 tends to overestimate the limiting concentrations for $D_{gr} < 60$. Better agreement is obtained at higher values of D_{gr}. Overall, Laursen's Eqn. 3.11 can produce a reasonably good prediction of the limiting concentrations over wide range of sediment sizes even though the equation itself does not include any effect of the particle size.

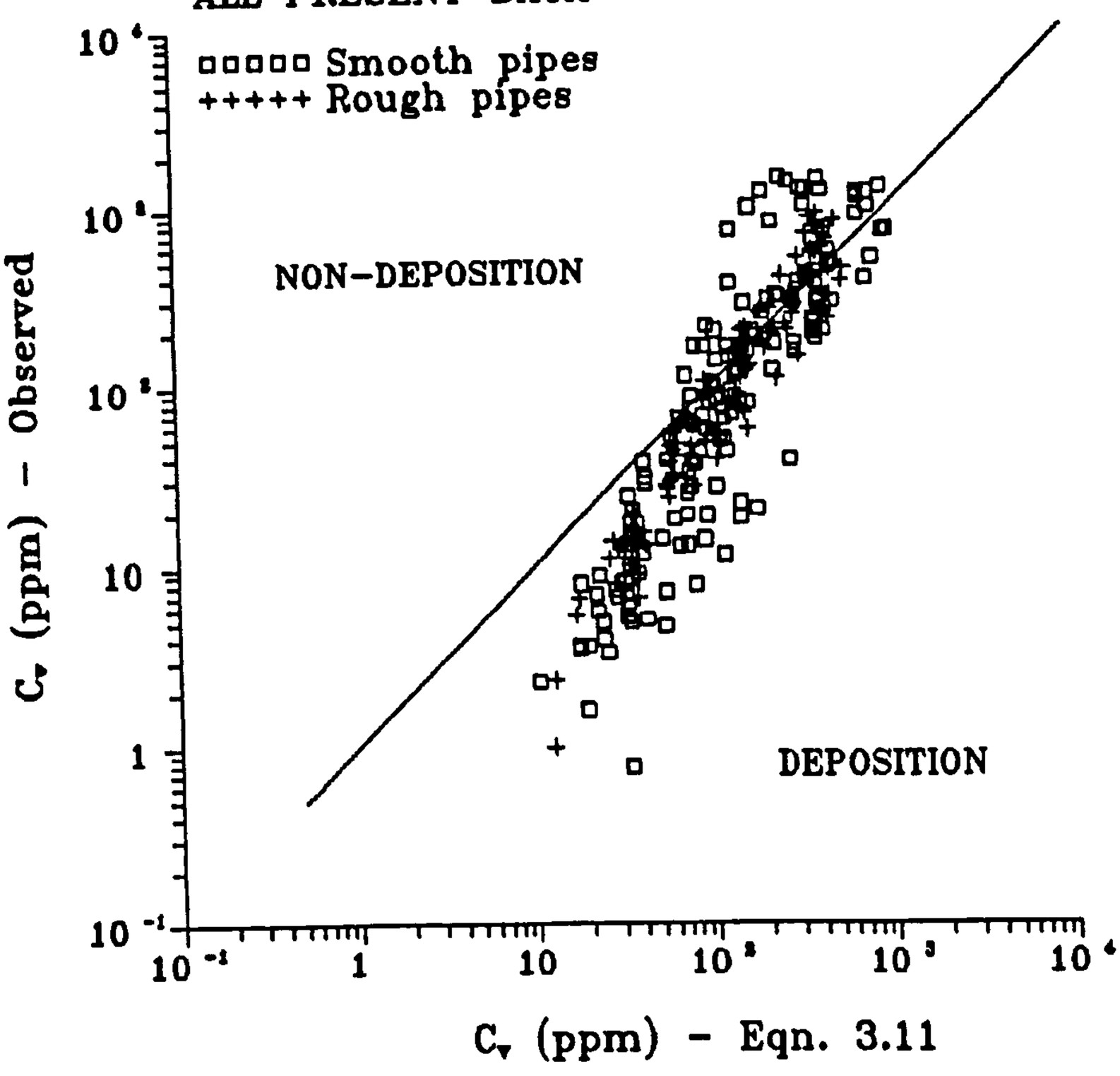

FIG. 6.1a Predicted C_v using Laursen's Eqn. 3.11

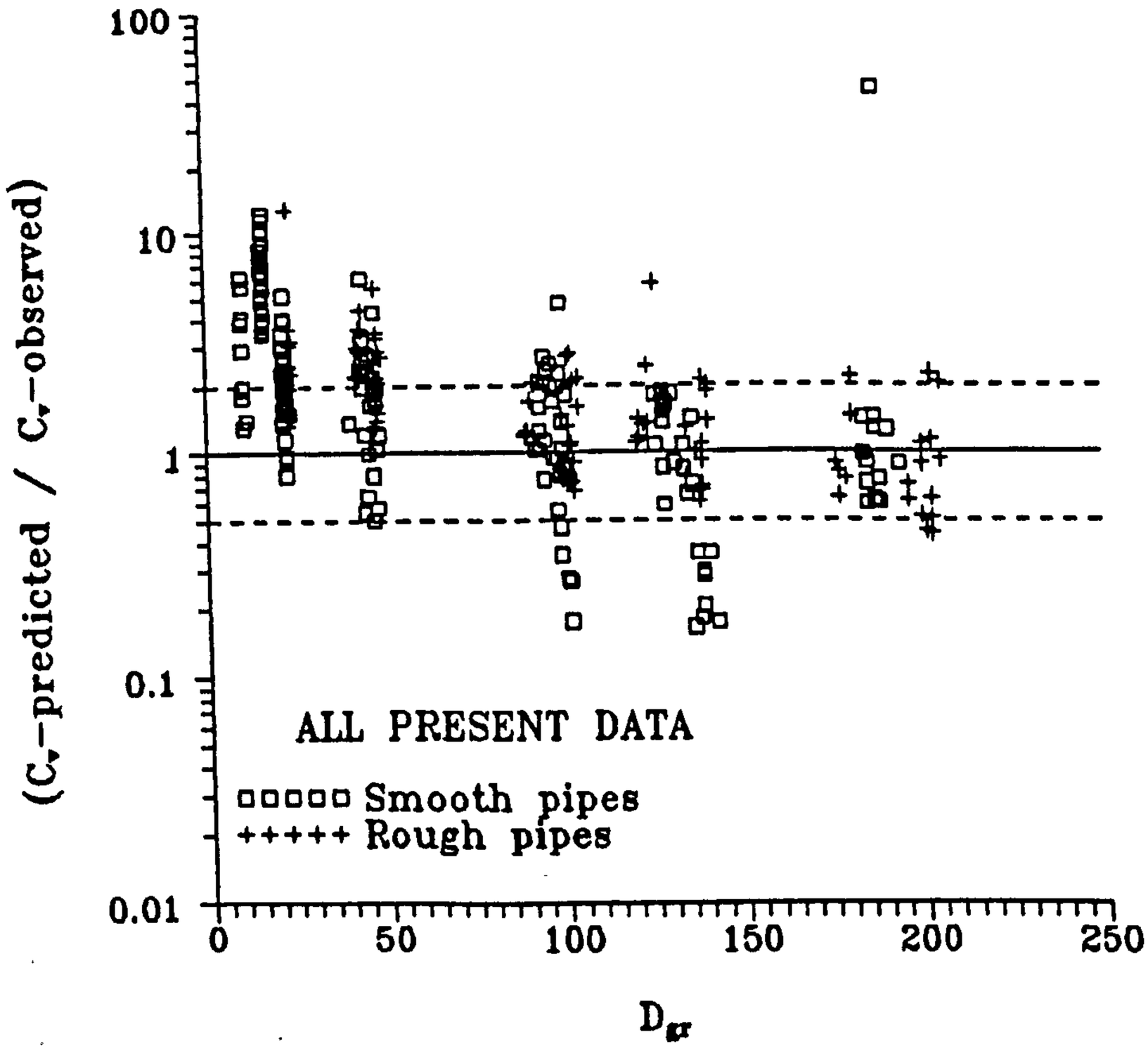

FIG. 6.1b Discrepancy ratio for Laursen's Eqn. 3.11 as a function of dimensionless particle size

Novak-Nalluri's Eqn. 3.15 in Fig. 6.2(a) shows more scatter than Laursen's Eqn. 3.11 and has a mean discrepancy ratio of 3.84. Only 38% (see Table 6.2) of the predicted concentrations are within the band error of 0.5 and 2 times the observed values. The equation tends to overestimate at low concentrations (C_v = 1ppm - 50ppm and underestimate at high concentrations (C_v > 500ppm). Fig. 6.2(a) also shows that Eqn. 3.15 correlates well both smooth and rough bed data. Fig. 6.2(b) shows that Eqn. 3.15 significantly overpredicts (i.e. discrepancy ratio larger than 2.0) the limiting concentrations for the majority of data in the range D_{gr} < 50. Beyond this, there is better agreement with fewer underestimation or overestimation of the limiting concentrations.

The results of the comparison between predicted and observed limiting concentrations for Mayerle's Eqn. 3.34 is shown in Fig. 6.3(a). This equation underestimates the limiting concentrations for smooth bed data in most cases. Reasonable agreement is shown for concentrations in the range 1ppm to 30ppm. By contrast, the equation overestimates all of the limiting concentrations for rough bed data. A close examination of the rough bed data results reveals that bigger discrepancies are obtained for the larger roughness used (k_o = 1.34mm). Overall, Mayerle's Eqn. 3.34 has a mean discrepancy ratio of 3.55 with 35% of data falling within the range of discrepancy ratio 0.5 - 2.0 (see Table 6.2). Fig. 6.3(b) shows that the Eqn. 3.34 underestimates the limiting concentrations for majority of the smooth bed data over the range

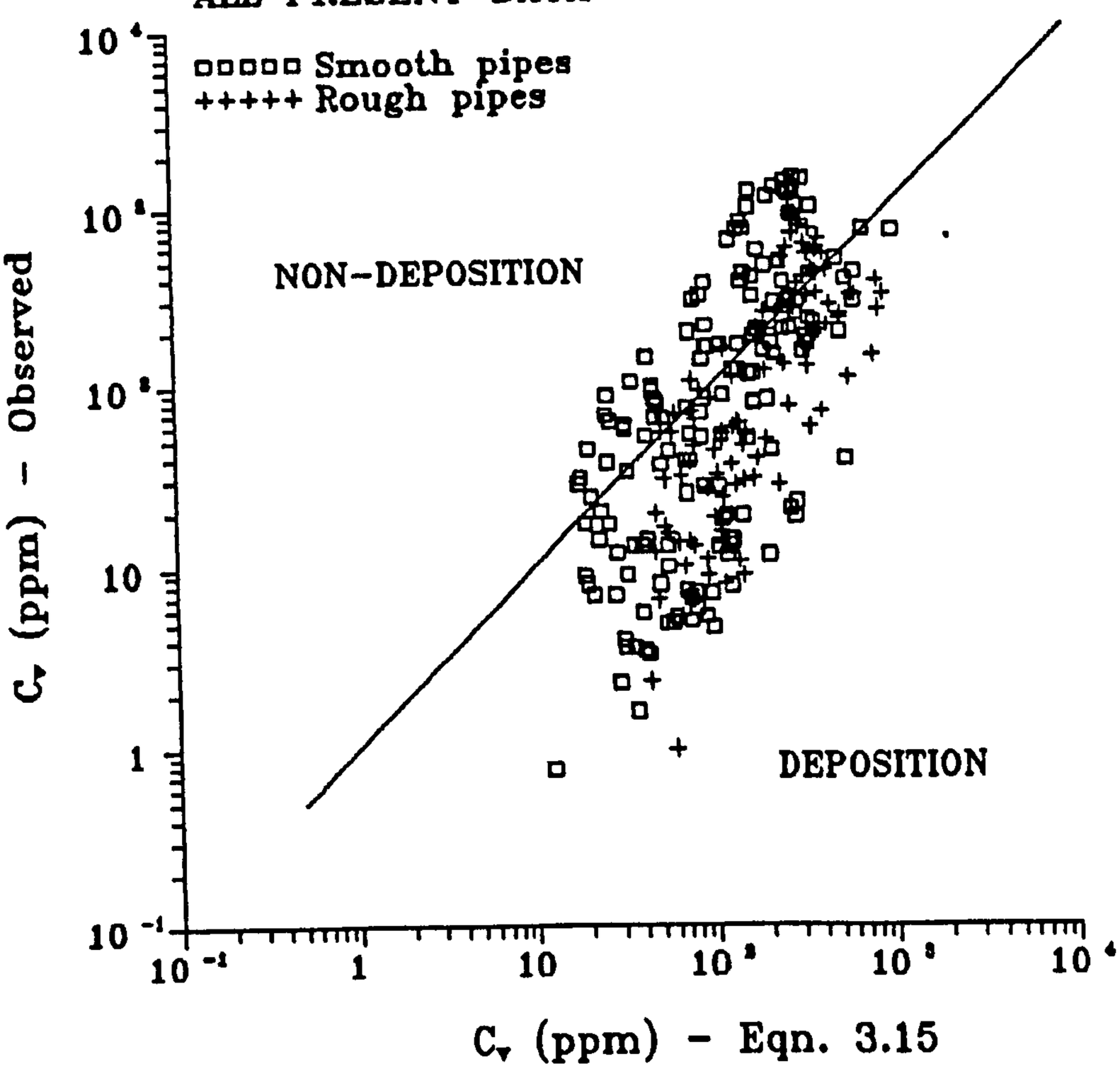

FIG. 6.2a Predicted C_v using Novak-Nalluri's Eqn. 3.15

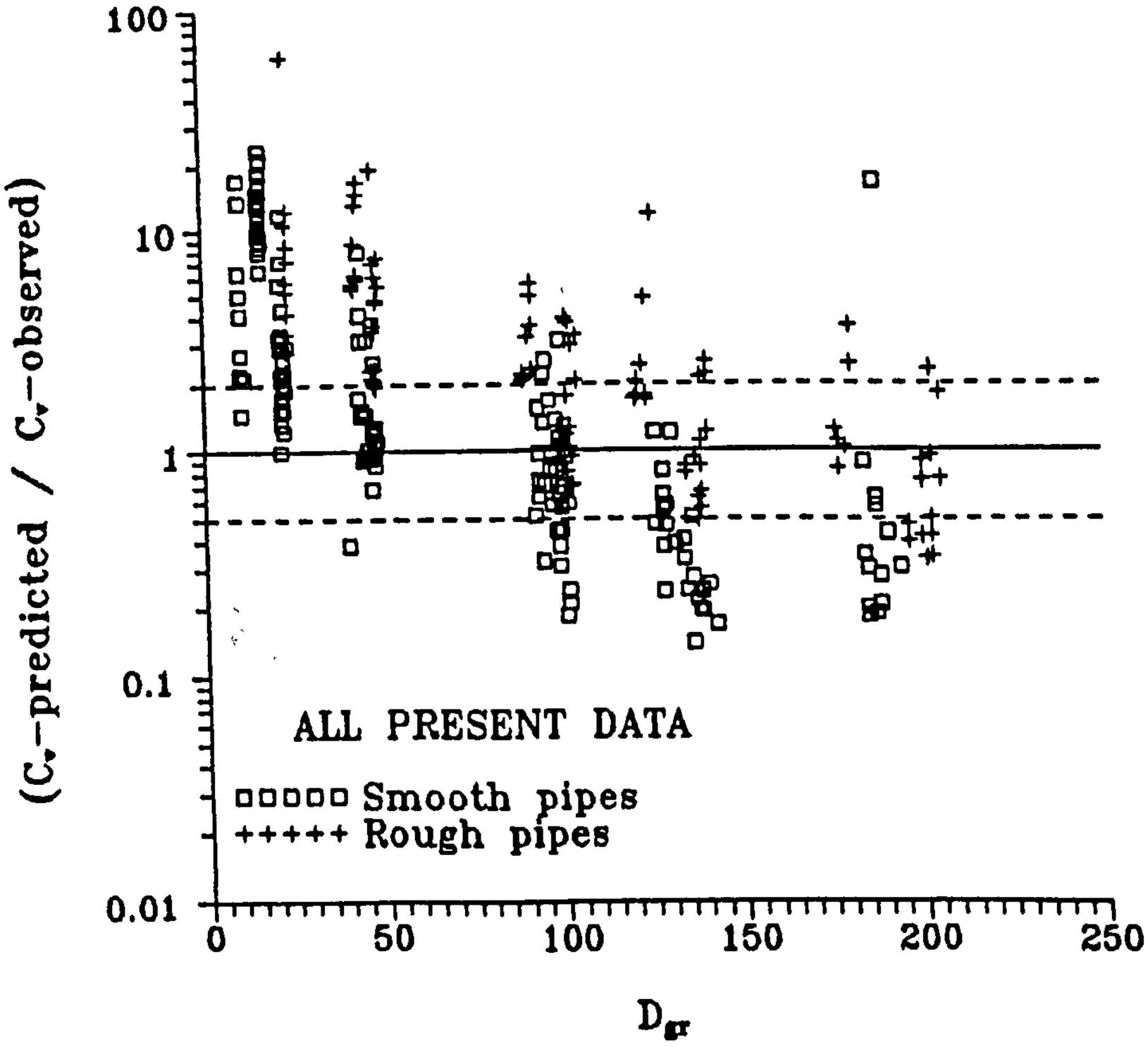

FIG. 6.2b Discrepancy ratio for Novak-Nalluri's Eqn. 3.15 as a function of dimensionless particle size

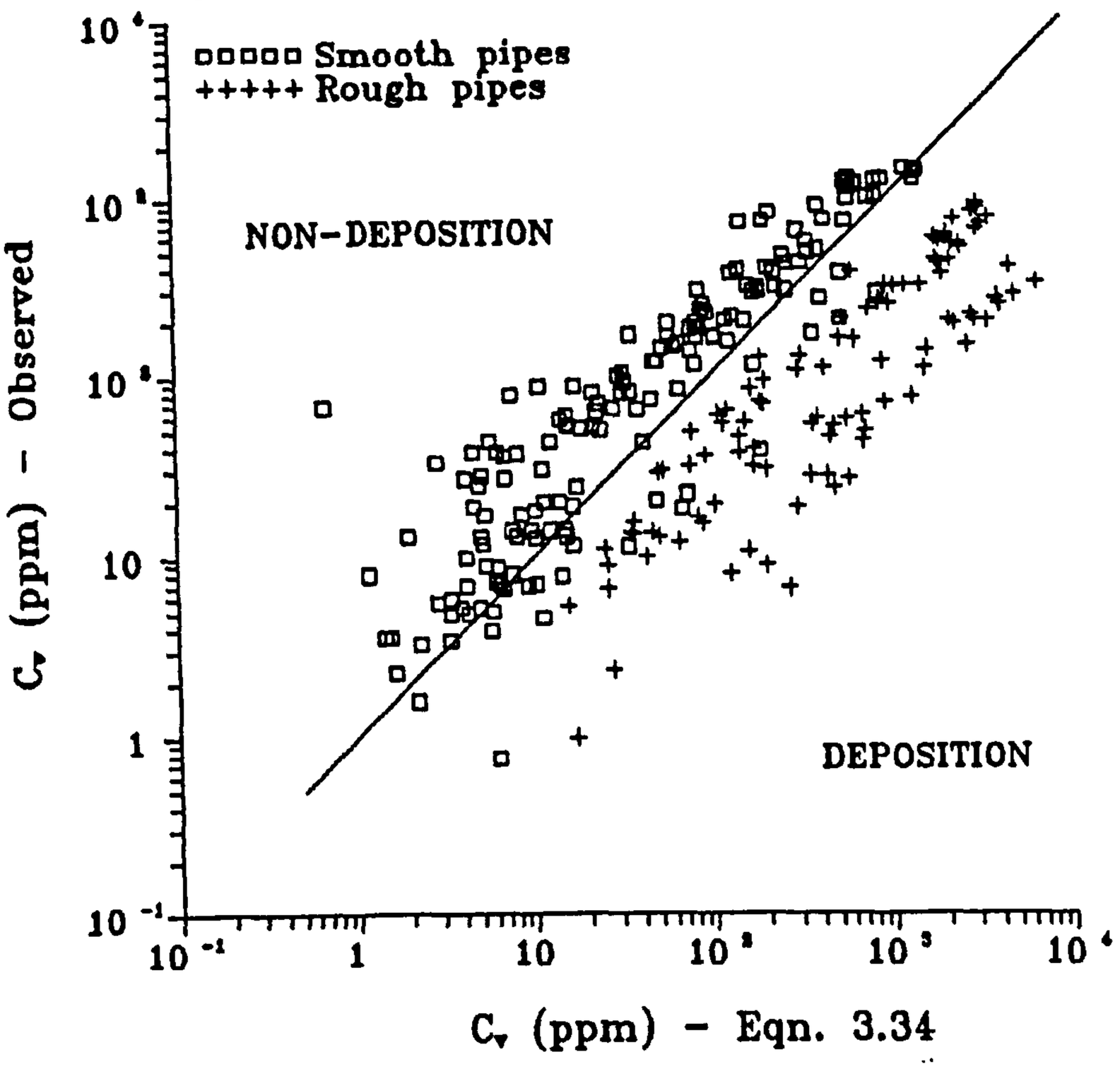

FIG. 6.3a Predicted C_v using Mayerle's Eqn. 3.34

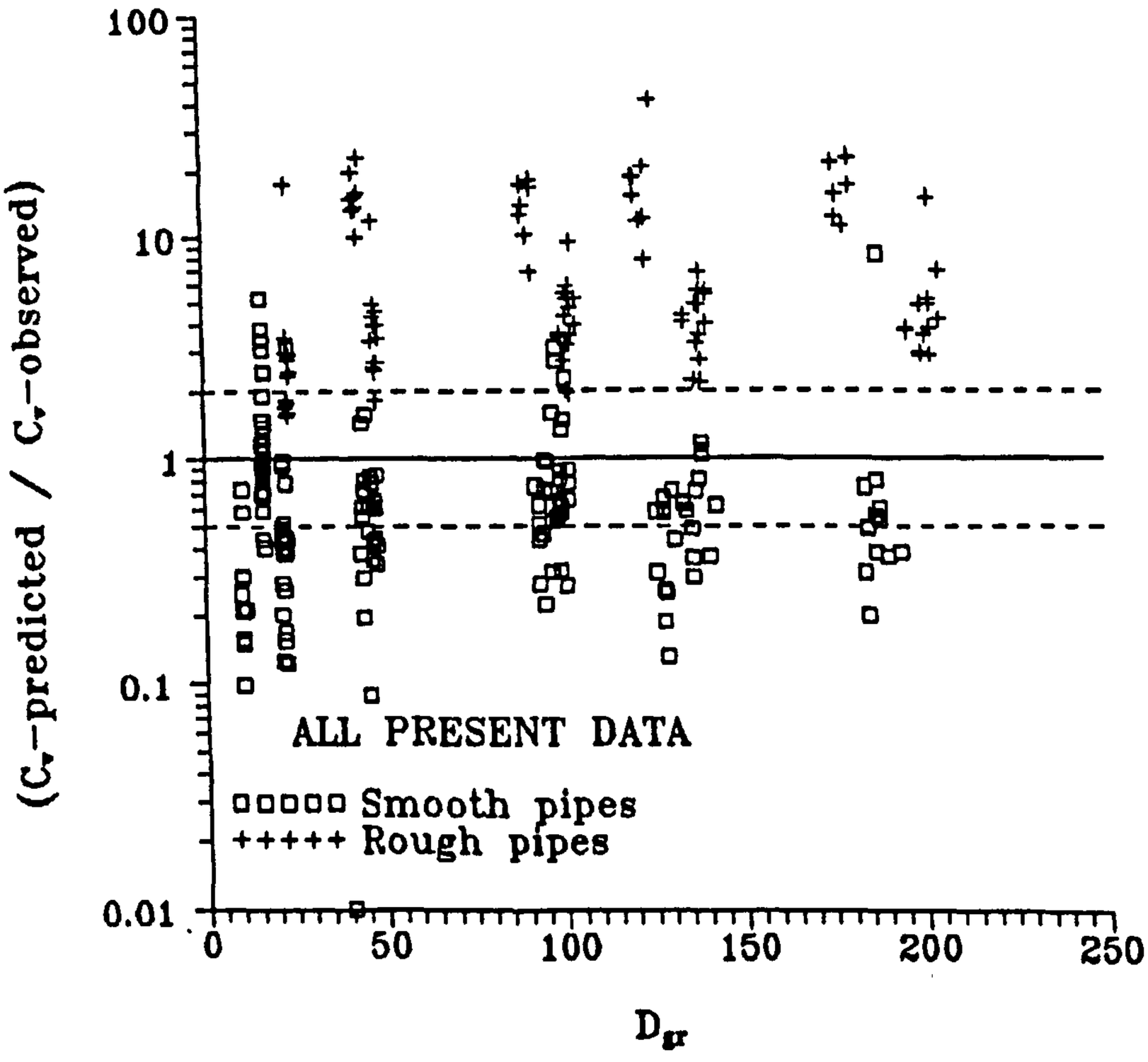

FIG. 6.3b Discrepancy ratio for Mayerle's Eqn. 3.34 as a function of dimensionless particle size

of particle size. On the other hand, over the range of particle sizes, the equation overestimates the limiting concentrations for all of rough bed data. The results of the comparison highlight the need to include the rough bed data in deriving an equation which has the form of Mayerle's Eqn. 3.34.

Mayerle's Eqn. 3.35 in Figure 6.4(a) underestimates the limiting concentrations in nearly all the data. The equation has a mean discrepancy ratio of 0.38 with only 22% of the data lie within the range of discrepancy ratio between 0.5 and 2.0 (see Table 6.2). However, the equation shows good correlation between the rough and smooth bed data. Fig. 6.4(b) shows that Eqn. 3.35 increasingly underpredicts the limiting concentrations as the particle size decreases. It is worthwhile mentioning that Eqn. 3.35 has the same form as that of Eqn. 3.34. However the poorer agreement between the predicted and observed limiting concentrations for Eqn. 3.35 could point to the way the coefficients of this equation was determined. In deriving Eqn. 3.35, Mayerle (1988) used the rectangular rough bed data to extrapolate his equation for smooth pipes to be applicable for both smooth and rough pipes. However, Loveless (1991) showed that different limiting velocities are needed for circular and rectangular rigid bed channels with the latter requiring a lower velocity to keep the sediment in motion. The results of this analysis indicate that the rectangular rough bed data cannot be used to reflect the effect of the roughness of the pipe wall.

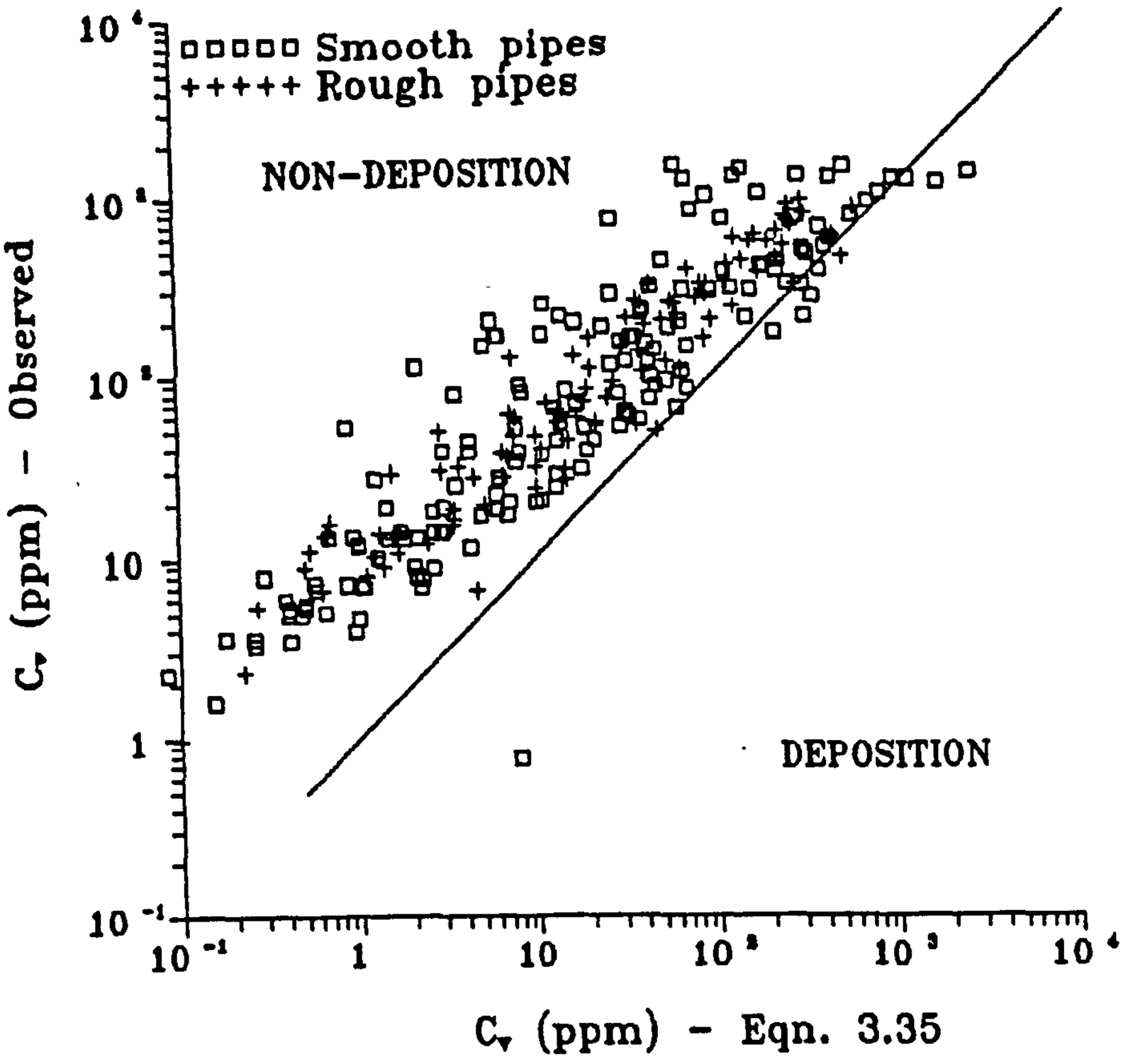

FIG. 6.4a Predicted C_v using Mayerle's Eqn. 3.35

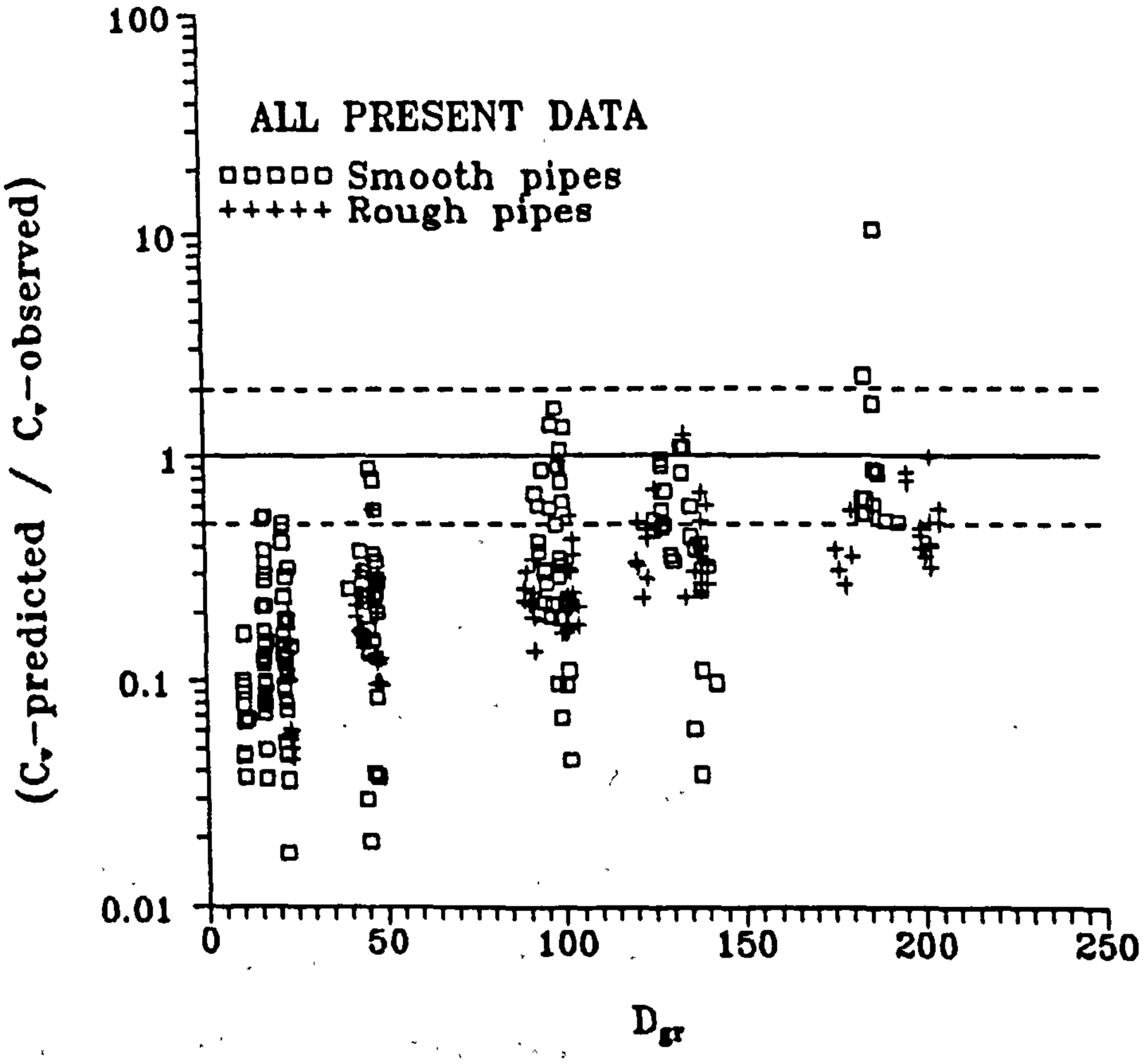

FIG. 6.4b Discrepancy ratio for Mayerle's Eqn. 3.35 as a function of dimensionless particle size

Fig. 6.5(a) shows the computed and observed limiting concentrations for May et al's Eqn. 3.19. As in the case of Mayerle's Eqn. 3.35, Eqn. 3.19 underpredicts the limiting concentrations in nearly all cases for both smooth and rough beds. The underpredictions get larger at concentrations less than 50ppm. Eqn. 3.19 was based on May's (1982) experimental data for pipes of diameter 77mm and 158mm. It was later (May et al 1989) shown that the equation could also work well for a larger pipe diameter (D = 300mm) provided a suitable equation for the threshold velocity (V_c) was used. The results obtained here seem to suggest that the choice of V_c would affect the accuracy of Eqn. 3.19 over the whole range of the limiting concentrations. Overall, only 6% of the predicted concentrations are within 0.5 to 2.0 times of the observed concentrations with the mean discrepancy ratio of 0.18 (see Table 6.2). Fig. 6.5(a) also shows that Eqn. 3.19 correlates both smooth and rough bed data equally well. Fig. 6.5(b) shows that the equations tend to have a similar degree of accuracy over the entire range of particle size.

Macke's Eqn. 3.17 in Fig. 6.6(a) underestimates the limiting concentrations for majority of the present data. Fig. 6.6(b) indicates that better agreement is obtained for $D_{gr} < 30$. This means that Eqn. 3.17, derived for suspended load transport, is also applicable for bed load transport in pipes as long as the sediment being transported is limited to sands of size up to about 1.2mm. The discrepancies get larger as the size of sediment increases as can be seen in Fig. 6.6(b). Fig. 6.6(a)

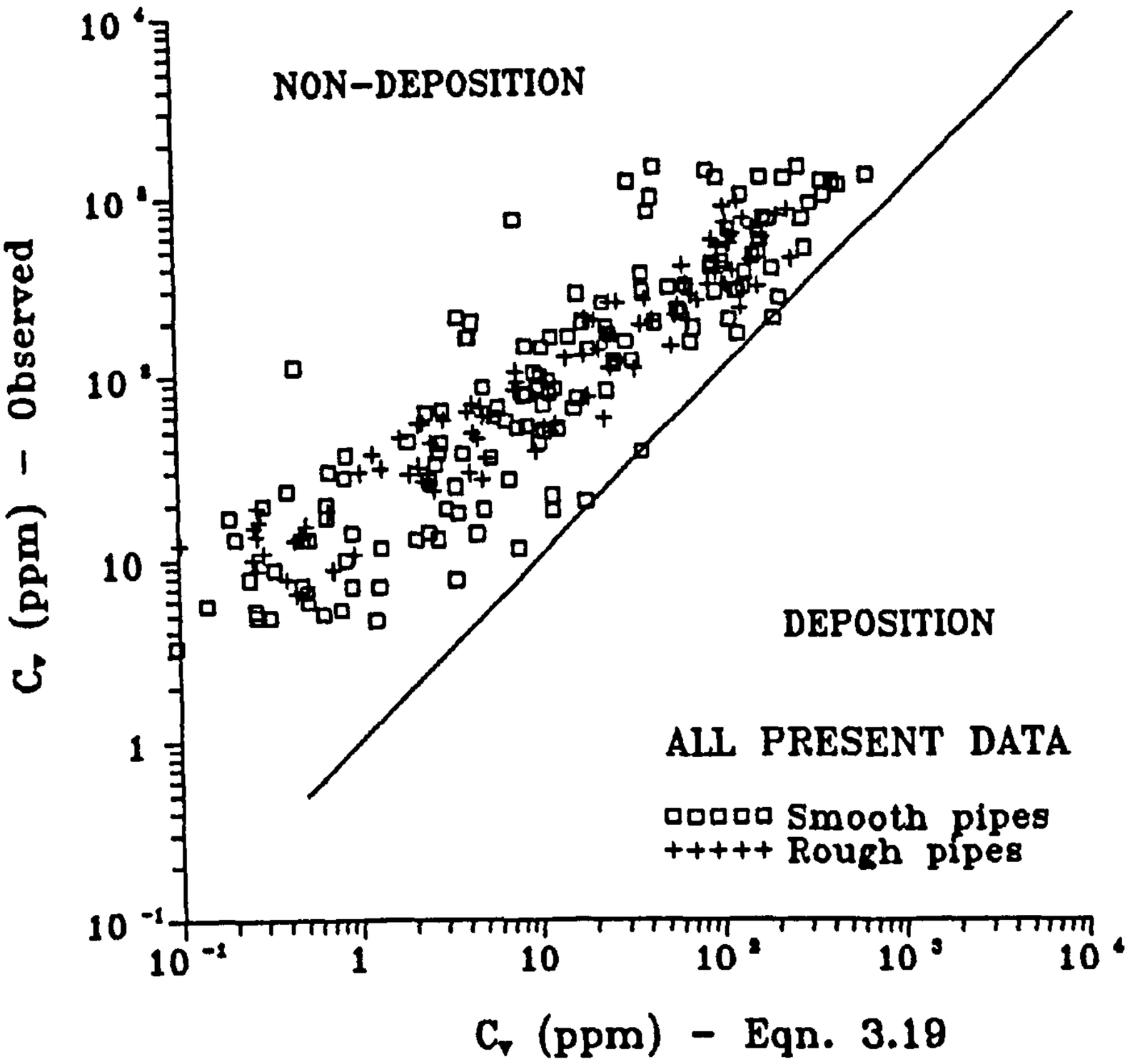

FIG. 6.5a Predicted C_v using May et al's Eqn. 3.19

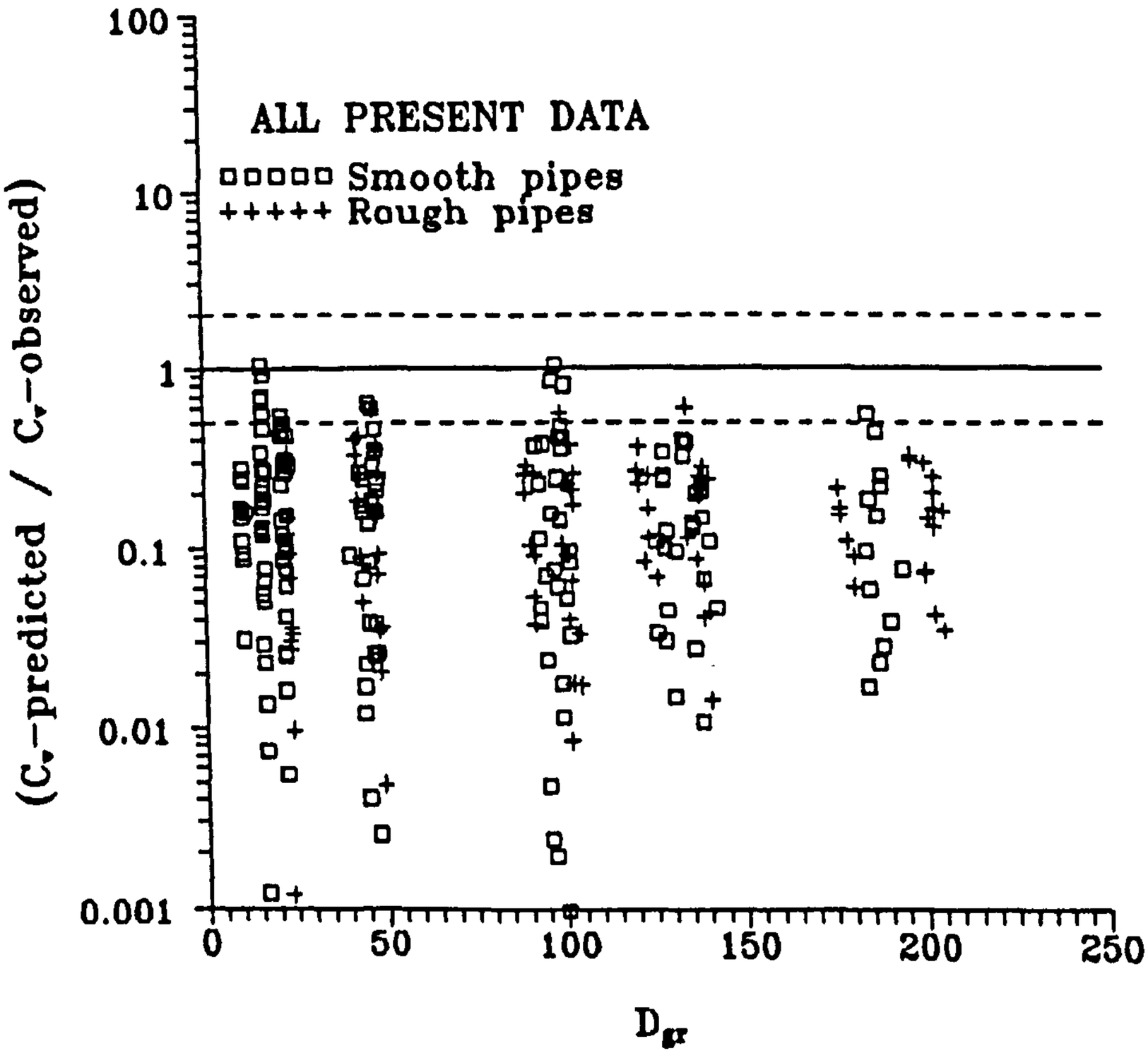

FIG. 6.5b Discrepancy ratio for May et al's Eqn. 3.19 as a function of dimensionless particle size

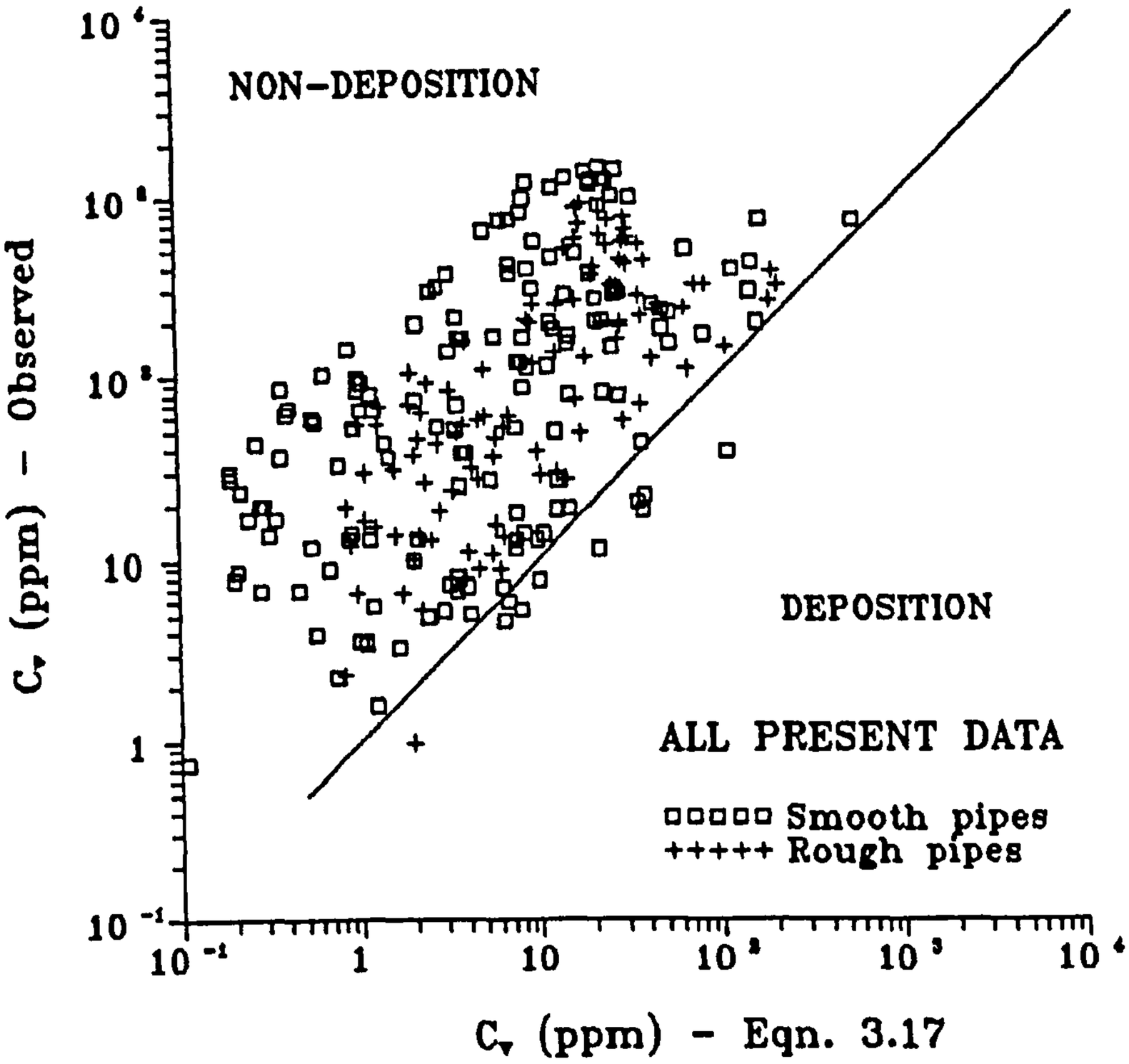

FIG. 6.6a Predicted C_v using Macke's Eqn. 3.17

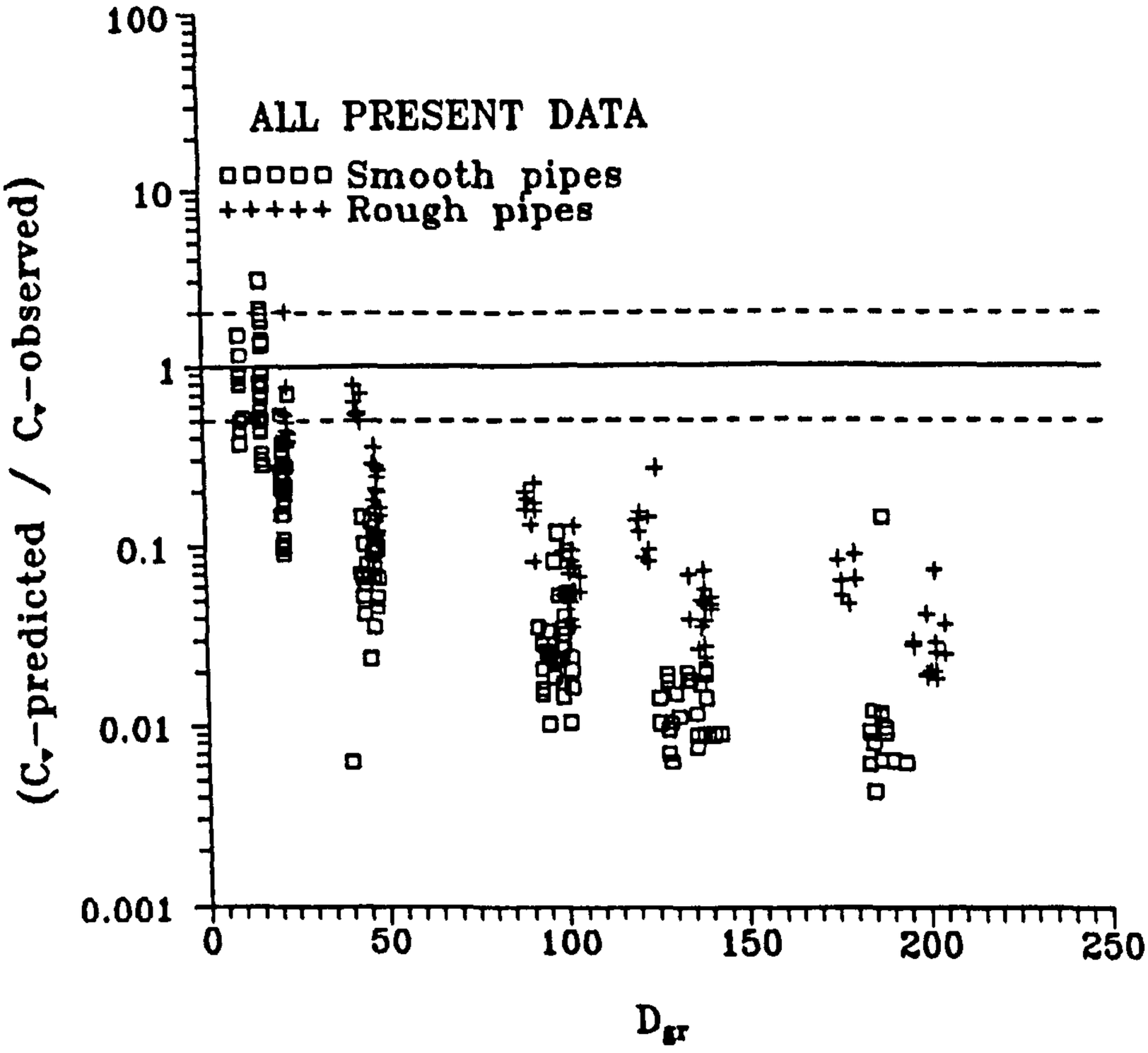

FIG. 6.6b Discrepancy ratio for Macke's Eqn. 3.17 as a function of dimensionless particle size

shows that Eqn. 3.17 tends to correlate the smooth and rough bed data well though there is significant scatter. Overall, Eqn. 3.17 has a mean discrepancy ratio of 0.24 with only 16% of the predicted concentrations fall within 0.5 to 2.0 times the observed concentrations (see Table 6.2).

The comparisons as presented above show that none of the existing equations adequately predicts the limiting concentrations for the present experimental data. In general, within the range of data tested, the equations that give the best results are fairly simple regression equations such as those of Laursen's Eqn. 3.11 and Novak-Nalluri's Eqn. 3.15 while the more complex equations such as that of May et al's Eqn. 3.19 and Macke's Eqn. 3.17 give poorer results. The effect of wall roughness on the limiting concentrations seems to be reflected in most of the equations tested with the exception of Mayerle's Eqn. 3.34.

6.1.3 Bed load Models for Clean Pipes

6.1.3.1 Introduction

As mentioned previously in Section 6.1.1, there are two most commonly used approaches in analysing the sediment transport data in clean pipe channels namely, dimensional and theoretical analyses.

Dimensional analysis involves the generation of functional relationships or models from which the resulting equations are obtained through statistical fittings (Robinson-Graf 1972, Mayerle 1988) or eye-fittings (Ambrose 1953, Novak-Nalluri 1975, Arora et al 1984) to transport data.

Theoretical analysis on the basic forces acting on a particle along the pipe invert usually leads to a complicated form of equation (May 1982-1993, Mat Suki 1987, Loveless 1991). This theoretical model usually requires many simplifications such that the performance of the resulting equation could be greatly affected.

In the present study dimensional analysis is used throughout to analyse the author's data as well as the data from other relevant studies which were considered appropriate. Several functional relationships were considered and multiple regression analyses were used to obtain the required equations. Attempts were also made to modify a loose bed model (Ackers 1991) to broaden its applicability to clean pipe channels. Furthermore an attempt was

BOX A1 Multiple Linear Regression Analysis

Basic form:

$$y = \beta_o + \beta_1 x_1 + \beta_2 x_2 + \ldots + \beta_k x_k + e \qquad (A1.1)$$

where y is the dependent variable, x_1, x_2, ..., x_k are the independent variables, β_0, β_1, ..., β_k are the regression coefficients, and ε is the error term denoting the discrepancy between the observed dependent variable and that computed by the best-fit line. In the regression analysis, unknown regression coefficients are determined using the "least squares principle" by which the sum of squares of differences between the observed and computed dependent variable y is minimized.

The aim of the present study is to obtain a power-law equation:

$$Y = b_o A_1^{b1} A_2^{b2} A_3^{b3} A_4^{b4} \qquad (A1.2)$$

where Y is the dominant variable, A_1, ..., A_4 are the independent variables, and b_0, ..., b_4 are the unknown regression coefficients. The application of the multiple regression analysis (Eqn. A1.1) will require Eqn. A1.2 to be expressed in the logarithmic form:

$$\log Y = \log 10^{b_o} + b_1 \log A_1 + b_2 \log A_2 + b_3 \log A_3 + b_4 \log A_4 \qquad (A1.3)$$

It should be noted that several previous works (Robinson-Graf 1972, Mayerle 1988, El-Zaemey 1991) used the multiple linear regression analysis to obtain the sediment transport relationships in the form of Eqn. A1.2.

There are many computer-software packages that can be used to perform a rather comprehensive regression analysis. In the present study, the author used STATGRAPHICS. This package is capable of handling large data sets, estimating regression parameters, computing confidence/prediction intervals, performing various statistical tests, selecting the best independent variables to name a few.

In the present study, the accuracy of the regression models was based on the values of adjusted determination coefficient (adj. r^2) and standard deviation (s). It should be noted that the value of adj. r^2 may decrease if the independent variables entered do not add significantly to the fit while the value of s indicates the portion of variation in the dependent variable not explained by the regression model.

made to obtain an equation applicable for all channel shapes for rigid boundary conditions. The present design practice was later appraised with the new transport models.

6.1.3.2 Proposed Sediment Transport Equations

As demonstrated in Section 6.1.2, the best results for predicting the limiting concentrations in clean pipes were given by simple regression equations. It is worthwhile stating that in deriving a sediment transport equation, a certain amount of scatter is inevitable and cannot be eliminated by increasing the complexity of the equation. It is therefore decided to keep the form of the equation as simple and as easy to use as possible.

In the following analysis, the overall performance of each regression model is assessed from the values of adj. r^2 and s. The discrepancy ratio in terms of the dependent variable is also given as further evidence of the accuracy of each model. In each case, the average, minimum, and maximum values of the discrepancy ratios for each group of data will be given together with the percentage of data falling within the different range of discrepancy ratios: ± 0.10, ± 0.25, ± 0.50, and 0.50 - 2.0. As mentioned earlier, due to the inevitable presence of scatter, the author believes that the percentage of data lying within the ± 0.25 range of discrepancy ratio should be used as an indication of the reliability of the equation. The final selection of the best-fit model will therefore be based on the equation's values

of adj. r^2, s and the percentage of data occurring within the ± 0.25 deviations.

Since several forms of functional relationships have already existed from earlier works, the author has decided to re-evaluate these forms with the present data. It should be made clear that the chosen functional relationships should include all parameters which contribute significantly to the sediment transport process in clean pipes. Also, the author favours the use of the mean flow velocity (V) instead of the mean shear stress (τ_o) as the dominant variable. This is because τ_o is not constant across the cross-section of the flow. An example of such functional relationship is given by Mayerle (1988):

$$Fr_m = \frac{V}{\sqrt{gd_{50}(S_s-1)}} = f\left(C_v, D_{gr}, \frac{R}{d_{50}}, \lambda_s\right) \qquad (6.1)$$

In Eqn. 6.1, the influence of the sediment concentration, sediment size, flow depth and pipe size, as well as flow resistance (i.e wall roughness and presence of sediment) on the limiting velocity (V) are represented by the dimensionless parameters C_v, D_{gr}, R/d_{50}, and λ_s respectively. The effects of the gravitational acceleration and specific gravity are incorporated in the modified Froude number parameter, Fr_m.

The form of Eqn. 6.1 was initially used to analyse the current experimental data. A summary of the ranges of the relevant parameters is given in Table 6.3. A multiple regression analysis

TABLE 6.3 PARAMETER RANGES - ALL PRESENT DATA (CLEAN PIPES)

(a) SMOOTH PIPES

PARAMETER	D (mm)		
	154	305	450
Fr_m	1.30 - 6.83	1.37 - 13.54	4.69 - 11.37
C_v (ppm)	38 - 1450	1 - 1280	1 - 38
D_{gr}	22.0 - 140.8	10.2 - 194.2	15.9 - 16.9
R/d_{50}	3.87 - 50.05	4.67 - 200.29	155.05 - 188.40
λ_s	0.0159 - 0.0480	0.0129 - 0.0263	0.0142 - 0.0182
D^2/A	1.57 - 13.18	1.48 - 8.32	1.58 - 2.58
y_o/d_{50}	6.57 - 125.42	7.77 - 500.65	308.75 - 468.75
y_o/D	0.157 - 0.757	0.210 - 0.805	0.494 - 0.750
D_h/y	0.69 - 0.98	0.70 - 1.06	0.78 - 0.97
d_{50}/D	0.0060 - 0.0370	0.0015 - 0.0370	0.0016
q/ν	3510 - 71941	6876 - 117296	79541 - 252641
S_c	0.0007 - 0.0034	0.0004 - 0.0034	0.0003 - 0.0019
NO. OF DATA	39	89	27

TABLE 6.3 (CONTINUED)

(b) ROUGH PIPES AND ENTIRE DATA

PARAMETER	D(mm)		ENTIRE DATA
	305 (ROUGHNESS 1)	305 (ROUGHNESS 2)	
Fr_m	1.61 - 7.94	1.87 - 4.78	1.30 - 13.54
C_v (ppm)	1 - 923	6 - 403	1 - 1450
D_{gr}	23.1 - 205.6	42.3 - 181.1	10.2 - 205.6
R/d_{50}	4.06 - 95.32	5.33 - 46.16	3.87 - 200.30
λ_s	0.0210 - 0.0316	0.0261 - 0.0392	0.0129 - 0.0480
D^2/A	1.54 - 10.62	1.55 - 6.75	1.48 - 13.18
y_o/d_{50}	6.66 - 242.58	9.07 - 116.50	6.57 - 500.65
y_o/D	0.177 - 0.772	0.244- 0.764	0.157 - 0.805
D_h/y	0.46 - 1.00	0.71 - 0.99	0.46 - 1.06
d_{50}/D	0.0032 - 0.0272	0.0066 - 0.0272	0.0016 - 0.0370
q/ν	21266 - 114951	29760 - 110845	3510 - 252641
S_c	0.0004 - 0.0036	0.0008 - 0.0036	0.0003 - 0.0036
NO. OF DATA	71	30	256

was performed using the entire present data to give an equation valid for both smooth and rough pipe channels (Fig. 6.7):

$$\frac{V}{\sqrt{gd_{50}(S_s-1)}} = 1.83\, C_v^{0.23}\, D_{gr}^{0.10} \left(\frac{R}{d_{50}}\right)^{0.69} \lambda_s^{-0.04} \qquad (6.2)$$

with adj. r^2 = 0.96 and s = 0.042. Table 6.4 gives the discrepancy ratio in terms of the modified Froude number. 98% of the predicted values of the modified Froude number shown in Fig. 6.7 lie within the ± 0.25 deviation of the observed values with a mean discrepancy ratio of 0.99. The results obtained show that the form of Eqn. 6.1 correlates very well the transport data for different pipe sizes and wall roughnesses. For smooth clean pipes (D = 154mm - 450mm), the percentage of data falling within the ± 0.25 range of discrepancy ratio are 92%, 99% and 100% for the 154mm, 300mm and 450mm dia. pipes respectively while for rough clean pipes (D = 305mm), both roughnesses (k_o = 0.53mm, 1.34mm) have 100% of the data occurring within the ± 0.25 range of discrepancy ratio.

In Eqn. 6.2, the shape effects due to the variation in flow depths were represented by the hydraulic radius (R) which is given by the dimensionless parameter, R/d_{50}, though other variables such as the hydraulic depth, D_h (= $A/\mathcal{B}$) could also be used to represent these shape effects . Several other conveyance shape parameters (as shown in Table 6.1) were then considered to take into account the shape effects by including them in the Mayerle 's function (Eqn. 6.1). Another dimensionless parameter also considered was the ratio of particle size to pipe size

TABLE 6.4 DISCREPANCY RATIO (Fr_*) FOR EQN. 6.2 - ALL PRESENT CLEAN PIPE DATA

D(mm)	Fr_* (predicted) / Fr_* (observed)							No. of data
	Mean	min	max	0.90-1.10 (%)	0.75-1.25 (%)	0.5-1.5 (%)	0.5-2.0 (%)	
154 (Smooth)	1.04	0.72	1.32	61	92	100	100	39
305 (Smooth)	0.99	0.50	1.17	81	99	100	100	89
450 (Smooth)	0.98	0.80	1.18	74	100	100	100	27
305 (k_0 = 0.53mm)	1.01	0.84	1.15	82	100	100	100	71
305 (k_0 = 1.34mm)	0.93	0.76	1.10	67	100	100	100	30
All	0.99	0.50	1.32	75	98	100	100	256

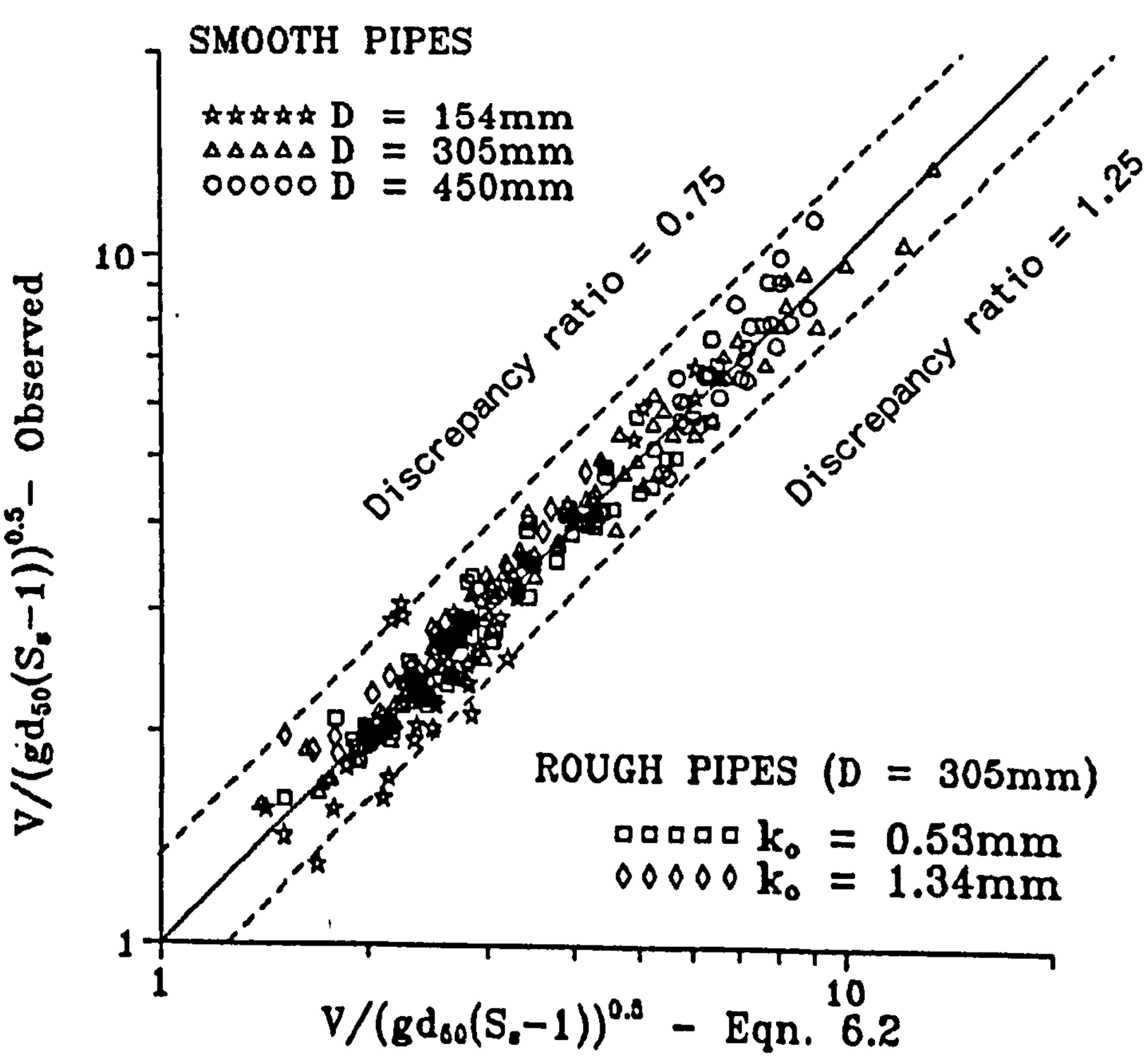

FIG. 6.7 Limiting velocity criterion - Eqn. 6.2 (All present data)

(d_{50}/D). This is used to reflect the effect of the variation in sediment size. The ranges of parameters used in the analysis are given in Table 6.3. The modified functional relationships considered are listed below:

$$\frac{V}{\sqrt{gd_{50}(S_s-1)}} = f\left(C_v, \frac{R}{d_{50}}, \frac{D^2}{A}, D_{gr}, \lambda_s\right) \quad (6.3)$$

$$\frac{V}{\sqrt{gd_{50}(S_s-1)}} = f\left(C_v, \frac{R}{d_{50}}, \frac{y_o}{d_{50}}, D_{gr}, \lambda_s\right) \quad (6.4)$$

$$\frac{V}{\sqrt{gd_{50}(S_s-1)}} = f\left(C_v, \frac{R}{d_{50}}, \frac{d_{50}}{D}, \lambda_s\right) \quad (6.5)$$

$$\frac{V}{\sqrt{gd_{50}(S_s-1)}} = f\left(C_v, \frac{y_o}{d_{50}}, \frac{d_{50}}{D}, D_{gr}, \lambda_s\right) \quad (6.6)$$

$$\frac{V}{\sqrt{gd_{50}(S_s-1)}} = f\left(C_v, \frac{D_h}{y}, \frac{y_o}{d_{50}}, D_{gr}, \lambda_s\right) \quad (6.7)$$

The resulting equations from multiple regression analyses on the entire present data are given in Table 6.5. For comparison, the equation from the original function (Eqn. 6.2) is also included. The performance of all the resulting equations (Eqns. 6.8 - 6.12) as given by a similar value of adj. r^2 shows that the different parameters of conveyance shape and sediment considered do not

TABLE 6.5 TRANSPORT EQUATIONS BASED ON MODIFIED FUNCTIONAL RELATIONSHIPS FOR ENTIRE PRESENT DATA

DEPENDENT VARIABLE	MULTIPLE REGRESSION EQUATION	adj. r^2	s	EQN. NO.
$\frac{V}{\sqrt{gd_{50}(S_s-1)}}$	$1.83\ C_v^{0.23}\left(\frac{R}{d_{50}}\right)^{0.69} D_{gr}^{0.10}\ \lambda_s^{-0.04}$	0.96	0.042	6.2
	$1.35\ C_v^{0.22}\left(\frac{R}{d_{50}}\right)^{0.71}\left(\frac{D^2}{A}\right)^{0.04} D_{gr}^{0.13}\ \lambda_s^{-0.05}$	0.96	0.042	6.8
	$1.64\ C_v^{0.218}\left(\frac{R}{d_{50}}\right)^{0.91}\left(\frac{y_o}{d_o}\right)^{-0.20} D_{gr}^{0.12}\ \lambda_s^{-0.05}$	0.96	0.042	6.9
	$2.90\ C_v^{0.21}\left(\frac{R}{d_{50}}\right)^{0.60}\left(\frac{d_{50}}{D}\right)^{0.01}\ \lambda_s^{-0.08}$	0.96	0.044	6.10
	$0.68\ C_v^{0.24}\left(\frac{y_o}{d_{50}}\right)^{0.44}\left(\frac{d_{50}}{D}\right)^{-0.26} D_{gr}^{0.12}\ \lambda_s^{-0.08}$	0.96	0.044	6.11
	$1.06\ C_v^{0.22}\left(\frac{D_h}{y_o}\right)^{-0.03}\left(\frac{y_o}{d_{50}}\right)^{0.07} D_{gr}^{0.08}\ \lambda_s^{-0.05}$	0.96	0.043	6.12

make any significant improvement. It is therefore decided to use the original function (Eqn. 6.1) for further data analysis.

When an equation is based primarily on dimensional and regression analyses, it becomes extremely important to have a data base containing a wide range of data. The importance of a sufficient data base has been demonstrated in the appraisals of the alluvial channel relationships (White et al 1975, Brownlie 1981, Yang-Molinas 1982). The results show that those equations based on dimensional analysis and a large data base such as that by Yang (1973) and Brownlie (1981) were found to give a high percentage of data falling within the range of discrepancy ratio of between 0.5 and 2.0.

It is therefore decided to include experimental data from earlier works of Mayerle (1988), May et al (1989) and Loveless (1991) to give a revised relationship which could be applicable over a wider range of conditions. All data from these works were collected in smooth pipe channels with the exception of Loveless's which has both smooth and limited rough data. The ranges of parameters for the combined data are given in Table 6.6. The combination of these data yielded the following best-fit relationship (Fig. 6.8):

TABLE 6.6 RANGES OF PARAMETERS FOR COMBINED DATA (CLEAN PIPES)

PARAMETER	MAYERLE (1988)	MAY ET AL (1989)	LOVELESS (1991)	PRESENT DATA
Fr_m	1.31 - 12.50	4.63 - 14.00	2.02 - 12.77	1.30- 13.54
C_v (ppm)	20 - 1275	1 - 507	74 - 2010	1 - 1450
D_{gr}	12.5 - 215.6	14.2 - 17.0	10.5 - 147.8	10.2 - 205.6
R/d_{50}	2.43 - 91.36	49.87 - 125.28	3.28 - 103.85	3.87 - 200.30
λ_s	0.0158 - 0.0338	0.0158 - 0.0234	0.0148 - 0.0695	0.0129 - 0.0480
q/v	8037 - 122900	18576 - 214148	3907 - 61822	3510 - 252641
y_o/d_{50}	4.12 - 224.00	91.34 - 311.46	5.28 - 193.33	6.57 - 500.65
S_c	0.0009 - 0.0037	0.0005- 0.0055	0.0020 - 0.0090	.0003 - .0036
D_h/y_o	0.70 - 1.06	0.74 - 1.01	0.69 - 0.84	0.46 - 1.06
NO. OF DATA	106	51	46	256

$$\frac{V}{\sqrt{gd_{50}(S_s-1)}} = 3.08\ C_v^{0.21}\ D_{gr}^{-0.09} \left(\frac{R}{d_{50}}\right)^{0.53} \lambda_s^{-0.21} \qquad (6.13)$$

with adj. $r^2 = 0.95$ and $s = 0.057$. The results shown in Fig. 6.8 have a perfect average discrepancy ratio of 1.0 (see Table 6.7) where 94% of the combined data occur within the ± 0.25 range of discrepancy ratio.

When assessing the statistics given in Table 6.7, it is worthwhile remembering that each investigator used different experimental techniques. More importantly, the criterion used for the determination of the limit of deposition is subjective as it is based on the observations of each investigator. These differences could account for the scatter shown in Fig. 6.8. Table 6.7 shows that each investigator's data has more than 90% of them lying within the ± 0.25 range of discrepancy ratio while the average discrepancy ratio varies from 0.89 to 1.05. Due to its large data base (a total of 459 data) covering different experimental techniques, these results suggest that Eqn. 6.13 would be applicable over a wide range of conditions in sewers with clean inverts.

The application of Eqn. 6.13 requires a separate equation for the computation of the friction factor with sediment, λ_s. This required equation could be evaluated from a functional relationship proposed by Nalluri and Kithshiri (1992):

$$\lambda_s = f\ (\lambda_o, C_v, D_{gr}) \qquad (6.14)$$

TABLE 6.7 DISCREPANCY RATIO (Fr_m) FOR EQN. 6.13 - COMBINED DATA (CLEAN PIPES)

Source of data	Fr_s (predicted) / Fr_s (observed)							No. of data
	Mean	min	max	0.90-1.10 (%)	0.75-1.25 (%)	0.5-1.5 (%)	0.5-2.0 (%)	
Present	1.05	0.57	1.38	57	91	100	100	256
Mayerle (1988)	0.95	0.75	1.19	66	100	100	100	106
May et al (1989)	0.89	0.64	1.18	39	94	100	100	51
Loveless (1991)	0.97	0.78	1.41	80	100	100	100	46
Combined	1.00	0.57	1.41	59	94	100	100	459

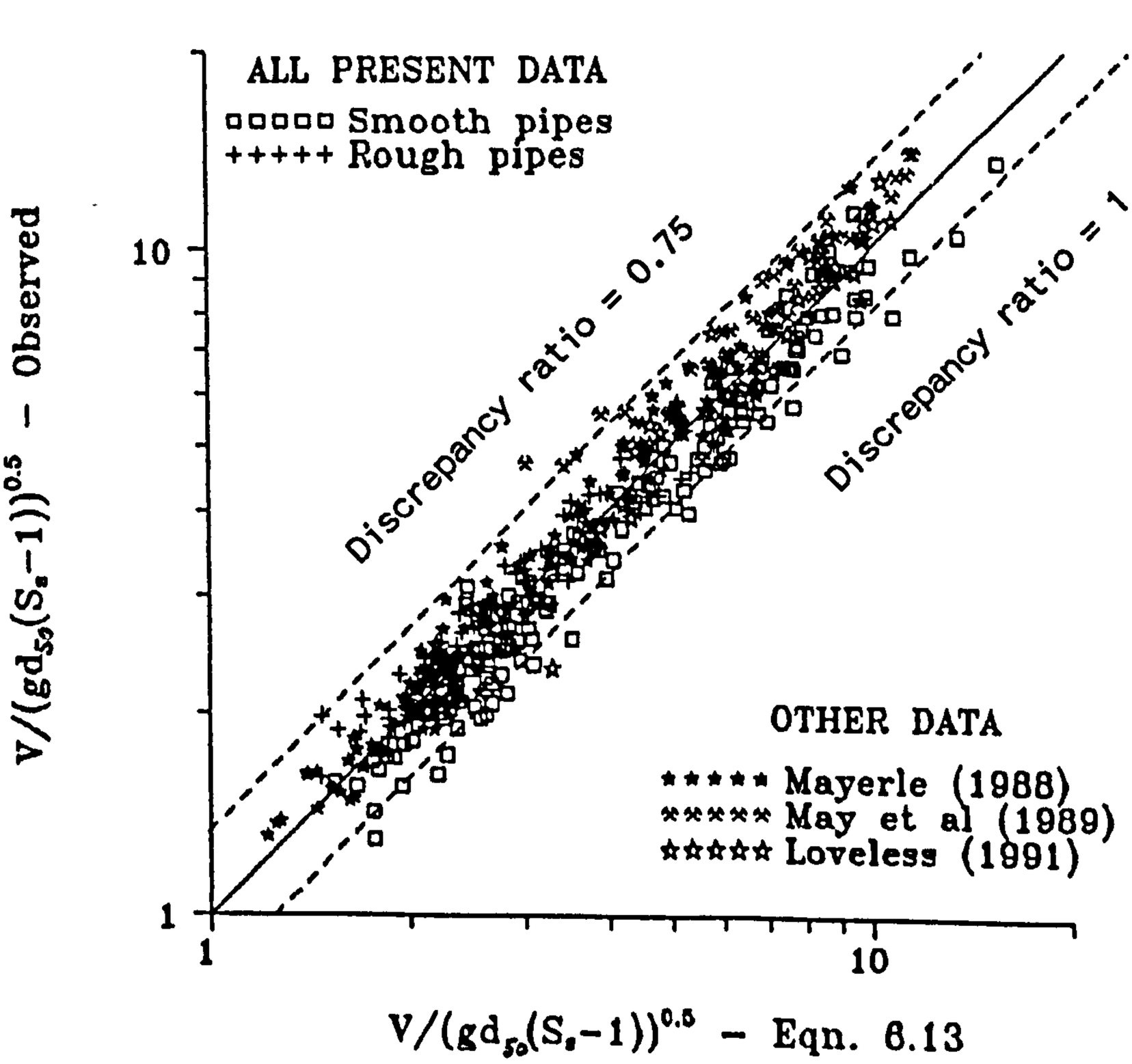

FIG. 6.8 Limiting velocity criterion - Eqn. 6.13 (Combined data)

λ_o being the clear-water friction factor of the channel. A multiple regression analysis was applied to the entire present data. The resulting best-fit equation (adj. r^2 = 0.96, s = 0.023) was given as:

$$\lambda_s = 1.15\ \lambda_o^{0.99}\ C_v^{0.02}\ D_{gr}^{0.01} \qquad (6.15)$$

Utilising the combined data (see Table 6.6) the regression yielded (adj. r^2 = 0.95, s = 0.023):

$$\lambda_s = 1.13\ \lambda_o^{0.98}\ C_v^{0.02}\ D_{gr}^{0.01} \qquad (6.16)$$

Loveless (1991) did not produce the information on the clear water friction factor preceding transport tests. His data were therefore omitted in the derivation of Eqn. 6.16. Fig. 6.9 shows the predicted λ_s using Eqn. 6.16 plotted against observed λ_s. The discrepancy ratios in terms of λ_s are given in Table 6.8. The results shown in Fig. 6.9 have an average discrepancy ratio of 1.0 where 94% of the data fall within ± 0.10 range of discrepancy ratio. Eqn. 6.16 suggests that the presence of sediment in the flow would increase the friction factor by about 13% to that of clear water flow. This is consistent with the findings from previous works (Laursen 1956, May 1982, Mat Suki 1987) where it was found that the increase in the friction factor varies from 5% to 20%. Due to the low scatter and minimum asymmetry of the deviation in deriving Eqn. 6.16, it should be applied with confidence to any sediment transport equation. The friction factor for clear water conditions should be computed from the Colebrook-White's Eqn. 5.7.

TABLE 6.8 DISCREPANCY RATIO (λ_s) FOR EQN. 6.16 - COMBINED DATA (CLEAN PIPES)

Source of data	λ_s (predicted) / λ_s (observed)							No. of data
	Mean	min	max	0.90-1.10 (%)	0.75-1.25 (%)	0.5-1.5 (%)	0.5-2.0 (%)	
Present	1.00	0.85	1.21	94	100	100	100	256
Mayerle (1988)	1.00	0.86	1.03	99	100	100	100	106
May et al (1989)	1.01	0.87	1.23	84	100	100	100	51
Combined	1.00	0.85	1.23	94	100	100	100	413

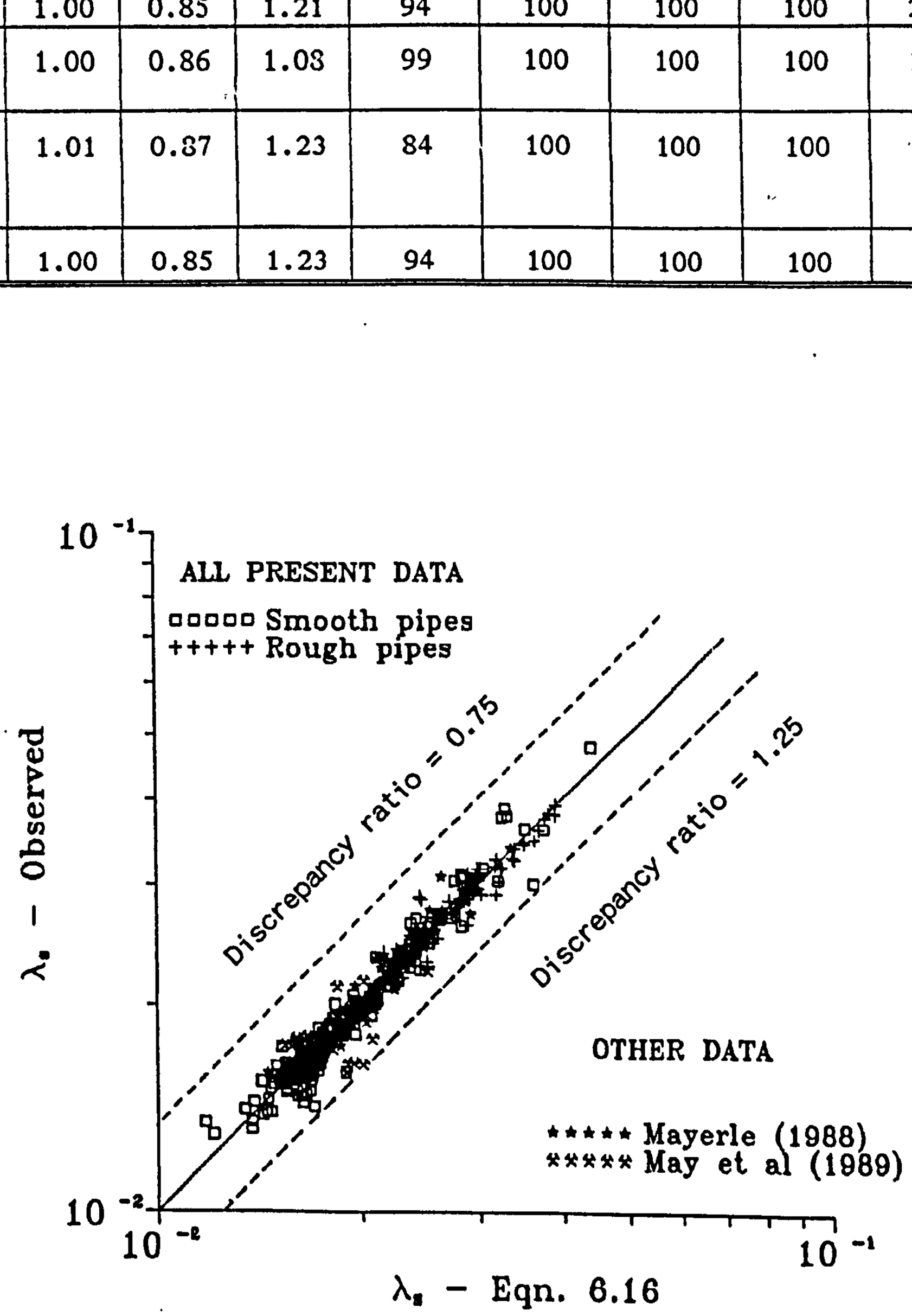

FIG. 6.9 Friction factor with sediment model – Eqn. 6.16 (Combined data)

Mayerle's function (Eqn. 6.1) utilises Fr_* as the dependent variable. The function was then re-evaluated with C_v as the dependent variable:

$$C_v = f\left(\frac{V}{\sqrt{gd_{50}(S_s-1)}}, D_{gr}, \frac{R}{d_{50}}, \lambda_s\right) \qquad (6.17)$$

For comparison, the regression was performed on the entire present data and this yielded (adj. $r^2 = 0.94$, $s = 0.192$):

$$C_v = 0.28\left(\frac{V}{\sqrt{gd_{50}(S_s-1)}}\right)^{3.81} D_{gr}^{-0.70}\left(\frac{R}{d_{50}}\right)^{-3.00}\lambda_s^{0.13} \qquad (6.18)$$

The high value of adj. r^2 obtained in Eqn. 6.18 suggests that it correlates well the present data. The applicability of the form of Eqn. 6.17 for a wider range of data is assessed by applying the regression on the combined data (Table 6.6). The resulting equation was given as:

$$C_v = 0.03\left(\frac{V}{\sqrt{gd_{50}(S_s-1}}\right)^{3.54} D_{gr}^{-0.11}\left(\frac{R}{d_{50}}\right)^{-2.47}\lambda_s^{0.57} \qquad (6.19)$$

with adj. $r^2 = 0.89$ and $s = 0.236$. Fig. 6.10 compares the limiting concentrations predicted by Eqn. 6.19 with the observed values. The values of the discrepancy ratios in terms of volumetric sediment concentration (C_v) are given in Table 6.9. It was found that few data had very low values of the discrepancy ratios. It was therefore decided to include only those data that lie within the range of discrepancy ratio of 0.2 - 5.0. The

TABLE 6.9 DISCREPANCY RATIO (C_v) FOR EQN. 6.19 - COMBINED DATA (CLEAN PIPES)

Source of data	C_v (predicted) / C_v (observed)							No. of data
	Mean	min	max	0.90-1.10 (%)	0.75-1.25 (%)	0.5-1.5 (%)	0.5-2.0 (%)	
Present	0.89	0.21	2.94	12	43	81	86	254
Mayerle (1988)	1.40	0.60	3.11	17	38	64	87	105
May et al (1989)	1.51	0.70	4.62	25	46	63	75	48
Loveless (1991)	1.01	0.24	1.84	17	50	87	96	46
Combined	1.10	0.21	4.63	15	43	76	86	454

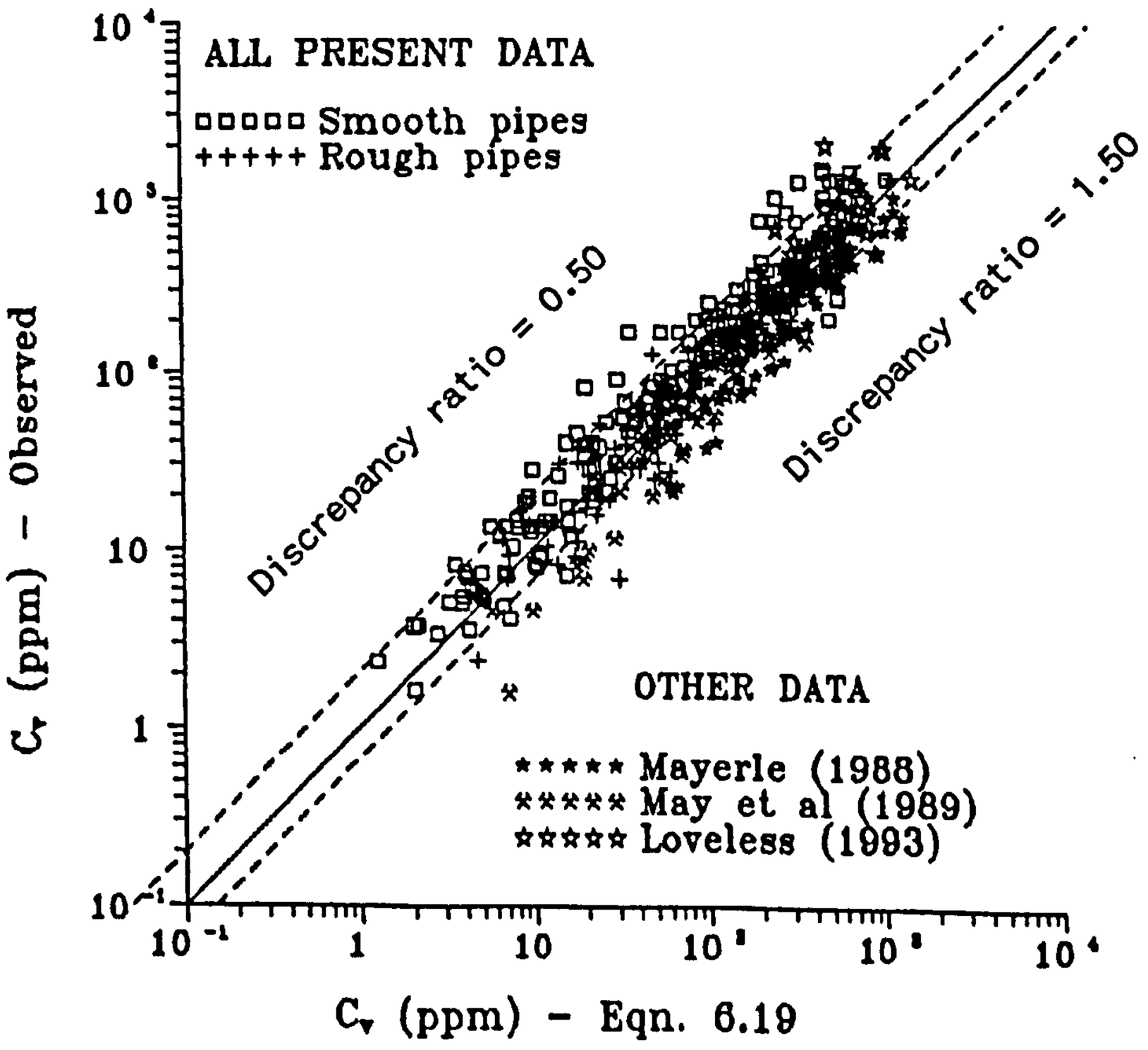

FIG. 6.10 Transport capacity criterion – Eqn. 6.19 (Combined data)

omitted data were found to be in the range of C_v less than 2ppm. The results shown in Fig. 6.10 have an average discrepancy ratio of 1.10. Only 43% of the combined data shown in Fig. 6.10 fall within the ± 0.25 range of the discrepancy ratio. An examination on each of the investigator's data also reveals poor results where 41% to 50% occur within the ± 0.25 range of the discrepancy ratio while the average discrepancy ratio varies from 0.89 to 1.51. Fig. 6.10 reveals that better agreement is obtained at higher limiting concentrations (C_v > 100ppm). The above analysis suggests that the form of Eqn. 6.17 does not represent the bed load transport process in clean pipes well. This is due to its inability to cope with both a large number and wider range of data.

An attempt was then made to re-evaluate another function with C_v as the dependent variable. Paul-Sakhuja (1990) proposed a function which was intended to be applicable for various channel shapes:

$$C_v = f\left(\frac{q}{v}, \frac{y_o}{d_{50}}, S_c, \lambda_s, \frac{D_h}{y_o}\right) \qquad (6.20)$$

There are two main differences between this function (Eqn. 6.20) and that of the modified Mayerle's function (Eqn. 6.17). Firstly, the effects of flow depth and pipe size are accounted for by both parameters D_h/y_o and y_o/d_{50} with the latter also reflecting the effect of particle size. Secondly, both the slope parameter, S_c, and the friction factor parameter, λ_s, are expected to take into account the effect of flow resistance.

A multiple regression analysis on the entire present data resulted in the following best-fit equation (adj. $r^2 = 0.94$, s = 0.172):

$$C_v = 15.26 \left(\frac{q}{v}\right)^{-0.41} \left(\frac{y_o}{d_{50}}\right)^{-0.44} S_c^{2.02} \lambda_s^{-2.01} \left(\frac{D_h}{y_o}\right)^{0.85} \qquad (6.21)$$

This high value of adj. r^2 suggests further analysis using the combined data (Table 6.6). The regression then yielded (Fig. 6.11):

$$C_v = 0.63 \left(\frac{q}{v}\right)^{-0.02} \left(\frac{y_o}{d_{50}}\right)^{-0.59} S_c^{1.75} \lambda_s^{-1.26} \left(\frac{D_h}{y_o}\right)^{-0.31} \qquad (6.22)$$

with adj. $r^2 = 0.89$ and s = 0.538. It is interesting to note that the value of adj. r^2 of Eqn. 6.22 is similar to that of Eqn. 6.19. A comparison of the discrepancy ratios (see Table 6.9 and 6.10) for these two equations (Eqns. 6.19 and 6.22) indicates that they have almost identical accuracies . Both equations have an average discrepancy ratio of 1.10 and with 43%-45% of the combined data falling within the ± 0.25 range of the discrepancy ratio. The results suggests that the complexity of the form of an equation (such as Eqn. 6.20) does not necessarily increase its performance. The analyses done on both forms of functional relationships (Eqns. 6.17 and 6.20) with C_v as the dependent variable show that neither of them represent the bed load process in clean pipes well.

TABLE 6.10 DISCREPANCY RATIO (C_v) FOR EQN. 6.22 - COMBINED DATA (CLEAN PIPES)

Source of data	C_v (predicted) / C_v (observed)							No. of data
	Mean	min	max	0.90-1.10 (%)	0.75-1.25 (%)	0.5-1.5 (%)	0.5-2.0 (%)	
Present	0.92	0.23	2.80	18	43	81	87	254
Mayerle (1988)	1.36	0.59	3.25	18	41	69	89	105
May et al (1989)	1.51	0.72	4.11	21	44	62	75	48
Loveless (1991)	1.04	0.22	1.95	24	50	83	91	46
Combined	1.09	0.22	4.31	19	43	76	86	453

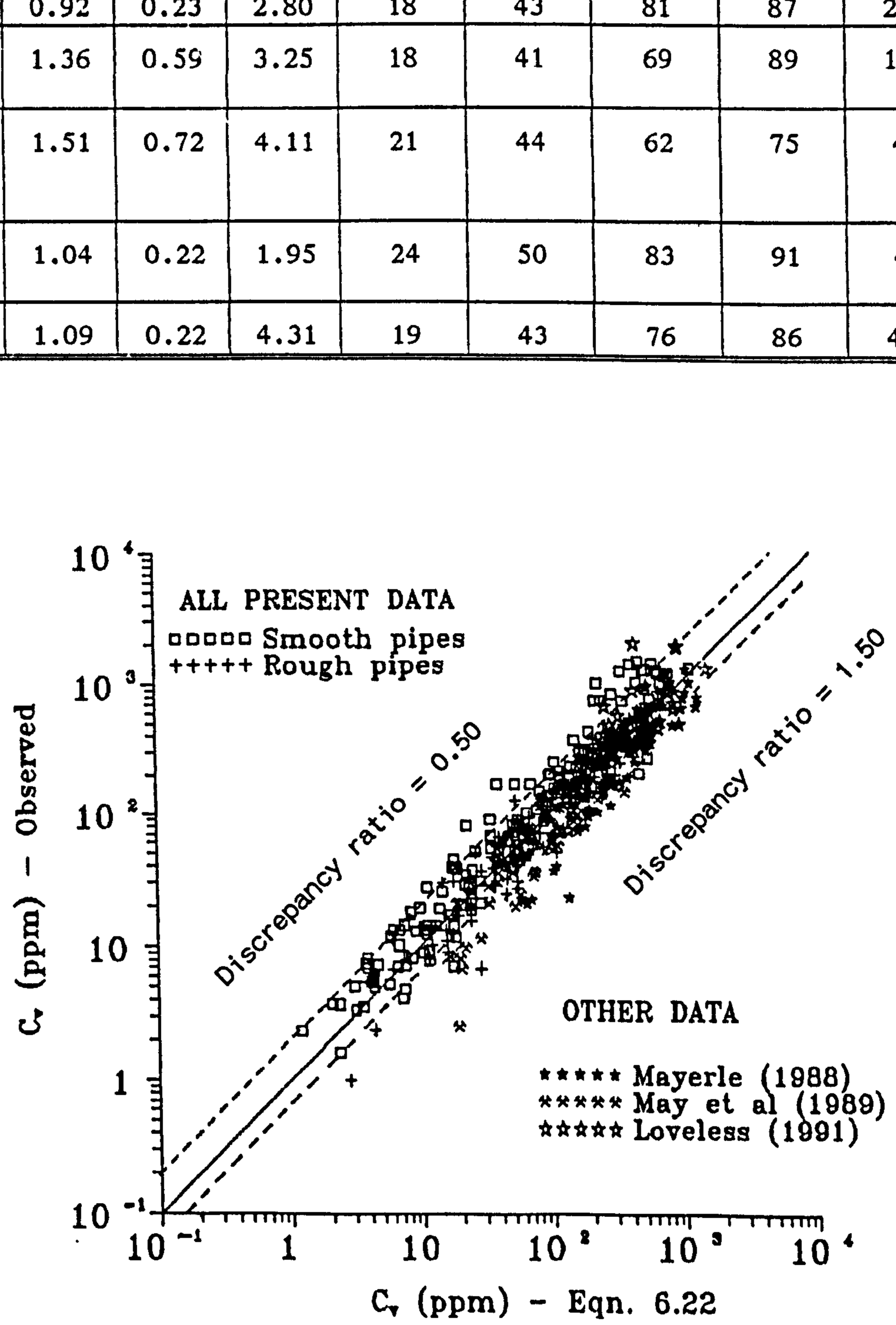

FIG. 6.11 Transport capacity criterion – Eqn. 6.22 (Combined data)

The preceding analyses using functional relationships with C_v as the dependent variable (Eqns. 6.19 and 6.22) indicate that the discrepancies between the predicted and observed limiting concentrations get larger with decreasing sediment concentration. This can be seen in Figs. 6.10 and 6.11 where more scatter is present for C_v less than 50ppm. Attempts were then made to assess the effect of including an incipient motion criterion in a sediment transport equation to improve the accuracy of predicting the limiting sediment concentration when the concentration is low.

It was decided to introduce the critical modified Froude number, $Fr_{m,cr}$ ($= V_c/[gd_{50}(S_s-1)]^{0.5}$) in the Mayerle's function (Eqn. 6.1) due to its simple form. Two modified functions were considered: one with the excess Fr_m as the dependent variable:

$$\frac{V - V_c}{\sqrt{gd_{50}(S_s-1)}} = f\left(C_v, D_{gr}, \frac{R}{d_{50}}, \lambda_s\right) \qquad (6.23)$$

and the other with C_v as the dependent variable:

$$C_v = f\left(\frac{V - V_c}{\sqrt{gd_{50}(S_s-1)}}, D_{gr}, \frac{R}{d_{50}}, \lambda_s\right) \qquad (6.24)$$

Multiple regression analyses were later applied to these two functions to obtain the required equations. For each function, the regressions were first done with the entire present data and then with the combined data (Table 6.6).

Initially, Novak-Nalluri equation (Eqn. 3.5) was chosen as the required criterion for incipient motion:

$$\frac{V_c}{\sqrt{gd_{50}(S_s-1)}} = 0.50\left(\frac{R}{d_{50}}\right)^{0.40} \qquad (3.5)$$

Table 6.11 gives the results of the regression analyses. Considering the analysis of the combined data, Eqn. 6.26 shows that both of the modified functions give relationships with similar values of adj. r^2. Hence either of the resulting equations (Eqn. 6.26a or Eqn. 6.26b) may be used for predicting the limiting concentrations. It is useful to compare the performance of Eqns. 6.19 and 6.26b to assess directly the effect of the inclusion of the incipient motion criterion. The comparison between the observed and predicted concentrations using Eqn. 6.26b is shown in Fig. 6.12. Table 6.12 gives the corresponding discrepancy ratios in terms of C_v. The results shown in Fig. 6.12 have an average discrepancy ratio of 1.10 with 45% of the combined data lying within ± 0.25 deviations. Comparisons of the discrepancy ratios for Eqn. 6.26b (Table 6.12) and Eqn. 6.19 (Table 6.9) show that there is no substantial improvement in the prediction of the limiting concentrations with the introduction of Novak-Nalluri's incipient motion criterion in Eqn. 6.26b.

An alternative incipient motion criterion could be found from the interpolation of the transport data. Plots of C_v vs. $\{Fr_m * (R/d_{50})^a\}$ were executed where the coefficient 'a' was adjusted for all data to collapse into a single line (see Fig. 6.13).

TABLE 6.11 EXCESS VELOCITY EQUATIONS USING NOVAK-NALLURI'S EQN. 3.5 FOR INCIPIENT MOTION

DATA SOURCE	MULTIPLE REGRESSION EQUATION	adj. r^2	s	EQN. NO.
PRESENT DATA	$\frac{V - V_c}{\sqrt{gd_{50}(S_s-1)}} = 1.63\, C_v^{0.57} \left(\frac{R}{d_{50}}\right)^{1.14} D_{gr}^{0.30}\, \lambda_s^{-0.07}$	0.88	0.110	6.25a
	$C_v = 1.10 \left[\frac{V - V_c}{\sqrt{gd_{50}(S_s-1)}}\right]^{1.49} \left(\frac{R}{d_{50}}\right)^{-2.17} D_{gr}^{-0.18}\, \lambda_s^{-0.02}$	0.94	0.179	6.25b
COMBINED DATA	$\frac{V - V_c}{\sqrt{gd_{50}(S_s-1)}} = 5.43\, C_v^{0.452} \left(\frac{R}{d_{50}}\right)^{0.67} D_{gr}^{-0.18}\, \lambda_s^{-0.43}$	0.87	0.127	6.26a
	$C_v = 0.11 \left[\frac{V - V_c}{\sqrt{gd_{50}(S_s-1)}}\right]^{1.60} \left(\frac{R}{d_{50}}\right)^{-1.60} D_{gr}^{-0.17}\, \lambda_s^{0.51}$	0.88	0.239	6.26b

TABLE 6.12 DISCREPANCY RATIO FOR EQN. 6.26b - COMBINED DATA (CLEAN PIPES)

Source of data	C_v(predicted) / C_v (observed)							No. of data
	Mean	min	max	0.90-1.10 (%)	0.75-1.25 (%)	0.5-1.5 (%)	0.5-2.0 (%)	
Present	0.92	0.13	3.69	16	50	79	85	255
Mayerle (1988)	1.43	0.52	3.79	17	35	64	90	105
May et al (1989)	1.50	0.45	3.76	9	28	64	79	47
Loveless (1991)	0.89	0.28	1.56	30	54	83	87	46
Combined	1.10	0.13	3.79	17	45	74	85	453

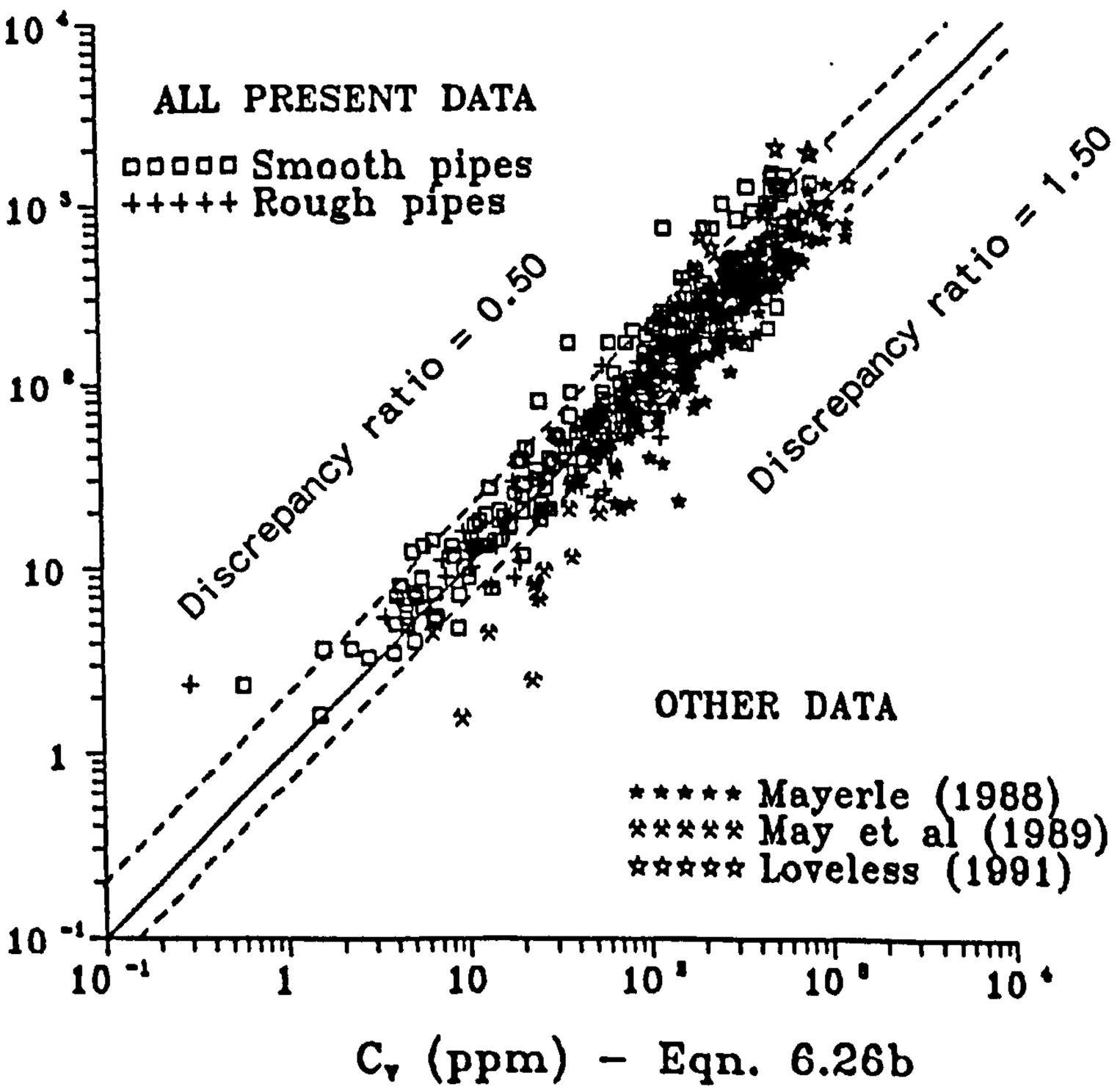

FIG. 6.12 Excess velocity criterion - Eqn. 6.26b with Novak-Nalluri's Eqn. 3.5 (Combined data)

Assuming that the incipient motion occurs at a selected low sediment concentration, an equation similar to that of Novak-Nalluri (Eqn. 3.5) would be obtained:

$$\frac{V_c}{\sqrt{gd_{50}(S_s-1)}} = b\left(\frac{R}{d_{50}}\right)^a \qquad (6.27)$$

At the chosen value of C_v which represents the point of the incipient motion, the corresponding constant 'b'is obtained on the abscissa. Based on the entire present data as shown in Fig. 6.13a, the incipient motion is assumed to occur at C_v = 1ppm (which was the lowest concentration obtained in the present study). This yielded:

$$\frac{V_c}{\sqrt{gd_{50}(S_s-1)}} = 0.189\left(\frac{R}{d_{50}}\right)^{0.60} \qquad (6.28)$$

Performing similar analysis on the combined data produced (Fig. 6.13b):

$$\frac{V_c}{\sqrt{gd_{50}(S_s-1)}} = 0.146\left(\frac{R}{d_{50}}\right)^{0.65} \qquad (6.29)$$

Fig. 6.14 shows values of $Fr_{*,cr}$ computed using different incipient motion criteria over the range of R/d_{50} (= 2 - 200) for the combined data (Table 6.6). As expected, the author's Eqns. 6.28 and 6.29 give lower values of $Fr_{*,cr}$ compared to those of Novak-Nalluri's Eqn. 3.5. The lift force required to start the motion of particles is relatively larger than the one at the

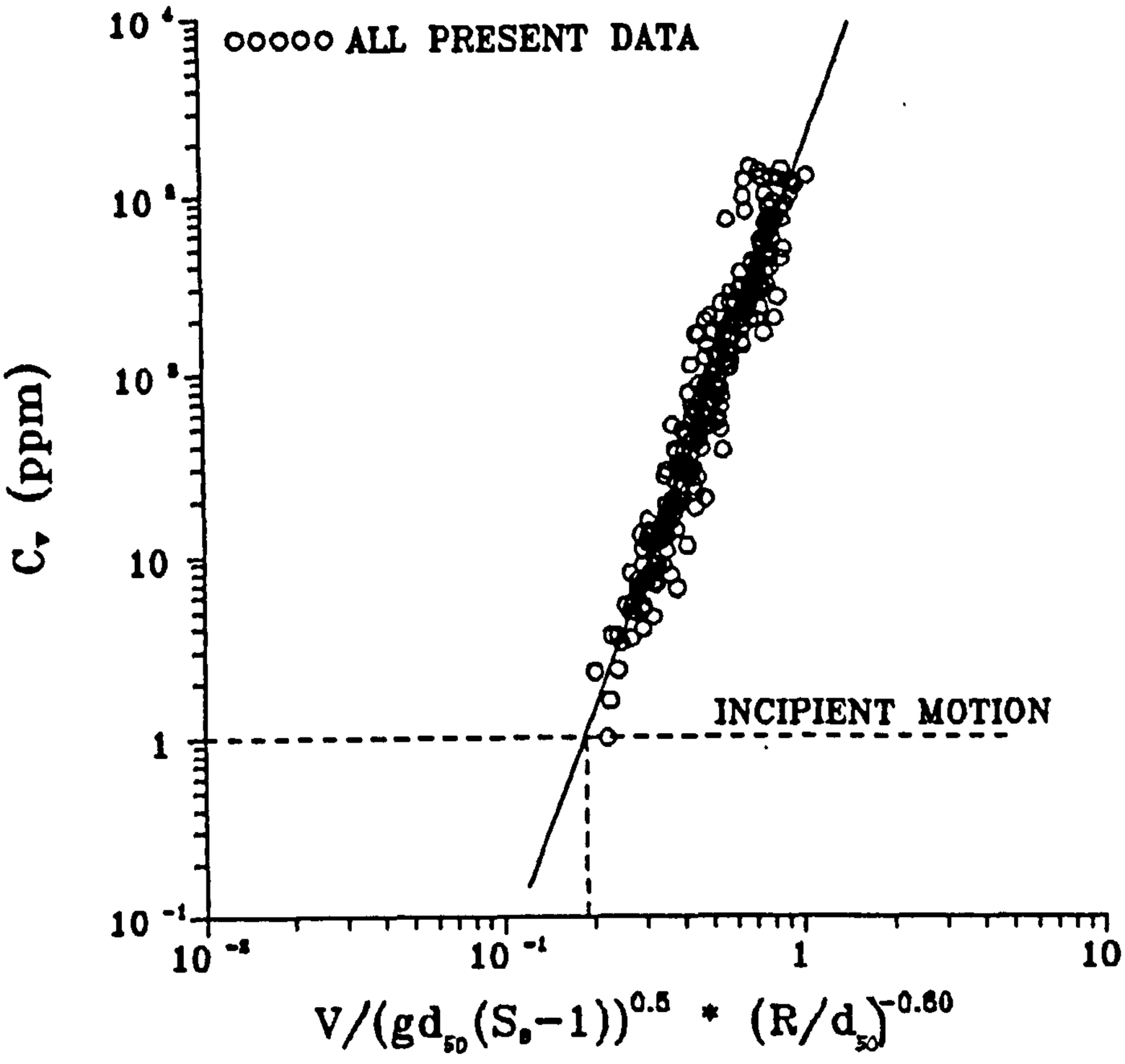

FIG. 6.13a Interpolation of critical velocity for incipient motion from entire present data – Eqn. 6.28

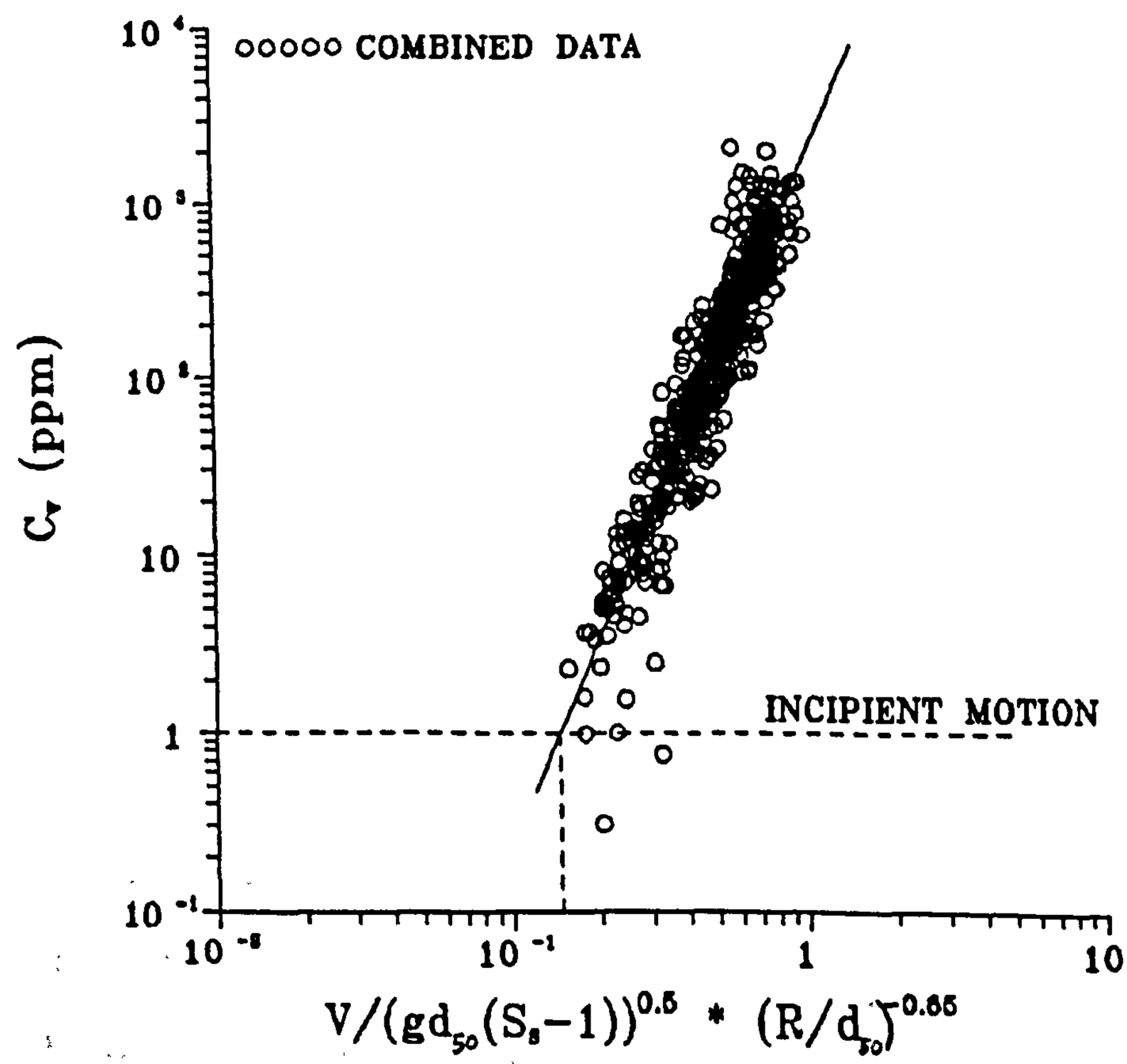

FIG. 6.13b Interpolation of critical velocity for incipient motion from the combined data – Eqn. 6.29

limit of deposition (Loveless 1991). This might explain the higher threshold velocity given by Novak-Nalluri's Eqn. 3.5.

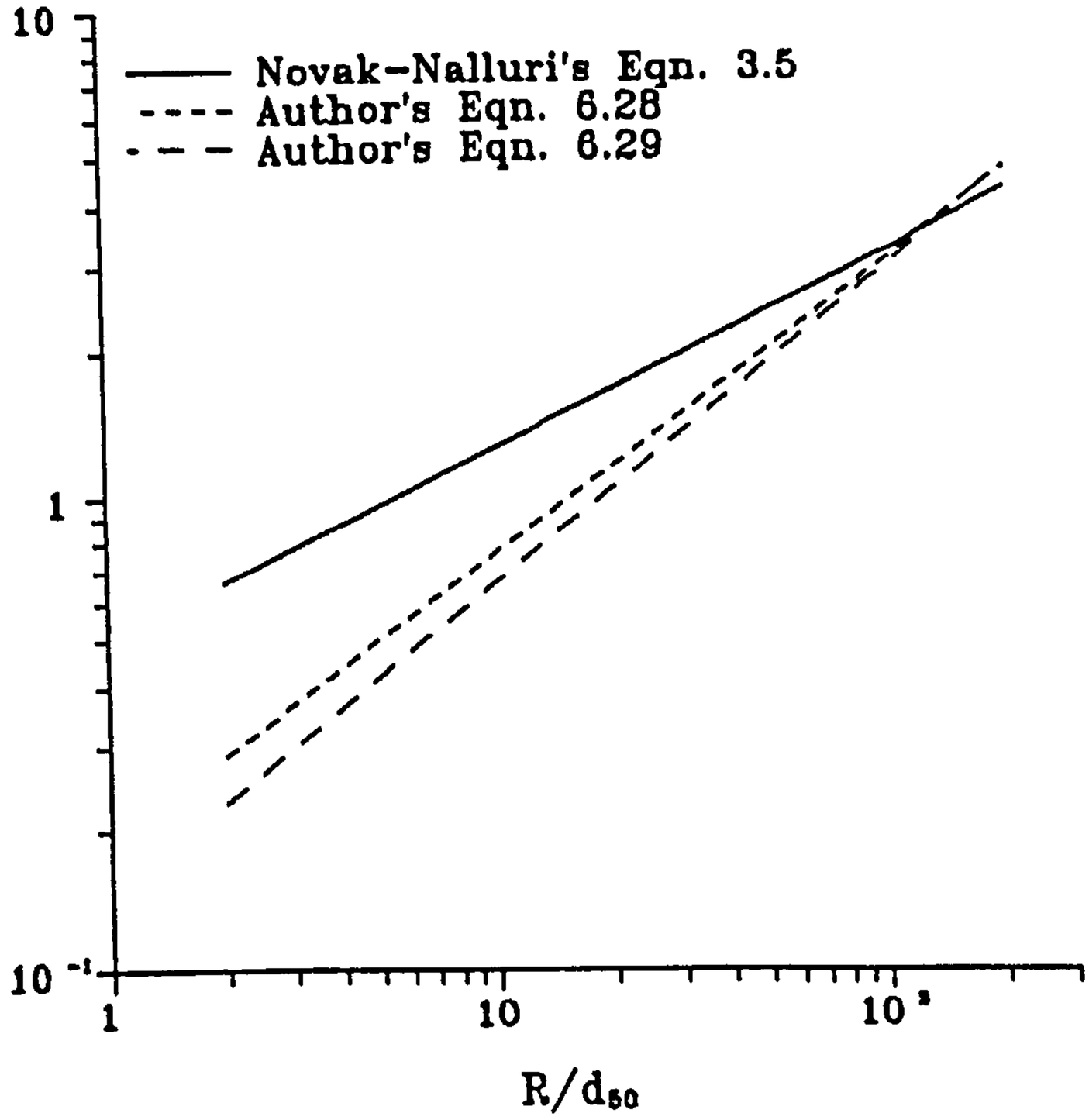

FIG. 6.14 Incipient motion criteria for clean pipes

The results of multiple regression analyses on the modified functions (Eqns. 6.23 and 6.24) using these two alternative incipient motion criteria (Eqns. 6.28 and 6.29) are given in Tables 6.13 and 6.14. Considering the results of the combined data, the equations with C_v as the dependent variable (Eqns. 6.31b and 6.33b) have a slightly higher adj. r^2 (= 0.86 and 0.87 respectively) than those with excess Fr_* as the dependent variable (Eqns. 6.31a and 6.33a). However, these values of adj. r^2 are very similar to the one obtained from the equation which

TABLE 6.13 EXCESS VELOCITY EQUATIONS USING INTERPOLATED INCIPIENT MOTION'S EQN. 6.28

DATA SOURCE	MULTIPLE REGRESSION EQUATION	$adj.\ r^2$	s	EQN. NO.
PRESENT DATA	$\frac{V - V_*}{\sqrt{gd_{50}(S_s-1)}} = 2.86\, C_v^{0.40} \left(\frac{R}{d_{50}}\right)^{0.74} D_{gr}^{0.18}\, \lambda_s^{-0.09}$	0.82	0.096	6.30a
	$C_v = 0.42 \left[\frac{V - V_*}{\sqrt{gd_{50}(S_s-1)}}\right]^{1.89} \left(\frac{R}{d_{50}}\right)^{-2.04} D_{gr}^{-0.83}\, \lambda_s^{-0.01}$	0.92	0.209	6.30b
COMBINED DATA	$\frac{V - V_*}{\sqrt{gd_{50}(S_s-1)}} = 6.91\, C_v^{0.35} \left(\frac{R}{d_{50}}\right)^{0.46} D_{gr}^{-0.83}\, \lambda_s^{-0.36}$	0.84	0.109	6.31a
	$C_v = 0.04 \left[\frac{V - V_*}{\sqrt{gd_{50}(S_s-1)}}\right]^{1.94} \left(\frac{R}{d_{50}}\right)^{-1.80} D_{gr}^{-0.19}\, \lambda_s^{0.49}$	0.87	0.257	6.31b

TABLE 6.14 EXCESS VELOCITY EQUATIONS USING INTERPOLATED INCIPIENT MOTION'S EQN. 6.29

DATA SOURCE	MULTIPLE REGRESSION EQUATION	adj. r^2	s	EQN. NO.
PRESENT DATA	$\frac{V - V_c}{\sqrt{gd_{50}(S_s-1)}} = 3.08\, C_v^{0.38} \left(\frac{R}{d_{50}}\right)^{0.69} D_{gr}^{0.17}\, \lambda_s^{-0.09}$	0.80	0.097	6.32a
	$C_v = 0.38 \left[\frac{V - V_c}{\sqrt{gd_{50}(S_s-1)}}\right]^{1.94} \left(\frac{R}{d_{50}}\right)^{-2.04} D_{gr}^{-0.86}\, \lambda_s^{-0.02}$	0.91	0.220	6.32b
COMBINED DATA	$\frac{V - V_c}{\sqrt{gd_{50}(S_s-1)}} = 7.14\, C_v^{0.34} \left(\frac{R}{d_{50}}\right)^{0.45} D_{gr}^{-0.18}\, \lambda_s^{-0.35}$	0.83	0.108	6.33a
	$C_v = 0.04 \left[\frac{V - V_c}{\sqrt{gd_{50}(S_s-1)}}\right]^{1.98} \left(\frac{R}{d_{50}}\right)^{-1.61} D_{gr}^{-0.22}\, \lambda_s^{0.47}$	0.86	0.263	6.33b

was based on Novak-Nalluri's criterion (Eqn. 6.26b). Figs. 6.15 and 6.16 show the predicted limiting concentrations using Eqns. 6.31b and 6.33b plotted against their observed values respectively. The discrepancy ratios in terms of C_v are given in Tables 6.15 (Eqn. 6.31b) and 6.16 (Eqn. 6.33b). The results shown in Figs. 6.15 and 6.16 have an average discrepancy ratio of 1.12 with 41% of the combined data lie within the ± 0.25 deviations. Based on the values of adj. r^2 and the percentage of data falling within the ± 0.25 deviations, it can be concluded that Eqns. 6.31b and 6.33b have accuracies similar to Eqn. 6.19. Again this shows that it is not necessary to include an incipient motion criterion to predict the limiting sediment concentrations for the range of the combined data.

Having considered several functional relationships to analyse the present and data from other studies, the best-fit models representing the different form of functions are listed in Table 6.17. It must be emphasized that the choice of parameters will play an important role in the accuracy of an equation in the prediction of either limiting velocity or sediment concentration. Also, as has been demonstrated in the foregoing analyses, the complexity of an equation does not necessarily increase its accuracy. Based on the values of adj. r^2, s, and the discrepancy ratio, the author therefore proposes Eqn. 6.13, in conjunction with Eqn. 6.16 for λ_s, to be used for the design of new sewers and also in the evaluation of the transport capacity of the in-use sewers with clean inverts. Both equations were derived from a large number and wide range of data (see Table 6.6) hence

TABLE 6.15 DISCREPANCY RATIO FOR EQN. 6.31b - COMBINED DATA (CLEAN PIPES)

Source of data	C_v (predicted) / C_v (observed)							No. of data
	Mean	min	max	0.90-1.10 (%)	0.75-1.25 (%)	0.5-1.5 (%)	0.5-2.0 (%)	
Present	0.94	0.20	2.81	15	38	75	84	253
Mayerle (1988)	1.40	0.48	3.90	13	43	67	86	105
May et al (1989)	1.66	0.59	4.72	21	33	56	75	48
Loveless (1991)	0.90	0.26	1.81	35	63	89	89	46
Combined	1.12	0.20	4.72	17	41	73	84	452

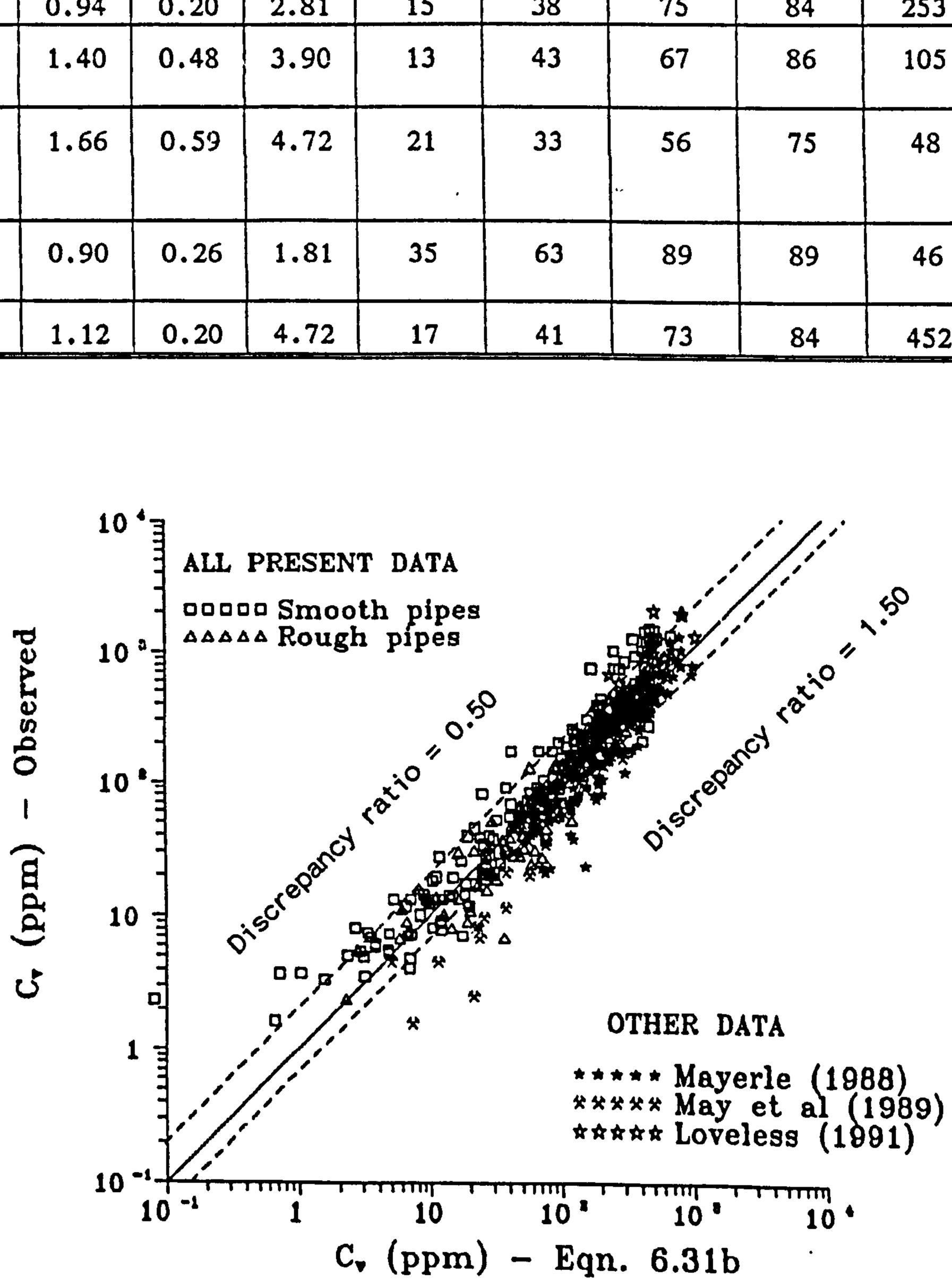

FIG. 6.15 Excess velocity criterion - Eqn. 6.31b with author's Eqn. 6.28 (Combined data)

TABLE 6.16 DISCREPANCY RATIO FOR EQN. 6.33b - COMBINED DATA (CLEAN PIPES)

Source of data	C_v (predicted) / C_v (observed)							No. of data
	Mean	min	max	0.90-1.10 (%)	0.75-1.25 (%)	0.5-1.5 (%)	0.5-2.0 (%)	
Present	0.95	0.19	2.91	15	38	74	83	253
Mayerle (1988)	1.38	0.48	3.93	14	44	69	87	105
May et al (1989)	1.65	0.59	4.55	21	35	56	75	48
Loveless (1991)	0.89	0.26	1.81	35	63	89	91	46
Combined	1.12	0.19	4.55	17	41	72	84	452

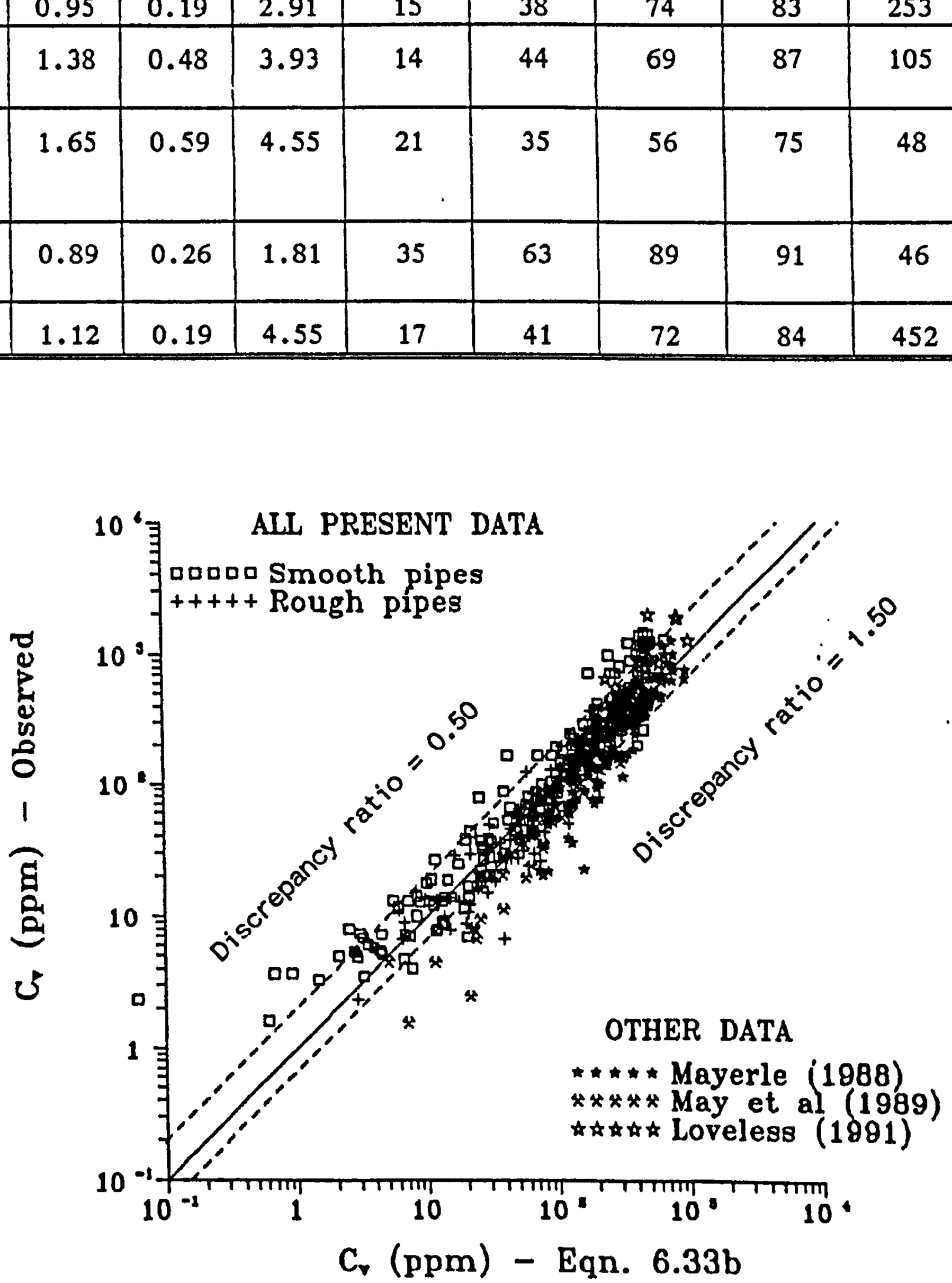

FIG. 6.16 Excess velocity criterion – Eqn. 6.33b with author's Eqn. 6.29 (Combined data)

ensuring their applications over a wide range of flow conditions in clean sewers.

TABLE 6.17 SELECTION OF THE BEST MODEL FOR SEDIMENT TRANSPORT IN CLEAN PIPES (COMBINED DATA)

TYPE OF EQUATION	MULTIPLE REGRESSION EQUATION	adj. r^2	s	EQN. NO.
TOTAL VELOCITY WITH Fr_m AS THE DEPENDENT VARIABLE	$\frac{V}{\sqrt{gd_{50}(S_s-1)}} = 3.08\, C_v^{0.21} \left(\frac{R}{d_{50}}\right)^{0.53} D_{gr}^{-0.08}\, \lambda_s^{-0.21}$	0.95	0.057	6.13
TOTAL VELOCITY WITH C_v THE DEPENDENT VARIABLE	$C_v = 0.03 \left(\frac{V}{\sqrt{gd_{50}(S_s-1)}}\right)^{3.54} D_{gr}^{-0.11} \left(\frac{R}{d_{50}}\right)^{-2.47} \lambda_s^{0.57}$	0.89	0.236	6.19
EXCESS VELOCITY WITH C_v AS THE DEPENDENT VARIABLE	$C_v = 0.11 \left[\frac{V - V_*}{\sqrt{gd_{50}(S_s-1)}}\right]^{1.00} \left(\frac{R}{d_{50}}\right)^{-1.00} D_{gr}^{-0.17}\, \lambda_s^{0.51}$	0.88	0.239	6.26b

To illustrate the applicability of Eqn. 6.13 over the range of the combined data, the discrepancy ratios in terms of Fr_m are evaluated as functions of dimensionless grain size (D_{gr}), proportional flow depth (y_o/D), velocity (V), and sediment concentrations (C_v). The measured values of λ_s were used in computing the predicted values of Fr_m. The results are given in Table 6.18 and plotted in Fig. 6.17.

Fig. 6.17a shows that a reasonably good agreement is obtained over the range of D_{gr}. The average discrepancy ratio varies from 0.95 to 1.03 where between 90% to 100% of the data lie within the ± 0.25 deviations.

Fig. 6.17b shows that the agreement is generally satisfactory over the full range of flow depths studied. The average discrepancy ratio for flows up to and beyond half-full depths is 1.0 with over 90% of the data for each region of flow fall within ± 0.25 deviations.

Fig. 6.17c indicates that the agreement is best for concentrations between 10ppm and 1000ppm where the average discrepancy ratio varies from 0.98 to 1.02 and over 94% of data occur within the ± 0.25 deviations.

Fig. 6.17d reveals that the agreement is reasonably good over the central range of velocities between 0.60 and 0.9m/s where the average discrepancy ratio varies from 0.96 to 1.04 with over 98% of data lie within the ± 0.25 deviations. There appear to be systematic errors at the extremes: overprediction for V < 0.6m/s and underprediction for V > 0.9m/s).

The presence of scatter as given by Eqn. 6.13 for certain conditions is usually due to the difficulties in determining accurately the limit of deposition. This involves the small particle size (D_{gr} < 25) or the extreme range of velocities (V < 0.6m/s or V > 0.9m/s).

TABLE 6.18 DISCREPANCY RATIO (Fr_s) FOR EQN. 6.13 AS FUNCTIONS OF RELEVANT PARAMETERS - COMBINED DATA (CLEAN PIPES).

Range of parameter		Fr_s (predicted) / Fr_s (observed)							No of data
		Mean	min	max	0.90-1.10 (%)	0.75-1.25 (%)	0.50 - 1.50 (%)	0.5-2.0 (%)	
D_{gr}	10-25	1.01	0.64	1.38	36	90	100	100	156
	26-50	1.00	0.78	1.41	69	96	100	100	103
	51-100	1.03	0.80	1.25	68	100	100	100	56
	101-150	1.01	0.75	1.36	70	95	100	100	91
	151-200	0.98	0.57	1.15	79	96	100	100	24
	201-250	0.95	0.77	1.11	72	100	100	100	29
y_0/D	≤ 0.5	1.00	0.57	1.41	59	92	100	100	293
	> 0.5	1.00	0.64	1.31	56	98	100	100	166
C_v (ppm)	1-10	1.01	0.57	1.34	40	85	100	100	47
	11-100	1.02	0.75	1.38	54	96	100	100	155
	101-500	0.98	0.76	1.37	62	96	100	100	186
	501-1000	1.00	0.77	1.36	75	94	100	100	52
	1001-2000	1.11	0.93	1.41	53	84	100	100	19
V(m/s)	0.200-0.500	1.09	0.57	1.41	46	73	100	100	59
	0.501-0.600	1.05	0.64	1.32	49	93	100	100	80
	0.601-0.700	1.04	0.76	1.38	71	97	100	100	99
	0.701-0.800	0.98	0.78	1.18	64	100	100	100	89
	0.801-.900	0.96	0.79	1.31	74	98	100	100	62
	0.901-1.000	0.89	0.76	1.13	45	100	100	100	49
	1.001-1.500	0.91	0.76	1.17	43	100	100	100	21

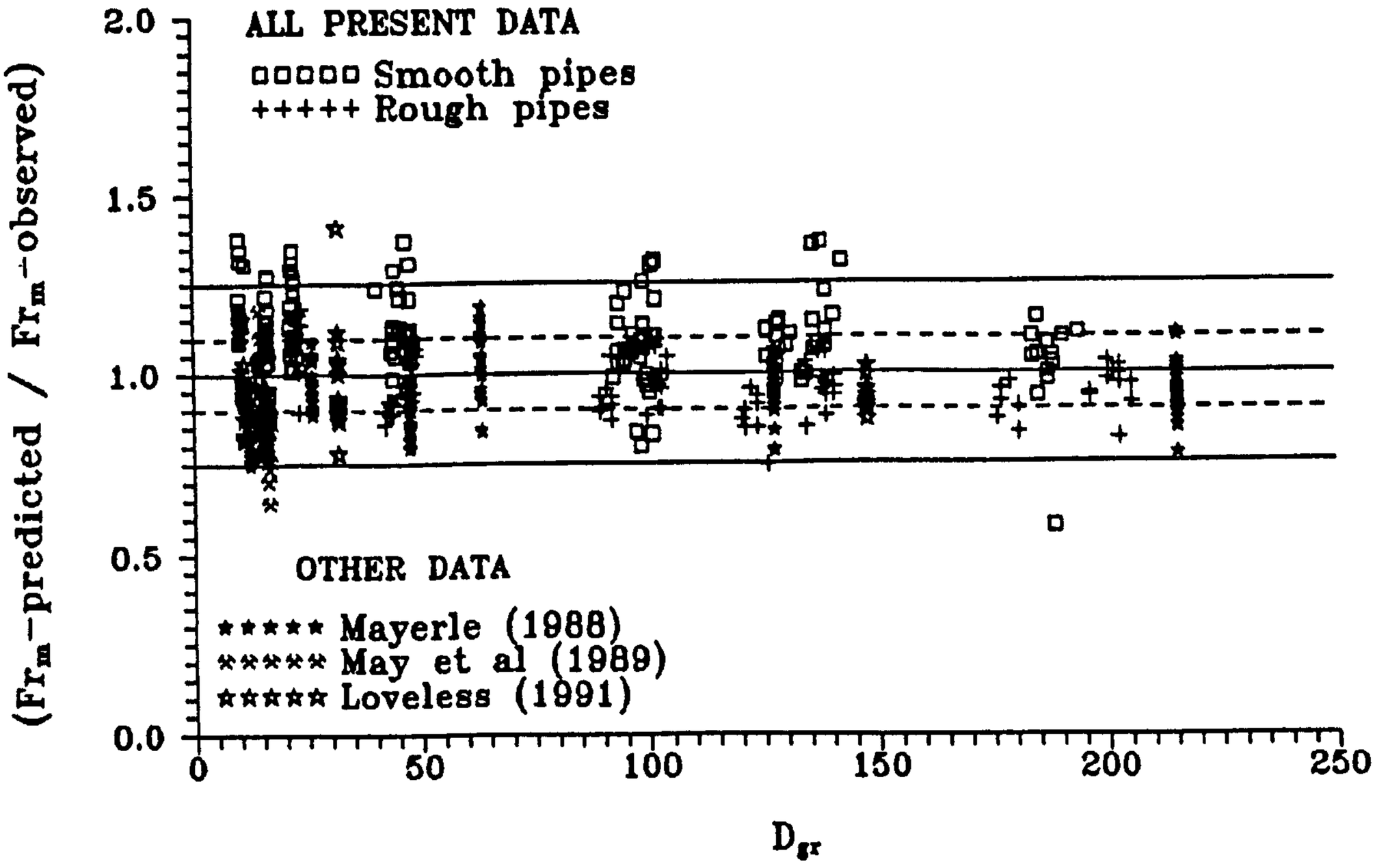

FIG. 6.17a Discrepancy ratio for Eqn. 6.13 as a function of dimensionless particle size

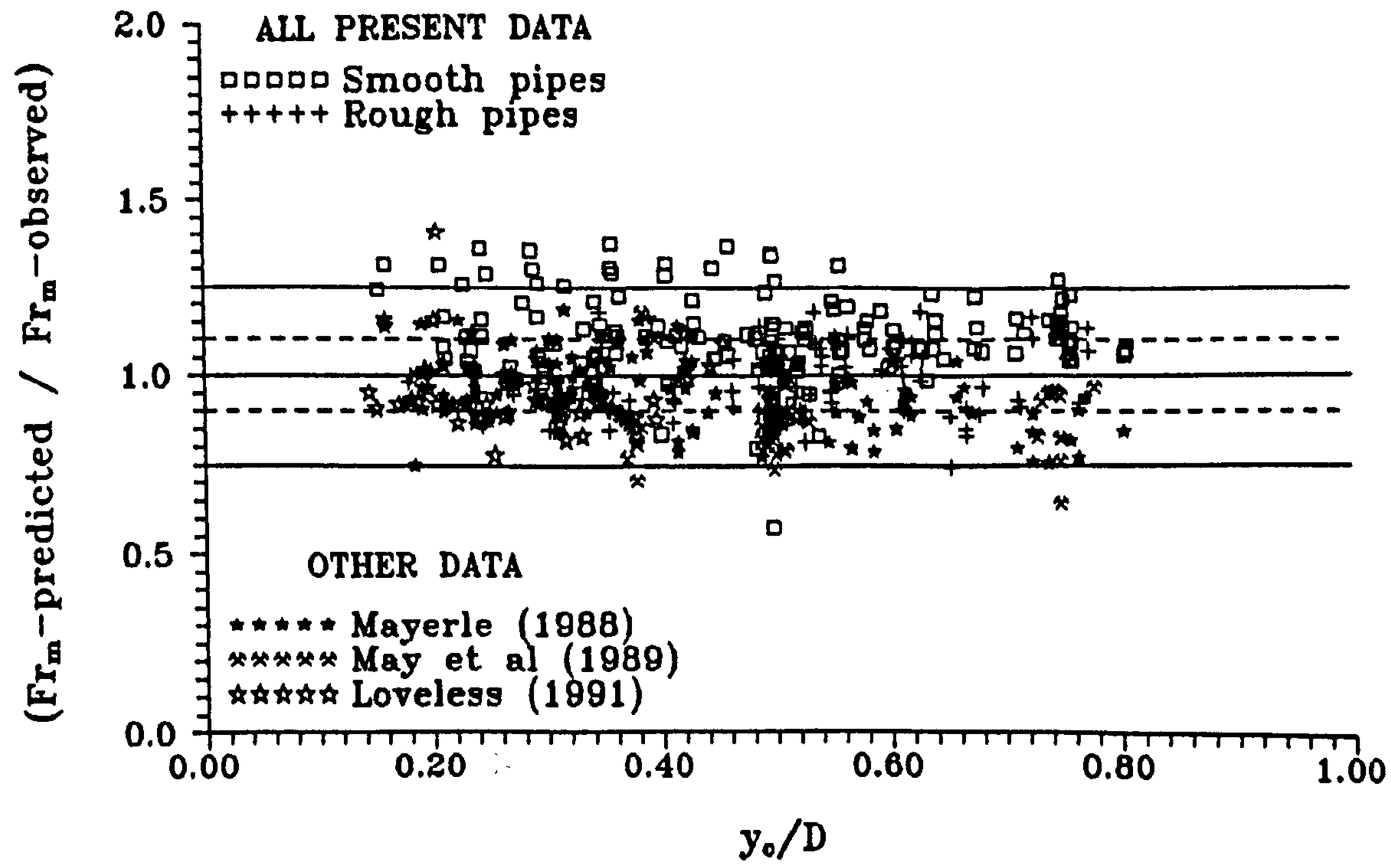

FIG. 6.17b Discrepancy ratio for Eqn. 6.13 as a function of proportional flow depth

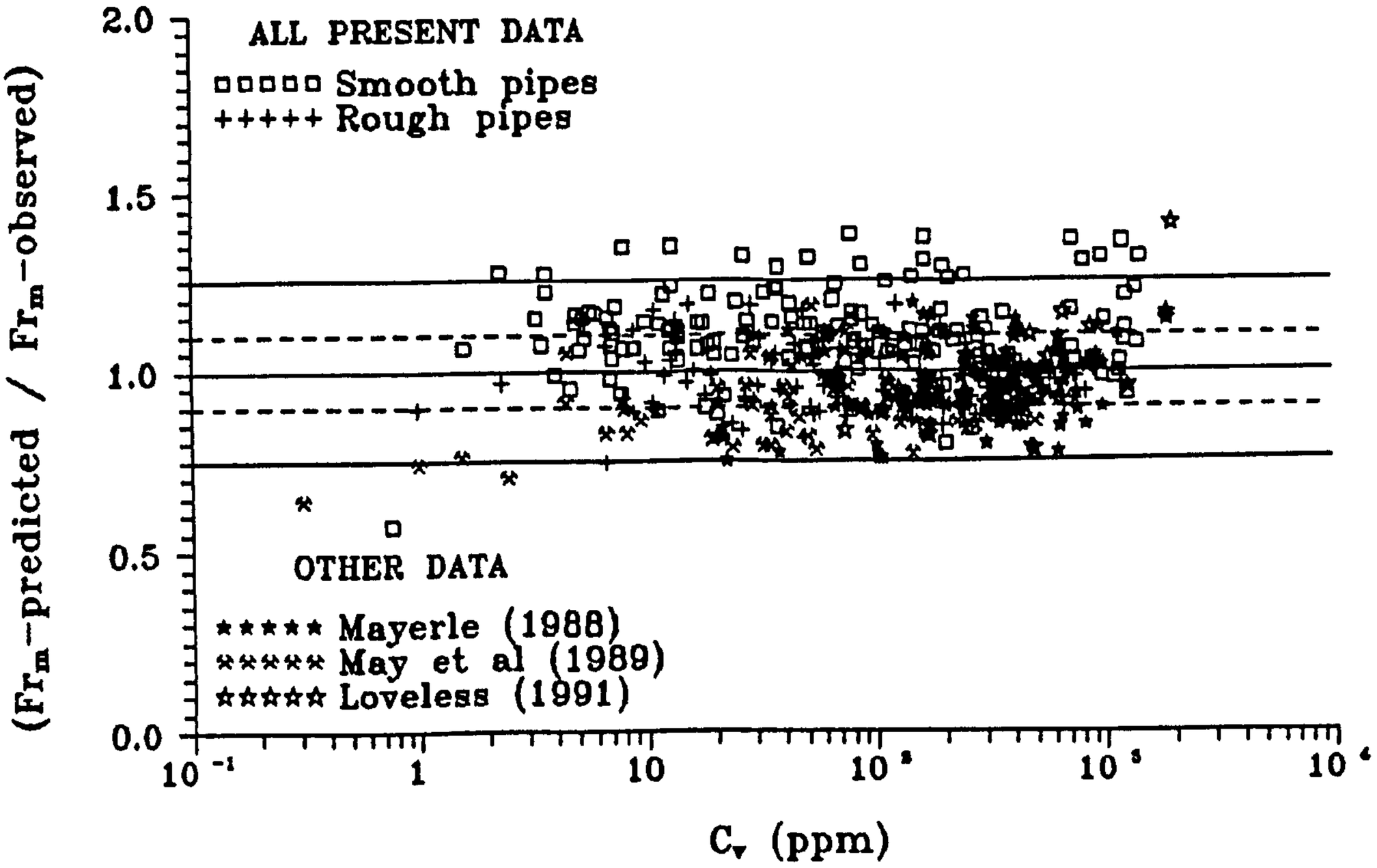

FIG. 6.17c Discrepancy ratio for Eqn. 6.13 as a function of observed volumetric concentration

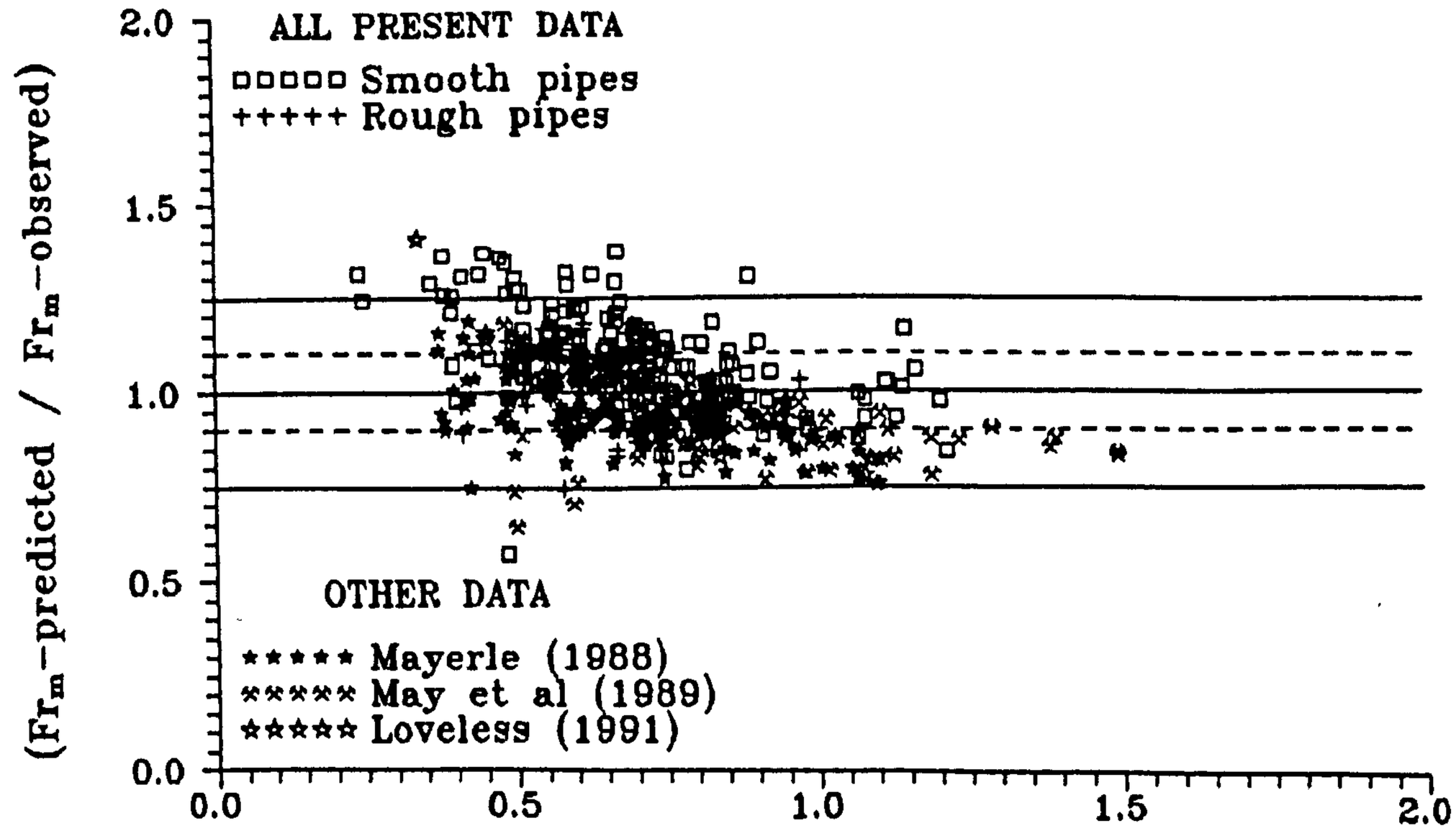

FIG. 6.17d Discrepancy ratio for Eqn. 6.13 as a function of observed velocity

6.1.3.3 Application of Ackers (1991) Equation to Clean Pipes

The Ackers-White (1973) equation has been shown to be a good predictor of sediment concentration for wide alluvial channels (White et al 1975, Brownlie 1981, Yang-Molinas 1982, Van Rijn 1984). Subsequently, as mentioned in Section 3.3.1, Ackers (1984, 1991) made the necessary modifications to Ackers-White (1973) equation with the aim of extending its applicability to non-rectangular channels.

The application of Ackers' Eqn. 3.29 to clean pipe channels requires a knowledge of an effective sediment transport width (W_e). Based on the pipe-full experimental data by May (1982) in pipes of diameter 77mm and 158mm using sediment sizes between 0.64mm and 7.9mm, Ackers (1984) proposed that $W_e = 10d_{50}$. A satisfactory agreement was found by Mat Suki-Nik Hassan (1990) between the measured and predicted limiting concentrations for Mat Suki's (1987) pipe-full data with sediment sizes of 1.3mm (D = 253mm) and 5.2mm (D = 164mm) using $W_e = 10d_{50}$ in the earlier version of Eqn. 3.29 (i.e. Eqn. 3.25).

Since the introduction of the concept of an effective width by Ackers (1984), several investigators have made measurements of the width of sediment spread (W_s) for part-full flow in clean pipes. Mayerle (1988) found that the relative spread over the particle size (W_s/d_{50}) varies between 3 and 186 in a 152mm dia. pipe for sediment sizes of between 0.5mm and 8.3mm. Loveless (1991) indicated that W_s varied between 0.11D and 0.20D with an

average value of 0.16D in a 220mm dia. semi-circular channel for the sediment sizes 0.45mm to 6.0mm. However, neither of these investigators made use of their part-full pipe data to evaluate the validity of Ackers (1984) equation.

The author measured the width of sediment spread (W_s) along the wetted perimeter for experiments in the 154mm and 305mm dia. pipes. Earlier measurements of W_s (Mayerle 1988, Loveless 1991) suggests that it is a function of the particle and pipe size. It was therefore decided to evaluate the author's values of measured W_s for each particle size in terms of the relative spread over the particle size (W_s/d_{50}) and over the pipe diameter (W_s/D). The results of this analysis are given in Table 6.19. The results indicate that, over the range of particle size tested, W_s/d_{50} tends to be inversely proportional to the sediment size and varies between 6 and 75 while W_s/D tends to vary between 0.08 and 0.22. This is consistent with the measurements made by Mayerle (1988) and Loveless (1991). Two probable values of W_e would be obtained by averaging all of the measured values of W_s/d_{50} and W_s/D (see Table 6.19): 1) $W_e = 15d_{50}$, and 2) $W_e = 0.12D$.

An attempt was then made to assess the applicability of the refined Ackers' Eqn. 3.29 for transport data in part-full flow in clean pipes. Initially only the author's data collected in a smooth 305mm dia. pipe data with a wide range of particle sizes of between 0.5mm and 8.3mm (see Table 6.3) were used. In this analysis, it was assumed that $W_e = 10d_{50}$ as suggested by Ackers (1984).

TABLE 6.19 VALUES OF MEASURED WIDTH OF SEDIMENT SPREAD (W_s)

D (mm)	d_{50} (mm)	RANGES OF W_s (mm)	AVERAGE W_s (mm)	AVERAGE W_s/d_{50}	AVERAGE W_s/D
154 (SMOOTH)	0.93	9 - 22	14	15	0.09
	2.00	10 - 20	14	7	0.09
	4.20	10 - 28	20	5	0.13
	5.70	28 - 42	34	6	0.22
305 (SMOOTH)	0.46	20 - 80	35	75	0.11
	0.97	20 - 80	36	38	0.12
	2.00	20 - 60	35	18	0.11
	4.20	10 - 60	35	8	0.11
	5.70	30 - 60	42	7	0.14
	8.30	20 - 80	42	5	0.14
305 (ROUGHNESS 1)	0.97	10 - 40	24	25	0.08
	2.00	20 - 40	28	14	0.09
	4.20	15 - 45	33	8	0.11
	5.70	20 - 55	37	7	0.12
	8.30	30 - 75	52	6	0.17
305 (ROUGHNESS 2)	2.00	20 - 40	29	14	0.09
	4.20	30 - 45	37	9	0.12
	5.70	15 - 50	40	7	0.13
	8.30	25 - 70	52	6	0.17
OVERALL AVERAGE				15	0.12

Fig. 6.18 compares the measured and predicted limiting concentration using Eqn. 3.29. In general, the results indicate that Eqn. 3.29 underestimates the limiting concentrations for the majority of the data and that the disagreement between the measured and predicted limiting concentrations increases with increasing sediment size.

The poor agreement obtained by Ackers' Eqn. 3.29 for the above data especially for coarse sediments (d_{50} > 2.0mm) suggests that

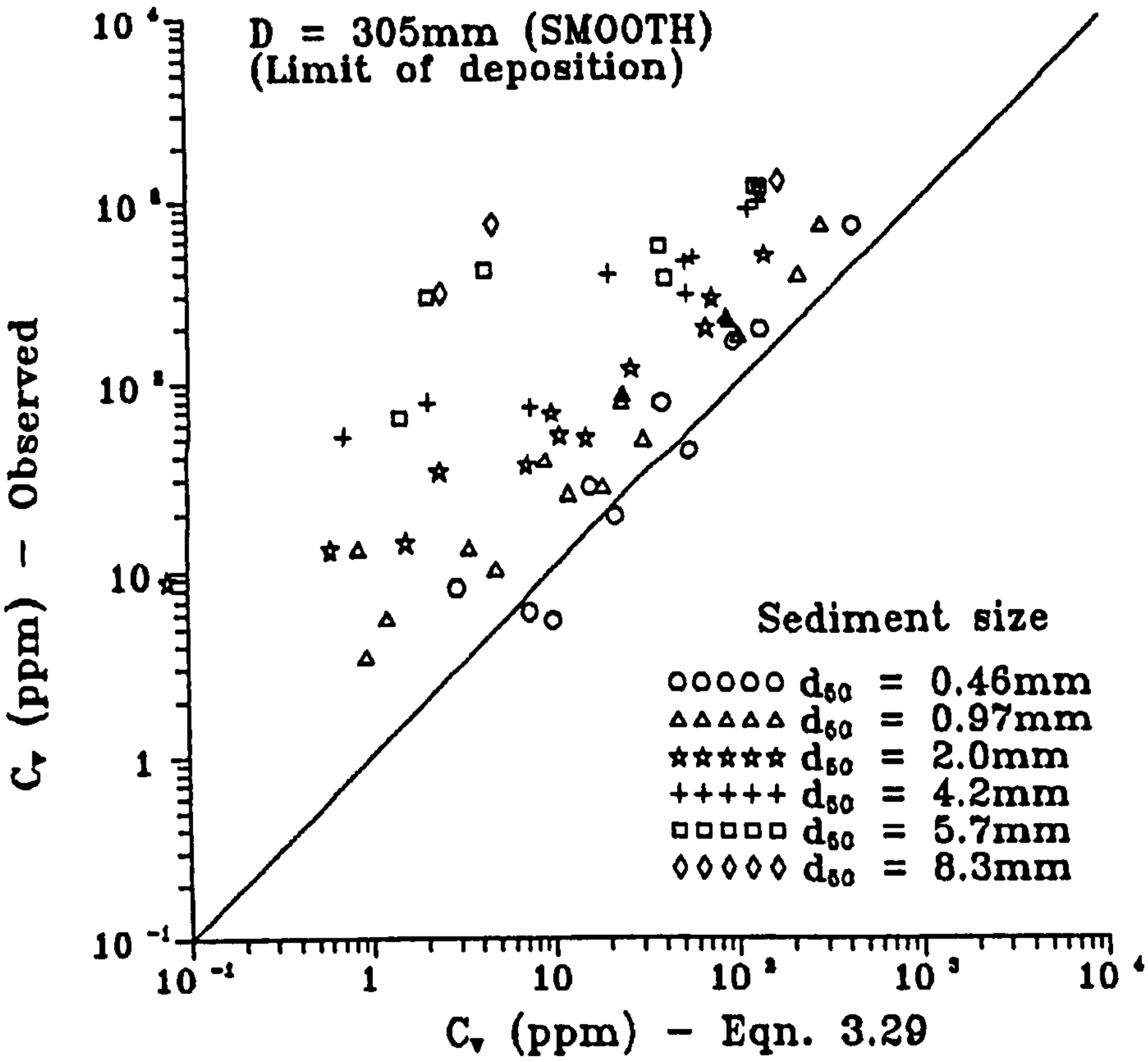

FIG. 6.18 Predicted C_v using Ackers' Eqn. 3.29 for author's smooth 305mm dia. pipe ($W_s = 10d_{50}$)

the form of the equation should be re-examined. Ackers' Eqn. 3.29 can be re-written as:

$$C_v = \left[\frac{\left(\frac{Fr_m}{K} - 1 \right)}{J} \right]^m \qquad (6.34)$$

where K and J are as defined earlier (Eqns. 3.30 and 3.31 respectively). The form of the equation (Eqn. 6.34) indicates that it will predict no movement of sediment if the threshold condition as given by K is larger than the total mobility number, Fr_m. Figs. 6.19 and 6.20 show the plots of Fr_m/K as a function of D_{gr} and R/d_{50} for the data from author's smooth 305mm dia. pipe

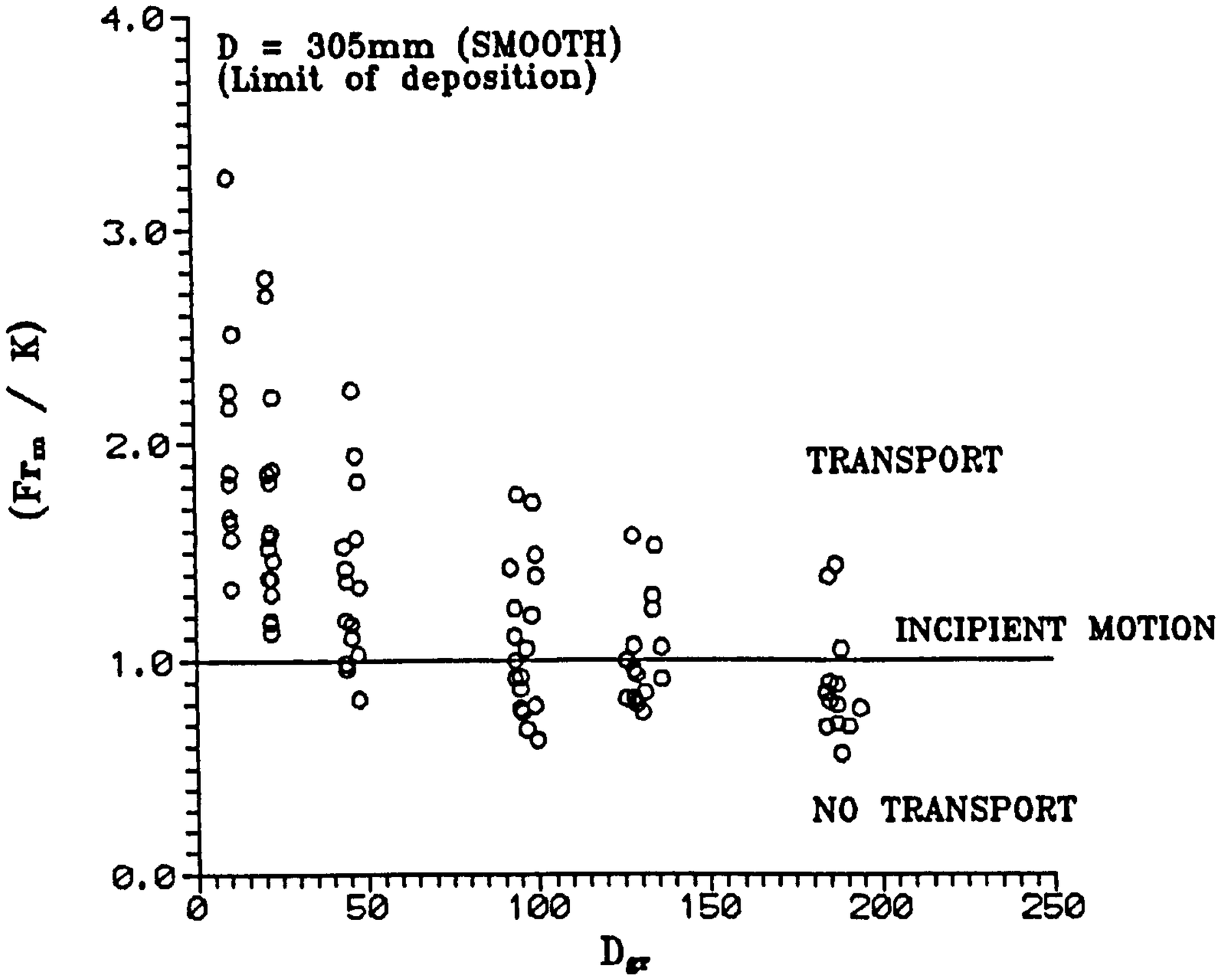

FIG. 6.19 Ratio of measured total mobility to critical mobility computed by Ackers' Eqn. 3.30 as a function of dimensionless particle size for author's smooth 305mm dia. data

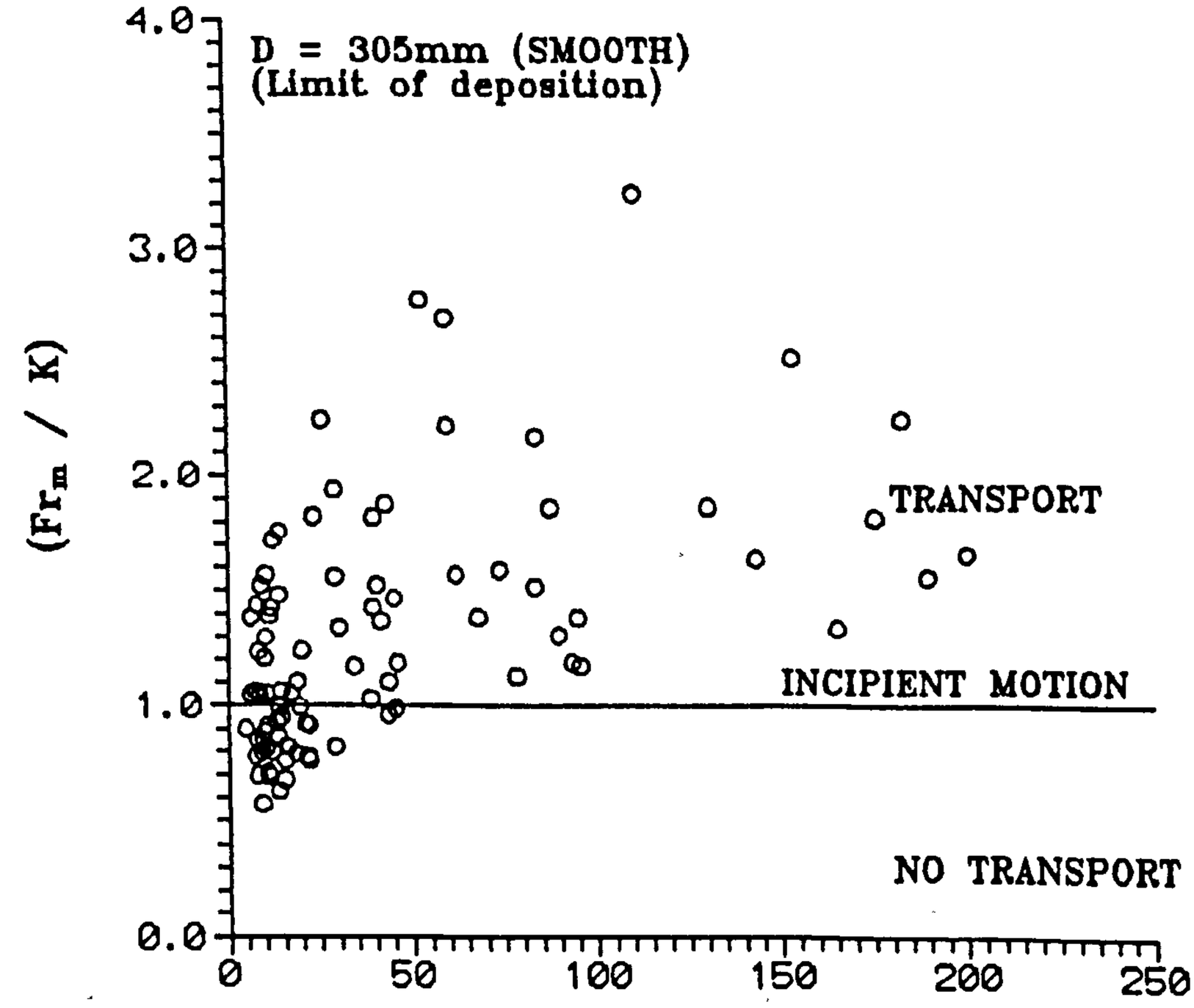

FIG. 6.20 Ratio of measured total mobility to critical mobility computed by Ackers' Eqn. 3.30 as a function of dimensionless particle size in smooth 305mm dia. data

could be explained by the much higher resistance due to the presence of bedforms in the alluvial channels upon which Ackers' Eqn. 3.29 was originally derived. It should also be noted that the range

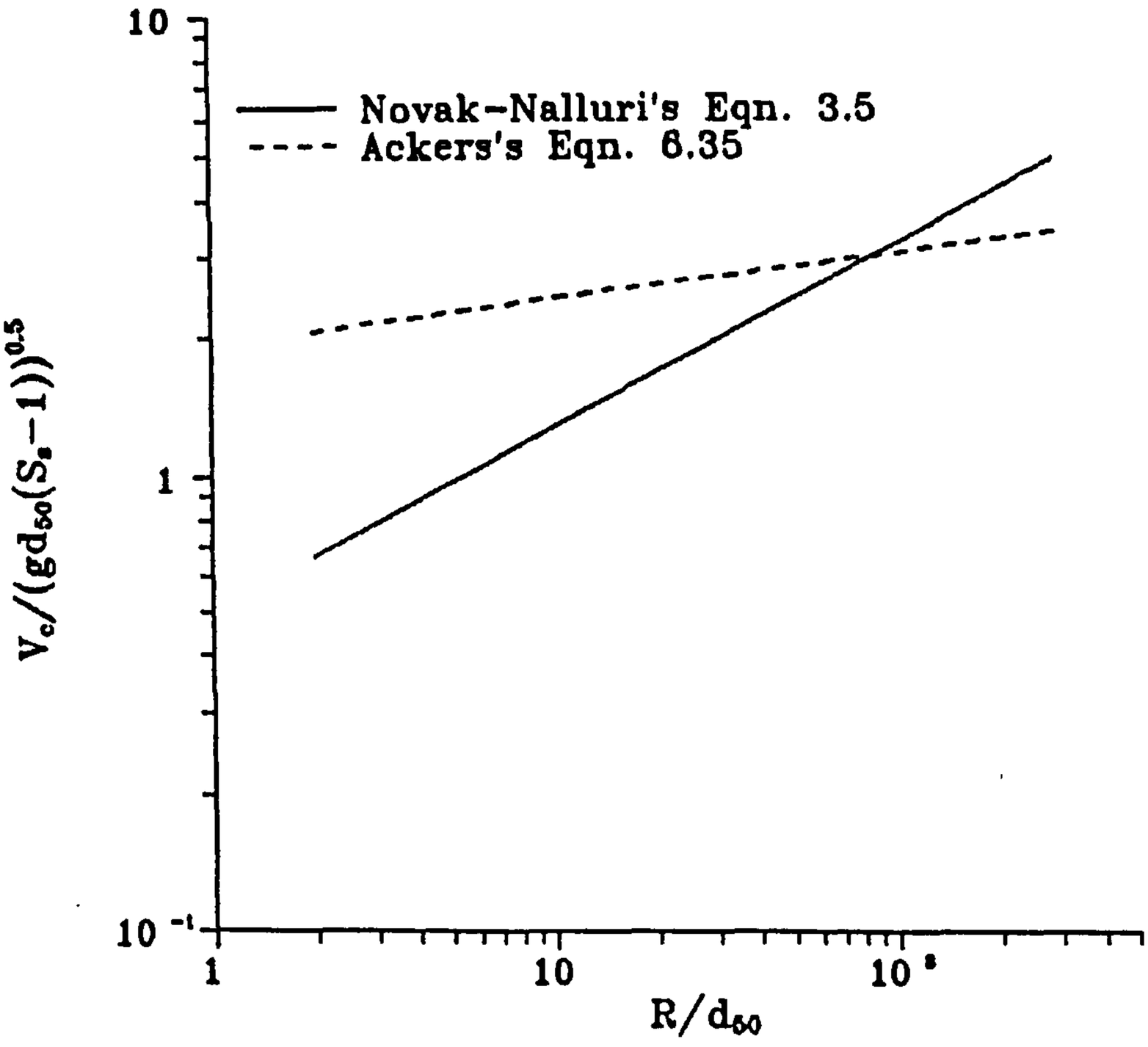

FIG. 6.21 Comparison of incipient motion criteria for loose and rigid boundaries

of applicability of Eqn. 3.30 is within $150 < R/d_{50} < 30000$ (Ackers 1991). Since the majority of the available data for transport in clean pipes (see Table 6.6) is within the range of $R/d_{50} < 100$, it seems appropriate to define K in terms of Novak-Nalluri's Eqn. 3.5 for the whole range of D_{gr}. Figs. 6.22 and 6.23 suggest the applicability of this modification where all the author's data for smooth 305mm dia. pipe were located in the

where the values of K were computed from Eqn. 3.30. These plots reveal that Ackers' Eqn. 3.29 predicts that there should be no sediment movement for several proportion of data with the range of $100 < D_{gr} < 200$ and $R/d_{50} < 50$. It would therefore be of interest to examine the values of K (as given by Eqn. 3.30) for these ranges of D_{gr} and R/d_{50}.

As mentioned earlier in Section 3.3.1, K is defined as:

$$K = \frac{A_{gr}\left(11.3\left(\frac{R}{d_{50}}\right)^{0.1}\right)^{1-n}}{\left(\frac{\lambda_s}{8}\right)^{\frac{n}{2}}} \qquad (3.30)$$

Ackers defined the coarse sediment as those with dimensionless particle size larger than 60 (see Table 3.3). For this range of D_{gr}, the sediment is assumed to move as bed load. Hence for $D_{gr} > 60$, substituting $n = 0$ and $A_{gr} = 0.17$ (see Table 3.3), Eqn. 3.30 can be re-written as:

$$K = 1.92\left(\frac{R}{d_{50}}\right)^{0.10} \qquad (6.35)$$

Eqn. 6.35 resembles Novak-Nalluri's incipient motion criterion (Eqn. 3.5) for rigid boundary conditions. Fig. 6.21 shows a comparison of these two incipient motion criteria, namely Eqn. 6.35 and Eqn. 3.35. The results of the comparison indicate that Eqn. 6.35 gives a much higher value of critical mobility number, $Fr_{m,cr}$ than that of Eqn. 3.5 for $R/d_{50} < 100$. This difference

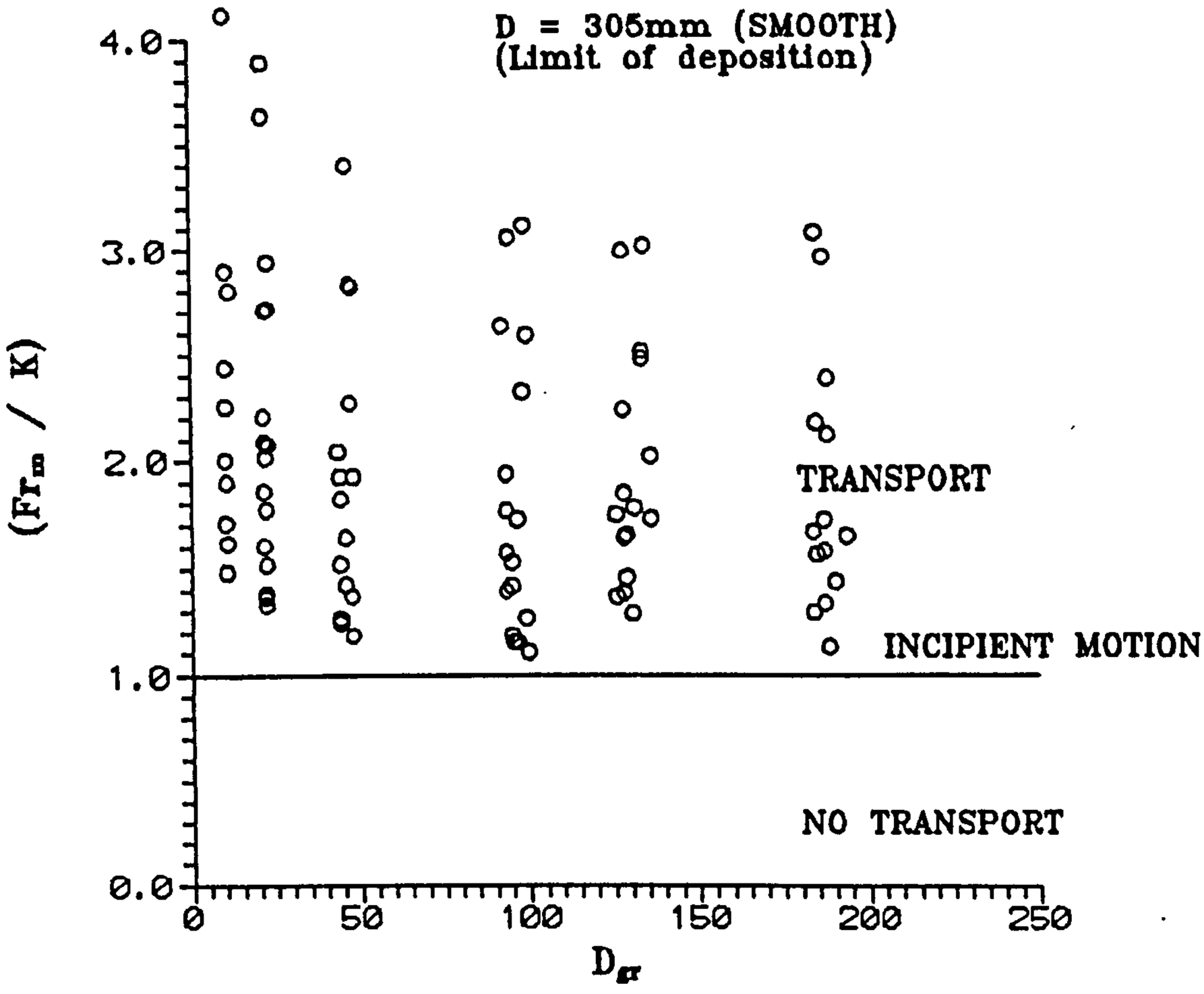

FIG. 6.22 Ratio of measured total mobility to critical mobility computed by Novak-Nalluri's Eqn. 3.5 as a function of dimensionless particle size for author's smooth 305mm dia. data

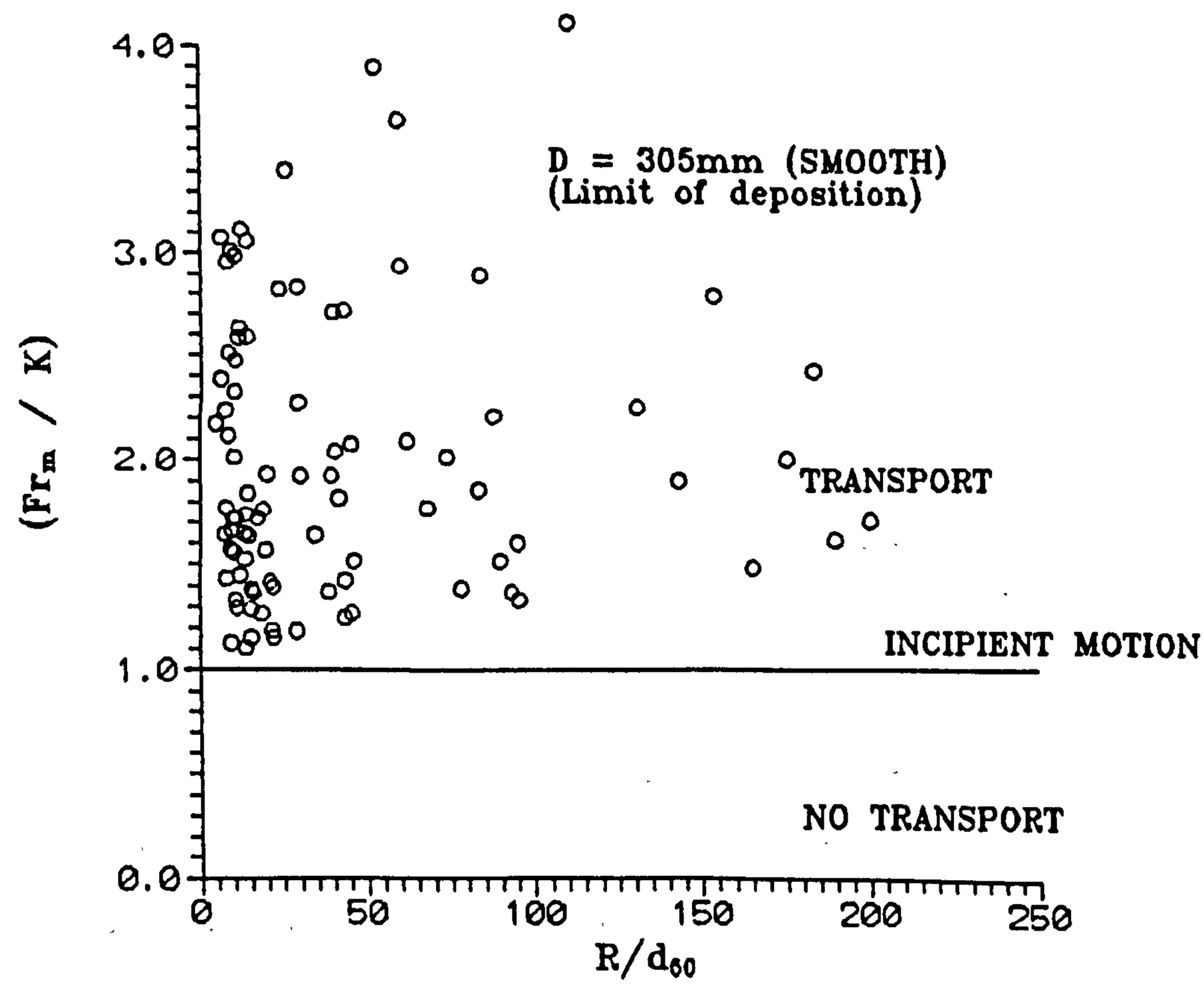

FIG. 6.23 Ratio of measured total mobility to critical mobility computed by Novak-Nalluri's Eqn. 3.5 as a function of relative roughness for author's smooth 305mm dia. data

transport region. It is expected that this modification will apply equally well to the data from other clean-pipe studies (see Table 6.6) since they have similar range of D_{gr} and R/d_{50} to those of author's. Henceforth, the term "modified Ackers' equation" will refer to Eqn. 3.29 with K and J as given by Eqns. 3.5 and 3.31 respectively.

Attempts were then made to find a suitable value of W_e to be used with the modified Ackers' equation so that it would be applicable for sediment transport in clean pipes. For the bed load process (i.e. n = 0.0), the form of Eqn. 3.29 (or Eqn. 6.34) predicts an increase in the sediment concentration with an increase in the effective width. This similar trend is known to occur for the transport of sediments over loose deposit beds with a finite sediment bed width as was mentioned earlier (Section 5.3.6). However, for transport in clean pipes, due to the absence of a finite sediment bed , it is therefore necessary to find a suitable definition of the effective width which will give a similar trend.

As shown earlier, Fig. 5.6 (see Section 5.3.3) indicates an increase in the sediment concentration with an increase in sediment size for a given flow condition. It is therefore likely that the effective width in clean pipes is dependent on the particle size such that different values of the effective width are required for different particle sizes (i.e. $W_e = f(d_{50})$).

Later, the following analysis was done on all of the author's data as well as the data from other studies (Mayerle 1988, May et al 1989, Loveless 1991); the ranges of relevant parameters for these data is as given in Table 6.6. The preceding analysis (Section 6.1.3.2) shows that the form of an equation with Fr_m as the dependent variable is more accurate in presenting the sediment transport process in clean pipes. Hence, for data from each study, the value of W_e (= $f(d_{50})$) was determined so as to minimise the proportionate errors in the predicted values of Fr_m using the modified Ackers' equation. The results of this analysis are given in plots of observed-Fr_m vs. predicted-Fr_m. The average, minimum and maximum values of the discrepancy ratios as well as the correlation coefficient (r) and standard deviation are also given for each set of data. Based on this analysis, it was hoped that the author would be able to suggest suitable values of W_e (= $f(d_{50})$) to be used in the application of the modified Ackers' equation.

Fig. 6.24 shows the results for the author's data. It was found that a reasonable agreement between the observed and predicted values of Fr_m was obtained for the majority of the data when W_e = $10d_{50}$. The average discrepancy ratio (see Table 6.20) for both rough and smooth pipes varies between 0.90 and 0.97 with the majority of the data lying within the ± 0.25 deviations (see Fig. 6.24). An examination of the discrepancy ratio for each sediment size shows that the ratio is larger for coarse sediment (d > 4.2mm). Due to this, it was then decided to re-evaluate the data of d_{50} > 4.2mm with W_e = 0.12D, the value of which was obtained from

TABLE 6.20 VERIFICATION OF MODIFIED ACKERS' EQUATION FOR PRESENT CLEAN PIPE DATA ($W_e = 10d_{50}$)

D (mm)	DISCREPANCY RATIO			r	s	NO. OF DATA
	AVERAGE	MIN	MAX			
154 (SMOOTH)	0.92	0.63	1.19	0.95	0.120	39
305 (SMOOTH)	0.95	0.71	1.15	0.99	0.096	89
450 (SMOOTH)	0.94	0.75	1.21	0.84	0.119	27
305 (ROUGHNESS 1)	0.97	0.72	1.21	0.97	0.126	71
305 (ROUGHNESS 2)	0.90	0.73	1.11	0.96	0.085	30

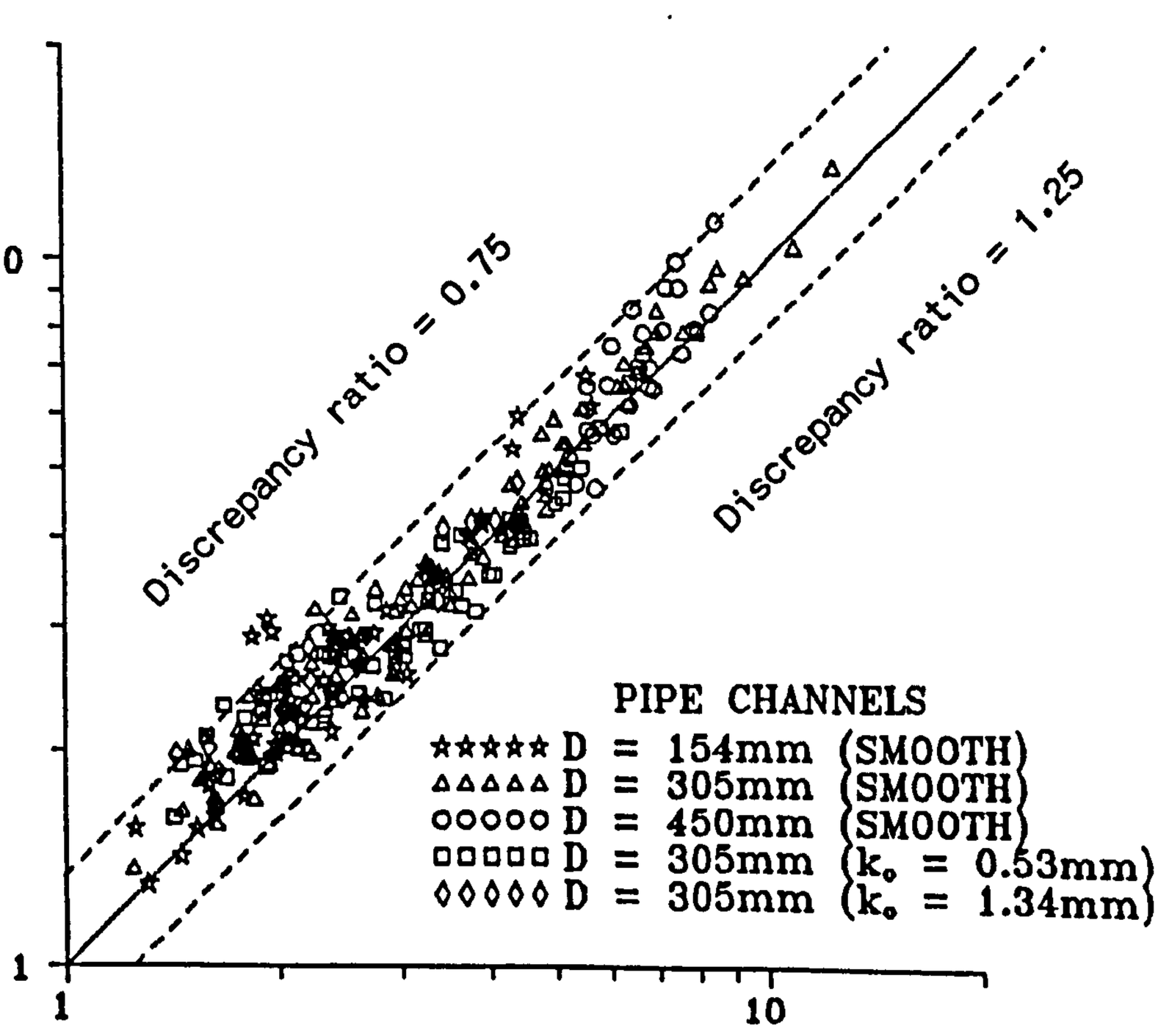

FIG. 6.24. Verification of modified Ackers' equation for all present data with $W_e = 10d_{50}$

the author's measurement of W_e (see Table 6.19). The results of this analysis are shown in Fig. 6.25. It is clear that there is better agreement when both definitions of W_e were used: 1) $W_e = 10d_{50}$ for $d_{50} \leq 4.2$mm and, 2) $W_e = 0.12D$ for $d_{50} > 4.2$mm. Table 6.21 shows that the average discrepancy ratio varies between 0.94 and 1.03. This suggests that for sediments with sizes of between 0.5mm and 4.2mm, the effective width is a function of particle size while for sediment with $d_{50} > 4.2$mm, the effective width depends on both particle and pipe size.

Fig. 6.26 compares the measured and predicted Fr_* using the modified Ackers' equation for Mayerle's (1988) data. The results show that different values of effective width were needed: 1) $W_e = d_{50}$ for $d_{50} = 0.50$mm, 2) $W_e = 4d_{50}$ for $d_{50} = 1.05$mm - 1.95mm, 3) $W_e = 10d_{50}$ for $d_{50} = 2.56$mm and, 4) $W_e = 0.12D$ for $d_{50} = 5.22$mm - 8.74mm. The application of modified Ackers' equation with these values of W_e yields (see Table 6.22) an average discrepancy ratio of 0.91 with a standard deviation of 0.084.

Fig. 6.27 illustrates the results of the comparison of measured and predicted Fr_m for May et al's (1989) data. The application of modified Ackers' equation requires $W_e = d_{50}$ for both particle sizes of 0.64mm (D = 158mm) and 0.72mm (D = 300mm). Table 6.22 shows that this gives an average discrepancy ratio of 1.06 with a standard deviation of 0.135.

TABLE 6.21 VERIFICATION OF MODIFIED ACKERS' EQUATION FOR PRESENT CLEAN PIPE DATA ($W_e = 10d_{50}$ OR $0.12D$)

D (mm)	DISCREPANCY RATIO			r	s	NO. OF DATA
	AVERAGE	MIN	MAX			
154 (SMOOTH)	1.00	0.63	1.63	0.87	0.227	39
305 (SMOOTH)	0.99	0.82	1.18	0.99	0.079	89
450 (SMOOTH)	0.94	0.72	1.21	0.84	0.119	27
305 (ROUGHNESS 1)	1.03	0.84	1.21	0.98	0.086	71
305 (ROUGHNESS 2)	0.95	0.83	1.11	0.97	0.065	30

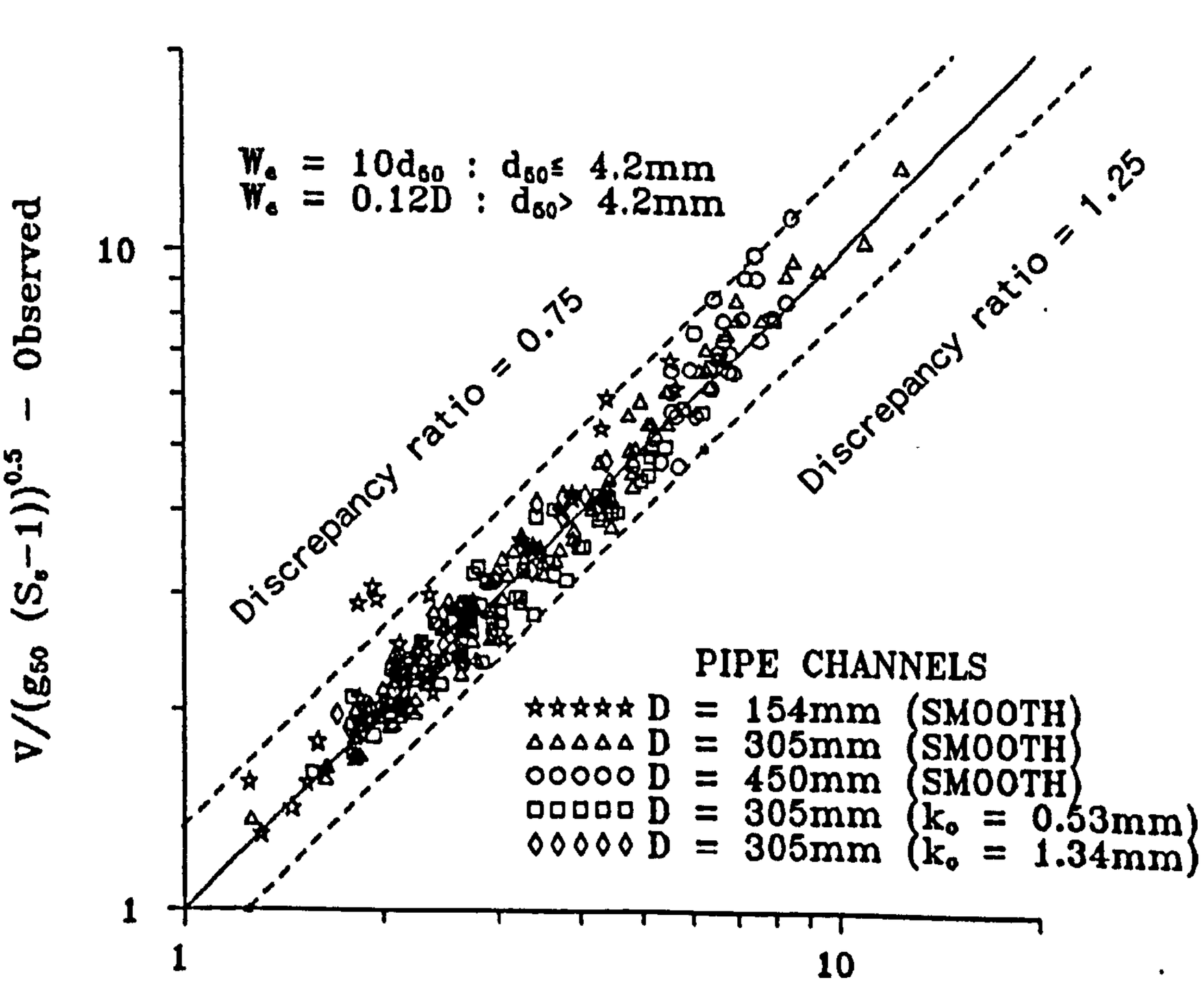

FIG. 6.25 Verification of modified Ackers' equation for all present data with $W_e = 10d_{50}$ or $0.12D$

TABLE 6.22 VERIFICATION OF MODIFIED ACKERS' EQUATION FOR OTHER CLEAN PIPE DATA

AUTHORS	DISCREPANCY RATIO			r	s	NO. OF DATA
	AVERAGE	MIN	MAX			
MAYERLE (1988)	0.91	0.67	1.10	0.98	0.084	106
MAY ET AL (1989)	1.06	0.77	1.53	0.94	0.135	51
LOVELESS (1991)	0.96	0.54	1.15	0.95	0.175	46

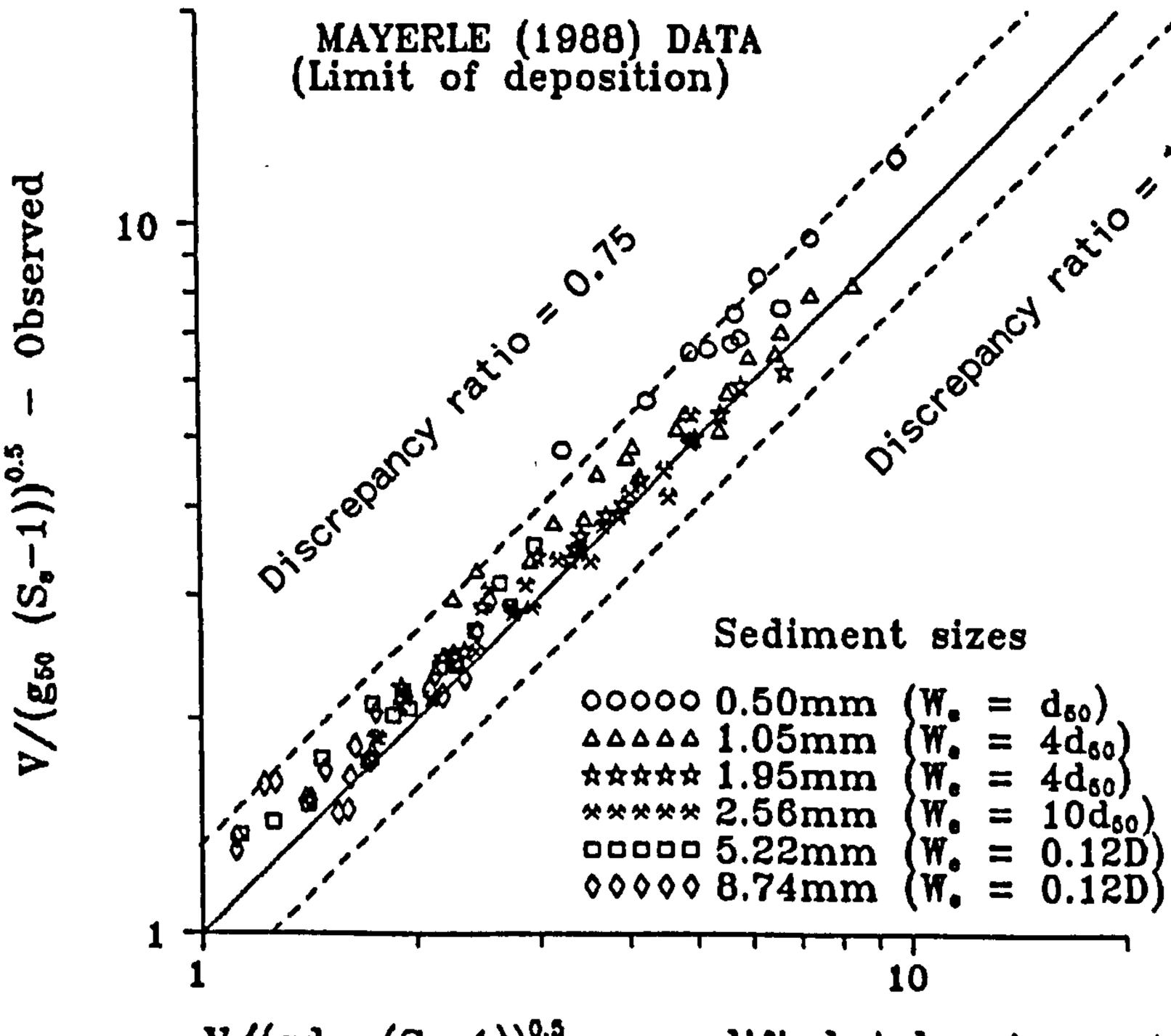

FIG. 6.26 Verification of modified Ackers' equation for Mayerle (1988) data

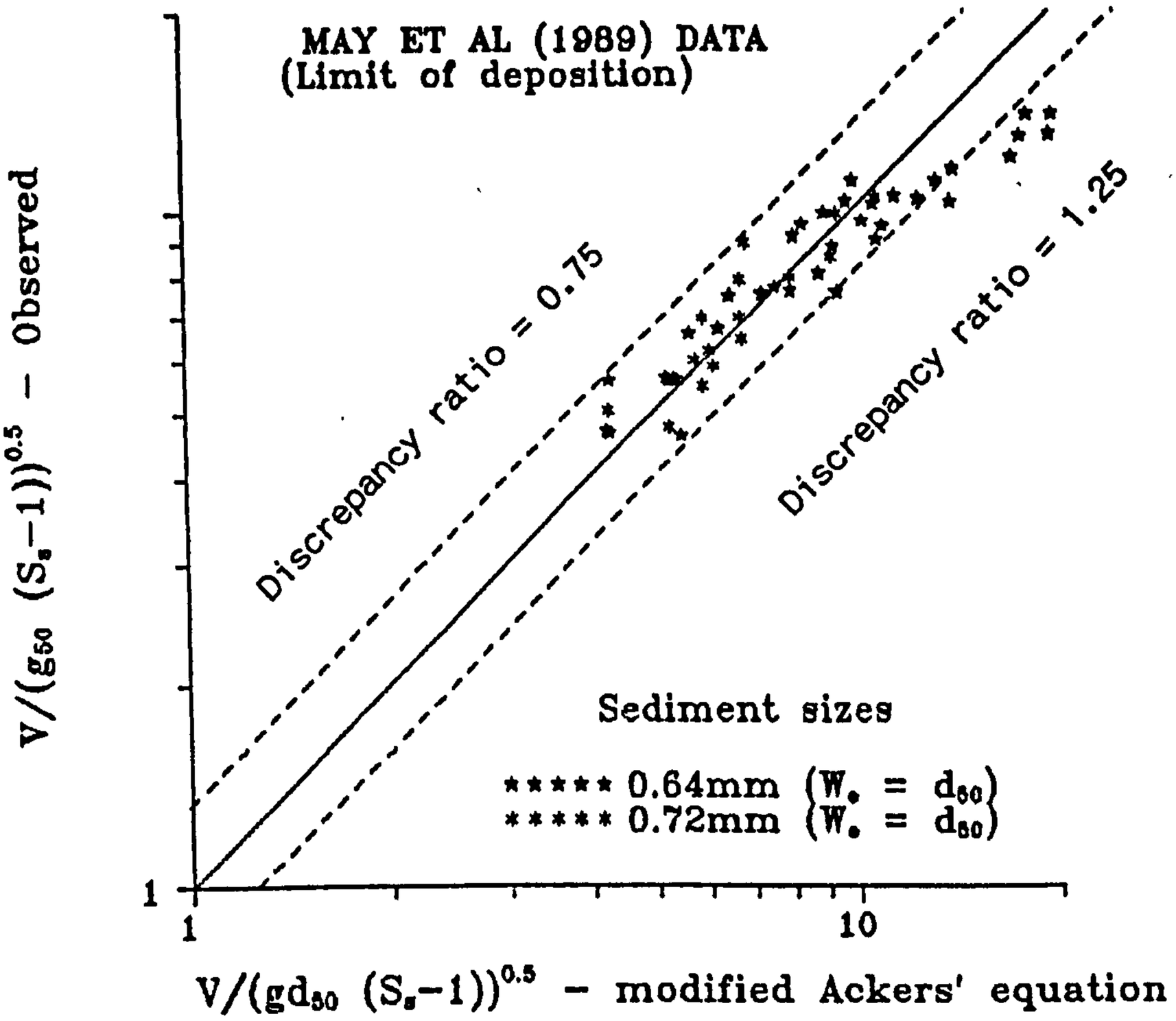

FIG. 6.27 Verification of modified Ackers' equation for May et al (1989) data

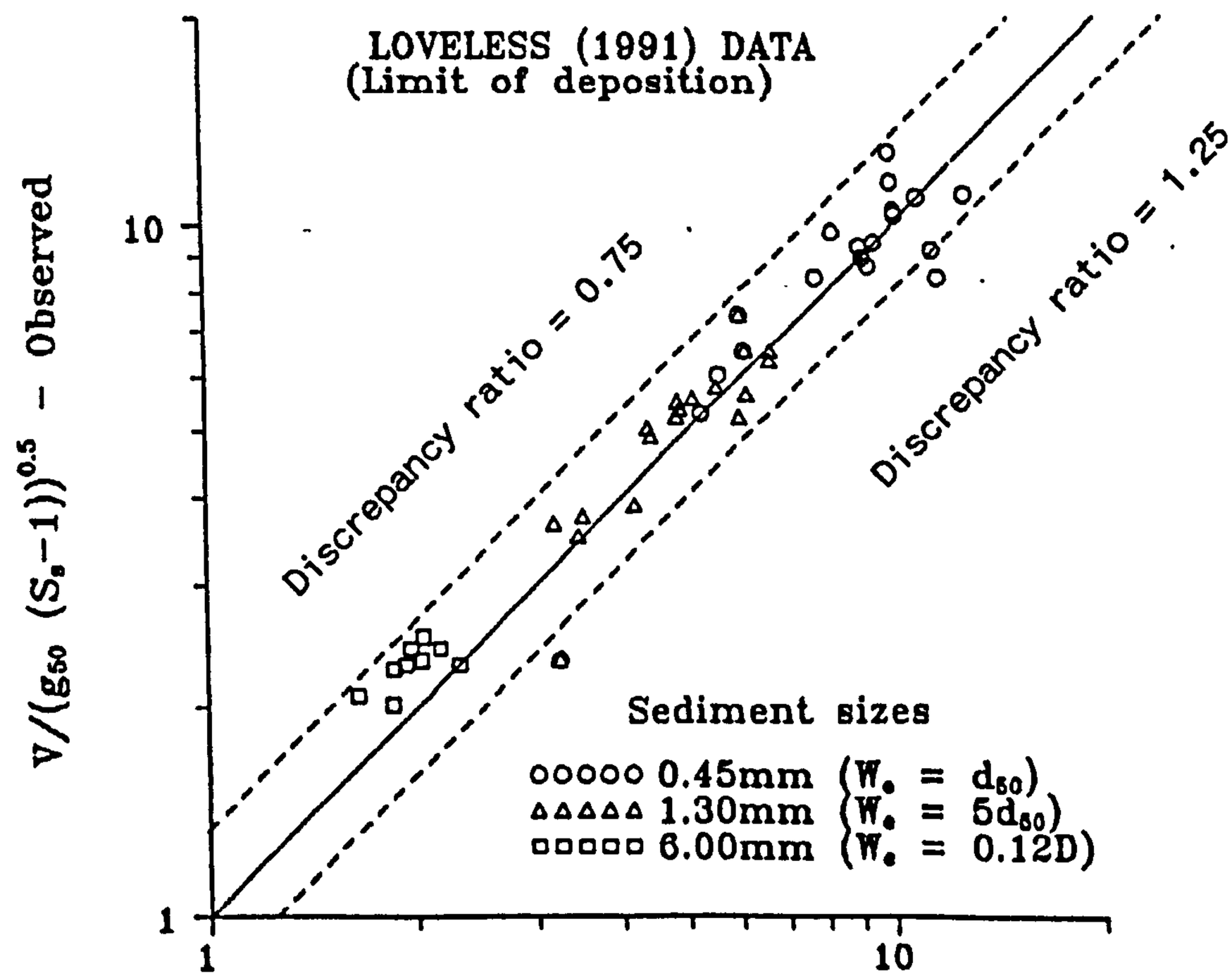

FIG. 6.28 Verification of modified Ackers' equation for Loveless (1991) data

Fig. 6.28 compares the measured and predicted Fr_m using modified Ackers' equation for Loveless' (1991) data. The required values of W_e were found to be: 1) $W_e = d_{50}$ for $d_{50} = 0.45$mm, 2) $W_e = 5d_{50}$ for $d_{50} = 1.30$mm and, 3) $W_e = 0.12D$ for $d_{50} = 6.0$mm. The application of modified Ackers' equation with these values of W_e yields (see Table 6.22) an average discrepancy ratio of 0.96 with a standard deviation of 0.175.

Based on the preceding analysis of the available data in clean pipe studies, it can be concluded that, depending on the particle size, four different values of W_e are needed to apply the modified Ackers' equation as given in Table 6.23. It should be noted that Eqn. 6.16 should be used to compute λ_s in the application of the modified Ackers' equation.

TABLE 6.23 VALUES OF EFFECTIVE WIDTH (W_e) TO BE USED IN THE MODIFIED ACKERS' EQUATION

SEDIMENT SIZE d_{50} (mm)	EFFECTIVE WIDTH W_e (m)
$0.5 \leq d_{50} < 1.0$	d_{50}
$1.0 \leq d_{50} < 2.0$	$5d_{50}$
$2.0 \leq d_{50} < 4.5$	$10d_{50}$
$d_{50} > 4.5$	0.12D

The assessment of the applicability of the modified Ackers' equation with the suggested values of W_e (Table 6.23) was then made using all available data (Table 6.6). The results shown in Fig. 6.29 have an average discrepancy ratio of 1.02 (see Table 6.24) where 89% of the combined data lie within the ± 0.25

TABLE 6.24 DISCREPANCY RATIO (Fr_*) FOR MODIFIED ACKERS' EQUATION - COMBINED DATA (CLEAN PIPES)

Source of data	Fr_* (predicted) / Fr_* (observed)							No. of data
	Mean	min	max	0.90-1.10 (%)	0.75-1.25 (%)	0.5-1.5 (%)	0.5-2.0 (%)	
Present	1.07	0.63	1.62	58	86	97	100	256
Mayerle (1988)	0.89	0.67	1.10	54	96	100	100	106
May et al (1989)	1.06	0.77	1.53	51	86	98	100	51
Loveless (1991)	0.97	0.78	1.39	54	96	100	100	46
Combined	1.02	0.63	1.63	56	89	98	100	459

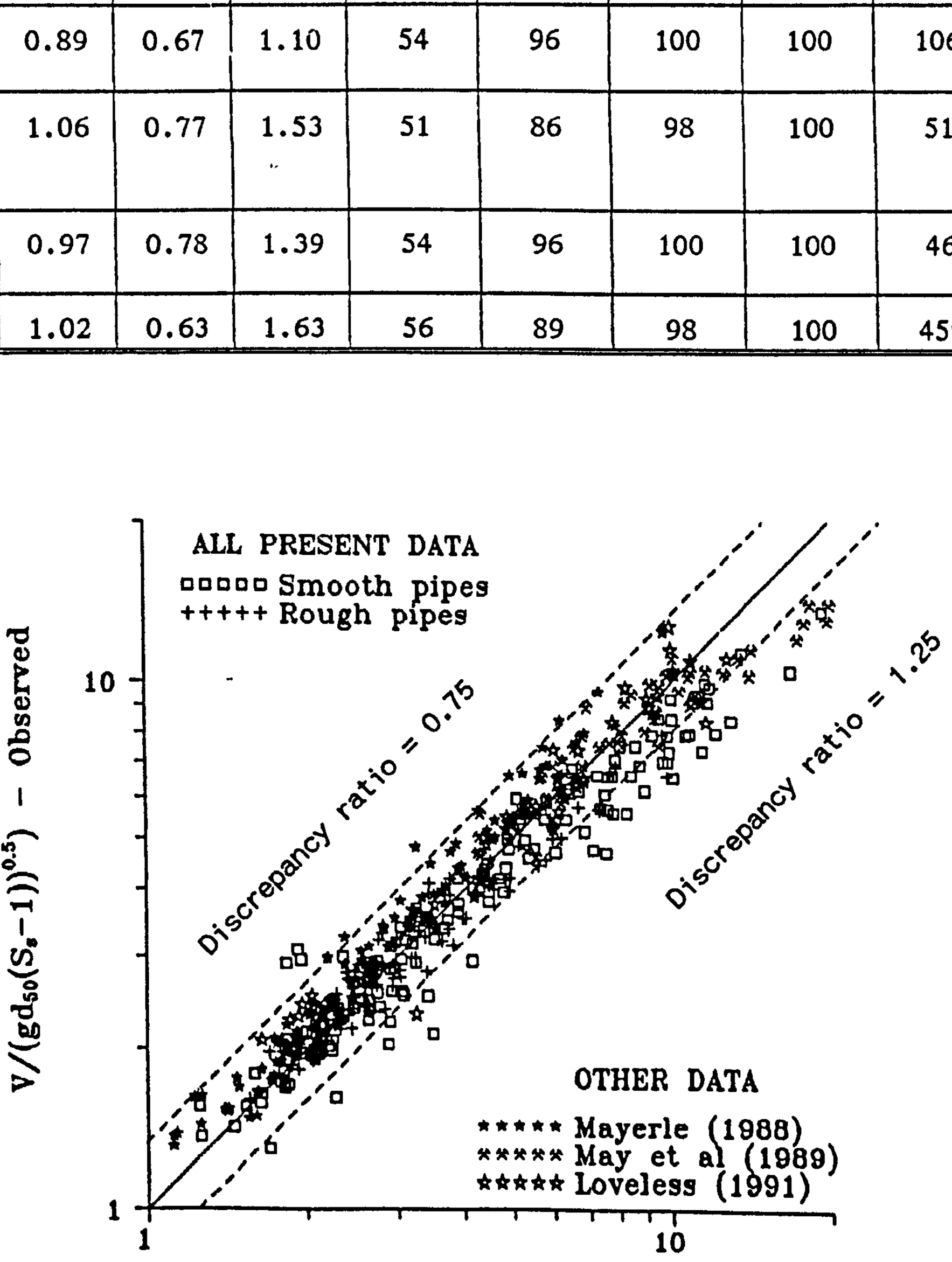

FIG. 6.29 Limiting velocity criterion due to modified Ackers' equation (Combined data)

deviations. The average discrepancy ratio for each investigator varies between 0.89 to 1.07 with between 86% and 96% of the data occurring within the ± 0.25 range of discrepancy ratio.

The applicability of the modified Ackers' equation over the range of the combined data is evaluated (with the discrepancy ratio computed in terms of Fr_*) as functions of dimensionless grain size (D_{gr}), proportional flow depth (y_o/D), velocity (V) and sediment concentrations (C_v). The results are given in Table 6.25 and plotted in Fig. 6.30.

Fig. 6.30a shows that the agreement is best over the range of 25 $\leq D_{gr} \leq$ 200 with the average discrepancy ratio varying from 0.97 to 1.01. A fairly good agreement is obtained outside this range of D_{gr} with the average discrepancy ratio varying between 0.94 to 1.09. The results also show that between 78% to 100% of the data over the particle size tested lie within the ± 0.25 deviation. It should also be noted that the modified Ackers' equation yields a reasonably good agreement for the range 51 $\leq D_{gr} \leq$ 100 with an average discrepancy ratio of 1.0 where 89% of the data occur within the ± 0.10 deviations.

Fig. 6.30b indicates that the agreement is generally satisfactory over the full range of flow depths studied. The average discrepancy ratio for flow up to half-full depths is 1.01 with over 90% of the data falling within the ± 0.25 deviation. A similar degree of accuracy is obtained for flow more than half-

full depths with an average discrepancy ratio of 1.04 and over 88% of the data lying within the ± 0.25 deviation.

Fig. 6.30c reveals that a good agreement is obtained for the range of 11 ≤ C_v (ppm) ≤ 1000 where the average discrepancy ratio varies between 1.0 and 1.02 and between 90% and 94% of data lie within the ± 0.25 deviations. A fairly reasonable agreement is shown outside of this range of C_v where the average discrepancy ratio varies between 0.99 and 1.12 and between 72% and 79% of the data lie within the ± 0.25 deviations.

Fig. 6.30d shows that the agreement is reasonably good for the range of 0.50 ≤ V (m/s) ≤ 1.10 where the average discrepancy ratio varies between 1.00 and 1.04 and between 87% and 96% of the data lie within the ± 0.25 range of the discrepancy ratio. It appears that there is no systematic error for the extremes.

Within the range of the combined data, the preceding analysis suggests the general applicability of the modified Ackers' equation for sediment transport in clean pipes provided that the suggested values of W_e as given in Table 6.23 are used. It must also be noted that the applicability of the modified Ackers' equation is affected greatly by its incipient motion criterion (Eqn. 3.5). Its applicability for $R/d_{50} > 200$ (see Fig. 6.21) should be assessed when such data are available.

TABLE 6.25 DISCREPANCY RATIO (Fr_m) FOR MODIFIED ACKERS' EQUATION AS FUNCTIONS OF RELEVANT PARAMETERS - COMBINED DATA (CLEAN PIPES)

Range of parameter		Fr_m (predicted) / Fr_m (observed)							No of data
		Mean	min	max	0.90-1.10 (%)	0.75-1.25 (%)	0.50 - 1.50 (%)	0.5-2.0 (%)	
D_{gr}	10-25	1.09	0.67	1.62	40	78	96	100	156
	26-50	0.97	0.66	1.39	51	93	100	100	103
	51-100	1.00	0.83	1.40	89	98	100	100	56
	101-150	0.98	0.63	1.63	58	93	99	100	91
	151-200	1.01	0.86	1.13	79	100	100	100	24
	201-250	0.94	0.76	1.08	69	100	100	100	29
y_0/D	≤ 0.5	1.01	0.63	1.62	49	90	99	100	293
	> 0.5	1.04	0.66	1.63	67	88	96	100	166
C_v (ppm)	1-10	1.12	0.77	1.61	49	72	96	100	47
	11-100	1.02	0.67	1.56	58	90	98	100	155
	101-500	1.00	0.66	1.62	57	92	99	100	186
	501-1000	1.00	0.76	1.63	54	94	98	100	52
	1001-2000	0.99	0.63	1.42	47	79	100	100	19
V(m/s)	0.200-0.500	0.95	0.63	1.39	47	90	100	100	59
	0.501-0.600	1.00	0.63	1.61	66	90	99	100	80
	0.601-0.700	1.02	0.76	1.63	60	92	99	100	99
	0.701-0.800	1.03	0.66	1.56	54	87	98	100	89
	0.801-.900	1.04	0.76	1.62	61	90	97	100	62
	0.901-1.000	1.01	0.77	1.54	51	96	99	100	49
	1.001-1.500	1.17	0.78	1.53	33	67	100	100	21

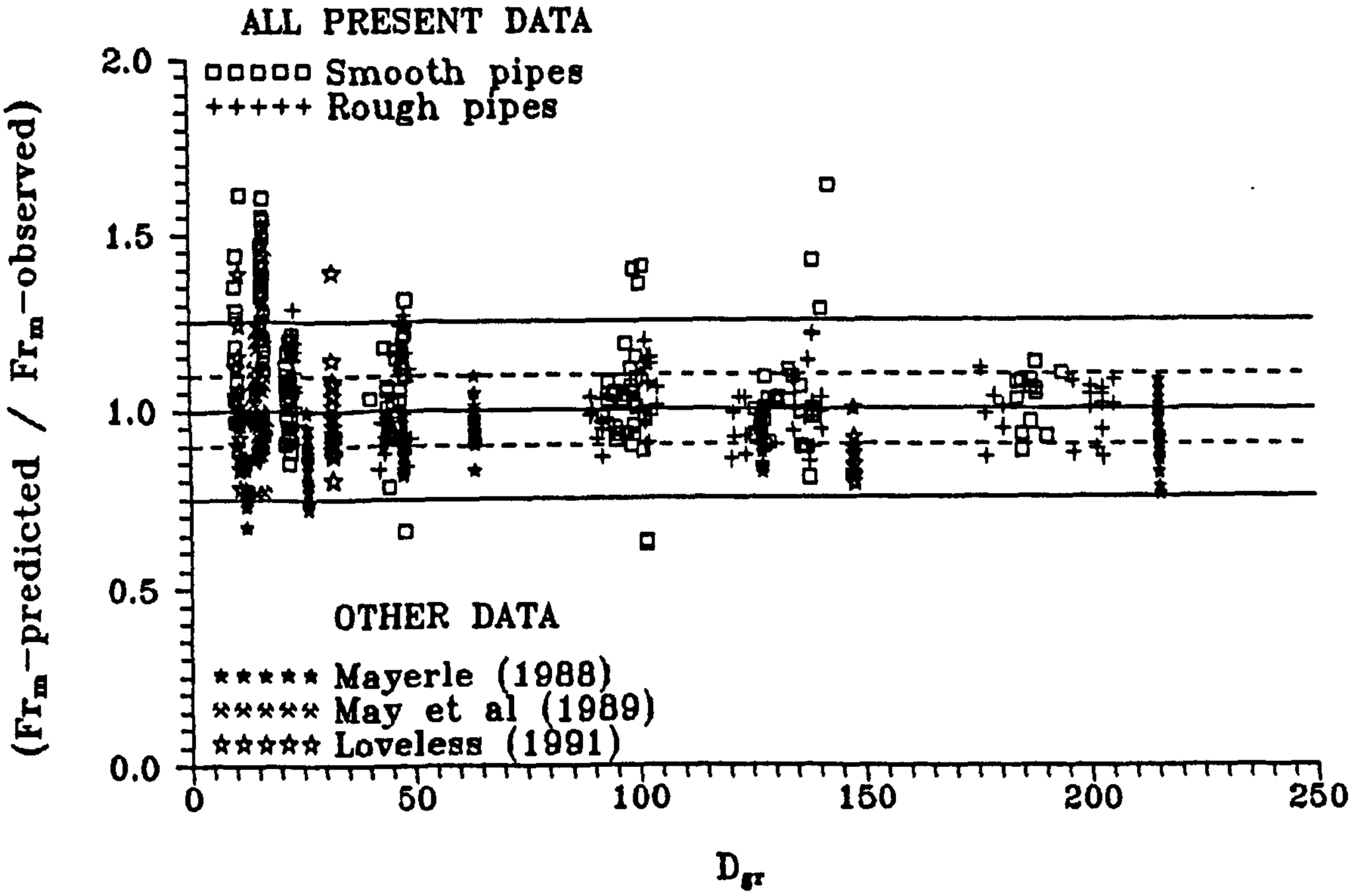

FIG. 6.30a Discrepancy ratio for modified Ackers' equation as a function of dimensionless particle size

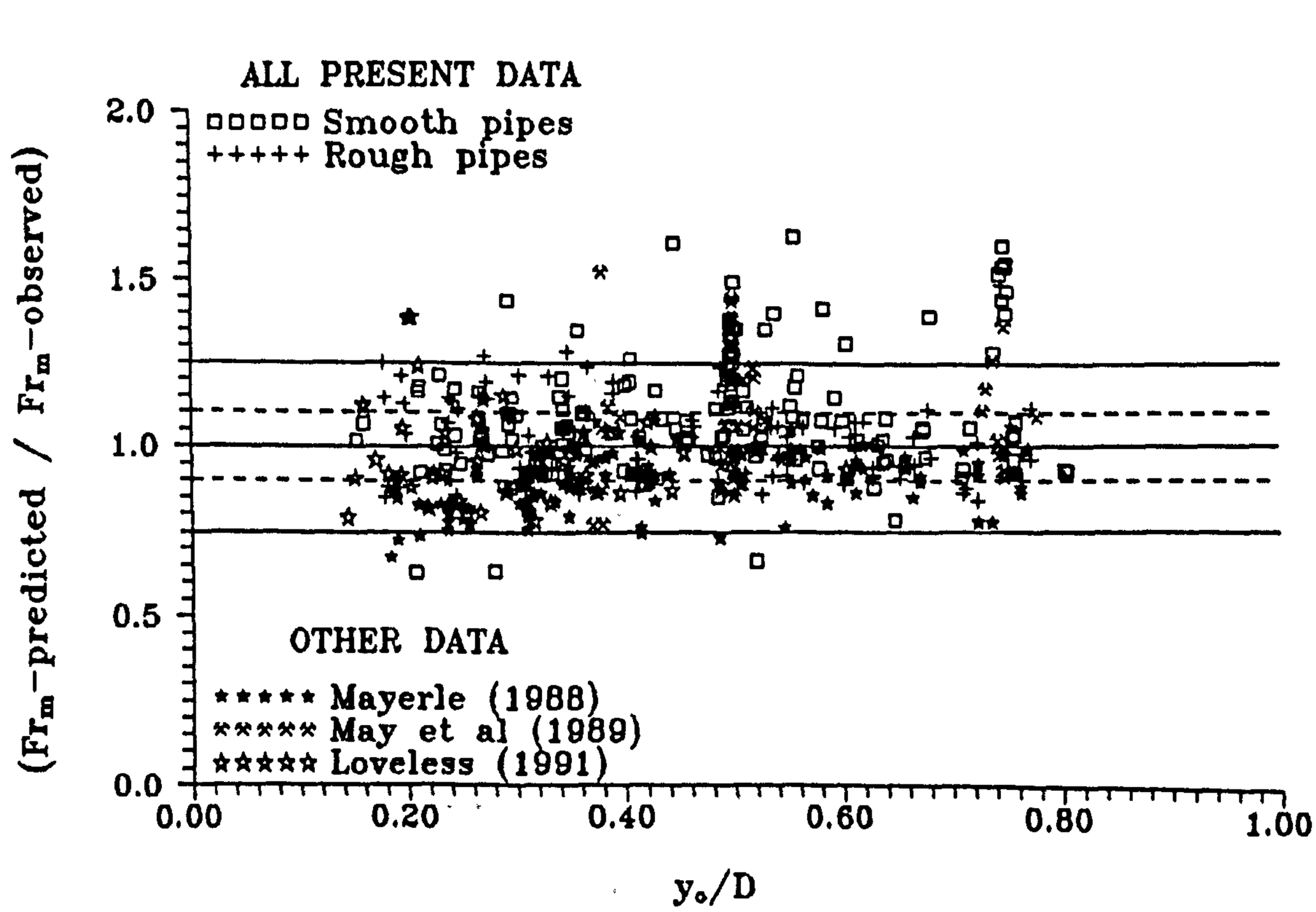

FIG. 6.30b Discrepancy ratio for modified Ackers' equation as a function of proportional flow depth

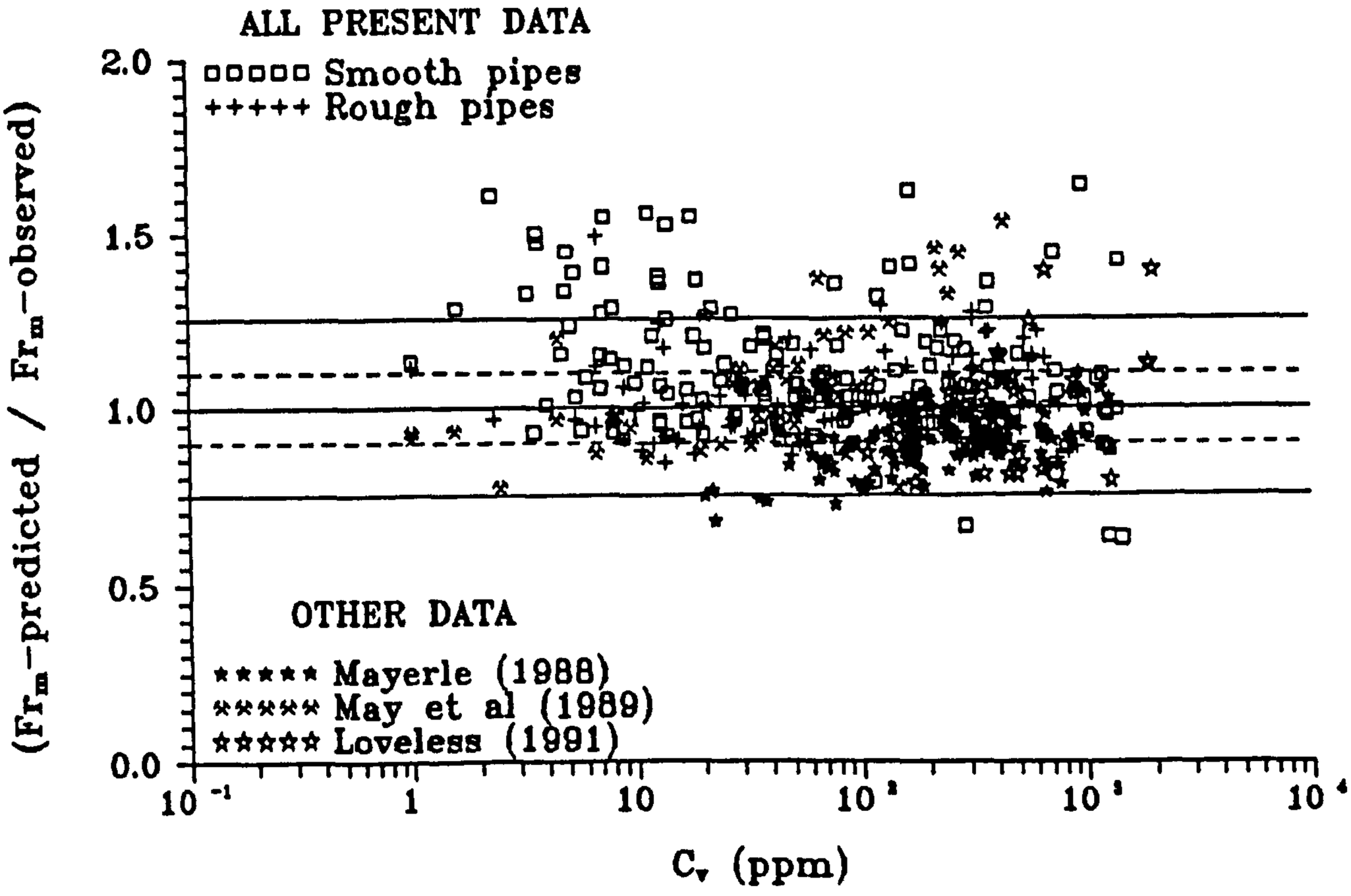

FIG. 6.30c Discrepancy ratio for modified Ackers' equation as a function of limiting concentration

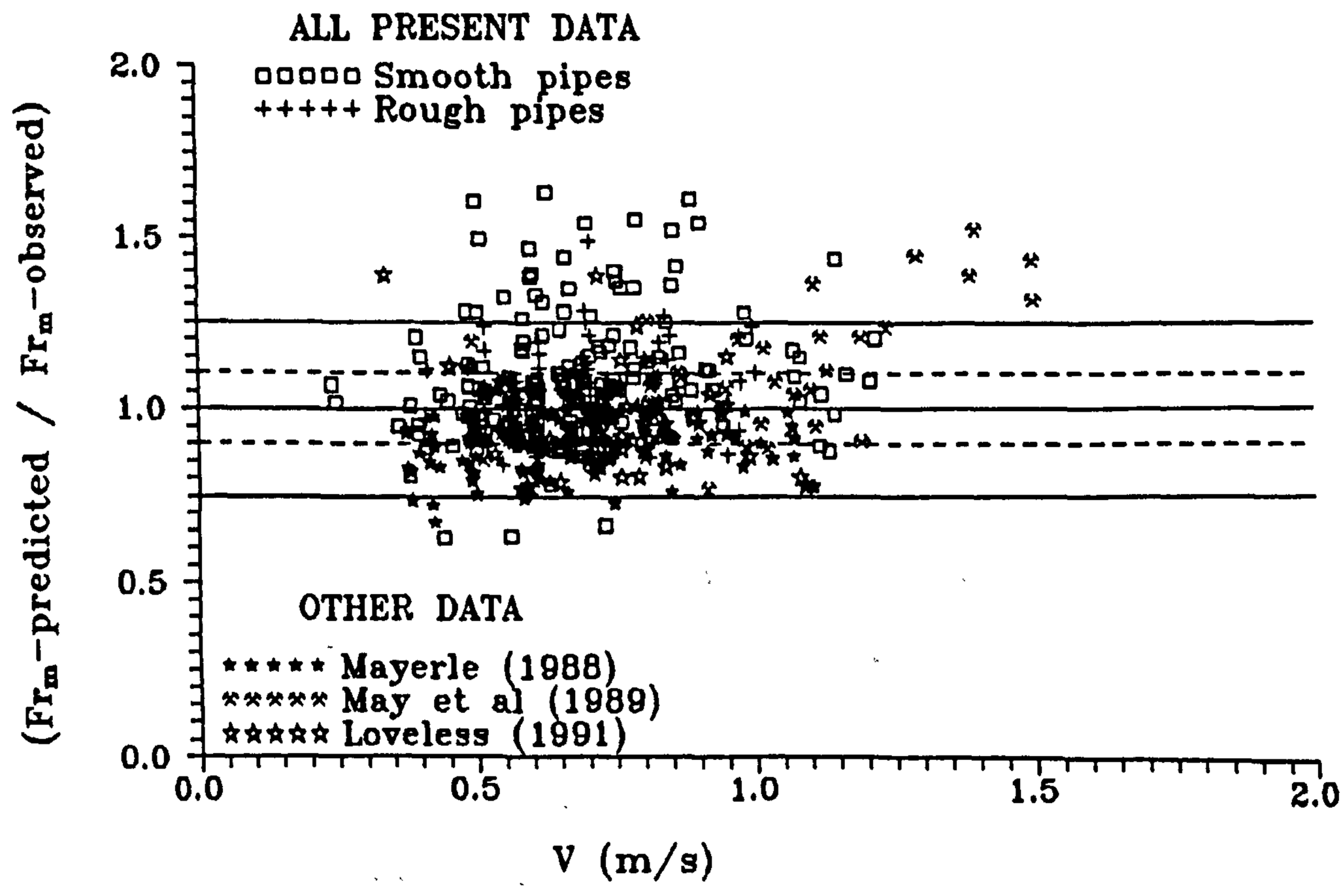

FIG. 6.30d Discrepancy ratio for modified Ackers' equation as a function of limiting velocity

6.1.3.4 Application of El-Zaemey (1991) Equations to Clean Pipe and Rigid Bed Rectangular Channels

6.1.3.4.1 Introduction

As mentioned in Section 3.3.2, El-Zaemey (1991) investigated the effect of permanent deposits on the invert of pipe channels on the sediment carrying capacity and hydraulic resistance to flow. Due to the intermittent nature of flow, the deposition of sediments occurs spasmodically in sewer networks, especially during dry weather flow. The longer the deposits remain in the sewer system the more likely that the sediment properties change and can eventually become consolidated or cemented.

El-Zaemey (1991) proposed a functional relationship to describe the sediment transport process in pipes with permanent deposits by utilising the bed shear stress (τ_b) as the dependent variable:

$$\frac{\tau_b}{\rho g(S_s-1)d_{50}} = f\left(C_v, \frac{b}{y_o}, \frac{d_{50}}{D}, \lambda_{sb}\right) \qquad (6.36)$$

He emphasized the importance of the width to depth parameter (b/y_o) to characterize the influence of bed width (b) and flow depth and hence the channel shape on sediment movement. In particular, the bed width could be related to the effective width (W_e) responsible for the movement of sediments. This concept of W_e have been touched on by earlier researchers (Ackers 1984, Paul-Sakhuja 1990, Loveless 1991). Another important parameter in Eqn. 6.36 is the relative particle size (d_{50}/D) which reflects

the influence of pipe diameter and particle size on sediment movement.

Based on his experimental data in a 305mm dia. pipe with a range of bed thicknesses of $0.154 < y_s/D < 0.393$, El-Zaemey (1991) obtained an equation for pipe channels with permanent deposits by the application of a multiple regression analysis on the functional relationship of Eqn. 6.36:

$$\frac{\tau_b}{\rho g(S_s-1)d_{50}} = 0.47\, C_v^{0.33} \left(\frac{b}{y_o}\right)^{-0.80} \left(\frac{d_{50}}{D}\right)^{-1.14} \lambda_{sb}^{1.2} \qquad (3.58)$$

This equation (Eqn. 3.58) is applicable for both rough and smooth flat fixed beds. Eqn. 3.58 may be transformed in terms of limiting velocity as:

$$\frac{V}{\sqrt{gd_{50}(S_s-1)}} = 1.94\, C_v^{0.17} \left(\frac{b}{y_o}\right)^{-0.40} \left(\frac{d_{50}}{D}\right)^{-0.57} \lambda_{sb}^{0.10} \qquad (6.37)$$

El-Zaemey (1991) also derived the best-fit equations to compute the overall and bed friction factors (λ_s and λ_{sb} respectively) to make use of Eqn. 3.58 or Eqn. 6.37:

$$\lambda_s = 0.88\, C_v^{0.01} \left(\frac{b}{y_o}\right)^{0.03} \lambda_o^{0.94} \qquad (3.57)$$

$$\lambda_{ab} = 6.6\ \lambda_s^{1.45} \qquad (3.59)$$

In the following sections, attempts were made to assess the applicability of El-Zaemey's equations (Eqns. 3.57-3.59) to other channel shapes.

6.1.3.4.2 Clean Pipe Channels

El-Zaemey (1991) utilised Mayerle's (1988) data in a smooth 152mm dia. pipe to widen the applicability of his equation (Eqn. 3.58) for transport data in clean pipes. The form of Eqn. 3.58 or Eqn. 6.37 suggests the possibility of its application to clean pipes provided that a suitable value of "bed width", b, could be found.

It has been observed that in rectangular channels or circular channels with flat beds (Mayerle 1988, Loveless 1991, El-Zaemey 1991) the sediments spread over the whole width of the bed. Hence it can be concluded that, for these channels, $W_e = b$. El-Zaemey (1991) therefore attempted to modify Eqn. 3.58 by relating the bed width (b) of the flat rigid bed to the effective width (W_e) of transport over the invert of clean pipes.

El-Zaemey (1991) re-analysed the measurements of the width of sediment spread (W_s) made by Mayerle (1988) in a 152mm dia. pipe channel for the range of sediment sizes of $0.5 < d(mm) < 8.74$. He found that the average value of the relative spread over pipe diameter (W_s/D) was 0.3 and confirmed this value by conducting a

few measurements of W_s in a 152mm dia. pipe. El-Zaemey (1991) then resolved that the effective width (W_e) should be slightly larger than 0.3D because the particles tend to touch each other while moving along the invert of circular channels.

El-Zaemey (1991) later found that the best agreement between Eqn. 3.58 and Mayerle's data was obtained when the bed width value (b) was replaced by 0.5D which he referred to as "the equivalent bed width". It is expected that this modification will remain valid in terms of limiting velocity. Substituting b = 0.5D, Eqn. 6.37 is then re-written as:

$$\frac{V}{\sqrt{gd_{50}(S_s-1)}} = 2.56\, C_v^{0.165} \left(\frac{D}{y_o}\right)^{-0.40} \left(\frac{d_{50}}{D}\right)^{-0.57} \lambda_{sb}^{0.10} \qquad (6.38)$$

for application to clean pipe data. It should be noted that in the application of Eqn. 6.38 to the available data in rough clean pipes (see Table 6.6) the overall friction factor (λ_s) should be used instead of the bed friction factor (λ_{sb}). This is because all available rough bed data (author's and Loveless' 1991) in clean pipes were obtained in uniformly roughened pipes.

Attempts were then made to verify the validity of applying Eqn. 6.38 to the available clean pipe data (see Table 6.6). The comparisons were made in plots of the observed Fr_m against the predicted values. The measured values of λ_s were used in the computation of the predicted values of Fr_m. As before, the discrepancy ratios in terms of Fr_m were also computed.

Fig. 6.31 confirms the good agreement obtained (see Table 6.26) between the predicted values of Fr_m using Eqn. 6.38 and the observed values from Mayerle data. The results shown in Fig. 6.31 have an average discrepancy ratio of 0.96 with 94% of the Mayerle's data falling within the ± 0.25 deviation.

TABLE 6.26 DISCREPANCY RATIO (Fr_m) FOR EL-ZAEMEY'S EQN. 6.38 - COMBINED DATA (CLEAN PIPES)

Source of data	Fr_m (predicted) / Fr_m (observed)							No. of data
	Mean	min	max	0.90-1.10 (%)	0.75-1.25 (%)	0.5-1.5 (%)	0.5-2.0 (%)	
Present	1.13	0.71	1.66	36	82	98	100	256
Mayerle (1988)	0.96	0.68	1.29	58	94	100	100	106
May et al (1989)	0.88	0.70	1.16	43	86	100	100	51
Loveless (1991)	0.98	0.68	1.76	61	93	99	100	46
Combined	1.05	0.68	1.76	44	88	99	100	459

Further verification of Eqn. 6.38 was made with the entire present data and data of May et al (1989) and Loveless (1991). Fig. 6.32 shows good correlation between Eqn. 6.38 and these independent data (see Table 6.26) where the average discrepancy ratios vary from 0.88 to 1.13 and between 82% and 93% of the data lie within the ± 0.25 deviation. Considering the combined data (see Table 6.26), the correlation in Eqn. 6.38 has an average discrepancy ratio of 1.05 with 88% of the data occurring within the ± 0.25 deviation.

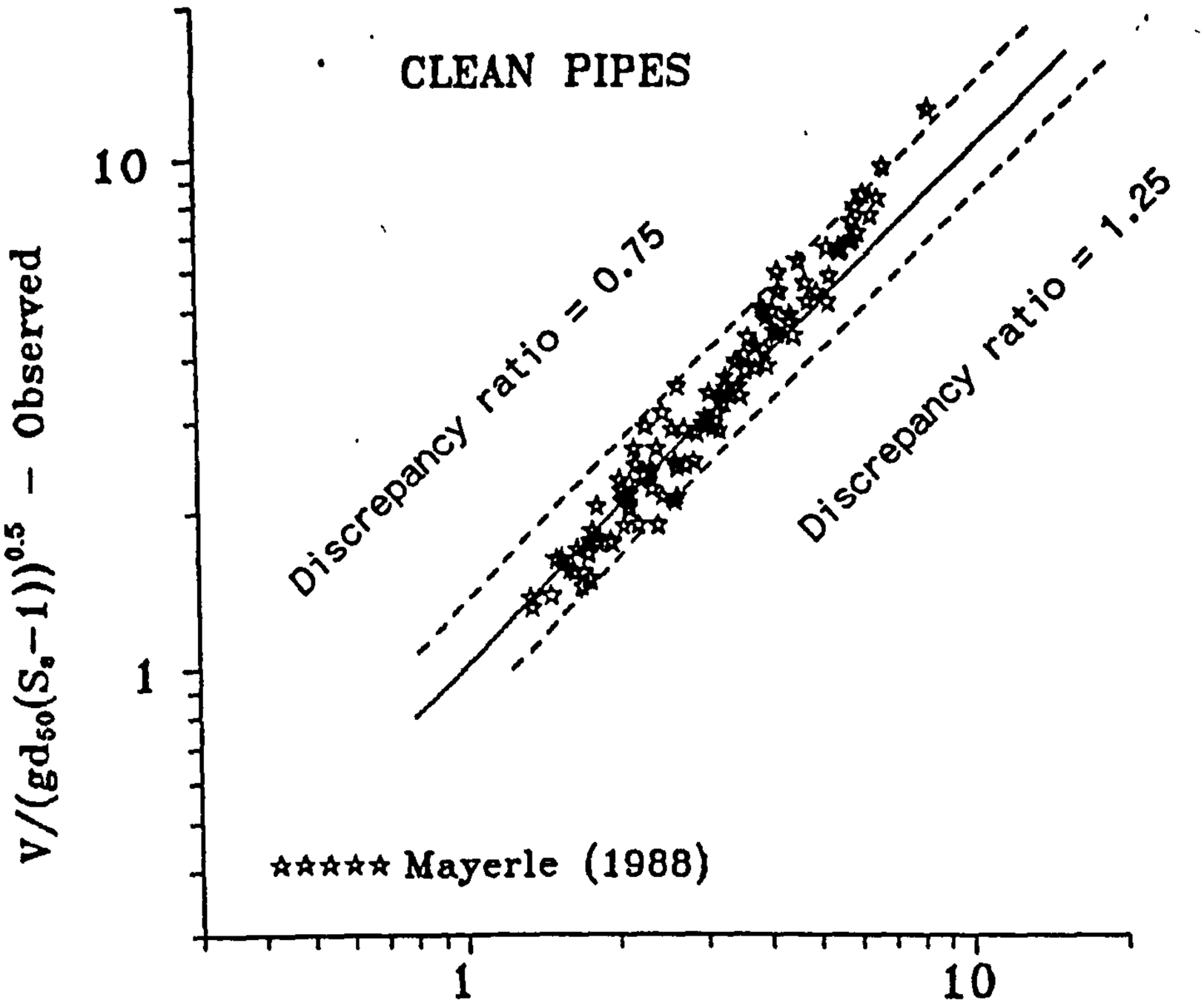

FIG. 6.31 Validity of Eqn. 6.37 for Mayerle's clean pipe data (b = 0.5D)

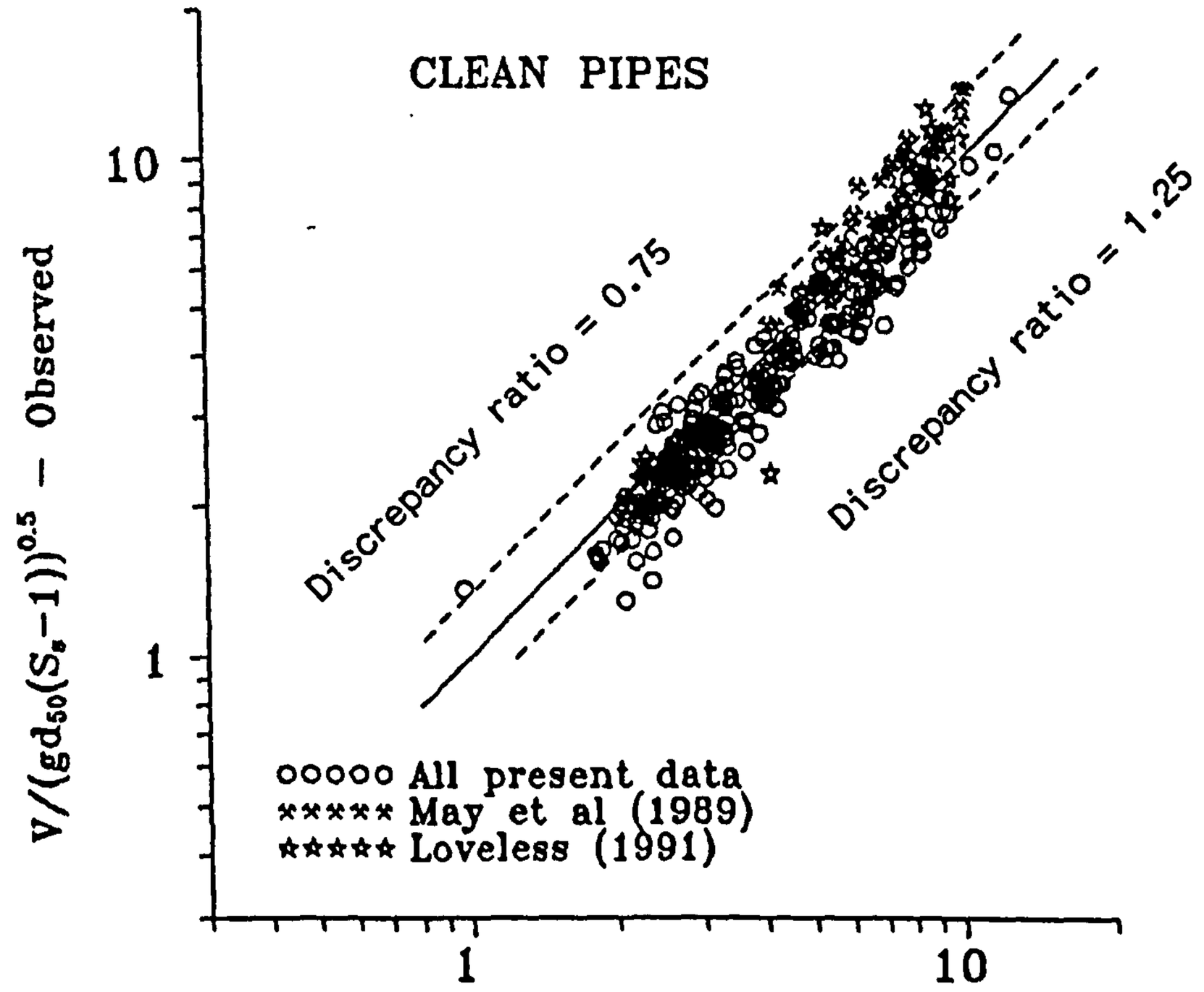

FIG. 6.32 Validity of Eqn. 6.37 for present, May et al and Loveless' clean pipe data (b = 0.5D)

The applicability of Eqn. 6.38 over the range of particle size, flow depth, sediment concentration and velocity is shown in Fig. 6.33 with the corresponding discrepancy ratios is listed in Table 6.27. All available data in clean pipes were used in the analysis.

Fig. 6.33a shows that the agreement is generally good over the range of particle size. The average discrepancy ratio varies from 1.01 to 1.10 with 80% - 100% of the data lying within the ± 0.25 deviation. Even though the average discrepancy ratios for the range of $51 < D_{gr} < 200$ are slightly high (1.07 - 1.10), the majority of the data for this region of D_{gr} fall within the ± 0.25 deviations (84% - 96%).

Fig. 6.33b indicates that better agreement is obtained for the data in the region of proportional flow depth up to half-full. This region of flow depth has an average discrepancy ratio of 1.04 with 88% of the data lie within the ± 0.25 deviations.

Fig. 6.33c reveals that the best agreement is obtained for the range of $101 < C_v$ (ppm) < 500 with a perfect average discrepancy ratio of 1.0 and 89% of the data in this region fall within the ± 0.25 deviation. At the extremes ($C_v < 10$ppm or $C_v > 1000$ppm), Eqn. 6.38 overpredicts the observed Fr_m on average by 15% and a smaller proportion of the data fall within the ± 0.25 deviations (64% - 74%). It should be noted that these extremes are outside El-Zaemey's experimental range of C_v (= 11ppm - 512ppm) and this might explain the poor agreement obtained.

TABLE 6.27 DISCREPANCY RATIO (Fr_s) FOR EL-ZAEMEY'S EQN. 6.38 AS FUNCTIONS OF RELEVANT PARAMETERS - COMBINED DATA (CLEAN PIPES)

Range of parameter		Fr_s (predicted) / Fr_s (observed)							No of data
		Mean	min	max	0.90-1.10 (%)	0.75-1.25 (%)	0.50 - 1.50 (%)	0.5-2.0 (%)	
D_{gr}	10-25	1.01	0.68	1.60	36	80	99	100	156
	26-50	1.05	0.71	1.76	52	89	98	100	103
	51-100	1.09	0.80	1.41	41	84	100	100	56
	101-150	1.10	0.76	1.60	49	91	99	100	91
	151-200	1.07	0.71	1.21	38	96	100	100	24
	201-250	1.03	0.79	1.21	66	100	100	100	29
y_0/D	≤ 0.5	1.04	0.68	1.76	49	88	99	100	293
	> 0.5	1.07	0.68	1.49	35	83	100	100	166
C_v (ppm)	1-10	1.15	0.71	1.49	21	64	100	100	47
	11-100	1.08	0.71	1.60	36	89	98	100	155
	101-500	1.00	0.68	1.66	53	89	99	100	186
	501-1000	1.03	0.74	1.60	60	92	98	100	52
	1001-2000	1.16	0.84	1.76	37	74	95	100	19
V(m/s)	0.200-0.500	1.21	0.71	1.76	25	59	93	100	59
	0.501-0.600	1.14	0.77	1.49	31	80	100	100	80
	0.601-0.700	1.10	0.80	1.37	40	93	100	100	99
	0.701-0.800	1.03	0.75	1.29	66	98	100	100	89
	0.801-.900	0.97	0.72	1.16	74	98	100	100	62
	0.901-1.000	0.85	0.68	1.14	37	84	100	100	49
	1.001-1.500	0.83	0.68	0.94	19	81	100	100	21

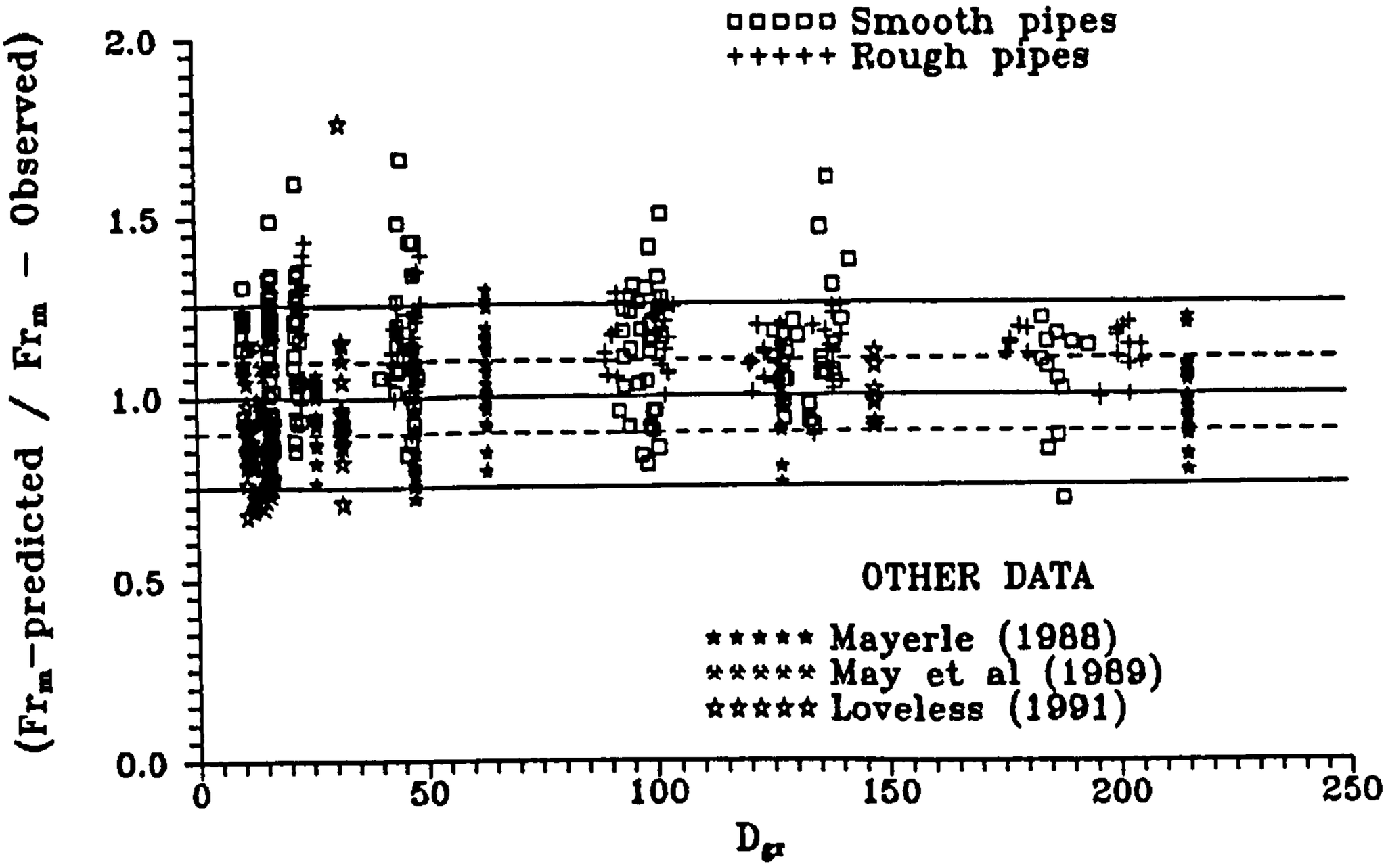

FIG. 6.33a Discrepancy ratio for El-Zaemey's Eqn. 6.37 with b = 0.5D (Eqn. 6.38) as a function of dimensionless particle size

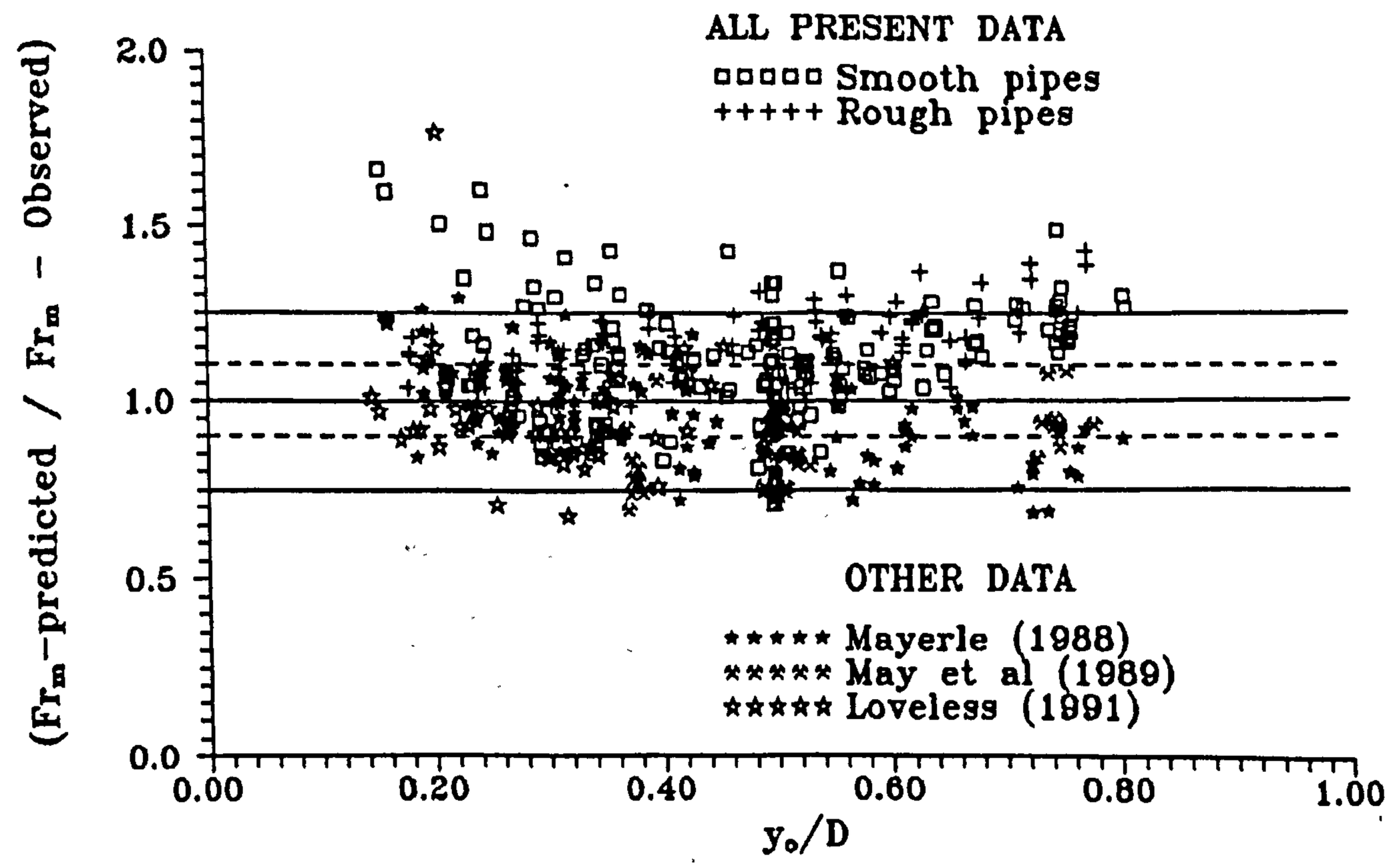

FIG. 6.33b Discrepancy ratio for El-Zaemey's Eqn. 6.37 with b = 0.5D (Eqn. 6.38) as a function of proportional flow depth

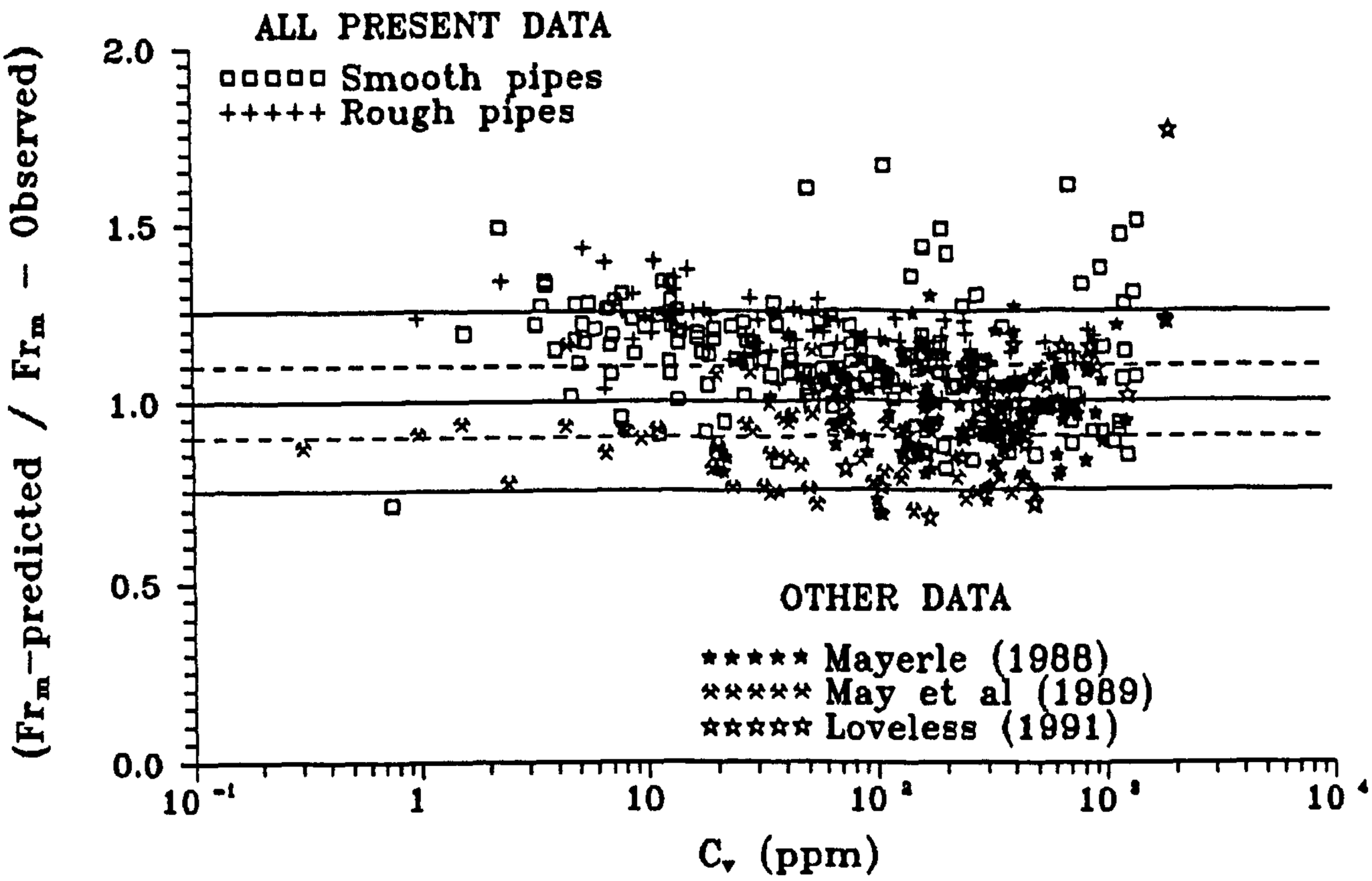

FIG. 6.33c Discrepancy ratio for El-Zaemey's Eqn. 6.37 with b = 0.5D (Eqn. 6.38) as a function of limiting sediment concentration

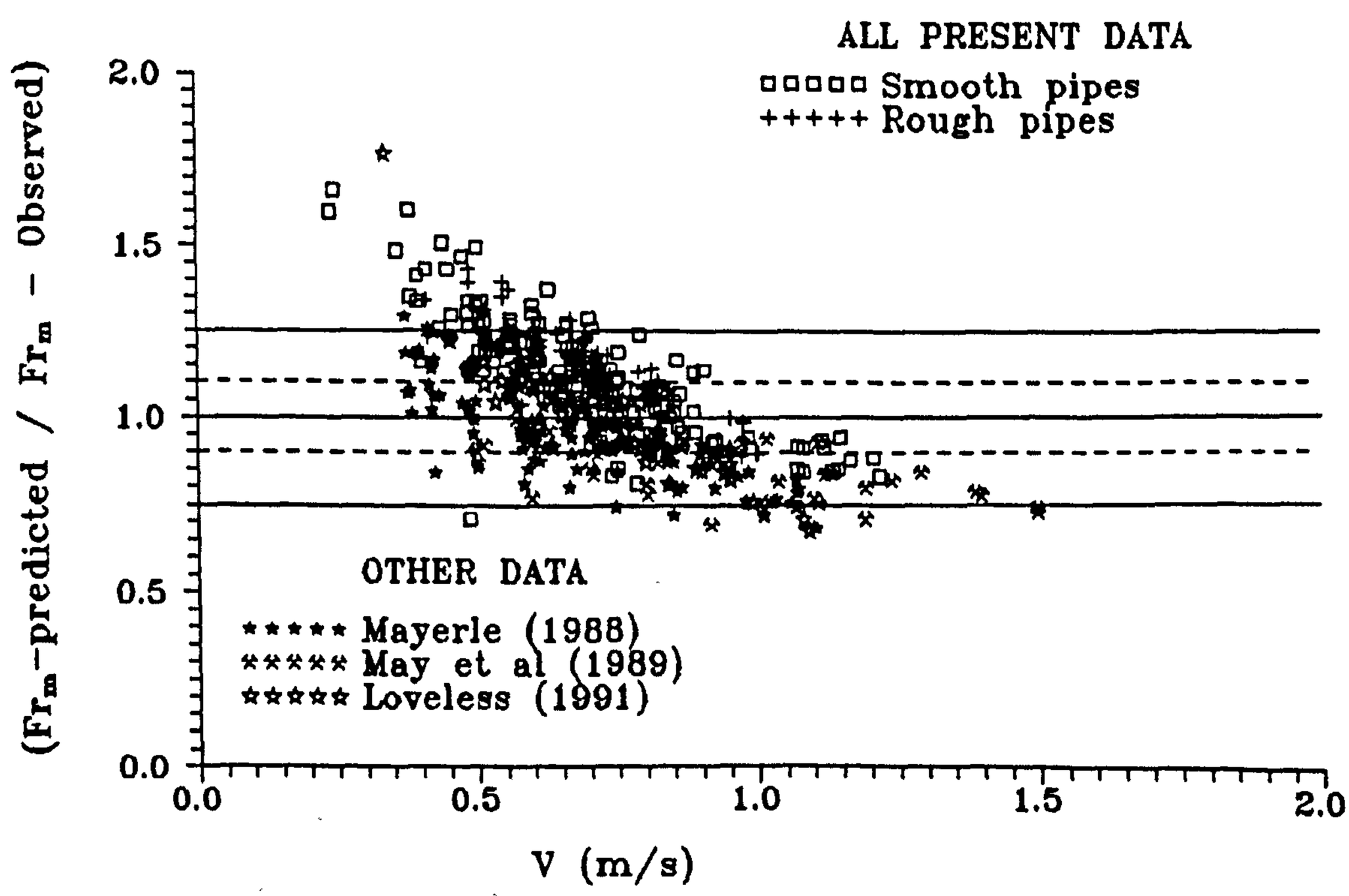

FIG. 6.33d Discrepancy ratio for El-Zaemey's Eqn. 6.37 with b = 0.5D (Eqn. 6.38) as a function of limiting velocity

Fig. 6.33d indicates that the agreement is reasonably good over the central range of velocities between 0.7m/s and 0.9m/s where the average discrepancy ratios vary from 0.97 to 1.03 with 98% of the data lie within the ± 0.25 deviations. There appears to be systematic errors at the extremes: overprediction for V < 0.7m/s and underprediction for V > 0.9m/s.

Overall Eqn. 6.38 provides a fairly good agreement over a range of sediments and flow conditions in clean pipes. This confirms the notional concept of substituting b = 0.5D in El-Zaemey's Eqn. 6.37 for its application to conditions in clean pipe channels.

An attempt was also made to test the applicability El-Zaemey's Eqn. 3.57 for the computation of the friction factor with sediment (λ_s) to clean pipe data. Substitution of b = 0.5D into Eqn. 3.57 yielded:

$$\lambda_s = 0.86\, C_v^{0.01} \left(\frac{D}{y_o}\right)^{0.03} \lambda_o^{0.94} \qquad (6.39)$$

The verification of Eqn. 6.39 for its application to clean pipe data is shown in Fig. 6.34. The good agreement obtained (see Table 6.28) with an average discrepancy ratio of 0.97 for all the data shown in Fig. 6.34 where 91% of them fall within the ± 0.25 deviations. This confirms once again the validity of the notional concept of substituting b = 0.5D in El-Zaemey's equations (Eqns. 6.37 and 3.57) for application to conditions in clean pipe channels.

TABLE 6.28 DISCREPANCY RATIO (λ_s) FOR EQN. 6.39 - COMBINED DATA (CLEAN PIPES)

Source of data	λ_s (predicted) / λ_s (observed)							No. of data
	Mean	min	max	0.90-1.10 (%)	0.75-1.25 (%)	0.5-1.5 (%)	0.5-2.0 (%)	
Present data	0.97	0.80	1.18	92	100	100	100	256
Mayerle (1988)	0.96	0.81	1.02	92	100	100	100	106
May et al (1989)	0.99	0.86	1.20	84	100	100	100	51
Combined	0.97	0.80	1.20	91	100	100	100	413

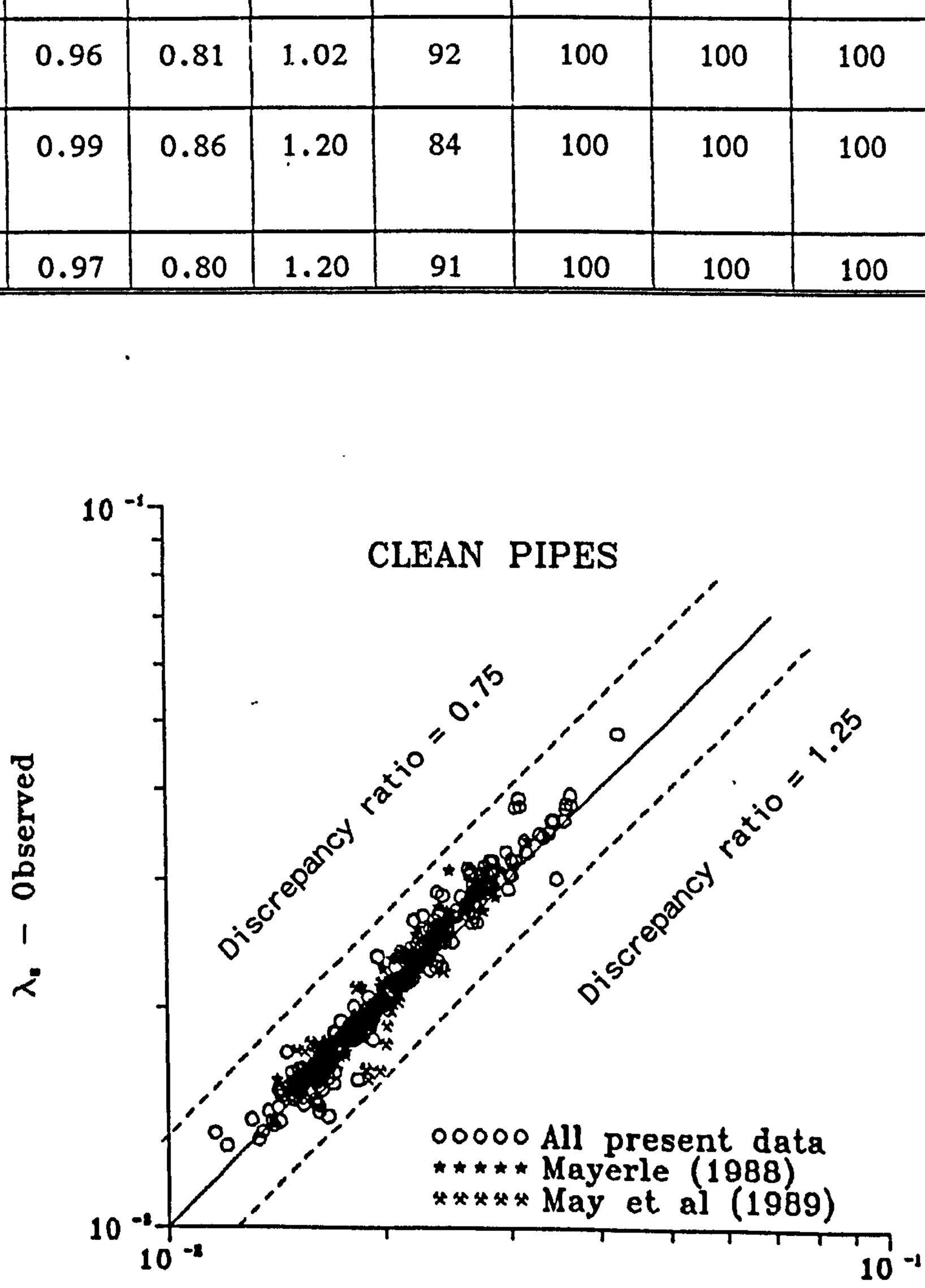

FIG. 6.34 Validity of Eqn. 3.57 for present, Mayerle and May et al's clean pipe data (b = 0.5D)

Initially, the data from Mayerle's (1988) studies in smooth and rough rigid bed rectangular were utilised. As mentioned in Section 3.3.3 (see Table 6.29), Mayerle (1988) performed his experiments over a wide range of sediment sizes (d_{50} = 0.5mm - 8.74mm) and three boundary roughness values (k_o = 0.0, 0.60mm, 0.73mm).

As shown earlier, the application of Eqn. 6.37 to conditions in clean pipe channels requires the substitution of b = 0.5D (Eqn. 6.38). It was then decided to substitute D = 2.0b, acting as a "shape factor", for the application of Eqn. 6.37 to Mayerle's data from smooth and rough rectangular channels. Figs. 6.35 and 6.36 show that this substitution results in the overprediction of the observed values of Fr_m for smooth and rough bed data. However, both plots show that the best-fit lines of the predicted values of Fr_m are parallel to the line of best agreement. This suggests the existence of a simple relationship between the pipe diameter (D) and the bed width (b) of the rigid bed rectangular channels.

Further analyses were made with different values of D as defined in terms of b. The results show that the best-fit lines of the predicted values of Fr_m approach the line of best agreement as the values of D get closer to the unity value of b. Figs. 6.37 and 6.38 compare the observed and predicted values of Fr_m for D = 1.5b. Better agreement is shown for rough bed data while the smooth bed results tend to scatter around the line of best agreement. An attempt was then made to improve the prediction

TABLE 6.29 RANGES OF PARAMETERS FOR RIGID BED RECTANGULAR CHANNELS

PARAMETER	MAYERLE (1988)	PEDROLI (1963)	NOVAK-NALLURI (1975)	LOVELESS (1991)	KITHSIRI (1990)
b (mm)	311.5 - 462.3	300.0 - 600.0	305.0	59.0 - 100.0	311.5
k_o (mm)	0.0 - 0.73	0.0	0.0	0.00	0.73 - 5.61
V (m/s)	0.411 - 1.042	0.437 - 2.147	0.560 - 0.710	0.240 - 0.660	0.463 - 0.925
d_{50} (mm)	0.50 - 8.74	1.10 - 11.10	0.15 - 2.04	0.45 - 1.30	0.99 - 8.40
S_s	2.49 - 2.61	2.70 - 2.72	2.56	2.65	2.62 - 2.63
Fr_*	1.79 - 11.28	1.68 - 13.74	3.19 - 14.71	1.65 - 7.26	1.50 - 5.44
b/y_o	2.94 - 12.49	1.28 - 28.17	3.35 - 4.69	0.76 - 8.33	2.68 - 7.00
d_{50}/D	0.0011 - 0.0281	0.0018 - 0.0185	0.0005 - 0.0067	0.0045 - 0.0220	0.0032 - 0.0270
D_{gr}	11.38 - 196.41	25.70 - 258.36	3.39 - 46.14	10.72 - 31.50	23.23 - 208.80
λ_s	0.0138 - 0.0483	0.0112 - 0.0513	0.0160 - 0.0222	0.0241 - 0.0929	0.0199 - 0.0698
C_v (ppm)	10 - 3034	16 - 13 860	182 - 394	170 - 1399	12 - 819
NO. OF DATA	273	204	6	25	166

6.1.3.4.3 Rigid Bed Rectangular Channels

It has been observed that, depending on the bed thickness and flow depth, the flows in a circular channel with flat beds will assume velocity and shear stress distributions close to that of a rectangular channel (El-Zaemey 1991, Alvarez 1990). Such conditions would occur for low bed thickness with large flow depth or large bed thickness with low flow depth. This suggests the possibility of extending the application of El-Zaemey's Eqn. 3.58 or Eqn. 6.37 to conditions in rigid bed rectangular channels. Also, Loveless (1991) has shown that the use of sewers with a rectangular cross section will result in milder slopes than those with a circular cross section. It is therefore decided to assess the applicability of El-Zaemey's Eqn. 3.58 or Eqn. 6.37 to conditions in rigid bed rectangular channels.

The form of Eqn. 6.37 suggests the possibility of its application to conditions in rigid bed rectangular channels provided that a suitable value of an "equivalent pipe diameter", D, can be found. As mentioned earlier, the parameter d_{50}/D in Eqns. 3.58 and 6.57 reflects the influence of the pipe diameter and particle size on the sediment movement in circular channels with flat rigid beds. It is therefore likely that a similar parameter (i.e. d_{50}/b) would be needed to characterize the influence of the bed width and sediment size on the sediment movement in rigid bed rectangular channels. It is then necessary to find a suitable relationship between the pipe diameter (D) and the bed width (b) of the rigid bed rectangular channels.

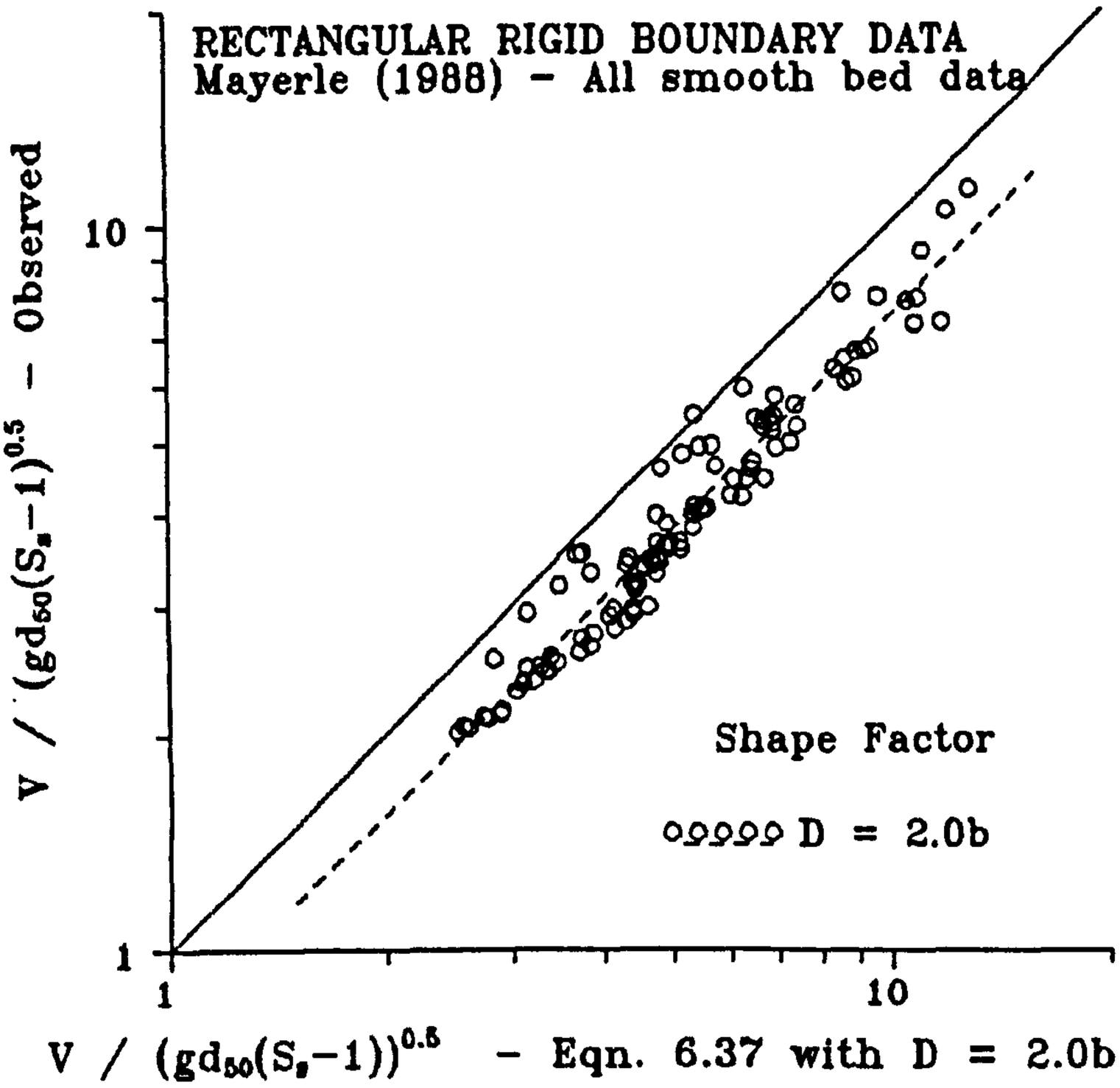

FIG. 6.35 Modification of El-Zaemey's Eqn. 6.37 for application to Mayerle's smooth rigid bed rectangular channels (D = 2.0b)

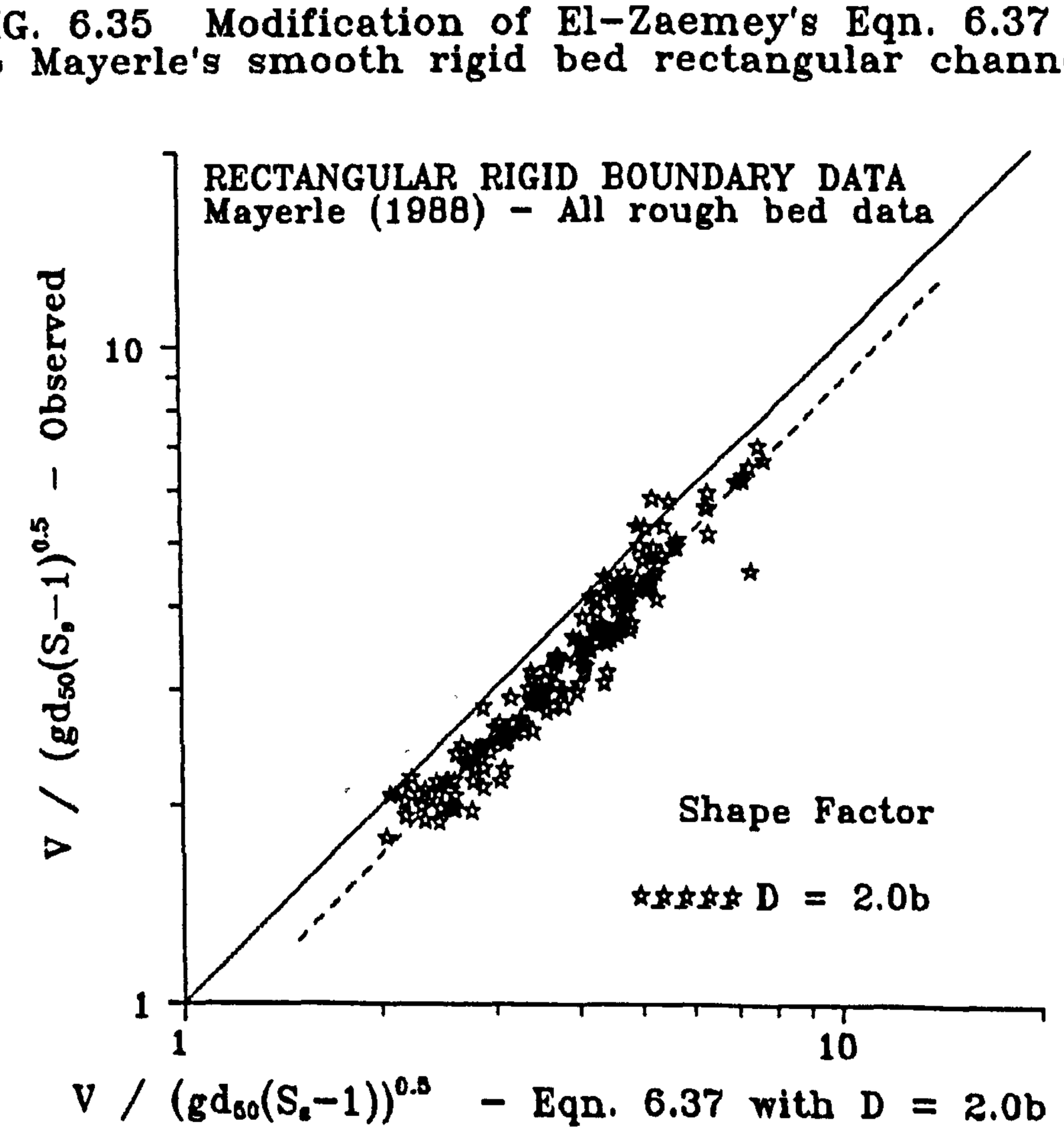

FIG. 6.36 Modification of El-Zaemey's Eqn. 6.37 for application to Mayerle's rough rigid bed rectangular channels (D = 2.0b)

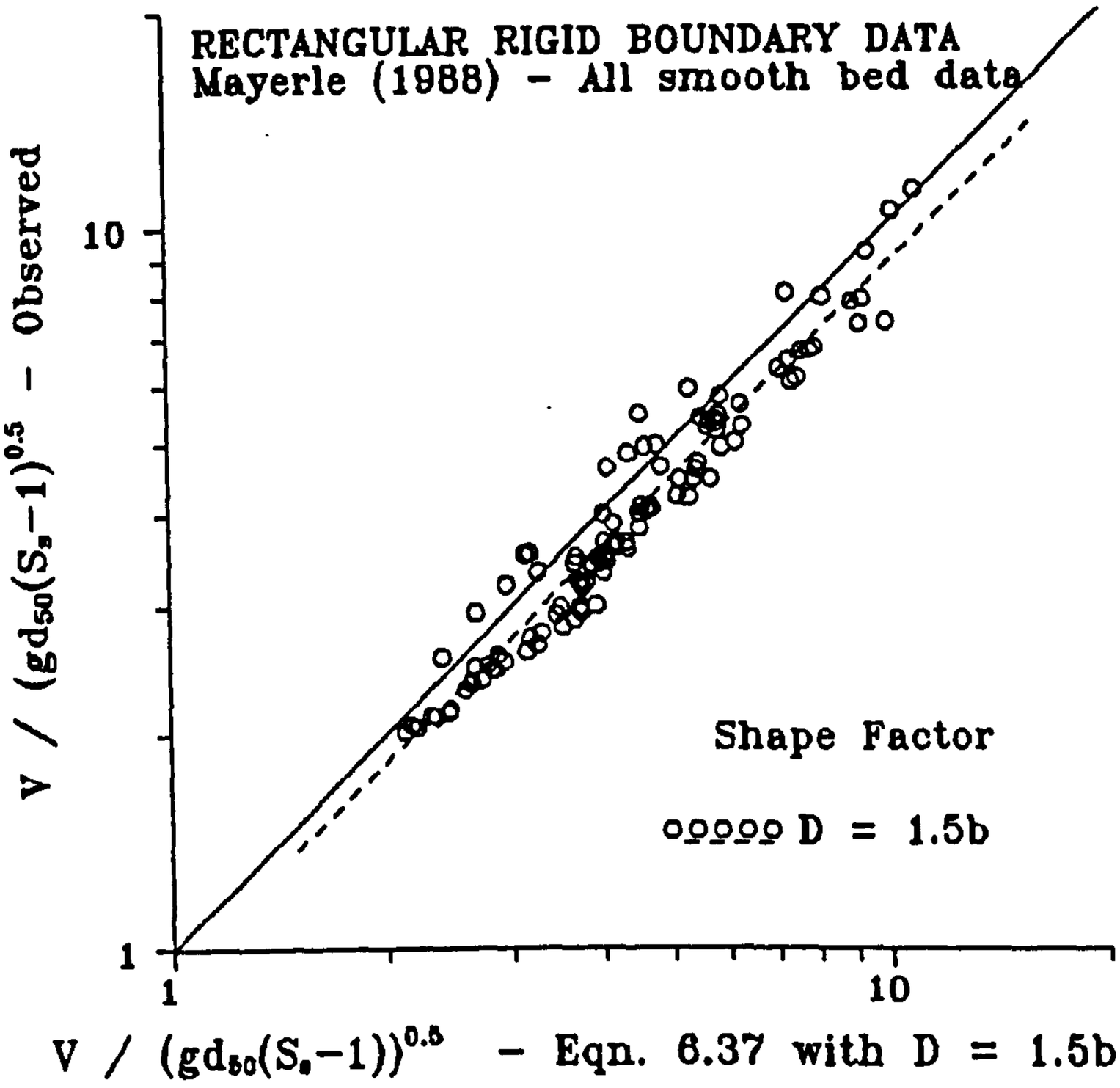

FIG. 6.37 Modification of El-Zaemey's Eqn. 6.37 for application to Mayerle's smooth rigid bed rectangular channels (D = 1.5b)

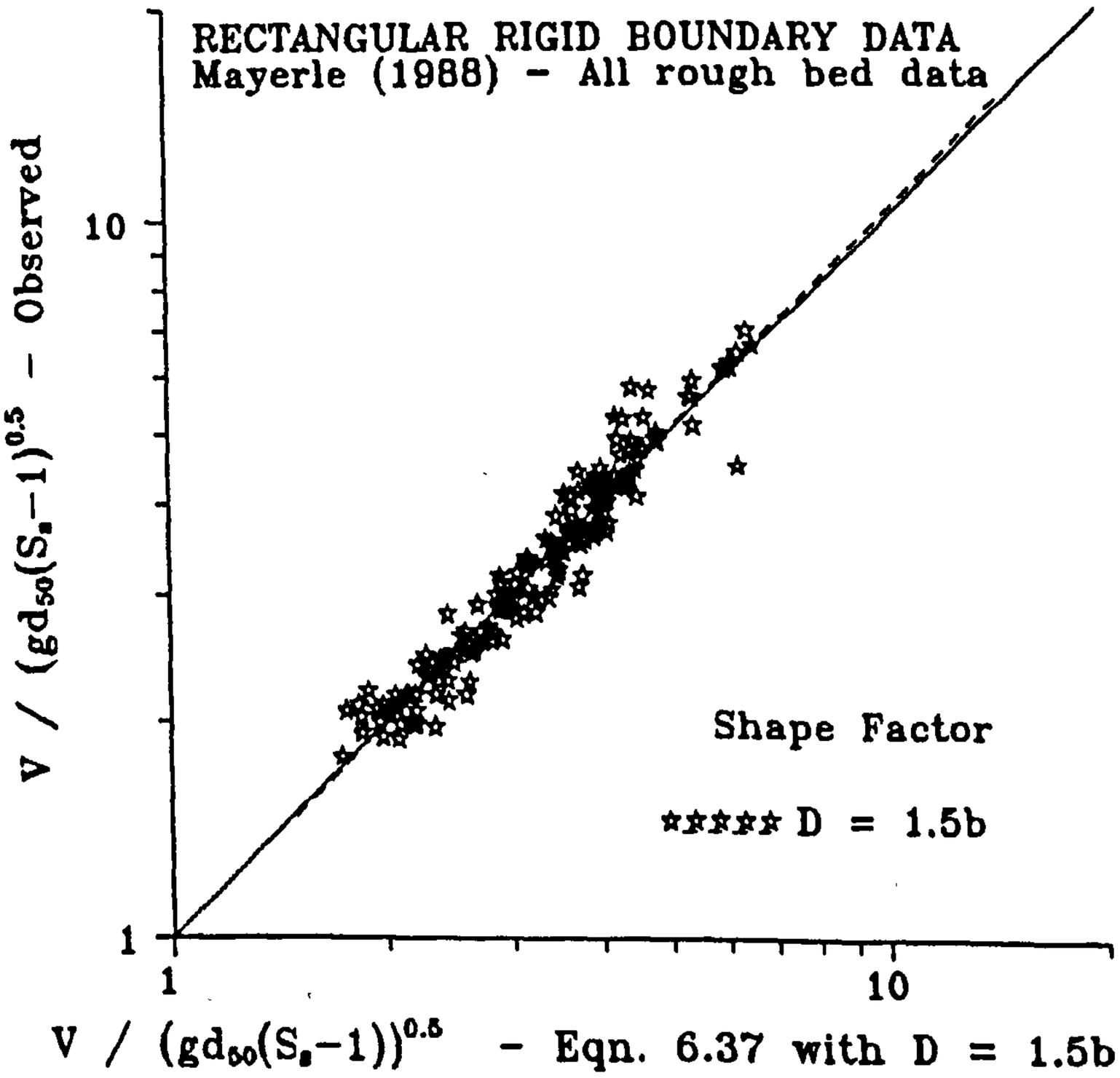

FIG. 6.38 Modification of El-Zaemey's Eqn. 6.37 for application to Mayerle's rough rigid bed rectangular channels (D = 1.5b)

of Fr_* for the smooth bed data while not compromising the good agreement obtained for the rough bed data. The results show that the substitution of D = 1.35 in Eqn. 6.37 yielded a good correlation for both smooth and rough bed data as shown in Figs. 6.39 and 6.40. The results shown in Figs. 6.39 and 6.40 have an average discrepancy ratio of 0.99 with 67% and 99% of the data falling within the ± 0.10 and ± 0.25 range of discrepancy ratios respectively (see Table 6.30). Eqn. 6.37 can then be re-written as:

$$\frac{V}{\sqrt{gd_{50}(S_s-1)}} = 2.30\, C_v^{0.165} \left(\frac{b}{y_o}\right)^{-0.40} \left(\frac{d_{50}}{b}\right)^{-0.57} \lambda_{sb}^{0.10} \qquad (6.40)$$

for its application to smooth and rough bed rectangular channels after substituting D = 1.35b.

Further verification of these modifications is shown in Figs. 6.41 and 6.42 (see Table 6.30) where independent data of Pedroli (1963), Novak-Nalluri (1975), Kithsiri (1990) and Loveless (1991) were utilised. The ranges of experimental data and relevant parameters are given in Table 6.29.

Fig. 6.41 compares the observed and predicted values of Fr_* using Eqn. 6.40 for other smooth rectangular channels' data (Pedroli 1963, Novak-Nalluri 1975, Loveless 1991). The results shown in Fig. 6.41 have a fairly good agreement (see Table 6.30) with the average discrepancy ratio varying from 0.97 to 1.16 where between 76% and 88% of the data for the different investigators fall

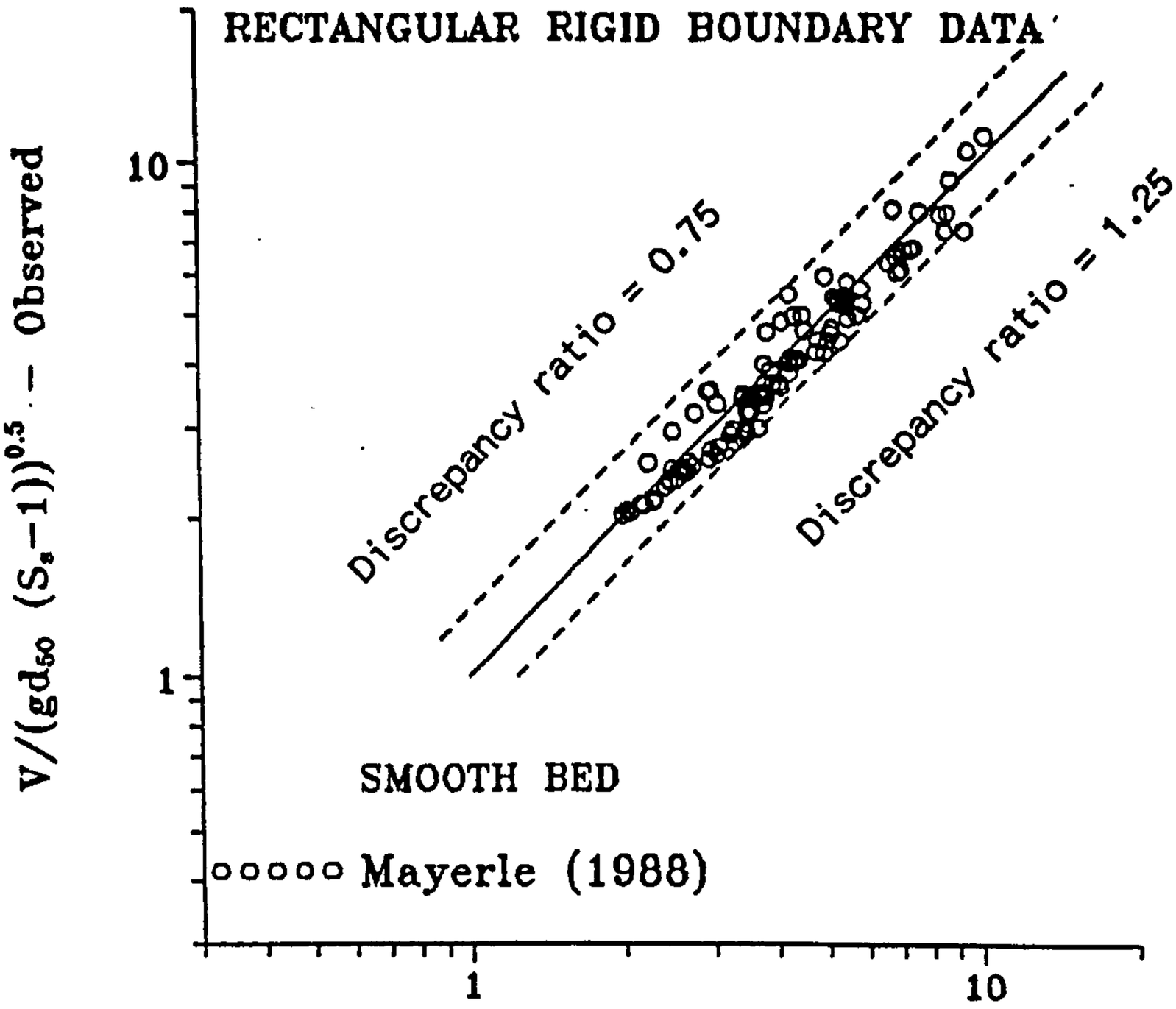

FIG. 6.39 Application of Eqn. 6.37 for Mayerle's smooth rectangular channel data (D = 1.35b)

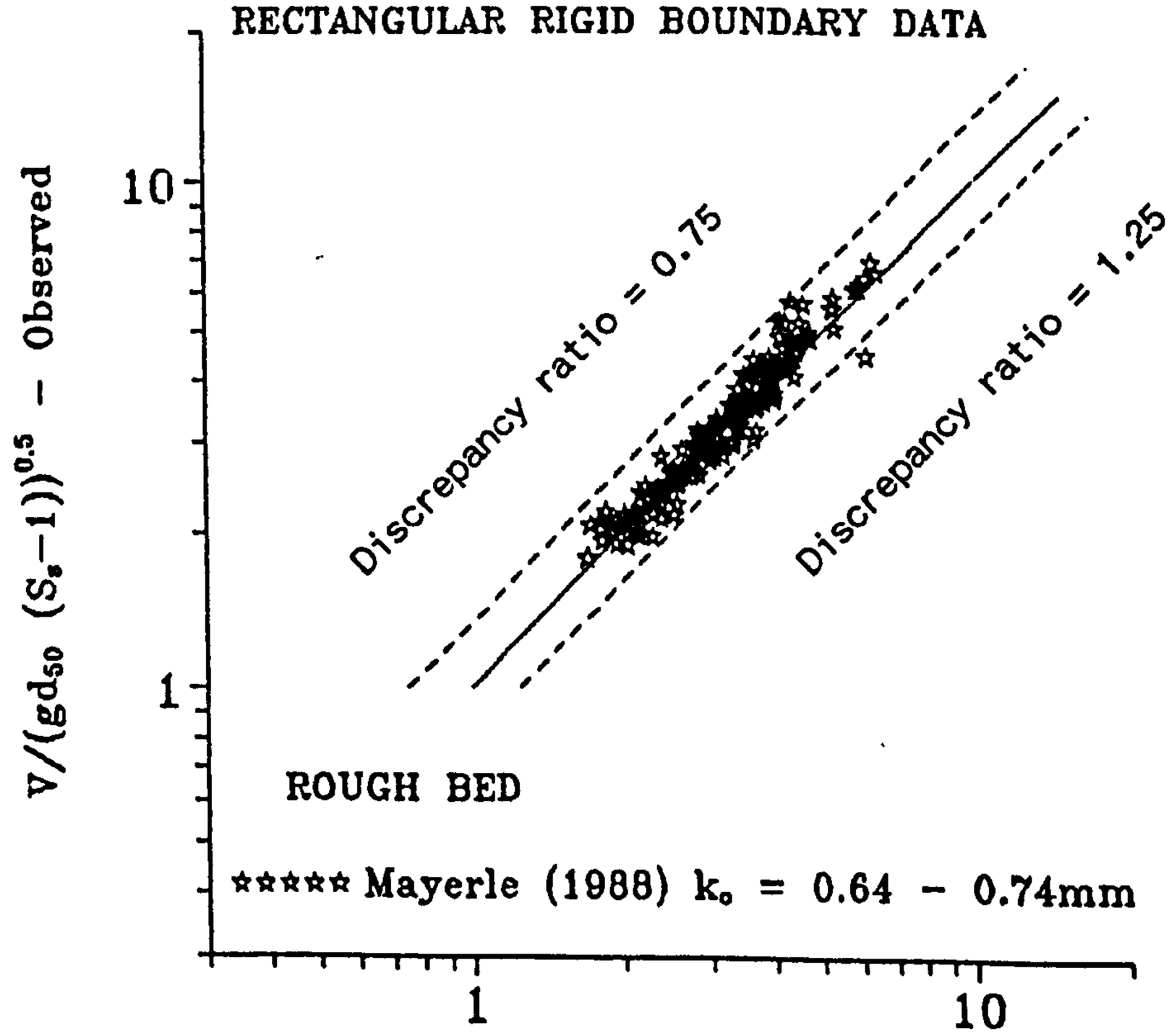

FIG. 6.40 Application of Eqn. 6.37 for Mayerle's rough rectangular channel data (D = 1.35b)

TABLE 6.30 DISCREPANCY RATIO (Fr_*) FOR EQN. 6.40 - COMBINED DATA (RIGID BED RECTANGULAR CHANNELS)

Source of data	Fr_* (predicted) / Fr_* (observed)							No. of data
	Mean	min	max	0.90-1.10 (%)	0.75-1.25 (%)	0.5-1.5 (%)	0.5-2.0 (%)	
Mayerle (1988)	0.99	0.72	1.31	67	99	100	100	273
Pedroli (1963)	0.97	0.72	1.34	50	88	100	100	204
Novak-Nalluri (1975)	1.13	1.01	1.28	50	83	100	100	6
Loveless (1991)	1.16	0.92	1.76	56	76	92	100	25
Kithsiri (1990)	0.92	0.53	1.52	55	86	99	100	166
Combined data	0.97	0.53	1.76	58	91	99	100	674

within the ± 0.25 deviation (see Table 6.30). The presence of scatter in the plot (Fig. 6.41) could be attributed to the different criteria used by each investigator to determine the limit of deposition. It should be noted that there is uncertainty in the criterion used by Pedroli (1963) as to whether the bed material was continuously moving or that some bed formations were allowed in his experiments (see Mayerle et al, 1991).

The verification of Eqn. 6.40 for other available rough bed data (Kithsiri, 1990) is shown in Fig. 6.42. The results show that a reasonable agreement (Table 6.30) is obtained with an average discrepancy ratio of 0.92 with 86% of the data lying within the ± 0.25 deviation. The best agreement is obtained for the data

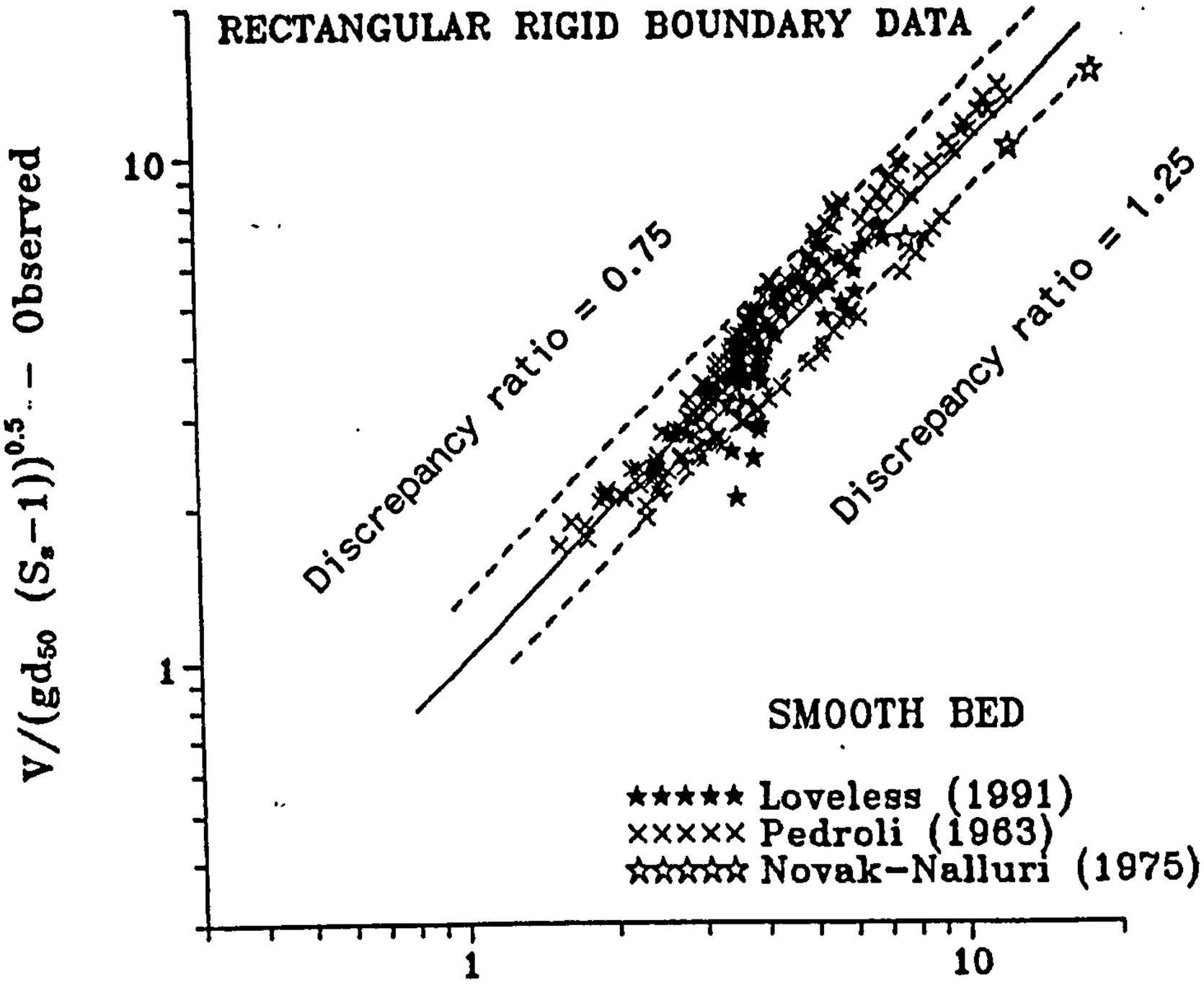

FIG. 6.41 Validity of Eqn. 6.37 for other smooth rectangular channels' data (D = 1.35b)

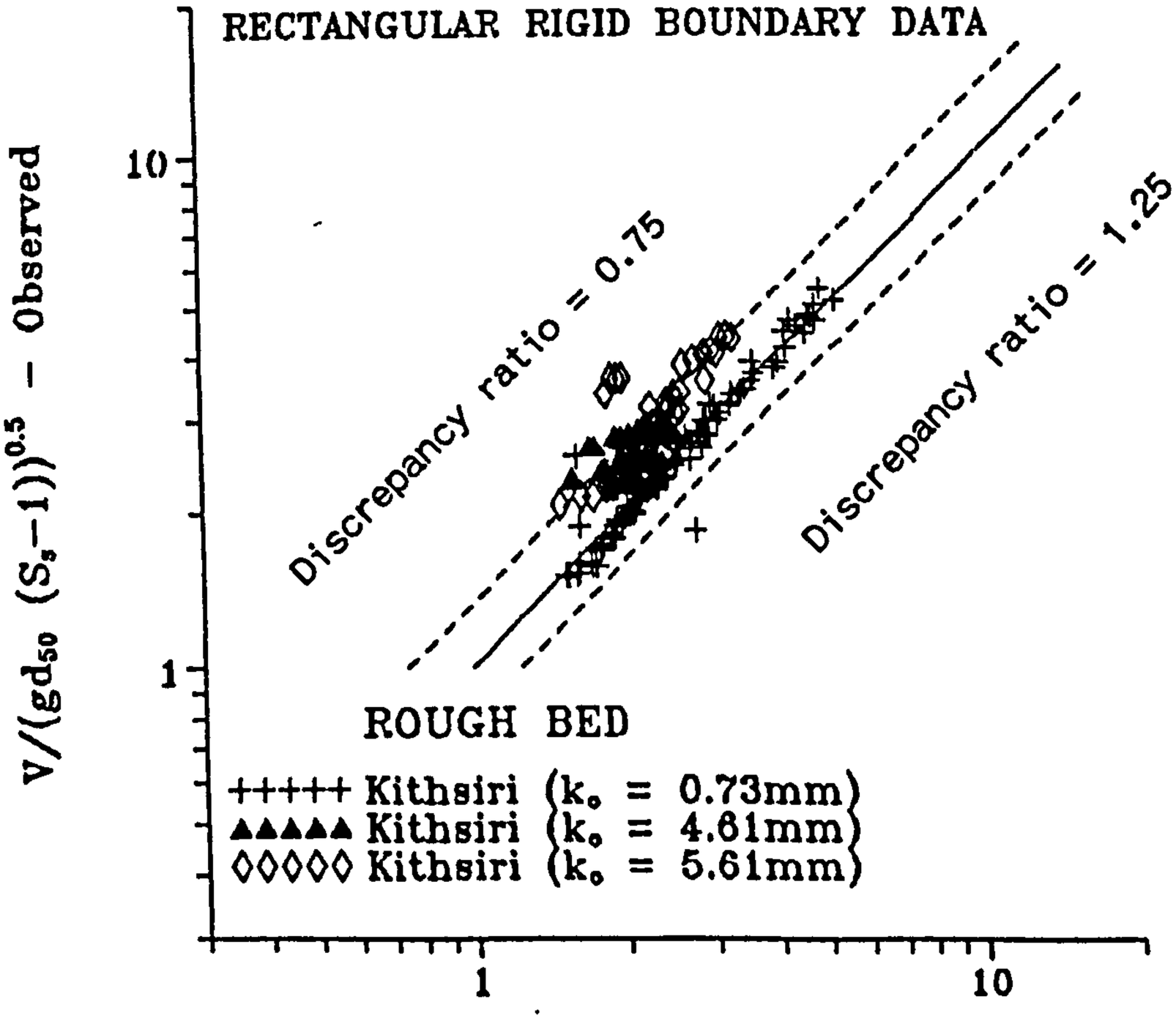

FIG. 6.42 Validity of Eqn. 6.37 for other rough rectangular channels' data (D = 1.35b)

with the smallest boundary roughness value (k_o = 0.73mm) as can be seen in Fig. 6.42. This could be explained by the similar range of conditions tested to that of Mayerle's. However, there appears to be an underprediction of the observed values of Fr_* for the data with the largest boundary roughness value (k_o = 5.61mm). It should be noted that the data collected for this bed roughness are doubtful due to the large physical boundary roughness element used in Kithsiri's experiments.

The applicability of Eqn. 6.40 over the range of particle size, flow depth, sediment concentration and velocity is as shown in Fig. 6.43. The corresponding values of the discrepancy ratios are listed in Table 6.31. All available data in rigid bed rectangular channels (Table 6.29) are used in this analysis.

Fig. 6.43a shows that the agreement is generally good over the range of particle sizes tested. The average discrepancy ratio varies from 0.93 to 1.03 with 86% - 99% of the data lying within the ± 0.25 range of discrepancy ratio.

Fig. 6.43b indicates that there is good agreement obtained for the whole range of aspect ratio. The average discrepancy ratio varies from 0.96 to 1.03 with over 87% of the data falling within the ± 0.25 deviations.

Fig. 6.43c reveals that the best agreement is obtained for the range of 101 < C_v (ppm) < 1000 where the average discrepancy ratio varies from 0.99 to 1.02 and over 92% of the data falling

within the ± 0.25 deviations. For C_v < 100ppm, the presence of Kithsiri's (1990) data where k_o = 5.61mm might have reduced the accuracy of the prediction. The average discrepancy ratio obtained is 0.95 with only 80% of the data lying within the ± 0.25 deviation. For C_v > 1000ppm, the uncertainty in the criterion used by Pedroli (1963) in the determination of the limit of deposition might explain the reduced accuracy with the average discrepancy ratio varying from 0.91 - 0.94 though almost all of the data falls within the ± 0.25 deviation.

Fig. 6.43d indicates that the agreement is reasonably good over the range of velocities of 0.50m/s - 0.80m/s where the average discrepancy ratio varies from 0.97 - 1.04 and over 91% of the data occurring within the ± 0.25 deviations. There appear to be systematic errors at the extremes. For V < 0.5m/s, the small particle sizes used by Loveless (1991) where D_{gr} < 50 might explain the overprediction obtained. For V > 0.8m/s, the presence of both Kithsiri's (1990) data where k_o = 5.61mm and Pedroli's (1963) data might account for the underprediction.

In general, Eqn. 6.40 provides a fairly good agreement over the range of sediments and flow conditions in rigid bed rectangular channels. This confirms the notional concept of substituting D = 1.35b in El-Zaemey's Eqn. 3.58 for its application to rigid bed rectangular channels.

An attempt was also made to evaluate the applicability of El-Zaemey's Eqn. 3.57 for the computation of the overall friction

TABLE 6.31 DISCREPANCY RATIO (Fr_*) FOR EQN. 6.40 AS FUNCTIONS OF RELEVANT PARAMETERS - COMBINED DATA (RIGID BED RECTANGULAR CHANNELS)

Range of parameter		Fr_* (predcited) / Fr_* (observed)							No of data
		Mean	min	max	0.90-1.10 (%)	0.75-1.25 (%)	0.50-1.50 (%)	0.5-2.0 (%)	
D_{gr}	3-25	1.03	0.83	1.31	63	97	98	100	86
	26-50	1.01	0.72	1.76	64	88	99	100	121
	51-100	0.97	0.53	1.52	56	86	100	100	184
	101-150	0.95	0.64	1.29	57	92	100	100	158
	151-200	0.94	0.69	1.12	58	99	100	100	81
	201-275	0.93	0.73	1.29	61	95	99	100	44
b/y_0	0-5.00	0.96	0.53	1.56	52	87	99	100	397
	5.01-10.0	0.99	0.72	1.76	63	98	100	100	228
	10.01-20.0	1.02	0.83	1.21	80	100	100	100	40
	20.01-30.00	1.03	0.94	1.17	78	100	100	100	9
C_v (ppm)	10-100	0.95	0.53	1.34	55	80	100	100	181
	101-500	1.02	0.72	1.41	62	94	99	100	276
	501-1000	0.99	0.75	1.76	46	92	100	100	37
	1001-2000	0.94	0.80	1.24	77	100	100	100	69
	> 2000	0.91	0.72	1.19	44	97	92	100	111
V (m/s)	0.200-0.500	1.12	0.82	1.76	54	81	100	100	37
	0.501-0.600	1.04	0.84	1.33	71	99	100	100	145
	0.601-0.700	1.03	0.81	1.34	75	95	100	100	126
	0.701-0.800	0.97	0.64	1.33	63	91	100	100	89
	0.801-0.900	0.89	0.55	1.31	45	85	100	100	108
	0.901-1.100	0.94	0.53	1.29	40	74	100	100	65
	1.101-2.500	0.87	0.72	0.99	43	98	100	100	104

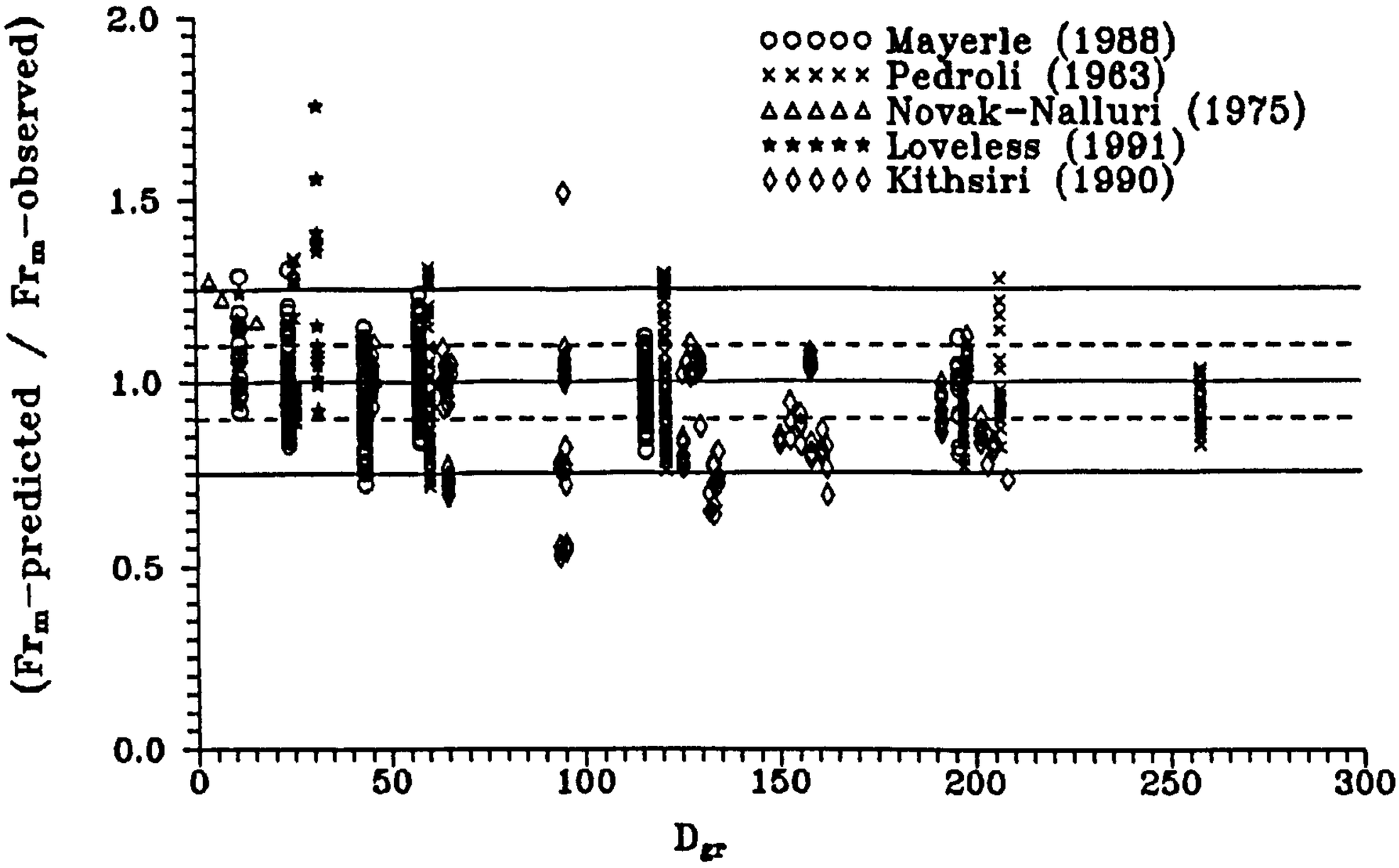

FIG. 6.43a Discrepancy ratio for El-Zaemey's Eqn. 6.37 with D = 1.35b or Eqn. 6.40 as a function of dimensionless particle size

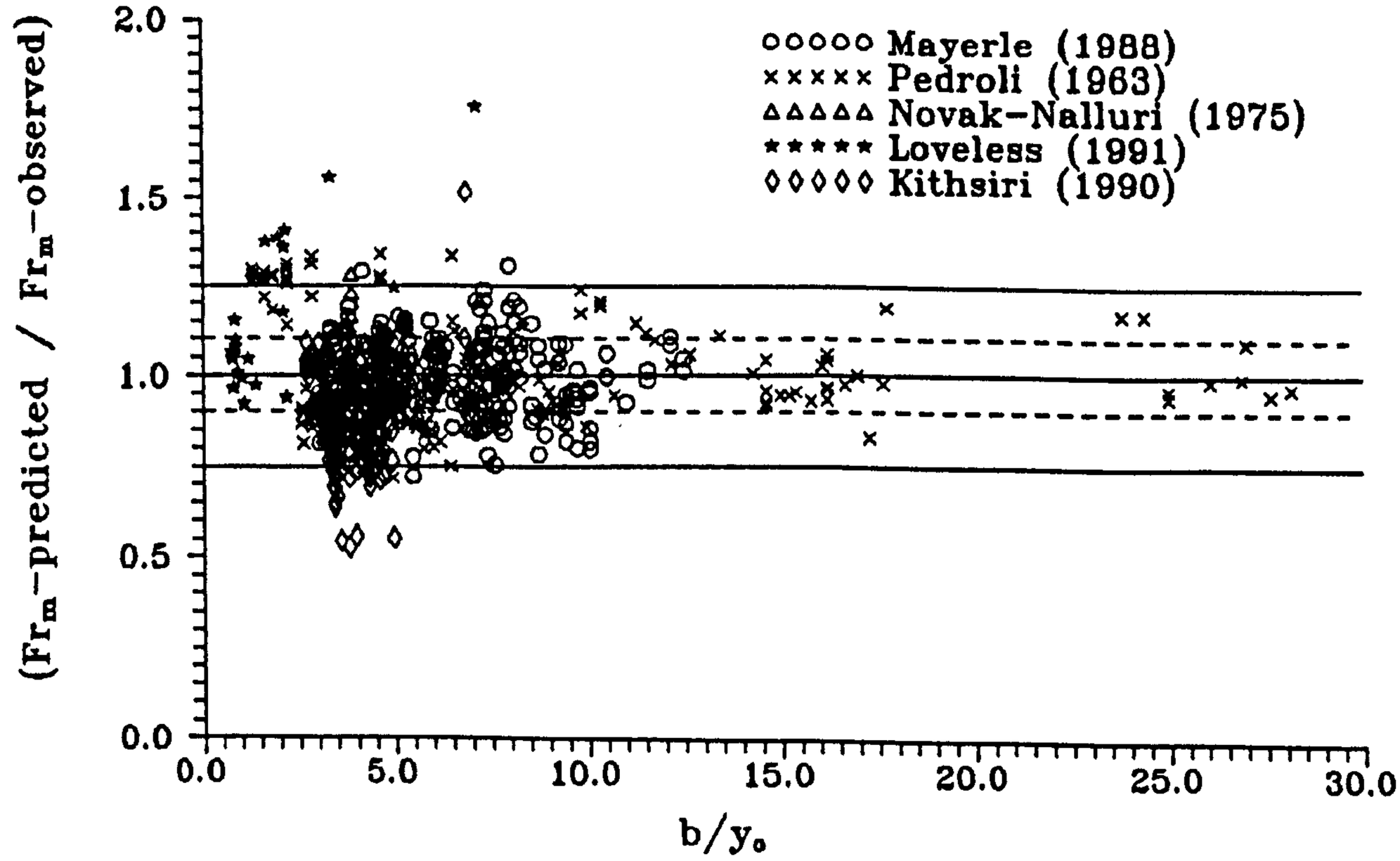

FIG. 6.43b Discrepancy ratio for El-Zaemey's Eqn. 6.37 with D = 1.35b or Eqn. 6.40 as a function of aspect ratio

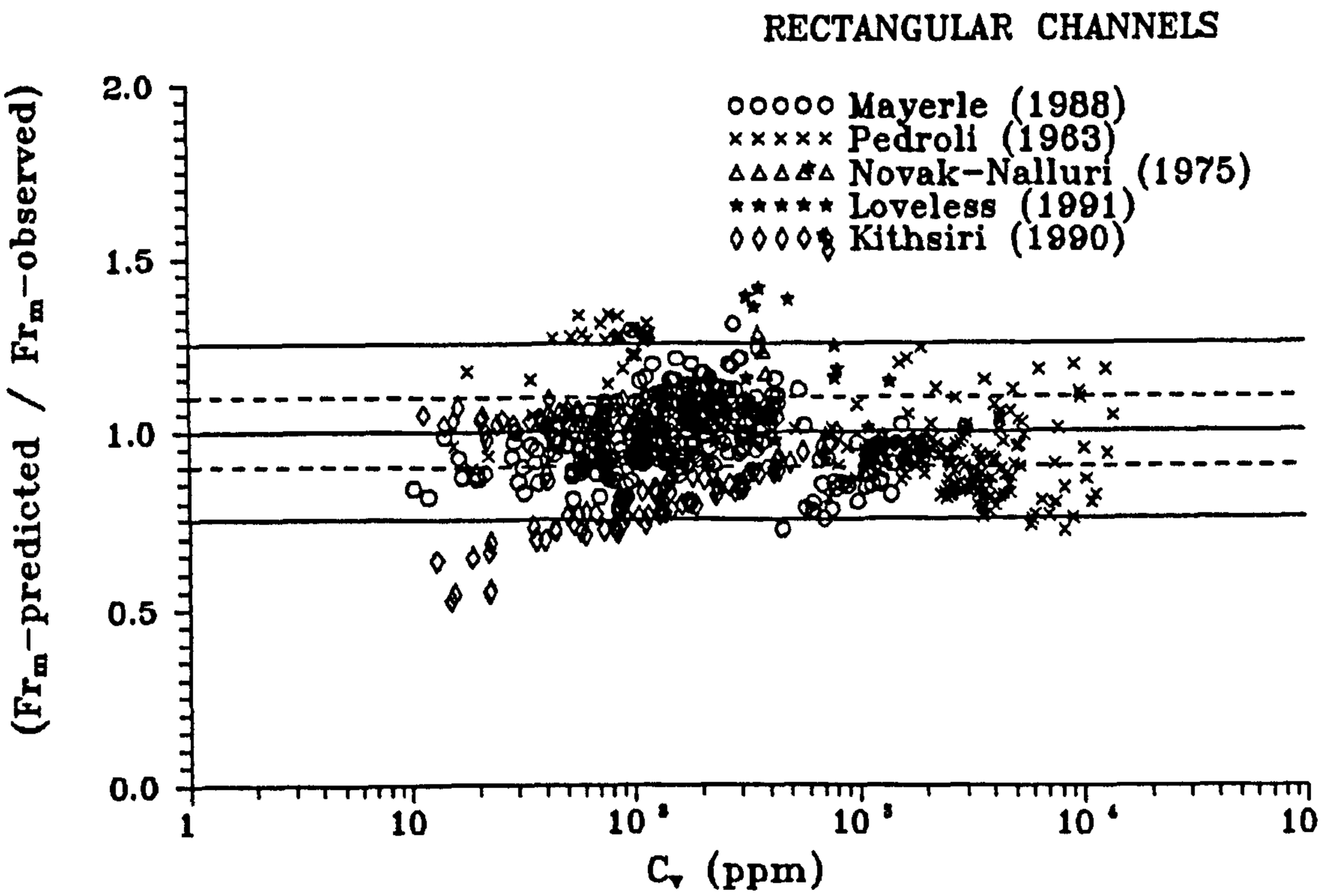

FIG. 6.43c Discrepancy ratio for El-Zaemey's Eqn. 6.37 with D = 1.35b or Eqn. 6.40 as a function of limiting concentration

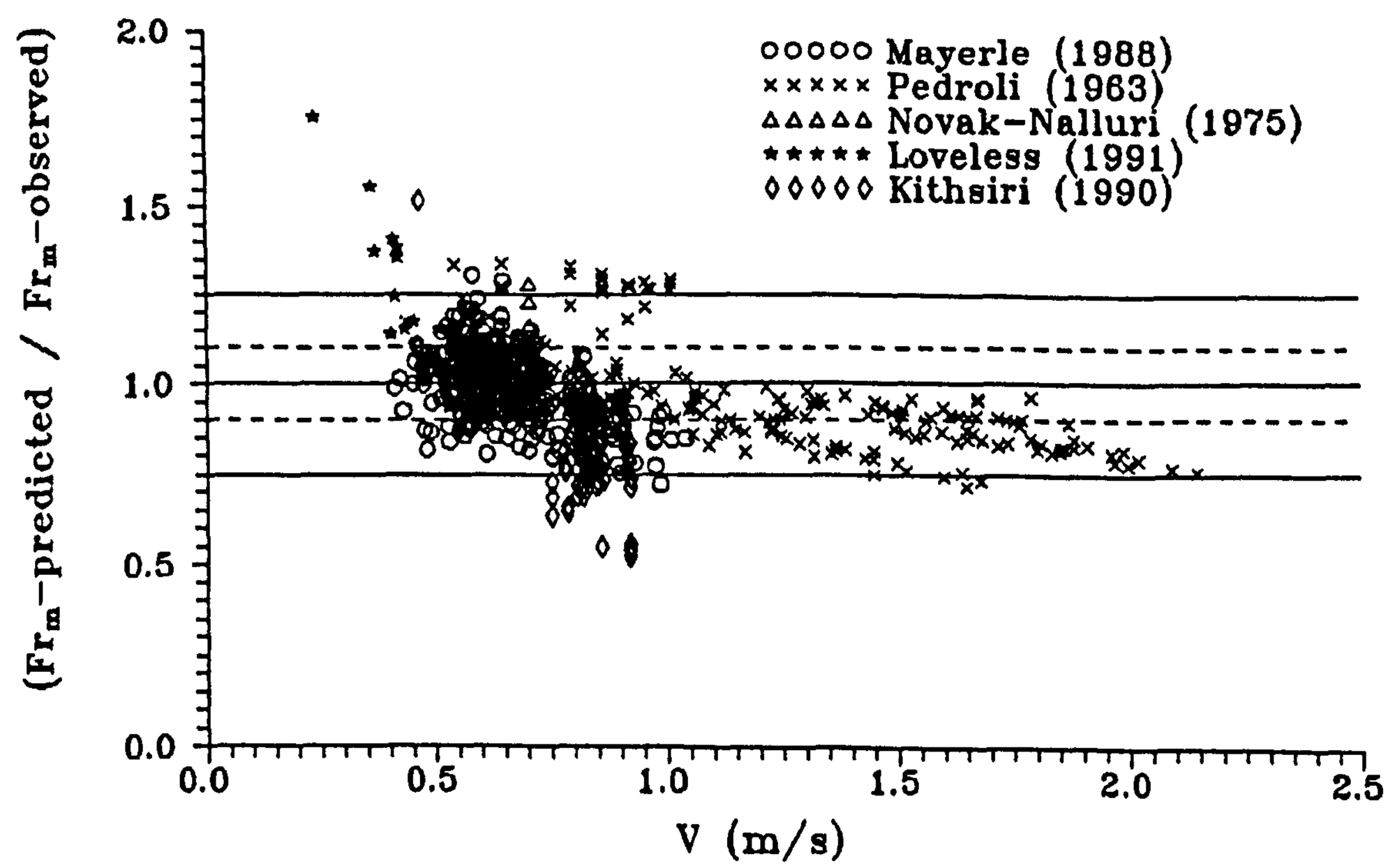

FIG. 6.43d Discrepancy ratio for El-Zaemey's Eqn. 6.37 with D = 1.35b or Eqn. 6.40 as a function of limiting velocity

factor with sediment (λ_s) for data from rigid bed rectangular channels. The format of Eqn. 3.57 suggests the possibility of its direct application to data from rigid bed rectangular channels. This possibility was tested using data of Mayerle (1988) and Kithsiri (1990). Other available data (Pedroli 1963, Novak-Nalluri 1975, Loveless 1991) however could not be used since they do not give any information on the clear water friction factor (λ_o). Fig. 6.44 shows that Eqn. 3.57 could be used satisfactorily (see Table 6.32) to compute λ_s for rectangular channels where the average discrepancy ratio is 0.95 and where 80% and 98% of the data lie within the ± 0.10 and ± 0.25 range of discrepancy ratios respectively.

TABLE 6.32 DISCREPANCY RATIO (λ_s) FOR EL-ZAEMEY'S EQN. 3.57 - COMBINED DATA (RIGID BED RECTANGULAR CHANNELS)

Source of data	λ_s (predicted) / λ_s (observed)							No. of data
	Mean	min	max	0.90-1.10 (%)	0.75-1.25 (%)	0.5-1.5 (%)	0.5-2.0 (%)	
Mayerle (1988)	0.94	0.69	1.13	74	98	100	100	273
Kithsiri (1990)	0.96	0.84	1.68	90	98	99	100	166
Combined	0.95	0.69	1.68	80	98	99	100	439

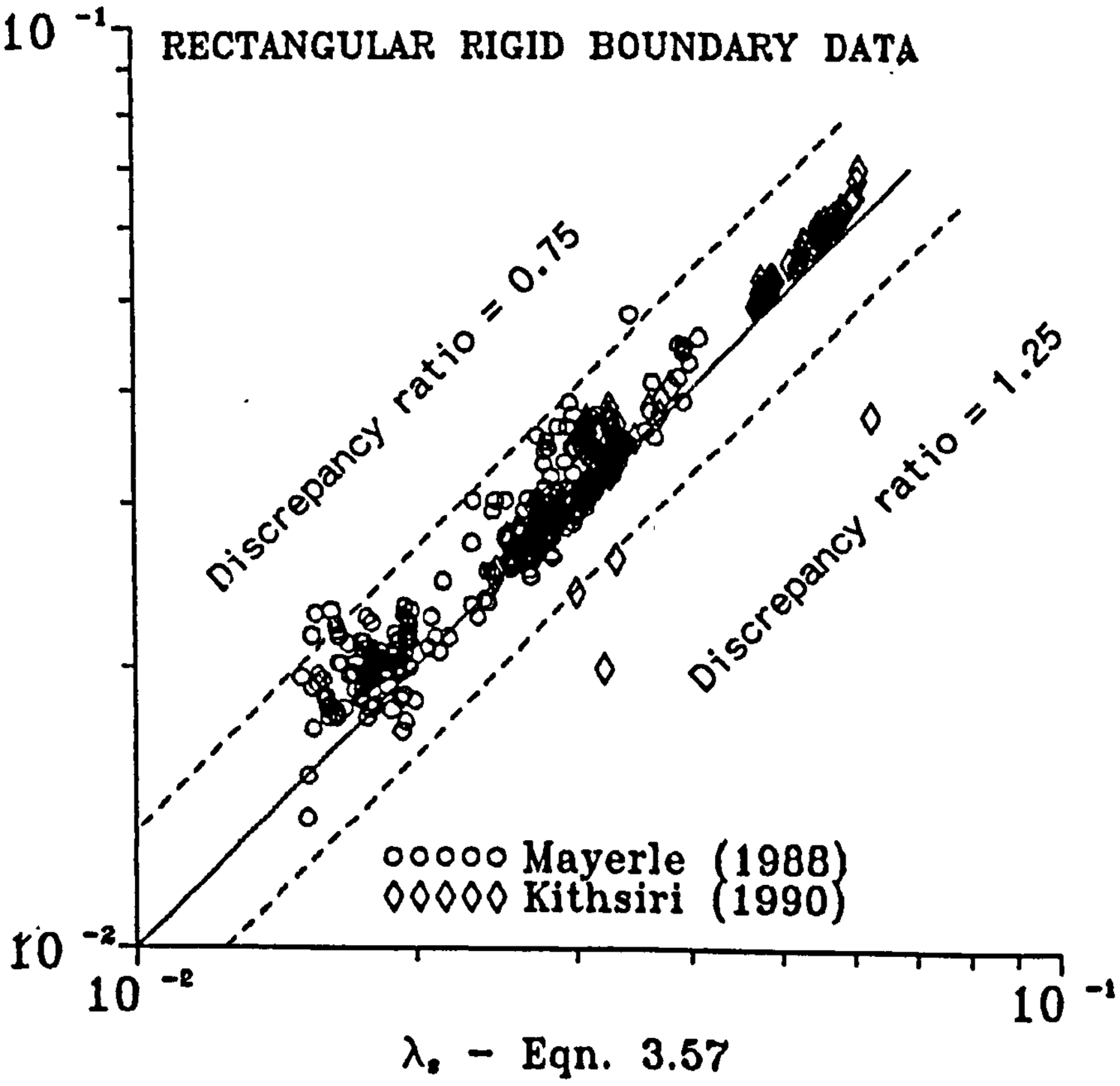

FIG. 6.44 Validity of Eqn. 3.57 for Mayerle and Kithsiri's rectangular channel data

6.2 Pipes with Deposited Beds

6.2.1 Background

The basic variables involved in the sediment transport process in sewers with deposited beds are the same as those in clean pipes (Section 6.1.1) with the addition of the bed formations. An important variable due to the presence of loose beds will be the width of the bed, W_b. El-Zaemey (1991) has shown the importance of the width (b) of the consolidated or cemented beds in sewers in determining the transporting capacity of the flow.

It must be noted that the presence of loose beds in sewers depends largely on the supply rate of sediment from the catchment of the sewerage systems. This supply rate could determine whether the formation of beds will either be dunes over continuous beds (henceforth called "continuous dunes") or trains of dunes with clean inverts between them (henceforth called "separated dunes"). The type of bed will in turn determine the effective flow resistance.

In the present studies limited data was obtained in the 450mm dia. pipe using a 0.72mm sand with the proportional sediment bed thickness (y_s/D) varying from 0.0002 to 0.23 (see Table 5.2c). These data were initially used to assess the applicability of several transport relationships for alluvial channels and also the recent equations for sewers with deposited beds (May 1993, Perrusquia 1992). As in the case of clean pipe channels, using the present and other available data in pipes with deposited

beds, multiple regression analyses were applied to several of the functions to obtain new and improved relationships.

6.2.2 Appraisals of Existing Equations

In this comparison, the volumetric sediment concentrations computed using the chosen equations were compared with the measured values obtained in the present studies. It should be noted that a proportion of the data from author's earlier work (Ab. Ghani, 1990) were also used in the comparison. The remaining data (Ab. Ghani, 1990) were omitted due to the uncertainty in the measured slopes of the water surface as explained in Section 5.3.7.

As in the case of clean pipe channels (Section 6.1.2), the overall performance of each equation is presented graphically in a plot of the observed concentrations against the computed values. Also, the discrepancy ratio in terms of C_v is plotted as a function of the proportional sediment bed depth (y_s/D). This is to highlight the applicability of the equations over the range of y_s/D studied. As mentioned in Section 5.3.6, the mean sediment thickness obtained by averaging the volume of sands over the measured section was used throughout in the analysis presented here.

The chosen alluvial channel equations were Graf-Acaroglu's Eqn. 3.63 and Ackers's (1991) Eqn. 3.29. It should be mentioned that

Graf-Acaroglu's Eqn. 3.63 also contains the loose bed data for pipe-full conditions in its derivation. This equation was chosen because it is simple to use and also to represent the commonly used form of equation for transport in alluvial channels (see Graf 1984, Raudkivi 1990). On the other hand, Ackers's (1991) Eqn. 3.29 has been shown to give promising results when applied to limited data from pipes with deposited beds (May 1993, Kleijwegt 1992).

The selected equations based on the recent experimental studies in pipes with deposited beds were Perrusquia's Eqn. 3.55 and May's Eqn. 3.46.

In the comparisons, the present data have been sorted according to the bed types, namely separated dunes and continuous dunes. The results of the comparisons are given in Table 6.33 and plotted on Figs. 6.45 - 6.50.

The Graf-Acaroglu's Eqn. 3.63 in Fig. 6.45a shows a fairly reasonable fit to the experimental data with a mean discrepancy ratio of 1.90. 51% of the data fall within the 0.5 - 2.0 range of discrepancy ratio, while 19% and 24% of the data are within the ± 0.10 and ± 0.25 range, respectively. An overprediction is obtained for y_s/D < 1% while majority of the data for y_s/D > 5% are in the 0.5 - 2.0 range of discrepancy ratio as can be seen in Fig. 6.45b. An examination of the data for y_s/D = 5% and 12% shows that better agreement (Fig. 6.45b) is obtained for overall flow depth at half-full (Y/D = 0.5). The results suggest the

TABLE 6.33 DISCREPANCY RATIO (C_v) FOR DIFFERENT EQUATIONS - ALL PRESENT DATA (PIPES WITH DEPOSITED BEDS)

Equations	C_v (predicted) / C_v (observed)							No. of data
	Mean	min	max	0.9-1.1 (%)	0.75-1.25 (%)	0.5-1.5 (%)	0.5-2.0 (%)	
Graf-Acaroglu (Eqn. 3.63)	1.90	0.46	4.95	19	24	41	51	37
Ackers[1] (Eqn. 3.29)	1.77	0.55	6.02	1	22	49	86	37
Ackers[2] (Eqn. 3.29)	0.89	0.36	1.91	16	59	86	92	37
May (Eqn.3.46)	1.36	0.37	3.42	24	38	73	78	37
Perrusquia[3] (Eqn. 3.55)	22.00	1.19	153.7	0	1	11	11	27
Perrusquia[4] (Eqn. 3.55)	3.29	0.56	15.20	0	14	14	51	37

NOTE:

(1) Used overall flow discharge (Q) in the computation of C_v

(2) Used effective flow discharge (Q_{eff}) in the computation of C_v

(3) Utilised bed friction factor (λ_{sb})

(4) Utilised overall frction factor (λ_s)

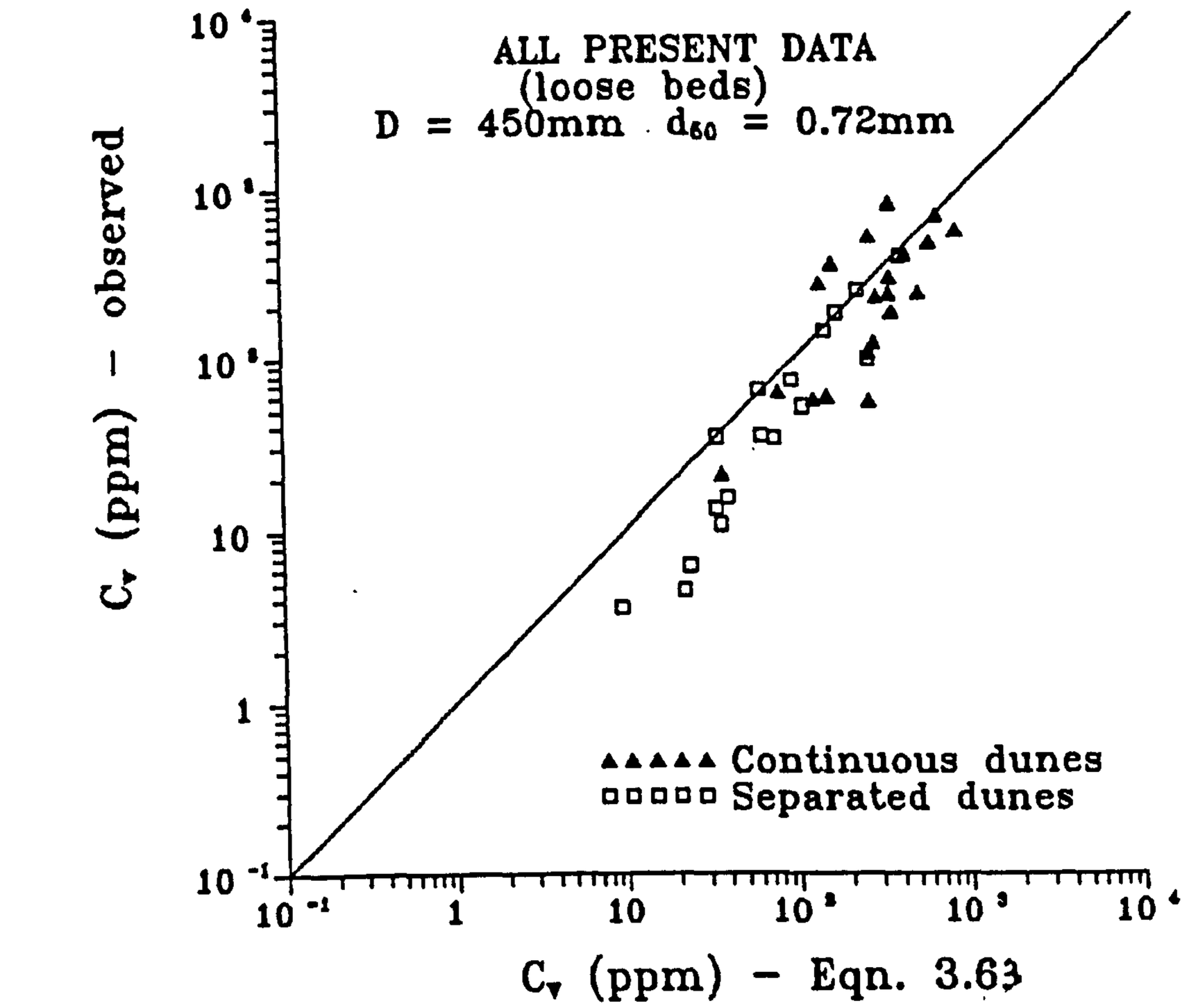

FIG. 6.45a Predicted C_v using Graf–Acaroglu's Eqn. 3.63

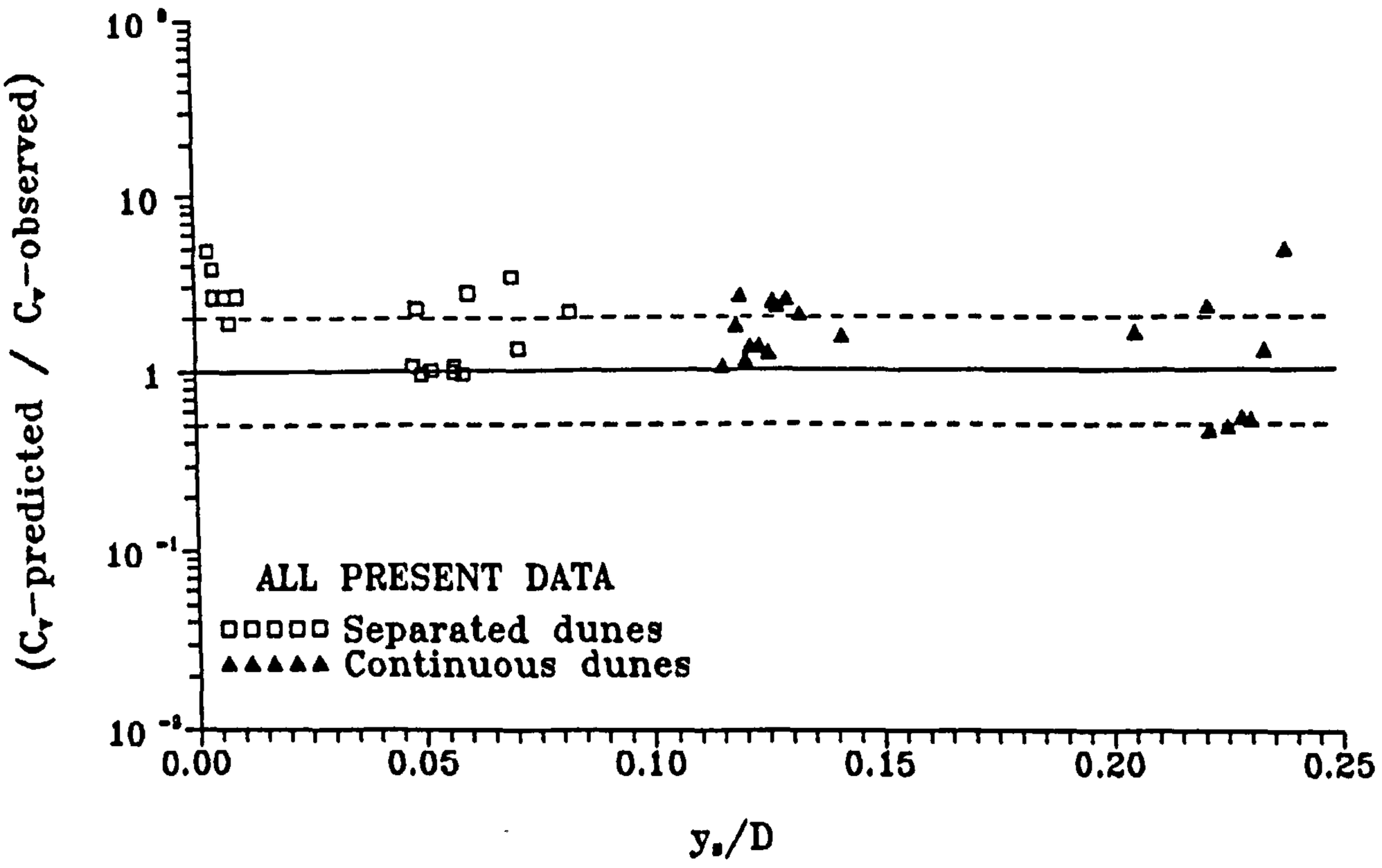

FIG. 6.45b Discrepancy ratio for Graf–Acaroglu's Eqn. 3.63 as a function of proportional sediment depth

possibility of using the Φ - Ψ form for further analysis (see Section 6.2.3.1).

Fig. 6.46a compares the observed and computed sediment concentrations for Ackers' Eqn. 3.29. In applying Eqn. 3.29 to the author's data, the Ackers's suggestion of using $W_e = 0.04D$ was applied for $y_o/D < 1\%$ while the actual widths of sediment bed (W_b) were used for $y_o/D > 1\%$. The results are generally quite good as is evidenced by Figs. 6.44a and 6.44b. Overall, the average discrepancy ratio for Ackers' Eqn. 3.29 is 1.77 with 86% of the data lying within the 0.50 - 2.0 range of discrepancy ratio. However, it should be noted that only 1% of the data falls within the ± 0.10 deviation (see Table 6.33) while 22% of the data occurs within the ± 0.25 deviation. An examination of the data shows that the predictions are equally well for both flow depths tested (Y/D = 0.50, 0.75).

Since Ackers's Eqn. 3.29 was originally derived for wide (rectangular) alluvial channels, an attempt was made to recompute the observed values of the volumetric sediment concentration (C_v) assuming that the pipe with sediment beds acts as a rectangular alluvial channel with the bed width of W_b. An effective flow discharge (Q_{eff}) is defined as the product of the mean flow velocity (V) and the effective flow area, A_{eff} (= W_b * y_o). The observed C_v is now given as the ratio of the volumetric sediment discharge (Q_s) to the effective flow discharge: $C_v = Q_s / Q_{eff}$. The main assumption is that the mean flow velocity remains the same over the actual flow area (A). Figs. 6.47a and 6.47b show

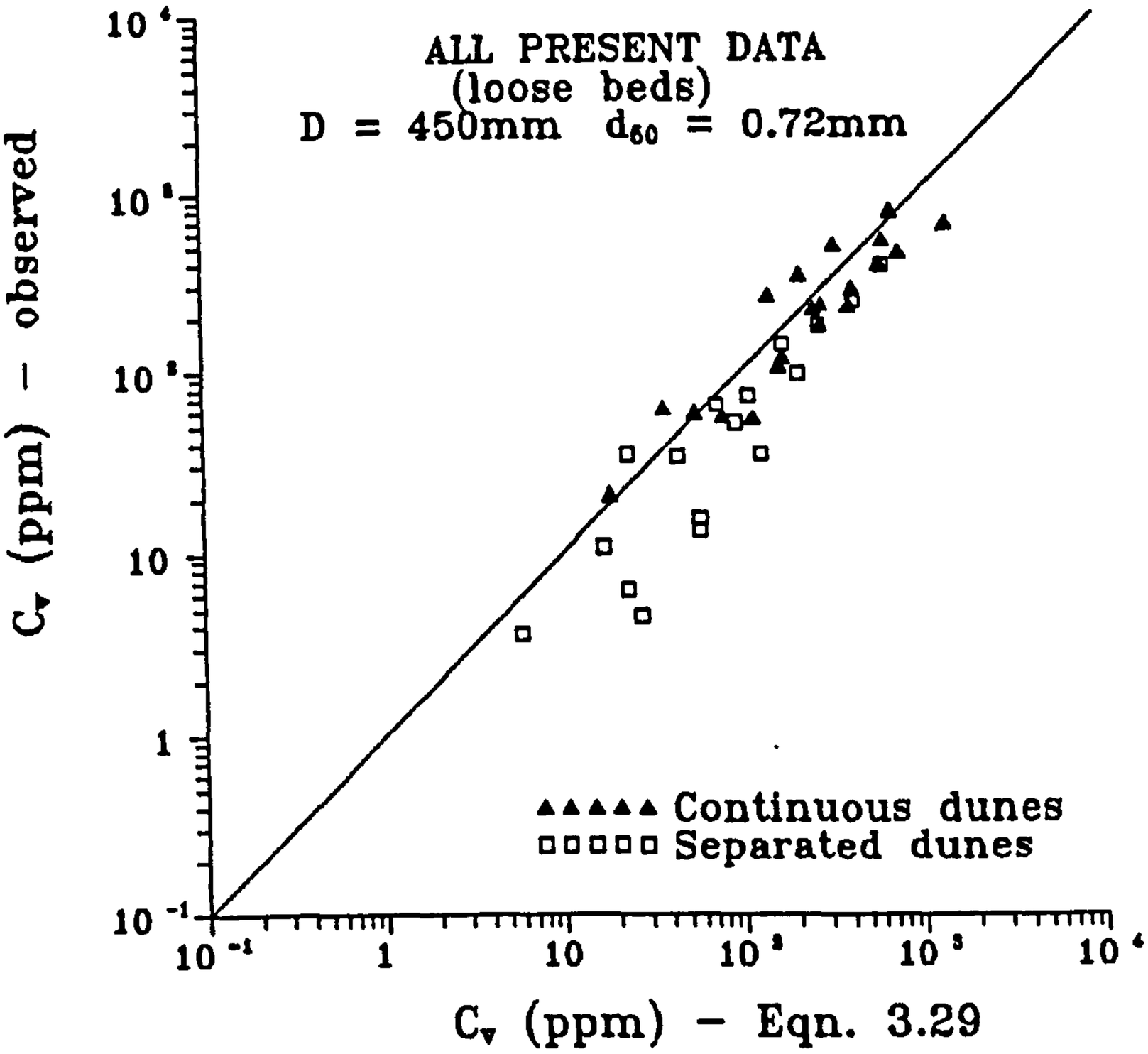

FIG. 6.46a Predicted C_v using Ackers' Eqn. 3.29

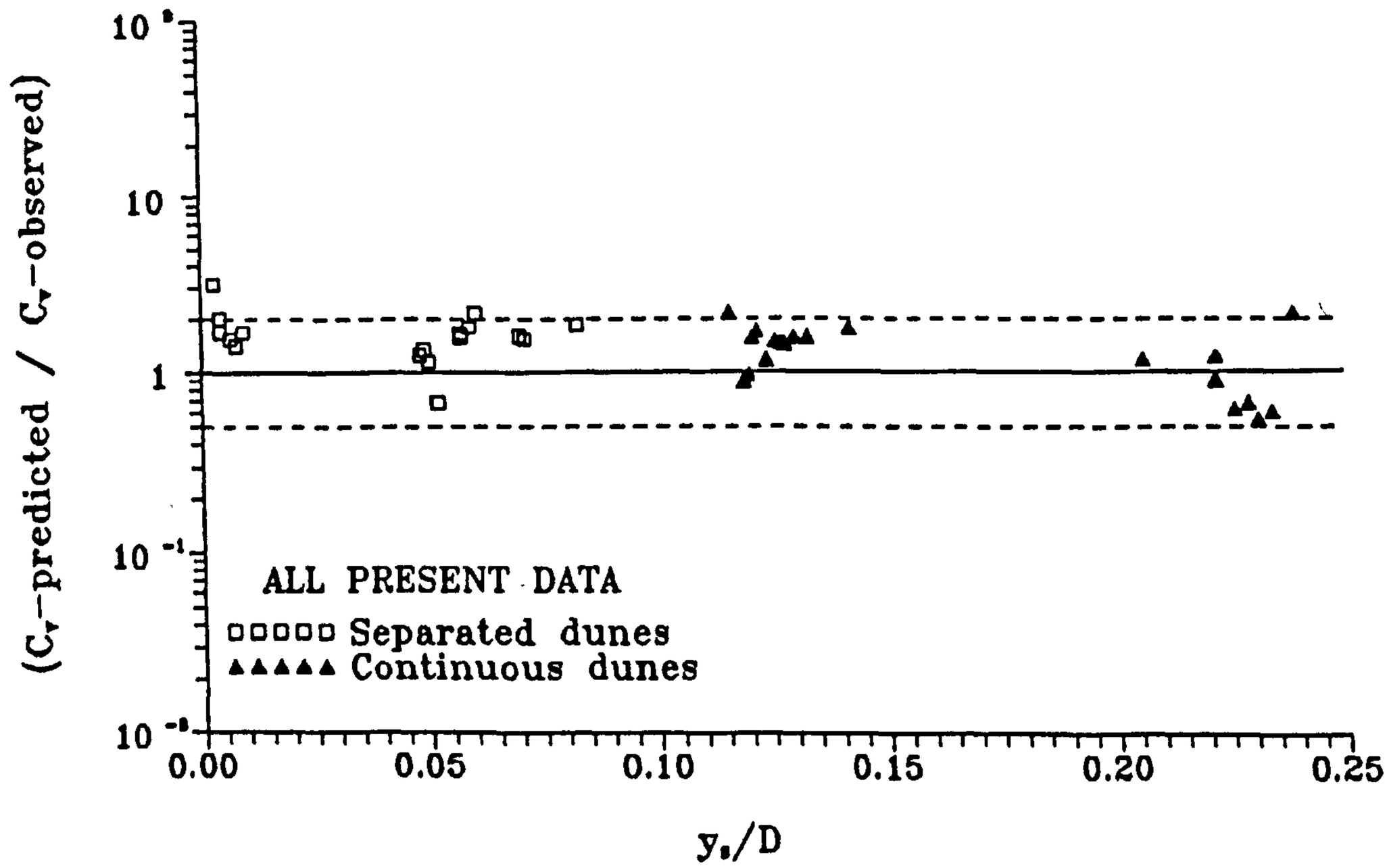

FIG. 6.46b Discrepancy ratio for Ackers' Eqn. 3.29 as a function of proportional sediment depth

that an improved result would be obtained with an average discrepancy ratio of 0.90. 92% of the data fall within the 0.5 - 2.0 range of discrepancy ratio, while 16% and 59% of the data are within ± 0.10 and ± 0.25 range of discrepancy ratio, respectively. The results imply that Ackers' Eqn. 3.29 actually predicts the volumetric concentration over the "idealized" rectangular alluvial channel.

May's Eqn. 3.46 in Fig. 6.48a gives promising results with an average discrepancy ratio of 1.36. 78% of the data fall within the 0.5 - 2.0 range of discrepancy ratio, while 24% and 38% of the data lie within the ± 0.10 and ± 0.25 range of discrepancy ratio, respectively. It should be noted that May's (1993) data in the 450mm dia. pipe were collected for y_s/D = 18% - 23%. Fig. 6.48b shows that Eqn. 3.46 applies equally well for y_s/D = 5% - 12% as studied by the author. May also suggested that for the case of separated dunes, the mean bed thickness (y_s) should be computed assuming that the total volume of sediment bed is spread only over the length of pipes covered by the dunes instead of over the length of the measurement section including the clean invert. It should be noted that for the author's data of y_s/D = 5%, the sediments were observed to move as separated dunes. The good agreement obtained by May's Eqn. 3.46 for this bed thickness suggests that the form of the equation rather than the definition of y_s will affect the accuracy of the prediction.

The comparison between the observed and computed sediment concentrations for Perrusquia's Eqn. 3.55 is shown in Fig. 6.49.

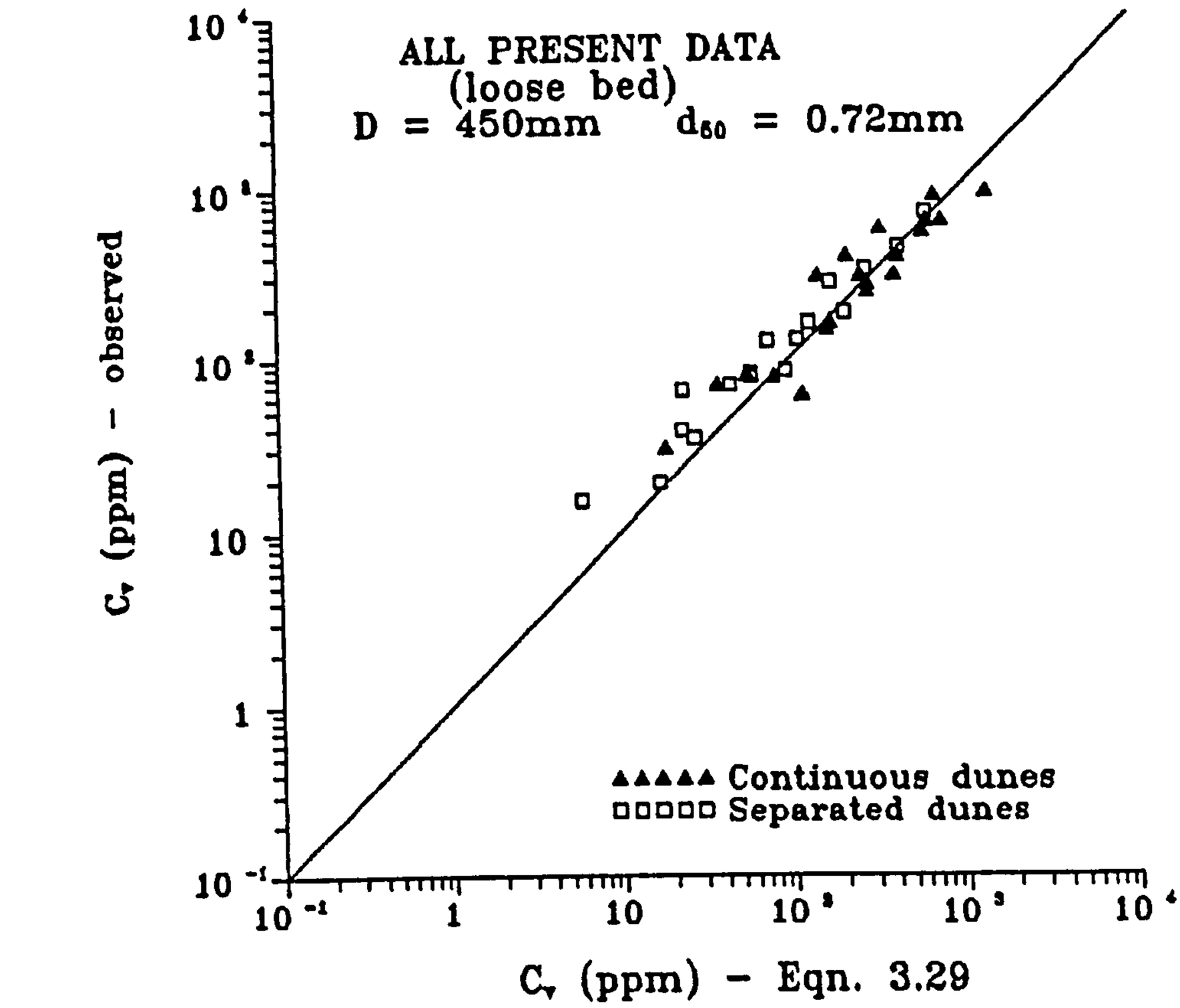

FIG. 6.47a Predicted C_v using Ackers' Eqn. 3.29 with observed C_v computed from effective discharge

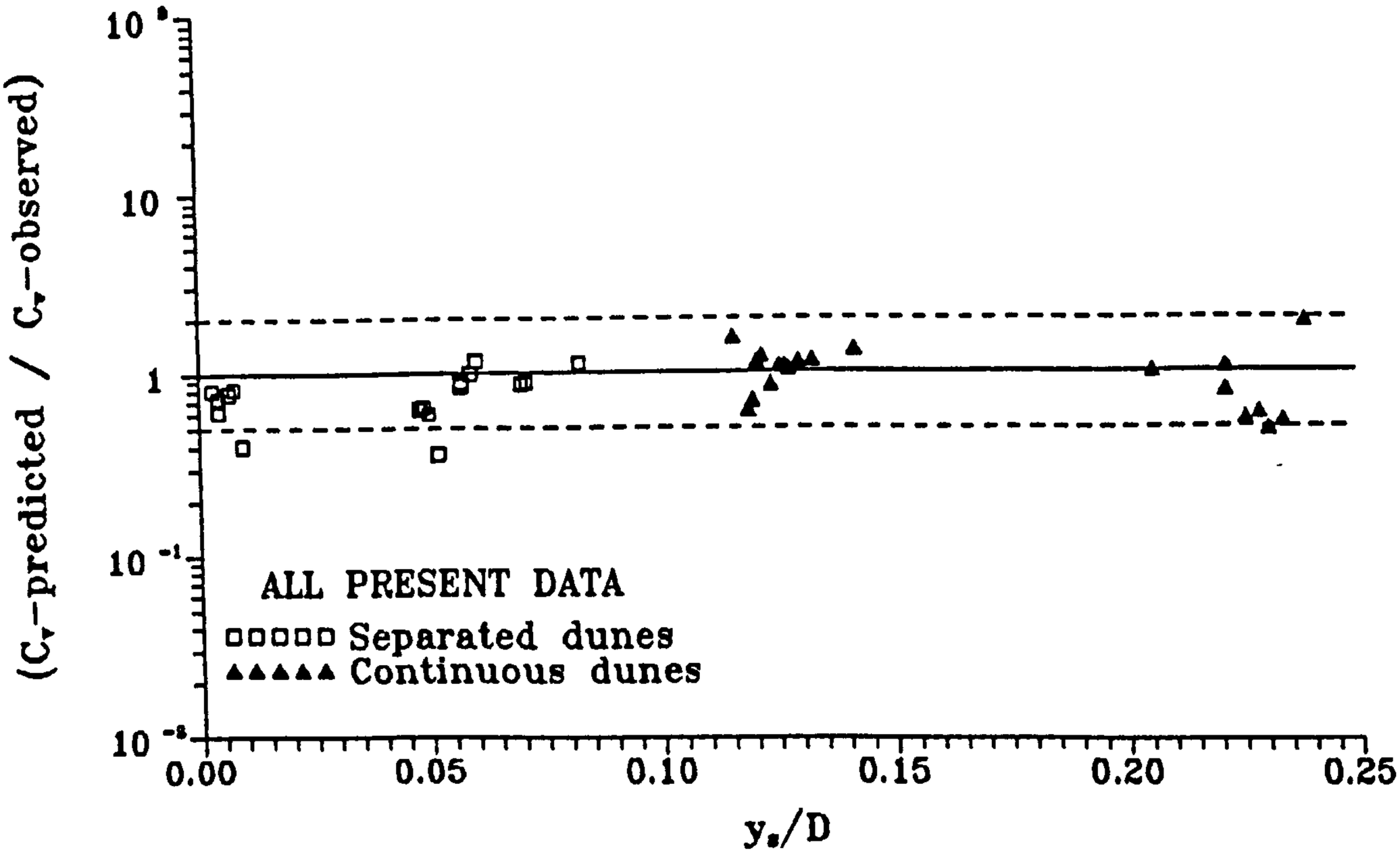

FIG. 6.47b Discrepancy ratio for Ackers' Eqn. 3.29, with observed concentrations computed using an effective flow discharge, as a function of proportional sediment depth

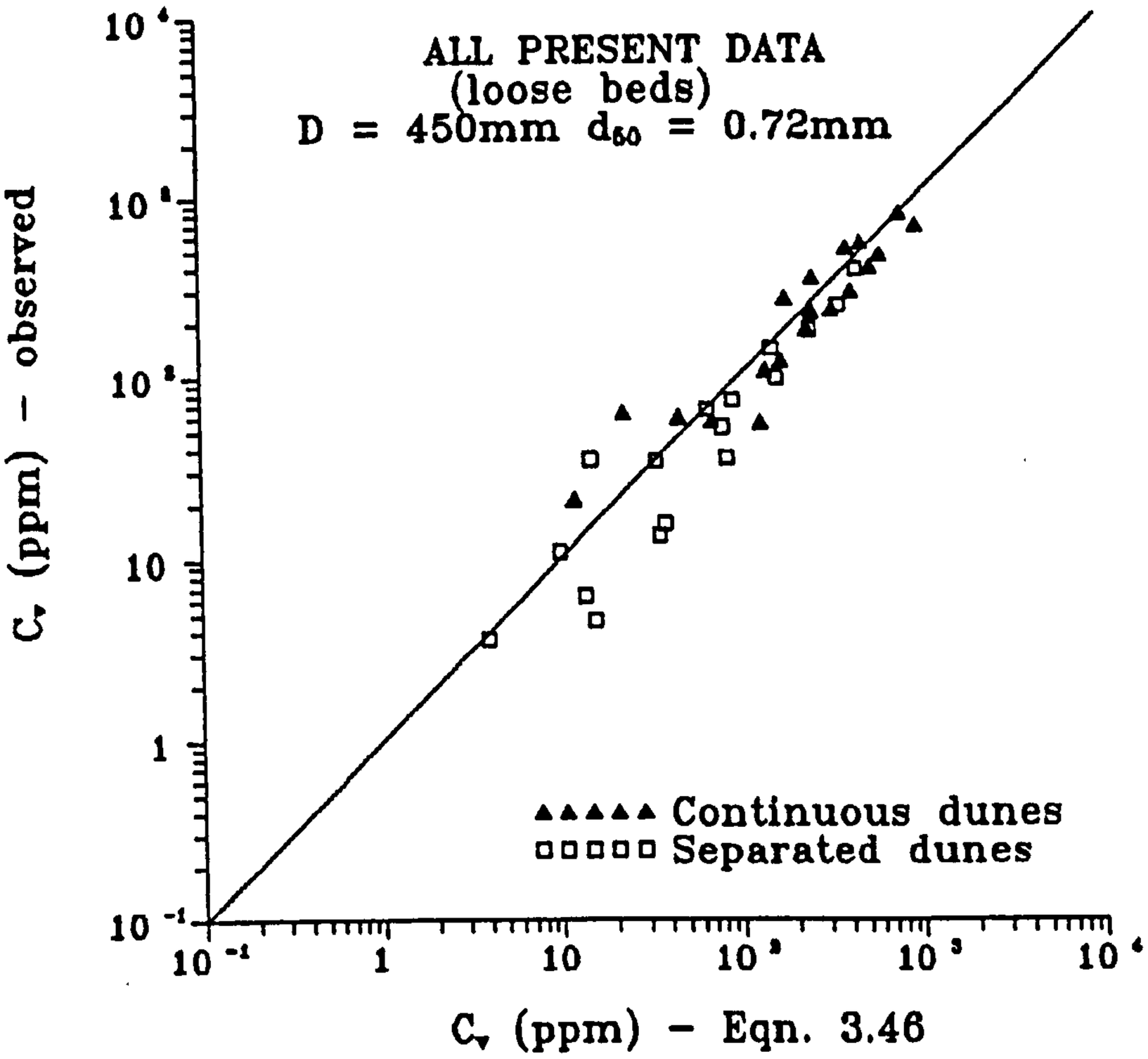

FIG. 6.48a Predicted C_v using May's Eqn. 3.46

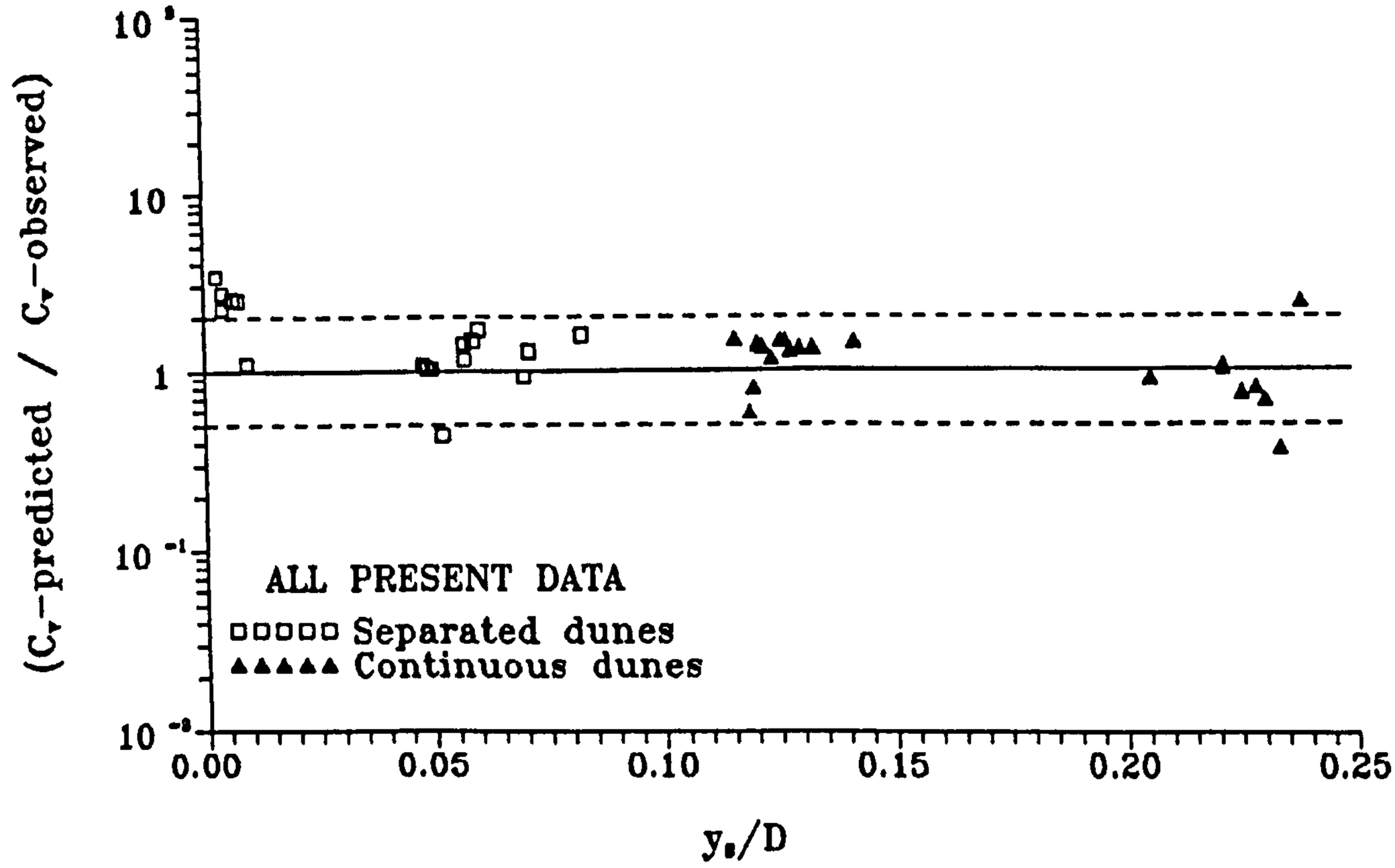

FIG. 6.48b Discrepancy ratio for May's Eqn. 3.46 as a function of proportional sediment depth

The bed friction factor (λ_{sb}) was computed from Visvalingam' Eqn. 5.11. Eqn. 3.55 overpredicts the observed concentrations in all cases where only 11% of the data lie in the 0.5 - 2.0 range of discrepancy ratio. Even though Perrusquia attempted to improve the form of Φ - Ψ equation by introducing several other parameters (y_o/d_{50}, y_o/D, y_s/D and D_{gr}), the results hardly suggest any improvement. The poor results obtained could have been due to the limited ranges of data used for the derivation of the equation. Eqn. 3.55 was re-evaluated using the overall friction factor (λ_s) instead of the bed friction factor. The results as shown in Fig. 6.50 shows some improvement with an average discrepancy ratio of 3.29 and 51% of the data lie within the 0.5 - 2.0 range of discrepancy ratio. However, none of the data fall in the ± 0.10 range of discrepancy ratio while only 14% of the data fall within the ± 0.25 range.

Based on the ± 0.25 range of discrepancy ratios, it can be concluded that the best performance is given by May's Eqn. 3.46 (38%) followed by Graf-Acaroglu's Eqn. 3.63 (24%) and Ackers' Eqn. 3.29 (22%). However, more analyses are needed to improve the prediction of the sediment concentrations for pipes with deposited beds.

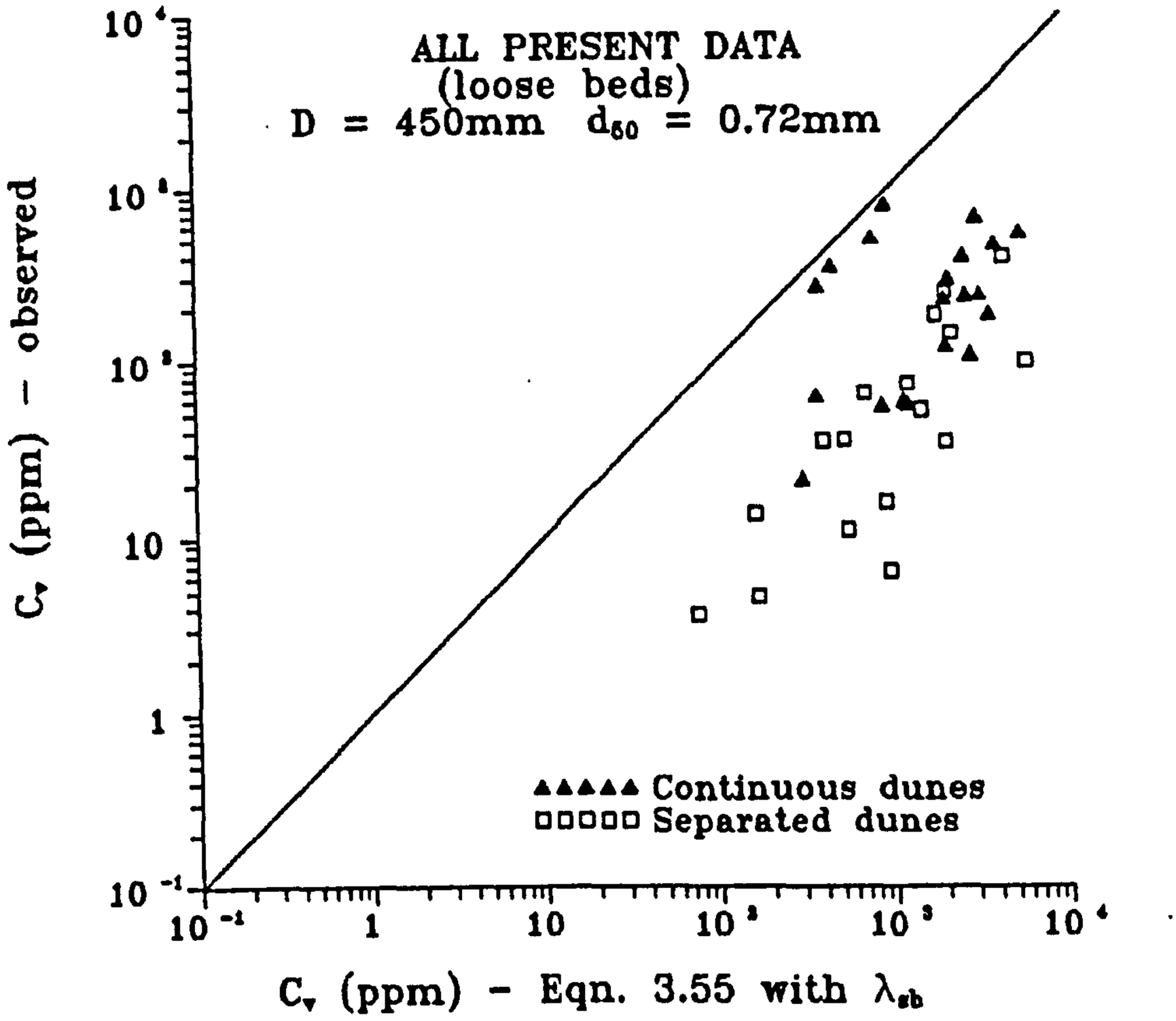

FIG. 6.49a Predicted C_v using Perrusquia's Eqn. 3.55 with bed friction factor

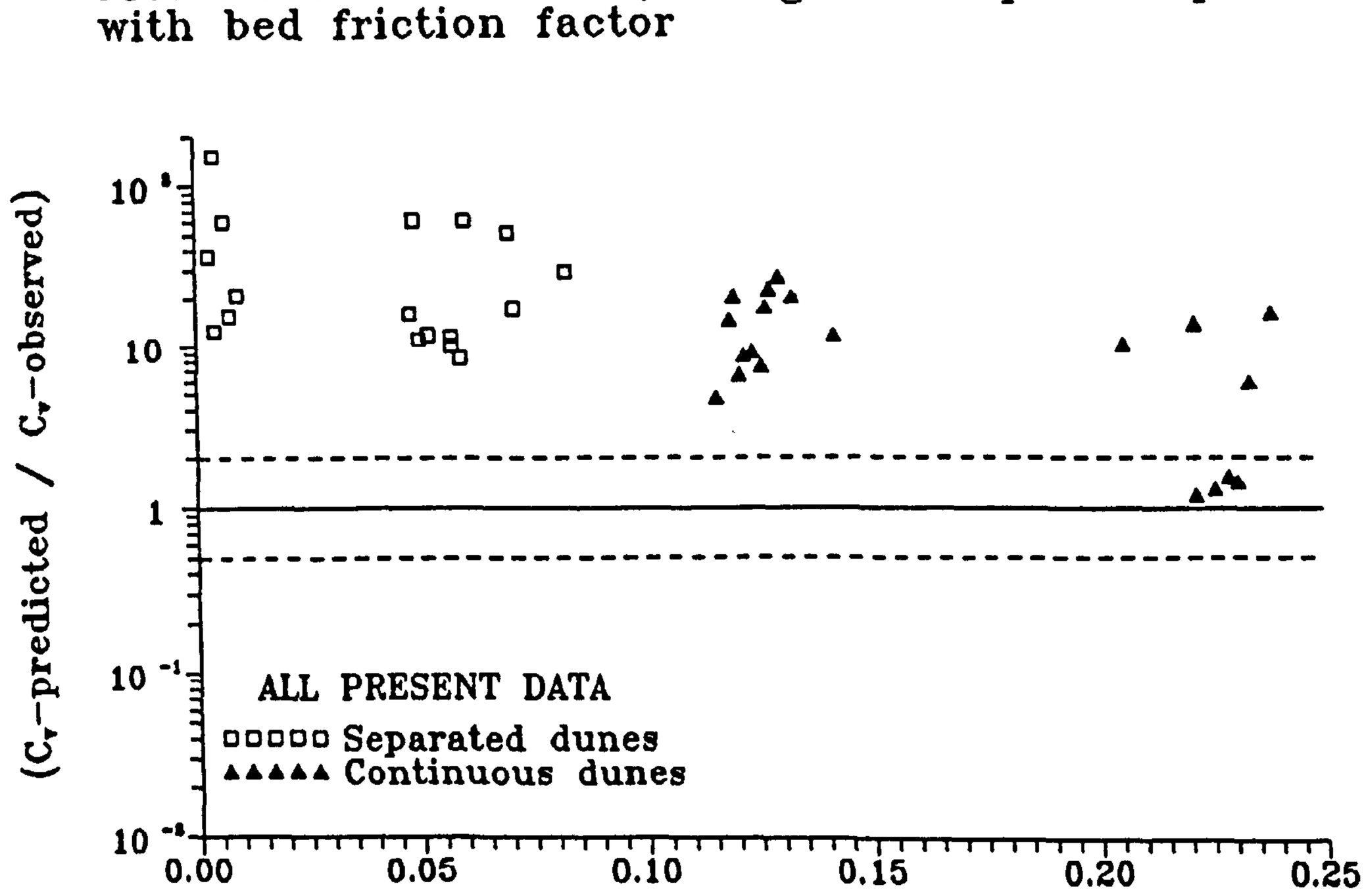

FIG. 6.49b Discrepancy ratio for Perrusquia's Eqn. 3.55, utilising bed friction factor, as a function of proportional sediment dept

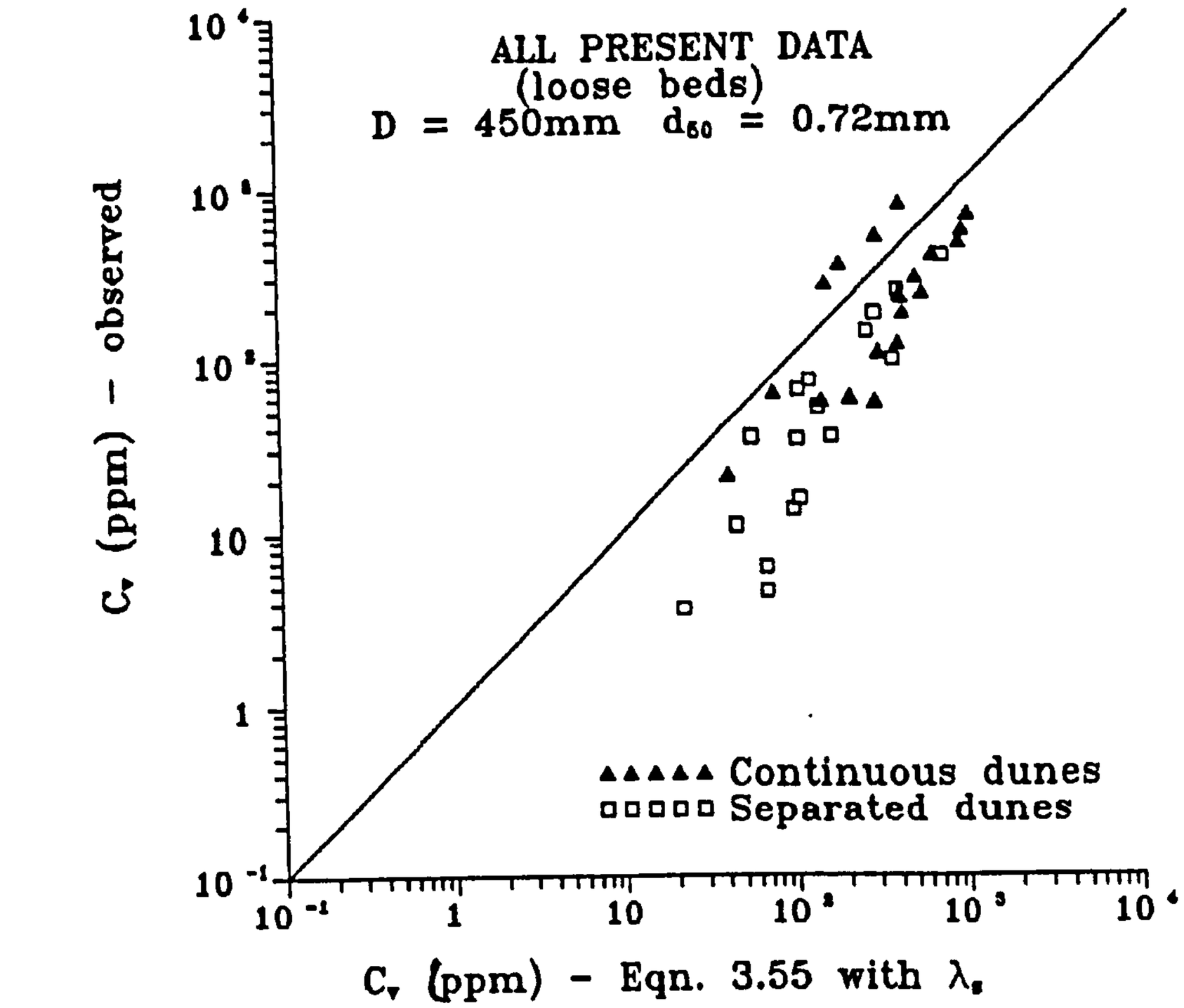

FIG. 6.50a Predicted C_v using Perrusquia's 3.55 with overall friction factor

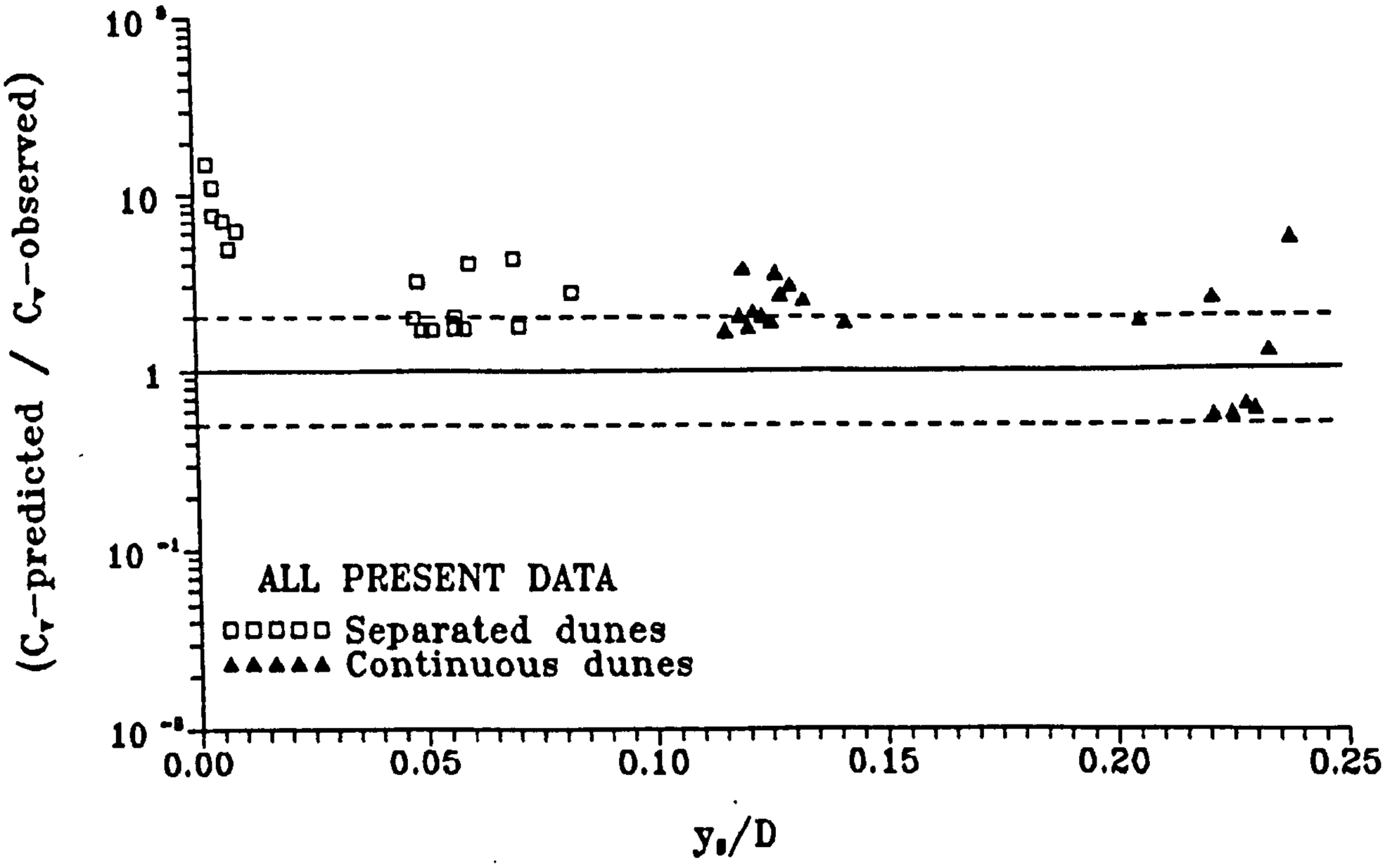

FIG. 6.50b Discrepancy ratio for Perrusquia's Eqn. 3.55, utilising overall friction factor, as a function of proportional sediment dept

6.2.3 Bed Load Models for Pipes with Deposited Beds

6.2.3.1 Proposed Sediment Transport Equations

The majority of the sediment transport equations for wide alluvial channels are expressed in the form:

$$\phi = f(\psi) \tag{6.41}$$

where $\Phi = C_v VR/(gd_{50}^3(S_s-1))^{0.5}$ and $\psi = (S_s-1)d_{50}/SR$. Graf-Acaroglu's Eqn. 3.63 is a common example of this format. As shown in Section 6.2.2, the results obtained for Graf-Acaroglu's Eqn. 3.63 suggests the possibility of applying the form of Eqn. 6.41 to the data from pipes with deposited beds. Due to its simplicity, the format of Eqn. 6.41 was initially used to analyse the present data. It should be mentioned here that the author did not make any use of the data from his earlier work (Ab. Ghani, 1990).

Fig. 6.51 shows the present data plotted in the format of Eqn. 6.41. Less scatter was present implying the suitability of the format of Eqn. 6.41 in analysing the present data. Also the data for separated and continuous dunes correlates well confirming the validity of using a unique definition of y_s for both type of beds as explained before (see Section 5.3.6). A power regression analysis on the plot (Fig. 6.51) yielded (adj. $r^2 = 0.86$, s = 0.24):

$$\phi = 11.71\ \psi^{-2.86} \qquad (6.42)$$

For comparison, the Φ - ψ plot using Graf-Acaroglu's Eqn. 3.63 is also shown in Fig. 6.51. It shows that the best agreement obtained with the present data is for the range of $10^{-1} < \phi < 1$.

As in the case of clean pipes, an attempt was then made to utilise all available data (see Table 6.34) for pipes with deposited beds by including independent data of Alvarez (1990), Perrusquia (1992) and May (1993). The plot of Φ - ψ was then made using all these data as shown in Fig. 6.52. The data from different investigators correlate well and the resulting equation is given as:

$$\phi = 6.14\ \psi^{-2.26} \qquad (6.43)$$

with adj. $r^2 = 0.83$ and $s = 0.36$. The plot in Fig. 6.52 shows that the data of Alvarez (1990) and Perrusquia (1992) approximately occupy the range of $10^{-4} < \Phi < 10^{-2}$ while the data of May (1993) and the author's occupy the range of $10^{-3} < \Phi < 2$. This illustrates the importance of using a wide range of data to obtain a reliable equation. Fig. 6.52 also shows that with a large number of data used for its derivation, Eqn. 6.43 approaches the wide alluvial channel relationship as given by the Graf-Acaroglu equation (Eqn. 3.63). The results imply the similarity of behaviour of the sediment movement in alluvial channels and that in sewers with deposited beds.

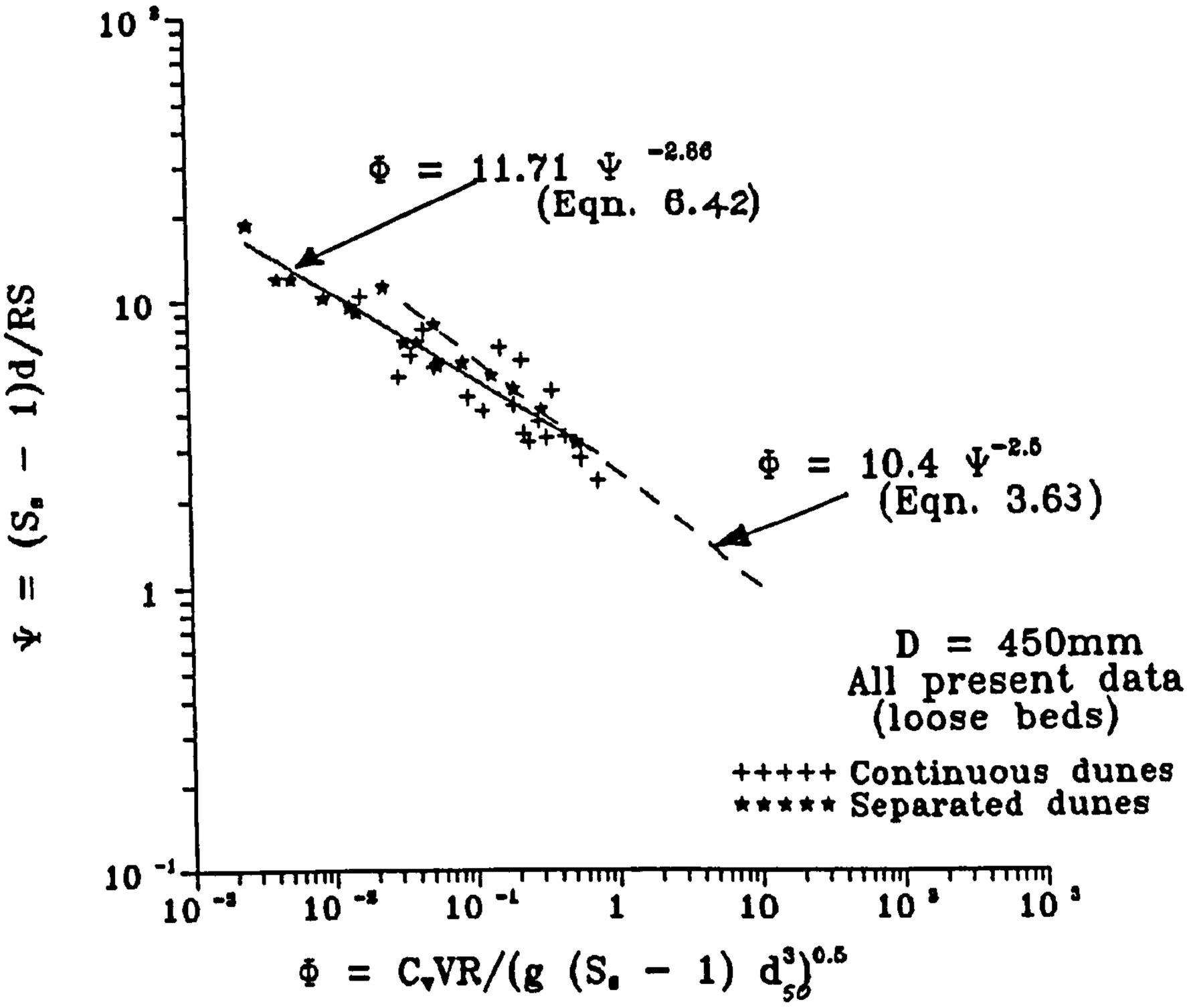

FIG. 6.51 Φ – Ψ plot for all present data

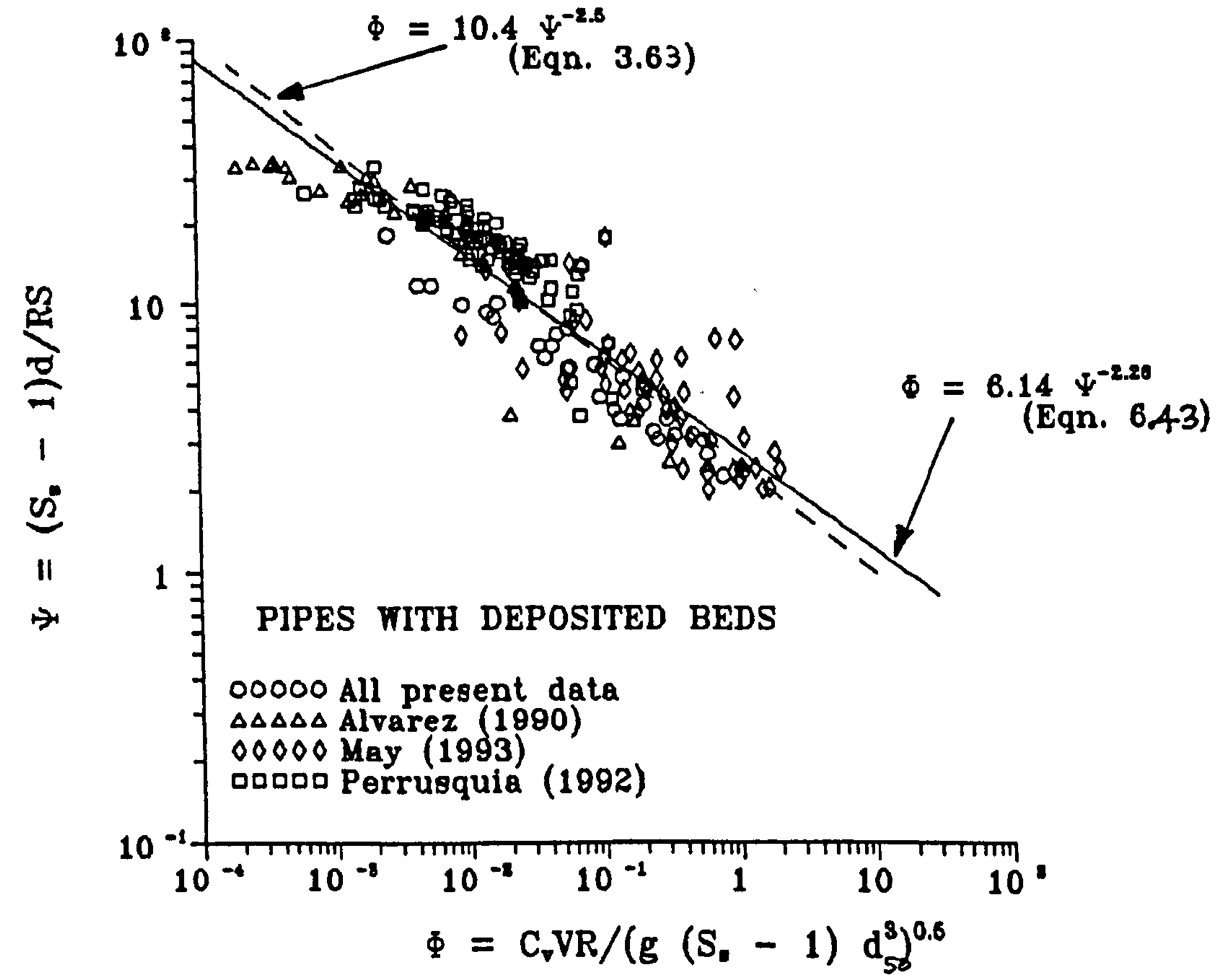

FIG. 6.52 Φ – Ψ plot for the combined data

TABLE 6.34 RANGES OF PARAMETER FOR THE COMBINED DATA (PIPES WITH DEPOSITED BEDS)

PARAMETER	ALVAREZ (1990)	PERRUSQUIA (1992)	MAY (1993)	PRESENT
D (mm)	154	154 - 450	300 - 450	450
y_s/D	0.11 - 0.39	0.20 - 0.40	0.0008 - 0.22	0.002 - 0.22
Y/D	0.51 - 0.76	0.32 - 0.86	0.5 - 1.0	0.5 - 0.75
d_{50} (mm)	0.50 - 2.90	0.72 - 2.5	0.47 - 0.72	0.72
Φ	$1.34X10^{-4}$ - $3.40X10^{-2}$	$6.56X10^{-4}$ - $1.71X10^{-1}$	$9.07X10^{-3}$ - 2.03	$2.64X10^{-3}$ - 1.09
ψ	11.84 - 42.54	3.72 - 33.56	2.04 - 19.49	2.31 - 18.53
Fr_m	2.53 - 4.77	2.08 - 5.19	4.79 - 14.22	4.60 - 11.27
C_v (ppm)	2 - 131	19 - 408	12 - 1187	4 - 672
W_b/y_o	0.93 - 6.29	0.74 - 9.80	0.12 - 3.57	0.21 - 1.78
d_{50}/D	0.0034 - 0.0188	0.0016 - 0.0111	0.001044 - 0.0024	0.0016
λ_s	0.0249 - 0.0410	0.0211 - 0.146	0.0131 - 0.0631	0.0176 - 0.0581
NO. OF DATA	30	79	52	32

Eqn. 6.43 can be re-written in terms of the limiting velocity as:

$$\frac{V}{\sqrt{gd_{50}(S_s-1)}} = 2.28\, C_v^{0.28} \left(\frac{R}{d_{50}}\right)^{0.28} \lambda_s^{-0.64} \qquad (6.44)$$

Fig. 6.53 compares the observed and computed Fr_* using Eqn. 6.44. The accuracy of Eqn. 6.44 was evaluated as before using the discrepancy ratio in terms of Fr_*. The results shown in Fig. 6.53 have an average discrepancy ratio of 1.03 where 78% of the data occur within the ± 0.25 deviation (see Table 6.35).

An attempt was then made to assess the applicability of Eqn. 6.44 over the range of the available data (Table 6.34). In this analysis, the discrepancy ratio in terms of Fr_* is plotted as functions of the volumetric sediment concentration (C_v), proportional sediment bed thickness (y_s/D), sediment bed width to flow depth ratio (W_b/y_o), dimensionless particle size (D_{gr}) and velocity (V). The results of this analysis are given in Table 6.36 and Fig. 6.54. It should be noted that the measured values of λ_s were used in the calculation of the predicted values of Fr_*.

Fig. 6.54a reveals that the agreement is best for concentrations between 51ppm and 100ppm with a perfect average discrepancy ratio of 1.00 where 93% of the data for this range of C_v lie within the ± 0.25 range of discrepancy ratio. A fairly reasonable agreement is obtained for the range of C_v = 11ppm - 50ppm and C_v = 101ppm - 500ppm with average discrepancy ratios of 0.85 and 1.10 respectively. 78% and 84% of the data for these ranges of C_v are

TABLE 6.35 DISCREPANCY RATIO (Fr_m) FOR EQN. 6.44 - COMBINED DATA (PIPES WITH DEPOSITED BEDS)

Source of data	Fr_s (predicted) / Fr_s (observed)							No. of data
	Mean	min	max	0.90-1.10 (%)	0.75-1.25 (%)	0.5-1.5 (%)	0.5-2.0 (%)	
Present	0.89	0.63	1.08	47	88	100	100	32
Alvarez (1990)	0.91	0.51	1.28	43	70	100	100	30
Perrusquia (1992)	1.10	0.62	2.08	32	82	97	99	79
May (1993)	1.07	0.48	2.17	38	69	90	96	52
Combined	1.03	0.48	2.17	38	78	96	98	193

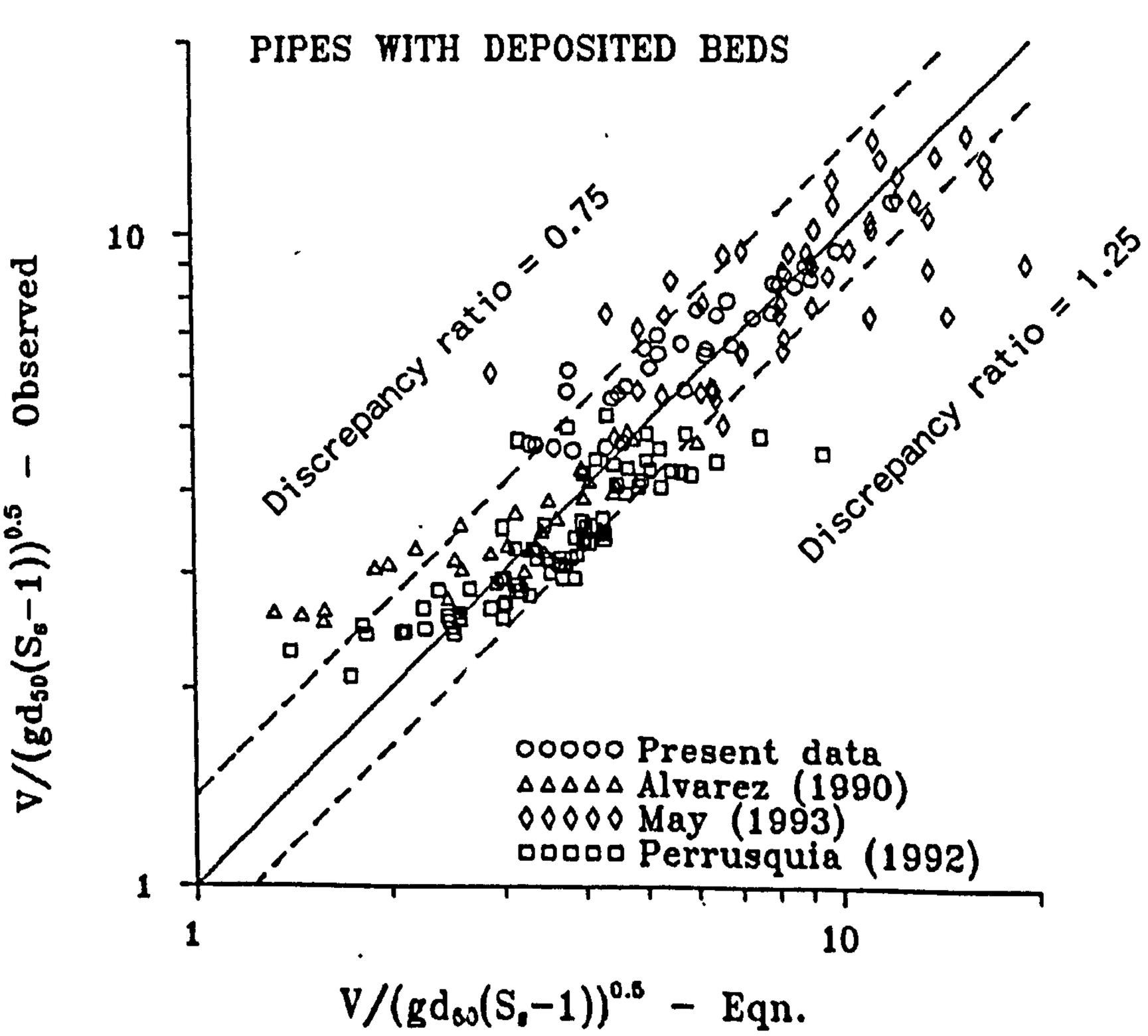

FIG. 6.53 Bed-load model for pipes with deposited beds - Eqn. 6.44 (Combined data)

within the ± 0.25 range of discrepancy ratio respectively. However, there is an underprediction for concentrations in the range of C_v < 10ppm and an overprediction for C_v > 501ppm. A possible explanation for these tendencies could be found by examining the plots of the discrepancy ratio as functions of y_s/D (Fig. 6.54b) and W_b/y_o (Fig. 6.54c).

Fig. 6.54b shows the presence of undeprediction (see Table 6.36) for y_s/D < 1% and the existence of overprediction for y_s/D = 15% - 20% with the average discrepancy ratios of 0.85 and 1.17 respectively. Similar trends of underprediction and overprediction could be found for W_b/y_o < 1.0 and W_b/y_o = 2.01 - 3.0 as can be seen in Fig. 6.54c. These trends suggest the inability of Eqn. 6.44 to cope with the variation in bed thickness and flow depth for a certain range of the available data. It should be stressed that the form of Eqn. 6.44 has only the parameter R/d_{50} to reflect any variation in the bed thickness and flow depth.

Fig. 6.54d indicates that the agreement is generally satisfactory over the range of particle sizes where the average discrepancy ratios vary from 0.94 to 1.09. Even though only 57% to 84% of the data lie within the ± 0.25 range of the discrepancy ratios, there appears no systematic errors.

Fig. 6.54e shows that the agreement is reasonably good for the range of V = 0.25m/s to 0.8m/s where the average discrepancy ratio varies from 0.98 to 1.05 and 68% - 87% of the data lie

TABLE 6.36 DICREPANCY RATIO (Fr_*) FOR EQN. 6.44
AS FUNCTIONS OF RELEVANT PARAMETERS - COMBINED DATA
(PIPES WITH DEPOSITED BEDS)

Range of parameter		Fr_* (predicted) / Fr_* (observed)							No of data
		Mean	min	max	0.90-1.10 (%)	0.75-1.25 (%)	0.50-1.50 (%)	0.5-2.0 (%)	
C_v (ppm)	1-10	0.64	0.51	0.73	0	0	100	100	10
	11-50	0.85	0.48	1.09	44	78	100	100	36
	51-100	1.00	0.72	1.51	48	93	99	100	29
	101-500	1.10	0.67	2.08	36	84	97	99	101
	501-1200	1.27	0.96	2.17	41	59	82	94	17
y_s/D (%)	<1.0	0.85	0.59	1.51	33	62	99	100	21
	1.05-10.0	1.03	0.70	1.34	56	93	100	100	27
	10.05-15.0	0.95	0.51	1.56	48	82	99	100	33
	15.05-20.0	1.17	0.67	2.17	20	73	91	95	44
	20.05-30.0	1.07	0.48	1.98	32	64	94	97	31
	30.05-40.0	1.00	0.57	1.23	43	89	100	100	37
W_b/y_o	0-1.0	0.93	0.59	1.51	45	81	98	100	47
	1.01-2.0	1.04	0.61	1.56	45	83	98	100	53
	2.01-3.0	1.13	0.48	2.17	27	65	90	98	48
	3.01-4.0	1.03	0.62	2.08	32	73	95	95	22
	4.01-10.0	0.98	0.57	1.20	35	91	100	100	23
D_{gr}	10-15	0.94	0.48	1.40	24	57	95	100	21
	16-20	1.01	0.59	2.17	42	78	92	98	85
	21-25	1.09	0.51	1.46	36	82	100	100	56
	26-80	1.02	0.61	1.32	39	84	100	100	31
V (m/s)	0.2-0.500	1.01	0.51	2.08	34	82	99	99	71
	0.501-0.600	1.05	0.48	1.57	39	68	95	100	44
	0.601-0.700	0.98	0.63	1.24	30	87	100	100	23
	0.701-0.800	1.04	0.59	1.98	40	76	88	100	25
	0.801-1.500	1.07	0.66	2.17	50	77	93	97	30

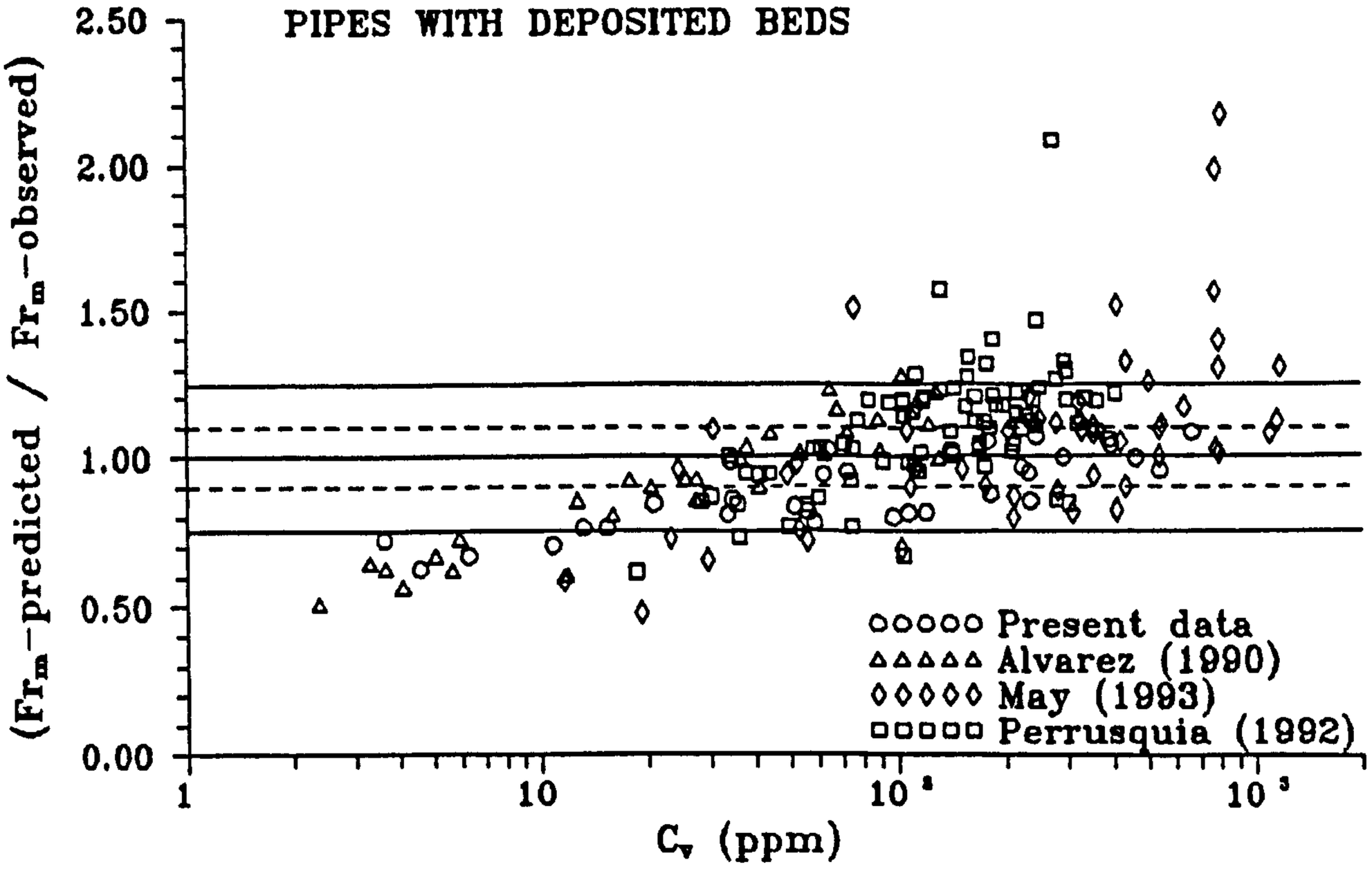

FIG. 6.54a Discrepancy ratio for Eqn. 6.44 as a function of sediment concentrations

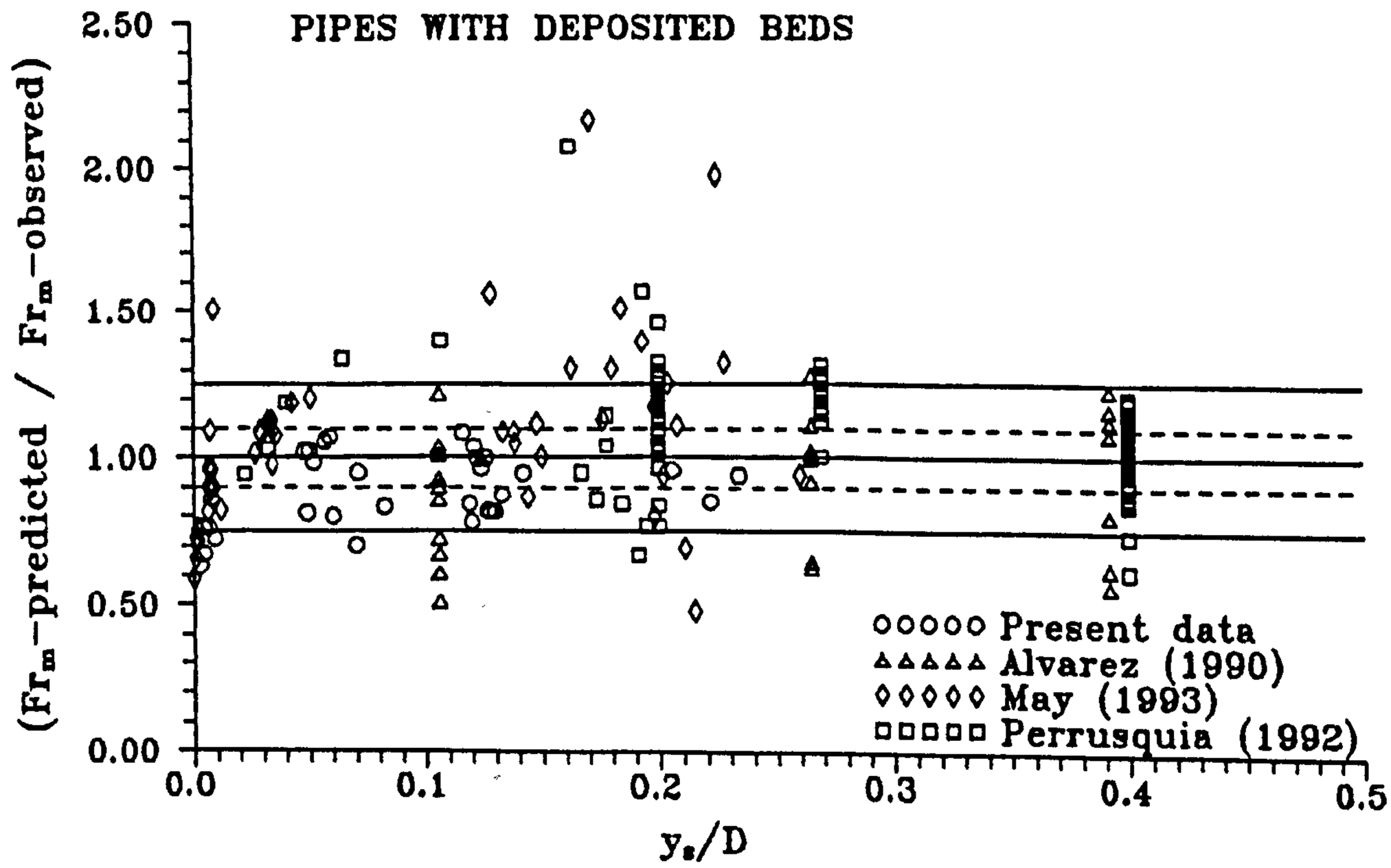

FIG. 6.54b Discrepancy ratio for Eqn. 6.44 as a function of proportional sediment depth

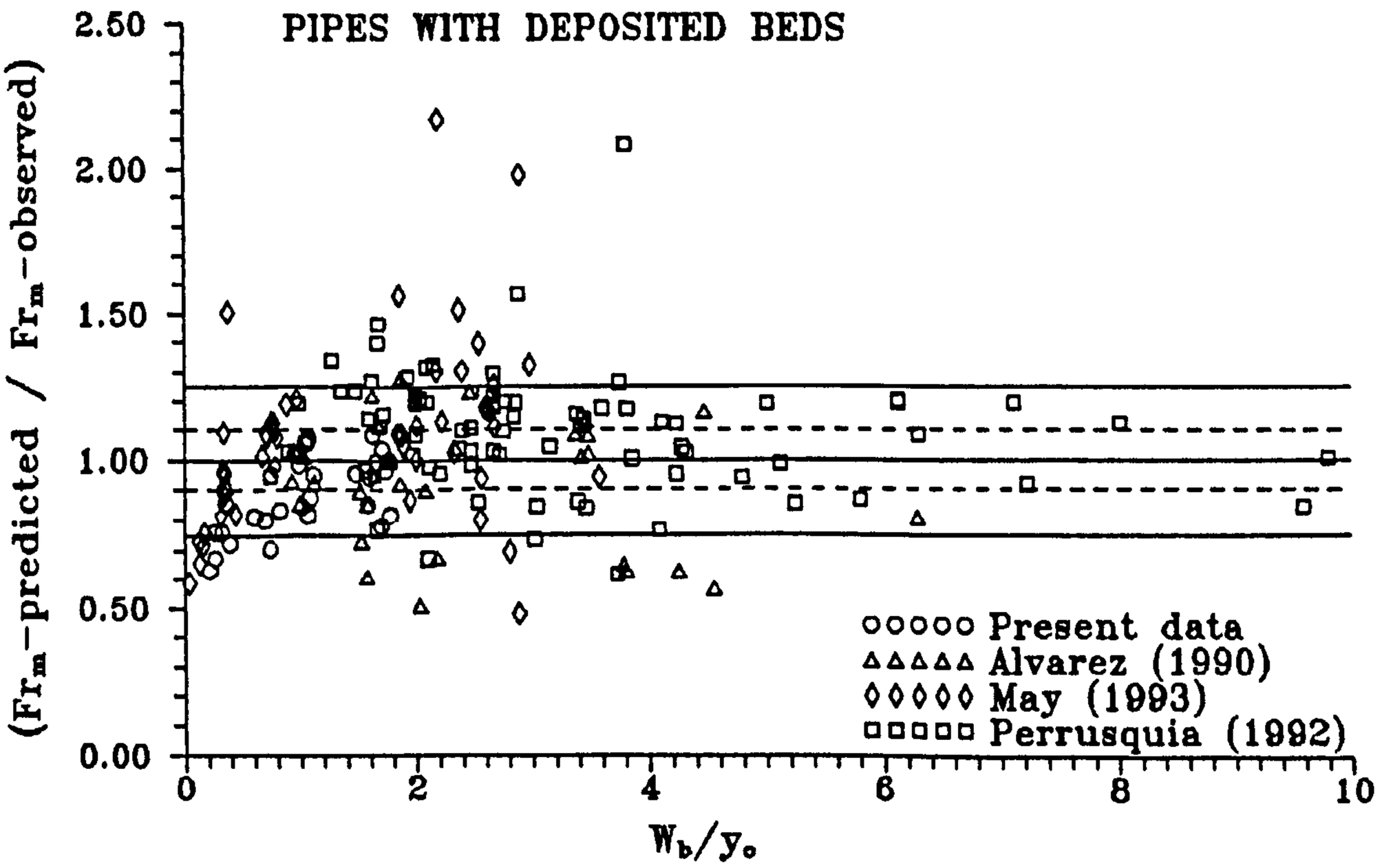

FIG. 6.54c Discrepancy ratio for Eqn. 6.44 as a function of sediment bed width to flow depth ratio

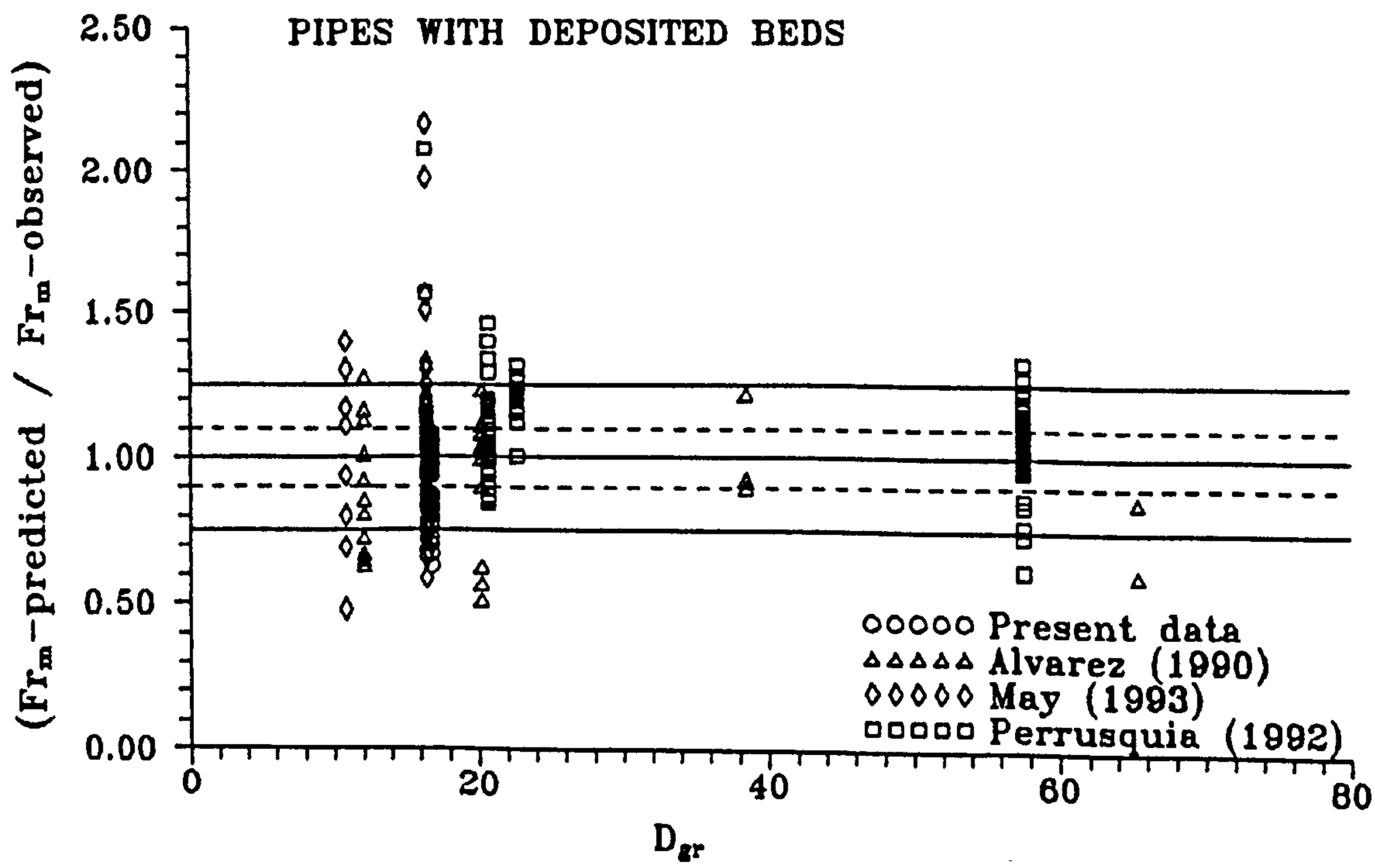

FIG. 6.54d Discrepancy ratio for Eqn. 6.44 as a function of dimensionless particle size

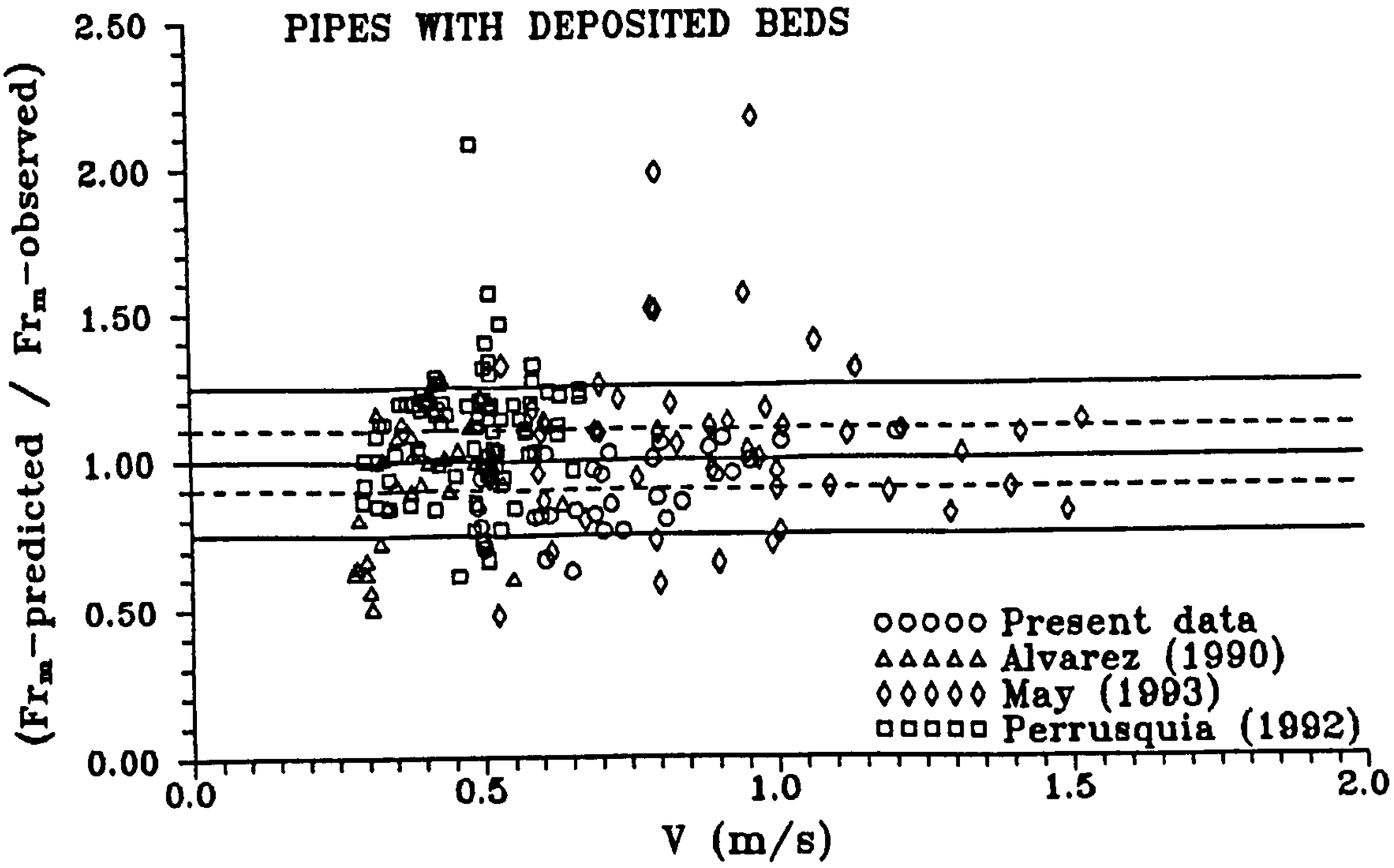

FIG. 6.54e Discrepancy ratio for Eqn. 6.44 as a function of velocity

within the ± 0.25 deviations. A slightly higher average discrepancy ratio for V > 0.8m/s could be attributed to the difficulties in obtaining the slopes of the water surface accurately.

Overall, Eqn. 6.44 provides a fairly good agreement over the range of sediments and flow conditions in pipes with deposited beds. This highlights the range of applicability of the ϕ - Ψ form of equation to data from pipes with deposited beds.

An attempt was then made to consider another function to account for the presence of sediment beds in pipes. As mentioned previously in Section 6.1.3.4, El-Zaemey (1991) proposed a function (Eqn. 6.36) for transport over cemented beds in sewers.

Utilising the limiting velocity instead of the shear stress as the dependent variable, Eqn. 6.36 can be re-written as:

$$\frac{V}{\sqrt{gd_{50}(S_s-1)}} = f\left(C_v, \frac{W_b}{y_o}, \frac{d_{50}}{D}, \lambda_s\right) \qquad (6.45)$$

It should be emphasized that the parameter W_b/y_o is considered to reflect the influence of the bed width and flow depth on sediment movement. The influence of pipe diameter and particle size on sediment movement is characterized by the parameter d_{50}/D. The effect of flow resistance due to the presence of sediment beds is incorporated in the overall friction factor parameter λ_s.

A multiple regression analysis using the combined data (see Table 6.34) produced:

$$\frac{V}{\sqrt{gd_{50}(S_s-1)}} = 1.18\, C_v^{0.16} \left(\frac{W_b}{y_o}\right)^{-0.18} \left(\frac{d_{50}}{D}\right)^{-0.34} \lambda_s^{-0.31} \qquad (6.46)$$

with adj. $r^2 = 0.93$ and $s = 0.057$. Fig. 6.55 compares the observed values of Fr_m against the computed values by Eqn. 6.46. Table 6.37 gives the discrepancy ratio in terms of Fr_m. The results shown in Fig. 6.55 have an average discrepancy ratio of 1.00 where 96% of the combined data are within the ± 0.25 range of discrepancy ratio.

The applicability of Eqn. 6.46 over the range of the combined data (Table 6.34) is evaluated with the discrepancy ratio plotted as functions of C_v, y_s/D, W_b/y_o, D_{gr} and V. The measured values

TABLE 6.37 DISCREPANCY RATIO (Fr_*) FOR EQN. 6.46 - COMBINED DATA (PIPES WITH DEPOSITED BEDS)

Source of data	Fr_* (predicted) / Fr_* (observed)							No. of data
	Mean	min	max	0.90-1.10 (%)	0.75-1.25 (%)	0.5-1.5 (%)	0.5-2.0 (%)	
Present	1.00	0.80	1.21	78	100	100	100	32
Alvarez (1990)	0.94	0.70	1.07	70	93	100	100	30
Perrusquia (1992)	1.06	0.77	1.56	68	97	99	100	79
May (1993)	0.96	0.69	1.30	42	94	100	100	52
Combined	1.00	0.69	1.56	62	96	99	100	193

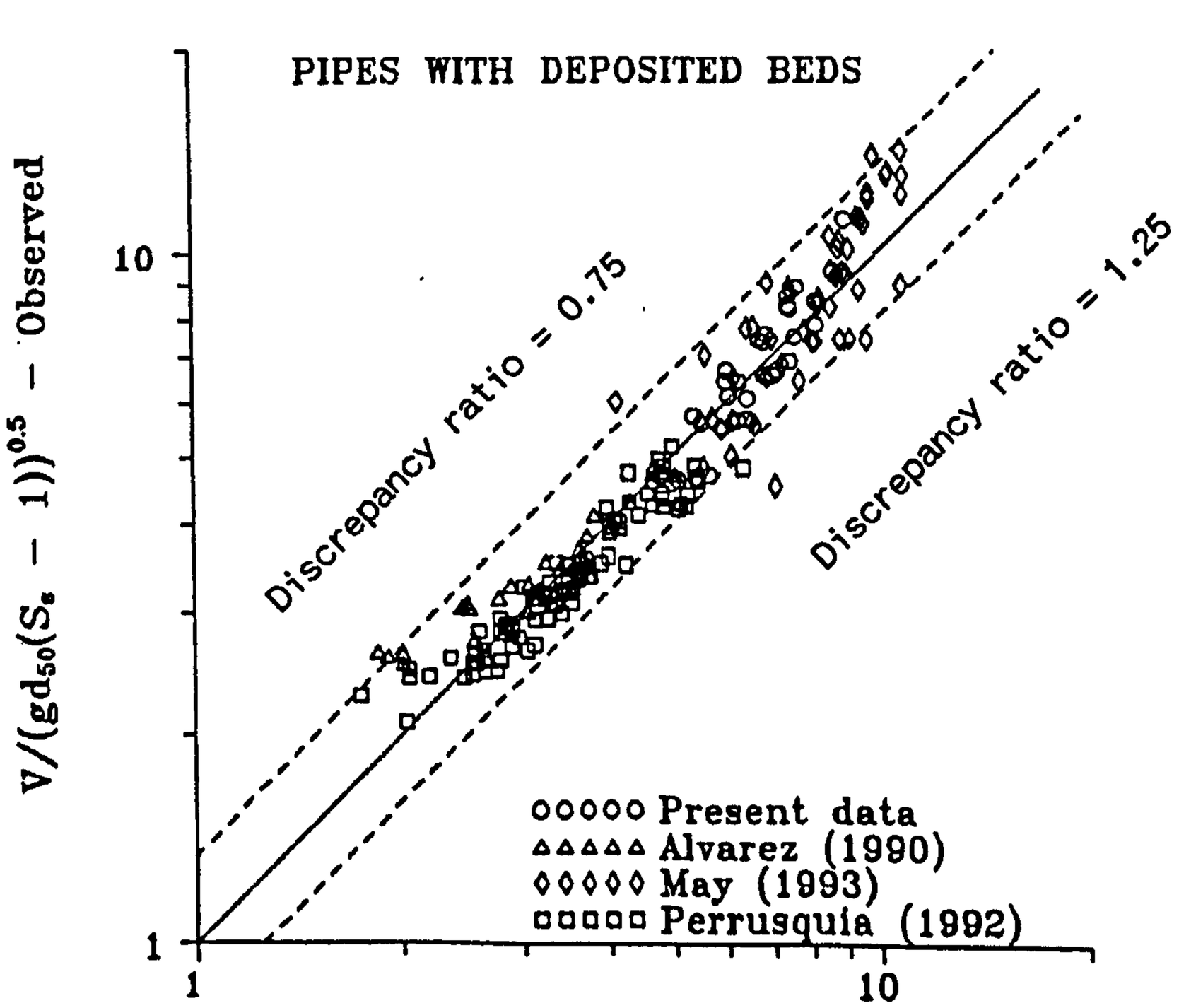

FIG. 6.55 Bed load model for pipes with deposited beds - Eqn. 6.46 (Combined data)

of λ_s were used in the computation of the predicted values of Fr_m. The results are given in Table 6.38 and Fig. 6.56.

Fig. 6.56a shows that the agreement is reasonably good over the whole range of C_v studied. The average discrepancy ratio varies from 0.90 to 1.04 with over 90% of the data for each range of C_v falling within the ± 0.25 range of discrepancy ratio.

Fig. 6.56b reveals that the agreement is also reasonably good over the whole range of y_s/D studied. The average discrepancy ratio varies from 0.94 to 1.04 with over 95% of the data for each range of y_s/D lying within the ± 0.25 range of discrepancy ratio.

Fig. 6.56c indicates that the agreement is very good over the range of W_b/y_o. The average discrepancy ratio varies from 1.00 to 1.02 with over 95% of the data for each range of W_b/y_o occurring within the ± 0.25 range of discrepancy ratio.

The good correlation shown for each range of C_v, y_s/D and W_b/y_o confirms the importance of these parameters in the sediment transport process in pipes with deposited beds.

Fig. 6.56d also reveals the good agreement obtained for the whole range of particle sizes tested. The average discrepancy ratio varies from 0.91 to 1.05 with over 95% of the data for each range of D_{gr} falling within the ± 0.25 range of discrepancy ratio.

TABLE 6.38 DICREPANCY RATIO (Fr_m) FOR EQN. 6.46 AS FUNCTIONS OF RELEVANT PARAMETERS - COMBINED DATA (PIPES WITH DEPOSITED BEDS)

Range of parameter		Fr_m (predicted) / Fr_m (observed)							No of data
		Mean	min	max	0.90-1.10 (%)	0.75-1.25 (%)	0.50-1.50 (%)	0.5-2.0 (%)	
C_v (ppm)	1-10	0.91	0.74	1.16	30	90	100	100	10
	11-50	1.00	0.69	1.21	67	94	100	100	36
	51-100	1.04	0.91	1.30	86	97	100	100	29
	101-500	1.02	0.72	1.57	67	97	99	100	101
	501-1200	0.90	0.77	1.23	12	100	100	100	17
y_s/D (%)	<1.0	1.04	0.80	1.30	57	95	100	100	21
	1.05-10.0	1.00	0.72	1.23	52	96	100	100	27
	10.05-15.0	0.94	0.70	1.22	70	97	100	100	33
	15.05-20.0	1.04	0.81	1.57	57	95	98	100	44
	20.05-30.0	0.99	0.69	1.23	65	97	100	100	31
	30.05-40.0	1.01	0.74	1.16	70	97	100	100	37
W_b/y_0	0-1.0	1.01	0.72	1.30	53	96	100	100	47
	1.01-2.0	1.00	0.70	1.23	77	98	100	100	53
	2.01-3.0	1.00	0.69	1.32	54	96	100	100	48
	3.01-4.0	1.00	0.77	1.57	73	95	95	100	22
	4.01-10.0	1.02	0.74	1.16	57	96	96	100	23
D_{gr}	10-15	0.91	0.69	1.08	43	95	100	100	21
	16-20	1.01	0.72	1.57	55	95	99	100	85
	21-25	1.05	0.74	1.23	70	98	100	100	56
	26-80	0.97	0.70	1.12	77	97	100	100	31
V (m/s)	0.2-0.500	1.02	0.74	1.57	68	97	99	100	71
	0.501-0.600	1.05	0.69	1.32	64	93	100	100	44
	0.601-0.700	1.01	0.79	1.19	70	100	100	100	23
	0.701-0.800	1.02	0.85	1.30	72	96	100	100	25
	0.801-1.500	0.88	0.72	1.21	37	97	100	100	30

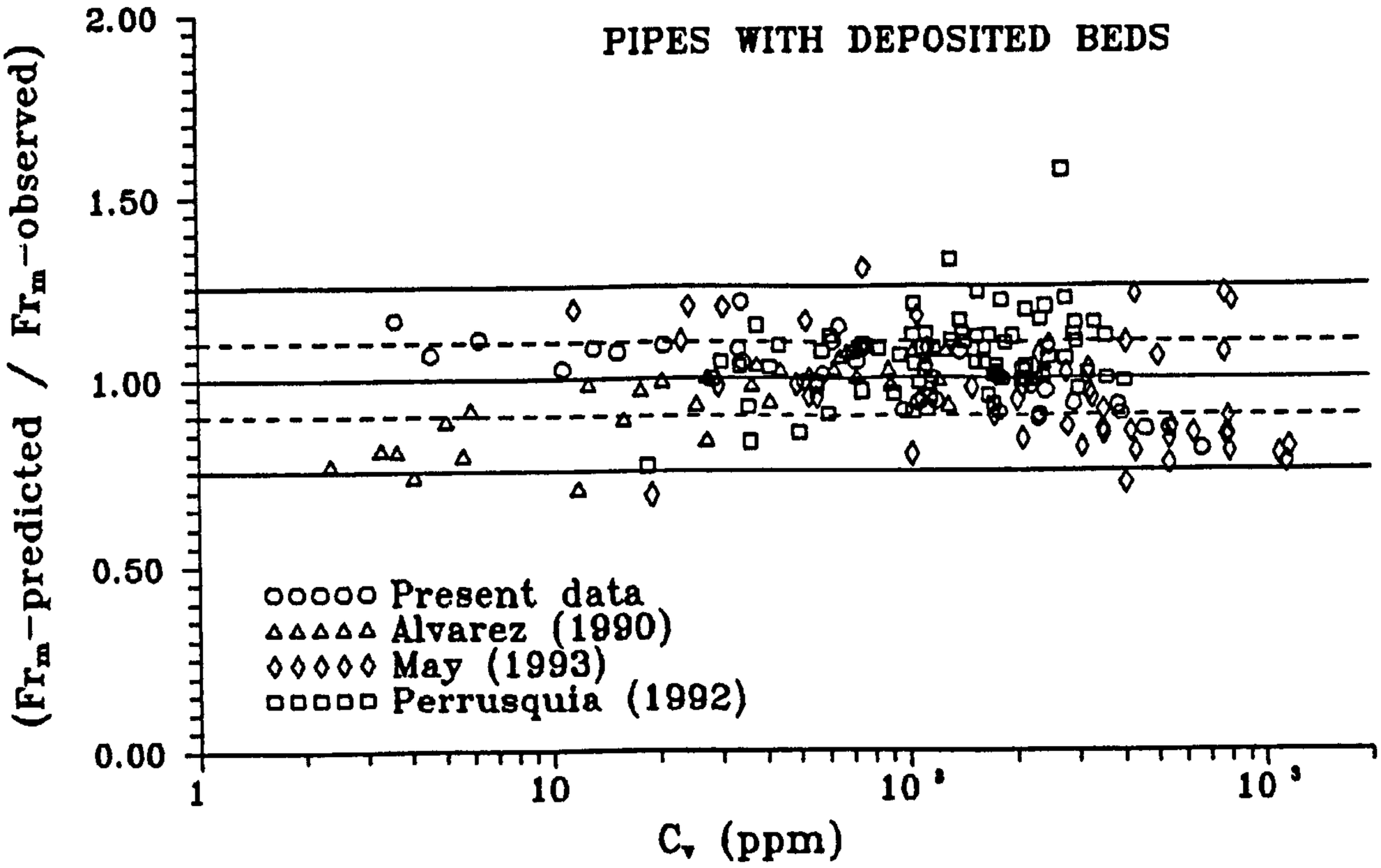

FIG. 6.56a Discrepancy ratio for Eqn. 6.46 as a function of sediment concentrations

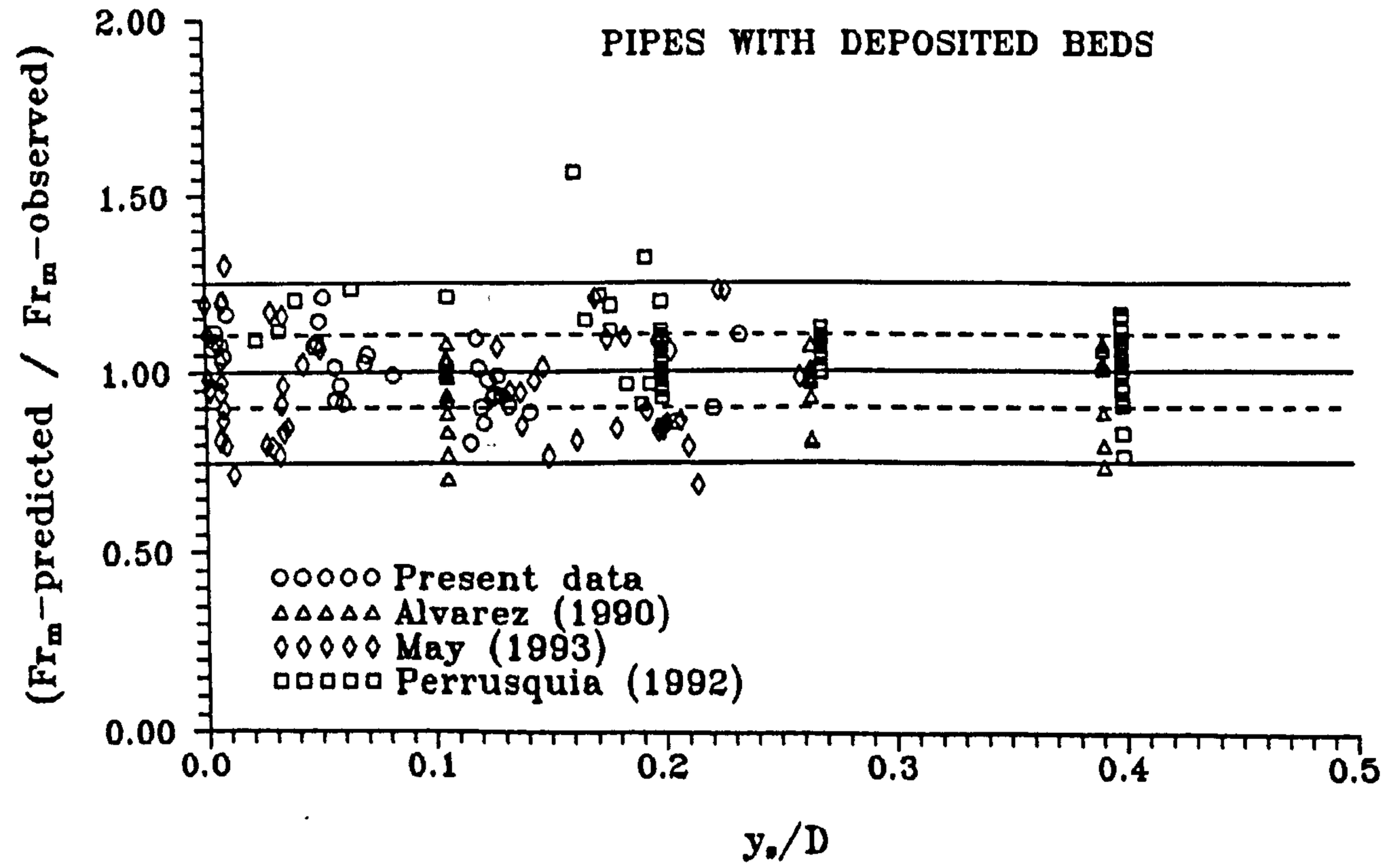

FIG. 6.56b Discrepancy ratio for Eqn. 6.46 as a function of proportional sediment depth

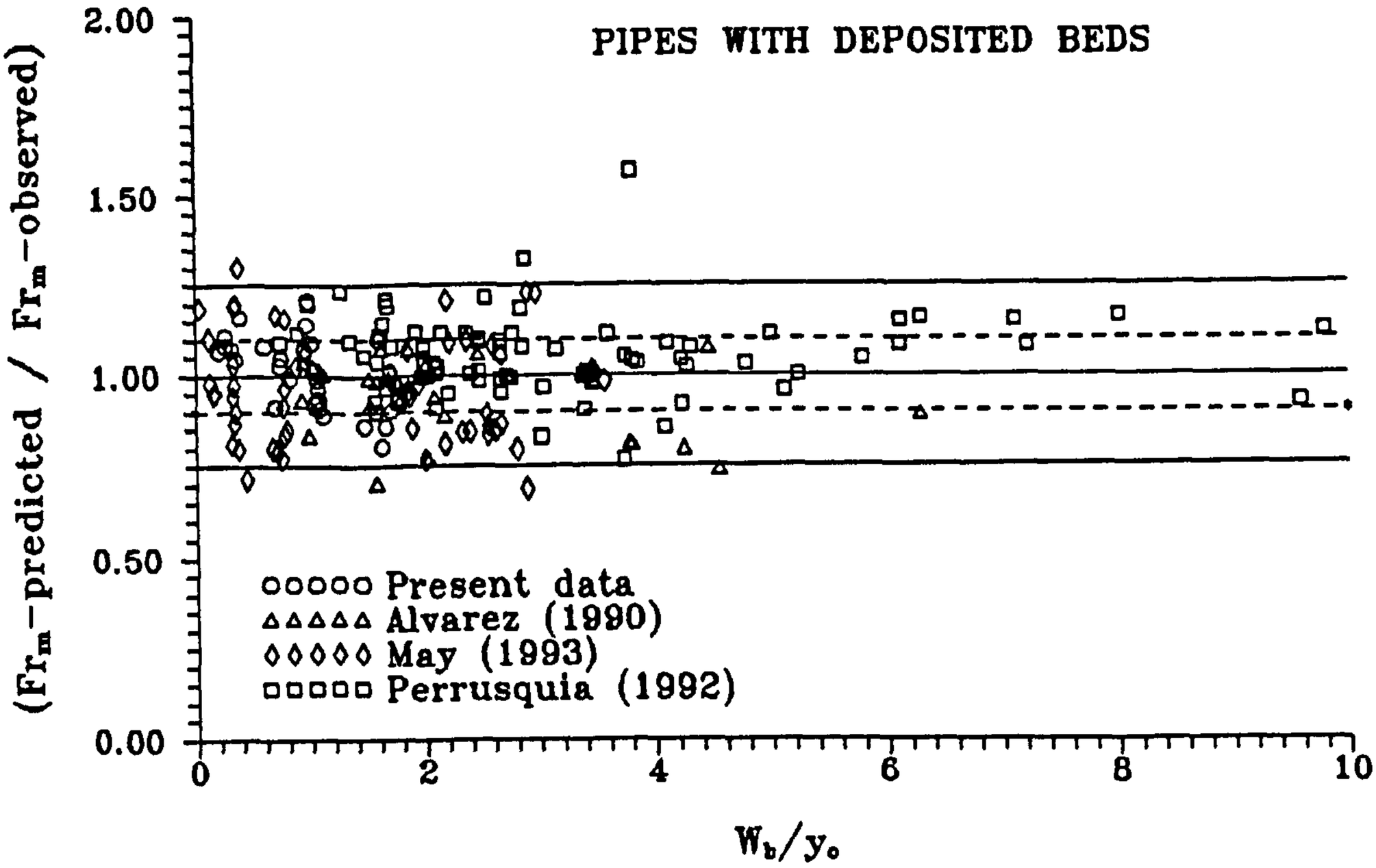

FIG. 6.56c Discrepancy ratio for Eqn. 6.46 as a function of sediment bed width to flow depth ratio

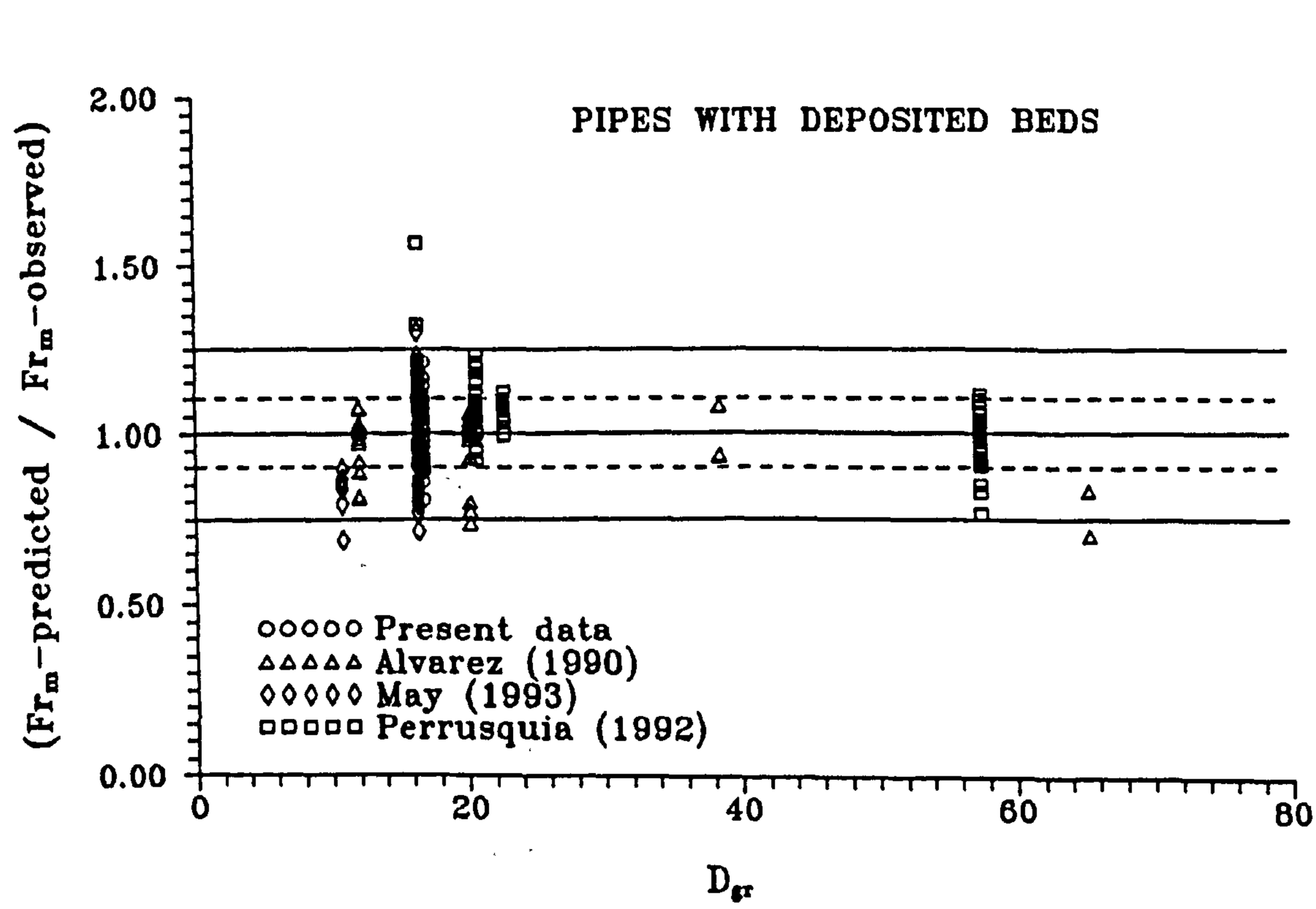

FIG. 6.56d Discrepancy ratio for Eqn. 6.46 as a function of dimensionless particle size

Fig. 6.56e shows the agreement is reasonably good for the range of V = 0.25m/s - 0.80m/s. The average discrepancy ratio varies from 1.01 to 1.05 with over 93% of the data for each range of V lying within the ± 0.25 range of discrepancy ratio. There is an underprediction for V > 0.8m/s. As mentioned previously, the probable explanation for this trend is the difficulties in obtaining the slope of the water surface accurately.

Overall, the preceding analysis suggests the general applicability of Eqn. 6.46 over wide range of sediments and flow conditions. The author therefore proposes Eqn. 6.46 to be used for the design of sewers with deposited loose beds. Due to its simplicity, it is also recommended that Eqn. 6.44 to be used as an alternative design criterion.

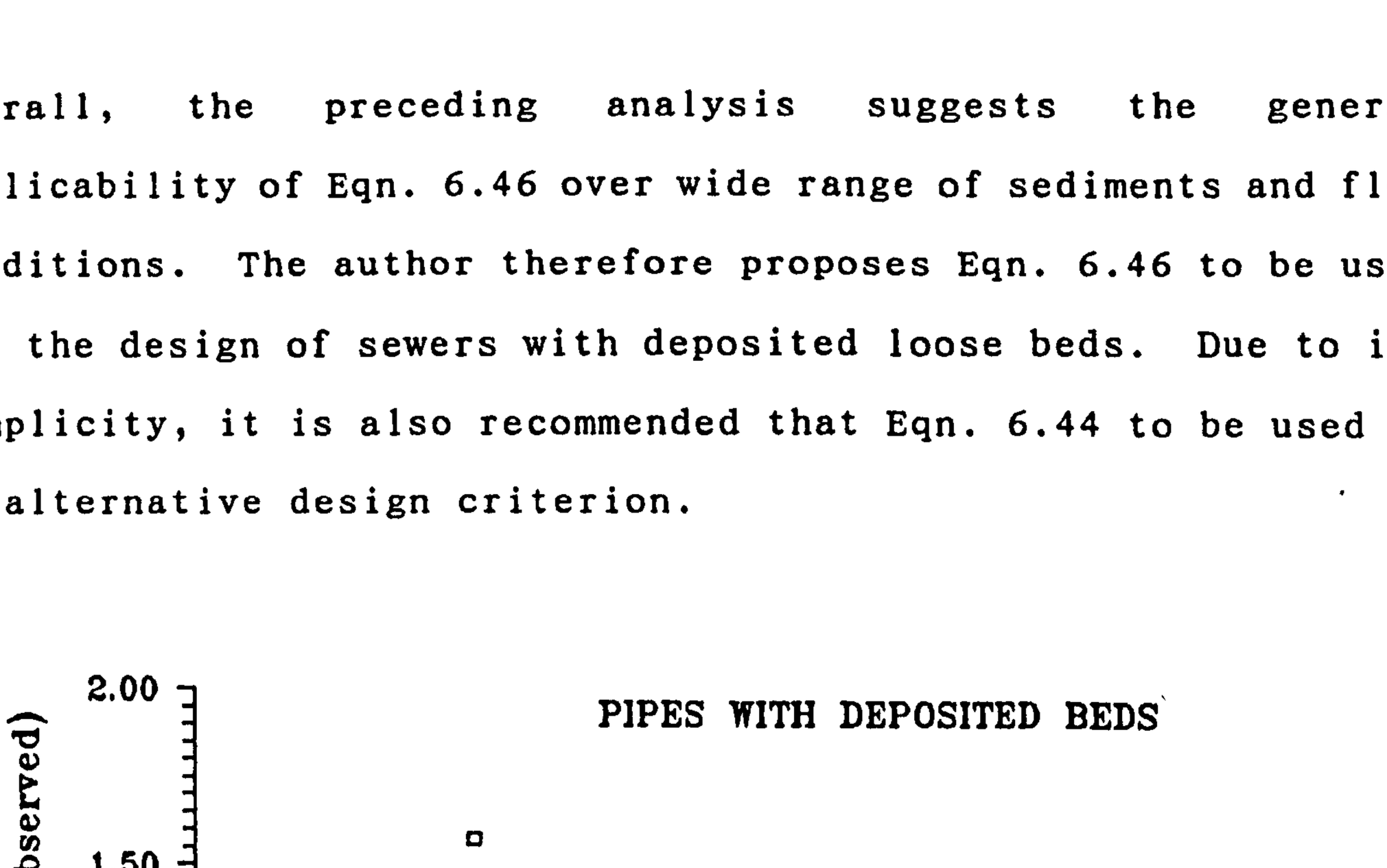

FIG. 6.56e Discrepancy ratio for Eqn. 6.46 as a function of velocity

The application of either Eqn. 6.46 or Eqn. 6.44 requires a separate equation for the computation of the overall friction factor (λ_s). As shown earlier in Fig. 5.16 (see Section 5.3.7), the overall friction factor is dependent mainly on the sediment bed thickness and to a lesser extent on the sediment concentration. This suggests the possibility of applying the parameters W_b/y_o and C_v to represent the variation in λ_s. A suitable parameter to characterize the influence of particle sizes on λ_s is also needed and two of the possible parameters are the ratio R/d_{50} and the dimensionless particle size D_{gr}. The author therefore proposes the following function to determine the overall friction factor for pipes with deposited beds:

$$\lambda_s = f\left(C_v, \frac{W_b}{y_o}, \frac{R}{d_{50}}, D_{gr} \right) \qquad (6.47)$$

A multiple regression analysis was performed using the combined data (Table 6.34) and the best-fit equation was found to be:

$$\lambda_s = 0.0014\, C_v^{-0.04} \left(\frac{W_b}{y_o}\right)^{0.34} \left(\frac{R}{d_{50}}\right)^{0.24} D_{gr}^{0.54} \qquad (6.48)$$

with adj. r^2 = 0.60 and s = 0.11. Fig. 6.57 compares the observed and predicted values of λ_s using Eqn. 6.48. The results shown in Fig. 6.57 have an average discrepancy ratio of 1.01 (see Table 6.40) where 78% of the combined data fall within the ± 0.25 range of discrepancy ratio.

TABLE 6.39 DISCREPANCY RATIO (λ_s) FOR EQN. 6.48 - COMBINED DATA (PIPES WITH DEPOSITED BEDS)

Source of data	λ_s (predicted) / λ_s (observed)							No. of data
	Mean	min	max	0.90-1.10 (%)	0.75-1.25 (%)	0.5-1.5 (%)	0.5-2.0 (%)	
Present	0.94	0.63	1.32	41	78	100	100	32
Alvarez (1990)	1.08	0.76	1.49	42	76	100	100	30
Perrusquia (1992)	0.95	0.59	1.93	50	83	97	100	79
May (1993)	1.11	0.55	2.72	31	63	85	94	52
Combined	1.01	0.55	2.72	43	78	95	98	193

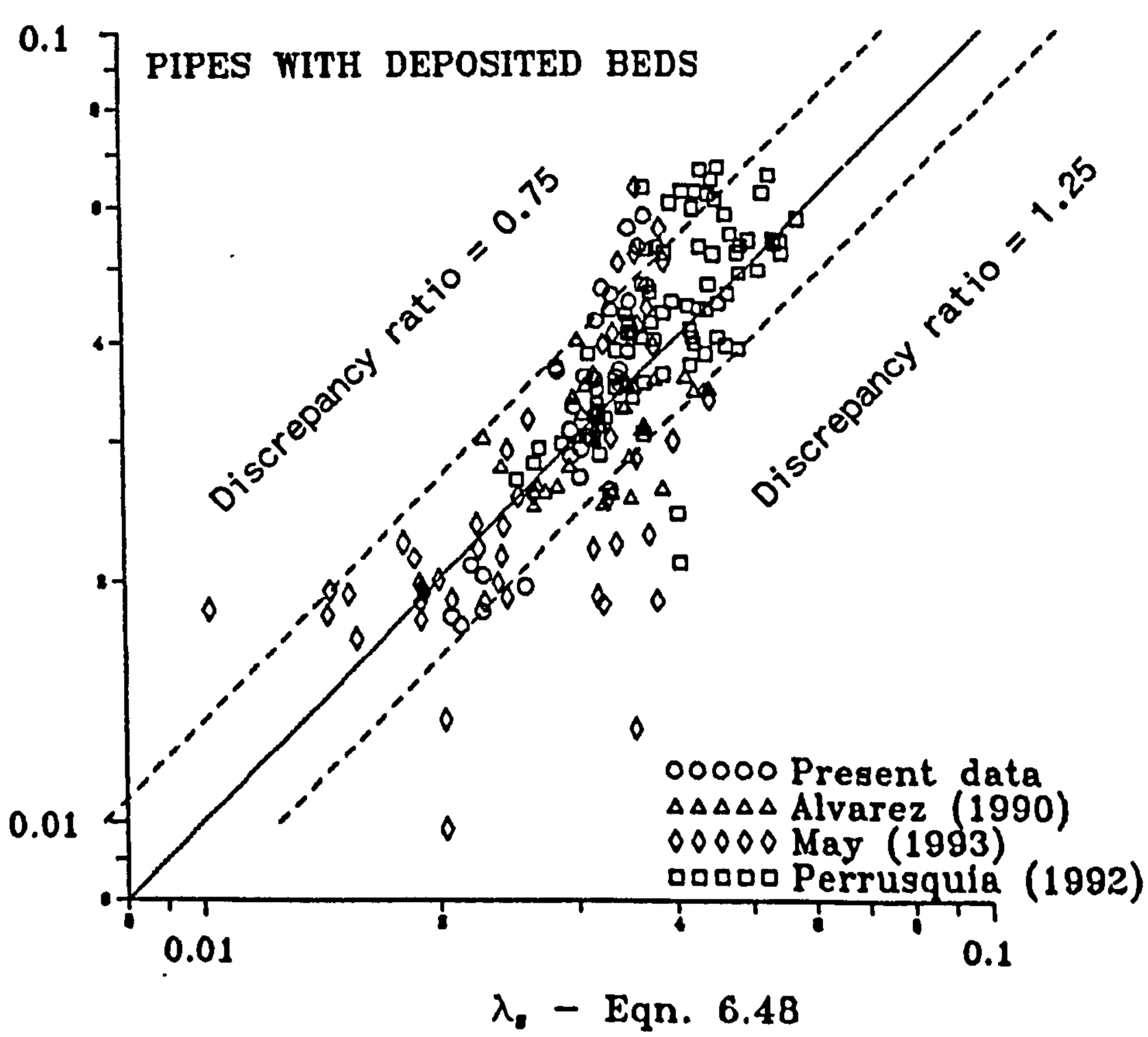

FIG. 6.57 Composite friction factor model for pipes with deposited beds (Combined data)

6.3 Implications for Sewer Design

6.3.1 General

The purpose of the following sections is to assess the UK code of practice (BS 8005, 1987), which requires the use of a constant velocity of 0.75m/s for stormwater sewer design (see Table 2.4), with regard to the equations derived in Sections 6.1 and 6.2. Other relevant equations were also used in the comparisons. Table 6.40 lists the equations used in the comparison.

Based on this assessment, design charts for sediment transport in clean pipes and in pipes with deposited beds were devised.

6.3.2 Assessment of the Constant Velocity Criterion

6.3.2.1 Clean Pipes

In this section (see Table 6.40), the criterion of V = 0.75m/s (with n = 0.012) is compared with author's Eqn. 6.13, Mayerle's Eqn. 3.35 and El-Zaemey's Eqn. 6.38. Eqn. 6.16 was used to evaluate the friction factor with sediment, λ_s.

The plots of discharge (Q) - slope (S_o) - diameter (D) were made for the following assumed conditions:

- volumetric sediment concentration	C_v = 50ppm
- pipe wall roughness value	k_o = 0.0, 0.6mm
- proportional flow depth	y_o/D = 0.50
- characteristic sediment size	d_{50} = 1.0mm
- specific gravity of sediment	S_s = 2.65

TABLE 6.40 EQUATIONS USED FOR THE APPRAISALS OF THE CONSTANT VELOCITY CRITERION

TYPE OF EQUATION	EQUATIONS	EQN. NO
UK CODE	$V = \frac{1}{n} R^{2/3} S_o^{1/2}$	5.2
CLEAN PIPES	$\frac{V}{\sqrt{gd_{50}(S_s-1)}} = 3.08\ C_v^{0.21}\ D_{gr}^{-0.09} \left(\frac{R}{d_{50}}\right)^{0.53} \lambda_s^{-0.21}$	6.13
	$\frac{V}{\sqrt{gd_{50}(S_s-1)}} = 2.56\ C_v^{0.165} \left(\frac{D}{y_o}\right)^{-0.40} \left(\frac{d_{50}}{D}\right)^{-0.57} \lambda_{sb}^{0.10}$	6.38
	$\frac{V}{\sqrt{g(S_s-1)d}} = 14.43\ C_v^{0.18} D_{gr}^{-0.14} \left(\frac{d}{R}\right)^{-0.56} \lambda_s^{0.18}$	3.35
	$\lambda_s = 1.13\ \lambda_o^{0.98}\ C_v^{0.02}\ D_{gr}^{0.01}$	6.16
PIPES WITH DEPOSITED BEDS	$\frac{V}{\sqrt{gd_{50}(S_s-1)}} = 2.28\ C_v^{0.28} \left(\frac{R}{d_{50}}\right)^{0.28} \lambda_s^{-0.64}$	6.44
	$\frac{V}{\sqrt{gd_{50}(S_s-1)}} = 1.18\ C_v^{0.16} \left(\frac{W_b}{y_o}\right)^{-0.18} \left(\frac{d_{50}}{D}\right)^{-0.34} \lambda_s^{-0.31}$	6.46
	$\frac{V}{\sqrt{g(S_s-1)d}} = K\left(1 + J\ C_v^{1/m}\right)$	3.29
	$\lambda_s = 0.0014\ C_v^{-0.04} \left(\frac{W_b}{y_o}\right)^{0.34} \left(\frac{R}{d_{50}}\right)^{0.24} D_{gr}^{0.54}$	6.48

It should be noted that somewhat different comparisons would emerge for other sediment sizes and concentrations, other pipe wall roughness values and proportional flow depths.

Fig. 6.58 shows the results of the comparison for the smooth clean pipes. This shows that the constant velocity criterion overdesigns the slope for D < 300mm. For large diameters, however, steeper slopes are required. Fig. 6.58 also shows that the author's Eqn. 6.13 has best agreement with El-Zaemey's Eqn. 6.38 for diameters up to 1.0m. On the other hand, Mayerle's Eqn. 3.35 gives the largest slopes for all pipe diameters considered.

Fig. 6.59 gives the results of the comparison for rough clean pipes. This shows that the constant velocity criterion overdesigns the slope for D < 200mm. This indicates that pipe wall roughness should be taken into consideration in the design of sewers with clean inverts. Fig. 6.59 also illustrates once again that author's Eqn. 6.13 has the best agreement with El-Zaemey's Eqn. 6.38 and that Mayerle's Eqn. 3.35 provides the largest slopes.

From these comparisons, it can be concluded that the constant velocity criterion is inadequate for pipe diameters larger than 300mm. Also, the pipe wall roughness should be considered when sizing the sewers with clean inverts. The best agreement with author's Eqn. 6.13 is given by El-Zaemey's Eqn. 6.38.

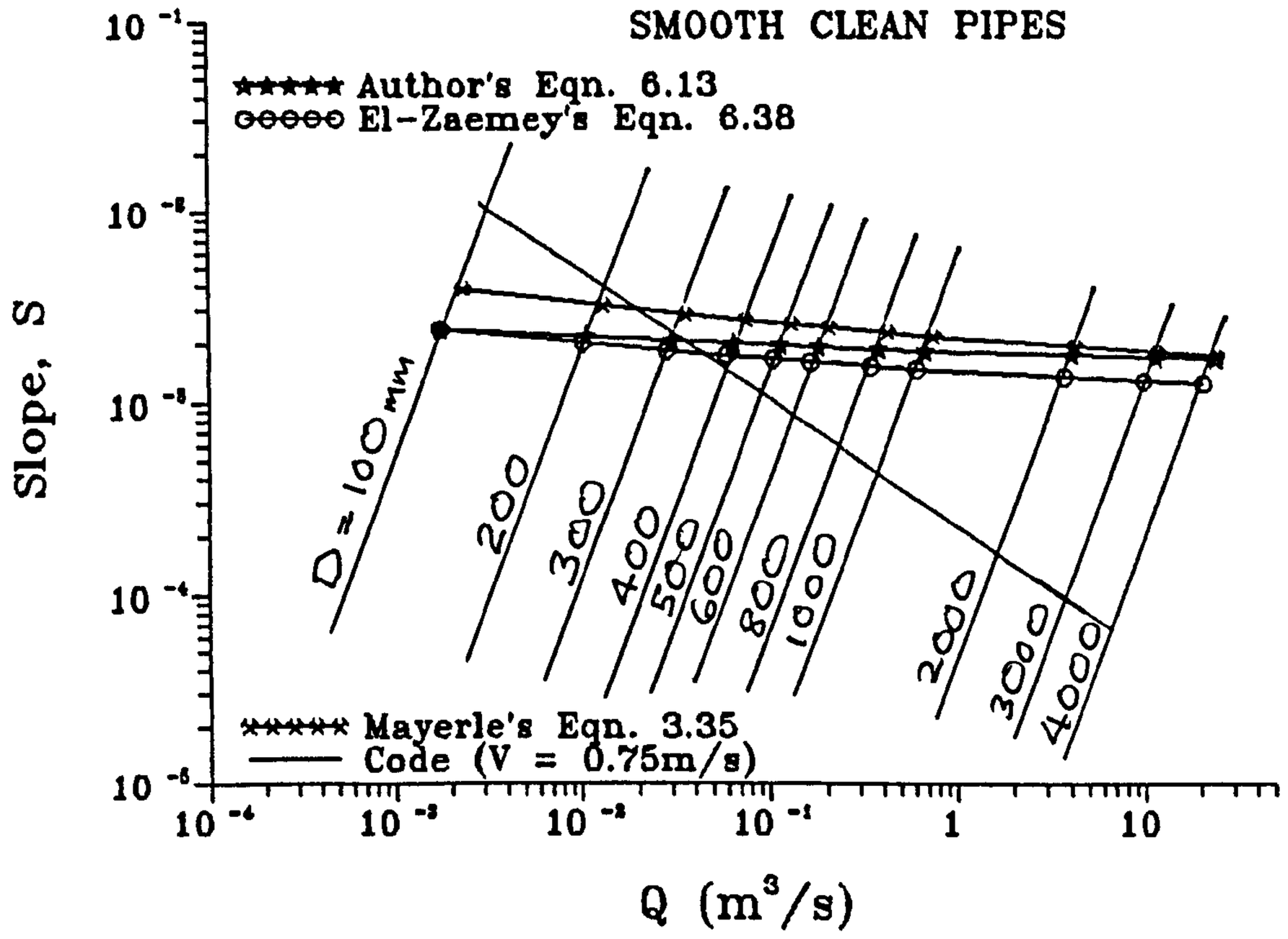

FIG. 6.58 Q–S–D Plot – d_{50} = 1.00mm
(C_v = 50ppm, y_o/D = 0.5, k_o = 0.0mm)

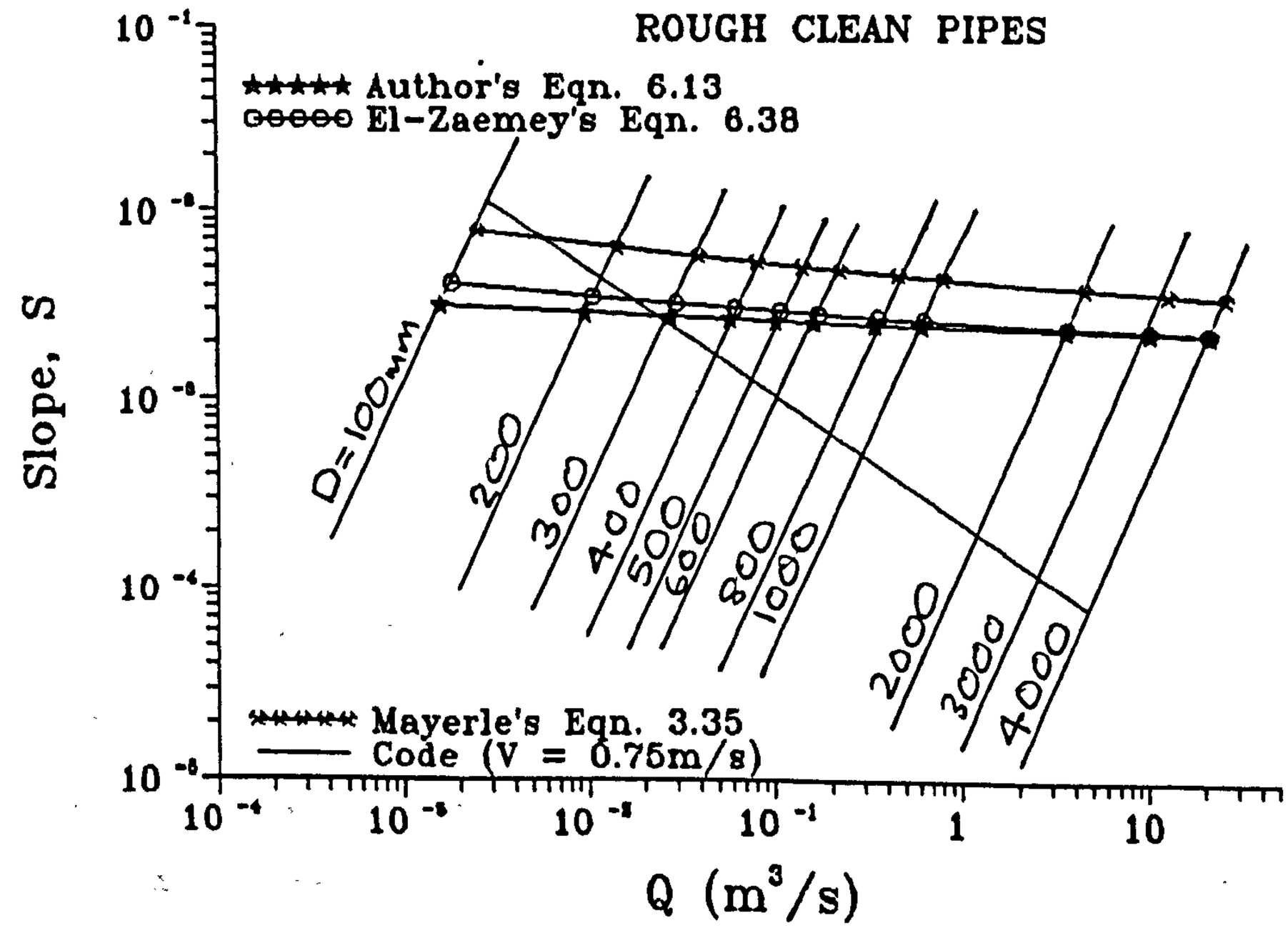

FIG. 6.59 Q–S–D Plot – d_{50} = 1.00mm
(C_v = 50ppm; y_o/D = 0.5, k_o = 0.6mm)

6.3.2.2 Pipes with Deposited Loose Beds

In this section (see Table 6.40), the criterion of V = 0.75m/s (with n = 0.012) is compared with author's Eqns. 6.46 and 6.44, and Ackers' Eqn. 3.29. The overall friction factor was computed from Eqn. 6.48. To illustrate the effect of sediment deposits on the sewer transporting capacity, the author's Eqn. 6.13 in conjunction with Eqn. 6.16 for λ_s is also considered.

The plots of Q - S - D were made for the following specified conditions:

- volumetric sediment concentration	C_v = 50ppm
- pipe wall roughness value	k_o = 0.6mm
- overall proportional flow depth	Y/D = 0.50
- proportional sediment bed depth	y_s/D = 0.01, 0.10
- characteristic sediment size	d_{50} = 1.0mm
- specific gravity of sediment	S_s = 2.65

It should be noted again that somewhat different comparisons would emerge for other sediment sizes and concentrations, sediment bed thickness and overall flow depth.

Fig. 6.60 shows the results of the comparison with small depth of sediment deposits (y_s/D = 1%). It should be noted that the Ackers' Eqn. 3.29 was computed assuming W_e = 0.04D. Considering the equations for pipes with sediment beds only (Eqns. 6.46, 6.44 and 3.29), Fig. 6.60 shows that the constant velocity criterion overdesigns the slope for D < 300mm and which is similar to that of smooth clean pipes. Also, Ackers' Eqn. 3.29 seems to give much higher slopes for D > 300mm compared to the slopes given by the author's Eqns. 6.46 and 6.44. Fig. 6.60 also shows that

author's Eqn. 6.46 agrees well with author's Eqn. 6.13 (clean pipes) for pipe diameters up to 1.0m. This suggests that for pipe diameters up to 1.0m, sewers can be designed with clean inverts. However, for larger diameters, the sewers should be designed with a proportion of its diameter covered with sediment bed.

Fig. 6.61 shows the results of the comparison with a significant depth of sediment deposits (y_s/D = 10%). It should be noted that the actual width of sediment bed was used in applying Ackers' Eqn. 3.29. The results show that the constant velocity criterion overdesigns the slope for D < 500mm. This indicates the advantage of having a proportion of sewers covered by the sediment bed. Also, the slopes provided by the equations for pipes with sediment beds (Eqns. 6.46, 6.44, 3.29) are much milder than those given by the clean pipe equation (Eqn. 6.13). This again suggests that for large pipe diameters, the sewers should be allowed to have a limited depth of sediment deposits. Fig. 6.61 also shows that author's Eqn. 6.46 has good agreement with Ackers' Eqn. 3.29 over the range of pipe diameters.

From these comparisons, it can be concluded that the sewers can be designed with clean inverts for diameters up to 1.0m while the larger diameters should be designed by allowing a limited depth of sediment deposits.

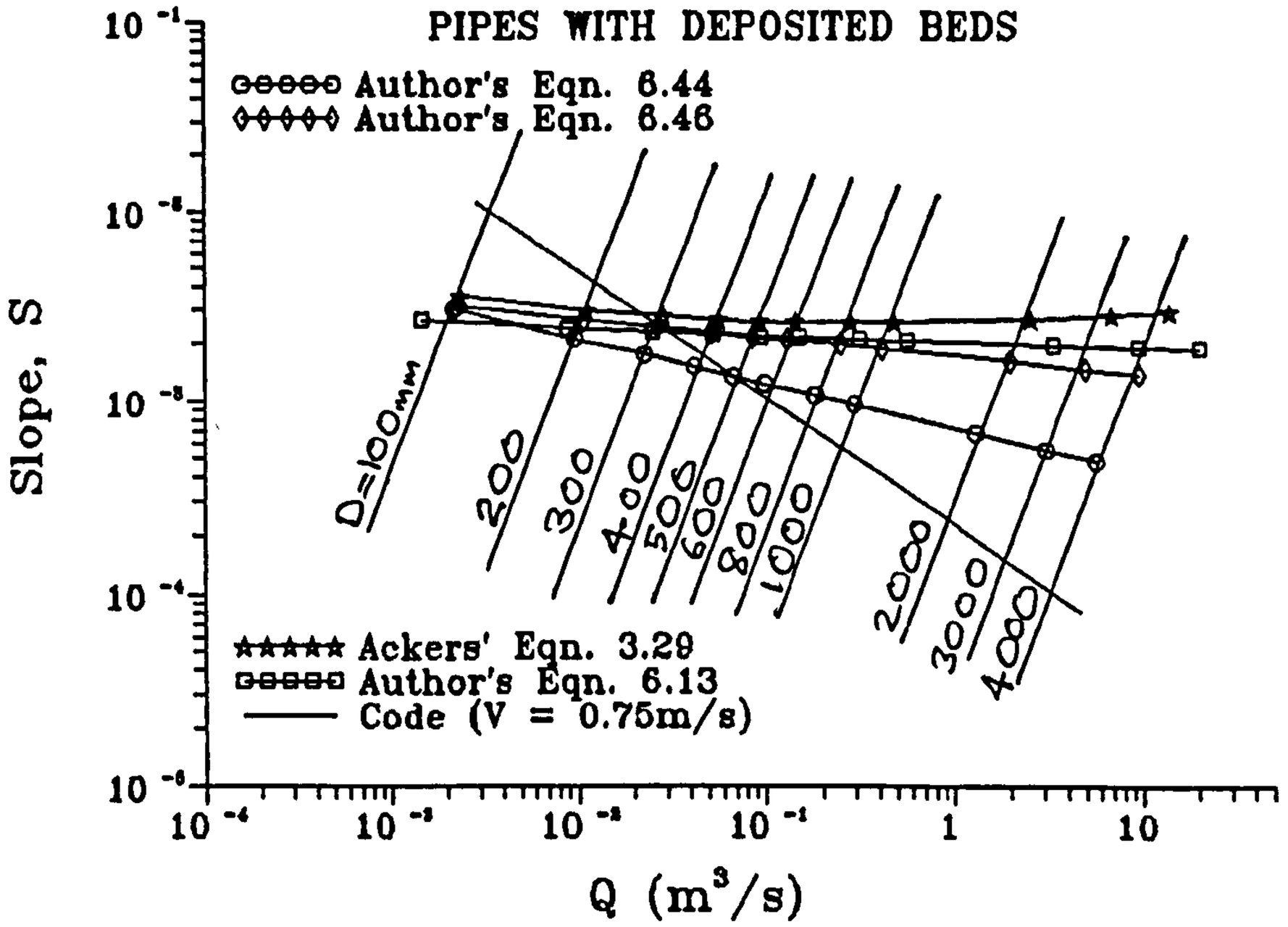

FIG. 6.60 Q–S–D Plot – d_{50} = 1.00mm
(C_v = 50ppm, Y/D = 0.5, y_s/D = 0.01)

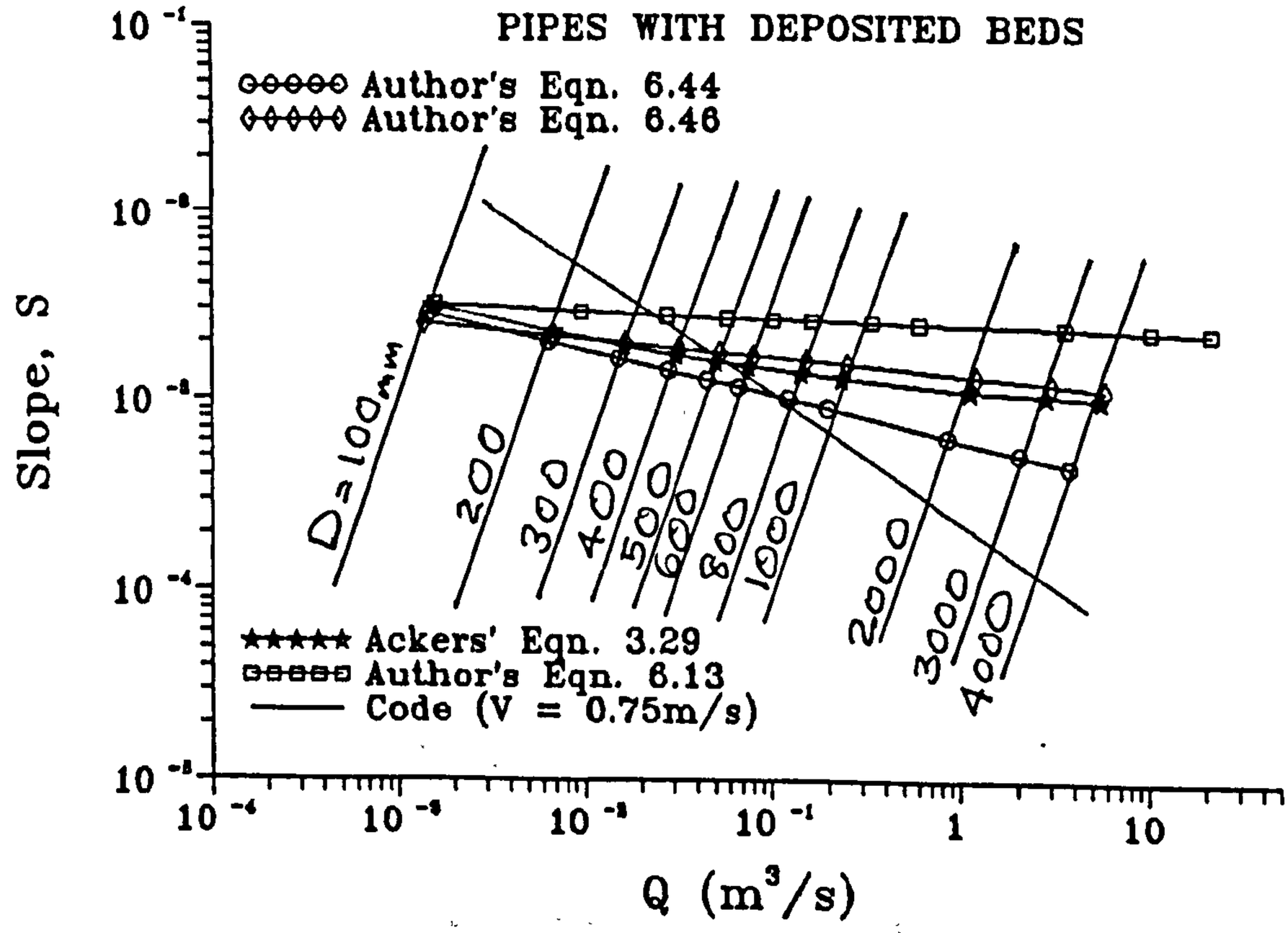

FIG. 6.61 Q–S–D Plot – d_{50} = 1.00mm
(C_v = 50ppm, Y/D = 0.5, y_s/D = 0.1)

6.3.3 Design Charts

Based on the comparisons in the previous sections, the design charts for clean pipes and pipes with deposited beds were devised considering the following specified conditions:

- volumetric sediment concentration	C_v = 50ppm
- pipe wall roughness value	k_o = 0.6mm
- overall proportional flow depth	Y/D = 0.25, 0.50, 0.75
- characteristic sediment size	d_{50} = 1.0mm
- specific gravity of sediment	S_s = 2.65

For diameters up to 1.0m, author's Eqn. 6.13 in conjunction with Eqn. 6.16 for λ_s was used to obtain the required slope. For diameters between 1.0m and 4.0m, author's Eqn. 6.46 in conjunction with Eqn. 6.48 for λ_s was used to compute the required slopes with a pre-determined "optimum" proportional bed thickness (y_s/D).

The following computations were made to obtain the "optimum" proportional sediment bed thickness. For a given overall flow depth, the required slope for each diameter was computed by assuming several values of y_s/D (see Fig. 6.62). It was found that the lowest slope on the curve for each pipe diameter occurs at a similar value of y_s/D which was then taken as the "optimum" depth. Fig. 6.62 illustrates the "optimum" y_s/D for each overall flow depth. This shows that the optimum y_s/D increases with an increase in overall flow depth. This trend is expected since the flow in sewers will adjust itself so as to obtain an equilibrium condition with a larger flow depth for the large y_s/D.

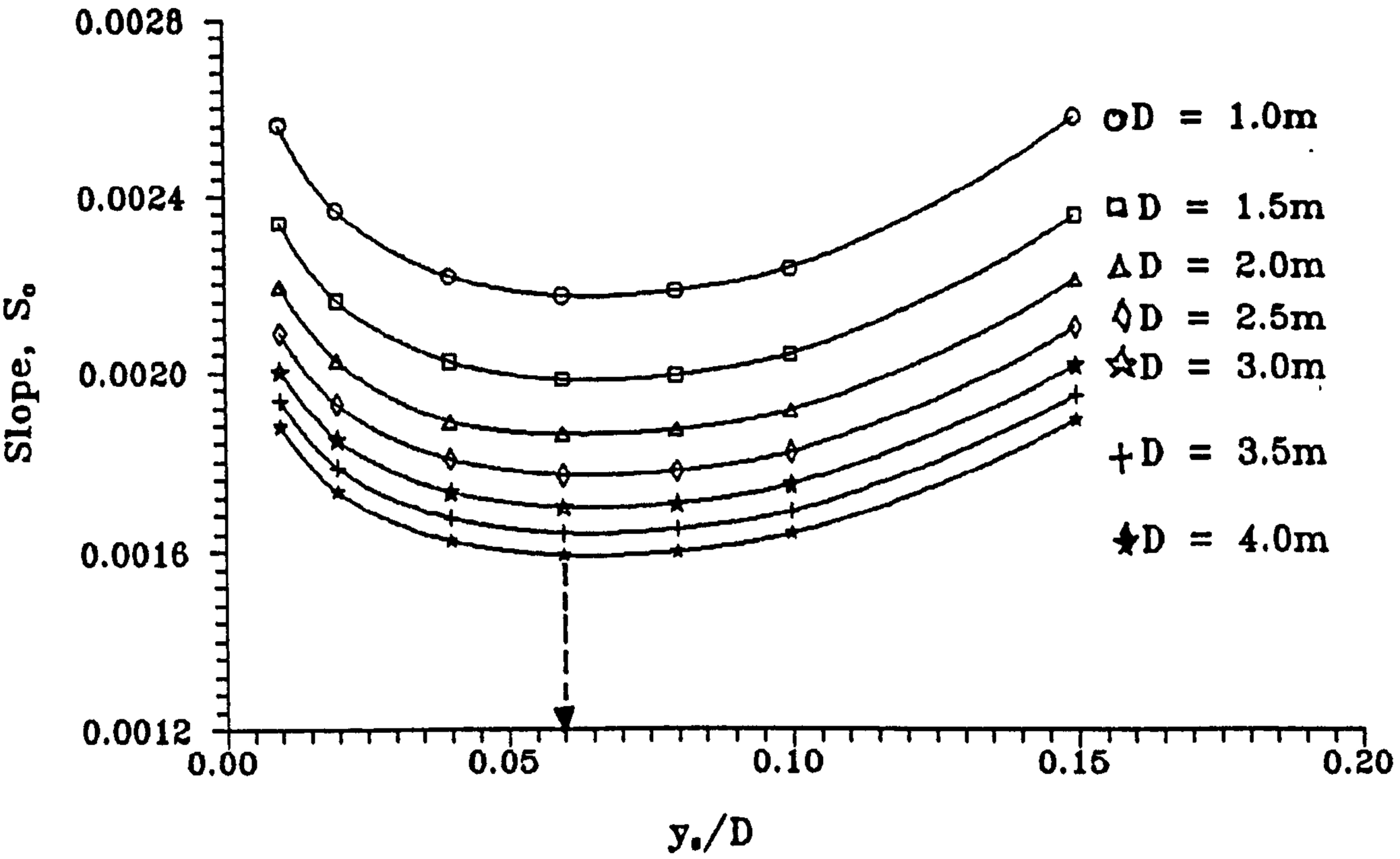

FIG. 6.62a Optimum sediment depth : d_{50} = 1.0mm
(C_v = 50ppm, Y/D = 0.25)

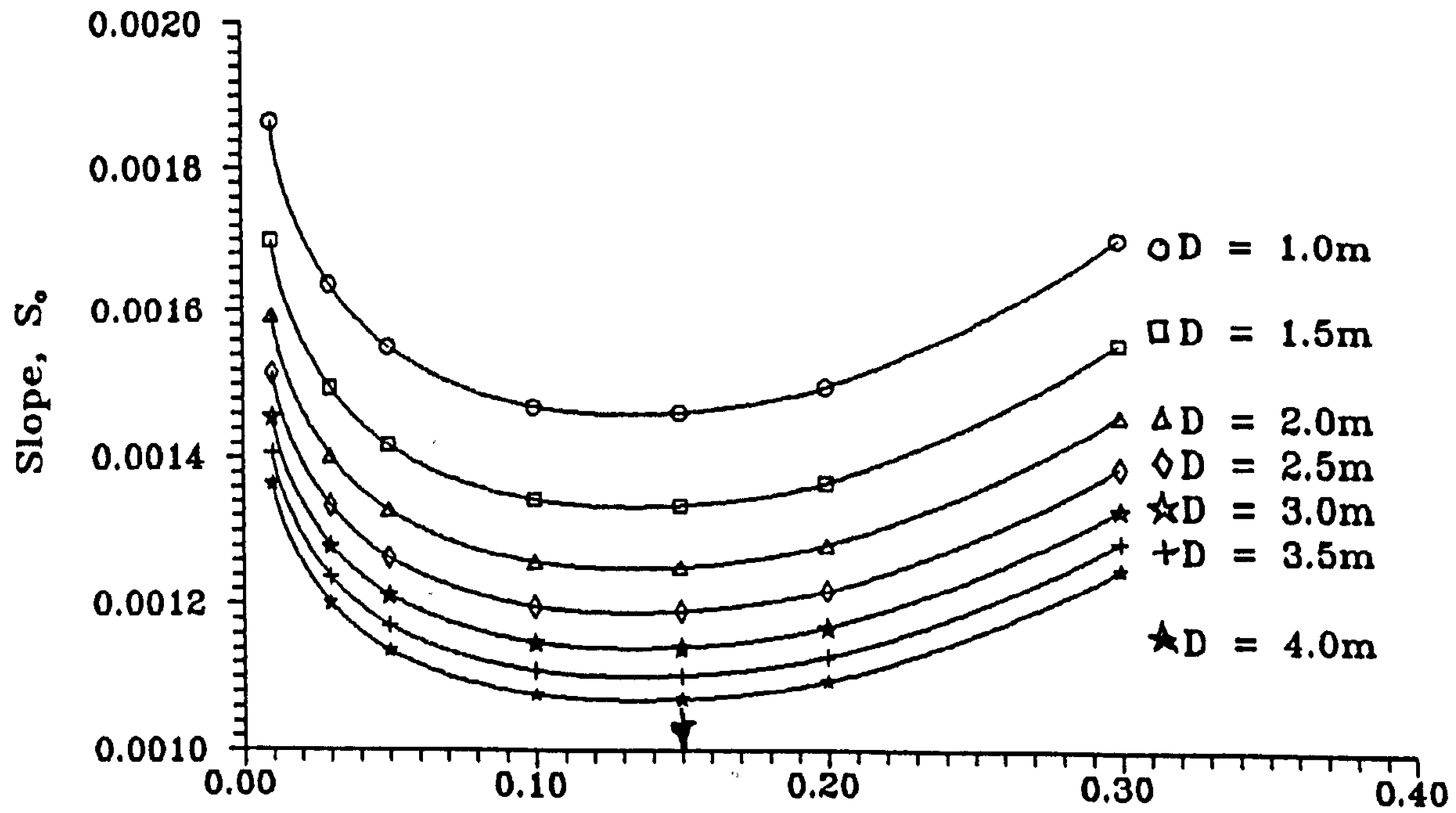

FIG. 6.62b Optimum sediment depth : d_{50} = 1.0mm
(C_v = 50ppm, Y/D = 0.50)

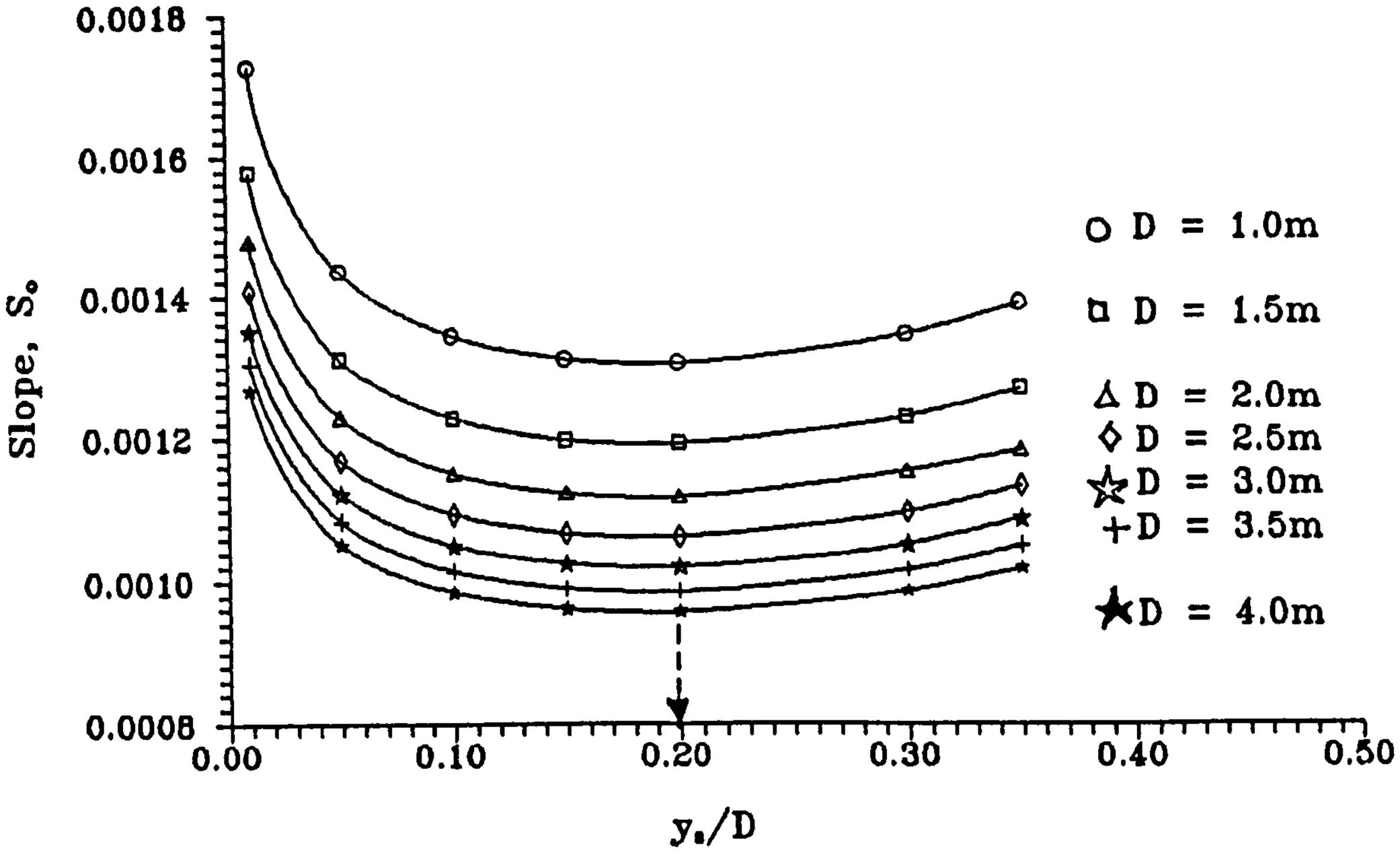

FIG. 6.62c Optimum sediment depth : d_{50} = 1.0mm
(C_v = 50ppm, Y/D = 0.75)

Figs. 6.63 and 6.64 show the design charts for clean pipes and pipes with deposited beds. Fig. 6.64 shows that sewers should be designed with continuous loose beds for overall flow depth larger than 0.5. Separated dunes should be expected for overall flow depth less than 0.5.

It should be re-affirmed that somewhat different positions of the curves would be obtained for different sediment sizes and concentrations.

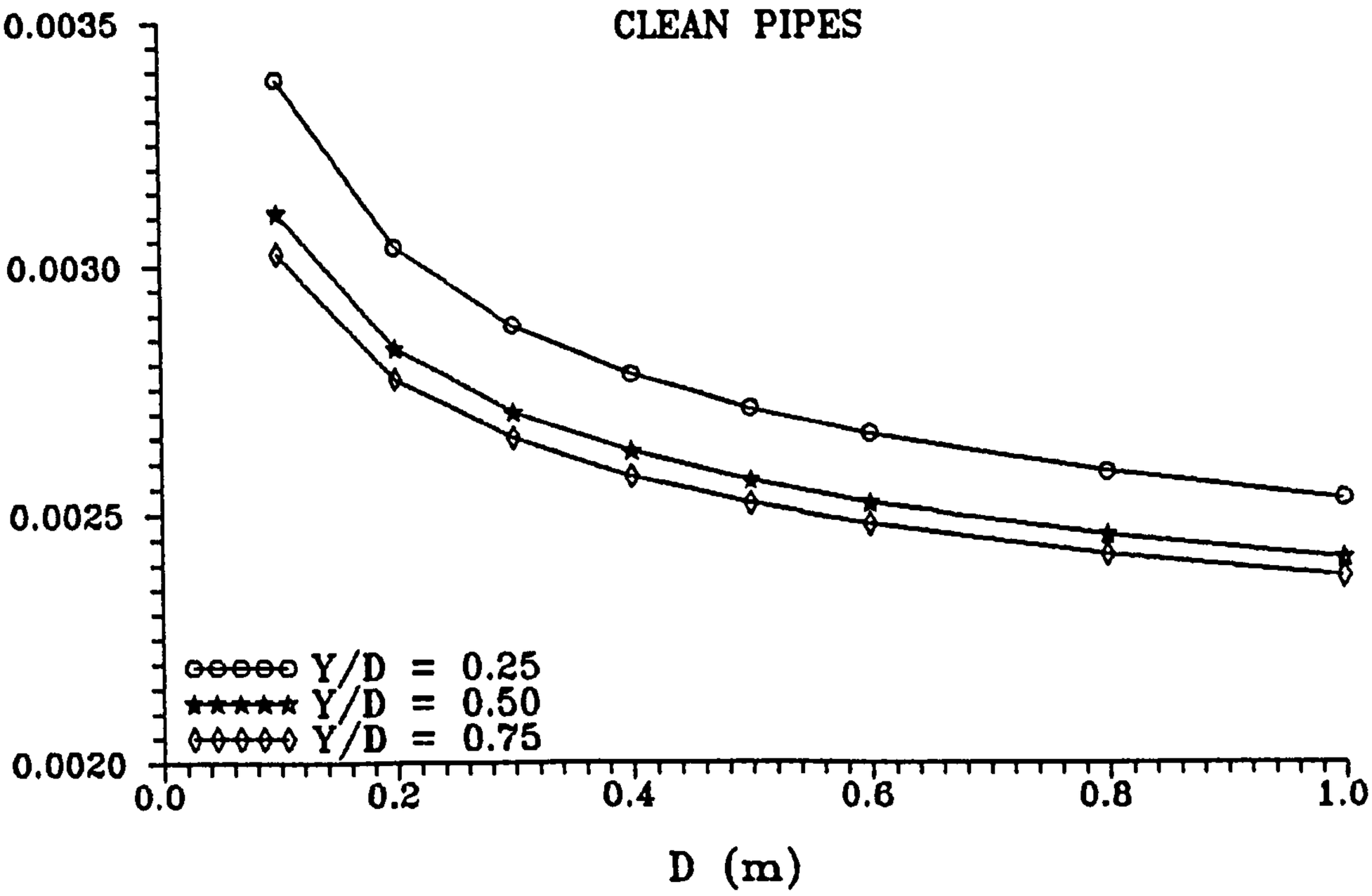

FIG. 6.63 Design chart for clean pipes
(C_v = 50ppm, d_{50} = 1.0mm, k_o = 0.6mm)

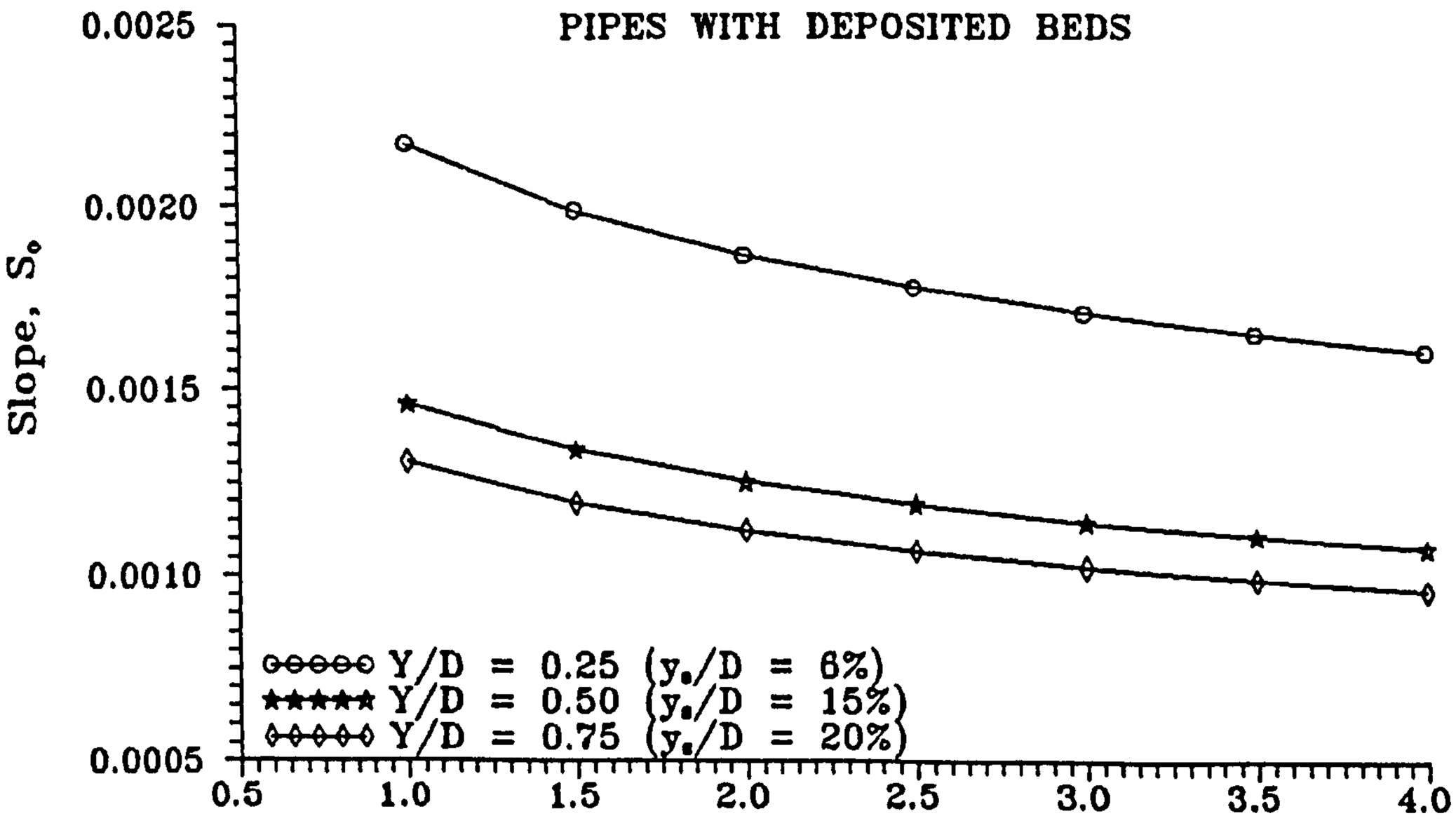

FIG. 6.64 Design chart for pipes with deposited beds
(C_v = 50ppm, d_{50} = 1.0mm)

CHAPTER 7

CONCLUSIONS AND RECOMMENDATIONS FOR FURTHER RESEARCH

7.1 Conclusions

The present experimental programme covered the sediment transport in pipes for both smooth (D = 154mm - 450mm) and rough (D= 305mm) rigid and loose (D = 450mm) boundaries. The results obtained in terms of new transport equations permit the appraisals of the present design and maintenance practice of sewers. The range of applicability of these new results will be for non-cohesive sediments moving as bed load either in clean pipes (no deposition) or pipes with deposited loose beds flowing part-full. The results from the present studies will be divided according to the type of boundary upon which the experiments have been conducted namely rigid and loose boundaries. Finally, the design implications based on the new transport equations are given.

7.1.1 Clean Pipes (Rigid Boundary)

The clear water experiments (see Section 5.2) conducted preceding sediment transport experiments allow the assessment of the current practice of applying Colebrook-White's equation (Eqn. 5.6) to compute the friction factor without sediment (λ_o) for part-full flows after substituting D = 4R (Eqn. 5.7). The present clear water data shows that the modified Colebrook-

White's Eqn. 5.7 applies equally well to part-full flows (Fig. 5.4).

Preliminary analyses (see Section 5.3) on the present data at the limit of deposition show that the self-cleansing velocity (V) is affected by the volumetric sediment concentration (C_v), flow depth (y_o), particle size (d_{50}), surface roughness (k_o) and pipe size (D). The results indicate that the required self-cleansing velocity increases as the volumetric sediment concentration, flow depth and pipe size increase, and decreases as the particle size increases. The presence of a rougher surface could either increase or decrease the required self-cleansing velocity depending on whether the effects of the increase in flow resistance or the additional turbulence due to secondary currents is more dominant. The sediment transport also causes the increase in friction factor as shown in Figs. 5.14 and 5.15.

Comparisons of the existing equations for clean pipes (see Section 6.1.2) shows that none of them agrees well with the present data. In general, within the range of the data tested, the equations that give the best results are fairly simple regression equations such as those of Laursen' Eqn. 3.11 and Novak-Nalluri's Eqn. 3.15. Also, the comparisons highlighted the important effect of boundary roughness in the prediction of the limiting concentrations.

Several forms of functional relationships (see Section 6.1.3.2) were evaluated to obtain the best-fit model representing the

sediment transport in clean pipes. In this analysis, extensive use of data from the present and other relevant studies were made. The proposed equation (Eqn. 6.13) includes all the important variables affecting the sediment transport in clean pipes as discussed in Section 5.3. The equation is based on a large number of experimental data (a total of 459) covering wide range of flow conditions and sediments expected to occur in sewers. Eqn. 6.13 is applied in conjunction with Eqn. 6.16 (for λ_s) to give the required slope for new sewers.

Ackers' Eqn. 3.29 was modified for use in clean pipes by replacing his definition of the incipient motion condition (Eqn. 3.30) with that of Novak-Nalluri's Eqn. 3.5 (see Section 6.1.3.3). Extensive analyses on all available data from clean pipe channels suggests that the values of effective width (W_e) to be used with the modified Ackers' equation are a function of sediment size (i.e. $W_e = f(d_{50})$). The suggested values of W_e are given in Table 6.23.

Attempts were also made to assess the applicability of El-Zaemey's (1991) equations for their applications to other channel shapes (see Section 6.1.3.4). El-Zaemey's suggestion of applying his equation (Eqn. 3.58) to clean pipes by replacing the bed width term by the value 0.5D (Eqn. 6.38) is further confirmed with author's and other data as shown in Figs. 6.31 and 6.32. El-Zaemey's Eqn. 3.57 for friction factor with sediment (λ_s) could also be modified with b = 0.5D (Eqn. 6.39) to be applicable for clean pipes (see Fig. 6.34). Further modification to Eqn.

3.58 was made to suit data from rigid bed rectangular channels (Figs. 6.39 - 6.42). Extensive analyses on the available data from several studies suggest that this can be achieved by substituting the pipe diameter (D) by 1.35b (Eqn. 6.40). It was also found that El-Zaemey's Eqn. 3.57 could be applied directly to compute λ_s in the case of rectangular channels (see Fig. 6.44).

7.1.2 Pipes with Deposited Beds (Loose Boundary)

In the present studies limited data was obtained in the 450mm dia. pipe using a 0.72mm sand with the proportional sediment bed thickness (y_s/D) varying from 0.0002 to 0.23 (see Table 5.2c). Both types of bed namely, separated dunes and continuous loose beds were observed.

In the presence of loose beds, the flow transporting capacity of the sewers could be affected in two ways (see Sections 5.3.6 and 5.3.7). Firstly, the increase in the width of sediment bed with sediment thickness (Fig. 5.13) will result in an increase in the flow transporting capacity. The increase in volumetric sediment concentration could be caused by the larger space available for the sediment to move. Secondly, the increase in the sediment thickness will also increase the overall friction factor with sediment as shown in Fig. 5.16. This might offset some or all the gain in the transporting capacity associated with the increase in the sediment bed width for large bed thickness. The

results suggest that an optimum sediment bed thickness would be obtained when the gain in the transporting capacity could be maintained without the necessity to increase the sewer slope.

Comparisons of the data from the present study with several transport equations show that the best performance is given by May's Eqn. 3.46 followed by Graf-Acaroglu's Eqn. 3.63 and Ackers' Eqn. 3.29. The results of the comparisons also suggest that a simple form of equation such as that of Graf-Acaroglu's (see Fig. 6.45) should be considered for further data analysis.

As in the case of clean pipes, several functions were considered to represent the sediment transport process in pipes with deposited beds (see Section 6.2.3.1). The commonly used function in the form of Φ - Ψ relationship (Eqn. 6.41) was initially utilised. The function correlates well the present data (Eqn. 6.42 - Fig. 6.51) and the combination of data from the present and other relevant studies (Eqn. 6.43 - Fig. 6.52). However, detailed analysis (Fig. 6.54) of the accuracy of Eqn. 6.43 in terms of the limiting velocity (Eqn. 6.44) reveals its inability to cope with the variation in bed thickness and flow depth for a certain range of the combined data (Table 6.34).

Further analysis was made based on the modified El-Zaemey's function (Eqn. 6.45). The resulting equation (Eqn. 6.46) from the regression analysis on the combined data (Table 6.34) has very

high correlation (see Fig. 6.56). This is attributed to the parameter W_b/y_o to account for the variation in the bed thickness and flow depth. The author therefore proposes Eqn. 6.46 to be used for the design of sewers with deposited loose beds. Due to its simplicity, it is also recommended that Eqn. 6.44 to be used as an alternative design criterion. The author also proposes Eqn. 6.48 to be used in the computation of the overall friction factor.

7.1.3 Design Implications

An attempt was made to assess the constant velocity criterion (V = 0.75m/s for half-full flows), suggested by the UK code of practice (BS 8005), with regards to the newly derived equations for clean pipes (Eqn. 6.13) and pipes with deposited beds (Eqn. 6.46). Other relevant equations (El-Zaemey's Eqn. 6.38, Mayerle's Eqn. 3.35, Ackers' Eqn. 3.29 and author's Eqn. 6.44) were also used in the assessment.

The results for clean pipes (Figs. 6.58 and 6.59) suggest that, for the assumed conditions, the constant velocity criterion is inadequate for pipe diameters larger than 300mm and that the pipe wall roughness should be considered when sizing the sewers with clean inverts.

For pipes with deposited beds, the results (Figs. 6.60 and 6.61) for the assumed conditions indicate that the sewers can be

designed with clean inverts for diameters up to 1.0m while the larger diameters should be designed by allowing a limited depth of sediment deposits.

Based on this assessment, the design charts (Figs. 6.63 and 6.64) for clean pipes and pipes with deposited beds were devised. In devising the design chart for pipes with deposited beds, it was found that the slopes of the sewers could be determined for an "optimum" depth of bed thickness (Fig. 6.62). This confirms the trends shown by the present data (Figs. 5.13 and 5.16) as mentioned earlier (see Section 7.1.2).

7.2 Recommendations for Further Research

The present studies have covered all factors affecting the transporting capacity of sewers in clean pipes flowing part-full with non-cohesive sediments moving as bed load. A supplementary study on the effect of deposits in sewers has also been covered. Several features of the sediment movement in sewers need to be dealt with in the future:

1) The experimental work with a large diameter of pipe should be attempted as this will verify the existing equations derived for diameters less than 500mm.

2) The field data should be collected in a format that they could be used to verify the established equations mainly derived from experimental works.

3) The experimental work for the case of suspended load should also be considered to complete the possible mode of transport in sewers with deposited beds.

4) The effect of flow resistance with sediment movement in sewers with deposited beds should be given a priority since the value of overall or composite friction factor is needed to evaluate the sewer transporting capacity or design slope for new sewers.

REFERENCES

Ab. Ghani, A. (1990) " Sediment transport in sewer with a sediment bed: half-full flow." University of Newcastle upon Tyne, England, MSc Thesis.

Ackers, P. (1958) " Resistance of fluids flowing in channels and pipes." Hygraulic Research Paper No. 1, HMSO, London.

Ackers, P (1961) " The hydraulic resistance of drainage conduits." Proc. Institution of Civil Engineers, Vol. 19, pp. 307-336.

Ackers, P (1978) " Urban drainage: the effects of sediment on performance and design criteria." Proc. 1st. Intern. Conf. on Urban Storm Drainage, Southampton, England, pp. 535-545.

Ackers, P (1984) " Sediment transport in sewers and the design implications." Intern. Conf. on Planning, Construction, Maintainence, and Operation of Sewerage Systems, BHRA/WRc, Reading, England, pp. 215-230.

Ackers, P (1991) " Sediment aspects of drainage and outfall design." Proc. Intern. Symposium on Environmental Hydraulics, Hong Kong.

Ackers, P. and White, W.R. (1973) " Sediment transport: new approach and analysis." Jnl. of Hydraulic Division, ASCE, Vol. 99, HY11, pp. 2041-2060.

Ackers, P., Crickmore, M.J., and Holmes, D.W. (1964) " Effects of use on the hydraulic resistance of drainage conduits." Proc. Institution of Civil Engineers, Vol. 28, pp. 339-360.

Alvarez, E.M. (1990) "The influence of cohesion on sediment movement in channels of circular cross-section." University of Newcastle upon Tyne, England, Ph.D thesis.

Ambrose, H.H. (1953) "The transportation of sand in pipes - free surface flow." Proc. 5th. Hydraulics Conf., State University of Iowa Studies in Engineering, Iowa, USA, pp. 77-88.

American Society of Civil Engineers/Water Pollution Control Federation (1969) " Design and construction of sanitary and storm sewers." ASCE manuals and reports on engineering practice, No. 37.

American Society of Civil Engineers/American Environment Federation (1992) "Design and Construction of Urban Stormwater Management Systems." ASCE manuals and reports on engineering practice, No. 77.

Arora, A.K., Ranga Raju, K.G., and Garde, R.J. (1984) "Criterion for deposition of of sediment transported in rigid boundary channels." Proc. 1st. Intern. Conf. on Channels and Channel Control Structures, Southampton, England, pp. 45-56.

Ashley, R.M. and Crabtree, R.W. (1992) "Sediment origins, deposition, and build-up in combined sewers systems." Water Science and Technology, Vol. 25, No. 8, pp. 1-12.

Ashley, R.M., Coghlan, B.P., and Jefferies, C. (1990) " The quality of sewerage flows and sediment in Dundee." Water Science and Technology, Vol. 22, No. 10/11, pp. 39-46.

Ashley, R.M., Arthur, S., Coghlan, B.P., and McGregor, I. "Fluid sediment in combined sewers." To be published in Water Science and Technology.

Ashley, R.M., Wotherspoon, D.J.J., Coghlan, B.P., and McGregor, I. (1992) " The erosion and movement of sediments and associated pollutants in combined sewers." Water Science and Technology, Vol. 25, No. 8, pp. 101-114.

Ashley, R.M., Wotherspoon, D.J.J., Goodison, M.J., McGregor, I., and Coghlan, B.P. (1992) " The deposition and erosion of sediment in sewers." Water Science and Technology, Vol. 26, No. 5-6, pp. 1283-1293.

Bachoc,A. (1992) " Location and general characteristics of sediment deposits into man-entry combined sewers." Water Science and Technology, Vol. 25, No. 8, pp. 47-56.

Bain, A.G. and Bonnington, S.T. (1970) The Hydraulic Transport of Solids by Pipeline, Pergamon Press, Oxford, England.

Bertrand-Krajewski, J.L. (1992) " A model for solid production and transport for small urban catchments: preliminary results." Water Science and Technology, Vol. 25, No. 8, pp. 29-36.

Bertrand-Krajewski,J.L., Briat, P., and Scrivener, O. (1993) " Sewer sediment production and transport modelling: A literature review." Jnl. of Hydraulic Research, Vol. 31, No. 4, pp. 435-460.

British Standard Institution (1987) " Sewerage - guide to new sewerage construction." BS 8005, Part 1.

Brownlie, W.R. (1981) " Prediction of flow depth and sediment discharge in open channels." California Institute of Technology, Pasadena, California, USA, Ph.D thesis.

Butler, D., Thedchanamoorthy, S., and Payne, J.A. (1992) " Aspects of surface sediment characteristics on an urban catchment in London." Water Science Technology, Vol. 25, No. 8, pp. 13-19.

Chadwick, A. and Morfett, J. (1993) Hydraulics in Civil Engineering. Allen & Unwin, London, England.

Chebbo,G., Musquere, P., and Bachoc, A. (1990) " Solids transferred into sewers." 5th. Intern. Conf. on Urban Storm Drainage, Osaka, Japan, pp. 885-890.

Chow, V.T. (1973) Open-Channel Hydraulics. Mc-Graw Hill, London, England.

Clark, P.B., Payne, J.A., and May, R.W.P. (1993) " Design of sewers to control sediment problems." Proc. 6th. Intern. Conf. on Urban Storm Drainage, Niagara Falls, Canada, pp. 851-856.

Construction Industry Research and Information Association (1987) "Sediment movement in combined sewerage and stormwater drainage systems." CIRIA, London, England, Project Report Phase 1.

Crabtree, R.W. (1988) " A classification of combined sewers sediment types and characteristics." WRc Engineering, Swindon, England, Report ER 324E.

Crabtree, R.W., Ashley, R.M., and Saul, A.J. (1991) " Review of research into sediments in sewers and ancilliary structures." Foundation for Water Research, Report FR0205.

Craven, J.P. (1953) "The transportation of sand in pipes - full-pipe flow." Proc. 5th. Hydraulic Conf., State University of Iowa Studies in Engineering, Iowa, USA, pp. 67-76.

Dake, J.M.K. (1983) Essentials of Engineering Hydraulics. MacMillan, 2nd. edition, London, England.

Daniel, C. and Wood, F.S. (1980) Fitting equations to data. John Wiley & Sons, 2nd. edition, New York, USA.

Durand, R (1953) " Basic relationships of the transportation of solids in pipes." 5th Congress, IAHR, Minneapolis, USA, pp. 89-103.

El-Zaemey, A.K.S. (1991) " Sediment transport over deposited beds in sewers." University of Newcastle upon Tyne, England, Ph.D thesis.

Engelund, F. and Hansen, E. (1967) " A monograph on sediment transport in alluvial streams." Teknisk Forlag, Copenhangen, Denmark.

Featherstone, R.E. and Nalluri, C. (1988) Civil Engineering Hydraulics, Blackwell Scientific Publication, Oxford, England.

Garde, R.J. and Ranga Raju, K.G. (1985) Mechanics of Sediment Transportation and Alluvial Stream Problems. John Wiley & Sons, 2nd. edition, New Delhi, India.

Graf, W.H. (1984) Hydraulics of Sediment Transport, Water Resources Publication, Fort Collins, USA.

Graf, W.H. and Acaroglu, E.R. (1968) " Sediment transport in conveyance systems." Bulletin IAHR, Part 1, Vol. XIII, No. 2, pp. 20-39.

Graf, W.H. and Suszka, L. (1987) " Sediment transport in steep channels." Jnl. of Hydroscience and Hydraulic Engineering, Vol. 5, No. 1, pp. 11-26.

Henderson, R.J. (1984) "A guide to hydraulic roughness in sewers." WRc Engineering, Swindon, England, External Report E. 131E.

Henderson, R.J. (1984) "The hydraulic roughness of used sewers." Proc. Intern. Conf. on Planning, Construction, Maintainence, and Operation of Sewerage Systems, BHRA/WRc, Reading, England, pp. 337-354.

Hines, W. H. and Montgomery, D.C. (1990) Probability and Statistics in Engineering and Management Science, John Wiley & Sons, New York, USA.

Hydraulics Research Ltd. (1990) "Charts for the hydraulic design of channels and pipes." 6th. edition, Thomas Telford Ltd., London, England.

Hydraulics Research Ltd. (1993) " Sediment transport: The Ackers and White theory revised." Hydraulics research Ltd., Wallingford, England, Report SR 237.

Kabir, M.R. and Torfs, H. (1992) "Comparisons of different methods to calculate bed shear stress." Water Science Technology, Vol. 25, No. 8, pp. 131-140.

Kithsiri, M.M.A.U. (1990) "Sediment transport in rectangular channels with rough rigid beds." University of Newcastle upon Tyne, England, PhD thesis.

Kleijwegt, R.A. (1992) "On sediment transport in circular sewers with non-cohesive deposits." Technical University of Delft, Ph.D Thesis.

Kleijwegt, R.A. (1992) "Sewer sediment models and basic knowledge." Water Science and Technology, Vol. 25, No. 8, pp. 123-130.

Laplace, D., Bachoc, A., Sanchez, Y., and Dartus, D. (1992) "Trunk sewer clogging development - description and solutions." Water Science and Technology, Vol. 25, No. 8, pp. 91-100.

Larson, M., Berndtsson, R., and Hogland, W. (1990) " Field measurements and mathematical modeling of pollution build-up and pipe-deposit wash-out in combined sewers." 5th. Intern. Conf. on Urban Storm Drainage, Osaka, Japan, pp. 325-332.

Laursen, E.M. (1956) " The hydraulics of a storm-drain system for sediment-transporting flow." Iowa Highway Research Board, USA, Bulletin No.5.

Lavelle, J.W. and Mofjeld, H.O. (1987) "Do critical stresses for incipient motion and erosion really exist?" Jnl. of Hydraulic Engineering, ASCE, Vol. 113, No. 3, pp. 370-385.

Loveless, J.H. (1986) " Sediment transport in circular and non-circular conduits." Proc. Conf. on Hydraulic Design: Land Drainage, Southampton, England, pp. 315-324.

Loveless, J.H. (1991) " Sediment transport in rigid boundary channels with particular reference to the condition of incipient deposition." University of London, Ph.D thesis.

Lyngfelt, S. (1990) "Hydraulic properties in sewers with sediment." 5th. Intern. Conf. on Urban Storm Drainage, Osaka, Japan, pp.921-925.

Macke, E. (1982) " About sedimentation at low concentrations in partly filled pipes." Technical University of Braunschweig, Germany, Ph.D thesis.

Macke, E. (1983) " Determination of sediment-free flow conditions in sewer pipes." Korrespondenz Abwasser, Vol. 30, No. 7, pp. 462-469.

Mat Suki, R.M. (1986) " Sediment transport in storm sewers." University of Salford, England, Ph.D thesis.

Mat Suki, R.M. and Nik Hassan, N.M.K. (1990) " Effective bed width of sediment transport in storm sewer design criterion." 5th. Proc. Intern. Conf. on Urban Storm Drainage, Osaka, Japan, pp. 879-884.

May, R.W.P (1975) " Deposition of grit in pipes: literature survey." Hydraulics Research Station, Wallingford, England, Report IT 139.

May, R.W.P. (1982) " Sediment transport in sewers." Hydraulic Research Station, Wallingford, England, Report IT 222.

May, R.W.P. (1993) " Sediment transport in pipes and sewers with deposited beds." Hydraulic Research Ltd., Wallingford, England, Report SR 320.

May, R.W.P., Brown, P.M., Hare, G.R., and Jones, K.D. (1989) " Self-cleansing conditions for sewers carrying sediment." Hydraulics Research Ltd., Wallingford, England, Report SR 221.

Mayerle, R. (1988) " Sediment transport in rigid boundary channels." University of Newcastle upon Tyne, England, Ph.D thesis.

Mayerle, R., Nalluri, C., and Novak, P. (1991) " Sediment transport in rigid bed conceyance." Jnl. of Hydraulic Research, Vol. 29, No. 4, pp. 475-495.

Montgomery, D.C. and Peck, E.A. (1992) Introduction to Linear Regression Analysis, John Wiley & Sons, New York, USA.

Novak, P. and Nalluri, C. (1974) "Correlation of sediment incipient motion and deposition in pipes and open channels with fixed smooth beds." Proc. 3rd. Intern. Conf. on the Hydraulic Transport of solids in Pipes, Hydrotransport 3, E4, pp. 45-56.

Novak, P. and Nalluri, C. (1975) " Sediment transport in smooth fixed bed channels." Jnl. of Hydraulic Division, ASCE, Vol. 101, HY9, pp. 1139-1154.

Novak, P. and Nalluri, C. (1978) " Sewer design for no sediment deposition." Proc. Institution of Civil Engineers, Vol. 65, Part 2, pp. 669-674.

Novak, P. and Nalluri, C. (1984) " Incipient motion of sediment particles over fixed beds." Jnl. of Hydraulic Research, Vol. 22, No. 3, pp. 181-197.

Novak, P. and Nalluri, C. (1987) "Sediment transport in sewers and their sea outfalls." Proc. 4th. Intern. Conf. on Urban Storm Drainage, Lausanne, Switzerland, pp. 337-342.

Paul, T.C. and Sakhuja, V.S. (1990) " Why sediment deposit in lined channels." Jnl. of Irrigation and Drainage Engineering, ASCE, Vol. 116, No. 5, pp. 589-602.

Perrusquia, G.S. (1991) " Bed load transport in storm sewers: steam traction in pipe channels." Chalmers University of Technology, Sweden, Ph.D thesis.

Perrusquia, G.S. (1992) " Sediment transport in pipe channels." Chalmers University of Technology, Sweden, Report B: 55.

Perrusquia, G.S. (1992)" An experimental studies from flume to stream traction in pipe channels." Chalmers University of Technology, Sweden, Report B: 57.

Perrusquia, G.S. (1992) "An experimental study on the transport of sediment in sewer pipes with a permanent deposit." Water Science and Technology, Vol. 25, No. 8, pp. 115-122.

Raphelt, N.K. (1990) " Guidance on the selection and use of sediment discharge formulas." Proc. National Conf. on Hydraulic Engineering, ASCE, San Diego, USA, pp. 198-203.

Robinson, M.P. and Graf,W.H. (1972) " Pipelining of low concentration sand-water mixtures." Jnl.of Hydraulic Division, ASCE, Vol. 98, HY7, pp. 1221-1240.

Nalluri, C. (1985) " Sediment transport in rigid boundary channels." Proc. Euromech 192: Transport of Suspended Solids in Open channels, Neubiberg, Germany, pp. 101-104.

Nalluri, C. and Ab. Ghani, A. (1993) " Shape effect on bed load transport in pipes." Proc. National Conf. on Hydraulic Engineering, ASCE, San Francisco, USA, pp. 1200-1205.

Nalluri, C. and Ab. Ghani, A. (1993) " Bed load transport without deposition in channels of circular cross section." Proc. 6th. Intern. Conf. on Urban Storm Drainage, Niagara Falls, Canada, pp. 625-630.

Nalluri, C., Ab. Ghani, A. and El-Zaemey, A.K.S. (1993) "Sediment transport over deposited beds in sewers." To be published in Water Science and Technology.

Nalluri, C. and Alvarez, E.M. (1992) "The influence of cohesion on sediment transport behaviour." Water Science and Technology, Vol. 25, No. 8, pp. 151-164.

Nalluri, C. and Dabrowski, W. " Need for new standards to prevent deposition in waste water sewers." To be published in Jnl. of Environmental Engineering, ASCE.

Nalluri, C. and Kithsiri, M.M.A.U. (1992) "Extended data on sediment transport in rigid bed rectangular channels." Jnl. of Hydraulic Research, Vol. 30, No. 6, pp. 851-856.

Novak, P. (1983) Development in Hydraulic Engineering - 1, Applied Science Publishers, London, England.

Novak, P. (1993) " Sediment transport in conveyances with fixed beds and implications for sewer design." Proc. Intern. Scientific Conf. on Fluid Mechanics and Hydrodynamial Aspects of Biosphere, Institute of Hydrodynamics, Academy of Sciences of the Chezk Republic, Bratislava, Chezk.

Novak, P. and Cabelka, J. (1981) Models in Hydraulic Engineering, Pitman, Boston, USA.

Novak, P. and Nalluri, C. (1972) " A study into the correlation of sediment motion in pipe and open channel flow." Proc. 2nd. Intern. Conf. on the Hydraulic Transport of Solids in Pipes, Hydrotransport 2, D4, pp. 33-51.

Raudkivi, A.J. (1990) Loose Boundary Hydraulics, Pergamon Press, Oxford, England.

Schlichting, H (1979) Boundary Layer Theory, McGraw Hill, 7th. edition, New York.

Simons, D.B. and Senturk. F. (1977) Sediment Transport Technology, Water Resources Publication, Fort Collins, USA.

Vanoni, V.A. (1975) Sedimentation Engineering, ASCE Manual no. 54.

van Rijn, L.C. (1984) " Sediment transport, Part I: Bed load transport." Jnl. of Hydraulic Engineering, ASCE, Vol. 110, No. 10, pp. 1431-1456.

van Rijn, L.C. (1989) " Handbook of sediment transport by currents and waves." Delft Hydraulics, Delft, Netherland, Report H 461.

Verbanck, M. (1990) " Sewer sediment and its relation with the quality characteristics of combined sewer flows." Water Science Technology, Vol. 22, No. 10/11, pp. 247-257.

Verbanck, M. (1992) " Field investigations on sediment occurrence and behaviour in Brussels combined sewers." Water Science Technology, Vol. 25, No. 8, pp. 71-82.

Water Authorities Association (1989) Sewers for Adoption, 3rd. edition, WRc, Swindon, England.

White, W.R., Milli, H., and Crabbe, A.D. (1975) " Sediment transport theories: a review." Proc. Instn. Civil Engineers, Part 2, Vol. 39, pp. 265-292.

Williams, D.T. (1990) " The relationships of milligrams per liter to parts per million." Proc. National Conf. on Hydraulic Engineering, ASCE, San Diego, USA, pp. 428-433.

Xanthopoulus,C. and Augustin, A. (1993) " Inputs and characterisation of sediments in urban sewer systems." Water Science Technology, Vol. 25, No. 8, pp. 21-28.

Yalin, M.S. (1972) Mechanics of Sediment Transport, Pergamon Press, Oxford, England.

Yang, C.T. (1973) " Incipient motion and sediment transport" Jnl. of Hydraulic Division, ASCE, Vol. 99, HY10, pp. 1679-1704.

Yang, C.T. (1979) " Unit stream power equations for total load" Jnl. of Hydrology, Vol. 40, pp. 123-138.

Yang, C.T. and Kong, X. (1991) " Energy dissipation rate and sediment transport" Jnl. of Hydraulic Research, Vol. 29, No. 4, pp. 457-474.

Yang, C.T. and Molinas, A. (1982) " Sediment transport and unit stream power function." Jnl. of Hydraulic Division, ASCE, Vol. 108, HY6, pp. 774-793.

Yao, K.M. (1974) " Sewer line design based on critical shear stress." Jnl. of Environmental Engineering Division, ASCE, Vol. 100, EE2, pp. 507-520.

BIBLIOGRAPHY

Bielecki, R. (1982) " Entwicklungstendenzen fur das Bertreiben von Anlagen der Abwasserableitungen." Korrespondenz Abwasser, Vol. 29.

Broecker, H.W. (1984) " Impact of depositions on sewer operation." Proc. 3rd. Intern. Conf. on Urban Storm Drainage, Goteberg, Sweden, pp. 879-887.

Escritt, L.B. (1979) Drainage and Sewerage, National Salt Glazed Pipe Manufacturing Association.

Lysne, D.K. (1969) " Hydraulic design of self-cleansing sewage tunnels." Jnl. of Sanitary Engineering Division, ASCE, Vol. 95, pp. 17-36.

Mittlestadt, M., Macke, E., and Stahn, R. (1979) " About methods to obtain flows free of sedimentation in large sewage siphons." Institut fur Wasserbau der Technischen Universitat Braunsschweigh, pp. 119-153.

Newitt, D.M., Richardson, J.F., and Abott, M. and Turtle, R.B. (1955) " Hydraulic conveying of solids in horizontal pipe." Trans. Institute of Chemical Engineers, Vol.33, part 2.

Novak, P. and Nalluri, C. (1973) " Turbulence characteristics in a smooth open channel of circular cross section.", Jnl. of Hydraulic Research, Vol. 11, No. 4.

Ojo, S.I.A. (1978) " Study of incipient motions and sediment transport over fixed beds." University of Newcastle upon Tyne, PhD thesis.

Pedroli, R. (1963) " Bed load transportation in channels with fixed and smooth inverts." Scuola Politecnica Federale, Zurigo, Switzerland, PhD thesis.

Shultz, M. (1983) " Vermeidung von Ablagerungen in kanalisationsleitungen" GWF-Wasser/Abwasser, Vol.124, No. 8, pp. 393-398.

Urcikan, D.P. (1984) " Frictional losses in pipe flow of stormwaters having various concentrations of sediments." Proc. 3rd. Intern. Conf. on Urban Storm Drainage, Goteberg, Sweden, Vol. 4, pp. 1475-1486.

Valentine, H.R. (1955) " Transportation of solids in pipelines"
Commonwealth Engineering.

APPENDIX A

CLEAR WATER EXPERIMENTAL DATA

TABLE A1 CLEAR WATER EXPERIMENTAL DATA IN 154mm PIPE - PRELIMINARY TESTS (SMOOTH RIGID BED)

Exp No	Q (l/s)	V (m/s)	y_o (mm)	y_o/D	Re	Fr	S_o	λ_o
3	6.53	0.781	70.83	0.460	104022	1.07	0.004179	0.0196
5	4.65	0.687	60.31	0.392	83691	1.03	0.004927	0.0266
6	2.88	0.583	47.85	0.310	59213	1.00	0.004341	0.0272
8	2.55	0.551	45.70	0.297	55216	0.97	0.003884	0.0262
10	5.73	0.741	66.72	0.433	94714	1.05	0.004413	0.0221
11	7.02	0.780	75.04	0.487	109300	1.03	0.004094	0.0200
17	3.14	0.621	48.65	0.316	63973	1.06	0.004900	0.0274
18	1.50	0.455	35.88	0.233	37132	0.91	0.004071	0.0328
1	6.53	0.667	80.08	0.520	96263	0.84	0.002932	0.0204
2	6.53	0.593	88.00	0.571	90449	0.71	0.002194	0.0204
4	8.81	0.718	96.40	0.626	113110	0.80	0.003281	0.0218
7	8.81	0.738	94.11	0.611	117983	0.84	0.004249	0.0264
9	7.24	0.739	80.15	0.520	105381	0.94	0.003389	0.0192
12	7.77	0.774	81.68	0.530	115932	0.97	0.003800	0.0199
13	10.12	0.889	90.52	0.588	141000	1.04	0.004558	0.0192
14	9.23	0.658	108.50	0.704	112744	0.67	0.002315	0.0192
15	8.11	0.636	99.61	0.647	106986	0.69	0.002273	0.0195
16	8.40	0.679	97.06	0.630	110080	0.75	0.002572	0.0192

Exp No	k_o (mm)	n_o	T (C)	A (m^2)	P (m)	R (m)	B (m)
3	0.052	0.0091	17.0	0.00836	0.2291	0.0364	0.1535
5	0.324	0.0104	18.0	0.00676	0.2086	0.0325	0.1503
6	0.268	0.0102	18.0	0.00493	0.1821	0.0271	0.1425
8	0.207	0.0099	19.0	0.00463	0.1780	0.0261	0.1407
10	0.130	0.0096	17.0	0.00774	0.2215	0.0350	0.1526
11	0.073	0.0092	17.5	0.00901	0.2380	0.0379	0.1539
17	0.289	0.0103	18.0	0.00505	0.1842	0.0275	0.1432
18	0.429	0.0108	19.0	0.00330	0.1556	0.0212	0.1302
1	0.078	0.0094	17.0	0.00979	0.2481	0.0395	0.1539
2	0.074	0.0095	17.0	0.01100	0.2640	0.0417	0.1524
4	0.169	0.0099	16.5	0.01227	0.2811	0.0436	0.1490
7	0.450	0.0109	17.5	0.01193	0.2773	0.0431	0.1501
9	0.044	0.0091	16.5	0.00980	0.2485	0.0395	0.1539
12	0.077	0.0093	18.0	0.01003	0.2513	0.0399	0.1537
13	0.072	0.0092	18.0	0.01139	0.2693	0.0423	0.1516
14	0.058	0.0093	18.0	0.01402	0.3062	0.0457	0.1405
15	0.062	0.0094	18.5	0.01274	0.2874	0.0443	0.1472
16	0.052	0.0093	17.5	0.01237	0.2825	0.0438	0.1487

TABLE A2 CLEAR WATER EXPERIMENTAL DATA IN 154mm PIPE - PRECEDING TRANSPORT TESTS (SMOOTH RIGID BED)

a) Flows up to half-full depth

Exp No	Q (l/s)	V (m/s)	y_o (mm)	y_o/D	Re	Fr	S_o	λ_o
21	0.46	0.244	24.50	0.159	13634	0.60	0.001728	0.0344
22	2.21	0.494	44.60	0.290	47337	0.88	0.003132	0.0258
23	5.73	0.754	65.82	0.427	99130	1.08	0.004738	0.0226
24	1.23	0.384	35.12	0.228	30801	0.78	0.003137	0.0347
25	6.45	0.723	74.42	0.483	99590	0.96	0.003279	0.0185
11	1.30	0.361	38.16	0.248	27724	0.70	0.002641	0.0357
12	0.44	0.256	23.00	0.149	12841	0.65	0.002498	0.0426
13	2.69	0.503	50.78	0.330	50929	0.83	0.002711	0.0239
14	4.41	0.620	62.60	0.406	74793	0.91	0.003491	0.0238
15	3.55	0.454	67.30	0.437	58403	0.64	0.001787	0.0239
16	2.45	0.421	53.98	0.351	47114	0.68	0.001982	0.0262
3	4.73	0.549	72.56	0.471	76177	0.74	0.002233	0.0216
4	5.15	0.746	61.26	0.398	86891	1.11	0.004543	0.0211
5	6.99	0.795	73.64	0.478	107313	1.06	0.004558	0.0212
6	2.22	0.478	45.75	0.297	45110	0.84	0.003383	0.0303
7	1.31	0.410	35.10	0.228	29659	0.83	0.002527	0.0246
8	2.00	0.405	47.90	0.311	39140	0.69	0.002312	0.0300
28	4.88	0.738	59.28	0.385	86516	1.12	0.004743	0.0219
29	2.25	0.532	42.80	0.278	49241	0.97	0.003751	0.0257
30	2.39	0.598	41.18	0.267	53646	1.11	0.004869	0.0255
31	1.25	0.487	30.18	0.196	33306	1.07	0.004934	0.0298
32	5.48	0.780	62.10	0.403	96947	1.15	0.004754	0.0204
33	1.33	0.424	34.70	0.225	34068	0.87	0.003366	0.0303
34	2.10	0.501	42.64	0.277	46225	0.91	0.003572	0.0275
35	6.46	0.777	70.48	0.458	111158	1.07	0.004859	0.0229
36	3.60	0.625	53.60	0.348	71206	1.01	0.004265	0.0255

TABLE A2 Continued a) Flows up to half-full depth

Exp No	k_o (mm)	n_o	T (C)	A (m^2)	P (m)	R (m)	B (m)
21	0.230	0.0104	17.5	0.00191	0.1264	0.0151	0.1126
22	0.166	0.0098	18.0	0.00448	0.1750	0.0256	0.1397
23	0.157	0.0097	18.5	0.00760	0.2195	0.0346	0.1524
24	0.507	0.0110	19.0	0.00320	0.1533	0.0209	0.1292
25	0.015	0.0089	17.0	0.00892	0.2367	0.0377	0.1539
11	0.590	0.0113	14.5	0.00360	0.1605	0.0224	0.1330
12	0.595	0.0115	15.5	0.00174	0.1222	0.0142	0.1097
13	0.113	0.0096	16.0	0.00536	0.1884	0.0284	0.1448
14	0.174	0.0099	16.5	0.00711	0.2129	0.0334	0.1513
15	0.160	0.0100	17.0	0.00782	0.2224	0.0352	0.1528
16	0.212	0.0102	18.0	0.00582	0.1951	0.0298	0.1470
3	0.093	0.0096	18.0	0.00863	0.2330	0.0370	0.1537
4	0.078	0.0093	15.8	0.00691	0.2102	0.0329	0.1507
5	0.114	0.0095	16.5	0.00880	0.2352	0.0374	0.1538
6	0.394	0.0107	16.5	0.00464	0.1775	0.0261	0.1407
7	0.035	0.0093	15.0	0.00320	0.1533	0.0208	0.1292
8	0.373	0.0107	16.0	0.00494	0.1822	0.0271	0.1426
28	0.106	0.0094	17.0	0.00661	0.2061	0.0321	0.1499
29	0.163	0.0098	18.0	0.00423	0.1710	0.0247	0.1380
30	0.159	0.0097	18.0	0.00400	0.1674	0.0239	0.1363
31	0.223	0.0100	18.0	0.00258	0.1412	0.0182	0.1223
32	0.066	0.0091	18.0	0.00703	0.2119	0.0332	0.1511
33	0.278	0.0103	19.5	0.00314	0.1523	0.0206	0.1287
34	0.235	0.0101	18.0	0.00420	0.1707	0.0246	0.1378
35	0.187	0.0098	20.0	0.00831	0.2288	0.0363	0.1534
36	0.226	0.0100	19.0	0.00577	0.1943	0.0297	0.1467

TABLE A2 Continued b) Flows more than half-full depth

Exp No	Q (l/s)	V (m/s)	y_o (mm)	y_o/D	Re	Fr	S_o	λ_o
20	8.04	0.828	79.56	0.517	117538	1.05	0.004747	0.0213
26	7.81	0.517	116.48	0.756	92371	0.49	0.001344	0.0184
27	8.12	0.665	96.04	0.624	108580	0.74	0.002279	0.0176
10	8.04	0.637	98.74	0.641	96437	0.70	0.002441	0.0208
17	7.17	0.743	79.16	0.514	109189	0.95	0.003541	0.0197
18	6.63	0.628	85.10	0.553	98750	0.76	0.002848	0.0232
19	7.28	0.626	92.04	0.598	104043	0.72	0.002132	0.0182
1	8.13	0.598	105.48	0.685	100336	0.62	0.001981	0.0197
2	7.62	0.776	80.29	0.521	112114	0.98	0.004243	0.0219
9	7.65	0.759	82.02	0.532	112553	0.95	0.003790	0.0206
37	9.70	0.931	84.22	0.547	149015	1.30	0.005128	0.0189
38	9.74	0.683	110.20	0.716	122061	0.68	0.002456	0.0190
39	6.67	0.694	78.90	0.512	108165	0.89	0.003373	0.0215

Exp No	k_o (mm)	n_o	T (C)	A (m^2)	P (m)	R (m)	B (m)
20	0.135	0.0096	16.5	0.00971	0.2470	0.0393	0.1539
26	0.004	0.0092	19.0	0.01511	0.3248	0.0465	0.1322
27	−0.001	0.0089	18.0	0.01221	0.2804	0.0436	0.1492
10	0.105	0.0097	14.5	0.01262	0.2860	0.0441	0.1477
17	0.064	0.0092	18.0	0.00965	0.2462	0.0392	0.1539
18	0.213	0.0101	19.0	0.01056	0.2581	0.0409	0.1531
19	0.011	0.0090	19.5	0.01161	0.2722	0.0427	0.1510
1	0.063	0.0095	17.5	0.01360	0.3002	0.0453	0.1431
2	0.154	0.0097	17.0	0.00982	0.2485	0.0395	0.1538
9	0.104	0.0095	17.5	0.01009	0.2519	0.0400	0.1536
37	0.065	0.0091	20.0	0.01042	0.2564	0.0407	0.1533
38	0.058	0.0093	19.5	0.01426	0.3106	0.0459	0.1389
39	0.132	0.0096	20.5	0.00961	0.2457	0.0391	0.1539

TABLE A3 CLEAR WATER EXPERIMENTAL DATA IN 305mm PIPE - PRELIMINARY TESTS (SMOOTH RIGID BED)

Exp No	Q (l/s)	V (m/s)	y_o (mm)	y_o/D	Re	Fr	S_o	λ_o
1	6.74	0.481	75.30	0.247	72898	0.66	0.001185	0.0178
2	11.99	0.566	101.10	0.332	109872	0.66	0.001351	0.0187
3	22.85	0.710	138.20	0.453	173995	0.70	0.001345	0.0150
4	10.10	0.798	70.00	0.230	113744	1.15	0.003267	0.0167
5	18.12	0.947	94.00	0.308	173247	1.16	0.003283	0.0153
6	30.55	1.080	125.10	0.410	247158	1.13	0.003229	0.0144
7	8.76	0.425	99.30	0.326	80094	0.50	0.000697	0.0169
8	19.36	0.541	150.00	0.492	138223	0.50	0.000684	0.0138
10	16.09	0.763	100.90	0.331	145753	0.90	0.002223	0.0169
11	21.98	0.829	121.70	0.399	180477	0.89	0.002280	0.0167
12	7.92	0.583	73.60	0.241	86804	0.82	0.002242	0.0224
13	10.19	0.399	116.00	0.380	85068	0.43	0.000608	0.0189
14	14.87	0.455	140.00	0.459	110915	0.44	0.000655	0.0179
15	7.02	0.479	77.70	0.255	73692	0.65	0.001307	0.0203
16	12.70	0.579	103.80	0.340	113172	0.67	0.001225	0.0166
17	21.13	0.678	134.80	0.442	161194	0.68	0.001300	0.0156
18	10.10	0.792	70.40	0.231	111925	1.13	0.003185	0.0167
19	19.69	0.942	100.30	0.329	179016	1.11	0.003164	0.0157
20	8.24	0.613	73.10	0.240	90614	0.86	0.001926	0.0174
21	15.85	0.751	134.90	0.442	145436	0.88	0.002124	0.0167
22	20.99	0.801	117.60	0.385	175531	0.86	0.002152	0.0168
9	22.41	0.492	182.20	0.597	142652	0.40	0.000650	0.0178

Exp No	k_o (mm)	n_o	T (C)	A (m^2)	P (m)	R (m)	B (m)
1	−0.052	0.0090	14.5	0.01402	0.3171	0.0442	0.2630
2	0.045	0.0096	14.5	0.02118	0.3744	0.0566	0.2872
3	−0.039	0.0089	14.5	0.03217	0.4504	0.0714	0.3036
4	−0.021	0.0086	14.5	0.01267	0.3048	0.0415	0.2565
5	−0.021	0.0086	14.5	0.01915	0.3591	0.0533	0.2816
6	−0.016	0.0086	14.5	0.02823	0.4240	0.0666	0.3000
7	0.000	0.0091	14.0	0.02065	0.3705	0.0557	0.2859
8	−0.110	0.0086	14.0	0.03575	0.4740	0.0754	0.3050
10	0.009	0.0091	14.0	0.02110	0.3738	0.0564	0.2870
11	0.027	0.0092	14.0	0.02651	0.4123	0.0643	0.2977
12	0.170	0.0100	14.5	0.01359	0.3132	0.0434	0.2610
13	0.013	0.0098	14.0	0.02552	0.4055	0.0629	0.2962
14	0.015	0.0097	14.0	0.03268	0.4538	0.0720	0.3039
15	0.048	0.0096	14.0	0.01466	0.3227	0.0454	0.2658
16	−0.036	0.0090	14.0	0.02194	0.3800	0.0577	0.2890
17	−0.027	0.0091	14.0	0.03116	0.4437	0.0702	0.3029
18	−0.025	0.0086	14.0	0.01277	0.3058	0.0418	0.2571
19	−0.007	0.0088	14.0	0.02092	0.3725	0.0562	0.2865
20	−0.032	0.0088	14.5	0.01345	0.3120	0.0431	0.2604
21	0.001	0.0090	14.5	0.02111	0.3739	0.0565	0.2870
22	0.027	0.0092	14.5	0.02619	0.4101	0.0639	0.2972
9	0.058	0.0100	14.5	0.04552	0.5388	0.0845	0.2992

TABLE A4 CLEAR WATER EXPERIMENTAL DATA IN 305mm PIPE - PRECEDING TRANSPORT TESTS (SMOOTH RIGID BED)

a) Flows up to half-full depth

Exp No	Q (l/s)	V (m/s)	y_o (mm)	y_o/D	Re	Fr	S_o	τ_o
80	8.08	0.743	63.00	0.206	97670	1.13	0.003511	0.0189
75	20.37	1.172	87.70	0.288	205009	1.49	0.004832	0.0139
81	15.67	0.684	107.20	0.351	137125	0.78	0.001523	0.0151
87	16.27	0.589	123.00	0.403	136391	0.62	0.001075	0.0160
76	27.92	0.912	133.10	0.436	223274	0.91	0.002258	0.0148
86	17.61	0.488	151.20	0.496	130136	0.45	0.000680	0.0170
79	8.08	0.742	63.00	0.206	97598	1.13	0.003506	0.0189
9	9.48	0.767	68.90	0.226	115633	1.11	0.003320	0.0182
20	8.08	0.607	71.60	0.235	95154	0.86	0.002061	0.0188
73	20.78	1.192	87.90	0.288	203481	1.51	0.005122	0.0143
21	25.03	1.157	102.80	0.337	224364	1.35	0.004243	0.0142
25	20.37	0.951	102.10	0.335	203132	1.11	0.003157	0.0156
82	15.67	0.688	106.70	0.350	139273	0.78	0.001469	0.0143
88	16.27	0.590	122.90	0.403	136455	0.62	0.001074	0.0159
4	22.34	0.686	139.50	0.457	168027	0.67	0.001335	0.0160
85	17.61	0.487	151.20	0.496	130105	0.45	0.000667	0.0167
35	13.44	0.884	79.70	0.261	155902	1.18	0.003718	0.0173
12	19.69	1.111	89.00	0.292	196628	1.40	0.004741	0.0154
26	20.78	0.951	103.60	0.340	202941	1.10	0.003106	0.0155
16	8.77	0.402	103.50	0.339	87366	0.47	0.000643	0.0180
17	16.87	0.770	103.80	0.340	158464	0.89	0.002101	0.0160
38	15.44	0.659	109.00	0.357	150007	0.74	0.001428	0.0155
11	17.49	0.586	130.60	0.428	143301	0.59	0.000739	0.0116
29	19.29	0.516	155.40	0.509	149172	0.47	0.000707	0.0161
8	9.48	0.761	69.30	0.227	113105	1.10	0.003276	0.0183
34	13.44	0.888	79.50	0.260	154277	1.19	0.003700	0.0171
1	14.42	0.923	81.30	0.266	145606	1.22	0.004133	0.0180
13	19.69	1.106	89.30	0.293	206523	1.39	0.004889	0.0160
6	11.70	0.552	101.30	0.332	104363	0.65	0.001271	0.0186
15	8.77	0.400	103.70	0.340	82371	0.46	0.000733	0.0207

TABLE A4 Continued a) Flows up to half-full depth

Exp No	Q (l/s)	V (m/s)	y_o (mm)	y_o/D	Re	Fr	S_o	λ_o
27	20.78	0.966	102.40	0.336	206866	1.13	0.003128	0.0150
22	25.34	1.164	103.30	0.339	229484	1.35	0.004275	0.0142
3	11.41	0.439	117.60	0.386	96962	0.47	0.000782	0.0203
5	22.34	0.690	138.90	0.455	174019	0.67	0.001171	0.0138
28	19.29	0.518	154.90	0.508	145798	0.47	0.000724	0.0163
7	9.48	0.753	69.80	0.229	105616	1.08	0.003278	0.0188
19	8.08	0.600	73.30	0.240	90700	0.84	0.002021	0.0191
33	13.44	0.886	79.60	0.261	149174	1.19	0.003677	0.0171
14	19.69	1.120	88.50	0.290	212825	1.42	0.004865	0.0154
24	20.37	0.947	102.40	0.336	195291	1.10	0.003118	0.0156
18	16.87	0.772	103.60	0.340	166798	0.90	0.002076	0.0158
23	25.43	1.164	103.30	0.339	232543	1.35	0.004106	0.0137
37	15.44	0.658	109.10	0.358	148069	0.74	0.001487	0.0162
10	17.24	0.584	129.40	0.424	136642	0.60	0.000708	0.0111
31	24.11	0.683	148.50	0.487	180170	0.64	0.001104	0.0139
78	8.08	0.743	63.00	0.206	96385	1.13	0.003488	0.0188
32	13.65	0.901	79.50	0.261	147054	1.21	0.003649	0.0164
74	20.37	1.173	87.60	0.287	202457	1.49	0.005268	0.0151
36	15.44	0.656	109.40	0.359	138783	0.74	0.001484	0.0163
83	35.11	1.255	120.10	0.394	281458	1.34	0.004421	0.0142
89	16.27	0.593	122.40	0.401	138544	0.63	0.001068	0.0156
77	27.92	0.912	133.10	0.437	226168	0.91	0.002240	0.0147
30	24.42	0.677	150.90	0.495	175982	0.63	0.001051	0.0136
84	17.61	0.486	151.60	0.497	128221	0.45	0.000619	0.0157

TABLE A4 Continued a) Flows up to half-full depth

Exp No	k_o (mm)	n_o	T (C)	A (m^2)	P (m)	R (m)	B (m)
80	0.024	0.0090	15.0	0.01088	0.2877	0.0378	0.2469
75	−0.035	0.0081	15.0	0.01738	0.3453	0.0503	0.2761
81	−0.055	0.0087	14.0	0.02291	0.3871	0.0592	0.2912
87	−0.034	0.0091	15.5	0.02760	0.4198	0.0657	0.2992
76	−0.014	0.0088	15.5	0.03063	0.4402	0.0696	0.3025
86	0.000	0.0096	15.5	0.03612	0.4764	0.0758	0.3050
79	0.026	0.0090	15.0	0.01091	0.2879	0.0379	0.2470
9	0.020	0.0089	17.3	0.01239	0.3022	0.0410	0.2551
20	0.022	0.0092	17.0	0.01334	0.3110	0.0429	0.2598
73	−0.028	0.0082	14.0	0.01744	0.3457	0.0504	0.2763
21	−0.025	0.0084	14.0	0.02163	0.3777	0.0573	0.2883
25	0.001	0.0087	18.0	0.02145	0.3764	0.0570	0.2878
82	−0.073	0.0084	14.5	0.02277	0.3860	0.0590	0.2909
88	−0.036	0.0090	15.5	0.02757	0.4196	0.0657	0.2992
4	−0.007	0.0092	14.3	0.03256	0.4530	0.0719	0.3039
85	−0.015	0.0095	15.5	0.03614	0.4765	0.0758	0.3050
35	0.026	0.0089	18.5	0.01521	0.3273	0.0465	0.2680
12	−0.008	0.0082	15.0	0.01773	0.3480	0.0509	0.2772
26	−0.001	0.0087	17.5	0.02188	0.3795	0.0576	0.2888
16	−0.021	0.0094	18.3	0.02185	0.3793	0.0576	0.2888
17	−0.011	0.0089	16.0	0.02192	0.3798	0.0577	0.2890
38	−0.034	0.0088	18.5	0.02343	0.3908	0.0600	0.2923
11	−0.142	0.0078	16.0	0.02987	0.4351	0.0686	0.3018
29	−0.020	0.0094	18.0	0.03741	0.4849	0.0772	0.3049
8	0.022	0.0090	16.5	0.01248	0.3031	0.0412	0.2556
34	0.016	0.0088	18.0	0.01514	0.3268	0.0463	0.2677
1	0.040	0.0091	13.5	0.01562	0.3308	0.0472	0.2697
13	0.013	0.0087	17.0	0.01781	0.3487	0.0511	0.2775
6	0.035	0.0095	13.5	0.02119	0.3745	0.0566	0.2872
15	0.105	0.0101	16.0	0.02190	0.3797	0.0577	0.2890
27	−0.013	0.0086	18.0	0.02153	0.3770	0.0571	0.2880
22	−0.023	0.0084	14.5	0.02179	0.3789	0.0575	0.2887
3	0.119	0.0102	15.0	0.02599	0.4087	0.0636	0.2969
5	−0.070	0.0086	15.5	0.03238	0.4518	0.0717	0.3038
28	−0.015	0.0094	17.0	0.03725	0.4838	0.0770	0.3050
7	0.032	0.0091	14.0	0.01262	0.3043	0.0414	0.2563
19	0.024	0.0092	15.3	0.01350	0.3124	0.0432	0.2605
33	0.014	0.0088	16.7	0.01519	0.3272	0.0464	0.2679
14	0.000	0.0085	18.0	0.01759	0.3469	0.0507	0.2768
24	−0.003	0.0087	16.5	0.02155	0.3771	0.0571	0.2880
18	−0.013	0.0088	18.0	0.02188	0.3795	0.0576	0.2889
23	−0.033	0.0082	15.0	0.02178	0.3788	0.0575	0.2886
37	−0.014	0.0090	18.0	0.02347	0.3910	0.0600	0.2924
10	−0.158	0.0076	14.5	0.02951	0.4327	0.0682	0.3015
31	−0.067	0.0087	15.5	0.03531	0.4711	0.0750	0.3049
78	0.019	0.0090	14.5	0.01089	0.2877	0.0378	0.2469
32	−0.007	0.0087	15.5	0.01516	0.3269	0.0464	0.2678
74	−0.012	0.0084	14.5	0.01736	0.3451	0.0503	0.2760
36	−0.018	0.0090	15.5	0.02356	0.3916	0.0601	0.2925
83	−0.010	0.0085	15.0	0.02671	0.4137	0.0646	0.2980
89	−0.044	0.0090	16.0	0.02742	0.4186	0.0655	0.2990
77	−0.016	0.0088	16.0	0.03064	0.4403	0.0696	0.3025
30	−0.079	0.0086	14.5	0.03605	0.4759	0.0757	0.3050
84	−0.062	0.0092	15.5	0.03626	0.4773	0.0760	0.3050

TABLE A4 Continued b) Flows more than half-full depth

Exp No	Q (l/s)	V (m/s)	y_o (mm)	y_o/D	Re	Fr	S_o	λ_o
71	27.59	0.670	167.70	0.550	180850	0.58	0.000996	0.0141
70	37.33	0.822	181.80	0.596	234878	0.67	0.001523	0.0149
61	27.59	0.562	194.20	0.637	174523	0.44	0.000788	0.0171
62	35.77	0.604	230.60	0.756	188281	0.40	0.000837	0.0166
72	27.59	0.675	166.70	0.547	183979	0.59	0.000977	0.0135
68	37.33	0.824	181.50	0.595	232037	0.68	0.001531	0.0149
58	27.59	0.563	194.00	0.636	172417	0.44	0.000787	0.0170
54	28.58	0.517	215.70	0.707	162979	0.37	0.000626	0.0166
67	36.16	0.610	230.60	0.756	190296	0.41	0.000844	0.0164
57	31.88	0.507	244.80	0.803	163532	0.32	0.000624	0.0177
48	28.25	0.734	158.90	0.521	194414	0.66	0.001234	0.0141
49	32.42	0.778	169.40	0.555	211128	0.67	0.001507	0.0159
39	30.64	0.706	175.10	0.574	200377	0.59	0.001016	0.0132
52	23.81	0.494	191.10	0.626	144696	0.39	0.000626	0.0174
60	27.59	0.561	194.40	0.637	174373	0.44	0.000789	0.0171
53	28.58	0.512	217.90	0.714	157513	0.36	0.000620	0.0169
66	36.16	0.609	230.90	0.757	190457	0.41	0.000786	0.0153
45	28.25	0.728	160.00	0.524	191090	0.65	0.001262	0.0147
2	27.26	0.651	170.00	0.558	179427	0.56	0.001061	0.0160
69	37.33	0.825	181.30	0.594	232231	0.68	0.001561	0.0152
44	32.05	0.613	205.40	0.673	189732	0.46	0.000795	0.0148
55	28.58	0.516	216.30	0.709	162637	0.37	0.000624	0.0167
65	36.16	0.610	230.60	0.756	190334	0.41	0.000791	0.0154
56	31.88	0.507	245.10	0.803	163350	0.32	0.000626	0.0178
47	28.25	0.730	160.00	0.524	193889	0.65	0.001204	0.0139
51	31.70	0.766	168.40	0.552	209999	0.66	0.001397	0.0151
41	30.64	0.712	174.00	0.570	204007	0.60	0.000996	0.0127
59	27.59	0.564	193.40	0.634	175039	0.44	0.000790	0.0169
42	32.78	0.627	205.00	0.673	194115	0.47	0.000740	0.0132
64	36.16	0.611	230.10	0.754	188152	0.41	0.000758	0.0147
46	28.25	0.729	160.00	0.524	191184	0.65	0.001351	0.0157
50	31.70	0.767	168.20	0.551	210173	0.66	0.001492	0.0161
40	30.64	0.712	174.00	0.570	201247	0.60	0.001059	0.0135
43	32.05	0.614	204.90	0.672	190076	0.46	0.000829	0.0154
63	35.77	0.604	230.50	0.756	188377	0.40	0.000840	0.0167

TABLE A5 CLEAR WATER EXPERIMENTAL DATA IN 450mm PIPE - PRELIMINARY TESTS (SMOOTH RIGID BED)

Exp No	Q (l/s)	V (m/s)	y_o (mm)	y/D	Re	Fr	S_o	λ_o
2	39.69	0.496	225.90	0.502	189450	0.38	0.000484	0.0174
3	55.91	0.694	227.25	0.505	282648	0.52	0.000860	0.0159
4	72.15	0.908	225.00	0.500	348516	0.69	0.001665	0.0178
5	86.47	1.080	226.35	0.503	402066	0.82	0.001941	0.0147
6	38.70	0.486	225.00	0.500	191794	0.37	0.000504	0.0188
7	70.83	0.887	225.90	0.502	336849	0.67	0.001551	0.0174
8	87.40	1.091	226.80	0.504	414959	0.82	0.002141	0.0159
12	32.36	0.408	225.00	0.500	161304	0.31	0.000340	0.0181
13	47.40	0.597	224.55	0.499	238331	0.45	0.000727	0.0180
14	63.48	0.801	224.55	0.499	302975	0.61	0.001285	0.0176
15	79.51	1.012	223.20	0.496	373204	0.77	0.001929	0.0165
18	31.53	0.395	225.45	0.501	158756	0.30	0.000344	0.0195
19	31.69	0.397	225.90	0.502	162952	0.30	0.000363	0.0204
20	41.80	0.524	225.90	0.502	207840	0.40	0.000549	0.0177
21	47.93	0.606	224.10	0.498	241311	0.46	0.000666	0.0160
22	48.30	0.609	224.55	0.499	242985	0.46	0.000672	0.0160
23	62.57	0.781	226.35	0.503	313173	0.59	0.001141	0.0166
24	78.33	0.996	223.20	0.496	397678	0.76	0.001824	0.0161
1	86.20	0.670	339.30	0.754	310643	0.37	0.000750	0.0178
9	65.70	0.514	337.50	0.750	237879	0.29	0.000474	0.0191
10	103.63	0.812	337.05	0.749	375626	0.45	0.001120	0.0181
16	77.06	0.602	337.95	0.751	274988	0.33	0.000558	0.0164
17	52.07	0.407	337.50	0.750	184558	0.23	0.000251	0.0161
25	128.00	1.017	332.55	0.739	469447	0.57	0.001661	0.0170

Exp No	k_o (mm)	n_o	T (C)	A (m^2)	P (m)	R (m)	B (m)
2	0.101	0.0103	14.0	0.07988	0.7084	0.1128	0.4495
3	0.062	0.0099	16.0	0.08056	0.7114	0.1132	0.4495
4	0.210	0.0105	14.0	0.07948	0.7067	0.1125	0.4495
5	0.041	0.0095	13.0	0.08006	0.7093	0.1129	0.4495
6	0.218	0.0108	15.0	0.07958	0.7071	0.1125	0.4495
7	0.178	0.0104	13.5	0.07983	0.7082	0.1127	0.4495
8	0.103	0.0099	13.5	0.08018	0.7098	0.1129	0.4494
12	0.124	0.0105	15.5	0.07941	0.7063	0.1124	0.4495
13	0.178	0.0105	15.5	0.07933	0.7060	0.1124	0.4495
14	0.182	0.0104	13.5	0.07924	0.7056	0.1123	0.4495
15	0.127	0.0101	13.0	0.07856	0.7026	0.1118	0.4495
18	0.249	0.0110	16.0	0.07981	0.7081	0.1127	0.4495
19	0.344	0.0112	16.5	0.07986	0.7083	0.1127	0.4495
20	0.140	0.0104	15.5	0.07981	0.7082	0.1127	0.4495
21	0.048	0.0099	15.5	0.07914	0.7051	0.1122	0.4495
22	0.047	0.0099	15.5	0.07927	0.7058	0.1123	0.4495
23	0.114	0.0101	15.5	0.08009	0.7093	0.1129	0.4495
24	0.109	0.0100	16.0	0.07862	0.7028	0.1119	0.4495
1	0.237	0.0108	14.0	0.12861	0.9470	0.1358	0.3865
9	0.333	0.0112	14.0	0.12786	0.9425	0.1357	0.3888
10	0.286	0.0109	14.0	0.12769	0.9416	0.1356	0.3893
16	0.108	0.0104	13.5	0.12804	0.9436	0.1357	0.3882
17	0.016	0.0103	13.5	0.12804	0.9436	0.1357	0.3882
25	0.213	0.0106	14.0	0.12581	0.9306	0.1352	0.3946

TABLE A6 Continued b) Flows at three quarter depth

Exp No	Q (l/s)	V (m/s)	y_o (mm)	y_o/D	Re	Fr	S_o	λ_o
14	63.91	0.502	336.15	0.747	241530	0.28	0.000400	0.0169
15	89.47	0.700	337.50	0.750	337047	0.39	0.000797	0.0173
16	102.26	0.798	337.95	0.751	374718	0.44	0.001004	0.0168
17	115.04	0.904	336.15	0.747	423597	0.51	0.001291	0.0168
18	76.68	0.600	337.50	0.750	277572	0.33	0.000560	0.0166
19	96.15	0.754	336.60	0.748	348818	0.42	0.000810	0.0152
20	83.08	0.652	336.15	0.747	301806	0.36	0.000646	0.0161
21	108.66	0.856	335.25	0.745	406312	0.48	0.001058	0.0154
22	89.48	0.703	336.15	0.747	333881	0.39	0.000791	0.0170

Exp No	k_o (mm)	n_o	T (C)	A (m^2)	P (m)	R (m)	B (m)
14	0.123	0.0105	15.5	0.12732	0.9394	0.1355	0.3904
15	0.206	0.0107	15.5	0.12784	0.9424	0.1356	0.3888
16	0.173	0.0105	14.5	0.12807	0.9438	0.1357	0.3882
17	0.188	0.0105	14.5	0.12730	0.9392	0.1355	0.3904
18	0.123	0.0104	14.0	0.12791	0.9429	0.1357	0.3886
19	0.057	0.0100	14.0	0.12756	0.9408	0.1356	0.3897
20	0.101	0.0103	14.0	0.12734	0.9395	0.1355	0.3903
21	0.085	0.0100	15.0	0.12694	0.9371	0.1355	0.3915
22	0.180	0.0106	15.0	0.12729	0.9392	0.1355	0.3905

TABLE A7 CLEAR WATER EXPERIMENTAL DATA IN 305mm PIPE - PRELIMINARY TESTS (ROUGHNESS 1; k_o = 0.53mm)

Exp No	Q (l/s)	V (m/s)	y_o (mm)	y_o/D	Re	Fr	S_o	λ_o
1	7.096	0.597	67.10	0.220	86210	0.88	0.003650	0.0322
11	7.923	0.624	70.30	0.230	93891	0.89	0.003273	0.0275
8	11.11	0.739	80.90	0.265	127172	0.98	0.003981	0.0269
5	16.99	0.944	90.00	0.295	177466	1.18	0.005412	0.0245
10	14.41	0.696	99.60	0.326	140402	0.82	0.002574	0.0237
7	15.90	0.674	110.00	0.360	148436	0.76	0.002303	0.0239
4	26.29	0.991	120.00	0.392	230249	1.06	0.004608	0.0237
12	33.14	1.109	130.70	0.429	278483	1.12	0.005297	0.0232
13	20.91	0.621	143.20	0.469	168240	0.60	0.001554	0.0232
2	17.23	0.468	153.40	0.503	131094	0.43	0.000970	0.0266
14	26.77	0.718	155.00	0.508	204793	0.66	0.001729	0.0203
19	24.62	0.611	162.80	0.534	184290	0.54	0.001401	0.0234
9	20.22	0.481	170.70	0.560	141680	0.41	0.001004	0.0278
17	21.76	0.504	174.50	0.572	155936	0.42	0.000978	0.0250
6	33.69	0.727	185.00	0.606	223461	0.59	0.001490	0.0188
18	28.41	0.567	197.70	0.648	186602	0.44	0.001092	0.0234
16	21.19	0.407	204.60	0.671	137473	0.30	0.000603	0.0254
3	21.90	0.390	218.80	0.717	128360	0.28	0.000594	0.0278
15	26.61	0.449	230.70	0.756	155086	0.30	0.000615	0.0221

Exp No	k_o (mm)	n_o	T (C)	A (m^2)	P (m)	R (m)	B (m)
1	0.869	0.0118	16.5	0.01191	0.2977	0.0400	0.2526
11	0.496	0.0110	16.5	0.01274	0.3054	0.0417	0.2568
8	0.539	0.0111	17.0	0.01553	0.3301	0.0470	0.2693
5	0.418	0.0108	17.0	0.01801	0.3502	0.0514	0.2782
10	0.339	0.0106	16.5	0.02072	0.3710	0.0558	0.2860
7	0.426	0.0109	17.0	0.02360	0.3920	0.0602	0.2926
4	0.472	0.0110	16.5	0.02657	0.4127	0.0644	0.2977
12	0.473	0.0110	17.0	0.02991	0.4354	0.0687	0.3018
13	0.454	0.0111	17.5	0.03369	0.4604	0.0732	0.3044
2	0.836	0.0120	17.0	0.03680	0.4809	0.0765	0.3050
14	0.254	0.0105	17.5	0.03729	0.4841	0.0770	0.3050
19	0.525	0.0113	18.5	0.03969	0.4998	0.0794	0.3043
9	1.085	0.0124	16.5	0.04207	0.5156	0.0816	0.3028
17	0.718	0.0118	18.0	0.04322	0.5233	0.0826	0.3018
6	0.184	0.0103	16.5	0.04635	0.5445	0.0851	0.2980
18	0.589	0.0115	18.0	0.05012	0.5709	0.0878	0.2913
16	0.814	0.0120	18.5	0.05209	0.5853	0.0890	0.5867
3	1.197	0.0126	16.5	0.05609	0.6162	0.0910	0.2747
15	0.442	0.0113	18.0	0.05929	0.6433	0.0922	0.2618

TABLE A8 CLEAR WATER EXPERIMENTAL DATA IN 305mm PIPE - PRECEDING TRANSPORT TESTS (ROUGHNESS 1; k_o = 0.53mm)

a) Flows up to half-full depth

Exp No	Q (l/s)	V (m/s)	y_o (mm)	y_o/D	Re	Fr	S_o	λ_o
14	10.93	0.844	71.20	0.233	138281	1.20	0.005627	0.0261
19	18.25	0.520	147.80	0.485	151116	0.49	0.001105	0.0240
32	16.15	0.616	118.50	0.388	153068	0.66	0.001776	0.0235
33	15.67	0.711	104.20	0.342	156249	0.82	0.002660	0.0239
38	13.44	0.858	81.40	0.267	155998	1.14	0.005132	0.0258
67	18.12	0.983	91.50	0.300	192143	1.22	0.005412	0.0229
1	11.89	0.694	87.00	0.285	130019	0.89	0.003278	0.0267
30	18.25	0.518	148.30	0.486	150836	0.49	0.001126	0.0247
31	16.15	0.620	117.80	0.386	151692	0.67	0.001788	0.0232
34	15.67	0.705	104.80	0.344	155813	0.81	0.002582	0.0237
37	13.44	0.861	81.20	0.266	156193	1.14	0.005107	0.0255
43	6.12	0.716	53.20	0.174	90603	1.19	0.005530	0.0275
70	24.11	1.013	110.20	0.361	229807	1.13	0.004437	0.0205
2	11.89	0.683	87.90	0.288	129246	0.87	0.003269	0.0277
15	10.93	0.838	71.50	0.234	137949	1.19	0.005485	0.0259
21	7.10	0.725	58.40	0.192	101110	1.15	0.005164	0.0273
22	12.50	0.931	79.10	0.259	151046	1.12	0.004895	0.0257
27	18.89	0.576	140.20	0.460	165642	0.56	0.001455	0.0248
28	18.25	0.524	147.00	0.482	149830	0.49	0.001137	0.0242
35	15.67	0.709	104.40	0.342	156144	0.82	0.002593	0.0235
36	13.44	0.869	80.70	0.264	156773	1.16	0.005103	0.0249
42	6.12	0.720	53.00	0.174	90764	1.20	0.005497	0.0270
71	24.11	1.016	110.00	0.361	230099	1.14	0.004522	0.0208
3	11.89	0.686	87.70	0.288	129425	0.87	0.003257	0.0274
16	10.93	0.840	71.40	0.234	138026	1.19	0.005560	0.0262
17	17.86	0.880	98.20	0.322	191290	1.05	0.004369	0.0245
20	7.10	0.725	58.50	0.192	101104	1.15	0.005154	0.0272
23	12.50	0.829	79.30	0.260	150882	1.11	0.004873	0.0257
26	18.89	0.571	141.30	0.463	164912	0.55	0.001390	0.0243
41	6.12	0.721	53.00	0.174	90831	1.20	0.005484	0.0268
66	18.12	0.984	91.40	0.300	192262	1.22	0.005454	0.0230
18	17.86	0.876	98.50	0.323	190993	1.04	0.004341	0.0246
19	7.10	0.728	58.30	0.191	101274	1.15	0.005175	0.0270
24	12.50	0.828	79.40	0.260	150804	1.11	0.004865	0.0258
25	18.89	0.581	139.40	0.457	166272	0.57	0.001429	0.0239
39	13.44	0.857	81.50	0.267	155868	1.13	0.005143	0.0260
40	6.12	0.720	53.00	0.174	90766	1.20	0.005553	0.0273
68	18.12	0.977	91.90	0.301	191709	1.21	0.005482	0.0236
69	24.11	1.016	110.00	0.361	230100	1.14	0.004515	0.0207

TABLE A8 Continued a) Flows up to half-full depth

Exp No	k_o (mm)	n_o	T (C)	A (m^2)	P (m)	R (m)	B (m)
14	0.434	0.0108	19.5	0.01296	0.3075	0.0421	0.2580
19	0.537	0.0114	19.5	0.03510	0.4697	0.0747	0.3049
32	0.416	0.0109	19.5	0.02622	0.4103	0.0639	0.2973
33	0.414	0.0109	18.5	0.02206	0.3809	0.0579	0.2893
38	0.472	0.0109	19.0	0.01566	0.3311	0.0473	0.2698
67	0.319	0.0105	18.0	0.01845	0.3537	0.0522	0.2796
1	0.560	0.0112	18.0	0.01719	0.3437	0.0500	0.2754
30	0.611	0.0115	19.5	0.03523	0.4706	0.0749	0.3049
31	0.392	0.0109	19.0	0.02604	0.4091	0.0636	0.2970
34	0.393	0.0108	18.5	0.02220	0.3820	0.0582	0.2897
37	0.446	0.0108	19.0	0.01561	0.3307	0.0472	0.2696
43	0.387	0.0106	19.5	0.00855	0.2629	0.0325	0.2315
70	0.222	0.0101	18.0	0.02381	0.3935	0.0605	0.2931
2	0.653	0.0114	18.0	0.01745	0.3457	0.0504	0.2762
15	0.420	0.0107	19.5	0.01304	0.3083	0.0423	0.2584
21	0.413	0.0107	20.0	0.00979	0.2764	0.0354	0.2401
22	0.446	0.0108	20.0	0.01504	0.3259	0.0461	0.2673
27	0.614	0.0115	20.5	0.03280	0.4546	0.0722	0.3040
28	0.556	0.0114	19.0	0.03484	0.4680	0.0744	0.3048
35	0.376	0.0108	18.5	0.02211	0.3812	0.0580	0.2894
36	0.398	0.0107	19.0	0.01547	0.3295	0.0469	0.2690
42	0.356	0.0105	19.5	0.00851	0.2624	0.0324	0.2312
71	0.236	0.0102	18.0	0.02374	0.3930	0.0604	0.2929
3	0.619	0.0113	18.0	0.01739	0.3452	0.0503	0.2760
16	0.437	0.0108	19.5	0.01302	0.3081	0.0423	0.2583
17	0.452	0.0109	20.0	0.02033	0.3681	0.0552	0.2850
20	0.410	0.0107	20.0	0.00979	0.2764	0.0354	0.2401
23	0.453	0.0109	20.0	0.01509	0.3263	0.0462	0.2675
26	0.559	0.0114	20.5	0.03310	0.4566	0.0725	0.3042
41	0.344	0.0104	19.5	0.00849	0.2622	0.0324	0.2311
66	0.325	0.0105	18.0	0.01842	0.3534	0.0521	0.2795
18	0.461	0.0109	20.0	0.02043	0.3688	0.0554	0.2852
19	0.397	0.0106	20.0	0.00975	0.2760	0.0353	0.2398
24	0.456	0.0109	20.0	0.01511	0.3265	0.0463	0.2671
25	0.517	0.0113	20.5	0.03254	0.4528	0.0719	0.3039
39	0.487	0.0110	19.0	0.01569	0.3314	0.0473	0.2699
40	0.372	0.0105	19.5	0.00851	0.2624	0.0324	0.2312
68	0.364	0.0106	18.0	0.01856	0.3545	0.0523	0.2799
69	0.234	0.0102	18.0	0.02374	0.3930	0.0604	0.2929

TABLE A8 Continued b) Flows more than half-full depth

Exp No	Q (l/s)	V (m/s)	y_o (mm)	y_o/D	Re	Fr	S_o	λ_o
4	21.76	0.414	206.10	0.676	138628	0.37	0.000630	0.0257
7	24.42	0.619	162.10	0.532	188282	0.55	0.001359	0.0221
13	32.96	0.706	186.10	0.610	231625	0.57	0.001536	0.0207
45	21.76	0.516	170.90	0.560	162074	0.44	0.001072	0.0258
54	26.93	0.560	190.80	0.626	192838	0.44	0.001068	0.0231
57	30.99	0.548	220.50	0.723	196805	0.38	0.001006	0.0240
58	29.43	0.489	233.90	0.767	180168	0.32	0.000721	0.0218
5	21.76	0.412	207.20	0.679	138094	0.36	0.000604	0.0250
6	24.42	0.621	161.70	0.530	188638	0.55	0.001395	0.0225
12	32.96	0.705	186.40	0.611	231406	0.57	0.001540	0.0208
44	21.76	0.519	170.30	0.558	162452	0.44	0.001011	0.0240
55	26.93	0.561	190.60	0.625	192987	0.44	0.001047	0.0226
56	30.99	0.552	219.10	0.718	197753	0.39	0.000940	0.0221
59	29.43	0.486	235.50	0.772	179141	0.32	0.000737	0.0226
60	28.92	0.756	158.20	0.519	232156	0.68	0.002280	0.0244
8	24.42	0.619	162.00	0.531	188406	0.55	0.001418	0.0230
9	32.96	0.698	187.80	0.616	232972	0.56	0.001528	0.0211
46	21.76	0.514	171.70	0.563	161602	0.44	0.001012	0.0246
47	28.75	0.721	163.40	0.536	220566	0.64	0.001735	0.0208
53	26.93	0.560	190.90	0.626	192795	0.44	0.001048	0.0227
61	28.92	0.742	160.60	0.526	229923	0.66	0.002079	0.0234
10	32.96	0.697	188.10	0.617	235536	0.56	0.001549	0.0215
48	28.75	0.719	163.80	0.537	220257	0.64	0.001736	0.0210
51	29.43	0.647	182.00	0.597	215144	0.53	0.001296	0.0205
52	26.93	0.561	190.60	0.624	193004	0.44	0.001055	0.0227
62	28.92	0.743	160.40	0.526	230084	0.66	0.001989	0.0223
65	30.99	0.821	156.50	0.513	253526	0.74	0.002412	0.0218
11	32.96	0.706	186.00	0.609	231718	0.57	0.001588	0.0213
49	28.75	0.720	163.60	0.536	220367	0.63	0.001707	0.0206
50	29.43	0.656	180.00	0.590	216790	0.54	0.001352	0.0207
63	28.92	0.745	159.90	0.524	230524	0.67	0.002134	0.0237
64	30.99	0.827	155.60	0.510	254497	0.75	0.002471	0.0219

TABLE A8 Continued b) Flows more than half-full depth

Exp No	k_o (mm)	n_o	T (C)	A (m^2)	P (m)	R (m)	B (m)
4	0.858	0.0121	18.0	0.03684	0.5886	0.0892	0.2855
7	0.400	0.0110	19.0	0.03947	0.4984	0.0792	0.3044
13	0.325	0.0108	19.0	0.04670	0.5469	0.0854	0.2975
45	0.812	0.0119	19.0	0.04213	0.5160	0.0817	0.3028
54	0.548	0.0114	20.5	0.04810	0.5566	0.0864	0.2952
57	0.687	0.0117	20.0	0.05655	0.6200	0.0912	0.2730
58	0.437	0.0112	20.5	0.06013	0.6509	0.0924	0.2579
5	0.762	0.0119	18.0	0.03706	0.5909	0.0894	0.2847
6	0.435	0.0111	19.0	0.03933	0.4975	0.0791	0.3044
12	0.336	0.0108	19.0	0.04677	0.5474	0.0854	0.2974
44	0.598	0.0115	19.0	0.04195	0.5148	0.0815	0.3029
55	0.492	0.0113	20.5	0.04804	0.5562	0.0864	0.2953
56	0.469	0.0113	20.0	0.05619	0.6170	0.0911	0.2744
59	0.523	0.0114	20.5	0.06053	0.6546	0.0925	0.2559
60	0.652	0.0115	20.0	0.03827	0.4905	0.0780	0.3048
8	0.484	0.0112	19.0	0.03942	0.4981	0.0791	0.3044
9	0.364	0.0109	19.5	0.04720	0.5504	0.0858	0.2967
46	0.671	0.0117	19.0	0.04236	0.5175	0.0819	0.3026
47	0.311	0.0107	19.0	0.03985	0.5009	0.0796	0.3042
53	0.503	0.0113	20.5	0.04812	0.5567	0.0864	0.2952
61	0.540	0.0113	20.0	0.03899	0.4952	0.0787	0.3046
10	0.402	0.0110	20.0	0.04730	0.5510	0.0858	0.2966
48	0.323	0.0107	19.0	0.03996	0.5016	0.0797	0.3042
51	0.303	0.0107	20.0	0.04549	0.5386	0.0845	0.2992
52	0.508	0.0113	20.5	0.04803	0.5561	0.0864	0.2953
62	0.434	0.0110	20.0	0.03894	0.4949	0.0787	0.3046
65	0.393	0.0109	20.5	0.03775	0.4871	0.0775	0.3049
11	0.382	0.0109	19.0	0.04667	0.5466	0.0854	0.2975
49	0.291	0.0106	19.0	0.03992	0.5014	0.0796	0.3042
50	0.319	0.0108	20.0	0.04489	0.5345	0.0840	0.3000
63	0.573	0.0114	20.0	0.03880	0.4940	0.0785	0.3046
64	0.401	0.0109	20.5	0.03747	0.4852	0.0772	0.3049

TABLE A9 CLEAR WATER EXPERIMENTAL DATA IN 305mm PIPE - PRELIMINARY TESTS (ROUGHNESS 2; k_o = 1.34mm)

Exp No	Q (l/s)	V (m/s)	y_o (mm)	y_o/D	Re	Fr	S_o	λ_o
1	7.85	0.532	78.00	0.256	84332	0.72	0.002701	0.0341
2	12.19	0.517	109.40	0.359	108168	0.58	0.001779	0.0314
3	16.27	0.441	153.70	0.504	117378	0.41	0.000995	0.0308
4	5.05	0.486	61.00	0.200	62082	0.75	0.003736	0.0458
5	14.98	0.805	92.20	0.302	142906	1.00	0.005212	0.0331
6	27.59	0.661	169.60	0.556	181900	0.57	0.002131	0.0311

Exp No	k_o (mm)	n_o	T (C)	A (m^2)	P (m)	R (m)	B (m)
1	1.211	0.0125	15.0	0.01474	0.3233	0.0456	0.2661
2	1.223	0.0125	15.0	0.02357	0.3918	0.0602	0.2926
3	1.470	0.0129	15.0	0.03690	0.4815	0.0766	0.3050
4	2.403	0.0139	15.0	0.01041	0.2829	0.0368	0.2440
5	1.312	0.0126	14.0	0.01863	0.3551	0.0525	0.2801
6	1.670	0.0131	14.0	0.04174	0.5134	0.0813	0.3031

TABLE A10 CLEAR WATER EXPERIMENTAL DATA IN 305mm PIPE - PRECEDING TRANSPORT TESTS (ROUGHNESS 2; k_o = 1.34mm)

a) Flows up to half-full depth

Exp No	Q (l/s)	V (m/s)	y_o (mm)	y_o/D	Re	Fr	S_o	λ_o
9	9.83	0.723	73.60	0.241	99402	1.01	0.005546	0.0360
15	14.09	0.741	93.70	0.307	126324	0.91	0.004424	0.0336
20	20.78	0.742	124.40	0.408	160014	0.78	0.003241	0.0306
21	30.99	0.834	154.50	0.507	214297	0.76	0.003132	0.0272
8	9.83	0.725	73.50	0.241	99467	1.02	0.005553	0.0359
13	14.09	0.742	93.50	0.306	124725	0.91	0.004410	0.0331
19	20.78	0.742	124.40	0.408	160000	0.78	0.003291	0.0311
24	19.03	0.834	107.00	0.351	155940	0.95	0.004741	0.0316
7	9.83	0.721	73.80	0.242	99269	1.01	0.005556	0.0365
14	14.09	0.738	94.00	0.308	126077	0.90	0.004437	0.0341
18	20.78	0.745	124.10	0.407	160224	0.79	0.003255	0.0305
22	30.99	0.826	155.60	0.510	213283	0.75	0.003070	0.0272
23	19.03	0.832	107.10	0.351	155826	0.95	0.004746	0.0318
10	9.83	0.722	73.80	0.242	99297	1.01	0.005550	0.0363
16	14.09	0.734	94.20	0.309	125863	0.90	0.004419	0.0343
17	20.78	0.751	123.30	0.404	160812	0.79	0.003241	0.0297
25	19.03	0.836	106.70	0.350	158324	0.95	0.004741	0.0314

Exp No	k_o (mm)	n_o	T (C)	A (m^2)	P (m)	R (m)	B (m)
9	1.405	0.0127	11.5	0.01359	0.3132	0.0434	0.2610
15	1.394	0.0127	12.0	0.01906	0.3583	0.0532	0.2813
20	1.268	'0.0126	12.5	0.02800	0.4225	0.0663	0.2997
21	0.970	0.0121	13.5	0.03714	0.4831	0.0769	0.3050
8	1.387	0.0127	11.5	0.01356	0.3130	0.0433	0.2609
13	1.344	0.0126	11.5	0.01900	0.3579	0.0531	0.2812
19	1.345	0.0127	12.5	0.02801	0.4226	0.0663	0.2998
24	1.273	0.0125	11.5	0.02285	0.3866	0.0591	0.2910
7	1.465	0.0128	11.5	0.01365	0.3137	0.0435	0.2612
14	1.461	0.0128	12.0	0.01912	0.3589	0.0533	0.2816
18	1.252	0.0125	12.5	0.02791	0.4219	0.0662	0.2996
22	0.987	0.0122	13.5	0.03749	0.4854	0.0772	0.3049
23	1.300	0.0126	11.5	0.02289	0.3869	0.0592	0.2911
10	1.445	0.0128	11.5	0.01363	0.3136	0.0435	0.2612
16	1.500	0.0128	12.0	0.01921	0.3595	0.0534	0.2818
17	1.138	0.0124	12.5	0.02769	0.4204	0.0659	0.2993
25	1.233	0.0125	12.0	0.02278	0.3860	0.0590	0.2909

TABLE A10 Continued b) Flows more than half-full depth

Exp No	Q (l/s)	V (m/s)	y_o (mm)	y_o/D	Re	Fr	S_o	λ_o
2	29.26	0.580	198.70	0.652	172844	0.44	0.001412	0.0289
3	33.88	0.571	231.00	0.756	168798	0.38	0.001281	0.0285
4	27.92	0.682	166.80	0.547	178789	0.59	0.002131	0.0289
30	33.70	0.605	217.40	0.713	181176	0.43	0.001508	0.0294
5	27.92	0.681	167.20	0.548	178537	0.59	0.002246	0.0307
12	30.99	0.671	184.50	0.605	187956	0.54	0.001843	0.0273
28	34.63	0.672	202.50	0.664	196494	0.51	0.001822	0.0280
29	33.70	0.606	216.80	0.711	181502	0.43	0.001481	0.0287
1	29.26	0.583	198.00	0.649	173296	0.45	0.001468	0.0298
6	27.92	0.680	167.20	0.548	178509	0.59	0.002248	0.0307
27	34.63	0.673	202.40	0.664	196546	0.51	0.001828	0.0281
11	30.99	0.669	184.90	0.606	187652	0.54	0.001875	0.0280
26	34.63	0.673	202.20	0.663	196674	0.51	0.001908	0.0293

Exp No	k_o (mm)	n_o	T (C)	A (m^2)	P (m)	R (m)	B (m)
2	1.386	0.0128	14.0	0.05041	0.5730	0.0880	0.2907
3	1.366	0.0128	12.0	0.05938	0.6441	0.0922	0.2614
4	1.271	0.0126	12.5	0.04090	0.5079	0.0805	0.3036
30	1.522	0.0130	13.0	0.05570	0.6131	0.0909	0.2760
5	1.574	0.0130	12.5	0.04101	0.5086	0.0806	0.3036
12	1.090	0.0124	13.0	0.04621	0.5435	0.0850	0.2982
28	1.256	0.0126	13.0	0.05150	0.5810	0.0886	0.2881
29	1.392	0.0128	13.0	0.05557	0.6120	0.0908	0.2765
1	1.542	0.0130	14.0	0.05020	0.5715	0.0878	0.2911
6	1.583	0.0130	12.5	0.04102	0.5086	0.0807	0.3036
27	1.267	0.0126	13.0	0.05148	0.5808	0.0886	0.2882
11	1.196	0.0125	13.0	0.04634	0.5444	0.0851	0.2980
26	1.470	0.0129	13.0	0.05143	0.5804	0.0886	0.2883

APPENDIX B

BED LOAD TRANSPORT EXPERIMENTAL DATA

TABLE B1 BED LOAD EXPERIMENTAL DATA IN 154mm PIPE - (SMOOTH RIGID BED)

a) Flows up to half-full depth

Exp No	d50 (mm)	Q (l/s)	V (m/s)	y/D	Re	Fr	S_o	λ_s	k_s (mm)
21	0.93	0.46	0.240	0.159	13591	0.59	0.001756	0.0361	0.305
22	0.93	2.21	0.487	0.293	47653	0.86	0.003129	0.0267	0.210
23	0.93	5.73	0.746	0.433	99508	1.05	0.004785	0.0239	0.219
24	0.93	1.22	0.382	0.228	30546	0.78	0.002673	0.0299	0.250
25	0.93	6.45	0.719	0.486	101808	0.95	0.003268	0.0188	0.024
11	2.00	1.30	0.360	0.248	27698	0.70	0.002646	0.0360	0.612
12	2.00	0.44	0.248	0.153	12715	0.62	0.002596	0.0480	0.928
13	2.00	2.69	0.497	0.332	50680	0.82	0.002694	0.0245	0.139
14	2.00	4.41	0.610	0.413	75913	0.88	0.003463	0.0250	0.238
15	2.00	3.75	0.449	0.459	60493	0.61	0.001832	0.0260	0.290
16	2.00	2.45	0.412	0.356	47260	0.66	0.002170	0.0303	0.462
3	4.20	4.73	0.532	0.483	76924	0.71	0.002198	0.0229	0.159
4	4.20	5.15	0.740	0.400	88178	1.10	0.004569	0.0216	0.098
5	4.20	6.99	0.784	0.483	107992	1.04	0.004562	0.0219	0.146
6	4.20	2.22	0.457	0.307	44834	0.79	0.003738	0.0376	0.935
7	4.20	1.32	0.396	0.235	30662	0.79	0.002490	0.0266	0.113
8	4.20	2.00	0.396	0.316	40273	0.67	0.002199	0.0303	0.397
28	4.20	4.70	0.681	0.398	82848	1.01	0.004789	0.0267	0.332
29	4.20	2.23	0.500	0.288	48437	0.89	0.003260	0.0260	0.179
30	4.20	2.39	0.562	0.280	53612	1.02	0.004946	0.0306	0.409
31	4.20	1.23	0.441	0.207	32453	0.94	0.004991	0.0387	0.703
32	5.70	5.48	0.743	0.418	97260	1.08	0.004859	0.0235	0.193
33	5.70	1.33	0.381	0.243	32702	0.75	0.003177	0.0378	0.745
34	5.70	2.10	0.476	0.287	45903	0.85	0.003604	0.0316	0.463
35	5.70	6.46	0.740	0.478	108547	0.99	0.004913	0.0263	0.375
36	5.70	3.55	0.600	0.364	70118	0.91	0.004304	0.0309	0.557

TABLE B1 Continued a) Flows up to half-full depth

Exp No	n_s	Cv (ppm)	Ws (mm)	T (C)	A (m^2)	P (m)	R (m)	B (m)
21	0.0107	52	9	18.0	0.00191	0.1264	0.0151	0.1126
22	0.0100	249	10	18.5	0.00454	0.1760	0.0258	0.1401
23	0.0099	426	13	19.0	0.00774	0.2213	0.0350	0.1526
24	0.0102	147	10	19.0	0.00319	0.1531	0.0208	0.1291
25	0.0090	151	13	18.0	0.00897	0.2375	0.0378	0.1539
11	0.0114	200	10	14.5	0.00361	0.1607	0.0224	0.1330
12	0.0122	113	10	15.5	0.00180	0.1236	0.0145	0.1107
13	0.0098	186	15	16.0	0.00542	0.1894	0.0286	0.1451
14	0.0101	309	20	17.5	0.00727	0.2151	0.0338	0.1517
15	0.0105	167	13	17.5	0.00835	0.2294	0.0364	0.1535
16	0.0110	167	10	18.5	0.00595	0.1969	0.0302	0.1475
3	0.0099	164	NA	19.0	0.00890	0.2366	0.0376	0.1539
4	0.0094	268	NA	16.5	0.00696	0.2109	0.0330	0.1509
5	0.0097	205	NA	17.0	0.00891	0.2367	0.0377	0.1539
6	0.0120	285	NA	17.0	0.00485	0.1808	0.0268	0.1420
7	0.0097	163	10	16.5	0.00333	0.1558	0.0214	0.1305
8	0.0108	212	10	17.5	0.00505	0.1839	0.0275	0.1432
28	0.0104	1014	25	17.5	0.00691	0.2103	0.0329	0.1508
29	0.0099	822	28	18.5	0.00445	0.1747	0.0255	0.1395
30	0.0107	1260	28	19.0	0.00426	0.1717	0.0248	0.1382
31	0.0115	1450	28	19.0	0.00279	0.1456	0.0192	0.1248
32	0.0099	1237	28	19.0	0.00738	0.2165	0.0341	0.1519
33	0.0116	734	30	19.5	0.00350	0.1588	0.0220	0.1321
34	0.0109	1221	30	18.5	0.00442	0.1741	0.0254	0.1393
35	0.0106	1258	36	20.0	0.00874	0.2344	0.0373	0.1538
36	0.0107	1382	36	20.0	0.00613	0.1995	0.0307	0.1482

TABLE B1 Continued b) Flows more than half-full depth

Exp No	d50 (mm)	Q (l/s)	V (m/s)	y/D	Re	Fr	S_o	λ_s	k_s (mm)
20	0.93	8.04	0.824	0.519	118724	1.04	0.004768	0.0217	0.152
26	0.93	7.81	0.516	0.757	95565	0.49	0.001161	0.0159	-0.073
27	0.93	7.96	0.646	0.628	107237	0.72	0.002289	0.0188	0.036
10	2.00	8.04	0.631	0.647	95811	0.68	0.002433	0.0213	0.126
17	2.00	7.17	0.732	0.520	109713	0.93	0.003513	0.0203	0.086
18	2.00	6.63	0.620	0.558	98066	0.75	0.002677	0.0225	0.178
19	2.00	7.28	0.620	0.603	103408	0.71	0.002150	0.0188	0.031
1	4.20	8.13	0.603	0.680	100906	0.63	0.002064	0.0201	0.081
2	4.20	7.62	0.762	0.529	114467	0.95	0.004197	0.0226	0.193
9	4.20	7.65	0.751	0.537	114746	0.93	0.003812	0.0213	0.135
37	5.70	9.70	0.862	0.582	142918	1.01	0.005281	0.0235	0.267
38	5.70	9.74	0.661	0.738	122009	0.64	0.002325	0.0193	0.072
39	5.70	6.67	0.628	0.556	105177	0.76	0.003223	0.0263	0.409

Exp No	n_s	Cv (ppm)	Ws (mm)	T (C)	A (m^2)	P (m).	R (m)	B (m)
20	0.0097	296	15	17.0	0.00976	0.2477	0.0394	0.1539
26	0.0085	38	22	19.0	0.01514	0.3252	0.0465	0.1320
27	0.0092	82	22	18.5	0.01232	0.2819	0.0437	0.1488
10	0.0098	115	10	14.5	0.01275	0.2876	0.0443	0.1472
17	0.0094	291	20	18.5	0.00979	0.2481	0.0395	0.1538
18	0.0099	155	13	19.0	0.01070	0.2599	0.0411	0.1529
19	0.0092	121	20	19.5	0.01174	0.2739	0.0429	0.1507
1	0.0096	138	NA	17.5	0.01348	0.2986	0.0452	0.1437
2	0.0099	373	NA	18.2	0.01001	0.2509	0.0399	0.1537
9	0.0097	168	10	18.5	0.01020	0.2534	0.0402	0.1535
37	0.0102	1415	36	20.0	0.01125	0.2673	0.0421	0.1519
38	0.0094	369	33	20.5	0.01473	0.3183	0.0463	0.1354
39	0.0107	989	42	21.5	0.01063	0.2591	0.0410	0.1529

TABLE B2 BED LOAD EXPERIMENTAL DATA IN 305mm PIPE - (SMOOTH RIGID BED)

a) Flows up to half-full depth

Exp No	d50 (mm)	Q (l/s)	V (m/s)	y_o/D	Re	Fr	S_o	λ_s	k_s (mm)
80	0.46	8.08	0.721	0.211	96548	1.08	0.003448	0.0200	0.062
75	0.46	20.37	1.146	0.292	203182	1.45	0.005339	0.0163	0.017
81	0.46	15.67	0.670	0.357	135922	0.76	0.001525	0.0160	−0.032
87	0.46	16.27	0.586	0.405	136072	0.62	0.001081	0.0163	−0.023
76	0.46	27.92	0.888	0.445	220578	0.88	0.002301	0.0161	0.028
86	0.46	17.61	0.485	0.498	129796	0.45	0.000622	0.0158	−0.056
79	0.97	8.08	0.724	0.210	96770	1.09	0.003513	0.0202	0.069
9	0.97	9.48	0.749	0.230	115270	1.08	0.003319	0.0193	0.058
20	0.97	8.08	0.584	0.244	94955	0.81	0.002012	0.0202	0.078
73	0.97	20.78	1.165	0.293	201603	1.47	0.005317	0.0157	0.003
21	0.97	25.03	1.143	0.340	226105	1.33	0.004439	0.0154	0.003
25	0.97	20.37	0.925	0.341	200697	1.07	0.003074	0.0163	0.021
82	0.97	15.67	0.667	0.358	137451	0.75	0.001493	0.0158	−0.036
88	0.97	16.27	0.587	0.404	137940	0.62	0.001080	0.0162	−0.025
4	0.97	22.34	0.690	0.455	174040	0.67	0.001220	0.0144	−0.055
85	0.97	17.61	0.486	0.497	129884	0.45	0.000634	0.0160	−0.045
35	2.00	13.44	0.865	0.265	154575	1.15	0.003668	0.0181	0.050
12	2.00	19.56	1.080	0.295	200482	1.36	0.005080	0.0175	0.053
26	2.00	20.78	0.943	0.342	204782	1.09	0.003132	0.0160	0.013
16	2.00	8.72	0.395	0.342	86916	0.46	0.000687	0.0200	0.076
17	2.00	16.87	0.758	0.344	165541	0.87	0.002102	0.0167	0.015
38	2.00	15.44	0.651	0.360	151087	0.73	0.001491	0.0167	0.005
11	2.00	17.49	0.585	0.428	143293	0.59	0.000821	0.0129	−0.116
29	2.00	19.29	0.513	0.512	149460	0.46	0.000719	0.0166	0.003
8	4.20	9.48	0.741	0.232	113384	1.06	0.003301	0.0198	0.074
34	4.20	13.44	0.865	0.265	152734	1.15	0.003661	0.0181	0.047
1	4.20	14.42	0.889	0.274	143460	1.16	0.004035	0.0193	0.092
13	4.20	19.56	1.080	0.296	206317	1.35	0.005300	0.0184	0.088
6	4.20	11.70	0.550	0.330	108340	0.64	0.001401	0.0207	0.143
15	4.20	8.77	0.401	0.340	86673	0.46	0.000733	0.0206	0.109

TABLE B2 Continued a) Flows up to half-full depth

Exp No	d50 (mm)	Q (l/s)	V (m/s)	y_d/D	Re	Fr	S_o	λ_s	k_s (mm)
27	4.20	20.78	0.941	0.342	204577	1.09	0.003161	0.0163	0.020
22	4.20	25.34	1.118	0.349	227473	1.28	0.004442	0.0164	0.034
3	4.20	11.41	0.436	0.388	99184	0.47	0.000752	0.0199	0.098
5	4.20	22.34	0.683	0.459	175430	0.66	0.001201	0.0146	-0.050
28	4.20	19.29	0.516	0.509	147404	0.47	0.000681	0.0155	-0.047
7	5.70	9.48	0.730	0.234	107152	1.04	0.003300	0.0205	0.100
19	5.70	8.08	0.587	0.244	92735	0.82	0.002020	0.0201	0.069
33	5.70	13.44	0.858	0.267	150350	1.14	0.003690	0.0186	0.065
14	5.70	19.69	1.070	0.299	209166	1.34	0.004888	0.0173	0.053
24	5.70	20.37	0.919	0.343	197709	1.06	0.003091	0.0167	0.032
18	5.70	16.87	0.750	0.347	167633	0.86	0.002045	0.0167	0.018
23	5.70	25.34	1.115	0.349	228318	1.27	0.004652	0.0173	0.066
37	5.70	15.44	0.650	0.361	149123	0.73	0.001428	0.0160	-0.018
10	5.70	17.24	0.576	0.429	139359	0.58	0.000829	0.0135	-0.108
31	5.70	24.11	0.679	0.489	179675	0.63	0.001090	0.0140	-0.066
78	8.30	8.08	0.715	0.212	94988	1.07	0.003439	0.0204	0.077
32	8.30	13.44	0.851	0.269	142389	1.12	0.003712	0.0191	0.082
74	8.30	20.37	1.133	0.295	199610	1.42	0.005051	0.0159	0.006
36	8.30	15.44	0.647	0.362	143364	0.72	0.001515	0.0172	0.019
83	8.30	33.51	1.205	0.406	276449	1.26	0.004379	0.0156	0.027
89	8.30	16.27	0.584	0.406	137606	0.62	0.001085	0.0165	-0.014
77	8.30	27.92	0.886	0.446	220276	0.88	0.002330	0.0165	0.040
30	8.30	24.11	0.676	0.491	176971	0.63	0.001066	0.0138	-0.073
84	8.30	17.61	0.486	0.497	129901	0.45	0.000625	0.0158	-0.055

TABLE B2 Continued a) Flows up to half-full depth

Exp No	n_s	Cv (ppm)	Ws (mm)	T (C)	A (m^2)	P (m)	R (m)	B (m)
80	0.0093	197	30	15.5	0.01120	0.2909	0.0385	0.2487
75	0.0088	730	80	15.0	0.01777	0.3483	0.0510	0.2774
81	0.0089	79	30	14.0	0.02339	0.3904	0.0599	0.2922
87	0.0092	27	30	15.5	0.02774	0.4207	0.0659	0.2994
76	0.0092	168	40	15.5	0.03143	0.4455	0.0705	0.3031
86	0.0092	8	20	15.5	0.03631	0.4776	0.0760	0.3050
79	0.0093	222	35	15.0	0.01118	0.2906	0.0385	0.2485
9	0.0092	232	40	17.5	0.01267	0.3049	0.0416	0.2566
20	0.0095	80	30	17.5	0.01383	0.3154	0.0438	0.2621
73	0.0086	734	80	14.0	0.01784	0.3489	0.0511	0.2776
21	0.0087	388	70	14.5	0.02191	0.3798	0.0577	0.2890
25	0.0090	183	40	18.0	0.02204	0.3807	0.0579	0.2892
82	0.0089	88	30	14.5	0.02349	0.3912	0.0601	0.2924
88	0.0091	38	30	16.0	0.02769	0.4204	0.0659	0.2994
4	0.0087	27	40	15.5	0.03237	0.4518	0.0717	0.3038
85	0.0093	13	20	15.5	0.03626	0.4773	0.0760	0.3050
35	0.0091	294	40	18.5	0.01554	0.3302	0.0471	0.2693
12	0.0091	503	60	16.3	0.01804	0.3505	0.0515	0.2783
26	0.0089	202	40	18.0	0.02207	0.3809	0.0579	0.2893
16	0.0099	12	25	18.5	0.02208	0.3810	0.0579	0.2894
17	0.0091	121	50	18.0	0.02225	0.3823	0.0582	0.2897
38	0.0091	70	40	19.0	0.02371	0.3928	0.0604	0.2929
11	0.0082	33	30	16.0	0.02987	0.4351	0.0687	0.3018
29	0.0095	9	20	18.2	0.03763	0.4863	0.0774	0.3049
8	0.0093	394	40	17.0	0.01282	0.3062	0.0419	0.2573
34	0.0091	461	40	18.0	0.01555	0.3302	0.0471	0.2693
1	0.0095	486	NA	13.5	0.01622	0.3358	0.0483	0.2719
13	0.0093	997	60	17.5	0.01810	0.3510	0.0516	0.2785
6	0.0101	43	40	15.0	0.02129	0.3752	0.0567	0.2875
15	0.0101	7	10	18.0	0.02187	0.3795	0.0576	0.2889
27	0.0090	308	40	18.0	0.02212	0.3813	0.0580	0.2894
22	0.0090	903	60	14.8	0.02268	0.3853	0.0588	0.2907
3	0.0101	14	30	16.0	0.02617	0.4100	0.0638	0.2972
5	0.0088	52	40	16.0	0.03271	0.4540	0.0720	0.3040
28	0.0092	17	20	17.5	0.03737	0.4846	0.0771	0.3049
7	0.0095	418	40	15.0	0.01302	0.3080	0.0422	0.2582
19	0.0095	196	40	16.5	0.01378	0.3149	0.0437	0.2618
33	0.0093	566	50	17.5	0.01567	0.3312	0.0473	0.2698
14	0.0091	1183	60	18.0	0.01837	0.3530	0.0520	0.2793
24	0.0091	374	40	17.5	0.02219	0.3818	0.0581	0.2896
18	0.0091	298	60	18.7	0.02251	0.3841	0.0586	0.2903
23	0.0093	1190	60	15.0	0.02275	0.3859	0.0589	0.2908
37	0.0090	93	40	18.5	0.02376	0.3931	0.0604	0.2930
10	0.0084	44	30	15.5	0.02992	0.4354	0.0687	0.3019
31	0.0087	57	40	15.5	0.03551	0.4724	0.0752	0.3049
78	0.0094	647	40	14.5	0.01130	0.2918	0.0387	0.2493
32	0.0094	755	60	15.5	0.01581	0.3324	0.0476	0.2704
74	0.0087	1280	80	14.5	0.01798	0.3500	0.0514	0.2781
36	0.0093	144	40	17.0	0.02387	0.3939	0.0606	0.2932
83	0.0090	1128	60	15.0	0.02781	0.4212	0.0660	0.2995
89	0.0092	63	30	16.0	0.02784	0.4214	0.0661	0.2996
77	0.0093	316	40	15.5	0.03152	0.4461	0.0707	0.3032
30	0.0086	68	40	15.0	0.03567	0.4735	0.0753	0.3049
84	0.0092	0.759	20	15.5	0.03625	0.4772	0.0760	0.3050

TABLE B2 Continued b) Flows more than half-full depth

Exp No	d50 (mm)	Q (l/s)	V (m/s)	y_o/D	Re	Fr	S_o	λ_s	k_s (mm)
71	0.46	27.59	0.670	0.550	180869	0.58	0.001093	0.0154	−0.021
70	0.46	37.33	0.829	0.592	235904	0.68	0.001589	0.0153	0.005
61	0.46	27.59	0.559	0.639	173998	0.44	0.000787	0.0172	0.059
62	0.46	35.77	0.604	0.755	188507	0.40	0.000840	0.0168	0.049
72	0.97	27.59	0.668	0.551	183001	0.58	0.001013	0.0144	−0.055
68	0.97	37.33	0.810	0.603	229888	0.66	0.001618	0.0164	0.050
58	0.97	27.59	0.562	0.637	174534	0.44	0.000789	0.0171	0.050
54	0.97	28.58	0.515	0.710	162451	0.37	0.000629	0.0169	0.031
67	0.97	36.16	0.608	0.758	189895	0.41	0.000799	0.0156	−0.008
57	0.97	31.88	0.506	0.805	165218	0.32	0.000621	0.0177	0.083
48	2.00	28.25	0.724	0.526	193098	0.65	0.001284	0.0151	−0.023
49	2.00	32.42	0.778	0.556	211024	0.67	0.001405	0.0148	−0.023
39	2.00	30.64	0.700	0.578	199439	0.59	0.001015	0.0135	−0.072
52	2.00	23.81	0.489	0.632	143773	0.38	0.000648	0.0185	0.104
60	2.00	27.59	0.559	0.640	173945	0.43	0.000784	0.0172	0.057
53	2.00	28.58	0.506	0.717	157088	0.36	0.000620	0.0170	0.035
66	2.00	36.16	0.609	0.756	189965	0.41	0.000822	0.0161	0.012
45	4.20	28.25	0.724	0.526	193064	0.65	0.001279	0.0151	−0.025
2	4.20	27.75	0.655	0.563	181488	0.56	0.001172	0.0176	0.078
69	4.20	37.33	0.817	0.599	234048	0.67	0.001579	0.0157	0.021
44	4.20	32.05	0.612	0.674	189539	0.46	0.000798	0.0149	−0.036
55	4.20	28.58	0.516	0.709	162686	0.37	0.000626	0.0167	0.023
65	4.20	36.16	0.610	0.756	190358	0.41	0.000788	0.0153	−0.021
56	4.20	31.88	0.507	0.803	164725	0.32	0.000624	0.0177	0.082
47	5.70	28.25	0.729	0.524	193739	0.65	0.001322	0.0153	−0.016
51	5.70	32.42	0.781	0.554	220028	0.67	0.001439	0.0150	−0.012
41	5.70	30.64	0.701	0.578	202168	0.59	0.001057	0.0140	−0.055
59	5.70	27.59	0.562	0.637	174480	0.44	0.000787	0.0171	0.049
42	5.70	32.05	0.610	0.676	189222	0.45	0.000700	0.0132	−0.094
64	5.70	36.16	0.610	0.756	190260	0.41	0.000799	0.0155	−0.011
46	8.30	28.25	0.726	0.526	193312	0.65	0.001281	0.0150	−0.027
50	8.30	31.70	0.760	0.556	214676	0.65	0.001493	0.0165	0.043
40	8.30	30.64	0.697	0.580	198968	0.58	0.001040	0.0140	−0.059
43	8.30	32.05	0.612	0.674	189679	0.46	0.000788	0.0147	−0.044
63	8.30	35.77	0.602	0.758	187898	0.40	0.000824	0.0165	0.031

TABLE B3 BED LOAD EXPERIMENTAL DATA IN 450mm PIPE - (SMOOTH RIGID BED)

a) Flows at half-full depth

Exp No	d50 (mm)	Q (l/s)	V (m/s)	y_o/D	Re	Fr	S_o	λ_s	k_s (mm)
1	0.72	48.02	0.609	0.497	242326	0.46	0.000677	0.0160	0.050
2	0.72	62.88	0.786	0.503	314821	0.59	0.001173	0.0168	0.131
3	0.72	77.29	0.983	0.496	392164	0.75	0.002006	0.0182	0.247
4	0.72	40.51	0.510	0.500	206283	0.39	0.000476	0.0161	0.031
5	0.72	55.93	0.709	0.497	285694	0.54	0.000978	0.0171	0.138
6	0.72	63.81	0.808	0.498	321554	0.62	0.001193	0.0161	0.088
7	0.72	71.51	0.912	0.495	361775	0.70	0.001609	0.0169	0.151
8	0.72	78.41	0.986	0.500	390679	0.75	0.001983	0.0180	0.232
9	0.72	87.12	1.069	0.509	439273	0.80	0.001994	0.0156	0.089
10	0.72	55.73	0.705	0.498	288093	0.54	0.000981	0.0174	0.157
11	0.72	40.12	0.504	0.500	204077	0.38	0.000507	0.0176	0.128
13	0.72	47.22	0.600	0.497	238245	0.46	0.000715	0.0175	0.144
23	0.72	95.22	1.216	0.494	459563	0.93	0.003054	0.0181	0.249
24	0.72	59.51	0.754	0.497	288446	0.57	0.001058	0.0164	0.091
25	0.72	67.47	0.853	0.500	326795	0.65	0.001320	0.0159	0.081
26	0.72	43.90	0.553	0.499	209314	0.42	0.000573	0.0165	0.061
27	0.72	51.08	0.652	0.495	241777	0.49	0.000820	0.0169	0.106
28	0.72	66.91	0.843	0.499	319149	0.64	0.001234	0.0153	0.045

Exp No	n_s	Cv (ppm)	T (C)	A (m^2)	P (m)	R (m)	B (m)
1	0.0094	5	15.5	0.07878	0.7035	0.1120	0.4495
2	0.0102	13	15.5	0.08003	0.7091	0.1129	0.4495
3	0.0106	22	16.0	0.07859	0.7027	0.1118	0.4495
4	0.0100	4	16.0	0.07937	0.7062	0.1124	0.4495
5	0.0103	7	16.0	0.07891	0.7041	0.1121	0.4495
6	0.0099	8	16.0	0.07899	0.7045	0.1121	0.4495
7	0.0102	11	15.5	0.07842	0.7020	0.1117	0.4495
8	0.0105	18	15.5	0.07949	0.7067	0.1125	0.4495
9	0.0098	20	16.5	0.08136	0.7151	0.1138	0.4494
10	0.0103	5	16.5	0.07904	0.7047	0.1122	0.4495
11	0.0104	2	16.0	0.07955	0.7070	0.1125	0.4495
13	0.0104	5	15.5	0.07880	0.7036	0.1120	0.4495
23	0.0105	38	14.0	0.07834	0.7016	0.1116	0.4494
24	0.0100	13	14.0	0.07892	0.7042	0.1121	0.4495
25	0.0099	19	14.0	0.07904	0.7046	0.1122	0.4495
26	0.0101	3	13.5	0.07939	0.7063	0.1124	0.4495
27	0.0102	5	13.0	0.07841	0.7019	0.1117	0.4495
28	0.0097	14	13.5	0.07934	0.7060	0.1124	0.4495

TABLE B3 Continued b) Flows at three-quarter depth

Exp No	d50 (mm)	Q (l/s)	V (m/s)	y_o/D	Re	Fr	S_o	λ_s	k_s (mm)
14	0.72	63.91	0.502	0.747	239726	0.28	0.000413	0.0174	0.166
15	0.72	89.47	0.701	0.749	337495	0.39	0.000753	0.0163	0.126
16	0.72	101.00	0.790	0.750	370630	0.44	0.001039	0.0177	0.250
17	0.72	115.04	0.904	0.747	420234	0.51	0.001091	0.0142	0.028
18	0.72	76.68	0.600	0.750	277795	0.33	0.000498	0.0147	0.002
19	0.72	96.15	0.753	0.749	348444	0.42	0.000826	0.0155	0.079
20	0.72	84.13	0.662	0.746	306114	0.37	0.000668	0.0162	0.107
21	0.72	108.66	0.857	0.744	406772	0.48	0.001108	0.0160	0.127
22	0.72	89.61	0.706	0.745	334926	0.40	0.000775	0.0165	0.143

Exp No	n_s	Cv (ppm)	T (C)	A (m^2)	P (m)	R (m)	B (m)
14	0.0107	2	15.5	0.12721	0.9387	0.1355	0.3907
15	0.0103	7	15.5	0.12763	0.9412	0.1356	0.3895
16	0.0108	12	14.5	0.12785	0.9425	0.1357	0.3888
17	0.0096	18	14.5	0.12728	0.9391	0.1355	0.3905
18	0.0098	4	14.0	0.12778	0.9421	0.1356	0.3890
19	0.0101	7	14.0	0.12773	0.9418	0.1356	0.3892
20	0.0103	5	14.0	0.12725	0.9383	0.1356	0.3918
21	0.0102	14	15.0	0.12676	0.9361	0.1354	0.3920
22	0.0104	7	15.0	0.12701	0.9375	0.1355	0.3913

TABLE B4 BED LOAD EXPERIMENTAL DATA IN 305mm PIPE - (ROUGHNESS 1; k_o = 0.53mm)

a) Flows at half-full depth

Exp No	d50 (mm)	Q (l/s)	V (m/s)	y_o/D	Re	Fr	S_o	λ_s	k_s (mm)
14	0.97	10.93	0.821	0.238	136831	1.16	0.005535	0.0276	0.552
29	0.97	18.25	0.517	0.486	150741	0.48	0.001163	0.0256	0.714
32	0.97	16.15	0.613	0.390	152770	0.66	0.001817	0.0243	0.490
33	0.97	15.67	0.697	0.346	155006	0.80	0.002678	0.0253	0.534
38	0.97	13.44	0.844	0.270	154991	1.11	0.005154	0.0271	0.580
67	0.97	18.12	0.973	0.302	191340	1.20	0.005221	0.0227	0.307
1	2.00	11.89	0.675	0.291	128534	0.85	0.003244	0.0284	0.727
30	2.00	18.25	0.516	0.488	150514	0.48	0.001131	0.0251	0.653
31	2.00	16.15	0.614	0.389	152898	0.66	0.001787	0.0238	0.442
34	2.00	15.67	0.693	0.348	154601	0.79	0.002679	0.0257	0.576
37	2.00	13.44	0.840	0.271	154629	1.10	0.005191	0.0277	0.633
43	2.00	6.12	0.699	0.177	89804	1.15	0.005546	0.0294	0.514
70	2.00	24.11	0.997	0.366	228227	1.11	0.004526	0.0218	0.306
2	4.20	11.89	0.671	0.292	128199	0.85	0.003312	0.0294	0.834
15	4.20	10.93	0.821	0.238	136846	1.16	0.005561	0.0277	0.562
21	4.20	7.10	0.694	0.198	99447	1.08	0.005175	0.0308	0.682
22	4.20	12.50	0.802	0.266	149041	1.06	0.004884	0.0281	0.654
27	4.20	18.89	0.570	0.463	164844	0.55	0.001460	0.0256	0.698
28	4.20	18.25	0.519	0.485	150973	0.49	0.001184	0.0258	0.743
35	4.20	15.67	0.690	0.349	154288	0.79	0.002758	0.0268	0.683
36	4.20	13.44	0.831	0.273	154030	1.09	0.005160	0.0283	0.689
42	4.20	6.12	0.690	0.179	89380	1.13	0.005492	0.0301	0.570
71	4.20	24.11	1.000	0.364	228825	1.19	0.004553	0.0216	0.291
3	5.70	11.89	0.669	0.292	128119	0.84	0.003256	0.0291	0.801
16	5.70	10.93	0.806	0.241	135873	1.13	0.005550	0.0291	0.683
17	5.70	17.86	0.849	0.330	188363	1.00	0.004338	0.0267	0.654
20	5.70	7.10	0.705	0.195	100044	1.10	0.005195	0.0296	0.581
23	5.70	12.50	0.798	0.267	148680	1.06	0.004893	0.0286	0.703
26	5.70	18.89	0.573	0.462	165168	0.56	0.001460	0.0253	0.668
41	5.70	5.12	0.691	0.179	89409	1.13	0.005534	0.0303	0.582
66	5.70	18.12	0.971	0.303	191212	1.20	0.005285	0.0231	0.332
18	8.30	17.86	0.844	0.332	187927	0.99	0.004346	0.0271	0.699
19	8.30	7.10	0.688	0.199	99150	1.07	0.005212	0.0316	0.754
24	8.30	12.50	0.788	0.270	147938	1.04	0.004893	0.0294	0.795
25	8.30	18.89	0.571	0.463	165006	0.55	0.001449	0.0252	0.662
39	8.30	13.44	0.824	0.275	153516	1.07	0.005153	0.0289	0.756
40	8.30	6.12	0.678	0.181	88793	1.10	0.005494	0.0316	0.688
68	8.30	18.12	0.950	0.308	189497	1.16	0.005391	0.0250	0.474
69	8.30	24.11	0.974	0.372	225912	1.07	0.004595	0.0235	0.439

TABLE B4 Continued a) Flows at half-full depth

Exp No	n_s	Cv (ppm)	Ws (mm)	T (C)	A (m^2)	P (m)	R (m)	B (m)
14	0.0111	320	30	19.5	0.01332	0.3108	0.0429	0.2597
29	0.0117	14	20	19.5	0.03528	0.4709	0.0749	0.3049
32	0.0111	49	20	19.5	0.02634	0.4112	0.0641	0.2975
33	0.0112	125	30	18.5	0.02248	0.3839	0.0585	0.2903
38	0.0112	262	30	19.5	0.01593	0.3334	0.0478	0.2708
67	0.0104	379	35	18.0	0.01863	0.3551	0.0525	0.2801
1	0.0116	161	30	18.0	0.01766	0.3474	0.0508	0.2770
30	0.0116	13	20	19.5	0.03539	0.4716	0.0750	0.3049
31	0.0110	61	30	19.5	0.02629	0.4108	0.0640	0.2974
34	0.0113	129	30	18.5	0.02262	0.3850	0.0588	0.2906
37	0.0113	318	35	19.0	0.01602	0.3341	0.0479	0.2712
43	0.0110	318	30	19.5	0.00876	0.2652	0.0330	0.2330
70	0.0105	235	40	18.0	0.02419	0.3962	0.0611	0.2938
2	0.0118	252	30	18.0	0.01775	0.3482	0.0510	0.2773
15	0.0111	437	45	19.5	0.01332	0.3108	0.0429	0.2597
21	0.0114	562	40	20.0	0.01024	0.2811	0.0364	0.2429
22	0.0114	419	40	20.0	0.01560	0.3306	0.0472	0.2695
27	0.0117	37	30	20.5	0.03313	0.4568	0.0725	0.3042
28	0.0118	15	15	19.5	0.03517	0.4702	0.0748	0.3049
35	0.0115	207	40	18.5	0.02273	0.3857	0.0589	0.2908
36	0.0115	542	40	19.0	0.01618	0.3355	0.0482	0.2718
42	0.0111	586	30	19.5	0.00887	0.2665	0.0333	0.2339
71	0.0104	313	40	18.0	0.02405	0.3951	0.0609	0.2935
3	0.0117	254	40	18.0	0.01780	0.3485	0.0511	0.2774
16	0.0114	662	55	19.5	0.01358	0.3132	0.0434	0.2609
17	0.0114	366	50	20.0	0.02106	0.3735	0.0564	0.2869
20	0.0112	617	40	20.0	0.01007	0.2794	0.0360	0.2419
23	0.0115	537	40	20.0	0.01570	0.3314	0.0473	0.2699
26	0.0116	31	20	20.5	0.03300	0.4559	0.0724	0.3041
41	0.0111	745	40	19.5	0.00887	0.2664	0.0333	0.2338
66	0.0105	443	45	18.0	0.01867	0.3554	0.0525	0.2802
18	0.0115	516	55	20.0	0.02118	0.3744	0.0566	0.2872
19	0.0116	867	40	20.0	0.01031	0.2819	0.0366	0.2434
24	0.0117	705	60	20.0	0.01588	0.3330	0.0477	0.2706
25	0.0116	30	30	20.5	0.03306	0.4563	0.0725	0.3041
39	0.0116	765	50	19.0	0.01063	0.3368	0.0485	0.2724
40	0.0114	923	50	19.5	0.00903	0.2683	0.0337	0.2350
68	0.0109	837	75	18.0	0.01909	0.3586	0.0532	0.2815
69	0.0109	583	75	18.0	0.02477	0.4002	0.0619	0.2949

TABLE B4 Continued b) Flows more than half-full depth

Exp No	d50 (mm)	Q (l/s)	V (m/s)	y_o/D	Re	Fr	S_o	λ_s	k_s (mm)
4	0.97	21.76	0.413	0.677	140088	0.31	0.000691	0.0284	1.289
7	0.97	24.42	0.615	0.534	187742	0.54	0.001420	0.0234	0.528
13	0.97	32.96	0.705	0.611	231428	0.57	0.001558	0.0210	0.357
45	0.97	21.76	0.514	0.563	161595	0.44	0.001008	0.0245	0.659
54	0.97	26.93	0.558	0.627	192514	0.44	0.001115	0.0243	0.684
57	0.97	30.99	0.547	0.723	196669	0.38	0.000977	0.0234	0.610
58	0.97	29.43	0.487	0.771	179304	0.32	0.000775	0.0237	0.655
5	2.00	21.76	0.411	0.680	139653	0.30	0.000690	0.0287	1.338
6	2.00	24.42	0.614	0.535	187534	0.54	0.001402	0.0232	0.511
12	2.00	32.96	0.705	0.611	231499	0.57	0.001591	0.0215	0.395
44	2.00	21.76	0.516	0.561	161977	0.44	0.001024	0.0247	0.675
55	2.00	26.93	0.557	0.628	192259	0.44	0.001065	0.0233	0.572
56	2.00	30.99	0.547	0.724	196598	0.38	0.000957	0.0229	0.557
59	2.00	29.43	0.486	0.772	179206	0.32	0.000784	0.0241	0.695
60	2.00	28.92	0.736	0.530	229068	0.65	0.001987	0.0227	0.478
8	4.20	24.42	0.614	0.535	187516	0.54	0.001478	0.0245	0.649
9	4.20	32.96	0.694	0.619	232214	0.55	0.001529	0.0214	0.392
46	4.20	21.76	0.513	0.564	161423	0.44	0.001028	0.0252	0.735
47	4.20	28.75	0.716	0.539	219626	0.63	0.001778	0.0218	0.390
53	4.20	26.93	0.557	0.628	192219	0.44	0.001112	0.0244	0.695
61	4.20	28.92	0.743	0.526	230165	0.66	0.002287	0.0256	0.789
10	5.70	32.96	0.693	0.619	234832	0.55	0.001588	0.0223	0.480
48	5.70	28.75	0.712	0.541	219054	0.62	0.001758	0.0218	0.394
51	5.70	29.43	0.643	0.600	214320	0.52	0.001352	0.0218	0.412
52	5.70	26.93	0.558	0.628	192412	0.44	0.001116	0.0244	0.696
62	5.70	28.92	0.746	0.524	230683	0.67	0.002095	0.0232	0.519
65	5.70	30.99	0.814	0.516	252492	0.74	0.002371	0.0218	0.399
11	8.30	32.96	0.704	0.612	231254	0.57	0.001581	0.0214	0.390
49	8.30	28.75	0.714	0.540	219380	0.63	0.001846	0.0227	0.480
50	8.30	29.43	0.652	0.593	216165	0.54	0.001408	0.0219	0.420
63	8.30	28.92	0.743	0.526	230160	0.66	0.002291	0.0256	0.795
64	8.30	30.99	0.810	0.518	251860	0.73	0.002450	0.0228	0.492

TABLE B4 Continued b) Flows more than half-full depth

Exp No	n_s	Cv (ppm)	Ws (mm)	T (C)	A (m^2)	P (m)	R (m)	B (m)
4	0.0127	1	10	18.5	0.05268	0.5897	0.0893	0.2852
7	0.0113	29	20	19.0	0.03969	0.4998	0.0794	0.3043
13	0.0109	30	40	19.0	0.04676	0.5473	0.0854	0.2974
45	0.0117	9	20	19.0	0.04236	0.5176	0.0819	0.3026
54	0.0117	16	20	20.5	0.04823	0.5575	0.0865	0.2950
57	0.0116	11	20	20.0	0.05660	0.6204	0.0912	0.2728
58	0.0117	5	20	20.5	0.06047	0.6540	0.0925	0.2562
5	0.0128	2	20	18.5	0.05292	0.5916	0.0895	0.2845
6	0.0113	32	30	19.0	0.03977	0.5004	0.0795	0.3043
12	0.0110	36	40	19.0	0.04674	0.5472	0.0854	0.2974
44	0.0117	10	20	19.0	0.04218	0.5163	0.0817	0.3027
55	0.0115	14	20	20.5	0.04834	0.5583	0.0866	0.2948
56	0.0115	14	20	20.0	0.05663	0.6206	0.0912	0.2727
59	0.0118	7	20	20.5	0.06051	0.6544	0.0925	0.2560
60	0.0111	39	30	20.0	0.03927	0.4971	0.0790	0.3045
8	0.0116	45	30	19.0	0.03978	0.5004	0.0795	0.3043
9	0.0110	64	40	19.5	0.04746	0.5522	0.0860	0.2963
46	0.0118	12	20	19.0	0.04245	0.5181	0.0819	0.3025
47	0.0109	84	35	19.0	0.04018	0.5030	0.0799	0.3041
53	0.0117	16	20	20.5	0.04835	0.5584	0.0866	0.2947
61	0.0118	52	30	20.0	0.03891	0.4947	0.0787	0.3046
10	0.0112	71	40	20.0	0.04753	0.5527	0.0860	0.2962
48	0.0109	93	30	19.0	0.04038	0.5044	0.0801	0.3039
51	0.0110	54	30	20.0	0.04579	0.5406	0.0847	0.2988
52	0.0117	19	20	20.5	0.04827	0.5578	0.0865	0.2949
62	0.0112	54	30	20.0	0.03874	0.4936	0.0785	0.3047
65	0.0109	109	40	20.5	0.03806	0.4891	0.0778	0.3048
11	0.0110	69	40	19.0	0.04682	0.5477	0.0855	0.2973
49	0.0112	106	50	19.0	0.04026	0.5036	0.0799	0.3040
50	0.0110	55	40	20.0	0.04511	0.5360	0.0842	0.2997
63	0.0119	50	45	20.0	0.03891	0.4947	0.0787	0.3046
64	0.0112	158	60	20.5	0.03824	0.4903	0.0780	0.3048

TABLE B5 BED LOAD EXPERIMENTAL DATA IN 305mm PIPE - (ROUGHNESS 2; k_o = 1.34mm)

a) Flows up to half-full depth

Exp No	d50 (mm)	Q (l/s)	V (m/s)	y/D	Re	Fr	S_o	λ_s	k_s (mm)
9	2.00	9.83	0.714	0.243	98851	0.99	0.005556	0.0375	1.606
15	2.00	14.09	0.730	0.310	125615	0.89	0.004341	0.0342	1.487
20	2.00	20.78	0.734	0.411	161297	0.76	0.003271	0.0318	1.467
21	2.00	30.99	0.827	0.510	210505	0.75	0.002994	0.0265	0.891
8	4.20	9.83	0.709	0.245	98603	0.98	0.005550	0.0381	1.696
13	4.20	14.09	0.728	0.311	123751	0.89	0.004345	0.0345	1.532
19	4.20	20.78	0.736	0.410	161547	0.77	0.003283	0.0317	1.439
24	4.20	19.03	0.823	0.354	157210	0.93	0.004731	0.0327	1.430
7	5.70	9.83	0.710	0.244	98668	0.99	0.005556	0.0379	1.675
14	5.70	14.09	0.730	0.310	125556	0.89	0.004396	0.0347	1.560
18	5.70	20.78	0.738	0.410	161718	0.77	0.003295	0.0316	1.426
22	5.70	30.99	0.826	0.510	210457	0.75	0.002943	0.0261	0.836
23	5.70	19.03	0.826	0.353	157454	0.94	0.004754	0.0325	1.401
10	8.30	9.83	0.701	0.246	98206	0.97	0.005554	0.0392	1.870
16	8.30	14.09	0.719	0.314	124768	0.87	0.004380	0.0360	1.764
17	8.30	20.78	0.733	0.411	159085	0.76	0.003338	0.0325	1.583
25	8.30	19.03	0.811	0.358	156250	0.91	0.004716	0.0338	1.616

Exp No	n_s	Cv (ppm)	Ws (mm)	T (C)	A (m^2)	P (m)	R (m)	B (m)
9	0.0130	145	30	11.5	0.01378	0.3150	0.0438	0.2619
15	0.0128	109	30	12.0	0.01932	0.3604	0.0536	0.2821
20	0.0128	70	30	13.0	0.02833	0.4247	0.0667	0.3002
21	0.0120	57	30	13.0	0.03748	0.4853	0.0772	0.3049
8	0.0131	246	40	11.5	0.01388	0.3158	0.0439	0.2623
13	0.0129	190	40	11.5	0.01938	0.3608	0.0537	0.2823
19	0.0128	76	40	13.0	0.02823	0.4241	0.0666	0.3000
24	0.0127	215	40	12.0	0.02316	0.3888	0.0595	0.2917
7	0.0131	278	50	11.5	0.01385	0.3156	0.0439	0.2622
14	0.0129	201	50	12.0	0.01933	0.3605	0.0536	0.2822
18	0.0128	138	40	13.0	0.02817	0.4236	0.0665	0.3000
22	0.0119	119	40	13.0	0.03749	0.0485	0.0772	0.3049
23	0.0127	199	40	12.0	0.02331	0.3881	0.0594	0.2915
10	0.0133	323	60	11.5	0.01403	0.3172	0.0442	0.2630
16	0.0132	267	55	12.0	0.01962	0.3627	0.0541	0.2830
17	0.0130	200	60	12.5	0.02835	0.4249	0.0667	0.3002
25	0.0130	403	70	12.0	0.02350	0.3912	0.0600	0.2924

TABLE B5 Continued b) Flows more than half-full depth

Exp No	d50 (mm)	Q (l/s)	V (m/s)	y_o/D	Re	Fr	S_o	λ_s	k_s (mm)
2	2.00	29.26	0.580	0.652	172684	0.44	0.001511	0.0311	1.794
3	2.00	33.88	0.566	0.764	176807	0.38	0.001298	0.0294	1.542
4	2.00	27.92	0.679	0.549	178336	0.59	0.002163	0.0297	1.402
30	2.00	33.70	0.605	0.713	181127	0.43	0.001486	0.0290	1.446
5	4.20	27.92	0.681	0.548	178630	0.59	0.002126	0.0290	1.280
12	4.20	30.99	0.669	0.606	187704	0.54	0.001929	0.0288	1.322
28	4.20	34.63	0.670	0.666	196036	0.50	0.001915	0.0297	1.555
29	4.20	33.70	0.606	0.711	181515	0.43	0.001571	0.0304	1.724
1	5.70	29.26	0.580	0.652	172708	0.44	0.001434	0.0295	1.485
6	5.70	27.92	0.680	0.548	178485	0.59	0.002212	0.0303	1.498
27	5.70	34.63	0.670	0.666	196010	0.50	0.001868	0.0290	1.423
11	8.30	30.99	0.663	0.611	186672	0.53	0.001979	0.0302	1.582
26	8.30	34.63	0.670	0.666	196010	0.50	0.001868	0.0290	1.424

Exp No	n_s	Cv (ppm)	Ws (mm)	T (C)	A (m^2)	P (m)	R (m)	B (m)
2	0.0133	9	20	14:0	0.05048	0.5735	0.0880	0.2905
3	0.0130	8	30	14.0	0.05989	0.6487	0.0923	0.2590
4	0.0128	27	40	12.5	0.04110	0.5091	0.0807	0.3035
30	0.0129	11	20	13.0	0.05572	0.6133	0.0909	0.2760
5	0.0126	46	45	12.5	0.04098	0.5084	0.0806	0.3036
12	0.0127	58	30	13.0	0.04631	0.5442	0.0851	0.2981
28	0.0130	27	30	13.0	0.05169	0.5823	0.0888	0.2877
29	0.0132	18	30	13.0	0.05556	0.6120	0.0908	0.2765
1	0.0129	7	15	14.0	0.05047	0.5734	0.0880	0.2905
6	0.0129	61	50	12.5	0.04103	0.5087	0.0807	0.3036
27	0.0128	24	35	13.0	0.05170	0.5824	0.0888	0.2877
11	0.0130	43	25	13.0	0.04675	0.5472	0.0854	0.2974
26	0.0128	26	40	13.0	0.05170	0.5824	0.0888	0.2877

TABLE B6 BED LOAD EXPERIMENTAL DATA IN 450mm - SEPARATED DUNES

a) Flows at half-full depth

Exp No	d50 (mm)	Q (l/s)	V (m/s)	y_s/D	y_o/D	Y/D	Re	Fr	So
1	0.72	51.57	0.652	0.003	0.495	0.500	241179	0.50	0.000873
2	0.72	58.88	0.740	0.004	0.496	0.500	278150	0.56	0.001092
3	0 72	66.91	0.841	0.008	0.494	0.501	315969	0.64	0.001470
4	0.72	47.62	0.606	0.004	0.492	0.496	226287	0.46	0.000876
5	0.72	56.24	0.706	0.006	0.495	0.501	265480	0.54	0.001144
6	0.72	39.71	0.501	0.009	0.490	0.500	185368	0.38	0.000561
7	0.72	38.30	0.504	0.052	0.446	0.498	188371	0.39	0.000961
8	0.72	46.00	0.607	0.050	0.446	0.496	220703	0.47	0.001305
9	0.72	54.30	0.717	0.048	0.447	0.496	264152	0.56	0.001985
10	0.72	61.30	0.805	0.057	0.444	0.501	300525	0.63	0.002217
11	0.72	69.00	0.911	0.059	0.441	0.500	334502	0.71	0.002622
12	0.72	76.70	1.011	0.057	0.443	0.500	371688	0.79	0.003430

Exp No	λ_s	k_s (mm)	n_s	Cv (ppm)	T (C)	A (m^2)	P (m)	R (m)
1	0.0181	0.187	0.0105	5	13.0	0.07906	0.7049	0.1122
2	0.0176	0.170	0.0104	13	13.5	0.07957	0.7072	0.1125
3	0.0184	0.241	0.0106.	35	13.5	0.07959	0.7076	0.1125
4	0.0210	0.455	0.0113	6	13.5	0.07863	0.7031	0.11'8
5	0.0203	0.401	0.0112	15	13.5	0.07965	0.7078	0.1125
6	0.0197	0.292	0.0110	4	13.0	0.07924	0.7062	0.1122
7	0.0323	2.545	0.0140	34	14.5	0.07604	0.6981	0.1089
8	0.0302	2.025	0.0135	65	13.5	0.07575	0.6965	0.1088
9	0.0330	2.762	0.0142	142	14.0	0.07581	0.6964	0.1088
10	0.0292	1.828	0.0133	180	14.5	0.07608	0.6992	0.1088
11	0.0269	1.364	0.0128	247	14.0	0.07576	0.6983	0.1085
12	0.0286	1.714	0.0132	391	14.0	0.07585	0.6983	0.1086

Exp No	B (m)	As (m)	Ps (m)	Wb (m)	λ_{sb}	k_{sb} (mm)	H (mm)	L (mm)	H/L
1	0.450	0.00004	0.0475	0.047	0.0252	1.56	15	198	0.076
2	0.450	0.00007	0.0585	0.058	0.0211	0.63	14	290	0.048
3	0.450	0.00018	0.0789	0.079	0.0285	2.75	22	367	0.060
4	0.450	0.00007	0.0585	0.058	0.0574	37.18	15	192	0.078
5	0.450	0.00014	0.0723	0.072	0.0459	17.46	17	237	0.072
6	0.450	0.00024	0.0871	0.087	0.0313	3.85	18	223	0.079
7	0.450	0.00312	0.2064	0.199	0.0679	40.89	38	447	0.084
8	0.450	0.00297	0.2030	0.196	0.0618	32.11	53	633	0.084
9	0.450	0.00282	0.1995	0.193	0.0735	51.43	51	518	0.099
10	0.450	0.00358	0.2163	0.208	0.0574	25.86	50	413	0.122
11	0.450	0.00381	0.2210	0.212	0.0492	16.57	40	480	0.083
12	0.450	0.00362	0.2172	0.209	0.0559	24.17	39	400	0.098

TABLE B6 Continued b) Flow at three-quarter depth

Exp No	d50 (mm)	Q (l/s)	V (m/s)	y_s/D	y_o/D	Y/D	Re	Fr	S_o
1	0.72	62.50	0.503	0.070	0.688	0.757	226615	0.28	0.000868
2	0.72	75.00	0.590	0.049	0.712	0.761	271511	0.33	0.001231
3	0.72	87.50	0.704	0.071	0.686	0.757	319800	0.40	0.001470
4	0.72	80.20	0.658	0.083	0.667	0.751	296273	0.38	0.001518
5	0.72	100.00	0.813	0.060	0.684	0.744	369813	0.46	0.002334

Exp No	λ_s	k_s (mm)	n	Cv (ppm)	T (C)	A (m^2)	P (m)	R (m)
1	0.0357	4.316	0.0152	11	14.2	0.12435	0.9387	0.1325
2	0.0371	4.956	0.0156	34	14.5	0.12704	0.9477	0.1340
3	0.0308	2.678	0.0141	73	14.5	0.12423	0.9385	0.1324
4	0.0361	4.435	0.0153	52	14.5	0.12191	0.9291	0.1312
5	0.0368	4.768	0.0155	98	14.5	0.12299	0.9274	0.1326

Exp No	B (m)	As (m)	Ps (m)	Wb (m)	λ_{sb}	k_{sb} (mm)	H (mm)	L (mm)	H/L
1	0.386	0.00486	0.2404	0.229	0.0926	115.81	55	537	0.102
2	0.384	0.00286	0.2004	0.194	0.1155	208.49	68	488	0.139
3	0.386	0.00498	0.2426	0.231	0.0738	67.69	52	514	0.101
4	0.389	0.00624	0.2623	0.248	0.0888	100.46	69	502	0.137
5	0.393	0.00393	0.2234	0.214	0.1041	156.89	55	469	0.118

TABLE B7 BED LOAD EXPERIMENTAL DATA IN 450mm - CONTINUOUS LOOSE BEDS

a) Flows at half-full depth

Exp No	d50 (mm)	Q (l/s)	V (m/s)	y_s/D	y_o/D	Y/D	Re	Fr	S_o
1	0.72	34.20	0.497	0.120	0.381	0.500	172221	0.41	0.001811
2	0.72	41.77	0.615	0.127	0.374	0.501	208150	0.50	0.002556
3	0.72	47.60	0.690	0.124	0.380	0.504	235803	0.56	0.002710
4	0.72	53.96	0.792	0.126	0.375	0.501	268629	0.65	0.003100
5	0.72	61.41	0.888	0.121	0.382	0.503	304302	0.72	0.003507
6	0.72	68.71	0.958	0.122	0.394	0.516	321700	0.77	0.004081
7	0.72	86.04	1.206	0.116	0.394	0.511	409980	0.97	0.004658
8	0.72	28.75	0.514	0.239	0.289	0.528	154366	0.46	0.002539
9	0.72	30.18	0.560	0.231	0.280	0.511	166929	0.52	0.002061
10	0.72	32.90	0.611	0.226	0.281	0.508	177027	0.56	0.002274
11	0.72	37.32	0.673	0.229	0.288	0.517	204919	0.61	0.002862
12	0.72	35.69	0.808	0.216	0.240	0.456	202678	0.81	0.002394
13	0.72	45.22	0.830	0.222	0.285	0.507	250314	0.76	0.003496
14	0.72	49.64	0.892	0.215	0.292	0.507	268577	0.81	0.001672
15	0.72	41.84	0.940	0.204	0.250	0.454	250142	0.93	0.000689
16	0.72	54.43	0.981	0.220	0.289	0.509	294030	0.89	0.001050
17	0.72	60.90	1.016	0.210	0.313	0.523	322037	0.89	0.002493
18	0.72	68.70	1.332	0.206	0.274	0.480	376536	1.25	0.000860

Exp No	λ_s	k_s (mm)	n_s	Cv (ppm)	T (C)	A (m^2)	P (m)	R (m)
1	0.0581	12.506	0.0186	59	14.5	0.06883	0.6814	0.1010
2	0.0531	9.940	0.0177	120	14.0	0.06796	0.6794	0.1000
3	0.0451	6.539	0.0164	224	14.0	0.06900	0.6834	0.1010
4	0.0389	4.246	0.0152	294	14.0	0.06814	0.6800	0.1002
5	0.0353	3.192	0.0145	398	14.0	0.06912	0.6832	0.1012
6	0.0360	3.481	0.0147	465	12.5	0.07173	0.6948	0.1032
7	0.0260	1.144	0.0125	672	13.0	0.07137	0.6918	0.1032
8	0.0644	13.451	0.0190	55	15.5	0.05603	0.6563	0.0854
9	0.0432	4.769	0.0155	269	16.0	0.05393	0.6447	0.0836
10	0.0401	3.853	0.0149	349	14.8	0.05398	0.6436	0.0838
11	0.0422	4.562	0.0154	508	16.1	0.05545	0.6511	0.0852
12	0.0216	0.342	0.0108	1036	13.6	0.04535	0.6023	0.0749
13	0.0336	2.284	0.0137	794	16.0	0.05462	0.6455	0.0846
14	0.0142	−0.019	0.0089	935	15.3	0.05584	0.6490	0.0860
15	0.0047	−0.166	0.0050	1096	15.0	0.04689	0.6057	0.0766
16	0.0073	−0.124	0.0064	919	15.3	0.05551	0.6486	0.0856
17	0.0170	0.117	0.0099	940	15.5	0.05994	0.6659	0.0901
18	0.0031	−0.145	0.0042	1269	14.5	0.05194	0.6292	0.0824

TABLE B7 Continued a) Flows at half-full depth

Exp No	B (m)	As (m2)	Ps (m)	Wb (m)	λ_{sb}	k_{sb} (mm)	H (mm)	L (mm)	H/L
1	0.450	0.01077	0.3179	0.292	0.1110	90.09	55	505	0.109
2	0.450	0.01171	0.3275	0.299	0.0976	68.34	63	938	0.067
3	0.450	0.01141	0.3246	0.297	0.0806	46.26	45	795	0.057
4	0.450	0.01162	0.3267	0.299	0.0660	28.48	44	755	0.058
5	0.450	0.01101	0.3204	0.294	0.0590	21.76	25	612	0.041
6	0.450	0.01103	0.3207	0.294	0.0616	25.17	42	737	0.057
7	0.450	0.01030	0.3129	0.288	0.0386	6.42	46	646	0.071
8	0.449	0.02916	0.4596	0.384	0.0967	46.70			
9	0.450	0.02775	0.4509	0.379	0.0602	15.77			
10	0.450	0.02690	0.4455	0.376	0.0552	12.67			
11	0.450	0.02754	0.4496	0.378	0.0593	15.61			
12	0.447	0.02523	0.4348	0.370	0.0233	0.55			
13	0.450	0.02629	0.4416	0.374	0.0449	7.25			
14	0.450	0.02507	0.4336	0.370	0.0113	−0.09			
15	0.446	0.02334	0.4220	0.363					
16	0.450	0.02590	0.4396	0.373					
17	0.449	0.02427	0.4284	0.367	0.0166	0.09			
18	0.449	0.02360	0.4239	0.364					

TABLE B7 Continued b) Flows at three-quarter depth

Exp No	d50 (mm)	Q (l/s)	V (m/s)	y_s/D	y_o/D	Y/D	Re	Fr	So
1	0.72	58.25	0.492	0.119	0.637	0.756	210800	0.28	0.000887
2	0.72	69.95	0.599	0.128	0.626	0.754	254519	0.35	0.001579
3	0.72	81.08	0.692	0.130	0.628	0.758	294035	0.40	0.002251
4	0.72	93.52	0.798	0.133	0.628	0.761	338313	0.46	0.002719
5	0.72	104.98	0.898	0.142	0.624	0.766	373901	0.52	0.002828
6	0.72	50.72	0.497	0.234	0.530	0.764	184125	0.31	0.001287
7	0.72	72.72	0.719	0.222	0.525	0.746	264162	0.45	0.003189
8	0.72	97.36	0.928	0.206	0.547	0.754	352560	0.57	0.004265

Exp No	λ_s	k_s (mm)	n_s	Cv (ppm)	T (C)	A (m^2)	P (m)	R (m)
1	0.0368	4.580	0.0154	21	13.5	0.11830	0.9231	0.1282
2	0.0440	7.685	0.0168	56	13.5	0.11682	0.9181	0.1272
3	0.0469	9.143	0.0173	108	13.5	0.11712	0.9213	0.1271
4	0.0426	7.031	0.0165	182	13.5	0.11726	0.9235	0.1270
5	0.0348	3.820	0.0149	234	13.0	0.11691	0.9256	0.1263
6	0.0473	8.455	0.0171	62	12.0	0.10208	0.8840	0.1155
7	0.0561	13.234	0.0187	237	11.5	0.10111	0.8715	0.1160
8	0.0460	8.115	0.0170	544	12.0	0.10491	0.8862	0.1184

Exp No	B (m)	As (m2)	Ps (m)	Wb (m)	λ_{sb}	k_{sb} (mm)	H (mm)	L (mm)	H/L
1	0.386	0.01069	0.3170	0.291	0.0785	66.50	43	608	0.071
2	0.387	0.01181	0.3287	0.300	0.0991	109.55	56	761	0.074
3	0.386	0.01220	0.3324	0.303	0.1078	129.98	71	784	0.090
4	0.384	0.12595	0.3364	0.306	0.0948	99.50	76	940	0.081
5	0.381	0.14167	0.3473	0.314	0.0701	48.83	83	870	0.094
6	0.382	0.02836	0.4548	0.381	0.0858	60.96	55	1272	0.043
7	0.391	0.02622	0.4412	0.374	0.1077	98.74	74	1460	0.051
8	0.388	0.02369	0.4245	0.364	0.0878	68.70	51	1090	0.047

APPENDIX C

CROSS-SECTIONAL GEOMETRY OF PIPES

C.1 CLEAN PIPES

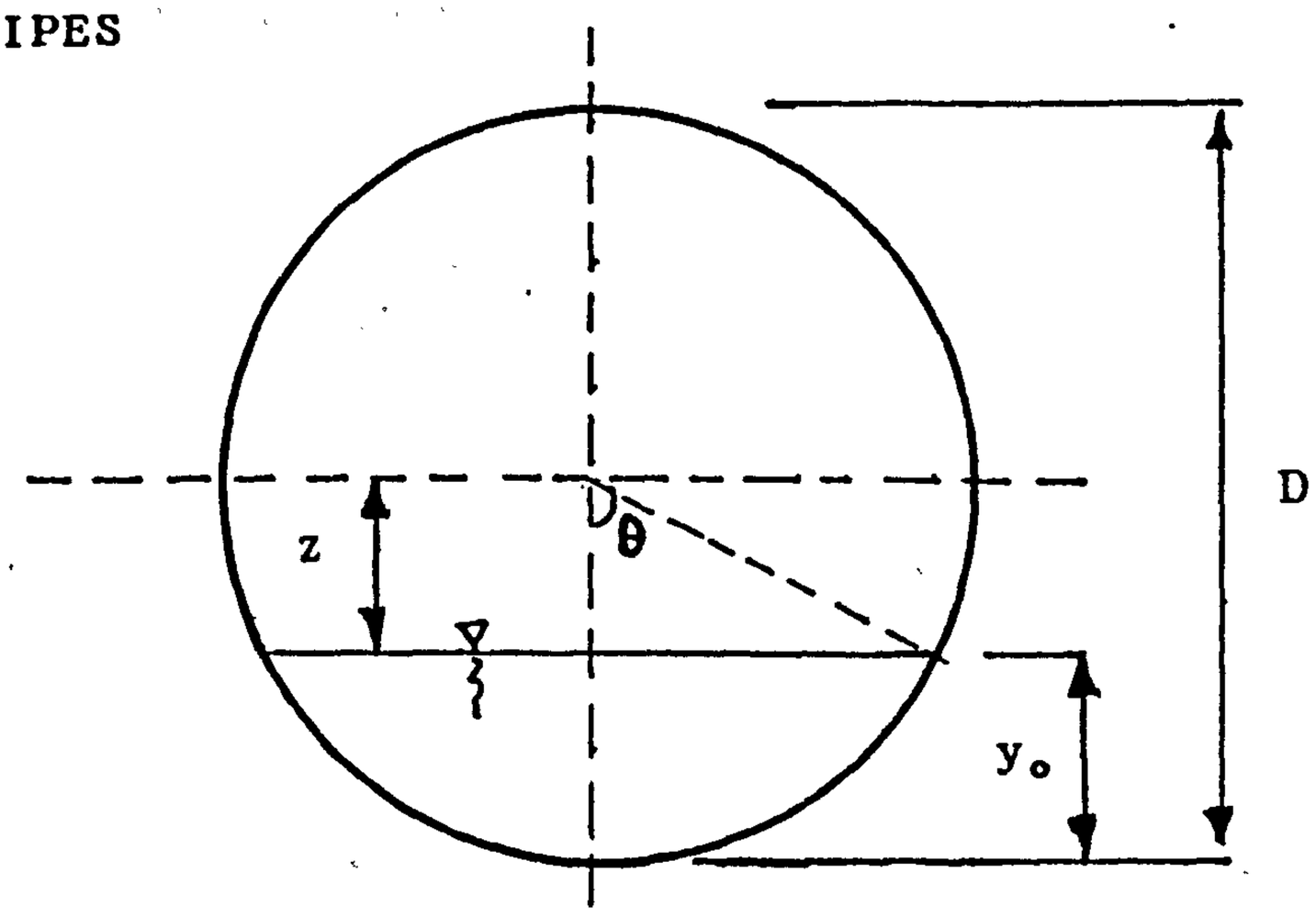

Fig. C.1 Circular channel section

The geometry properties of the flows in clean pipes (Fig. C.1) are computed as follow (see Featherstone-Nalluri, 1988):

$$z = \frac{D}{2} - y_o \qquad (C.1)$$

$$\theta = \cos^{-1}\left(\frac{2z}{D}\right) \qquad (C.2)$$

$$A = \left(\frac{D}{2}\right)^2 \left(\theta - \frac{\sin 2\theta}{2}\right) \qquad (C.3)$$

$$P = D\,\theta \qquad (C.4)$$

$$R = \frac{A}{P} \qquad (C.5)$$

$$B = D \sin\theta \qquad (C.6)$$

C.2 PIPES WITH DEPOSITED BEDS

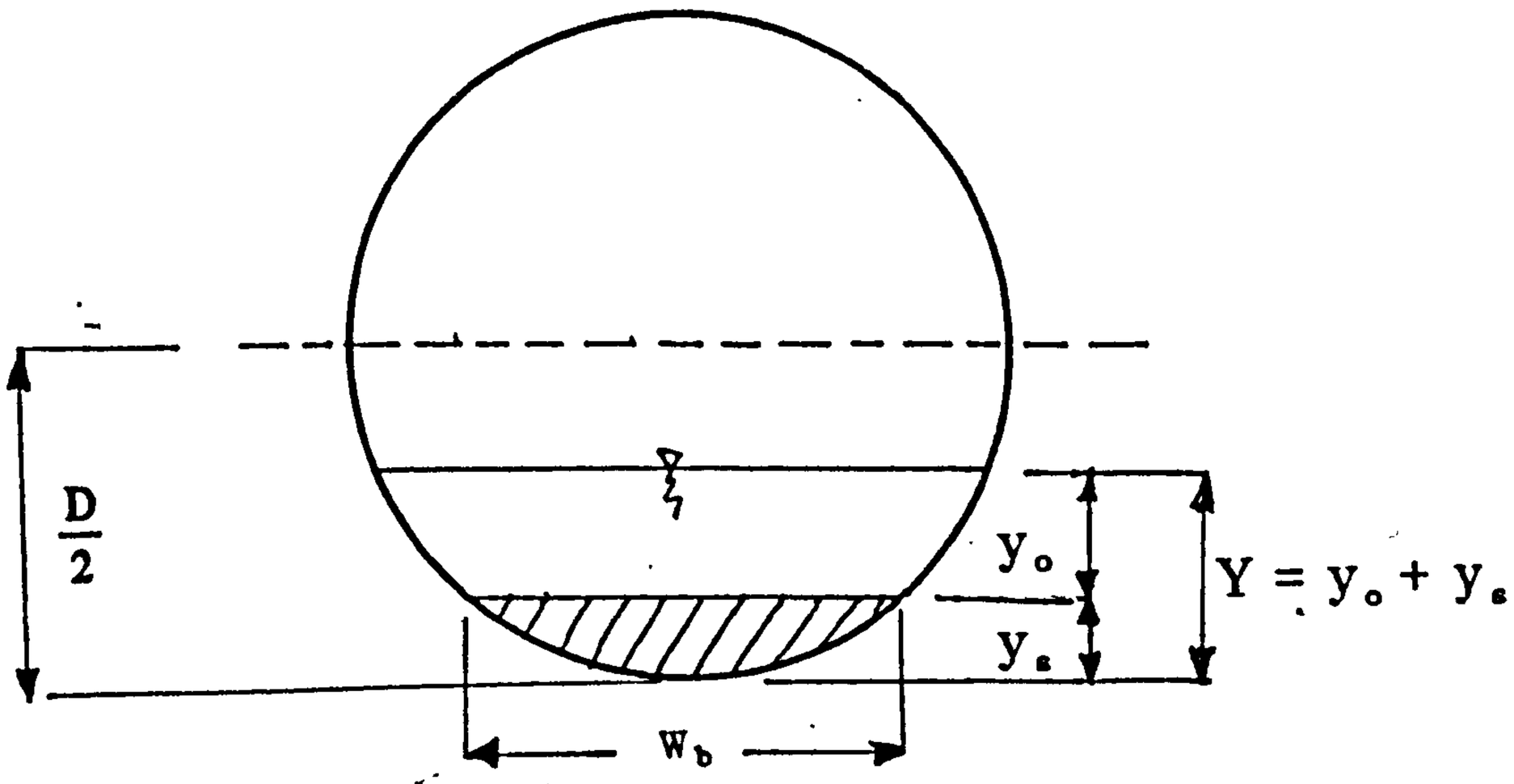

Fig. C.2 Pipes with deposited beds -

The computations of the flow geometry properties of the pipe with deposited beds are as follow:

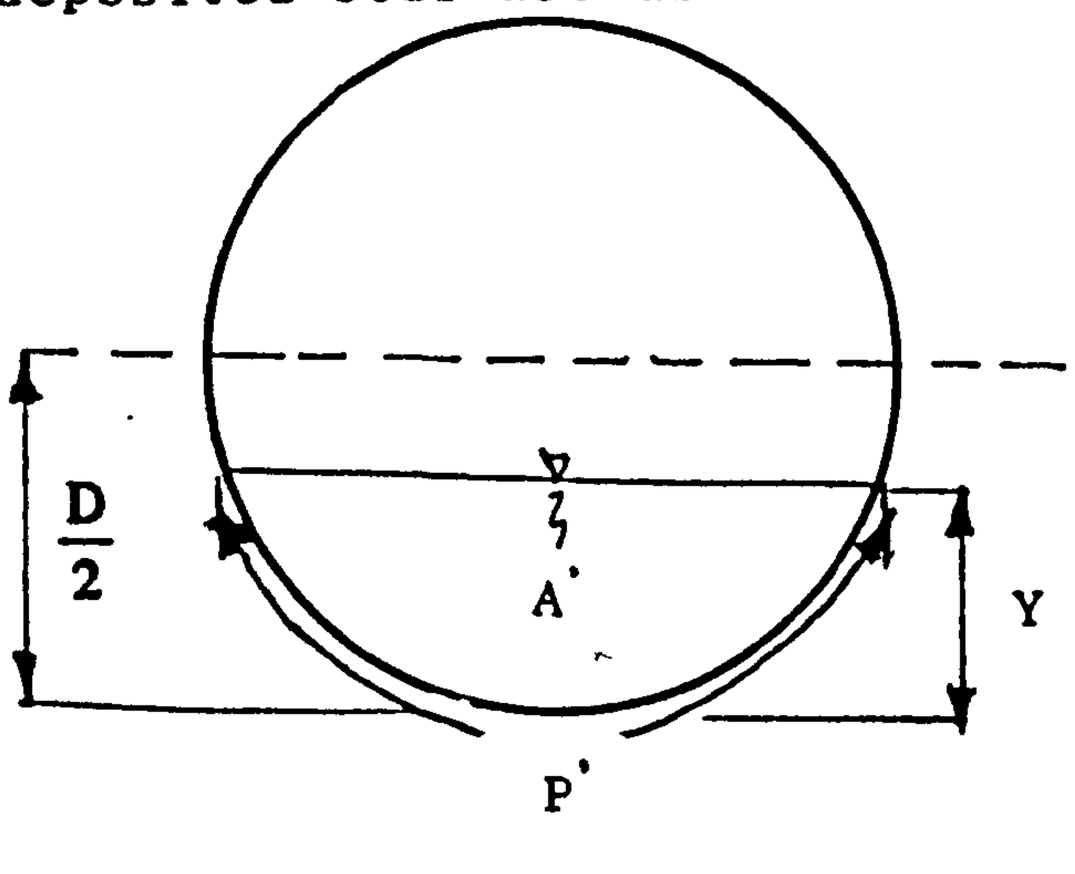

Fig. C.3 Overall flow geometry

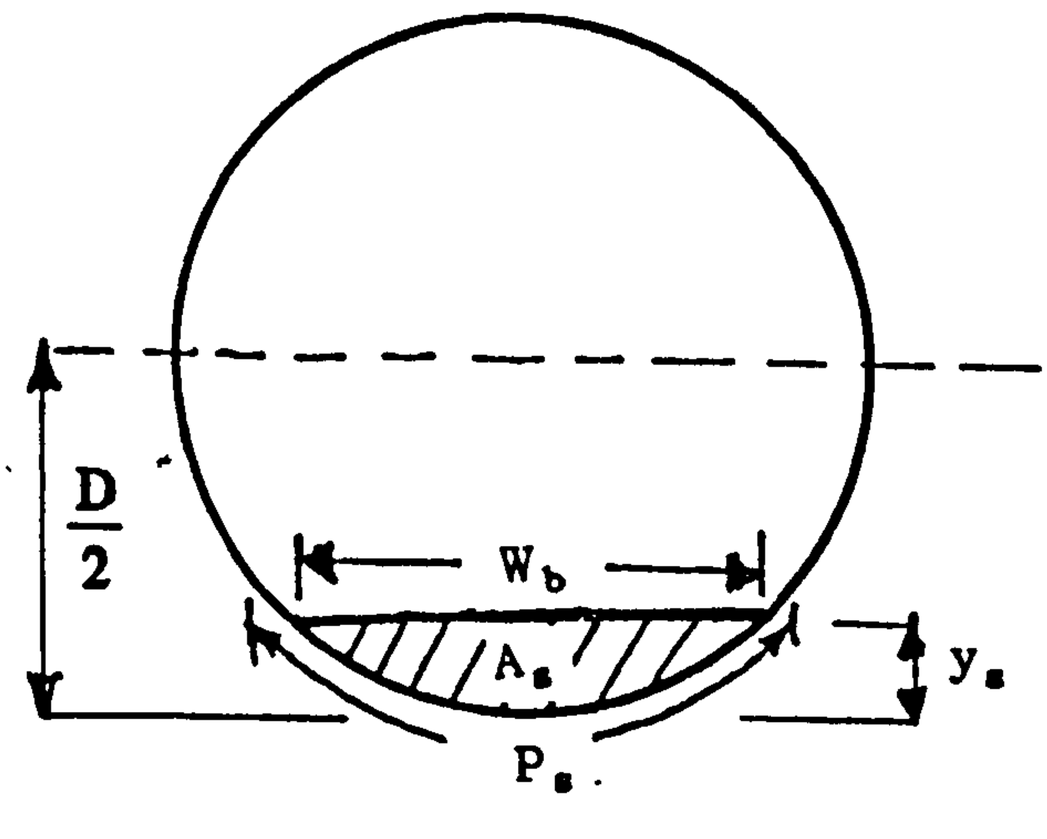

Fig. C.4 Sediment bed geometry

a) Overall flow geometry (Fig. C.3)

The required properties are flow depth (Y), flow area (A'), and wetted perimeter (P'). A' and P' can be computed from Eqns. C.3 and C.4 respectively.

b) Sediment bed geometry (Fig. C.4)

The required properties are sediment bed thickness (y_s), sediment bed area (A_s), the part of the pipe perimeter covered by the sediment (P_s), and the bed width, W_b. A_s, P_s and W_b can be computed from Eqns. C.3, C.4 and C.6 respectively.

c) Hydraulic flow geometry (Fig. C.2)

The geometry properties of the flow over the sediment bed are given by the following equations:

$$y_o = Y - y_s \tag{C.7}$$

$$A = A' - A_s \tag{C.8}$$

$$P = P' - P_s + W_b \tag{C.9}$$

$$R = \frac{A}{P} \tag{C.5}$$